land

Special Issue Reprint

Eco-Sensitive Areas

Ecosystem Services, Protected Lands, and Current Challenges

Edited by
Shicheng Li, Chuanzhun Sun, Qi Zhang, Basanta Paudel and Lanhui Li

mdpi.com/journal/land

MDPI

Eco-Sensitive Areas: Ecosystem Services, Protected Lands, and Current Challenges

Eco-Sensitive Areas: Ecosystem Services, Protected Lands, and Current Challenges

Editors

Shicheng Li
Chuanzhun Sun
Qi Zhang
Basanta Paudel
Lanhui Li

MDPI

Basel • Beijing • Wuhan • Barcelona • Belgrade • Novi Sad • Cluj • Manchester

Editors

Shicheng Li
China Univeristy of Geosciences
Wuhan
China

Basanta Paudel
Chinese Academy of Sciences
Beijing
China

Chuanzhun Sun
South China Agriculture University
Guangzhou
China

Lanhui Li
Xiamen University of Technology
Xiamen
China

Qi Zhang
University of North Carolina at Chapel Hill
Chapel Hill
USA

Editorial Office
MDPI
St. Alban-Anlage 66
4052 Basel, Switzerland

This is a reprint of articles from the Special Issue published online in the open access journal *Land* (ISSN 2073-445X) (available at: https://www.mdpi.com/journal/land/special_issues/protected_lands).

For citation purposes, cite each article independently as indicated on the article page online and as indicated below:

Lastname, A.A.; Lastname, B.B. Article Title. *Journal Name* **Year**, *Volume Number*, Page Range.

ISBN 978-3-7258-0557-0 (Hbk)
ISBN 978-3-7258-0558-7 (PDF)
doi.org/10.3390/books978-3-7258-0558-7

Contents

land

MDPI

Article

Spatial Differentiation and Driving Mechanisms of Ecosystem Service Value Change in Rural Land Consolidation: Evidence from Hubei, China

Mingqing Liu [1], Chaozheng Zhang [2,3], Xiaoyu Sun [3], Xupeng Zhang [4], Dongming Liao [3], Jiao Hou [5,*], Yaya Jin [2], Gaohui Wen [6] and Bin Jiang [7]

[1] College of Marxism, Wuhan Institute of Technology, Wuhan 430205, China; 21091601@wit.edu.cn
[2] College of Economics and Management, Northwest A&F University, Xianyang 712100, China; weirdo08@nwafu.edu.cn (C.Z.); jinyaya99@nwafu.edu.cn (Y.J.)
[3] College of Public Administration, Huazhong Agricultural University, Wuhan 430070, China; sdwfzcsxy@webmail.hzau.edu.cn (X.S.); l.dongming@webmail.hzau.edu.cn (D.L.)
[4] College of Public Administration, China University of Geosciences, Wuhan 430074, China; zhangxupeng@cug.edu.cn
[5] College of Management, Wuhan Polytechnic University, Wuhan 430074, China
[6] College of Geographical Science, Hunan Normal University, Changsha 410081, China; wgh@hunnu.edu.cn
[7] College of Public Management, Huazhong University of Science and Technology, Wuhan 430074, China; d201781034@hust.edu.cn
* Correspondence: houjiao@mails.ccnu.edu.cn

Abstract: Rural land consolidation projects (RLCPs) have become one of the largest organized human activities to change land use patterns and impact terrestrial ecosystems, and it may also be an important precondition to improving ecosystem service value (ESV). Evaluating the change in ecosystem service value (ESV) is an important basis for measuring the effectiveness of RLCPs. Therefore, this paper, taking RLCPs implemented at County Level in Hubei Province, China, as an example, uses the improved ESV evaluation model to analyze the spatial differentiation of ESV change in RLCPs and then adopts geographic detectors and a geographically weighted regression model to identify the dominant factors affecting the ESV change in RLCPs. The results showed that (1) although RLCPs make the unevenness of land use obvious, they reduce the complexity of land use evidently and improve the dominance of land use significantly; (2) The ESV of RLCPs in 71 counties of Hubei Province increased, with an average increase of USD 2.37×10^7 a^{-1}. The ESV increase is large in central Hubei, while small in eastern and western Hubei. However, the increase rate of ESV is high in eastern and central-north Hubei, while low in western and central-south Hubei. This indicates that RLCPs can effectively promote ESV, but there are significant regional differences, and (3) the ESV increase is positively correlated with GDP and construction scale, but negatively linked with investment and per capita income of rural residents. The ESV increase rate is negatively associated with cultivated land proportion and land use diversification index change, but it is positively related to the change in the land use evenness index. However, their driving effects have significant spatial heterogeneity.

Keywords: rural land consolidation projects; ecosystem service value; spatial differentiation; driving mechanisms; equivalent factor method; geographically weighted regression model

Citation: Liu, M.; Zhang, C.; Sun, X.; Zhang, X.; Liao, D.; Hou, J.; Jin, Y.; Wen, G.; Jiang, B. Spatial Differentiation and Driving Mechanisms of Ecosystem Service Value Change in Rural Land Consolidation: Evidence from Hubei, China. *Land* **2023**, *12*, 1162. https://doi.org/10.3390/land12061162

Academic Editors: Shicheng Li, Chuanzhun Sun, Qi Zhang, Basanta Paudel and Lanhui Li

Received: 27 April 2023
Revised: 28 May 2023
Accepted: 30 May 2023
Published: 31 May 2023

1. Introduction

Ecosystem services refer to natural environmental conditions and their utility that are formed and maintained by ecosystems and their processes [1], including support services, regulation services, supply services, and cultural services [2]. With the rapid increase in population and development of the economy, ecosystem services are constantly being utilized by human beings. The Millennium Ecosystem Assessment points out that more

than 60% of the global ecosystem services are declining, and the trend is expected to continue indefinitely [1,2]. As an important basis for natural asset accounting and ecological environment protection, the quantitative assessment of ecosystem service value (ESV) can be more persuasive in terms of the ecological benefits obtained by adhering to high-quality economic development and enhancing public awareness of environmental protection [3,4]. At present, the ESV evaluation is mainly based on three aspects. The first aspect is evaluating the comprehensive value of ecosystem services at different spatial scales, i.e., global, regional, and local [5–9]. The second aspect is assessing the comprehensive ESV of different ecosystem types, i.e., cultivated land, forest land, grassland, wetland, and unused land [10–14]. The third is evaluating the value of individual ecosystem services, such as primary product production, gas regulation, soil and water conservation, and biodiversity maintenance [14–19]. However, it should be emphasized that the purpose of ESV assessment is not to put an accurate and absolute price tag on ecosystem services, but to allow marginal changes in ESV to be reflected in the decision-making process on ecosystem conservation and land management [20–22]. The evaluation accuracy of ESV has not been effectively solved in previous studies, which is why future research should focus on analyzing the marginal change in ESV brought about by public policies or project implementation in order to weaken the error of absolute value to a certain extent, and provide policy implications for continued and effective implementation of public policies or projects [11,12].

Rural land consolidation projects (RLCPs), as sustainability-oriented projects, have been implemented worldwide to promote agricultural production and achieve rural development [23,24]. With the strategic adjustment of land use policy in China, RLCPs have acquired richer connotations and functions, which enabled comprehensive RLCPs. The RLCPs required by the Ministry of Natural Resources of the People's Republic of China refer to a governance activity that combines the comprehensive application of relevant policies and the adoption of advanced engineering technologies to adjust the land use structure and optimize the spatial layout of the land to ensure sustainable land use, ultimately meeting people's production, life, and ecological needs, including comprehensive effects such as food security, modern agriculture, precision poverty alleviation, and ecological restoration. Combining the above definition with the actual situation of RLCPs in China, In terms of RLCP objects, besides increasing the area and improving the quality of cultivated land, increasing the income of farmers, accelerating the internal adjustment of agriculture, promoting the migration of labor force, and improving the living environment in rural areas are also involved [25–27]. In terms of the contents of RLCPs, they are projects that mainly involve the implementation of agricultural land consolidation, construction land consolidation, area environmental consolidation, ecological restoration, and historical and cultural protection [28–30]. Among them, agricultural land consolidation refers to supplementing the quantity of cultivated land, improving the quality of cultivated land, and improving land utilization efficiency through land consolidation, reclamation, and development. Construction land consolidation refers to idle and inefficient construction land consolidation to meet the dual goals of regional development land demand and cultivated land protection. Ecological protection and restoration refer to a comprehensive improvement in the rural environment to improve rural ecological functions and maintain biodiversity, improving the ability to prevent natural disasters, and maintaining the rural natural landscape. Historical and cultural protection in RLCPs aim to enable rural areas to achieve industrial development led by distinctive rural culture, which requires the protection and utilization of rural natural and cultural resources, and the preservation of rural unique local culture.

RLCPs have become one of the largest organized human activities to change land use patterns and impact terrestrial ecosystems [31–34]. RLCPs will inevitably have direct or indirect positive or negative impacts on hydrology, soil, vegetation, atmosphere, organisms, and other environmental conditions in the project and surrounding areas [33–36]. The study of the ecological impact of RLCPs has become an important concern in the evaluation

of the benefits of land consolidation projects. Especially in China, quantitatively evaluating the economic effects of RLCPs by analyzing ESV changes has become a major concern for many scholars to provide a reference for policymakers in conducting post-RLCP benefit evaluations. For example, Lu et al. used an improved equivalent factor method to reveal the ESV profit and loss patterns of land consolidation projects with different properties and landforms, and effectively quantitatively evaluated the ecological environment changes caused by the implementation of land consolidation projects in villages in plains, hills, and mountainous areas of Hubei Province, China [19]. Liu et al. used GIS and landscape indicators to evaluate the ecological effects of RLCPs in typical RLCP locations [37]. Zhou et al. evaluated the ecological benefits of an RLCP at a township level [38]. However, the existing research mainly focuses on small areas such as villages and towns [19,37,38] and pays less attention to the county level. Specifically, these studies ignored the characteristics of China's RLCPs in terms of regions, types, goals, and modes, leading to an inaccurate assessment of the ecological effects of RLCPs. On the other hand, the driving mechanisms in ESV change in RLCPs at the county level remain unexplored. Taking Hubei Province, one of the pioneering zones for RLCP implementation in China, as a case study, we use the modified ESV evaluation model to analyze the spatial differentiation of ESV change in RLCPs. Then, we adopt a geographic detector and a geographically weighted regression model to identify the dominant factors affecting the ESV change in RLCPs, which is suitable for promoting the ecological transformation of RLCPs. Additionally, it also provides a scientific basis and support for strengthening the construction of ecological civilization and protecting the ecological environment.

2. Materials and Methods

2.1. The Effects of RLCPs on ESV

Based on the theory of ecosystem services, RLCPs will promote changes in ESV by changing land use patterns and causing ecosystem changes that affect support services, regulation services, supply services, and cultural services of the ecosystem.

Implementing RLCPs can have an impact on ecosystem support services. RLCPs supplement the quantity and improve the quality of cultivated land by implementing land consolidation, land reclamation, and land development. This has increased food production capacity. The result of improving food production capacity means that RLCPs can improve ecosystem support services.

The implementation of RLCPs has an impact on both ecosystem regulation and supply services. RLCPs affect soil physicochemical properties and hydrological processes such as surface runoff, soil infiltration, and deep infiltration by changing land use/cover types. These changes in soil habitats have an impact on the above ecosystem services in the area where RLCPs are implemented, specifically manifested as direct impacts on crop production, climate challenges, soil and water conservation, and other aspects.

The implementation of RLCPs will also have an impact on ecosystem cultural services. In practice, RLCPs focus on the improvement and protection of rural landscapes, manifested as promoting the development of industries such as ecotourism while emphasizing the protection of existing rural landscapes and culture. From this, the role of RLCPs in improving ecosystem cultural services is becoming increasingly evident.

Above all, this paper proposes that while RLCPs have an effect on the ecosystem service, there is an ESV change in RLCPs.

2.2. Study Area

Hubei Province, located in central China and the middle reaches of the Yangtze River, is one of the major grain-producing areas in China. It extends over an area of 18.59×10^4 km^2, equivalent to 1.94% of the national territory, of which mountains account for 55.5%, hills and hillocks comprise 24.5%, and plains and lakes encompass 20%. Hubei is one of the provinces with the earliest start, numerous projects, and remarkable effects in RLCPs in China, and it is also one of the pioneers and demonstration provinces for

RLCP implementation mode innovation. The RLCPs in Hubei Province is divided into 3 first-level types: low mountain and hilly consolidation type areas in eastern Hubei (I), plain consolidation type areas in central Hubei (II), and mountain plateau consolidation type area in western Hubei (III); it can be further subdivided into 7 secondary modes: low mountain consolidation mode areas (I-1), hilly consolidation mode areas (I-2), hillock consolidation mode areas (II-1), plain consolidation mode areas (II-2), water network polder consolidation mode areas (II-3), river (ditch) valley basin consolidation mode areas (III-1), and karst dam consolidation mode areas (III-2). According to the Department of the Natural Resources of Hubei Province, Hubei carried out 406 key RLCPs in 2013, with a cumulative construction scale of 461,190 hectares, a total investment of USD 2041.16 million, and 11,069 hectares of newly cultivated land, which were completed by the end of 2016. For the convenience of research, we have merged the municipal districts and the counties that have not implemented land consolidation projects, and we obtained a total of 71 county-level units. The serial numbers of each research unit and its consolidation mode are shown in Figure 1. Considering that the construction period of RLCPs takes half a year to three years, we chose 2012 and 2017 to represent the year before and after RLCPs, respectively.

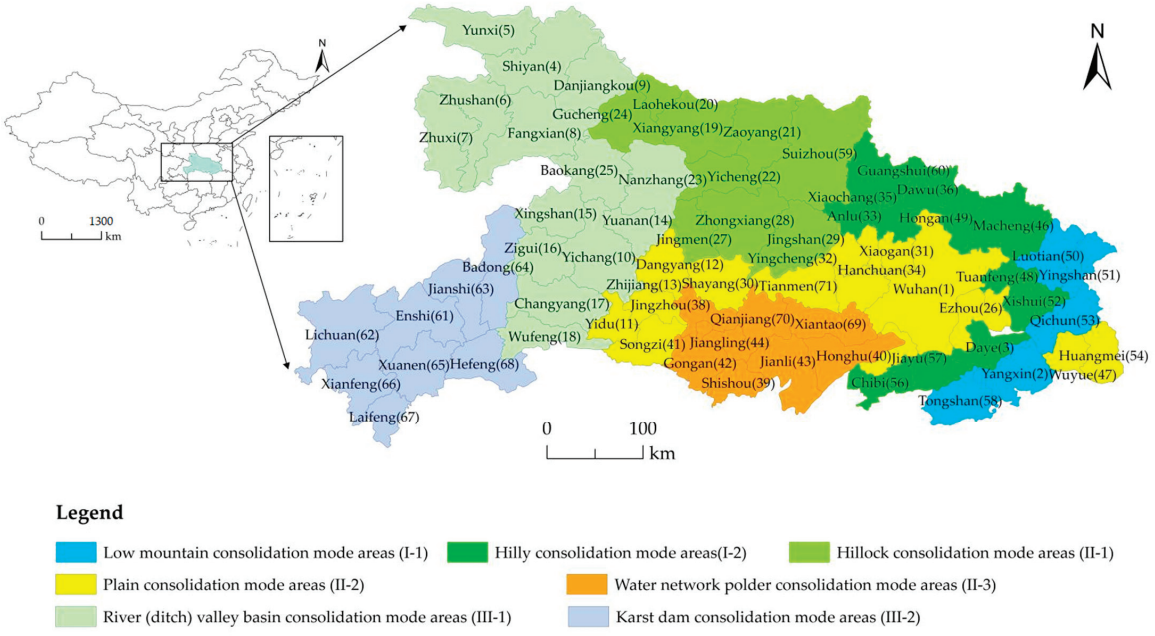

Figure 1. Location and zoning map of research unit for RLCPs in Hubei Province.

2.3. Research Methods

2.3.1. Indices of Land Use Structure

A change in land use structure will change ecosystem function and structure, leading to a change in ESV. The land use diversification index (LDI), land use diversity index (LVI), land use dominance index (LAI), and land use evenness index (LEI) are widely used to characterize land use structure from a macro perspective [39,40]. Both LDI and LVI indicate the complexity and richness of land use types, and the higher the value, the more complex the land use types. LAI refers to the difference between the maximum and actual LVI values. LEI is defined as the uneven distribution degree of various land use type areas. Their formulas are as follows.

$$LDI = 1 - \sum S_i^2 / \sum S_i^2 \quad (1)$$

$$LVI = -\sum P_i ln P_i \tag{2}$$

$$LAI = lnm + \sum P_i ln P_i \tag{3}$$

$$LEI = -\sum P_i ln P_i / lnm \tag{4}$$

where S_i and P_i represent the area and proportion of the *i*-th land use type, respectively; *m* represents the maximum area of each type of land use.

2.3.2. ESV Calculation

The equivalent factor method, derived from the unit value-based approach, has been widely applied for the calculation of the comprehensive ESV. Xie et al. developed a method based on a survey of 700 ecological experts to estimate the ESV in China [41–43]. This method is convenient and cost-effective for performing a comprehensive assessment of ESV. However, a growing body of research reveals that ecosystem service functions are regulated by different ecological mechanisms and processes, which are closely related to local ecological conditions [41]. Thus, assessment based on regional uniform equivalent factors cannot reflect regional differences in ecosystem services functions, thus limiting the practical application of ESV assessment in environmental management. To address these limitations, Xie et al. [41–43] updated equivalent coefficients of ecosystem services in China based on a combination of methods. This study obtained the table of equivalent ecosystem services coefficients in Hubei Province [41–43]. The specific steps are as follows.

First, we selected the indicators of average precipitation, food production, and social development stage to adjust the equivalent coefficients of ecosystem services [19,43,44], by which the adjusted equivalent coefficients can reflect the regional variations of ecological conditions in Hubei Province. The formulas are as follows:

$$\lambda_t = G_t / G_{0t} = W_t / W_{0t} \tag{5}$$

where λ_t is the regional correction coefficient in year *t*; G_t and G_{0t} are the average grain yield (kg/hm^2) of Hubei Province and China in year *t*, respectively; and W_t and W_{0t} are the average annual precipitation (mm) of Hubei Province and China in year *t*, respectively.

$$l_t = H_t L / \left(1 + e^{-(1/E_{nt} - 3)}\right) + h_t L / \left(1 + e^{-(1/E_{0nt} - 3)}\right) \tag{6}$$

$$T_t = l_{1t} / l_{0t} \tag{7}$$

$$P_t = GDP_{1t} / GDP_{0t} \tag{8}$$

where l_t is the coefficient of the social development stage in year *t*; T_t is the coefficient of regional willingness to pay for ecological environmental protection in year *t*; P_t is the coefficient of regional payment capacity in year *t*; *L* is the value of the social development coefficient in the ideal stage; H_t and h_t are the proportion of the urban and rural population in the total population in year *t*, respectively; E_{nt} and E_{0nt} are Engel's coefficients of urban and rural areas in year *t*, respectively; l_{1t} and l_0 are the coefficients of the social development stage in Hubei Province and China in year *t*, respectively; and GDP_{1t} and GDP_{0t} are the GDP per capita of Hubei Province and China in year *t*, respectively.

Second, Xie et al. defined that the ESV of the standard equivalent factor is equal to 1/7 of the food production value that farmland can provide [19,41–43]. We select the sowing area and output value of rice, wheat, and corn in Hubei Province to adjust the economic value of one equivalent factor. The formulas are as follows:

$$V_t = \frac{1}{7} \sum_{m=0}^{n} \left(\frac{A_{mt} P_{mt} Q_{mt}}{M_t} \right) \tag{9}$$

$$VC_{ijt} = \lambda_t \times T_t \times P_t \times V_t \times E_{0ijt} \quad (10)$$

where V_t is the economic value of one equivalent factor in year t (USD/hm^2 a^{-1}); VC_{ijt} is the economic value of one equivalent factor of the i-th ecosystem type (or land use type) and the j-th service type in year t; A_{mt}, P_{mt}, and Q_{mt} are the sown area, selling price, and total output of the m-th crops in year t, respectively; and M_t is the total sown area of three crops in year t.

Third, Xie et al. [43] divided the ecosystem types or land use types into 6 categories in the equivalent table of terrestrial ecosystem services in China, which differs from the land use type in the project area, so it is necessary to readjust them. Specifically, ESV of cultivated land is the average value of water fields and dry land; ESV of garden land is weighted with 80% of the corresponding value of forest land and 20% of the corresponding value of grassland; ESV of forest land is the average value of broad-leaved forests and shrub forests; ESV of grass land is the average value of grasslands, shrubs, and meadows; ESV of traffic land is replaced by the corresponding value of bare land; other land types include field ridge, sandy land, and bare land, and their ESV is replaced by the corresponding value of bare land; and the ESV of construction land is zero.

Forth, based on the modified equivalent coefficients of ecosystem services and areas of different land use types, the ESV formulas are as follows.

$$ESV_0 = \sum_i \sum_j A_{0i} \times VC_{0ij} \quad (11)$$

$$ESV_1 = \sum_i \sum_j A_{1i} \times VC_{1ij} \quad (12)$$

$$ESV_{gl} = ESV_1 - ESV_0 \quad (13)$$

$$ESV_{gl1} = ESV_1 - ESV_0 / ESV_0 \times 100 \quad (14)$$

where ESV_0 and ESV_1 are the total ESV before and after RLCP; A_{0i} and A_{1i} are the areas of the i-th ecosystem type before and after RLCP; VC_{0ij} and VC_{1ij} refer to the value coefficient of the i-th ecosystem type and the j-th service type before and after RLCP; and ESV_{gl} and ESV_{gl1} represent the amount and rate of change in ESV, respectively.

2.3.3. Spatial Autocorrelation

Spatial autocorrelation is commonly used to calculate the correlation degree of spatially dependent or heterogeneous data and interpret their spatial mechanism [45]. It can be divided into global spatial autocorrelation and local spatial autocorrelation [45]. The former can be used to investigate the overall spatial correlation and differences in ESV change, as expressed by Moran's I statistic [46]. The latter can be used to further explain the spatially non-stationary and heterogeneous characteristics of ESV change, which can be described by local Moran's I [46]. The formulas are as follows:

$$I = n \frac{\sum_{i=1}^{n} \sum_{j=1}^{n} W_{ij}(x_i - \overline{x})(x_j - \overline{x})}{\sum_{i=1}^{n} \sum_{j=1}^{n} W_{ij}(x_i - \overline{x})^2} \quad (15)$$

$$I_i = \frac{n(x_i - \overline{x}) \sum_{j=1}^{n} (x_j - \overline{x})}{\sum_{j=1}^{n} (x_j - \overline{x})^2} \quad (16)$$

where I and I_i are Moran's I and local Moran's I indices, respectively; n is the number of research units; x_i and x_j are the attribute values of spatial units I and j, respectively; x is the average value of x_i; and W_{ij} is the spatial weight matrix.

2.3.4. Geographic Detector and Geographically Weighted Regression Model

The geographic detector is widely used to detect spatial heterogeneity and discover its driving factors, and it is based on the assumption that if the independent variable has a significant effect on the dependent variable, the spatial distribution of the independent and dependent variables should be similar or even highly consistent [47,48]. Therefore, we use the geographic detector to determine the dominant factors affecting the ESV change in RLCPs. The expression is as follows:

$$q = 1 - \frac{1}{N\sigma^2} \sum_{h=1}^{L} N_h \sigma_H^2 \quad (17)$$

where q is the explanatory power of explanatory variables for ESV change or change rate, whose values range from 0 to 1; h = 1, ..., L is the stratification of variable Y or factor X; N_h and N are the numbers of cells in stratum h and full area, respectively; and σ_h^2 and σ^2 are the variances of Y values in stratum h and full area, respectively.

The geographic detector is a method of global spatial analysis, in which the regression parameters are the same in different geographic locations. However, the regression parameters differ in different geographical locations [49]. If we would only adopt the geographic detector, the estimated parameters would be the average values of the regression parameters in the whole study area, which cannot reflect the real spatial characteristics of the regression parameters of the driving factors that affect ESV change in RLCPs. To solve this problem, Fortheringham et al. presented a geographically weighted regression (GWR) model, which is an extension of the ordinary linear square model and incorporates the geographic location of the sample data into the regression parameters [50,51]. Therefore, we use the GWR model to analyze the heterogeneity of the influence of the driving factors that affect ESV change. The formula is as follows:

$$Y_i = \beta_0(u_i, v_i) + \sum_{i=1}^{k=1} \beta_k(u_i, v_i) X_{ik} + \varepsilon_i \quad (18)$$

where Y_i is the explained variable, i.e., the ESV change amount or rate of the i-th county; X_{ik} is the explanatory variable, i.e., the k-th explanatory variable of the i-th county; (u_i, v_i) is the geographic location of the i-th county; $\beta_0(u_i, v_i)$ and $\beta_k(u_i, v_i)$ are the constant and the k-th regression parameter of the i-th county; and ε_i is random error item.

2.4. Data Source

The data used in this paper include RLCP data and socioeconomic data. The RLCP data were obtained from the Department of Natural Resources of Hubei Province. The socioeconomic data were derived from China Statistical Yearbook, China Water Conservancy Statistical Yearbook, Hubei Statistical Yearbook, and National Agricultural Products Cost–benefit Data Compilation.

3. Results

3.1. Characteristics of Land Use Change

Table 1 shows the areas of different land use types before and after RLCPs. After RLCPs, the area of cultivated land and rural roads increased, while the area of other lands, barren grassland, water, forest, construction land, garden, and ditch decreased. However, the increase rate of rural roads is significantly higher than that of cultivated land, which indicates that the main purpose of RLCPs in Hubei Province is no longer to increase the area of cultivated land and promote agricultural production, but to pay more attention to the construction and improvement in rural infrastructure [28,39,40].

Table 1. The area of different land use types before and after land consolidation.

	Cultivated Land	Garden Land	Forest Land	Water	Ditch	Grassland	Rural Roads	Other Lands	Construction Land
Before consolidation/hm^2	366,944	14,949	2624	28,966	14,957	4709	10,273	16,894	871
After consolidation/hm^2	374,371	14,786	1587	27,471	14,933	1719	11,431	13,968	659
Area change/hm^2	7427	−163	−1037	−1495	−24	−2990	1158	−2925	−211
Range change/%	2.02	−1.09	−39.52	−5.16	−0.16	−63.50	11.27	−17.32	−24.26

Figure 2 shows the changes in land use structure indices before and after RLCPs. After RLCPs, the LDI, LVI, and LEI indices of each county show a decreasing trend, while the LAI index shows an increasing trend. RLCPs can promote the transformation of land use types, such as barren grassland, water, and forest converted into cultivated land, which increases the proportion of cultivated land. Although RLCPs can reduce the complexity of land use and significantly improve the dominance of land use, they can also lead to uneven land use.

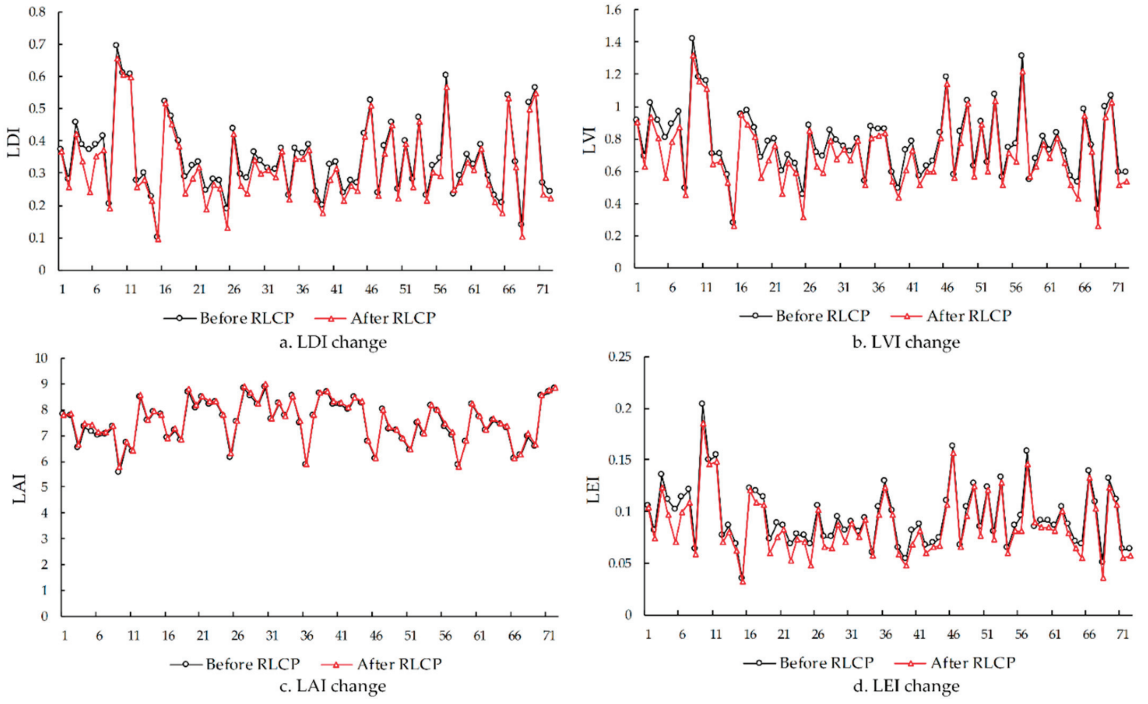

Figure 2. Land use structure indices change before and after RLCP.

3.2. Spatial Differentiation of ESV Change

3.2.1. Spatial Distribution Characteristics of ESV Change

Figure 3 shows the spatial distribution of the amount and rate of ESV increase. Grading similar amounts and rates of ESV increase to the same level is convenient for comparison. Therefore, using the Jenks natural breaks classification method [52,53], the amounts and rates of ESV increase were divided into four levels: low, medium-low, medium-high, and high. As can be seen in Figure 3a, the amount of ESV increase is characterized as high

in the middle, while low in the east and west. Specifically, the ESV amount in the whole province, the low mountain and hilly areas in eastern Hubei, the plain areas in central Hubei, and the mountainous plateau area in western Hubei increased by an average of USD 3.54×10^6 a^{-1}, USD 2.84×10^6 a^{-1}, USD 5.28×10^6 a^{-1}, and USD 1.52×10^6 a^{-1}, respectively. The high-level zones are only found in Xiantao City, the medium-high-level zones are mainly located in the small hillock areas, the medium-low zones are mainly distributed in the plain and water network polder areas, and the low-level zones are mainly distributed in eastern and western Hubei. As shown in Figure 3b, the increasing rate of ESV is high in eastern and central-northern Hubei, while low in western and central-southern Hubei. Specifically, the entire province, the low mountainous and hilly areas in eastern Hubei, the plain areas in central Hubei, and the mountain plateau area in western Hubei are characterized by an average increase rate of 10.49%, 12.46%, 10.63%, and 8.76%, respectively. Additionally, the low and medium-low level zones are mainly concentrated in western Hubei, while the zones with medium-high and high levels are mainly distributed in central and eastern Hubei.

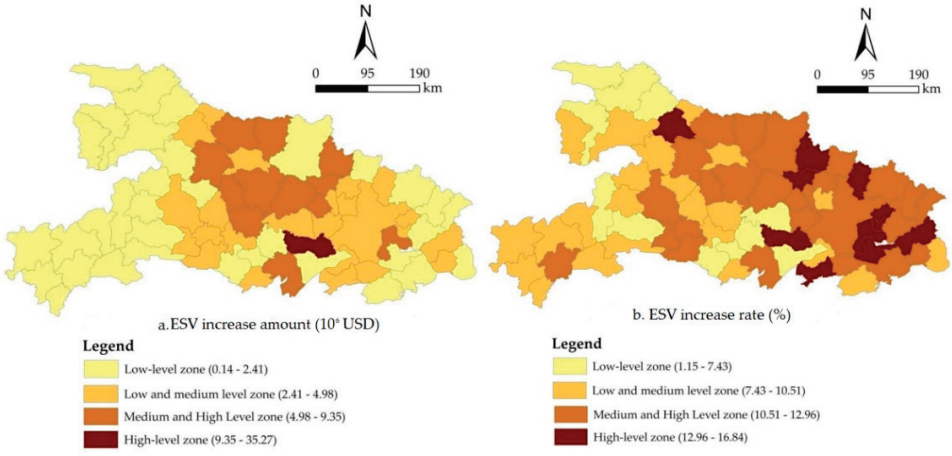

Figure 3. Spatial distribution of ESV increase amount (**a**) and rate (**b**).

3.2.2. Spatial Agglomeration Characteristics of ESV Change

Figure 4 shows the Lisa cluster map of the amount and rate of increase in ESV. Moran's I value of the amount of ESV increase was 0.1041, passing the significance test at 0.01 levels. Moran's I value of the rate of ESV increase was 0.3396, passing the significance test at 0.001 levels. These results show that there is an obvious spatial autocorrelation between the amount of ESV increase amount and the rate of ESV increase. In terms of the amount of ESV increase, the high-high and low-high areas are relatively small and mainly distributed in central Hubei, while the low-low areas are relatively large and mainly concentrated in northeast and southwest Hubei. This indicates that RLCPs in Hubei Province were widely distributed with an obvious diffusion effect. In terms of the rate of ESV increase, the high-high areas are mainly located in Wuhan, Ezhou, and Huanggang, and these areas are the hot spots of high-standard farmland construction in Hubei Province. The low-low areas are mainly located in Shiyan. The low-high and high-low areas are mainly concentrated in southern Hubei. These results suggest that with the economic development, each county increased its RLCPs investment, and regional differences gradually decreased.

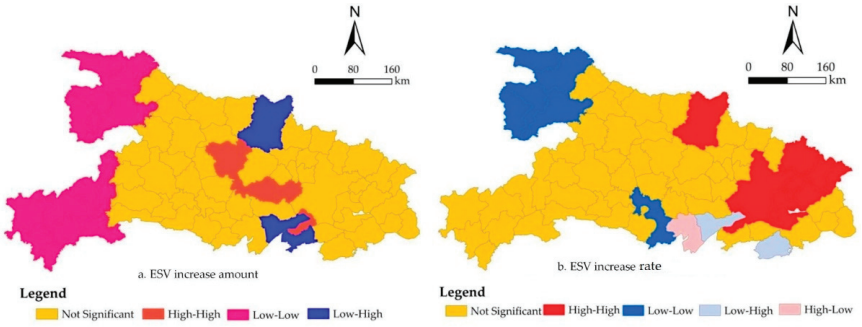

Figure 4. The Lisa cluster map of ESV increase amount (**a**) and rate (**b**).

3.3. Driving Mechanism of ESV Change

3.3.1. Driving Factors Selection

In addition to RLCPs, natural, economic, social, policy, and other factors will influence the change in ESV. Firstly, natural factors, especially cultivated land factors, are the sufficient conditions for RLCPs. The main purpose of RLCPs is to improve the quality of cultivated land and increase the area of cultivated land. Secondly, RLCPs belong to the engineering measures of capital investment, and good economic conditions are a necessary condition for its implementation. Thirdly, RLCPs are an important tool for promoting rural revitalization and achieving regional sustainable development. Therefore, social factors such as population and farmers' income are also important factors influencing the layout of RLCPs. Fourthly, policy factors, especially investment scale and construction scale, not only indicate the frequency of RLCPs, but also represent the difficulty of RLCPs. Finally, an apparent linear relationship is noticed between indicators of land use change and ESV change. Based on the above analysis, 15 factors were selected as the driving factors of ESV change (Table 2).

Table 2. Driving factors of ESV change in RLCPs.

Driving Factors		Factors Definition/Unit	Code
Natural factors	Cultivated land area	Cultivated land area (hm^2)	X_1
	Cultivated land proportion	Cultivated land area/Total land area (%)	X_2
	Per capita cultivated land area	Cultivated land area/Total population ($hm^2 \cdot person^{-1}$)	X_3
Economic factors	GDP	GDP (USD 100 million)	X_4
	Per capita GDP	Total GDP/Total population ($USD \cdot person^{-1}$)	X_5
	Average investment in fixed assets	Social fixed assets investment/Total land area (10^4 $USD \cdot km^{-2}$)	X_6
Social factors	Per capita income of rural residents	Per capita net income of rural residents (USD)	X_7
	Population density	Total population/Total land area ($person \cdot km^{-2}$)	X_8
	Urbanization rate	Non-agricultural population/Total population (%)	X_9
Policy factors	Investment scale	Total investment scale of RLCPs (10^4 USD)	X_{10}
	Construction scale	Total construction scale of RLCPs (hm^2)	X_{11}
Land use change factors	*LDI* variation	*LDI* before RLCP-*LDI* after RLCP	X_{12}
	LAI variation	*LAI* before RLCP-*LAI* after RLCP	X_{13}
	LEI variation	*LEI* before RLCP-*LEI* after RLCP	X_{14}

3.3.2. Geographical Detector Results

The geographical detector is used to identify the driving factors of the increase in ESV amount and rate, and the results are shown in Table 3. In terms of the amount of ESV increase, X4, X7, X10, and X11 pass the significance test at 0.05 level, and the order of q

values from large to small is X11, X10, X7, and X4. This indicates that the amount of ESV increase is significantly affected by policy, social, and economic factors. In terms of the rate of ESV increase, only X2, X13, and X14 passed the significance test at 0.05 level, and the order of q values from large to small is X14, X13, and X2. This shows that the rate of ESV increase is significantly affected by land use change factors and natural factors.

Table 3. Estimated results of geographical detector.

Increase Amount	X_1	X_2	X_3	X_4	X_5	X_6	X_7	X_8	X_9	X_{10}	X_{11}	X_{12}	X_{13}	X_{14}
q value	0.11	0.14	0.01	0.16	0.11	0.09	0.17	0.10	0.06	0.27	0.57	0.03	0.03	0.03
sig.	0.14	0.05	0.86	0.04	0.12	0.22	0.01	0.16	0.30	0.00	0.00	0.60	0.63	0.53
Increase Rate	X_1	X_2	X_3	X_4	X_5	X_6	X_7	X_8	X_9	X_{10}	X_{11}	X_{12}	X_{13}	X_{14}
q value	0.01	0.24	0.12	0.10	0.05	0.09	0.12	0.08	0.07	0.02	0.07	0.13	0.24	0.28
sig.	0.99	0.03	0.25	0.83	0.83	0.99	0.23	0.74	0.38	0.81	0.89	0.13	0.01	0.00

3.3.3. GWR Results

Spatial Differentiation of the Dominant Factor Affecting the Amount of ESV Increase

Figure 5 describes the spatial differentiation of the dominant influencing the amount of ESV increase. It can be seen in Figure 5a that there is a positive correlation between GDP and the amount of ESV increase, indicating that the higher the level of economic development, the higher the total amount of ESV increased by RLCPs. Specifically, RLCPs belong to the capital investment engineering measures, and the higher the regional GDP, the greater the scale and amount of investment in RLCPs, and the greater the ecological effect of RLCPs. From the spatial perspective, the impact intensity of GDP on the amount of ESV increase shows a decreasing trend from southwest to northeast, which is opposite to the GDP of each unit. This is because the lower the economic level, the stronger the motivation for promoting the economy by RLCPs. The per capita income of rural residents is negatively correlated with the amount of ESV increase (Figure 5b). The impact intensity of per capita income of rural residents on ESV increases from west to east, which is consistent with the income level of rural residents in each unit. It may be that the higher the farmers' income, the higher their awareness of RLCPs. There is a negative correlation between the investment scale and the amount of ESV increase (Figure 5c), which may be that the higher the investment, the higher the cost of RLCPs, and then the number of projects or the construction scale is reduced. The effect of investment scale on the amount of ESV increase shows a decreasing trend from southeast to northwest, which is in direct proportion to the investment scale of RLCPs. At the same time, the positive impact of construction scale on the amount of ESV increase gradually increased from west to east (Figure 5d). The reason is that RLCPs mainly affect ESV by changing the land use structure, so its construction scale has a substantial impact on the amount of ESV increase [28,34,36].

Spatial Differentiation of the Leading Factor Affecting the Rate of ESV Increase

Figure 6 describes the spatial differentiation of the dominant factors influencing the rate of ESV increase. In plains and hilly areas, the cultivated land proportion is negatively correlated with the rate of ESV increase (Figure 6a). The impact intensity of cultivated land proportion on the rate of ESV increase gradually weakens around the Jianghan Plain. This is mainly due to the high proportion of cultivated land and low proportion of ecological land in these areas. The RLCPs of each unit are mainly based on the internal potential, and the rate of ESV increase is low. There is a positive correlation between the cultivated land proportion and the rate of ESV increase in mountainous areas. The more the terrain fluctuates, the lower the rate of land use. Each unit increases the cultivated land proportion through RLCPs, which will improve ESV. The relationship between LDI variation and the rate of ESV increase is similar to the cultivated land proportion. Except for some units in

Enshi Prefecture and Shiyan City, the LEI variation is positively correlated with the rate of ESV increase. A common general rule is that the more the LEI index decreases, the lower the rate of ESV increase. The influence intensity is the strongest in the water network polder areas, and gradually weakens in a semicircular shape from south to north and from east to west, which is consistent with the distribution of cultivated land resources and the land use intensity in each unit.

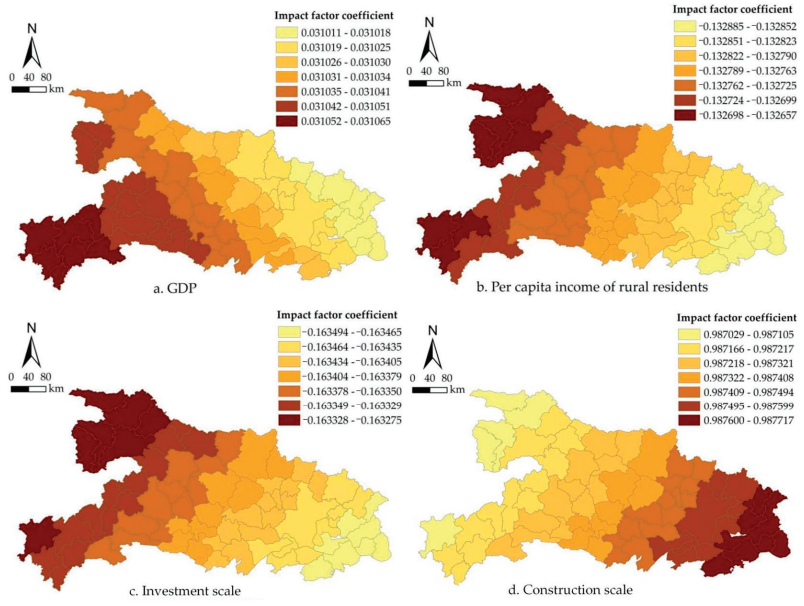

Figure 5. Spatial differentiation of dominant factor affecting ESV increase amount.

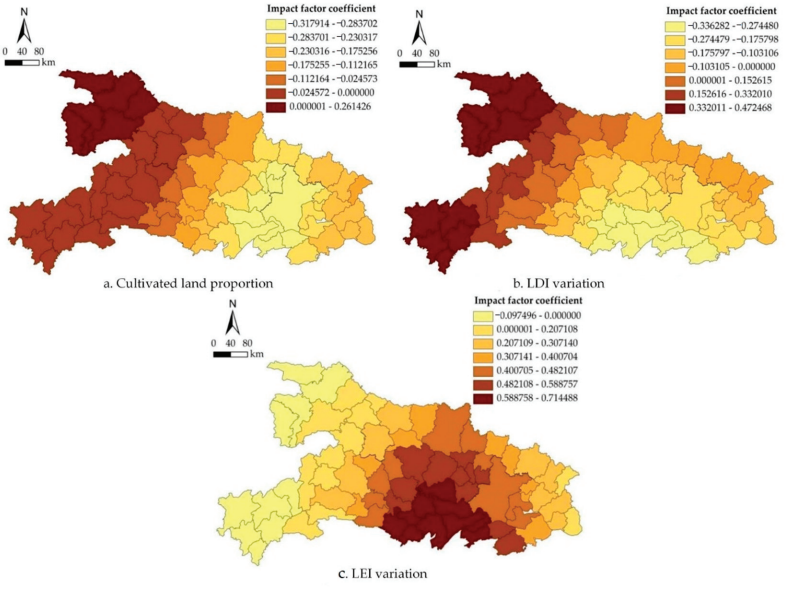

Figure 6. Spatial differentiation of dominant factor affecting ESV increase rate.

4. Discussion

4.1. Strengthening Research on ESV Change under the Background of RLCP

We have made corresponding modifications to the ESV evaluation method, which is realized by modifying the average precipitation, food production, socioeconomic development stage, as well as land use type, etc. The improved evaluation method is more consistent with the actual situation of Hubei Province in terms of specific application scales. The empirical results based on the improved value equivalent method show that after RLCPs, the ESV of the RLCP areas in 71 counties of Hubei Province increased. This result indicated that RLCPs can effectively improve the ecological environmental quality.

Currently, China is vigorously promoting the implementation of RLCPs, which is characterized by rich content, diverse models, diverse objectives, and comprehensive means. It has played an important role in optimizing spatial land layout, ensuring food security, and improving rural production and the living environment and ecosystem. At present, China is in a critical period of economic transformation. While ensuring sustained and stable economic growth, it is also implementing relevant policy measures such as RLCPs to reduce the damage caused by economic development to resources and the environment, ensure food demand, narrow development gaps, and improve the quality of economic development. Studying the ESV variation patterns and driving mechanisms in China's RLCPs provides a reference for other developing countries to achieve these goals in their development process.

However, this study has several research limitations. First, due to the limitation of data acquisition, the first year after the RLCPs were put into use was selected to represent the year after consolidation, which results in a smaller change in the amount and rate of ESV. After RLCPs, the supply, regulatory, and cultural services are in dynamic change. The changes in supply and partial cultural services can be observed in a short time, but the changes in regulatory and partial cultural services need to be reflected over a long period of time [19,25,26,38]. Therefore, the ESV change in RLCPs requires long-term fixed-point observation and analysis. Second, the change in the relationship between ecosystem services under the background of RLCPs was not quantitatively analyzed. The relationship between supply, regulatory, and cultural services is contradictory and antagonistic; that is, these three categories of ecosystem services do not increase or decrease simultaneously, with some services increasing, some services decreasing, and some services remaining unchanged [6,12,18]. In practice, the impact of RLCPs on ecosystem supply and regulatory services is reflected in ensuring the food production and quality of the region. Therefore, the development of the region relies on agricultural planting. The impact of RLCPs on ecosystem cultural services is reflected in strengthening the natural resources and historical and cultural characteristics of the region through relevant measures, vigorously developing the ecological tourism industry, etc. Its characteristic is that it will, to some extent, abandon the grain cultivation it originally relied on for rural development. Ensuring food security and development are equally important. Hence, the trade-offs, dependencies, or synergy relationships between ecosystem services affected by RLCPs should be deeply explored to provide support and guidance for the spatial layout of RLCPs and the optimal management of ecosystem services. Similarly, in the selection of content and policy formulation for the implementation of future RLCPs in China, appropriate content needs to be selected through the balance of these contents to ensure the positive benefits brought by the implementation of RLCPs.

4.2. Implementing Differentiated RLCPs Policy

Continue to implement the high-standard basic farmland consolidation projects in central Hubei: Central Hubei includes the Jianghan Plain and the middle and lower reaches of the Hanjiang River Plain, with flat terrain, abundant cultivated land resources, and a high level of economic development. The investment scale and the construction scale of RLCPs far exceed those in eastern or western Hubei. The amount of ESV increase in central Hubei is much larger than that in eastern or western Hubei, but the rate of ESV increase is

relatively low. Additionally, the proportion of cultivated land and the land use diversity index change has a significant impact on ESV change in Central Hubei. Therefore, we should continue with the implementation of basic farmland consolidation projects, but we should also strengthen the protection of land use diversity in the RLCP process and try to retain water areas and other land types that have a greater impact on the ecosystem in order to achieve good ecological effects.

Expanding the implementation of low hilly consolidation projects in eastern Hubei: The terrain of eastern Hubei is mainly hilly, with a small number of plains and mountains. Although the investment scale and the construction scale of RLCPs are far smaller than those of central or western Hubei, the newly increased rate of cultivated land is much higher than that of central or western Hubei, and the rate of ESV increase is also higher than that of central and western Hubei. Therefore, we should expand the implementation of consolidation projects in the area of low hills in eastern Hubei in order to ensure the dynamic balance of cultivated land in Hubei Province and achieve the dual effects of production and ecology.

Strengthen the investment in ecological conservation projects in western Hubei: Western Hubei includes Qinba Mountain and Wuling Mountain, and is characterized by poor natural conditions, weak ecological foundation, and low per capita income. Meanwhile, both the investment and construction scale of RLCPs are relatively small. The amount and rate of ESV increase in western Hubei are low; GDP and construction scale are positively correlated with the amount of ESV increase, while the investment scale and per capita income of rural residents are negatively correlated with the amount of ESV increase. Therefore, western Hubei can more actively implement small-scale RLCPs. What should be emphasized the most is the protection of natural forests and water conservation, while increasing the area and improving the quality of cultivated land.

5. Conclusions

RLCPs have become one of the largest organized human activities aiming to change land use patterns and impact terrestrial ecosystems. This study used Hubei Province as a case study to explore the spatial differentiation and driving mechanisms of ESV change in RLCPs. We use the improved ESV evaluation model to analyze the spatial differentiation of the amount and rate of ESV change due to RLCPs, and then adopt the geographic detectors and the geographically weighted regression model to identify the dominant factors affecting the amount and rate of ESV change due to RLCPs. The main results and conclusions are as follows:

(1) Although RLCPs make the unevenness of land use obvious, they evidently reduce the complexity of land use and significantly improve the dominance of land use. After RLCPs, the land use diversification index, land use diversity index, and land use dominance index of each county decreased, while the land use dominance index increased. This also indicates that RLCPs can improve ecosystem complexity and stability, and ultimately improve ESV;

(2) The ESV of the RLCPs areas in 71 counties of Hubei Province increased, with an average increase of USD $2.37 \times 107\ a^{-1}$. The amount of ESV increase is large in central Hubei, while small in eastern and western Hubei. The rate of ESV increase is high in eastern and central-northern Hubei, while low in western and central-southern Hubei. This implies that RLCPs can improve ESV, but the improvement effect has significant regional differences;

(3) The amount of ESV increase is positively corrected with GDP and construction scale, but is negatively correlated with investment scale and per capita income of rural residents. The rate of ESV increase is negatively correlated with the proportion of cultivated land and the change in the land use diversification index, but positively correlated with the change in the land use evenness index. However, their driving effects have significant spatial heterogeneity. Therefore, governments should carry

out differentiated RLCPs according to regional natural geographical conditions and socioeconomic development levels in order to protect the ecological environment.

Author Contributions: Conceptualization, M.L. and C.Z.; methodology, Y.J., X.S. and J.H.; software, D.L. and X.Z.; validation, M.L. and J.H.; formal analysis, G.W., X.S. and B.J.; investigation, Y.J.; resources, C.Z.; data curation, J.H. and X.Z.; writing—original draft preparation, M.L. and C.Z.; writing—review and editing, M.L. and C.Z.; visualization, C.Z. and J.H.; supervision, C.Z.; project administration, M.L., C.Z. and Y.J.; funding acquisition, M.L. and C.Z. All authors have read and agreed to the published version of the manuscript.

Funding: This research is funded by the National Natural Science Foundation of China (Project No. 42101307); the Humanity and Social Science Research Funds of Ministry of Education of China (Project No. 21YJC790006); the Fundamental Research Funds for the Central Universities (Project No. 2662020GGQD001); the Natural Science Foundation of Shaaxi Province (Project No. 2022JQ-747); the Major Theoretical and Practical Problems of Philosophy and Social Sciences of Shaanxi Province (Project No. 2022ND0342); the Doctoral Research Start-up Fund Project of Northwest A&F University (Project No. 2452023038); and the Science Foundation for The Excellent Youth Scholars of China University of Geosciences (Project No. CUGGG-2204).

Data Availability Statement: The data presented in this study are available on request from the first author.

Conflicts of Interest: The authors declare no conflict of interest.

References

1. Wang, L.; Zheng, H.; Chen, Y.; Ouyang, Z.; Hu, X. Systematic review of ecosystem services flow measurement: Main concepts, methods, applications and future directions. *Ecosyst. Serv.* **2022**, *58*, 101479. [CrossRef]
2. Daily, G.C. *Nature's Services: Societal Dependence on Natural Ecosystem*; Island Press: Washington, DC, USA, 1997.
3. Costanza, R.; d'Arge, R.; De Groot, R.; Farber, S.; Grasso, M.; Hannon, B.; Van Den Belt, M. The value of the world's ecosystem services and natural capital. *Nature* **1997**, *387*, 253–260. [CrossRef]
4. Costanza, R.; de Groot, R.; Sutton, P.; van der Ploeg, S.; Anderson, S.J.; Kubiszewski, I.; Farber, S.; Turner, R.K. Changes in the global value of ecosystem services. *Glob. Environ.* **2014**, *26*, 152–158. [CrossRef]
5. Filho, L.M.; Roebeling, P.; Villasante, S.; Bastos, M.I. Ecosystem services values and changes across the Atlantic coastal zone: Considerations and implications. *Mar. Policy* **2022**, *145*, 105265. [CrossRef]
6. He, Z.; Shang, X.; Zhang, T.; Yun, J. Coupled regulatory mechanisms and synergy/trade-off strategies of human activity and climate change on ecosystem service value in the loess hilly fragile region of northern Shaanxi, China. *Ecol. Indic.* **2022**, *143*, 109325. [CrossRef]
7. Mengist, W.; Soromessa, T.; Feyisa, G.L. Estimating the total ecosystem services value of Eastern Afromontane Biodiversity Hotspots in response to landscape dynamics. *Environ. Sustain. Indic.* **2022**, *14*, 100178. [CrossRef]
8. Braun, D.; de Jong, R.; Schaepman, M.E.; Furrer, R.; Hein, L.; Kienast, F.; Damm, A. Ecosystem service change caused by climatological and non-climatological drivers: A Swiss Case Study. *Ecol. Appl.* **2019**, *29*, e01901. [CrossRef]
9. Scheiter, S.; Schulte, J.; Pfeiffer, M.; Martens, C.; Erasmus, B.; Twine, W. How does climate change influence the economic value of ecosystem services in Savanna Rangelands? *Ecol. Econ.* **2019**, *157*, 342–356. [CrossRef]
10. Zhang, R.; Li, P.; Xu, L.; Zhong, S.; Wei, H. An integrated accounting system of quantity, quality and value for assessing cultivated land resource assets: A case study in Xinjiang, China. *Glob. Ecol. Conserv.* **2022**, *36*, e02115. [CrossRef]
11. Cheng, Q.; Zhou, L.; Wang, T. Assessment of ecosystem services value in Linghekou wetland based on landscape change. *Environ. Sustain. Indic.* **2022**, *15*, 100195. [CrossRef]
12. Long, X.; Lin, H.; An, X.; Chen, S.; Qi, S.; Zhang, M. Evaluation and analysis of ecosystem service value based on land use/cover change in Dongting Lake wetland. *Ecol. Indic.* **2022**, *136*, 108619. [CrossRef]
13. Gu, X.; Long, A.; Liu, G.; Yu, J.; Wang, H.; Yang, Y.; Zhang, P. Changes in ecosystem service value in the 1 km lakeshore zone of Poyang Lake from 1980 to 2020. *Land* **2021**, *10*, 951. [CrossRef]
14. Zhou, P.; Zhang, H.; Huang, B.; Ji, Y.; Peng, S.; Zhou, T. Are productivity and biodiversity adequate predictors for rapid assessment of forest ecosystem services values? *Ecosyst. Serv.* **2022**, *57*, 101466. [CrossRef]
15. Dominati, E.J.; Mackay, A.; Lynch, B.; Heath, N.; Millner, I. An ecosystem services approach to the quantification of shallow mass movement erosion and the value of soil conservation practices. *Ecosyst. Serv.* **2014**, *9*, 204–215. [CrossRef]
16. Chen, H.; Costanza, R.; Kubiszewski, I. Legitimacy and limitations of valuing the oxygen production of ecosystems. *Ecosyst. Serv.* **2022**, *58*, 101–485. [CrossRef]
17. Bruijnzeel, L. Hydrological functions of tropical forests: Not seeing the soil for the trees? *Agric. Ecosyst. Environ.* **2004**, *104*, 185–228. [CrossRef]

18. Jiang, W.; Gao, G.; Wu, X.; Lv, Y. Assessing temporal trade-offs of ecosystem services by production pssibility frontiers. *Remote Sens.* **2023**, *15*, 749. [CrossRef]
19. Lu, X.; Jiang, B.; Liu, M.; Li, Y.; Chen, D. A study on the gains and losses of the ecosystem service value of the land consolidation projects of different properties in Hubei Province: An empirical comparison based on plains, mountains and hills. *Land* **2022**, *11*, 1015. [CrossRef]
20. Zhen, H.; Gao, W.; Yuan, K.; Ju, X.; Qiao, Y. Internalizing externalities through net ecosystem service analysis: A case study of greenhouse vegetable farms in Beijing. *Ecosyst. Serv.* **2021**, *50*, 101323. [CrossRef]
21. Li, J.; Dong, S.; Li, Y.; Wang, Y.; Li, Z.; Li, F. Effects of land use change on ecosystem services in the China–Mongolia–Russia economic corridor. *J. Clean. Prod.* **2022**, *360*, 132175. [CrossRef]
22. Tian, Y.; Xu, D.; Song, J.; Guo, J.; You, X.; Jiang, Y. Impacts of land use changes on ecosystem services at different elevations in an ecological function area, northern China. *Ecol. Indic.* **2022**, *140*, 109003. [CrossRef]
23. Wójcik-Leń, J.; Leń, P.; Sobolewska-Mikulska, K. The proposed algorithm for identifying agricultural problem areas for the needs of their reasonable management under land consolidation works. *Comput. Electron. Agric.* **2018**, *152*, 333–339. [CrossRef]
24. Hu, X.; Su, K.; Chen, W.; Yao, S.; Zhang, L. Examining the impact of land consolidation titling policy on farmers' fertiliser use: Evidence from a quasi-natural experiment in China. *Land Use Policy* **2021**, *109*, 105645. [CrossRef]
25. Zhong, L.; Wang, J.; Zhang, X.; Ying, L. Effects of agricultural land consolidation on ecosystem services: Trade-offs and synergies. *J. Clean. Prod.* **2020**, *264*, 121412. [CrossRef]
26. Guo, B.; Fang, Y.; Jin, X. Monitoring the effects of land consolidation on the ecological environmental quality based on remote sensing: A case study of Chaohu Lake Basin, China. *Land Use Policy* **2020**, *95*, 104569. [CrossRef]
27. Shi, Y.; Cao, X.; Fu, D.; Wang, Y. Comprehensive value discovery of land consolidation projects: An empirical analysis of Shanghai, China. *Sustainability* **2018**, *10*, 2039. [CrossRef]
28. Stręk, Ż.; Noga, K. Method of delimiting the spatial structure of villages for the purposes of land consolidation and exchange. *Remote Sens.* **2019**, *11*, 1268. [CrossRef]
29. Yin, Q.; Sui, X.; Ye, B.; Zhou, Y.; Li, C.; Zou, M.; Zhou, S. What role does land consolidation play in the multi-dimensional rural revitalization in China? A research synthesis. *Land Use Policy* **2022**, *120*, 106261. [CrossRef]
30. Tran, D.; Vu, T.H.; Goto, D. Agricultural land consolidation, labor allocation and land productivity: A case study of plot exchange policy in Vietnam. *Econ. Anal. Policy* **2022**, *73*, 455–473. [CrossRef]
31. Yu, G.; Feng, J.; Che, Y.; Lin, X.; Hu, L.; Yang, S. The identification and assessment of ecological risks for land consolidation based on the anticipation of ecosystem stabilization: A case study in Hubei Province, China. *Land Use Policy* **2010**, *27*, 293–303. [CrossRef]
32. Janus, J.; Ertunç, E. Impact of land consolidation on agricultural decarbonization: Estimation of changes in carbon dioxide emissions due to farm transport. *Sci. Total Environ.* **2023**, *873*, 162391. [CrossRef] [PubMed]
33. Shan, W.; Jin, X.B.; Ren, J.; Wang, Y.C.; Xu, Z.G.; Fan, Y.T.; Gu, Z.M.; Hong, C.Q.; Lin, J.H.; Zhou, Y.K. Ecological environment quality assessment based on remote sensing data for land consolidation. *J. Clean. Prod.* **2019**, *239*, 118126. [CrossRef]
34. Feng, W.L.; Li, Y.R. Measuring the ecological safety effects of land use transitions promoted by land consolidation projects: The case of Yan'an city on the Loess Plateau of China. *Land* **2021**, *10*, 783. [CrossRef]
35. Yang, Z.; Yang, L.; Zhang, B. Soil erosion and its basic characteristics at karst rocky-desertified land consolidation area: A case study at Muzhe Village of Xichou County in Southeast Yunnan, China. *J. Mt. Sci.* **2010**, *7*, 55–72. [CrossRef]
36. Zhong, L.; Wang, J.; Zhang, X.; Ying, L.; Zhu, C. Effects of agricultural land consolidation on soil conservation service in the Hilly Region of Southeast China: Implications for land management. *Land Use Policy* **2020**, *95*, 104637. [CrossRef]
37. Liu, Y.; Wu, C.; Yue, W.; Ye, Y. Evaluation of ecological effect and landscape pattern in land consolidation project. *Acta Ecol. Sin.* **2008**, *5*, 2261–2269.
38. Zhou, X.; Feng, Y.; Luo, W.; Jia, W.; Yang, J.; Li, H. Comparing two ecosystem service evaluation methods of the ecological benefits from a land consolidation project at a township level: A case study in Sanxing Town, Jintang County of Sichuan Province. *Acta Ecol. Sin.* **2020**, *40*, 1799–1809.
39. Wang, K.; Shi, H.; Zhou, W.; Zheng, F.; Sun, H. Study on the relationship between land use structure change and ecological services value in the arid inland basin area: A case study of Jiuquan, China. *Pop. Res. Environ.* **2011**, *21*, 124–128.
40. Kuchma, T.; Tarariko, O.; Syrotenko, O. Landscape diversity indexes application for agricultural land use optimization. *Procedia Tech.* **2013**, *8*, 566–569. [CrossRef]
41. Xie, G.; Zhen, L.; Lu, C.; Xiao, Y.; Chen, C. Expert knowledge-based valuation method of ecosystem services in China. *J. Nat. Resour.* **2008**, *3*, 911–919.
42. Xie, G.; Zhang, C.; Zhang, L.; Chen, W.; Li, S. Improvement of the Evaluation Method for Ecosystem Service Value Based on Per Unit Area. *J. Nat. Resour.* **2015**, *30*, 1243–1254.
43. Xie, G.; Zhang, C.; Zhen, L.; Zhang, L. Dynamic changes in the value of China's ecosystem services. *Ecosyst. Serv.* **2017**, *26*, 146–154. [CrossRef]
44. Li, J.; Huang, L.; Cao, W. An influencing mechanism for ecological asset gains and losses and its optimization and promotion pathways in China. *J. Geogr. Sci.* **2022**, *32*, 1867–1885. [CrossRef]
45. Li, L.; Tang, H.; Lei, J.; Song, X. Spatial autocorrelation in land use type and ecosystem service value in Hainan Tropical Rain Forest National Park. *Ecol. Indic.* **2022**, *137*, 108727. [CrossRef]

46. Ren, H.; Shang, Y.; Zhang, S. Measuring the spatiotemporal variations of vegetation net primary productivity in Inner Mongolia using spatial autocorrelation. *Ecol. Indic.* **2020**, *112*, 106108. [CrossRef]
47. Peng, W.; Fan, Z.; Duan, J.; Gao, W.; Wang, R.; Liu, N.; Li, Y.; Hua, S. Assessment of interactions between influencing factors on city shrinkage based on geographical detector: A case study in Kitakyushu, Japan. *Cities* **2022**, *131*, 103958. [CrossRef]
48. Shi, S.; Wang, X.; Hu, Z.; Zhao, X.; Zhang, S.; Hou, M.; Zhang, N. Geographic detector-based quantitative assessment enhances attribution analysis of climate and topography factors to vegetation variation for spatial heterogeneity and coupling. *Glob. Ecol. Conserv.* **2023**, *42*, e02398. [CrossRef]
49. Gao, F.; Yang, L.; Han, C.; Tang, J.; Li, Z. A network-distance-based geographically weighted regression model to examine spatiotemporal effects of station-level built environments on metro ridership. *J. Transp. Geogr.* **2022**, *105*, 103472. [CrossRef]
50. Fotheringham, A.S.; Charlton, M.; Brunsdon, C. The geography of parameter space: An investigation of spatial non-stationarity. *Int. J. Geogr. Inf. Sci.* **1996**, *10*, 605–627. [CrossRef]
51. Zhang, R.; Chen, M. Spatial differentiation and driving mechanism of agricultural multi-functions in economically developed areas: A case study of Jiangsu Province, China. *Land* **2022**, *11*, 1728. [CrossRef]
52. Liu, Y.; Li, T.; Zhao, W.; Wang, S.; Fu, B. Landscape functional zoning at a county level based on ecosystem services bundle: Methods comparison and management indication. *J. Environ. Manag.* **2019**, *249*, 109315. [CrossRef] [PubMed]
53. Zhang, C.; Su, Y.; Yang, G.; Chen, D.; Yang, R. Spatial-temporal characteristics of cultivated land use efficiency in major function-oriented zones: A case study of Zhejiang Province, China. *Land* **2020**, *9*, 114. [CrossRef]

land

MDPI

Article

Assessment of Conservation Effectiveness of the Qinghai–Tibet Plateau Nature Reserves from a Human Footprint Perspective with Global Lessons

Mingjun Jiang [1], Xinfei Zhao [1], Run Wang [2], Le Yin [1] and Baolei Zhang [1,*]

[1] School of Geography and Environment, Shandong Normal University, Jinan 250014, China; yinl.16b@igsnrr.ac.cn (L.Y.)
[2] Shandong Provincial Territorial Spatial Ecological Restoration Center, Jinan 250014, China
* Correspondence: blzhangsd01@sdnu.edu.cn

Abstract: The intensity of human pressure (HP) has an important impact on the biodiversity and ecosystem services of nature reserves (NRs), and the conflict and the coordination between NRs and human activities are now key issues to solve in the construction of NR systems. This study improved and applied a human footprint (HF) model that considers population density, land use, night light, grazing intensity, and road construction as indicators of human activity to evaluate the effectiveness of NRs in the Qinghai–Tibet Plateau in mitigating HP from 2000 to 2020. The results indicated that during this period, the average HP in the national NRs of the plateau increased from 1.47646 to 1.76687, where values were generally high in the east and low in the west. The average value in wetland NRs was the largest and had the smallest growth rate, while that in desert NRs was the smallest and had the largest growth rate. From 2000 to 2020, the average HP in the core areas, buffer areas, and experimental areas of the NRs increased by 0.12969, 0.29909, and 0.44244, respectively. It is a challenge for the Chinese government to strengthen the ability of NRs to mitigate HP on the wetland reserves and experimental zones in the Qinghai–Tibet Plateau region.

Keywords: protection effectiveness; nature reserve; human pressure; Qinghai–Tibet Plateau

Citation: Jiang, M.; Zhao, X.; Wang, R.; Yin, L.; Zhang, B. Assessment of Conservation Effectiveness of the Qinghai–Tibet Plateau Nature Reserves from a Human Footprint Perspective with Global Lessons. *Land* **2023**, *12*, 869. https://doi.org/10.3390/land12040869

Academic Editor: Benedetto Rugani

Received: 10 March 2023
Revised: 10 April 2023
Accepted: 10 April 2023
Published: 12 April 2023

1. Introduction

Nature reserves (NRs) are considered cornerstones of biodiversity conservation, and their number and extent are expanding rapidly worldwide [1,2]. In 2020, more than 200,000 NRs have been established globally, covering 15.4% of the land and 7.5% of the marine environments [3]. While the international community has made important progress toward placing more land under protection, global biodiversity continues to decline, and the effectiveness of NRs has been questioned [4–6]. To address this crucial issue, there is a growing call for empirical evaluations of NRs' effectiveness in achieving their intended conservation goals and to understand the reasons behind their success or failure [7–9]. Climate change and human activities are important factors affecting biodiversity and ecosystem services [10–13]. With the rapid development of global society and continuous population growth, the conflict between protection and economic development has become increasingly prominent, and human activities increased by about 55% in spite of the establishment of more than 20,000 global reserves [14]. The fragmentation of habitat patches caused by human activities such as urbanization, deforestation, and road construction has been recognized as the biggest threat to ecological diversity within NRs [15,16]. Therefore, the assessment of HP is an important means of evaluating their effectiveness.

In recent years, a series of studies has been carried out on the impact of human activities on the ecological environment from the perspectives of biodiversity [17,18], biological habitat [19–21], and ecosystem services and their value [22,23]. With the rapid development of relevant theories, a new method of measuring HP, known as the human footprint (HF)

model, has been recently proposed [24]. This model quantifies the disturbance degree of the ecosystem and then accumulates different human interference factors. It can comprehensively measure multiple HPs on the environment [24,25], as well as the intensity of cumulative disturbance caused by some HP categories to ecosystems, including construction sites, crop and pasture lands, population density, nighttime lights, roads and railways, and navigable waterways [25]. The HF model has been widely used since the beginning of the 21st century [26,27], providing a reference for the study of HP interference [28]. It has also been widely adopted for the protection of NRs in China [29], the Qilian Mountains [30,31], the southeastern coast of Bangladesh [32], and the Yellow River Delta [33], where it was shown to be advantageous to evaluate the effectiveness of reserves. With time, increasing numbers of interference factors have been used as impact factors in the HF model to evaluate HP, including land use [34], road construction [35], grazing intensity [36], energy consumption (such as night light), and population density [37]. However, most studies have only investigated one or two influencing factors, so the assessment results are not perfect. It is urgent to consider all the abovementioned factors to evaluate HP in NRs and fill the gap in the existing data set for this complex parameter.

The Qinghai–Tibet Plateau is the largest plateau in China and an important ecological security barrier in both China and the Asian continent [38]. The plateau is not only a key area for the distribution of alpine ecosystems and endemic animal and plant species but also one of the regions with the richest biodiversity in the world [39]; it also has the highest concentration of threatened terrestrial ecosystems [40]. Since the establishment of the first national NR on the Qinghai–Tibet Plateau in 1963, 150 additional NRs have been created, accounting for 31.63% of the plateau area [41]. In recent years, domestic and foreign research groups have carried out relevant research on species protection, ecological and environmental changes, protection measures, and the effects of NRs in the Qinghai–Tibet Plateau region, where the impact of human activities has become an important part of the evaluation [42,43]. For example, it has been found that the damage to the normal growth of vegetation caused by long-term overgrazing is the main factor leading to grassland degradation in these reserves [44]; road traffic facilities can directly or indirectly modify the habitat of wild animals and plants and can even lead to habitat fragmentation and loss [45]; tourism-related activities will disturb the habitats of animals and plants in the NRs, directly destroy the surface vegetation, and alter the physical and chemical properties of soil [46,47]; and, finally, the development of the mineral extraction industry will have a serious impact on the migration of wild animals in the NRs [48]. In addition, engineering construction and urbanization processes also to varying degrees threaten the NRs of the Qinghai–Tibet Plateau [49]. Although numerous studies have been conducted on HP in the area, as far as we know, no systematic report is available on the current situation in the whole plateau in terms of the effects of constructing NRs, the protection they ensure, and the existing problems. Therefore, by comprehensively considering multiple interference factors examined in previous studies, we can adequately estimate what has been the level of HP in the national NRs of the Qinghai–Tibet Plateau in recent years. Because of the increasing population density and continuous expansion of production and living space in the region, we hypothesized that although HP increases less inside than outside, this parameter would have still slightly increased in the reserves during the period examined. To verify this hypothesis, we comprehensively considered five interference factors to assess HP in the national NRs of the Qinghai–Tibet Plateau.

The main aims of this study were to (1) improve and apply a human footprint (HF) model that considers population density, land use, night light, grazing intensity, and road construction as indicators of human activity to evaluate the effectiveness of NRs in the Qinghai–Tibet Plateau region and (2) compare and analyze the variation of HP values inside and outside the reserves and in each functional area to evaluate the effectiveness of NRs in reducing human impacts from 2000 to 2020. The paper is structured as follows: Section 1 introduces the background of the analysis; Section 2 presents the methodological approach;

Section 3 summarizes the results; and Section 4 discusses those results. Concluding remarks are presented in the final section.

2. Materials and Methods

2.1. Study Area

The Qinghai–Tibet Plateau (73.43~104.67° E, 25.98~39.82° N), in the southeast of China, is a unique geographical unit with the highest average altitude in China and even in the world, with an average altitude of more than 4000 m. The Qinghai–Tibet Plateau includes Qinghai Province, Tibet Autonomous Region, Sichuan Province, Yunnan Province, Gansu Province, Xinjiang Autonomous Region, and other regions, with a total area of 2,500,000 km^2, accounting for 26% of China's total land area. The uplift of the Qinghai–Tibet Plateau has blocked the Indian Ocean monsoon from moving northward and the low-level westerly flow in China, forming a unique plateau climate, which combines subtropical, temperate, and other climatic zones with complex hydrothermal conditions. The vegetation types include mainly forests, shrubs, meadows, and deserts, and the alpine meadows are the most widely distributed, accounting for about 60%.

The population density in the Qinghai–Tibet Plateau is relatively low, with less than 2 people/km^2 in the central and western regions and slightly more than 10 people/km^2 in the southeast regions. The Qinghai–Tibet Plateau lags in urbanization and industrialization; it is rich in minerals, oil, natural gas, and other energy resources; and its economic development level is lower than the national average. However, its overall development speed is higher than the national average. The construction of NRs in the Qinghai–Tibet Plateau began in 1963, and there were 56 national NRs in 2022. In this research, 32 national NRs completely located in the Qinghai–Tibet Plateau with clear three functional zones were selected as the study objects. The selected NRs were divided into five categories [50], including 4 integrated ecosystems (TIEs), 13 wildlife ecosystems (TWEs), 7 forest ecosystems (TFEs), 2 desert ecosystems (TDEs), and 6 inland wetlands and water ecosystems (TWWEs) (Figure 1).

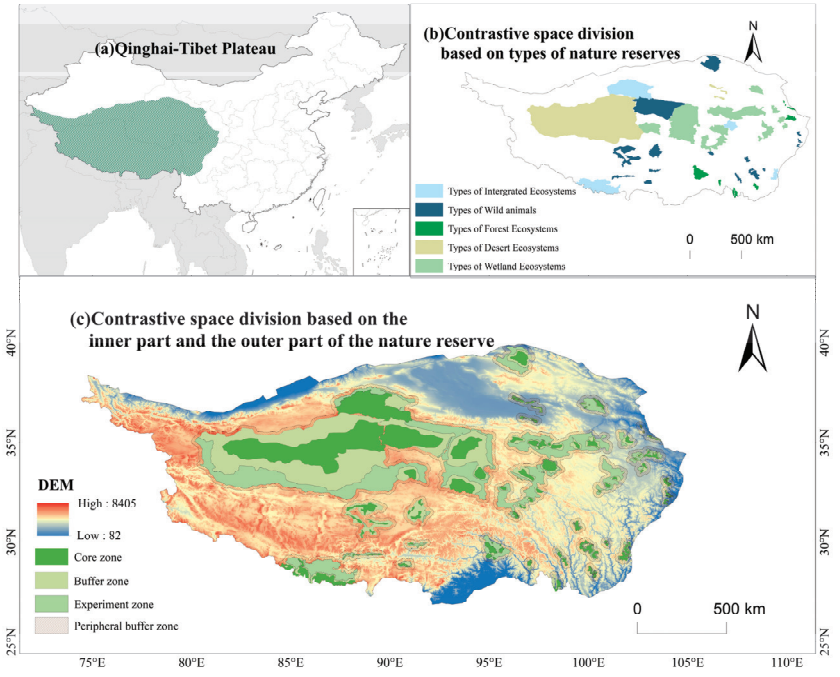

Figure 1. Location of the Qinghai–Tibet Plateau and the distribution of NRs and their functional zones.

2.2. Data

The data include mainly population density data, land-use data, grazing intensity data, night-light data, road data, etc. The data source is shown in Table 1.

Table 1. Data source and time.

Data Type	Time	Data Sources
Population density data	2000–2020	World Pop data set
Land-use data	2000–2020	Resource and Environmental Science Data Center of the Chinese Academy of Sciences
Grazing intensity data	2000–2020	Global Ecosystems and Environment observation Analysis Research Cooperation
Night-light data	2000–2020	National Oceanic and Atmospheric Administration (NOAA)
Road data	2002–2020	Open Street Map

2.3. Methods

Based on the local conditions of the Qinghai–Tibet Plateau and the availability of data, this study uses the HF model [25], taking into account five interference factors, namely population density, night light, road construction, land use, and grazing intensity, and first measures the respective HP values of the NRs of the Qinghai–Tibet Plateau. It then compares and analyzes the changes in HP values inside and outside the reserve and in each functional area and evaluates the effectiveness of the national NRs on the Qinghai Tibet Plateau in reducing cumulative impacts on the HP.2.3.1 population density.

The growth of the population density increases the demand for ecosystem services. Therefore, we take population density as an evaluation factor of HP. The population distribution in the Qinghai–Tibet Plateau is uneven, and the population in different regions greatly varies. Logarithmic processing can better represent the variability of population data without changing the nature and correlation of the data. Concerning the global model method [25,51–53], the grid with a population density greater than 1000 people/km^2 was assigned 10 points, and the grid with a population density less than or equal to 1000 people/km^2 is assigned by the following formula to calculate the population pressure score of the ecosystem:

$$\mathrm{popd}(i,t) = 3.333 \times \log_{10}(\mathrm{popden}(i,t) + 1) \quad (1)$$

where $\mathrm{popd}(i,t)$ is the value of the population pressure intensity of grid i for year t and $\mathrm{popden}(i,t)$ is the population density of grid i for year t.

2.3.1. Land-Use Activity

Human land-use activities have great impacts on the ecological environment, so we apply land-cover types to the HF model. 0–10 points were assigned different land-use types on the Qinghai–Tibet Plateau on the basis of relevant research [54,55]. The impact of grazing on the ecosystem in the NRs was considered because there were many pastoral areas distributed in this region. However, by using only satellite-based land-use data, it is difficult to distinguish whether grassland is used for grazing. The grassland was temporarily assigned a value of 0 in this section.

2.3.2. Grazing Intensity

The Qinghai–Tibet Plateau is a traditional grazing area in China and also the most developed area of animal husbandry in China. Grazing has a great impact on the grassland ecosystem. We choose grazing intensity as the interference indicator to describe the grassland ecosystem. The pressure scores caused by grazing intensity are calculated by

normalizing the data to 0–10 through the following formula and on the basis of relevant research on data scale conversion [56]:

$$Norgrad(i,t) = \frac{grazd(i,t) - grazd(i,t)_{min}}{grazd(i,t)_{max} - grazd(i,t)_{min}} * 10 \quad (2)$$

where $Norgrad(i,t)$ is the normalized grazing density of grid i for year t, ranging from 0 to 10; $grazd(i,t)$ is the grazing density of grid i for year t, which is the rasterized county-level data; and $grazd(i,t)_{max}$ and $grazd(i,t)_{min}$ are the maximum and minimum values of the original data set, respectively.

2.3.3. Nighttime Light Activities

Nighttime lights indicate how much electrical energy is consumed. Its spatial resolution is 1 km, and the years are from 2000 to 2020. The nighttime light images were calibrated by using the pseudoinvariant pixel method [57] and were grouped by using the classification interval determined by the natural discontinuities method, and the disturbance scores to the ecosystem were assigned a value from 0 to 10.

2.3.4. Distance from Road

The impact of roads on ecosystems accounts for at least 15~20% of the global land [58]. Roads and railways have great impacts on the surrounding ecosystems [59–61], and the interference distance even reaches 5 km [61]. Owing to the lack of road data in 2000, this paper selects road data in 2002 to represent roads in 2000. According to the global human footprint data set [25,62], we classify roads as a category of HP and assign different scores, on a 0–10 scale, to different levels of road buffers (Table 2).

Table 2. Human influence scores of different road levels on the ecosystem.

Road Categories	Buffer Distance		
	0–1 km	**1–2 km**	**2–5 km**
Freeways	10	6	3
National roads	8	4	2
Provincial roads	4	2	1
County roads	2	1	0
Railways	8	4	1

2.3.5. HP Calculation

Five interference factors of human pressures, i.e., population density, grazing intensity, land-use intensity, road construction, and nighttime lights were used to map HP according to the characteristics of the study area and data availability [25]. These interference factors were quantified by their disturbance degree to the ecosystem and then cumulatively summed. The spatial resolution of the HF map was determined as 1 km by using all available data sets of human pressures. Their disturbance to the ecosystem was quantified in the range of (0, 10) (0 is the minimum disturbance and 10 is the maximum; see Sections 2.3.1–2.3.5 for details) and accumulated in equal weight to measure the HP values. The equation was as below [51,52]:

$$HP(i,t) = \text{popd}(i,t) + \text{landuse}(i,t) + \text{graz}(i,t) + \text{road}(i,t) + \text{nightlight}(i,t) \quad (3)$$

where $HP(i,t)$ is the HP value of grid i for year t and $\text{popd}(i,t)$, $\text{landuse}(i,t)$, $\text{graz}(i,t)$, and $\text{nightlight}(i,t)$ are the disturbance intensities of population density, land use, roads construction, and energy consumption to the ecosystem in grid i for year t, respectively.

2.4. Changes in the Values of HP

The changes of the *HP* values were compared within the NRs of the Qinghai–Tibet Plateau for the period 2000–2020 by using the following equation:

$$\Delta HP(i, \Delta t) = HP(i, t_m) - HP(i, t_n) \quad (4)$$

where $\Delta HP(i, \Delta t)$ refers to the change in the HP value of grid i from t_m year to t_n year.

In addition, the types of nature reserves and different functional areas have different management requirements for human activities. Therefore, we further analyzed *HP* changes in different types of national NRs and three functional areas of the reserves on the Qinghai–Tibet Plateau from 2000 to 2020.

3. Results

3.1. Spatiotemporal Changes in the HP in the NRs of the Qinghai–Tibet Plateau for 2000–2020

From 2000 to 2020, HP on the national NRs of the Qinghai–Tibet Plateau has been high in the east and low in the west. Specifically, the NRs with low HP were in the western region thanks to its high altitude and harsh environments. HP in the NRs was generally low, with an average of 1.6434, reaching the lowest and highest values in 2005 and the highest value in 2015, respectively, and the variation exhibited an overall upward trend.

The average HP value in the NRs increased from 1.4765 in 2000 to 1.7669 in 2020, indicating an overall increasing trend throughout the period examined. The value decreased from 1.4765 in 2000 to 1.3326 in 2005, and next, the average increased to a maximum of 1.9326 in 2015. From 2015 to 2020, it slightly declined, reaching 1.7669 in 2020. In terms of spatial variation, although higher values were reported in the east, in general, the spatial pattern was relatively stable from 2000 to 2020 (Figure 2).

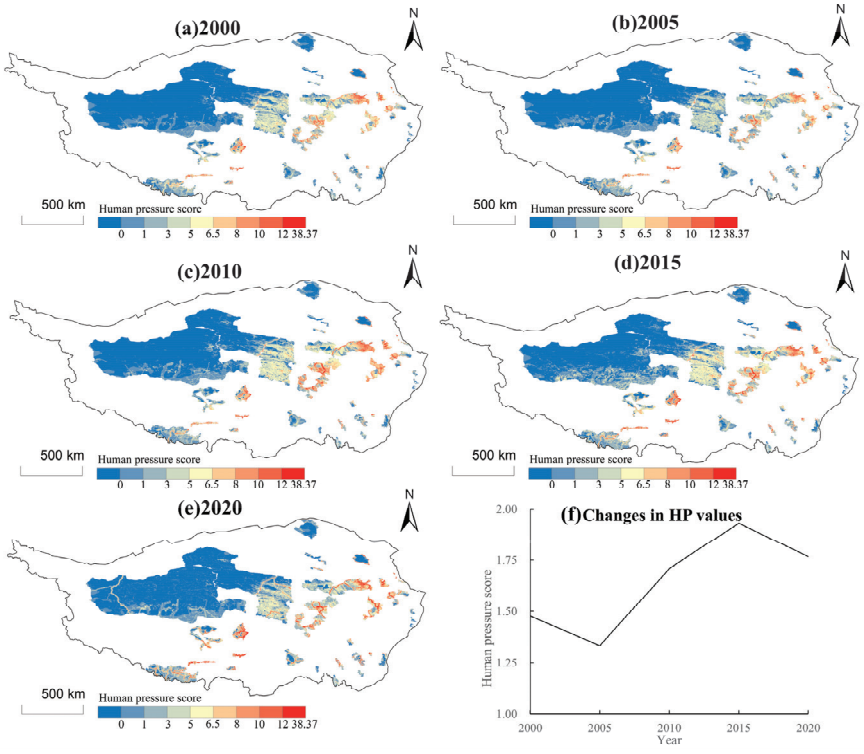

Figure 2. Spatiotemporal changes in HP in the NRs of the Qinghai–Tibet Plateau for 2000–2020.

In terms of the interference value of the five HP factors considered in this study, population density, land-use intensity, night light, and road construction showed an overall upward trend from 2000 to 2020. In particular, in this period, the pressure value of roads and the pressure value of population density increased by 0.2523 and by 0.10272 from 2000 to 2020, respectively. However, grazing intensity decreased year by year after increasing. This parameter showed an upward trend from 2005 to 2015, reaching the maximum value of 1.9326 in 2015 and decreasing to 0.8335 in 2020 (Table 3).

Table 3. Disturbance values of five HPs in the NRs of the Qinghai–Tibet Plateau for 2000–2020.

Human Pressures	2000	2005	2010	2015	2020
Roads	0.1213	0.1343	0.1397	0.1556	0.3738
Nighttime lights	0.0001	0.0002	0.0005	0.0006	0.0017
Population density	0.4102	0.4126	0.4178	0.4864	0.5129
Land-use activity	0.0377	0.0380	0.0380	0.0383	0.0655
Grazing intensity	0.9254	0.7731	1.1212	1.2757	0.8335
HP value	1.4765	1.3326	1.7085	1.9326	1.7669

The analysis of the spatial variation of the five HP interference types, from 2000 to 2020, showed that the overall changes in nighttime lighting and land use were relatively small, and the grazing intensity in most areas of the eastern region showed a downward trend; in contrast, the population density and road construction generally showed a significant upward trend in the same region. Overall, HP increased in the NRs in the eastern and southern parts and decreased in those in the central part of the Qinghai–Tibet Plateau (Figure 3).

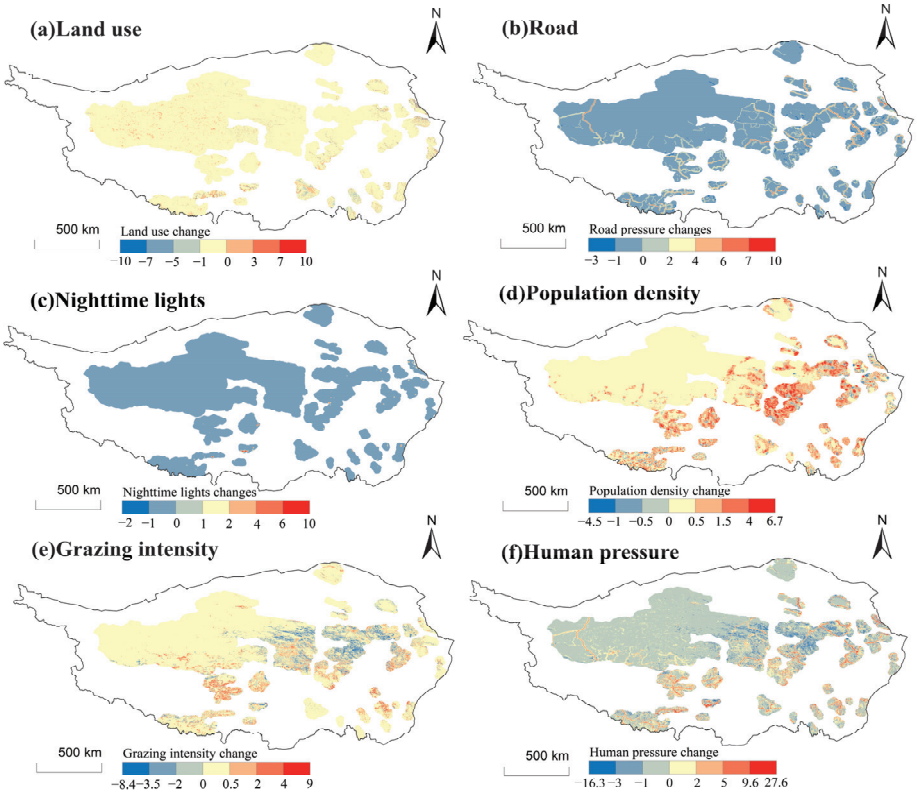

Figure 3. Spatiotemporal changes in five HPs in the NRs of the Qinghai–Tibet Plateau for 2000–2020.

3.2. HP Changes inside and outside the NRs of the Qinghai–Tibet Plateau

In the late 1990s and early 21st century, large national NRs such as Sanjiangyuan, Lalu Wetland, and Hoh Xil were established in the Qinghai–Tibet Plateau. From 2000 to 2005, the pressure of population growth in the internal and external buffer zones of the NRs showed a decreasing trend, which was greater outside than inside the national NRs, and was observed mainly in the central and eastern reserves of the plateau, especially in the Sanjiangyuan National NR (Figure 4). From 2005 to 2015, HP values in the internal and external buffer zones of the NRs increased, and in the latter, the values were considerably higher. From 2015 to 2020, the trend in both zones also increased because of road construction, and HP values increased less in the internal NR zones. From the aspect of spatial changes, HP mainly increased in the southern Qinghai–Tibet Plateau from 2000 to 2020.

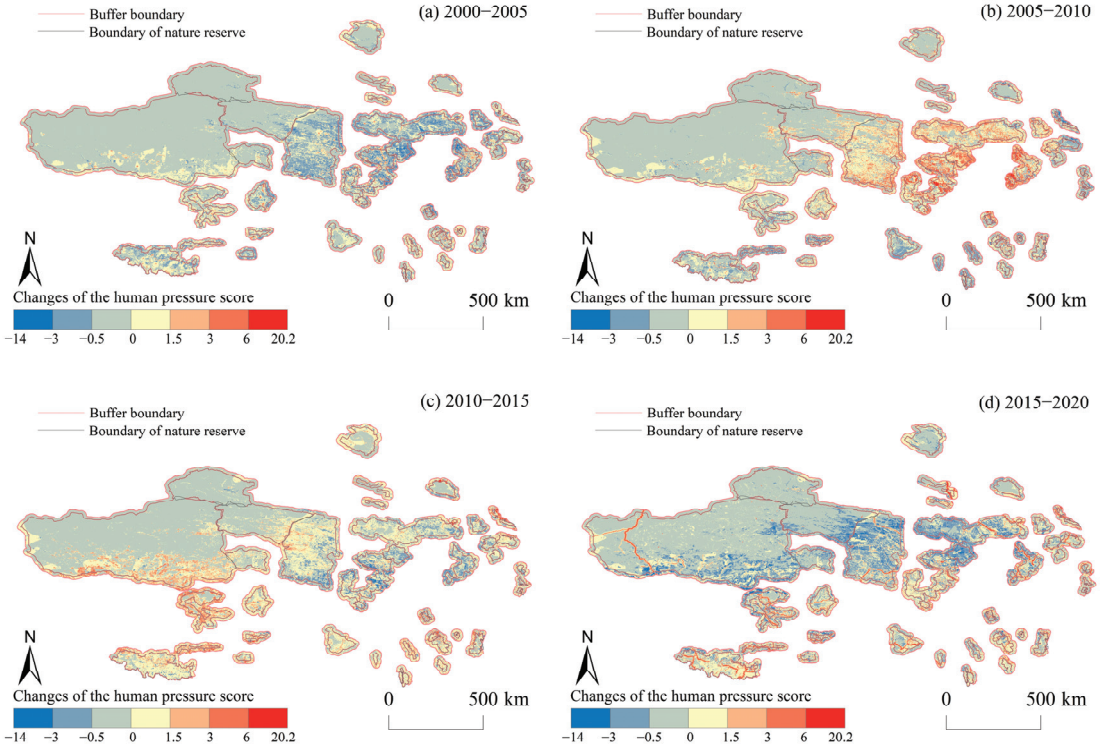

Figure 4. Spatiotemporal changes in HP inside and outside the NRs of the Qinghai–Tibet Plateau for 2000–2020.

The national NRs of the Qinghai–Tibet Plateau are partly positive in reducing the interference in the five HP types. From 2000 to 2020, the HP values for road construction were always lower inside the NRs than in the external buffer zones (Figure 5). From 2000 to 2015, these values inside the NRs and inside the external buffer zones increased by 0.0343 and 0.2024, respectively. However, from 2015 to 2020, the same parameter inside and outside the NRs increased by 0.2181 and 0.2854, respectively. The values inside and outside the NRs showed almost the same large increase, indicating that the regulatory capacity of protection measures to mitigate road construction decreased during these five years. The increase in night-light pressure was always lower in the NRs than in the external buffer zones from 2000 to 2020, and the increase rate was small (Figure 5). This indicated that the energy conservation measures adopted in the NRs effectively regulated the disturbance associated with of energy consumption in both the internal and external buffer zones.

From 2005 to 2010, population density without the NRs showed a decreasing trend, while the internal population density showed a growing trend (Figure 5), indicating that the measures aimed at controlling population growth did not work during the 2005–2010 period, but the effect of controlling population growth outside the NRs was good. During the 2000–2005 and 2010–2020 periods, population density always increased less in the NRs than in the external buffer zones, indicating that the plan to control population growth in the NRs was effective during these periods.

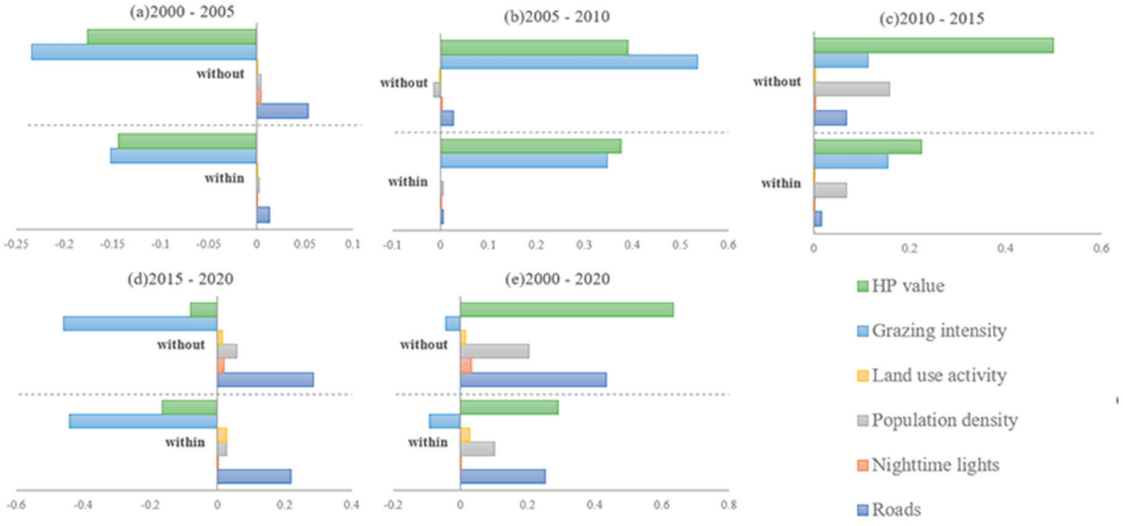

Figure 5. Changes in HP values inside and outside the NRs of the Qinghai–Tibet Plateau for 2000–2020.

From 2005 to 2010, land-use intensity in the internal and external buffer zones of the NRs showed a downward trend, and the decline in the latter was even greater (Figure 5), indicating that the protection measures were successful both inside and outside the NRs during this period. However, except for these 5 years, the land-use intensity showed an increasing trend in the rest of the research period, and from 2015 to 2020, the increase was greater in the NRs than in the external buffer zones. This shows that the proximity effect of the NRs is good but that protection measures still need to be strengthened.

Grazing intensity fluctuated and decreased from 2000 to 2020 (Figure 5). From 2005 to 2015, it significantly increased inside and outside the NRs. Moreover, thanks to the implementation of grazing prohibition measures, the situation improved from 2015 to 2020, where this parameter decreased to levels below those reported in 2000.

Overall, these results showed that the implementation of measures to reduce HP in the NRs of the Qinghai–Tibet Plateau has been partially effective. From 2000 to 2020, although all the HP factors except for grazing intensity showed an increasing trend inside the NRs, the increase was far lower than that in the external buffer zones. In 2020, the HP values in the internal and external buffer zones were 1.7669 and 4.2988, respectively. This huge difference indicates that the implementation of protective measures in the plateau's NRs was effective.

3.3. Temporal Variation in HP in Different Types of the NRs

The HP on different NR types in the Qinghai–Tibet Plateau increased from 2000 to 2020 (Figure 6), where the values in desert reserves exhibited the highest growth rate, 169.04%, and the lowest HP value, only 0.3316. HP in wetland NRs had a value of 4.0317 and showed the lowest growth rate, 5.23%. In comprehensive ecological reserves, wildlife

reserves and forest reserves the HP values were 1.4898, 2.2645, and 3.0886, respectively, from low to high, with growth rates of 22.79%, 33.78%, and 38.16%, respectively. HP values in all the NR types, except for the desert type, showed a downward trend from 2000 to 2005 and increased during during the 2005–2015 period.

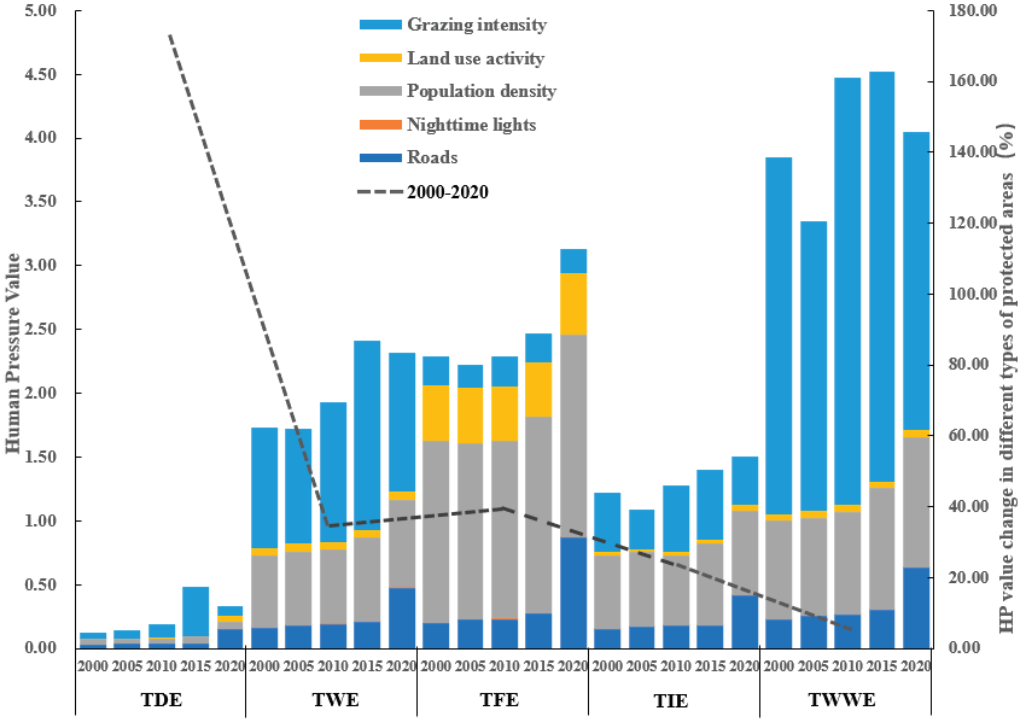

Figure 6. Temporal variation in HP in different types of the NRs for 2000–2020.

The increase in population density in all five types of NR was small, and in the comprehensive ecological reserves and forest reserves, this parameter even showed slight downward trends. The desert, wild animal, and wetland reserves significantly increased from 2005 to 2015 and then showed a downward trend from 2015 to 2020. The HP associated with land use was higher in forests than in other reserve types, and this was due mainly to the cultivation of farmland in the former. From 2000 to 2015, the interference from road construction in the five reserve types steadily increased, with a significant spike from 2015 to 2020, especially in forest reserves, where the value increased by 216.27%. Night-light interference accounted for a minimal proportion of HP in the different NRs and could therefore be ignored. The temporal variation in HP in different NR types showed that the current protection measures have effectively controlled population growth and the use of light at night in these reserves; however, road construction, grazing, and land-use activities, as well as production and daily living activities, still increased during the period examined.

3.4. Changes in HP in Various Functional Areas of the NRs

In each same period, the HP values in the three functional areas decreased, moving from the experimental area to the buffer area and core areas, in that order. These values showed a downward trend from 2000 to 2005, and the largest drop was detected in the experimental area (0.2321), followed by the core area and buffer area, in that order. From 2005 to 2015, the HP values in the three functional areas all increased, with the lowest increase detected in the core area, followed by the buffer area and experimental area

(Figure 7). From 2015 to 2020, the values declined in three functional areas, and the decrease was largest in the experimental area, followed by buffer area and core area, due mainly to the reduction in grazing intensity.

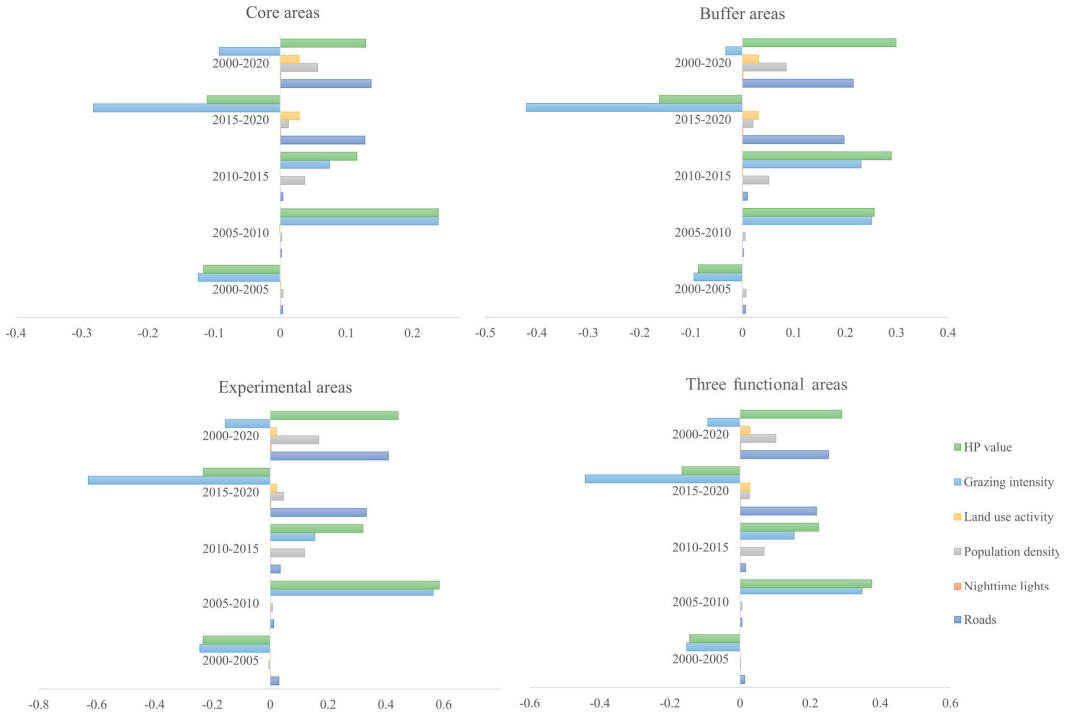

Figure 7. Changes in HP in various functional areas of the NRs for 2000–2020.

In the core zones of the NRs, grazing intensity significantly increased from 2000 to 2015 and then significantly decreased by 0.2825 from 2015 to 2020, which was still much lower than the decrease observed in 2000 (Figure 7). Land-use intensity from 2005 to 2015 was reduced to a better degree compared with that in the 2015–2020 period; the HP values for population density, road construction, and night light in 2020 were higher than those in 2000.

In the buffer zones of the NRs, grazing intensity was reduced by 0.2825 from 2015 to 2020 (Figure 7). The HP values associated with the intensity of land use, road construction, population density, and night light were all on the rise from 2000 to 2020, the most significant being road construction value, which increased by 0.2157.

In the experimental zones of the NRs, population density and grazing intensity were effectively alleviated from 2000 to 2005, and the HP values associated with each of them decreased by 0.005 and 0.24 37, respectively (Figure 7). The land-use intensity, road construction, population density, and night-light values increased by 0.4091, 0.0029, 0.1681, and 0.0227, respectively from 2000 to 2020, which indicated that the mitigation effect of protection measures on these four HP values was poor, especially for road construction from 2015 to 2020.

4. Discussion

4.1. Analyses of Differences in Conservation Effectiveness

The results of this study showed that the overall HP value on the NRs of the Qinghai–Tibet Plateau decreased from 2000 to 2005 and from 2015 to 2020, which indicates obvious

positive effects in mitigating human activities in these two periods. Similarly, the protection measures adopted in the reserves were also partially effective against the five types of human interference factors. HP on the NRs of the Qinghai–Tibet Plateau was high in the east and low in the west, results that are in line with recent studies, specifically with the global HF data reported in Venter [25].

Grazing intensity was significantly reduced during the 2000–2020 period because China implemented large-scale grassland restoration and ecological protection projects at the beginning of this century. Thanks to the launching of these projects, the number of livestock in and around the NRs has been reduced and grazing intensity alleviated. From 2005 to 2010, land use was effectively regulated, but it was not reduced to the original level. The main reason was that the economy of the Qinghai–Tibet Plateau developed rapidly, and the secondary and tertiary industries increased year by year. Especially after 2010, agricultural production activities decreased, driving the reduction of cultivated land, which has been converted into grassland, urban land, and forest land [63]. The reason was that the engineering buildings left behind by the original human production were still in the NRs [64]

China's implementation of the large-scale policy of returning farmland to forests at the end of the 20th century, and the prohibition of grazing as well as the enclosure of degraded grasslands at the beginning of the 21th century, represented incentives and subsidy policies for the protection of grasslands [65,66]. Road construction was greatly developed in the NRs from 2015 to 2020, due mainly to the construction of the G216 National Highway, which started in 2016 and spanned the Qiangtang NR. The building of both trunk roads and surrounding branch roads was necessary, and this led to an expansion of the road network in the reserves [62].

In terms of different functional areas, the growth of the HP index from 2000 to 2020 was considerably lower in the core zones than in the buffer zones and experimental areas. In the core zones, HP associated with land use showed a downward trend from 2005 to 2015, indicating that protection measures contributed to the growth of vegetation [67] and increased the coverage of the ecosystem [68]. Not only has grazing intensity decreased in the buffer and experimental zones, but the increase in the HP values associated with energy consumption, population density, land use, and grazing was considerably lower in these zones than in the external buffer zones. This was due mainly to the government's actions, which reduced the pressure of production and daily activities inside the NR [69].

This study also showed that the overall HP was considerably higher in wetland NRs than in the other four NR types examined. Specifically, grazing intensity and population density accounted for a large proportion of HP because wetland nature reserves are distributed mainly in the eastern part of the Qinghai–Tibet Plateau. Compared with the other regions of the Qinghai–Tibet Plateau, the eastern region is relatively flat with abundant rainfall [70]. The climate was therefore suitable for pasture growth [71]. In particular, population density in the Sanjiangyuan National NR increased year by year [56]. HP in desert NRs was the lowest, which was due mainly to the harsh climate and environment, which was not suitable for grazing and human living. Land use and population density in forest NRs accounted for a large proportion of HP, mainly because of the large area of cultivated land in these reserves and the high levels of production and living activities [72].

To achieve conservation objectives, the government must strengthen the management of NRs. China's implementation of the large-scale policy of returning farmland to forests at the end of the 20th century, as well as the prohibition against grazing and the enclosing of degraded grasslands in 2009, represented incentives and subsidy policies for the protection of grasslands. Although grazing intensity in the NRs of the Qinghai–Tibet Plateau was gradually reduced, the cultivated land area and road construction still increased [73]. To further achieve the protection goals, since the beginning of the 21st century, local governments have vigorously pursued ecological protection policies, such as returning farmland to pasture, enclosure protection, and ecological migration, so as to improve the vegetation coverage of the NRs and their surrounding areas [74]. In response to the national policy of

ecological civilization construction and development, in 2009 Tibet's government issued the Plan for the Protection and Construction of Tibet's Ecological Security Barrier (2008–2030), which divided the area into prohibition-restricted and conditional development zones. Researchers should also pay attention to ecological protection and water conservation.

The significance of the present study in terms of policies is that it recommends the implementation of more measures to manage NRs in China. Specifically, it is necessary to regularly assess the intensity of HP in and around the reserves, especially in the western region, where human activities continue to increase thanks to the urgent need for economic development. However, to protect biodiversity and natural resources without considering the quality of life of local residents is also inappropriate. Therefore, it is necessary to reasonably set the boundary of each reserve, establish the reserves in areas with high ecological service values, and reasonably develop the economy in the areas with low ecological service values [2].

4.2. Limitations and Future Works

While a data set for HP in the Qinghai–Tibet Plateau National NRs was developed in this study, a number of limitations were noted. First of all, the road construction data for the plateau region were missing for year 2000 and were therefore replaced with the data from 2002. Moreover, the road construction data after 2010 were obtained from OSM (Open Street Map), and there was no clear basis for the classification of roads below the provincial level. Therefore, more-accurate data were needed to correct possible errors. In addition, different measures implemented in different functional areas would have varying efficiencies. However, the existing information on ecological measures was related mainly to the overall evaluation of indicators, and there were only a few of these for each functional area. It is recommended that future studies obtain more data on ecological measures for different functional areas. Moreover, because HP is evaluated on the basis of different criteria in each NR type, this study did not consider the protection requirements of different NRs in detail, which needed further attention. Finally, more HP types could be included in the data set. In recent years, production activities, such as ore mining, tourism, livestock breeding, and other construction and development activities in the Qinghai–Tibet Plateau, especially in the Sanjiangyuan National NR, have grown rapidly [75]. Because of the difficulty in quantifying them, these activities have not been considered in this study; however, if they occur outside of protected areas, they will also pollute water sources in wetlands [76]. In the future, the impact that these human activities that take place outside the NRs have on the reserves should be comprehensively considered to obtain more-accurate and more-reliable estimates of the effectiveness of NRs.

This study showed that the correlation between population density and HP factors (such as land use) was high, and the absolute HF value obtained by direct equal weight space accumulation may also be high [77], especially in urban areas with high population density. In the future, spatial accumulation using the fuzzy algebraic sum method [78] may be used as an alternative method to obtain a more-accurate spatial mapping of the intensity of human activities.

Previous studies have shown that the application of the HF model to evaluate the effectiveness of NRs in China is highly feasible [25], and the results are accurate and reliable. Although the five HP categories used in the present study presented the problem of collinearity, the cumulative HP value did not change the overall trend for each of them. The model, which is easy to run, has already been used to evaluate the effects of some protected areas [52–54], and it is recommended to continue to adopt it to evaluate the effectiveness of all the protected areas in the vast territory of China and other parts of the world.

5. Conclusions

On the basis of the interference factors associated with human activities in the Qinghai–Tibet Plateau, this study evaluated the HP in the national NRs of the region from 2000 to

2020, specifically selecting road construction, night lighting, grazing intensity, land use, and population density as indicators. Variations in HP values were compared inside and outside the NRs and in each functional area to evaluate the effectiveness of the reserves in reducing human impacts during the period examined. The results showed that the average HP value in the NRs of the Qinghai–Tibet Plateau increased from 1.47646 in 2000 to 1.76687 in 2020. The increase in the road construction and population density values significantly contributed to the overall increase in HP, while the contribution of grazing intensity had a negative value. As for the NR types, the average HP in wetland NRs was the highest, and the growth rate was the lowest; population density and grazing intensity accounted for a large proportion of HP, which was the main reason for the high level of HP reported in wetlands. From 2000 to 2020, the increase in population density in the eastern and southern parts of the Qinghai–Tibet Plateau was the main reason for the rapid increase in HP in these regions. In the same period, the average increase in HP in the NRs' core areas, buffer areas, and experimental areas was 0.12969, 0.29909, and 0.44244, respectively. The increase in road construction pressure in the buffer zones was 0.21574, leading to an overall increase in HP in the NRs of the plateau. More efforts should be made to control human activities in wetland NRs and in the experimental zones of all NRs in the Qinghai–Tibet Plateau.

Author Contributions: Conceptualization, M.J. and X.Z.; methodology, M.J.; formal analysis, M.J.; investigation, L.Y.; resources, R.W. and L.Y.; data curation, M.J.; writing—original draft preparation, M.J. and X.Z.; writing—review and editing, M.J. and B.Z.; visualization, B.Z.; supervision, L.Y.; project administration, L.Y.; funding acquisition, B.Z. All authors have read and agreed to the published version of the manuscript.

Funding: This research was supported by the National Social Science Foundation of China [18BJY086] and the Natural Science Foundation of Shandong Province, China [ZR2021QD127, ZR2021ME203]. The authors gratefully acknowledge the anonymous reviewers and the members of the editorial team who helped to improve this paper through their thorough reviews.

Data Availability Statement: Not applicable.

Conflicts of Interest: The authors declare no conflict of interest in the publication of this paper.

References

1. Venter, O.; Watson, J.E.M.; Maxwell, S.L.; Cazalis, V.; Dudley, N.; Hoffmann, M.; Rodrigues, A.S.L.; Stolton, S.; Visconti, P.; Woodley, S.; et al. Area-based conservation in the twenty-first century. *Nature* **2020**, *586*, 217–227.
2. Jiang, M.K. Overview of research on evaluation of conservation effectiveness of natural reserves in China. *J. Ecol. Rural Environ.* **2015**, *31*, 789–790.
3. Tang, X.; Jiang, Y.; Liu, Z.; Chen, J.; Liang, B.; Lin, C. Top-level Design of the Natural Protected Area System in China. *For. Resour. Manag.* **2019**, *03*, 1–7. [CrossRef]
4. Mascia, M.B.; Pailler, S.; Krithivasan, R.; Roshchanka, V.; Burns, D.; Mlotha, M.J.; Murray, D.R.; Peng, N. Protected area downgrading, downsizing, and degazettement (PADDD) in Africa, Asia, and Latin America and the Caribbean, 1900–2010. *Biol. Conserv.* **2014**, *169*, 355–361. [CrossRef]
5. Yang, H.; Viña, A.; Winkler, J.A.; Chung, M.G.; Dou, Y.; Wang, F.; Zhang, J.; Tang, Y.; Connor, T.; Zhao, Z.; et al. Effectiveness of China's protected areas in reducing deforestation. *Environ. Sci. Pollut. Res.* **2019**, *26*, 18651–18661. [CrossRef]
6. Butchart, S.H.M.; Walpole, M.; Collen, B.; Van Strien, A.; Scharlemann, J.P.W.; Almond, R.E.A.; Baillie, J.E.M.; Bomhard, B.; Brown, C.; Bruno, J.; et al. Global Biodiversity: Indicators of Recent Declines. *Science* **2010**, *328*, 1164–1168. [CrossRef]
7. Leverington, F.; Costa, K.L.; Pavese, H.; Lisle, A.; Hockings, M. A Global Analysis of Protected Area Management Effectiveness. *Environ. Manag.* **2010**, *46*, 685–698. [CrossRef]
8. Watson, J.E.M.; Dudley, N.; Segan, D.B.; Hockings, M. The performance and potential of protected areas. *Nature* **2014**, *515*, 67–73. [CrossRef]
9. Coetzee, B.W.T. Evaluating the ecological performance of protected areas. *Biodivers. Conserv.* **2016**, *26*, 231–236. [CrossRef]
10. Pereira, H.M.; Navarro, L.M.; Martins, I.S. Global Biodiversity Change: The Bad, the Good, and the Unknown. *Annu. Rev. Environ. Resour.* **2012**, *37*, 25–50. [CrossRef]
11. Titeux, N.; Henle, K.; Mihoub, J.-B.; Regos, A.; Geijzendorffer, I.R.; Cramer, W.; Verburg, P.H.; Brotons, L. Biodiversity scenarios neglect future land-use changes. *Glob. Chang. Biol.* **2016**, *22*, 2505–2515. [CrossRef] [PubMed]
12. Pacifici, M.; Foden, W.B.; Visconti, P.; Watson, J.E.M.; Butchart, S.H.M.; Kovacs, K.M.; Scheffers, B.R.; Hole, D.G.; Martin, T.G.; Akçakaya, H.R.; et al. Assessing species vulnerability to climate change. *Nat. Clim. Chang.* **2015**, *5*, 215–224. [CrossRef]

13. Staudinger, M.D.; Carter, S.L.; Cross, M.S.; Dubois, N.; Duffy, J.E.; Enquist, C.; Griffis, R.; Hellmann, J.J.; Lawler, J.J.; O'Leary, J.; et al. Biodiversity in a changing climate: A synthesis of current and projected trends in the US. *Front. Ecol. Environ.* **2013**, *11*, 465–473. [CrossRef]
14. Jones, K.R.; Venter, O.; Fuller, R.A.; Allan, J.R.; Maxwell, S.L.; Negret, P.J.; Watson, J.E.M. One-third of global protected land is under intense human pressure. *Science* **2018**, *360*, 788–791. [CrossRef]
15. Mcdonald, R.I.; Kareiva, P.; Forman, R.T. The implications of current and future urbanization for global protected areas and biodiversity conservation. *Biol. Conserv.* **2008**, *141*, 1695–1703. [CrossRef]
16. Foley, J.A.; DeFries, R.; Asner, G.P.; Barford, C.; Bonan, G.; Carpenter, S.R.; Chapin, F.S.; Coe, M.T.; Daily, G.C.; Gibbs, H.K.; et al. Global consequences of land use. *Science* **2005**, *309*, 570–574. [CrossRef] [PubMed]
17. Martínez-Ramos, M.; Ortiz-Rodríguez, I.A.; Piñero, D.; Dirzo, R.; Sarukhán, J. Anthropogenic disturbances jeopardize biodiversity conservation within tropical rainforest reserves. *Proc. Natl. Acad. Sci. USA* **2016**, *113*, 5323–5328. [CrossRef]
18. Xu, W.-B.; Svenning, J.-C.; Chen, G.-K.; Zhang, M.-G.; Huang, J.-H.; Chen, B.; Ordonez, A.; Ma, K.-P. Human activities have opposing effects on distributions of narrow-ranged and widespread plant species in China. *Proc. Natl. Acad. Sci. USA* **2019**, *116*, 26674–26681. [CrossRef]
19. Wanghe, K.; Guo, X.; Hu, F.; Ahmad, S.; Jin, X.; Khan, T.U.; Xiao, Y.; Luan, X. Spatial coincidence between mining activities and protected areas of giant panda habitat: The geographic overlaps and implications for conservation. *Biol. Conserv.* **2020**, *247*, 108600. [CrossRef]
20. Di Minin, E.; Slotow, R.; Fink, C.; Bauer, H.; Packer, C. A pan-African spatial assessment of human conflicts with lions and elephants. *Nat. Commun.* **2021**, *12*, 2978. [CrossRef]
21. Ma, B.; Xie, Y.; Zhang, T.; Zeng, W.; Hu, G. Identification of conflict between wildlife living spaces and human activity spaces and adjustments in/around protected areas under climate change: A case study in the Three-River Source Region. *J. Environ. Manag.* **2020**, *262*, 110322. [CrossRef]
22. Zhang, Z.; Xia, F.; Yang, D.; Huo, J.; Wang, G.; Chen, H. Spatiotemporal characteristics in ecosystem service value and its interaction with human activities in Xinjiang, China. *Ecol. Indic.* **2019**, *110*, 105826. [CrossRef]
23. Li, Z.; Jun, X.; Deng, X.; Yan, H. Multilevel modelling of impacts of human and natural factors on ecosystem services change in an oasis, Northwest China. *Resour. Conserv. Recycl.* **2021**, *169*, 105474. [CrossRef]
24. Sanderson, E.W.; Jaiteh, M.; Levy, M.A.; Redford, K.H.; Wannebo, A.V.; Woolmer, G.; Notes, A. The Human Footprint and the Last of the Wild. *Bioscience* **2002**, *52*, 891–904. [CrossRef]
25. Venter, O.; Sanderson, E.W.; Magrach, A.; Allan, J.R.; Beher, J.; Jones, K.R.; Possingham, H.P.; Laurance, W.F.; Wood, P.; Fekete, B.M.; et al. Sixteen years of change in the global terrestrial human footprint and implications for biodiversity conservation. *Nat. Commun.* **2016**, *7*, 12558. [CrossRef] [PubMed]
26. Wang, J.; Zhang, G.; Nie, Z.; Yan, M. Quantintative assessment of human activity intensity in Hutuohe catchment. *J. Arid. Land Resour. Environ.* **2009**, *23*, 41–44.
27. Zhang, C.; Wang, Z. Quantitative assessment of human activity intensity in the Heihe catchment. *Adv. Earth Sci.* **2004**, *23*, 386–390.
28. Anderson, E.; Mammides, C. The role of protected areas in mitigating human impact in the world's last wilderness areas. *Ambio* **2019**, *49*, 434–441. [CrossRef]
29. Liu, X.; Fu, Z.; Wen, R.; Jin, C.; Wang, X.; Wang, C.; Xiao, R.; Hou, P. Characteristics of human activities and the spatio-temporal changes of national nature reserves in China. *Geogr. Res.* **2020**, *39*, 2391–2402.
30. Ren, B.; Park, K.; Shrestha, A.; Yang, J.; McHale, M.; Bai, W.; Wang, G. Impact of Human Disturbances on the Spatial Heterogeneity of Landscape Fragmentation in Qilian Mountain National Park, China. *Land* **2022**, *11*, 2087. [CrossRef]
31. Li, S.; Su, S.; Liu, Y.; Zhou, X.; Luo, Q.; Paudel, B. Effectiveness of the Qilian Mountain Nature Reserve of China in Reducing Human Impacts. *Land* **2022**, *11*, 1071. [CrossRef]
32. Al, M.A.; Akhtar, A.; Kamal, A.H.M.; AftabUddin, S.; Islam, S.; Sharifuzzaman, S. Assessment of benthic macroinvertebrates as potential bioindicators of anthropogenic disturbance in southeast Bangladesh coast. *Mar. Pollut. Bull.* **2022**, *184*, 114217. [CrossRef]
33. Lin, C.; Chunying, R.; Zongming, W.; Bai, Z.; Kaishan, S. Remote Sensing Monitoring and Analysis on Dynamics of Land Use of Human Disturbances in Coastal Area of the Yellow River Delta. *Wetland Science* **2017**, *15*, 613–621. [CrossRef]
34. Benavidez-Silva, C.; Jensen, M.; Pliscoff, P. Future Scenarios for Land Use in Chile: Identifying Drivers of Change and Impacts over Protected Area System. *Land* **2021**, *10*, 408. [CrossRef]
35. Poor, E.E.; Jati, V.I.M.; Imron, M.A.; Kelly, M.J. The road to deforestation: Edge effects in an endemic ecosystem in Sumatra, Indonesia. *PLoS ONE* **2019**, *14*, e0217540. [CrossRef] [PubMed]
36. Prowse, T.A.; O'Connor, P.J.; Collard, S.J.; Rogers, D.J. Eating away at protected areas: Total grazing pressure is undermining public land conservation. *Glob. Ecol. Conserv.* **2019**, *20*, e00754. [CrossRef]
37. Li, G.; Gao, J.; Li, L.; Hou, P. Human pressure dynamics in protected areas of China based on nighttime light. *Glob. Ecol. Conserv.* **2020**, *24*, e01222. [CrossRef]
38. Sun, H.; Zheng, D.; Yao, T.; Zhang, Y. Protection and construction of the national ecological security shelter zone on Tibetan Plateau. *Acta Geogr. Sin.* **2012**, *67*, 3–12.
39. Xu, Z.R.; Zhang, Y.L.; Cheng, S.K.; Zheng, D. Scientific basis and the strategy of sustainable development in Tibetan Plateau. *Sci. Technol. Rev.* **2017**, *35*, 108–114.

40. Myers, N.; Mittermeier, R.A.; Mittermeier, C.G.; da Fonseca, G.A.B.; Kent, J. Biodiversity hotspots for conservation priorities. *Nature* **2000**, *403*, 853–858. [CrossRef]
41. Zhang, Y.; Wu, X.; Qi, W.; Li, S.; Bai, W. Characteristics and protection effectiveness of nature reserves on the Tibetan Plateau, China. *Resour. Sci.* **2015**, *37*, 1455–1464.
42. Wang, W.; Xin, L.; Du, J.; Chen, B.; Liu, F.; Zhang, L.; Li, J. Evaluating conservation effectiveness of protected areas: Advances and new perspectives. *Biodivers. Sci.* **2016**, *24*, 1177–1188. [CrossRef]
43. Li, S.; Zhang, H.; Zhou, X.; Yu, H.; Li, W. Enhancing protected areas for biodiversity and ecosystem services in the Qinghai–Tibet Plateau. *Ecosyst. Serv.* **2020**, *43*, 101090. [CrossRef]
44. Li, G.Q.; Kan, A.K.; Wang, X.B.; Li, G.M.; Gao, Z.Y.; Wang, h.; Yong, Z. Distribution of degraded wetlands and their influence factors in Qomolangma National Nature Reserve. *Wetl. Sci.* **2010**, *8*, 110–114.
45. Zhu, L.; Zhan, X.; Meng, T.; Zhang, S.; Wei, F. Landscape features influence gene flow as measured by cost-distance and genetic analyses: A case study for giant pandas in the Daxiangling and Xiaoxiangling Mountains. *BMC Genet.* **2010**, *11*, 72. [CrossRef]
46. Cao, Y.; Wang, B.; Zhang, J.; Wang, L.; Pan, Y.; Wang, Q.; Jian, D.; Deng, G. Lake macroinvertebrate assemblages and relationship with natural environment and tourism stress in Jiuzhaigou Natural Reserve, China. *Ecol. Indic.* **2016**, *62*, 182–190. [CrossRef]
47. Li, W.; Zhang, Q.; Liu, C.; Xue, Q. Tourism's Impacts on Natural Resources: A Positive Case from China. *Environ. Manag.* **2006**, *38*, 572–579. [CrossRef]
48. Su, X.; Liu, S.; Dong, S.; Zhang, Y.; Wu, X.; Zhao, H.; Zhao, Z.; Sha, W. Effects of potential mining activities on migration corridors of Chiru (*Pantholops hodgsonii*) in the Altun National Nature Reserve, China. *J. Nat. Conserv.* **2015**, *28*, 119–126. [CrossRef]
49. Gui, J.; Gao, H.; Li, Z.; Zou, H.; Yuan, R. The impacts of hydropower development in Zhangye section of Qilian Mountains on regional eco-environment. *Chin. J. Ecol.* **2019**, *38*, 2159–2166.
50. Zhang, X.; Li, S.; Yu, H. Analysis on the ecosystem service protection effect of national nature reserve in Qinghai-Tibetan Plateau from weight perspective. *Ecol. Indic.* **2022**, *142*, 109225. [CrossRef]
51. Yin, L.; Dai, E.; Zheng, D.; Wang, Y.; Ma, L.; Tong, M. Spatio-Temporal analysis of the human footprint in the Hengduan Mountain region: Assessing the effectiveness of nature reserves in reducing human impacts. *J. Geogr. Sci.* **2020**, *30*, 1140–1154. [CrossRef]
52. Tapia-Armijos, M.F.; Homeier, J.; Munt, D.D. Spatio-temporal analysis of the human footprint in South Ecuador: Influence of human pressure on ecosystems and effectiveness of protected areas. *Appl. Geogr.* **2017**, *78*, 22–32. [CrossRef]
53. Azadeh, K.; Kendall, J. Assessing national human footprint and implications for biodiversity conservation in Iran. *Ambio* **2020**, *49*, 1506–1518.
54. Li, S.; Wu, J.; Gong, J.; Li, S. Human footprint in Tibet: Assessing the spatial layout and effectiveness of nature reserves. *Sci. Total Environ.* **2018**, *621*, 18–29. [CrossRef] [PubMed]
55. Li, S.; Bing, Z.; Jin, G. Spatially Explicit Mapping of Soil Conservation Service in Monetary Units Due to Land Use/Cover Change for the Three Gorges Reservoir Area, China. *Remote Sens.* **2019**, *11*, 468. [CrossRef]
56. Tan, L.; Guo, G.; Li, S. The Sanjiangyuan Nature Reserve Is Partially Effective in Mitigating Human Pressures. *Land* **2021**, *11*, 43. [CrossRef]
57. Wu, Y.; Shi, K.; Chen, Z.; Liu, S.; Chang, Z. Developing Improved Time-Series DMSP-OLS-Like Data (1992–2019) in China by Integrating DMSP-OLS and SNPP-VIIRS. *IEEE Trans. Geosci. Remote Sens.* **2022**, *60*, 5333. [CrossRef]
58. Zong, Y.G.; Zhou, S.Y.; Ping, P.; Liu, C.; Guo, R.H.; Cheng, H.C. Perspective of road ecology development. *Acta Ecol. Sinica* **2003**, *23*, 2396–2405.
59. Li, Y.; Zhou, J.; Wu, X. Effects of the construction of Qinghai-Tibet railway on the vegetation ecosystem and eco-resilience. *Geogr. Res.* **2017**, *36*, 2129–2140. [CrossRef]
60. Chen, H.; Li, S.; Zheng, D. Features of Ecosystems alongside Qinghai-Xizang Highway and Railway and the Impacts of Road Construction on Them. *J. Mt. Res.* **2003**, *21*, 559–567.
61. Yan, J.; Zhang, Y.; Liu, L.; Shen, Z.; Liu, Y.; Zheng, D. Main Effect of Plateau Traffic on Land Use and Landscape Pattern Change: From Lanzhou to Golmud. *Acta Geogr. Sin.* **2003**, *58*, 34–44.
62. Zhu, G.; Zhao, K.; Liu, J.; Yang, F.; Gao, Y.; Lin, J.; Han, D.; Xu, H.; Jiang, Y.; Sun, H. Study on Ecological Conflict and Coordination of Highway Network Planning—A Case Study of the Three-River Headwater Region of Qinghai-Tibet Plateau. *J. Cap. Norm. Univ. (Nat. Sci. Ed.)* **2020**, *41*, 57–63.
63. Peng, H.; Ren, Y.; Li, Q.; Wei, J. Spatial and Temporal Land Use/Cover Change Characteristics of Qinghai-Tibet Plateau. *J. Yangtze River Sci. Res. Inst.* **2022**, *39*, 41–49+57. [CrossRef]
64. Hong, L. Research on the compensation mechanism and policy of ecological migration in Sanjiangyuan. *J. South-Cent. Minzu Univ. (Humanit. Soc. Sci.)* **2013**, *33*, 101–105.
65. Li, S.; Liu, M. The Development Process, Current Situation and Prospects of the Conversion of Farmland to Forests and Grasses Project in China. *J. Resour. Ecol.* **2022**, *13*, 120–128.
66. Liu, D.; Ma, Y.; Dong, Q.; Shi, J. Effect of Forbidden Grazing and Exclusion Grassland on Communities Character of Artificial Pasture in "Back Soil Beach". *Chin. Qinghai J. Anim. Vet. Sci.* **2008**, *38*, 10–12.
67. Zhai, X.; Liang, X.; Yan, C.; Xing, X.; Jia, H.; Wei, X.; Feng, K. Vegetation Dynamic Changes and their Response to Ecological Engineering in the Sanjiangyuan Region of China. *Remote Sens.* **2020**, *12*, 4035. [CrossRef]

68. Han, S.; Meng, Q.; Liu, H.; Peng, Y.; Han, J.; Jin, S.; Fan, S.; Xin, B.; He, L.; Li, H. Refined land-cover classification mapping using a multi-scale transformation method from remote sensing, unmanned aerial vehicle, and field surveys in Sanjiangyuan National Park, China. *J. Appl. Remote Sens.* **2021**, *15*, 014513. [CrossRef]
69. Xia, S.; Yan, X.; Qian, K.; Liang, X. Management system of China's nature reserve. *J. Zhejiang A F Univ.* **2009**, *26*, 127–131.
70. Ma, Y.; Ma, J.; Li, F.; Ma, X. Spatial and Temporal Characteristics of Short-time Strong Rainfall and Its Altitude Distrbution Characteristics in Linxia at Plateau Slope. *Desert Oasis Meteorol.* **2022**, *16*, 68–74.
71. Zeng, Y.; Zhang, Q.; Hou, F. Effects of Climate Change on Pasture Production on Qinghai-Tibet Plateau based on Integratedanalyse of Database. *J. Grassl. Forage Sci.* **2022**, *266*, 13–23.
72. Zhu, P.; Huang, L.; Xiao, T.; Wang, J. Dynamic changes of habitats in China's typical national nature reserves on spatial and temporal scales. *J. Geogr. Sci.* **2018**, *28*, 778–790. [CrossRef]
73. Feng, Y.; Meng, L.; Li, S.; Di, Y. Effectiveness of grazing exclusion on the restoration of degraded alpine grasslands on the Northern Tibetan Plateau from 2010 to 2017. *Pratacultural Sci.* **2019**, *36*, 1148–1162.
74. Zu, D.; Luo, P.; Yang, H.; Mou, C.; Li, Y.; Mo, L.; Li, T.; Luo, C.; Li, H.; Wu, S. Assessing the space neighborhood effects and the protection effectiveness of a protected area—A case study from Zoige Wetland National Nature Reserve. *Chin. J. Appl. Environ. Biol.* **2019**, *25*, 0854–0862. [CrossRef]
75. Chung, M.G.; Pan, T.; Zou, X.; Liu, J. Complex Interrelationships between Ecosystem Services Supply and Tourism Demand: General Framework and Evidence from the Origin of Three Asian Rivers. *Sustainability* **2018**, *10*, 4576. [CrossRef]
76. Lu, S.-J.; Si, J.-H.; Hou, C.-Y.; Li, Y.-S.; Wang, M.-M.; Yan, X.-X.; Xie, M.; Sun, J.-X.; Chen, B.-J.; Li, S.-S. Spatiotemporal distribution of nitrogen and phosphorus in alpine lakes in the Sanjiangyuan Region of the Tibetan Plateau. *Water Sci. Technol.* **2017**, *76*, 396–412. [CrossRef]
77. Kennedy, C.M.; Oakleaf, J.R.; Theobald, D.M.; Baruch-Mordo, S.; Kiesecker, J. Managing the middle: A shift in conservation priorities based on the global human modification gradient. *Glob. Chang. Biol.* **2019**, *25*, 811–826. [CrossRef]
78. Theobald, D.M.; Kennedy, C.; Chen, B.; Oakleaf, J.; Baruch-Mordo, S.; Kiesecker, J. Earth transformed: Detailed mapping of global human modification from 1990 to 2017. *Earth Syst. Sci. Data* **2020**, *12*, 1953–1972. [CrossRef]

land

MDPI

Article

The Coupling Relationship between Green Finance and Ecosystem Service Demand in China Based on an Improved Coupling Coordination Degree Model

Haojia Wang [1], Dandan Zhao [2], Qiaowei Zhou [2], Qinhua Ke [2] and Guanglong Dong [3,*]

[1] College of Economics and Management, South China Agricultural University, Guangzhou 510642, China
[2] College of Public Management, South China Agricultural University, Guangzhou 510642, China
[3] School of Management Engineering, Shandong Jianzhu University, Jinan 250101, China
* Correspondence: dongguanglong18@sdjzu.edu.cn

Abstract: With the rapid development of society and economy, people's demand for ecosystem services is constantly increasing. All countries support this demand by vigorously developing green finance. The coordinated development of green finance and ecosystem service demand is of great significance for sustainable development. Most of the existing studies separately study green finance or ecosystem service demand, separating the relationship between the two. At present, there is still a lack of clear understanding of the coupling relationship between green finance and ecosystem service demand. In addition, in the existing coupling relationship calculation models, the setting of relevant parameters is subjective. Therefore, based on the green finance and ecosystem service demand database of 30 provinces in China from 2010 to 2017, this paper firstly evaluates the green finance and ecosystem service demand quantitatively, and then analyzes the coupling coordination relationship between them by using an improved coupling coordination degree model. The results show that: (1) compared with the traditional coupling coordination degree model, the contribution coefficient of each subsystem in the improved coupling coordination degree model has a more sufficient basis, and more objective evaluation results; (2) from 2010 to 2017, the level of green finance in China's provinces increased significantly, showing a spatial pattern of "high in the east and low in the west"; the ecosystem services demand increased first and then decreased, with an increase in nearly two-thirds of provinces; (3) the coupling coordination relationship between green finance and ecosystem service demand in China's provinces was optimized continuously from 2010 to 2017, showing the spatial differentiation of "eastern China > central China > northeast China > western China"; (4) in 2017, the coupling coordination degree of green finance and ecosystem service demand in Guangdong Province was the highest, reaching a high level of coordination, while Qinghai Province was the lowest, as a result of a serious level of incoordination. It is worth noting that the comprehensive development level of green finance in China is still low and seriously lags behind the development level of ecosystem services demand. In the future, green and low-carbon transformation should be accelerated to promote the sustainable development of financial ecology.

Keywords: green finance; ecosystem service demand; coupling coordination relationship

Citation: Wang, H.; Zhao, D.; Zhou, Q.; Ke, Q.; Dong, G. The Coupling Relationship between Green Finance and Ecosystem Service Demand in China Based on an Improved Coupling Coordination Degree Model. *Land* **2023**, *12*, 529. https://doi.org/10.3390/land12030529

Academic Editor: Teodoro Semeraro

Received: 2 February 2023
Revised: 20 February 2023
Accepted: 20 February 2023
Published: 22 February 2023

1. Introduction

The natural ecological environment provides essential ecosystem services for human beings [1], is the space for human survival, and is also the basis of sustainable economic and social development [2]. China's economy has maintained a fast growth rate in the past 40 years, with an average annual GDP growth rate of 10%. However, due to the long-term use of a factor input-driven economic growth mode characterized by sacrificing the ecological environment and consuming large amounts of resources, economic growth has gradually slowed down in recent years: GDP growth dropped to 6.7% in 2018, 6.0% in

2019, and 2.2% in 2020. At the same time, problems, such as resource shortage, environmental pollution, and ecological deterioration, have become increasingly prominent [3]. In response to the above problems, the Chinese government pointed out in the Boao Forum for Asia in 2010 that "green economy is the trend of the times in today's world" [4]. The adoption of the United Nations 2030 Agenda for Sustainable Development and the New Urban Agenda also show that the "green economy", as a new development model, has attracted global attention [5]. As the core of the modern economy, finance is an effective means to promote the coordinated development of the natural environment, economy, and society [6]. The transformation of the economic development mode from a high-carbon model to a low-carbon model is inseparable from the reform and innovation of finance. Based on the actual situation of economic development and ecological environment, China has proposed to develop green finance [7]. Green finance can not only promote high-quality economic development but also be the core driving factor for improving ecological environment [8]. It is an inevitable trend in China's economy to promote the coordinated development of ecological environment and economy and society through green finance.

As a bridge connecting natural environmental systems and economic and social systems, ecosystem service research includes two aspects: it not only pays attention to the supply of ecosystem services generated by the natural environment, but also pays attention to the ecosystem service demand for the benefit of economic and social activities [9]. In recent years, the research on ecosystem services has developed rapidly. Quantitative measurement of the correlation and collaborative evolution trend between ecosystem services and natural environment [10,11], economic, and social systems [12,13], as well as the supply and demand of ecosystem services [14,15], has become a research hotspot in this field. The eco-environmental protection principle adopted by green finance is very consistent with the concept of coordinated development [16]. However, at present, there are few studies on the coordinated development of green finance and ecosystem services in the world. Most of the existing studies study the relationship between green finance and the economic and social system from the external perspective of "economy explains economy". For example, Wang et al. studied the different stages of the integrated development degree of green finance and related industries, and believed that the initial stage should be resource-driven, and the later stage should strengthen the input of technical elements [17]. Yin et al. analyzed the close relationship between green finance and economy and pointed out that the two have an obvious synergistic effect and are in a highly coordinated and coupled development state [18]. Dong et al. studied the coordination with green finance from the perspective of urbanization, believing that the two have strong spatial agglomeration effects and spatial spillover effects, and urbanization generally lags behind green finance [19]. To sum up, existing research focuses on the single field of ecosystem services or green finance, ignored the organic connection between green development and financial innovation, and still lacks a clear understanding of the coupling relationship between ecosystem services and green finance.

Scale dependence and temporal-spatial heterogeneity are key characteristics of both natural environmental systems and economic and social systems [20], so they have significant time and space coupling characteristics. The quantitative measurement of the coupling relationship between the two is the focus of the cross-research of natural and social sciences. The coupled coordination degree model is widely used in the fields of ecology [21,22], environment [23,24], economy [25,26], society [27,28], and some scholars have also applied it to the study of green finance because of its advantages in a quantitative study of the interaction and interactive coupling relationship between two or more systems [29]. Yu et al. calculated the coupling degree and coordination degree between green finance and social development level and pointed out the positive promoting effect and threshold effect of green finance [30]. Wang et al. established a coupling coordination degree model between green finance and industrial technology innovation, and the results showed that there was strong regional heterogeneity between them [31]. Zhu et al. studied the coupling coordinated development degree of green finance and circular economy and believed that green

finance would fall into a "low development trap" if its development lagged [15]. However, the traditional coupling coordination degree model used in the above study regards the contributions of both subsystems as equally important. Some scholars have questioned this, pointing out that this assignment method is inconsistent with reality, and its distorted results may mislead policymakers to make wrong decisions [32]. Reasonable sub-system contribution coefficient assignments will directly affect the coupling coordination degree, and then affect the accurate evaluation of the coupling coordination relationship between ecosystem service demand and green finance. Therefore, the reasonable improvement of the coupling coordination degree model is still worth further discussion.

To sum up, most current studies focused on green finance or ecosystem service demand individually, and lacked a clear understanding of the coupling relationship between green finance and ecosystem service demand. Therefore, based on the panel data of 30 provinces in China from 2010 to 2017, this paper calculates the demand levels of green finance and ecosystem services by using the global principal component analysis and entropy method. Then, based on the improved coupling coordination degree model, the coupling coordination relationship between the two is quantitatively analyzed to provide scientific reference for the coordinated promotion of green finance and ecological environment construction.

2. Study Area and Data Sources

2.1. Study Area

In this paper, 30 provinces in mainland China, excluding Hong Kong, Macao, Taiwan, and Tibet Autonomous Region, are selected as research areas. According to economic regionalization of China, they can be divided into four regions: eastern China, central China, western China, and northeast China (Figure 1).

Figure 1. The four economic divisions of China.

In 2006, the International Finance Corporation (IFC) partnered with Industrial Bank to launch the first green credit product on the Chinese market. At its 18th National Congress in 2012, the CPC Central Committee included the construction of ecological civilization into the Five-sphere Integrated Plan which refers to China's overall plan for building socialism with Chinese characteristics. The China Banking Regulatory Commission issued

the Green Credit Guidelines, which became the programmed document of China's green credit system. China's green credit policy system began to be established, developed, and gradually improved. More banks are providing green credit, and green financial products are increasingly abundant. In August 2016, seven state ministries jointly issued the Guiding Opinions on Building a Green Finance System, which clarified the definition of green finance in China and established the top-level framework system of green finance. According to China Green Finance Development Report (2018), China issued more than 280 billion yuan of green bonds in 2018, with a stock of nearly 600 billion yuan, making it the country with the largest issuance of such bonds in the world [19]. At the same time, the ecosystem services demand in China also has strong spatial heterogeneity. The ecosystem services demand in most of the western and northern regions is at a low level, indicating that ecosystem services demand is relatively low. In contrast, the regions with high ecosystem services demand are mainly concentrated in the Yangtze River Delta, Pearl River Delta, Beijing-Tianjin-Hebei region, and some densely populated urban areas, as well as the Huang-Huai-Hai Plain [33].

2.2. Data Sources

The data used in this study mainly includes green finance and ecosystem service demand. Green finance data are mainly from the Wind database (www.wind.com.cn/, accessed from 5 September 2022 to 17 October 2022) and the China Environmental Statistical Yearbook (2011–2018). Data on ecosystem service demand are mainly derived from the China Statistical Yearbook (2011–2018), provincial statistical yearbooks of corresponding years, and the China Carbon Accounting Database (https://www.ceads.net.cn/, accessed on 12 November 2022).

3. Methods

3.1. Evaluation of Green Finance

Green financial instruments include a variety of products and mechanisms, including green credit, green securities, green insurance, green investment, carbon finance, etc. [34–36]. However, green finance in China is still in its development stage and relevant statistics are lacking. Therefore, referring to relevant studies [37] and following the principles of reflecting the basic connotation of green finance, covering the scope of green finance services, index representativeness and data accessibility, six indicators from four aspects of green credit, green securities, green investment, and carbon finance are selected to construct an evaluation index system of green finance (Table 1).

Table 1. China's provincial green finance evaluation index system.

Criterion	Index	Index Meaning	Unit	Efficiency
Green-credit policy	Green finance evaluation Total liabilities of listed companies in environmental protection industry	The total debt generates from *i*th province (city) registers environmental protection listed company in *t*th year	Yuan	−
Green securities	Total market value of listed companies in environmental protection industry	The total market value generates from *i*th province (city) registers the environmental protection listed company in *t*th year	Yuan	+
Green investment	Expenditure on energy conservation and environmental protection	The total expenditure on energy and environmental protection of the *i*th province (municipality) in *t*th year	Yuan	+
	Total investment in environmental pollution control	The total investment in pollution control of *i*th province (city) in *t*th year		
	Total equity investment of listed companies in environmental protection industry	The total equity investment of environmental protection listed companies register in the *i*th province (city) in the *t*th year	Yuan	+
Carbon finance	Carbon financial trading volume	Carbon financial trading volume in the *i*th province (city) in the *t*th year	Yuan	+

The global principal component analysis was used to calculate the comprehensive score of green finance, which is an improvement on traditional principal component analysis. It combines traditional principal component analysis and time series analysis [38]. Therefore, it can be used to process panel data, such as the green finance data of Chinese provinces from 2010 to 2017 in this paper.

3.2. Evaluation of Ecosystem Service Demand

Ecosystem service demand refers to the quantity and quality of services that humans expect to obtain from natural systems, namely the potential demand [39,40]. Typically, latent demand includes not only the actual demand that humans have consumed but also the unfulfilled demand that humans would like to consume within ecosystem services. Accounting for ecosystem service demand is required in terms of both consumption of ecosystem services and the amount expected to be obtained.

Ecosystem services can be divided into nine subtypes [41]. Among them, climate regulation and biodiversity maintenance services belong to the category of "global non-proximity" services [42], while the generation and acquisition of cultural services are subjective, and the consumption process is non-expendable, making it difficult to quantify their demands. Therefore, the supply and demand of these three services—climate regulation, biodiversity maintenance services and cultural services—are not carried out in this paper. Finally, six types of ecosystem services, including food demand, water conservation, carbon sequestration, raw material production, gas regulation, and waste treatment, are selected to analyze ecosystem service demand (Table 2).

Table 2. Index system of provincial ecosystem service demand evaluation in China.

Criterion	Index Meaning	Index Efficiency	Weights	Index Calculation Method
Food supply services	Total food demand in *i*th province (city) in *t*th year	+	0.156	Food demand = per capita food demand ∗population. Food demand is replaced by consumption (including consumption of grain, oil, vegetables, meat, aquatic products, eggs, milk, melons, and fruits) [43]
Water conservation services	Total water demand of *i*th province (city) in *t*th year	+	0.175	Water demand = per capitawater consumption ∗ population density. Per capita water consumption, including per capita agricultural, industrial, domestic and ecological water consumption [44]
Carbon sequestration services	Total carbon emissions of the *i*th province (city) in *t*th year	+	0.172	Carbon sequestration service = per capita carbon emission ∗ population [45]
Raw material production	Forestry output value of *i*th province (city) in *t*th year	+	0.171	The use of forestry output value represents provinces' demand for ecosystem raw material production services [14,46]
Gas regulation	Industrial airpollutants (including smoke dust, SO_2, NOx) discharges into the ecosystem in the *i*th province (city) in the *t*th year	+	0.150	The total emission of smoke dust, SO_2 and NOx is taken as the demand of ecosystem gas regulation service
Waste disposal	Wastes include solid wastes and wastewater discharges into the ecosystem in the *i*th province (city) in *t*th year	+	0.177	Since statistics show very little solid waste is discarded by industry in each province, only total wastewater discharges are calculated in the actual calculation [14]

The entropy method was used to determine the weight of the ecosystem service demand evaluation index. Based on the standardized values and weights of evaluation

indicators, the weighted sum model is adopted to calculate the comprehensive score of ecosystem service demand. The calculation formula is as follows:

$$V_i = \sum_{j=1}^{n} \left(W_{ij} \times x'_{ij} \right) \tag{1}$$

where V_i represents the comprehensive score of ecosystem service demand; n is the number of indicators; W_{ij} is the weight of indicators; and x'_{ij} represents the standardized value of evaluation indicators.

3.3. Coupling Coordination Degree Model

In this paper, the coupling coordination degree model is used to measure the coupling relationship between green finance and ecosystem service demand. The coupling coordination degree model is an effective method to analyze the interaction between two systems. Among them, the coupling degree reflects the degree of mutual restriction or dependence between two systems, and the coupling coordination degree reflects the degree of benign coupling interaction between systems [19,47].

3.3.1. Traditional Coupling Coordination Degree Model

The formula of traditional coupling coordination degree model is as follows:

$$C = 2\left\{ \frac{U \times A}{(U + A)^2} \right\}^{1/2} \tag{2}$$

$$T = \alpha U + \beta A \tag{3}$$

$$D = \sqrt{C \times T} \tag{4}$$

where C is the coupling degree; T is the comprehensive level of green finance and ecosystem service demand; D is the coupling coordination degree between green finance and ecosystem service demand; U and A are green finance comprehensive scores and ecosystem service demand comprehensive score respectively; α and β are contribution coefficients of green finance and ecosystem service demand, respectively. It is generally assumed that the green finance subsystem and ecosystem service demand subsystem are equally important, i.e., $\alpha = \beta = 0.5$.

3.3.2. Improved Coupling Coordination Degree Model

To objectively and accurately reflect the coupling relationship between green finance and ecosystem service demand, the corresponding contribution coefficient should be determined comprehensively according to the performance of green finance and ecosystem service demand. When a subsystem is relatively backward, it should be given a relatively large contribution coefficient, to attract more attention from the government and society, and then government and society take effective measures to promote the development of the system, narrow the gap between the systems, and realize the coordinated development of the systems [32,48]. Accordingly, the formula of the improved coupling coordination degree model is as follows:

$$T' = \alpha' U + \beta' A \tag{5}$$

$$\alpha' = \frac{A}{U + A} \tag{6}$$

$$\beta' = \frac{U}{U + A} \tag{7}$$

$$D' = \sqrt{C \times T} \tag{8}$$

where α' and β' are the improved contribution coefficients of green finance and ecosystem service demand, respectively. If the comprehensive score U of green finance is low, α' is relatively large, which reminds decision-makers to pay more attention to the development of green finance. If the comprehensive score of A of ecosystem services demand is low, β' is relatively large, which reminds policymakers to pay more attention to the improvement of the ecosystem services demand. Referring to relevant studies [24,49], the coupling coordination relationship between the green finance subsystem and the ecosystem service demand subsystem is divided into 3 categories, 8 subtypes, and 24 development modes according to the coupling coordination degree score and the role of the relationship between the two subsystems (Table 3).

Table 3. Green finance and coupling coordination degree types of ecosystem service demand.

Categories	D	Subgroup	Development Modes	
Balanced development	$0.8 < D \leq 1$	High-level coordination	U > A	High coordination—lagging ecosystem services demand
			U < A	High coordination—lagging green finance
			U = A	Advanced coordinated development of green finance and ecosystem service demand
	$0.7 < D \leq 0.8$	Favorably coordinated development	U > A	Good coordination—lagging ecosystem services demand
			U < A	Good coordination—lagging green finance
			U = A	Well coordinated development of green finance and ecosystem service demand
Transitional development	$0.6 < D \leq 0.7$	Moderate coordination	U > A	Moderate coordination—lagging ecosystem services demand
			U < A	Moderate coordination—lagging green finance
			U = A	The green finance and ecosystem services demand will be appropriately coordinated
	$0.5 < D \leq 0.6$	Basic coordination	U > A	Basic coordination—lagging ecosystem services demand
			U < A	Basic coordination—lagging green finance
			U = A	The green finance and ecosystem services demand is basically coordinated
	$0.4 < D \leq 0.5$	Low-level coordination	U > A	Low level of coordination—lagging ecosystem services demand
			U < A	Low level of coordination—lagging green finance
			U = A	Green finance and coordinated development of low ecosystem services demand

Table 3. *Cont.*

Categories	D	Subgroup	Development Modes	
Unbalanced development	$0.2 < D \leq 0.4$	Slightly uncoordinated	U > A	Mild incoordination—lagging ecosystem services demand
			U < A	Mild incoordination—lagging green finance
			U = A	Green finance and the ecosystem services demand developed slightly incongruously
	$0 < D \leq 0.2$	Seriously uncoordinated development	U > A	Serious incoordination—lagging ecosystem services demand
			U < A	Serious incoordination—lagging green finance
			U = A	There is serious incoordination between green finance and the development of the ecosystem services demand

4. Results

4.1. Temporal and Spatial Characteristics of Green Finance

From the time dimension, the development level of green finance in China's provinces improved significantly, showing a spatial distribution pattern of "high in the east and low in the west" (Figure 2). Among them, Guangdong had the best green finance development level, followed by Beijing, Shanghai, Jiangsu, Shandong, Zhejiang, and Hubei provinces. After 2015, the comprehensive scores of green finance in Guangdong Province, Beijing, and Shanghai all exceeded 0.6 and gradually approached 1. Jiangsu Province exceeded 0.5 in 2015. The comprehensive scores of green finance in other provinces were concentrated between 0 and 0.4.

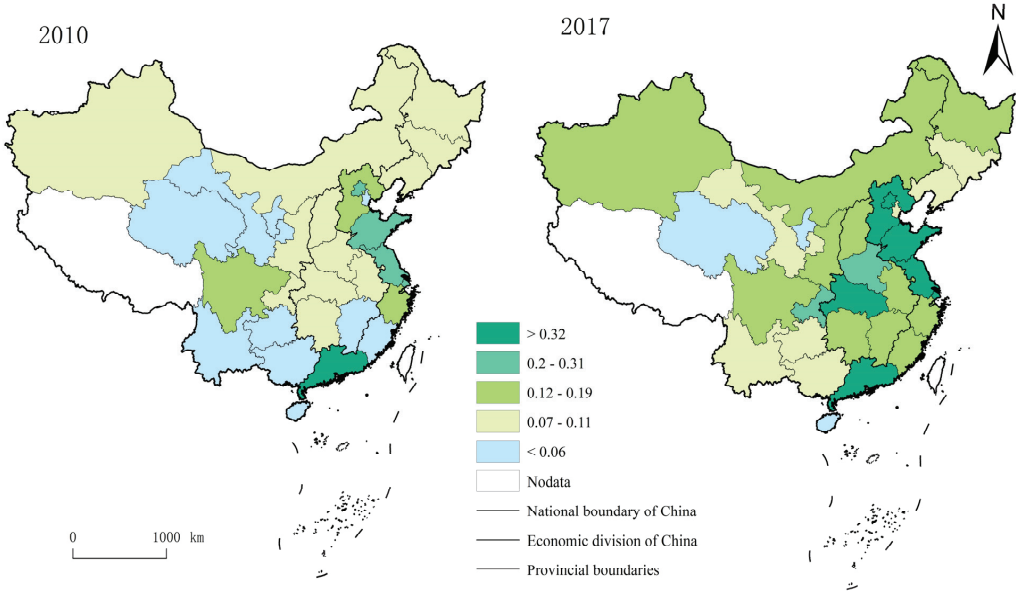

Figure 2. Spatial distribution of green finance in China from 2010 to 2017.

In 2010, the level of green finance in China was relatively low, with most provinces (21 provinces account for 70% of the studied provinces) scoring below 0.11. Only Guangdong Province had a high level of green finance development. The remaining eight

provinces (Shandong, Jiangsu, Beijing, Hebei, Fujian, Zhejiang, Henan, and Sichuan), which are all located in eastern China (except for Sichuan and Henan), had values between 0.12 and 0.31.

However, with the development of the national green economy, the development level of green finance in various places had improved significantly. In 2017, most provinces (20 provinces account for 66.7% of the studied provinces) scored above 0.12. Except for Fujian and Hainan, the scores in eastern China were all higher than 0.32. The spatial distribution of provinces with scores between 0.20 and 0.31 tended to move westward. Provinces with scores below 0.11 (Qinghai, Ningxia, Hainan, Gansu, Yunnan, Guizhou, Guangxi, Jilin, and Liaoning) were mainly located in western China.

4.2. Temporal and Spatial Characteristics of Ecosystem Service Demand

From 2010 to 2017, the comprehensive score that represented the ecosystem services demand in China rose and then slightly decreased. There was an upward trend from 0.27 in 2010 to 0.31 in 2015 and then to 0.29 in 2017. There were significant regional differences in China's ecosystem service demand, with the overall characteristics of "central > eastern > northeast > western"(Figure 3). The comprehensive score of ecosystem service demand in China in the central region was the highest, with a range of 0.36–0.41. The comprehensive level of demand for ecosystem services in Shanxi Province, Jiangxi Province, and Hubei Province was very similar, and the evolution trend was basically overlapping. The demand for ecosystem services in the eastern region was clearly polarized, with Guangdong Province having the highest level, reaching 0.7 in 2017. Jiangsu Province and Shandong Province followed, with an overall score between 0.53 and 0.56. However, the overall level of Hainan, Tianjin, and Beijing Provinces was low, remaining below 0.1. Between 2014 and 2015, demand for ecosystem services increased significantly in most provinces and then tended to decline. The overall demand for ecosystem services in China has developed slowly, and the changes in the demand for ecosystem services in the eastern, western, central, and northeastern regions are 33%, 38%, 67%, and 28%, respectively. Overall, demand for ecosystem services increased in most of China's provinces during the study period, with 19 provinces accounting for 63 percent.

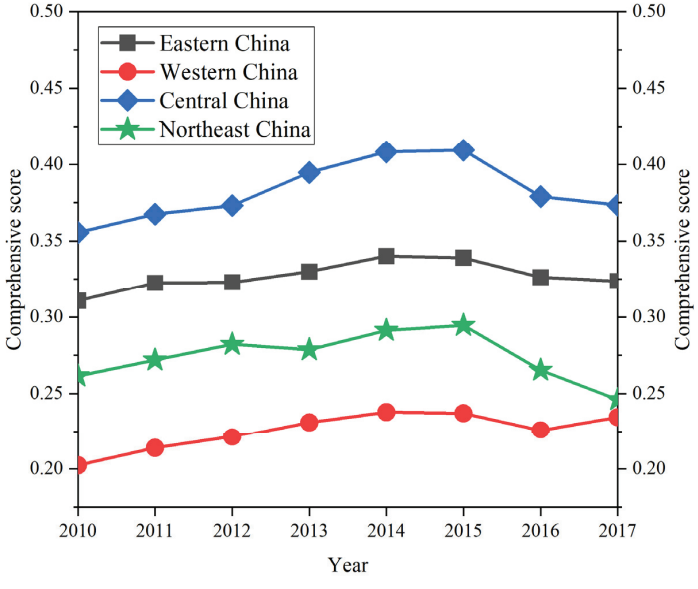

Figure 3. Temporal variation of ecosystem service demand in China from 2010 to 2017.

As can be seen from Figure 4, Guangdong has always been the province with the highest level of demand for ecosystem services. The biggest change in ecosystem services demand was in Guizhou, which saw a 44.19 % increase, followed by Sichuan, which saw a 30.98 % increase. Ningxia and Gansu saw a decrease of 15.3 % and 15.26%, respectively. In 2010, only three provinces—Fujian, Anhui, and Sichuan—had ecosystem service demand levels between 0.32 and 0.38. But in 2017, six more provinces—Zhejiang in the east, Guangxi and Yunnan in the west, and Shanxi, Jiangxi, and Hubei in the central region—were added. The spatial distribution shifted from east to east and central.

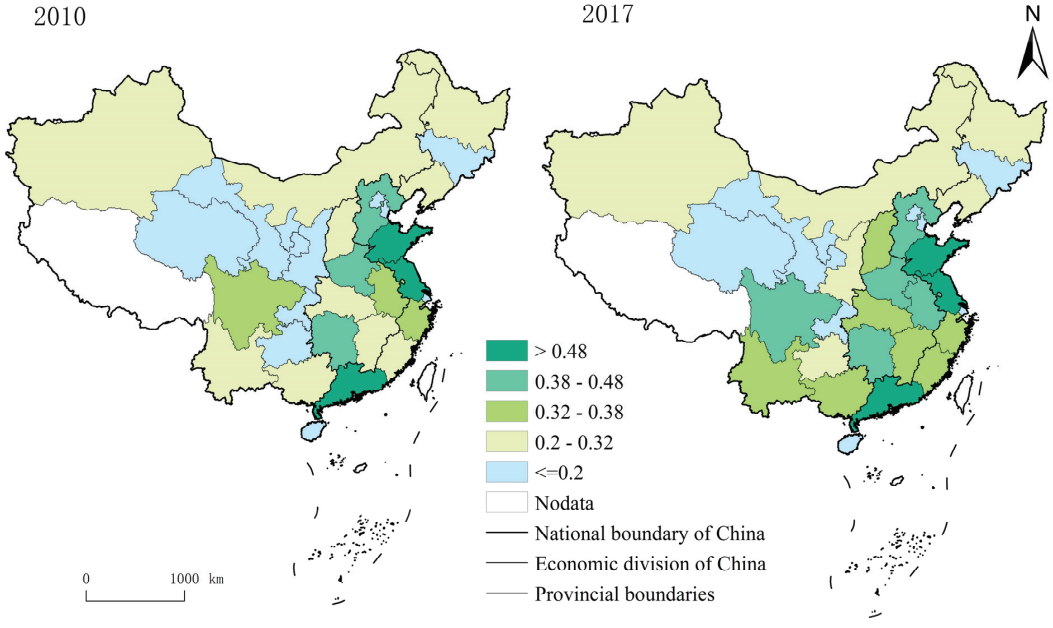

Figure 4. Spatial distribution of ecosystem service demand in China from 2010 to 2017.

4.3. The Coupling Coordination Relationship between Green Finance and Ecosystem Service Demand

4.3.1. Traditional Coupling Coordination Model

To verify whether the values of α and β have significant effects on the evaluation results of coupling coordination degree, five different combination scenarios were set (α = 0.2, β = 0.8; α = 0.4, β = 0.6; α = 0.5, β = 0.5; α = 0.6, β = 0.4; α = 0.8, β = 0.2), and the corresponding evaluation results of the coupling coordination degree were compared and analyzed. According to Formulas (2)–(8), the above values of α and β can be substituted to calculate the coupling coordination degree of green finance and ecosystem service demand and its type. Due to space limitation, only Jiangsu Province was selected here as an example to illustrate the results, as shown in Figure 5. The different values of α and β can lead to some differences in the size of coupling coordination degree, and the types of coupling coordination degree. Specifically, from the effects of different α and β values on the coupling coordination degree, when α = 0.2 and β = 0.8, the maximum value of the coupling coordination degree in Jiangsu Province was 0.77, and the minimum value was 0.69. When α = 0.8 and β = 0.2, the maximum and minimum of the coupling coordination degree in Jiangsu Province were 0.75 and 0.55. From the effects of different α and β values combinations on the coupling coordination types, when α = 0.2 and β = 0.8, the coupling coordination type of green finance and ecosystem service demand in 2010–2011 had moderate coordination and good coordination in 2012–2017. When α = 0.8 and β = 0.2, the coupling coordination type of green finance and ecosystem service demand was basic

coordination in 2010–2012, moderate coordination in 2013–2014, and had improved to good coordination in 2015–2017.

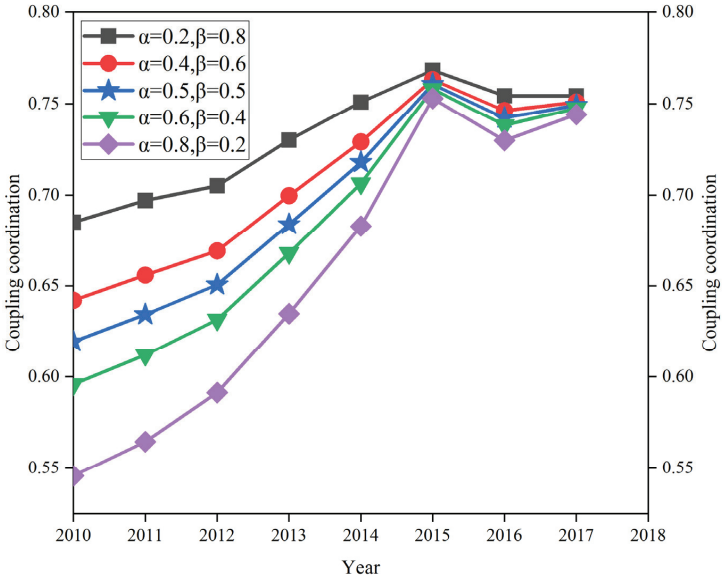

Figure 5. Change of coupling coordination degree of green finance and ecosystem service demand in Jiangsu Province based on traditional coupling coordination degree model.

4.3.2. Improved Coupling Coordination Degree Model

(1) Improved contribution coefficient (α', β')

Compared with the traditional coupling coordination degree model, which sets $\alpha = \beta = 0.5$, the improved coupling coordination model comprehensively determines the values of α' and β' according to the performance of green finance and ecosystem service demand. Based on the comprehensive evaluation results of green finance and ecosystem service demand, the contribution coefficients α' and β' of green finance and ecosystem service demand were calculated according to Formulas (7) and (8).

The result is shown in Figure 6. There was sustainable growth in both green finance and ecosystem service demand levels in Jiangsu Province, with the green finance evaluation index rising from 0.259 to 0.549, and the ecosystem service demand index rising from 0.568 to 0.574. The development level of green finance continues to increase, but α' was constantly decreasing, while β' was consistent with the changing trend of the demand level of ecosystem services. However, the green finance index was still smaller than the comprehensive index of ecosystem service demand, thus it was always a relatively large α' and a relatively small β'.

(2) Results of the improved coupling coordination degree model

The coupling coordination degree of ecosystem service demand and green finance saw a continuously optimal trend (Figure 7), but the regional differences of the coupling coordination degree were obvious. The coupling coordination degree of the eastern region was significantly higher than that of central, western, and northeast China. The coupling coordination degree of China's four major economic divisions was in the order of east–central–northeast–west from high to low, with an average of 0.45, 0.40, 0.34, and 0.32, respectively. Specifically, coordination levels in eastern and central regions experienced a process of "mild discoordination—low-level coordination—basic coordination". The northeast and western regions had been in a state of mild disharmony. In addition, the

coupling coordination degree of green finance and ecosystem service demand has been increased in China, but the coupling coordination degree is not high, indicating that the coupling coordination relationship between green finance and ecosystem service demand needs to be further optimized.

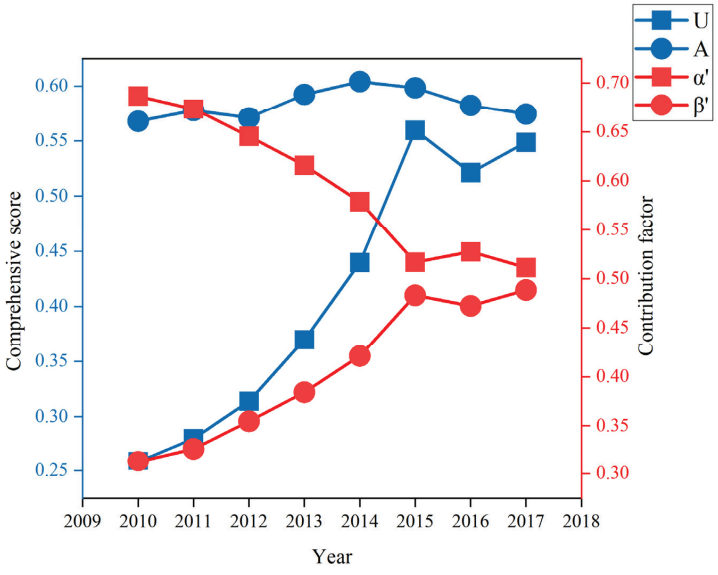

Figure 6. Changes of the improved contribution coefficient.

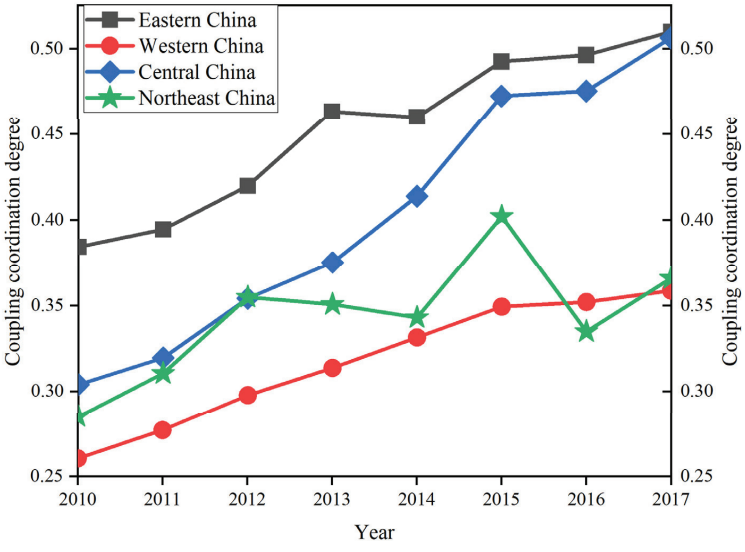

Figure 7. Temporal and spatial characteristics of the coupling coordination degree between green finance and ecosystem service demand in China from 2010 to 2017.

During the study period, the coupling coordination degree between green finance and ecosystem service demand increased significantly in the provinces, but there was an expanding trend in the inter-provincial differences.

In 2010, the coupling coordination relationship between green finance and ecosystem service demand in various provinces included six types: high coordination, moderate coordination, basic coordination, low level coordination, mild incoordination, and serious incoordination. Among them, serious incoordination and mild incoordination were the main types, with 11 and 13 provinces, respectively, accounting for 80% of the studied provinces. The 6 other provinces had moderate coordination (Guangdong), basic coordination (Shandong, Jiangsu), and low coordination (Hebei, Henan, Hunan), and were mainly distributed in the eastern region.

In 2017, only Qinghai was still in the stage of serious incoordination, the other provinces improved. The number of mild incoordination provinces decreased by 2, the number of provinces with low level coordination and basic coordination increased to 4, the number of provinces with moderate coordination increased to 3, and Guangdong Province was in the stage of moderate coordination to high coordination stage.

5. Discussion

5.1. Analysis of Reasons for Temporal and Spatial Differences between Green Finance and Ecosystem Service Demand

As is shown in Figure 8, the coupling coordination degree between green finance and ecosystem service demand was concentrated between 0.3 and 0.6, with a low level. From the provincial level, only Guangdong Province's coupling coordination degree had been in a state of medium–high coordinated development, while the coupling coordination degree of green finance level and ecosystem service demand of other provinces was still at a low level of development. The overall coupling coordination degree was lowered. At the national level, the coupling and coordination degree between green finance and ecosystem service demand in China was not high, but the overall level and the comprehensive development level of subsystems saw an increasing trend. Therefore, we believe that green finance, the ecosystem services demand, and the coordinated development of the two have bright prospects in the future.

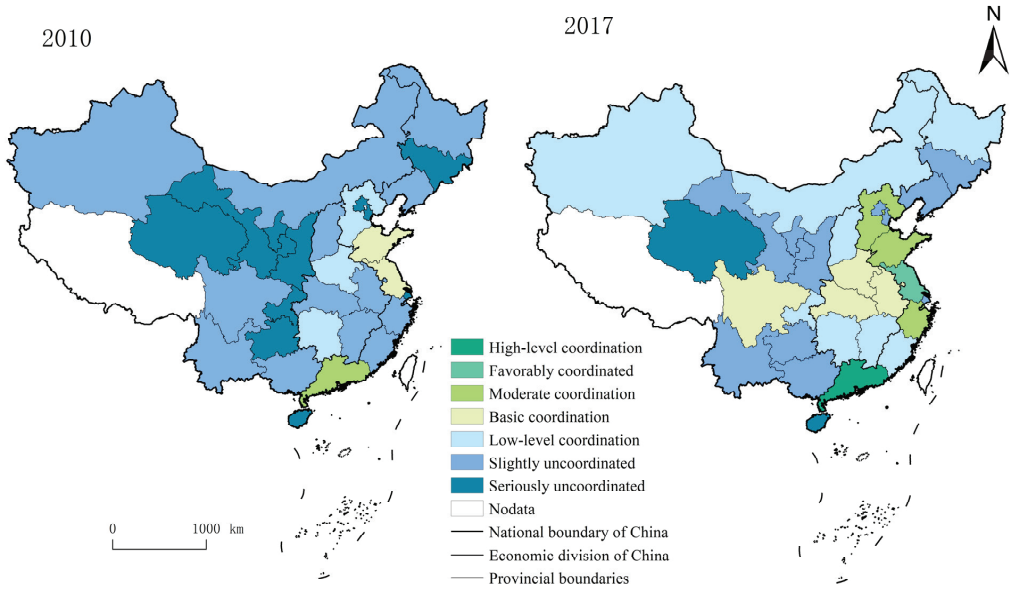

Figure 8. Spatial distribution of the coupling coordination degree of green finance and ecosystem service demand in China from 2010 to 2017.

In 2010, the coupling degree of green finance and ecosystem service demand was the lowest. The data analysis suggests that the reason was that the development level of green finance in various provinces lagged behind ecosystem services demand in 2010. From the perspective of policy, the reason was that the development of green finance in China started late, and the concept of green finance was not improved until 2016. Therefore, 2010 was just the beginning stage of green finance development, and all indicators were at a low level. In 2010, the coupling between green finance and ecosystem service demand was coordinated in only six provinces, distributed in the eastern coastal regions (Guangdong, Jiangsu, Shandong, Hebei, etc.), while the remaining severe uncoordinated areas were clustered in the western region (Chongqing, Guizhou, Shaanxi, Gansu, Qinghai, Ningxia, etc.). This was because the eastern region had a developed and stable financial system as well as a sound ecological environment foundation, and it attached more importance to the development of green finance under the guidance of national policies. The western region of China was not economically developed, the financial system was not active enough, and there was not a strong demand for green funds. Moreover, the westward migration of industries brought by China's western development strategy would also affect the development of green finance in the western region to a certain extent.

In 2017, the coupling coordination degree of green finance and ecosystem service demand was the highest. For the country as a whole, China introduced many policies in 2016 to encourage the development of green finance. For example, seven state ministries and commissions, including the People's Bank of China and the Ministry of Finance, issued the "Guidelines on Building a Green Finance System", which was the first time that the country systematically proposed the definition, incentive mechanism, development plan of green financial products, and risk monitoring measures of green finance. Therefore, the development level of green finance has been continuously improved under the incentive of relevant policies. At the provincial level, because the green finance development level of 1/5 provinces was ahead of the ecosystem service demand level, the coupling coordination degree of most provinces had been significantly improved. The coordination level of the two systems was more balanced. At that time, the provinces with high coupling coordination degrees were concentrated in East China (Jiangsu, Shandong, Zhejiang, Anhui, etc.) and central China (Henan, Hubei, etc.), which indicated the spatial diffusion from east to central China, which was also the achievement of China's coordinated development strategy.

5.2. Advantages of Improved Coupling Coordination Degree Model

Through comparative analysis, it found that the contribution coefficients α and β affect not only the coupling coordination degree, but also the coupling coordination type. However, the theoretical basis for the traditional coupling coordination degree model to set the same contribution coefficient of the two systems is not sufficient, and the calculation results struggle to reflect the coupling relationship between green finance and ecosystem service demand accurately and objectively [31]. Decision-makers are prone to make unreasonable or even wrong decisions that have a bad impact on the coordinated development of green finance and ecosystem services demand when facing such evaluation results.

To fill the subjective judgment of the contribution coefficients α and β in the traditional coupled coordination degree model, an improved coupled coordination degree model is introduced to determine the contribution coefficients according to the comprehensive performance of green finance and ecosystem service demand, which means that, with the continuous cooperation and competition between green finance and ecosystem service demand, the contribution coefficients of the two systems continue to develop and change. At the beginning of the study, the contribution coefficient of green finance (α') was much larger than the contribution coefficient of ecosystem services demand (β'). As time passed, China's ecological environment continued to improve, so the proportion of the contribution coefficient of this system rose constantly. At the end of the study, α' was almost equal to β'. Therefore, policymakers should focus on promoting ecological environment construction and achieving coordinated improvement of green finance and ecosystem service demand

on the premise of maintaining appropriate economic growth. In conclusion, the improved coupling coordination degree model can reflect the coordinated development of green finance and ecosystem service demands accurately, and help decision-makers to further develop more scientific and reasonable measures.

5.3. Limitations

Using data from 30 provinces in China, this paper evaluated the coupling relationship between green finance and ecosystem services demand in four major regions of China's economy, which made up for the shortcomings of the traditional coupling coordination model, but the research still has certain limitations. Firstly, considering the availability of data from 2018 to 2021, only the eight years from 2010 to 2017 were selected as the study period, and data from recent years should be supplemented for inclusion in the study in the future. Secondly, when constructing the indicator system for ecosystem service demand assessment, this paper used the actual human food consumption to measure food demand services, and replaced the demand with food consumption in the calculation process. Food consumption data (including grain, oil, vegetables, meat, aquatic products, eggs, milk, melons, and fruits) were all from the China and provincial statistical yearbooks. However, since some provinces (such as Heilongjiang Province, Sichuan Province, etc.) did not calculate the specific consumption of eggs, milk, melons, and fruits in 2013 and 2014, the missing data were replaced with data from adjacent years. The proportion of missing data is very small, so it has little impact on the calculation results. In the later stage, the method can be improved to make the empirical results more accurate by extrapolating the missing data.

6. Conclusions

This paper constructed a multi-index evaluation system for green finance and ecosystem service demand. Based on the panel data of 30 provinces in China from 2010 to 2017, the comprehensive development level of green finance and ecosystem service demand was evaluated by using the global principle component analysis and entropy method. Then, the improved coupling coordination degree model was used to explore the temporal and spatial evolution characteristics of the coupling coordination degree between green finance and ecosystem service demand in each province of China during the study period. The results show that:

(1) During the study period, the level of green finance in China's provinces improved significantly, showing a spatial pattern of "high in the east and low in the west". The ecosystem services demand in all provinces in China saw an initial increasing trend that eventually began decreasing. Nearly two-thirds of provinces had gradually increased the demand level for ecosystem services, showing a spatial pattern of "high demand for ecosystem services in East and South China and low ecosystem services demand in northwest and northeast China".

(2) The results of the improved coupling coordination degree model showed that the static coupling coordination relationship between green finance and ecosystem service demand in Chinese provinces continued to improve from 2010 to 2017, and the spatial distribution showed a spatial pattern of "high in eastern coastal and central China, low in western and northeast China".

(3) Contribution coefficients α and β not only affect the coupling coordination degree, but also affect the type of coupling coordination degree. Compared with the traditional coupling coordination degree model, the improved coupling coordination degree model can provide more effective information for decision-makers and help them to formulate more reasonable control measures.

Author Contributions: Conceptualization, H.W. and G.D.; methodology, H.W.; formal analysis, H.W., D.Z.; Q.Z. and Q.K.; writing—original draft preparation, H.W. and D.Z.; writing—review and editing, G.D.; supervision, G.D.; funding acquisition, G.D. All authors have read and agreed to the published version of the manuscript.

Funding: This research was funded by National Natural Science Foundation of China, grant number 41801173, Youth Innovation Science and Technology Support Plan of Colleges and Universities in Shandong Province, grant number 2021RW039, and Doctor foundation of Shandong Jianzhu University, grant number XNBS1803.

Data Availability Statement: The data presented in this study are available on request from the author.

Acknowledgments: Thanks to anonymous experts for their suggestions.

Conflicts of Interest: The authors declare no conflict of interest.

References

1. Assessment, M.E. *Ecosystems and Human Well-Being: A Framework for Assessment*, 1st ed.; Island Press: Washington, DC, USA, 2005; 81p.
2. Li, H.; Yuan, Y.; Wang, N. Evaluation of the coupling and coordinated development of regional green finance and ecological environment. *Stat. Decis. Mak.* **2019**, *8*, 161–164.
3. Shao, C.L.; Duan, B. A Study on Coupling Mechanisms og Green Finance and Innovation-driven Development. *J. Xi'an Univ. Financ. Econ.* **2019**, *32*, 5–12.
4. Lagoarde-Segot, T. Diversifying financere search: From financialization to sustainability. *Int. Rev. Financ. Anal.* **2015**, *39*, 1–6. [CrossRef]
5. He, X. The Origin, Development and Global Practice of Green Finance: A Literature Review. *J. Southwest Univ. (Soc. Sci. Ed.)* **2021**, *47*, 83–94+226.
6. Yu, B.; Fan, C.L. Green Finance, Technical Innovation and High-quality Economic Development. *Nanjing Soc. Sci.* **2022**, *9*, 31–43.
7. Wei, L.L.; Yang, Y. Green Finance:Developmental Logic, Theoretical Interpretation and Future Prospect. *J. Lanzhou Univ. (Soc. Sci.)* **2022**, *50*, 60–73.
8. Wang, X.X.; Lei, H.Y.; Wang, S.S. Green Finance, Digital Economy and Environmental Pollution. 2022, pp. 1–12. Available online: http://kns.cnki.net/kcms/detail/51.1268.G3.20220714.1707.010.html (accessed on 30 January 2023).
9. Boerema, A.; Rebelo, A.J.; Bodi, M.B.; Esler, K.J.; Meire, P. Are ecosystem services adequately quantified? *J. Appl. Ecol.* **2017**, *54*, 358–370. [CrossRef]
10. Sun, Y.; Liu, S.; Dong, Y.; An, Y.; Shi, F.; Dong, S.; Liu, G. Spatio-temporal evolution scenarios and the coupling analysis of ecosystem services with land use change in China. *Sci. Total Environ.* **2019**, *681*, 211–225. [CrossRef]
11. Liu, J.P.; Tian, Y.; Huang, K.; Yi, T. Spatial-temporal differentiation of the coupling coordinated development of regional energy-economy-ecology system: A case study of the Yangtze River Economic Belt. *Ecol. Indic.* **2021**, *124*, 107394. [CrossRef]
12. Xiao, R.; Lin, M.; Fei, X.; Li, Y.; Zhang, Z.; Meng, Q. Exploring the interactive coercing relationship between urbanization and ecosystem service value in theShanghai–Hangzhou Bay Metropolitan Region. *J. Clean. Prod.* **2020**, *253*, 119803. [CrossRef]
13. Zhao, X.Y.; Du, Y.X.; Li, H.; Wang, W.J. Spatio-temporal changes of the coupling relationship between urbanization and ecosystem services in the Middle Yellow River. *J. Nat. Resour.* **2021**, *36*, 131–147. [CrossRef]
14. Zhao, X.Y.; Ma, P.Y.; Li, W.Q. Spatiotemporal changes of supply and demand relationships of ecosystem services in the Loess Plateau. *Acta Geogr. Sin.* **2021**, *76*, 2780–2796.
15. Wu, J.S.; Men, X.N.; Liang, J.T.; Zhao, Y.H. Research on supply and demand equilibrium of ecosystem services in Guangdong Province based on the ginicoefficient. *Acta Ecol. Sin.* **2020**, *40*, 6812–6820.
16. Zhu, J.H.; Wang, H.J.; Zhen, P. Coupling and Coordinated Development of Circular Economy and Green Finance in Guizhou. *Econ. Georaphy.* **2019**, *39*, 119–128.
17. Wen, J.W.; Jing, C.L.; Tai, Y.H.; Hao, X.Z.; Xin, Z. Coupling coordination analysis of green finance and industrial technology innovation: A case study in Zhejiang Province, China. *Front. Environ. Sci.* **2022**, *10*, 958311.
18. Xiu, L.Y.; Zhao, R.X. An empirical analysis of the coupling and coordinative development of China's green finance and economic growth. *Resour. Policy* **2022**, *75*, 102476. [CrossRef]
19. Guang, L.D.; Yi, B.G.; Wei, Y.Z.; Yan, B.Q.; Wen, X.Z. Coupling Coordination and Spatiotemporal Dynamic Evolution Between Green Urbanization and Green Finance: A Case Study in China. *Front. Environ. Sci.* **2021**, *18*, 1601.
20. Qiu, J.J.; Liu, Y.H.; Yuan, L.; Chen, C.J.; Huang, Q.Y. Research progress and prospect of the interrelationship between ecosystem services and human well-being in the context of coupled human and natural system. *Prog. Geogr.* **2021**, *40*, 1060–1072. [CrossRef]
21. Jie, C.; Xiao, P.L.; Lan, J.L.; Ya, Z.C.; Xian, W.W.; Si, H.L. Coupling and coordinated development of new urbanization and agro-ecological environment in China. *Sci. Total Environ.* **2021**, *776*, 145837.
22. He, J.; Wang, S.; Liu, Y.; Ma, H.; Liu, Q. Examining the relationship between urbanization and theeco-environment using a coupling analysis: Case study of Shanghai, China. *Ecol. Indic.* **2017**.
23. Zhang, Z.; Li, Y. Coupling coordination and spatiotemporal dynamic evolution between urbanization and geological hazards–A case study from China. *Sci. Total Environ.* **2020**, *728*, 138825. [CrossRef]
24. Jiang, S.L.; Wei, S.; Ming, Y.L.; Meng, L. Coupling coordination degree of production, living and ecological spaces and its influencing factors in the Yellow River Basin. *J. Clean. Prod.* **2021**, *298*, 126803. [CrossRef]

25. Guang, L.D.; Wen, X.Z.; Xin, L.X.; Kun, J. Multi-Dimensional Feature Recognition and Policy Implications of Rural Human–Land Relationships in China. *Land* **2021**, *10*, 1086.
26. Liu, H.; Huang, B.; Yang, C. Climate Change; Researchers from Chinese University of Hong Kong Discuss Findings in Climate Change (Assessing the coordination between economic growth and urban climate change in China from 2000 to 2015). *Glob. Warm. Focus* **2020**, *732*, 139283.
27. Hong, W.L.; Erqi, X.; Hong, Q.Z. Examining the coupling relationship between urbanization and natural disasters: A case study of the Pearl River Delta, China. *Int. J. Disaster Risk Reduct.* **2021**, *55*, 102057. [CrossRef]
28. Han, H.; Li, G.; Ji, Q.Z.; Kaize, Z.; Ningbo, C. Spatiotempor alanalysis of the coordination ofeconomic development, resource utilization, and environmental quality in the Beijing-Tianjin-Hebei urban agglomeration. *Ecol. Indic.* **2021**, *127*, 107724. [CrossRef]
29. Zhang, Z.H.; Nie, T.T.; Gao, Y.; Sun, S.M.; Gao, J. Study on Temporal and Spatial Characteristics of Coupling Coordination Correlation Between Ecosystem Services and Economic—Social Development in the Yangtze River Economic Belt. *Resour. Environ. Yangtze Basin.* **2022**, *31*, 1086–1100.
30. Yu, P.; Zhang, J.P. Coupling and coordination evaluation of regional green finance and high-quality development. *Stat. Decis. Mak.* **2021**, *37*, 142–146.
31. Han, Y. An Empirical Study on the Coupling Development of Culture Industry and Green Finance Industry in Jiangsu Province. *Int. J. Soc. Sci. Educ. Res.* **2021**, *4*, 150–158.
32. Shen, L.; Huang, Y.; Huang, Z.; Lou, Y.; Ye, G.; Wong, S.W. Improved coupling analysis on the coordination between socio-economy and carbon emission. *Ecol. Indic.* **2018**, *94*, 357–366. [CrossRef]
33. Wang, J.; Zhai, T.L.; Lin, Y.F.; Kong, X.S.; He, T. Spatial imbalance and changes in supply and demand of ecosystem services in China. *Sci. Total Environment.* **2018**, *657*, 781–791. [CrossRef]
34. Zhang, D.; Zhang, Z.; Managi, S. A bibliometric analysis on green finance: Current status, development, and future directions. *Financ. Res. Lett.* **2019**, *29*, 425–430. [CrossRef]
35. Liu, N.; Liu, C.; Xia, Y.; Ren, Y.; Liang, J. Examining the Coordination between Green Finance and Green Economy Aiming for Sustainable Development: A Case Study of China. *Sustainability* **2020**, *12*, 3717. [CrossRef]
36. Zeng, X.W.; Liu, Y.Q.; Man, M.J.; Shen, Q.L. Measurement Analysis of the Development Level of China's Green Financs. *J. China Exec. Leadersh. Acad. Yan'an.* **2014**, *7*, 112–121+105.
37. Zhou, X.G.; Tang, X.M.; Zhang, R. Impact of green finance on economic development and environmental quality: A study based on provincial panel data from China. *Environ. Sci. Pollut. Res. Int.* **2020**, *27*, 1–18. [CrossRef] [PubMed]
38. Fan, W.; Wang, H.; Liu, Y.; Liu, H. Spatio-temporal variation of the coupling relationship between urbanization and air quality: A case study of Shandong Province. *J. Clean. Prod.* **2020**, *272*, 122812. [CrossRef]
39. Villamagna, A.M.; Angermeier, P.L.; Bennett, E.M. Capacity, pressure, demand, and flow: A conceptual framework for analyzing ecosystem service provision and delivery Ecol. *Complex.* **2013**, *15*, 114–121. [CrossRef]
40. Schröter, M.; Barton, D.N.; Remme, R.P.; Hein, L. Accounting for capacity and flow of ecosystem services: A conceptual model and a case study for Telemark, Norway. *Ecol. Indic.* **2014**, *36*, 539–551. [CrossRef]
41. Xie, G.D.; Lu, C.X.; Leng, Y.F.; Zhen, D.; Li, S.C. Ecological assets valuation of the Tibetan Plateau. *J. Nat. Resour.* **2003**, *2*, 189–196.
42. Costanza, R. Ecosystem services: Multiple classification systems are needed. *Biol. Conserv.* **2007**, *141*, 350–352. [CrossRef]
43. Liu, C.H.; Wang, W.T.; Liu, L.C.; Li, P.J. Supply-demand matching of county ecosystem services in Northwest China: A case study of Gulang county. *J. Nat. Resour.* **2020**, *35*, 2177–2190. [CrossRef]
44. Cui, F.; Tang, H.; Zhang, Q.; Wang, B.; Dai, L. Integrating ecosystem services supply and demand into optimized management at different scales: A case study in Hulunbuir, China. *Ecosyst. Serv.* **2019**, *39*, 100984. [CrossRef]
45. Zhang, P.T.; Liu, S.J.; Zhou, Z.; Liu, C.J.; Xu, L.; Gao, X. Supply and demand measurement and spatio-temporal evolution of ecosystem services in BeijingTianjin-Hebei Region. *Acta Ecol. Sinica.* **2021**, *41*, 3354–3367.
46. Zhang, X.L.; Xu, Z.J.; Zhang, Z.H.; Gu, D.Q.; Wang, L.H. Environment purification service value of urban green space ecosystem in Qingdao City. *Acta Ecol. Sin.* **2011**, *31*, 2576–2584.
47. Sun, Q.; Zhang, X.; Zhang, H.; Niu, H. Coordinated development of a coupled social economy and resource environment system: A case study in Henan Province, China. *Environ. Dev. Sustain.* **2018**, *20*, 1385–1404. [CrossRef]
48. Zhang, L.; Wu, M.Q.; Wuliyasu, B.; Jin, Y.Y.; Yu, M.Q.; Ren, J.Z. Measuring coupling coordination between urban economic development and air quality based on the Fuzzy BWM and improved CCD model. *Sustain. Cities Soc.* **2021**, *75*, 103283. [CrossRef]
49. Wang, Y.X.; Yao, L.; Xu, Y.; Sun, S.; Li, T. Potential heterogeneity in the relationship between urbanization and air pollution, from the perspective of urban agglomeration. *J. Clean. Prod.* **2021**, *298*, 126882. [CrossRef]

land

MDPI

Article

Land Use Function Transition and Associated Ecosystem Service Value Effects Based on Production–Living–Ecological Space: A Case Study in the Three Gorges Reservoir Area

Fangjie Pan [1], Nannan Shu [2], Qing Wan [1,*] and Qi Huang [3]

[1] School of Management, Wuhan Institute of Technology, Wuhan 430205, China
[2] Wuhan Agricultural Technology Extension Center, Wuhan 430012, China
[3] Institute of Economic Research on Changjiang River Valley, Hubei Academy of Social Sciences, Wuhan 430077, China
* Correspondence: wanqing@wit.edu.cn

Abstract: The transition of land use function and its effects on ecosystem services is a key issue in eco-environmental protection and is the basis of territorial space governance and optimization. Previous studies have typically selected land use types to evaluate ecosystem service value (ESV) and have overlooked comprehensive characteristics of ecosystem services and the mutual feedback relationship between human social systems and the ecosystem. Taking the Three Gorges Reservoir Area, Hubei section (TGRA-HS) as a case study, we used a transition matrix, the revised ESV method, and an ecological contribution rate model to explore land use function transition (LUFT) and its effects on the change in ESV based on the production–living–ecological space (PLES) classification system. The results show that: (1) The transition of land use function based on PLES was the mapping of the evolution of the human–nature relationship in the spatial pattern, which reflected the evolution of the spatial pattern caused by human interference with the continuous development of society; (2) The evolution of PLES showed the characteristics of a reduction in production space (P-space), and an expansion in living space (L-space) and ecological space (E-space). The distribution pattern of PLES from 1990 to 2020 was basically the same, and the characteristics of structural transform reflected the characteristics of project construction in different phases; (3) The E-space contributed the most to the total ESV, and it has risen by CNY 13.06×10^8. The transition of land use function caused by human construction projects impacts the spatiotemporal change in the regional ESV; (4) The change in ESV induced by LUFT revealed the whole dynamic process of the positive and negative effects of human construction projects on ecosystem services, and the two effects offset each other to keep the ESV relatively stable. The transition of E-space to P-space had the greatest impact on the reduction in ESV, whose contribution rate was 82.76%. The dynamic changes in land use function and ESV corresponding to the different stages of the Three Gorges Project's (TGP) construction reveals the important driving effect of human activities on ecosystem services. It reminds us that humans should not forget to protect the eco-environment when obtaining services from the ecosystem.

Keywords: production–living–ecological space (PLES); land use function transition (LUFT); ecosystem service value (ESV); Three Gorges Reservoir Area (TGRA); Three Gorges Project (TGP)

Citation: Pan, F.; Shu, N.; Wan, Q.; Huang, Q. Land Use Function Transition and Associated Ecosystem Service Value Effects Based on Production–Living–Ecological Space: A Case Study in the Three Gorges Reservoir Area. *Land* **2023**, *12*, 391. https://doi.org/10.3390/land12020391

Academic Editors: Shicheng Li, Chuanzhun Sun, Qi Zhang, Basanta Paudel and Lanhui Li

Received: 9 January 2023
Revised: 28 January 2023
Accepted: 29 January 2023
Published: 31 January 2023

1. Introduction

Land resources are the essential element and spatial carrier for human survival and development, and all human activities depend on land resources [1–3]. While economic and social developments have allowed for great achievements and promoted the profound transformation and spatial reconstruction of land use [4,5], this has brought about a lot of noticeable environmental problems, such as the overextraction of natural resources, water and soil loss, a decrease in biodiversity, and the degradation or loss of ecosystem functions [6–10], resulting in significant changes to ecosystem service functions. The most

severe problem is an unbalanced PLES in terms of its spatial structure and function, leading to severe challenges and crises in the sustainable development of territorial space. The important performance of land use transition is the dynamic process of the quantitative and spatial reallocation of limited land resources among different leading functions [11], thereby realizing the transition of the recessive form of land use function [12,13]. The transition of land use function is one of the important changes in land use in recessive patterns. That is, the dynamic process of quantitative re-proportion and spatial reallocation of land resources among production, living, and ecological functions reflect the different stages of regional economic and social transformation [14]. Land use transition not only causes a change in natural landscapes, but also causes a change in biodiversity, ecosystem service functions, and their stability, which threatens human health and ecological security [15–17]. The research on land use transition and its ecological effects has attracted increasing attention [18–21], and it has become an important research topic in current geography, landscape ecology, and ecological economics [22–25].

The LUFT is the further deepening and application of the land use theory in the research of territorial space in the new era. The existing research shows that land use has comprehensive production, living, and ecological functions, and it can be divided into PLES on the basis of the leading functions and use types [26,27]. The theory of PLES was proposed based on the view of element–structure–function in systematic [28]. The PLES was a comprehensive division method of territorial space, and the coordinated development of PLES will produce a synergistic effect where the total function is greater than the sum of its parts. Therefore, the PLES can reflect the complex characteristics of ecosystem services well, and its layout and evolution have a profound impact on the regional ecosystem services. Ecosystem service function is closely related to human welfare, and it is an important basis for human survival and development [29–31]. Under the influence of intrinsic and extrinsic factors [32], the changes in the spatial element and structure of PLES will lead to the transition of their functions, and the transition of the leading functions reflects the different stages of the evolution of regional ecosystem services. Essentially, the eco-environmental problem caused by the LUFT is due to the imbalance of PLES function. Therefore, based on the leading function classification system of PLES, the regional LUFT and the evolution of ecosystem service functions can be linked, giving a new perspective on studying the mutual feedback relationship between human social systems and ecosystems [33–35].

At the present stage, the research on LUFT and its regional ecological effects from the perspective of PLES is still in its infancy. Some researchers have analyzed the LUFT and its eco-environmental effects but have mainly focused on regions, basins, provinces, cities, and counties [36–40]. Furthermore, some researchers have also discussed it from different perspectives [20,41]. However, the existing research is mostly limited to the administrative areas undergoing rapid urbanization. Research on the LUFT in an important ecological function area has received less attention, and its effects on changes in ESV based on the PLES classification are still insufficiently studied [7]. Meanwhile, the ecological characteristics of the PLES classification system are not considered to be granular enough, and the internal connection between the production–living–ecological functions and ecosystem service function is ignored.

The TGRA is an important ecological function area that plays a vital role in ensuring the downstream ecological security and maintaining the ecosystem health of the Yangtze River [42]. The TGRA is also one of the most sensitive and vulnerable areas of the eco-environment in China, and the PLES competition is becoming increasingly fierce here. As the reservoir head of the TGRA, the Hubei section is most rapidly and directly affected by the project, and the issue of LUFT deserves much more attention. Therefore, it is of important theoretical and practical significance to explore the spatiotemporal characteristics of LUFT and its effects on the change in ESV based on the conception and identification of PLES in the TGRA-HS according to the construction stage division of the TGP.

Based on the above-mentioned state of research, this study aims to quantitatively analyze the structure and spatial characteristics of LUFT in the national key ecological

function area and its effects on changes in ESV from the perspective of PLES during the construction of the TGP from the project demonstration to the full operation stage. The contributions of this study are that: (1) The transition of land use function and the PLES are combined to analyze LUFT and its effects on ecosystem services, and it might provide a deeper understanding of the mutual feedback relationship between human social systems and ecosystems, especially the harmony between human development and biodiversity protection; (2) Taking the TGRA-HS as the study area, we analyzed the spatiotemporal evolution and structural transformation of PLES, and the assessment model was established and revised to analyze the quantity and spatial characteristics of ESV change; (3) This study also provides a scientific reference and practical guidance to support the optimization of the spatial development and eco-environmental protection patterns in the TGRA-HS.

2. Study Area

The TGRA-HS is located in the middle reaches of the Yangtze River in the southwest of Hubei Province (30°14′–31°34′ N, 110°06′–111°40′ E) and includes three counties (Badong, Zigui, and Xingshan counties) and five districts (Yiling, Dianjun, Xiling, Wujiagang, and Xiaoting districts) (Figure 1). It has a population of about 2.82 million and an area of about 1.21×10^4 km^2. The Hubei section is the reservoir head of the TGRA, and the landform types are complex and diverse, with more mountains and fewer plains. The mountains are high, the slopes are steep, and the valleys are deep. The climate is affected by topographic fluctuations, and the natural vegetation has the characteristics of vertical zoning. The dam site of the TGP is located in Sandouping Town, south-west of Yichang City, Hubei Province, China. The Gezhou dam, which is the regulating dam of the Three Gorges Dam, is located 38 km downstream. Since 1990, with the continuous advancement of the TGP and various ongoing construction projects, the PLES in the TGRA-HS have changed significantly and human activities have strongly interfered with the regional eco-environment. Under the dual drive of policy and economy, the land use pattern of the TGRA-HS has undergone significant changes, and the land use function has also undergone a transformation. In addition, due to the phased implementation of the TGP, the main projects have caused distress, such as the resettlement of immigrants, the submersion of water storage, and the relocation of facilities. This has further intensified the complexity of the study of regional ecological effect changes. The spatiotemporal characteristics of LUFT and the characteristics of the eco-environmental response show significant differences before and after the dam's construction [43,44].

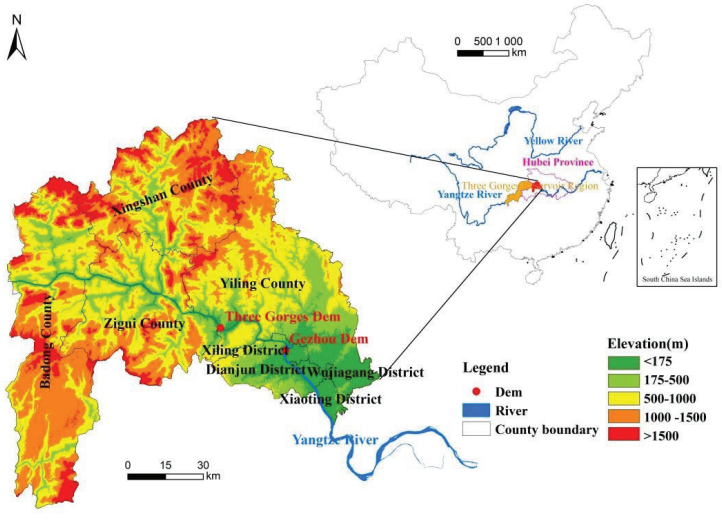

Figure 1. Location and elevation of the Three Gorges Reservoir area, Hubei section (TGRA-HS), China.

3. Materials and Methods

3.1. Research Framework

Different types of land use have various functions. Analyzing the evolution of spatial form and the structure of territorial space is an important way of exploring the process of space function change. One of the manifestations of the land use transition is the transformation between the three leading functions of production, living, and ecology [45]. Under different leading functions (spatial types), human beings have different impacts on the ecosystem, and the services provided by the ecosystem for human society are also significantly different. In general, anthropogenic interference (such as a large-scale construction project) will lead to the transformation of the three leading functions. The structure of PLES tends to be unbalanced, and thus, affects the components, structure, service value, and function of the ecosystem. It leads to changes in the supply capacity of regional ecosystem services and becomes the most direct driving factor affecting the function and value of ecosystem services [46,47]. This study was carried out according to the logic of the construction stage division of the TGP, the characteristics of LUFT, the spatiotemporal change in ESV, and the effects of LUFT in terms of changes in ESV (Figure 2). Thus, a framework of LUFT and its effects in terms of changes in ESV from the perspective of PLES in the TGRA-HS was developed as follows:

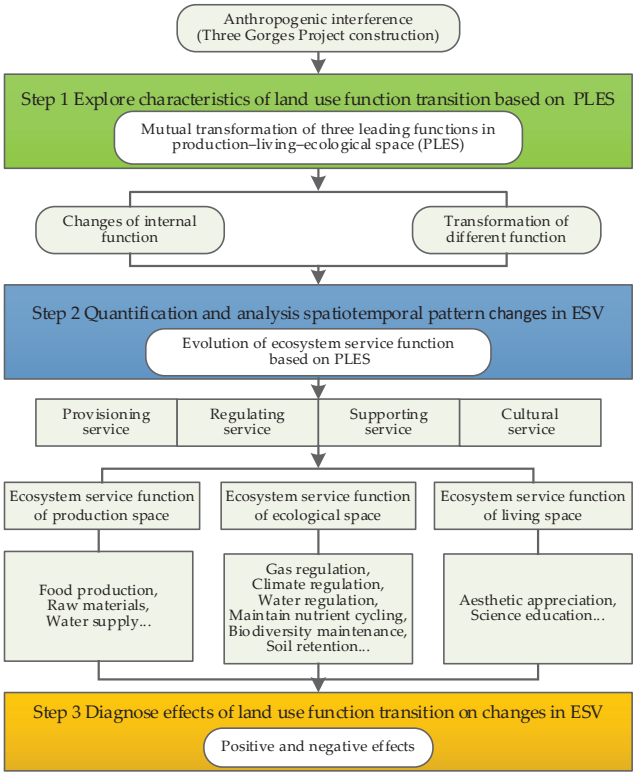

Figure 2. The conceptual framework of land use function transition (LUFT) and its effects on ecosystem service value (ESV).

Step 1: Explore the spatiotemporal evolution characteristics of LUFT during the different construction stages of the TGP from the perspective of PLES.

Step 2: Quantify ESV in the TGRA-HS from 1990 to 2020 using the revised assessment model and analysis of the evolution of its spatiotemporal pattern.

Step 3: Diagnose the effects of LUFT in terms of changes in ESV during the construction of the TGP in the TGRA-HS from 1990 to 2020.

3.2. Analysis of LUFT

3.2.1. PLES Classification System

The analysis of the PLES theory and the diagnosis of the relationships between land use types and functions are essential. This study referred to the PLES classification systems used in past studies [48,49]. On the basis of the leading function, and combined with the multi-functional attributes of land use [50,51], we divided land use types into different functional types of PLES [48,52]. Additionally, it was divided into 3 primary types (including P-space, L-space, and E-space) and 8 secondary types (including APS, IPS, ULS, RLS, FES, GES, WES, and OES) (Table 1). More specifically, P-space can be divided into APS and IPS, which primarily includes cultivated land and other construction land, such as mining land and transportation land. L-space can be divided into ULS and RLS and mainly includes urban land and rural residential land. E-space can be divided into FES, GES, WES, and OES and primarily includes all land types except cultivated land, rural and urban construction land, and industrial and mining land. According to the above criteria for PLES and the land use classification system in Table 1, this study used ArcGIS10.8 to obtain the PLES of the TGRA-HS in 1990, 2000, 2010, and 2020. The evaluation and structural transform characteristics of PLES in the TGRA-HS from 1990 to 2020 were obtained so as to lay the foundation for diagnosing the effects of LUFT on changes in ESV.

Table 1. Corresponding table of PLES and land use type.

Primary Type	Secondary Type	Land Use Interpretation and Classification
Production space (P-space)	Agricultural production space (APS)	Paddy field, dry land
	Industrial production space (IPS)	Industrial and mining land, transportation construction land
Living space (L-space)	Urban Living space (ULS)	Urban land
	Rural Living space (RLS)	Rural residential land
Ecological space (E-space)	Forestland Ecological space (FES)	Forestland, shrub land, sparse forestland, other forestland
	Grassland Ecological space (GES)	High-coverage grassland, medium-coverage grassland, low-coverage grassland
	Water Ecological space (WES)	Canals, lakes, permanent glaciers, snowfields, tidal flats, beaches, reservoirs and pond
	Other Ecological space (OES)	Sandy land, Gobi, saline–alkali land, marshland, bare land, bare rock texture, other land

3.2.2. Methods of LUFT

The transition of land use function is realized by a transition matrix, and it can calculate the amount and direction of transformation among land use function types [53]. This method is derived from the quantitative description of the system state and state transition in the system analysis, which can better describe changes in land use function type. Based on the PLES classification system in Table 1, this study adopts a transition matrix to represent the LUFT [54]. The characteristics of the PLES evaluation and structural transition in the TGRA-HS from 1990 to 2020 were obtained. The mathematical model is:

$$C_{ij} = 100A_{ij}^{t} + A_{ij}^{t+1} \tag{1}$$

$$C_{ij} = \begin{pmatrix} C_{11} & C_{12} & \cdots & C_{1n} \\ C_{21} & C_{22} & \cdots & C_{2n} \\ \cdots & \cdots & \cdots & \cdots \\ C_{n1} & C_{n2} & \cdots & C_{nn} \end{pmatrix} \tag{2}$$

where i and j are the two types of land use function, respectively; C_{ij} is the transition matrix; and A_{ij}^{t} and A_{ij}^{t+1} are the coding of land use function status at time t and $t+1$, respectively. For example, the coding of land use function status at time t and $t+1$ is 11 (representing APS) and 31 (representing FES), respectively, so C_{ij} is 1131, which represents the conversion from APS to FES.

3.2.3. Time Node Division

According to the stage deployment, the construction of the TGP can be divided into stages, such as the construction preparation and start of the first phase of the project (1993), the realization of the river closure and the start of the second phase of the project (1997), the start of water storage and the completion of the second phase of the project (2003), water storage of 175m and the completion of the third phase of the project (2009), and the realization of the full-scale operation of the TGP (2015) (Figure 3). There were obvious differences in the spatial pattern of PLES and its variation trend before and after the dam construction. However, it was difficult to carry out eco-environmental monitoring and change analysis in the whole process of project construction because of the difficulty of obtaining long-term data. Therefore, this study selected 1990, 2000, 2010, and 2020 as the time nodes to explore the characteristics of LUFT, the spatiotemporal change of ESV, and the effects of LUFT on the change in ESV from the project demonstration to the full operation stage according to the construction stage division of the TGP and the availability of data.

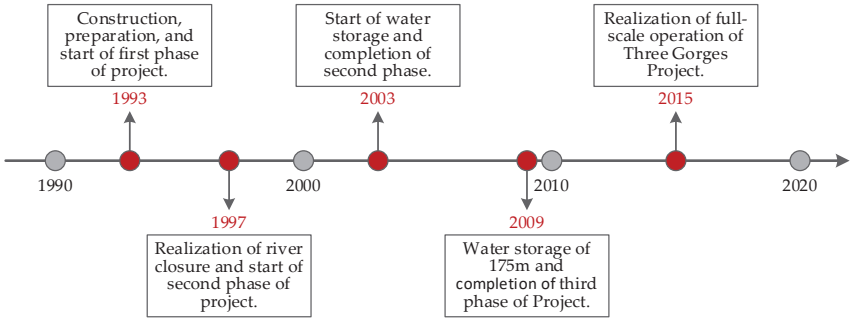

Figure 3. Division of the construction stage of the Three Gorges Project (TGP).

3.3. Assessment of ESV from the Perspective of PLES

The PLES can better reflect the comprehensive characteristics of ecosystem services. ESV is a quantitative assessment of ecosystem service capacity, and the quantitative assessment of ESV can help to transform ecological issues into indicators that are easy to understand for the public and that can help to identify problems. In this study, the equivalent factor of ESV per unit area was used to evaluate the ESV from the perspective of PLES in the TGRA-HS between 1990 and 2020. The outstanding advantage of the methods is their simplicity, and the value of ecosystem services in the form of currency. The equivalent value per unit area of APS, FES, GES, WES, and OES corresponded to the cultivated land, forestland, grassland, waters, and bare land in the existing studies, respectively. Additionally, they were modified and developed for the dynamic evaluation on Chinese terrestrial ecosystem service value. Among them, the equivalent value of APS was calculated based on the proportion composition of paddy field and dry land in the TGRA-HS. Although IPS, ULS, and RLS do not belong to natural ecological spaces, they still have various degree of ecosystem service function due to the existence of green space. This study refers to the equivalent value of construction land from the existing research [55,56] and adjusts the equivalent of different spaces according to the degree of human interference. In this way, the equivalent factor table of ecological services can be obtained (Table 2).

Table 2. Ecosystem service equivalent value per unit area in the TGRA-HS (unit: CNY/hm^2).

Category	Provision Service	Regulating Service	Supporting Service	Cultural Service
APS	145.73	8743.63	2477.35	233.17
IPS	−29,145.40	−32,059.95	408.04	29.15
ULS	−21,859.05	−14,222.96	1253.26	32.15
RLS	−8306.44	1165.81	1748.74	174.87
FES	3293.43	37,976.45	13,465.18	2710.53
GES	2215.05	22,704.27	8510.46	1719.58
WES	27,163.51	150,910.91	10,346.62	5508.48
OES	0.00	437.19	116.58	35.45

However, the vegetation coverage affected a variety of ecological processes and played an important role in ecosystem services. Owing to the differences in vegetation coverage flourishing in the types of cultivated land, forestland, and grassland covered with vegetation, the same types of land might provide significantly different levels of ecosystem service value [57]. Therefore, this study used NDVI to reflect the vegetation flourishing status in the TGRA-HS. The ESV was revised once again. Finally, the quantity and spatial characteristics of ESV from the perspective of the PLES of each period in the construction of the TGRA-HS was calculated using the ESV model. The mathematical ESV model is:

$$ESV = \sum_{i=1}^{m} \sum_{j=1}^{n} \sum_{k=1}^{o} A_{ij} B_{ik} C_{ik} \tag{3}$$

$$C_{ik} = \frac{NDVI_{ik}}{\overline{NDVI_i}} \tag{4}$$

where A_{ij} is the ESV coefficient of the j_{th} ecosystem services of the i_{th} PLES type; B_{ik} is the area of the i_{th} PLES type in the k_{th} research unit; C_{ik} is the revision coefficient of the *NDVI* of the i_{th} PLES type in the k_{th} research unit; $\overline{NDVI_i}$ is the mean of the i_{th} PLES type; $NDVI_{ik}$ is the *NDVI* value of the i_{th} PLES type in the k_{th} research unit; and *i, j,* and *k* are the PLES type, ecosystem services type, and number of research units, respectively. Then, a 1 km × 1 km vector grid was designed to cover the whole TGRA-HS, and it was divided into 11,612 grid units to explore spatial differences in ESV. Additionally, the ESV was divided into five levels (including slight, light, moderate, severe, and extreme levels) based on the natural breaks (Jenks) with the help of ArcGIS10.8.

3.4. The Effects of LUFT on Changes of ESV

The ecological contribution rate of LUFT refers to the change in the regional ESV caused by a certain land use function change. It can better identify the functional types that affect the change in ESV, which is conducive to the discussion of the leading factors of regional ecological environmental change [58]. Therefore, this study adopts the ecological contribution rate of LUFT to quantify the effects of LUFT on changes in regional ESV in the TGRA-HS. The mathematical model is [37]:

$$ESV_C = \frac{(ESV_{t+1} - ESV_t) \times CA}{TA} \tag{5}$$

where ESV_t and ESV_{t+1} are the ESV reflected by a certain LUFT at time *t* and *t+1*, respectively; ESV_C is the contribution rate of LUFT; *CA* is the transition area; and *TA* is the total area of the study area.

3.5. Data Sources

Data were collected from multiple sources (Table 3). The data on PLES in the TGRA-HS in 1990, 2000, 2010, and 2020 were taken from land use data, including 6 primary types and 25 secondary types, which were downloaded from the Geospatial Data Cloud. They were extracted at a resolution of 30 m × 30 m to explore the characteristics of

LUFT and the evolution of the ESV change, according to the construction stage division of the TGP. Meanwhile, the administrative map of the TGRA-HS was taken from the department of natural resources of the Hubei Province. Furthermore, the economic and social development data were taken from the Hubei Statistical Yearbook from 1990 to 2020 [59]. The geodatabase of the TGRA-HS was built in the ArcGIS10.8 software platform to process the above data.

Table 3. Data and sources.

Data	Sources
Land use data	Geospatial Data Cloud (http://www.gscloud.cn, accessed on 17 January 2023)
Digital elevation model data	
Administrative map	Department of Natural Resources of Hubei Province (https://zrzyt.hubei.gov.cn/, accessed on 17 January 2023)
Normalized difference vegetation index (NDVI) data	Resource and Environment Science and Data Center of the Chinese Academy of Sciences (http://www.resdc.cn/, accessed on 17 January 2023)
Economic and social development data	Hubei Statistical Yearbook

4. Results

4.1. Characteristics of the Transition of Land Use Function

4.1.1. Evaluation of Land Use Function in the TGRA-HS from 1990 to 2020

The spatiotemporal patterns of PLES were basically the same in the TGRA-HS, and they remained consistent as a whole in 1990, 2000, 2010, and 2020 (Table 4). The evolution of PLES showed characteristics of a reduction in P-space, and the expansion of L-space and E-space from 1990 to 2020. The structure of PLES was mainly dominated by FES, which accounted for over 77% of the total area of the TGRA-HS with an absolute dominant position during the study period (Figure 4). The P-space was mainly dominated by APS, presenting the characteristic of aggregated distribution, and its proportion was reduced from 12.86% to 11.59%. It was concentrated in the form of mass shape and mainly distributed in low-lying areas below 500 meters in the southeast and scattered in the west of the TGRA-HS in the form of point shapes. The E-space was mainly dominated by FES, which also presented the characteristic of aggregated distribution, and its proportion was reduced from 78.80% to 77.71%. It was mainly distributed in the mountain zone of the TGRA-HS. Meanwhile, the L-space was mainly dominated by ULS, presenting the characteristic of dotted distribution, and its proportion increased from 0.31% to 0.57%.

Table 4. The area proportion and change of production−living−ecological space (PLES) in the TGRA-HS between 1990 and 2020 (unit: %).

Years/Period	P-space		L-space		E-space			
	APS	IPS	ULS	RLS	FES	GES	WES	OES
1990	12.86	0.04	0.31	0.19	78.80	6.70	1.10	0.00
2000	12.85	0.32	0.39	0.20	78.44	6.70	1.11	0.00
2010	11.81	0.52	0.56	0.24	78.11	6.82	1.94	0.00
2020	11.59	1.12	0.57	0.24	77.71	6.80	1.96	0.00
1990–2000	–0.02	0.28	0.08	0.01	–0.35	0.00	0.00	0.00
2000–2010	–1.04	0.21	0.17	0.04	–0.33	0.12	0.83	0.00
2010–2020	–0.22	0.60	0.01	0.01	–0.40	–0.01	0.02	0.00
1990–2020	–1.28	1.08	0.26	0.06	–1.09	0.11	0.86	0.00

The expansion areas of ULS were concentrated in the southeast of the TGRA-HS and scattered throughout the rest of downtown Yichang. The spatial distribution of RLS was basically the same with the characteristics of agricultural production activities. It indicated that the regions that were suitable for agricultural production with relatively good natural conditions were usually suitable for harmonious human settlement. The regions had been developed into rural residential agglomerations gradually, and they remained relatively

stable. The evolution process of PLES showed the characteristics of two types down and five types up in the TGRA-HS from 1990 to 2020. The largest increase was in IPS, and the largest reduction was in APS, with a proportion of 1.08% and −1.28%, respectively. The evolution of PLES showed the characteristics of a reduction in P-space and the expansion of L-space and E-space from 1990 to 2010. This was mainly reflected in the continuous decline in APS and the continuous increase in ULS, RLS, and WES. While the P-space and L-space showed a trend of expansion, and the E-space mainly showed a trend of reduction from 2010 to 2020. The characteristics of the PLES evolution were closely related to the rapid development. The expansion of construction land had encroached on the land with relatively low economic benefits, which led to an increase in IPS, ULS, and RLS and a reduction in APS and FES.

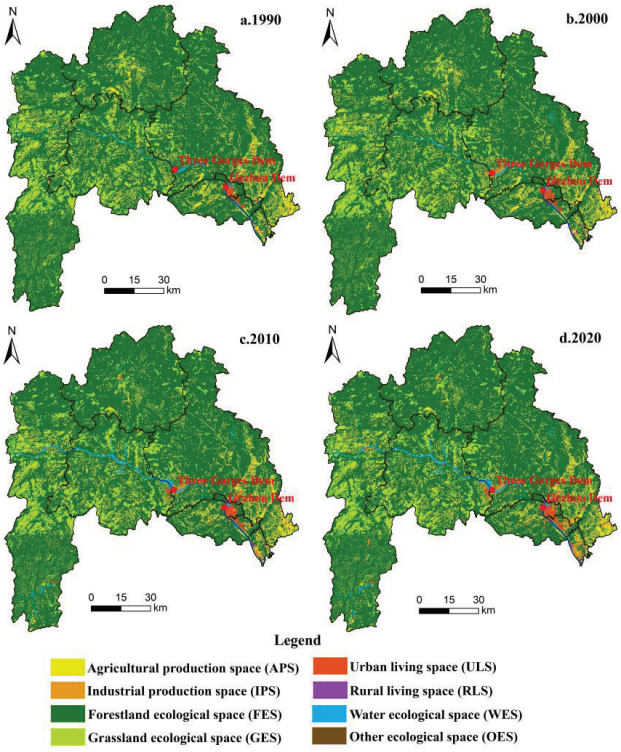

Figure 4. Characteristics of PLES in the TGRA-HS between 1990 and 2020.

4.1.2. Structural Transform of Land Use Function in the TGRA-HS from 1990 to 2020

For a further intuitive analysis, the structural transformation of the land use function in the TGRA-HS from 1990 to 2010 was calculated based on the mathematical model of LUFT. Compared with the data of the base period in 1990, the IPS and ULS increased significantly, and the growth rate was more than 85% during the study period (Table 5). Meanwhile, the FES and GES only showed minimal changes, and they were almost the same as the data of the base period. The differences in the spatial distribution characteristics of structural transform in different phases were obvious and were mainly reflected in the conversion of P-space and E-space in the TGRA-HS. From 1990 to 2000, the mutual conversion area was 6679.08 hm^2, which was mainly reflected in the conversion of APS, FES, and IPS, with a proportion of 70.84% of the total converted area. At this stage, the TGP and the resettlement of immigrants in the reservoir area had been implemented on a grand scale, resulting in the conversion of a large number of FES into IPS and APS. From 2000 to 2010, the mutual conversion area was 37,480.27 hm^2, which was mainly reflected in the conversion of APS

and FES, accounting for 66.88% of the total converted area during this period. The Grain for Green Project (GGP) was implemented, which resulted in a large amount of cultivated land being converted to forestland. At this stage, the Three Gorges Dam was officially closed for water storage, and the water level rose from 135 m to 175 m. This led to the transformation of an important proportion of APS into WES. Meanwhile, the mutual conversion area was 5916.48 hm^2 from 2010 to 2020, which was mainly reflected in the conversion of FES and IPS, accounting for 78.06% of the total converted area in the TGRA-HS. They were mainly concentrated in the urban area of Yichang around the Three Gorges Dam and the Gezhou Dam (Figure 5).

Table 5. Ordered Tupu table of land use transition in the TGRA-HS between 1990 and 2020 calculated based on Equations (1) and (2).

Period	Number	Transition Types	Area (hm^2)	Change Rates (%)	Accumulative Change Rates (%)
1990–2000	1	FES → IPS	2507.81	37.55	37.55
	2	FES → APS	1602.92	24.00	61.55
	3	APS → FES	620.96	9.30	70.85
	4	APS → ULS	548.97	8.22	79.07
	5	FES → ULS	352.47	5.28	84.34
	6	WES → IPS	287.52	4.30	88.65
	7	WES → APS	172.02	2.58	91.22
	8	APS → GES	134.79	2.02	93.24
	9	APS → WES	124.72	1.87	95.11
	10	FES → RLS	86.41	1.29	96.40
2000–2010	1	APS → FES	16,149.51	43.09	43.09
	2	FES → APS	8917.54	23.79	66.88
	3	FES → IPS	2452.59	6.54	73.43
	4	APS → GES	2415.21	6.44	79.87
	5	APS → WES	1544.04	4.12	83.99
	6	FES → ULS	907.02	2.42	86.41
	7	IPS → ULS	778.33	2.08	88.49
	8	APS → ULS	699.77	1.87	90.35
	9	IPS → WES	532.49	1.42	91.77
	10	FES → RLS	498.83	1.33	93.11
2010–2020	1	FES → IPS	4618.55	78.06	78.06
	2	APS → FES	219.98	3.72	81.78
	3	FES → APS	182.07	3.08	84.86
	4	FES → ULS	136.73	2.31	87.17
	5	WES → IPS	132.18	2.23	89.40
	6	APS → RLS	115.94	1.96	91.36
	7	IPS → FES	85.78	1.45	92.81
	8	APS → ULS	71.00	1.20	94.01
	9	FES → RLS	58.15	0.98	94.99
	10	RLS → APS	54.83	0.93	95.92

From the perspective of the structure characteristic of the PLES transform-in from 1990 to 2020, the APS was mainly converted from FES, and the proportion was 90.86%. The IPS was mainly converted from FES, and the proportion was as high as 93.11%. The ULS and RLS were mainly converted from APS and FES, while FES, GES, and WES were mainly converted from APS. From the perspective of the structural characteristics of the PLES transform-out from 1990 to 2020, the APS was mainly converted to FES, and the proportion of transition was 72.82%. The IPS was mainly converted to ULS, with a proportion of more than 82.49% of the total transition of this type. The RLS was mainly converted to IPS, with a transition ratio of 43.76%. The FES was mainly converted to APS and IPS. The GES was mainly converted to APS, and the WES was mainly converted to APS and IPS. The structural transform characteristics of PLES in different phases reflected the transformation of socio-economic development in the TGRA. We should pay more attention to the improvement of

the quality and the optimization of the structure. The win–win situation of PLES will be realized through the optimization of the structure in the whole area.

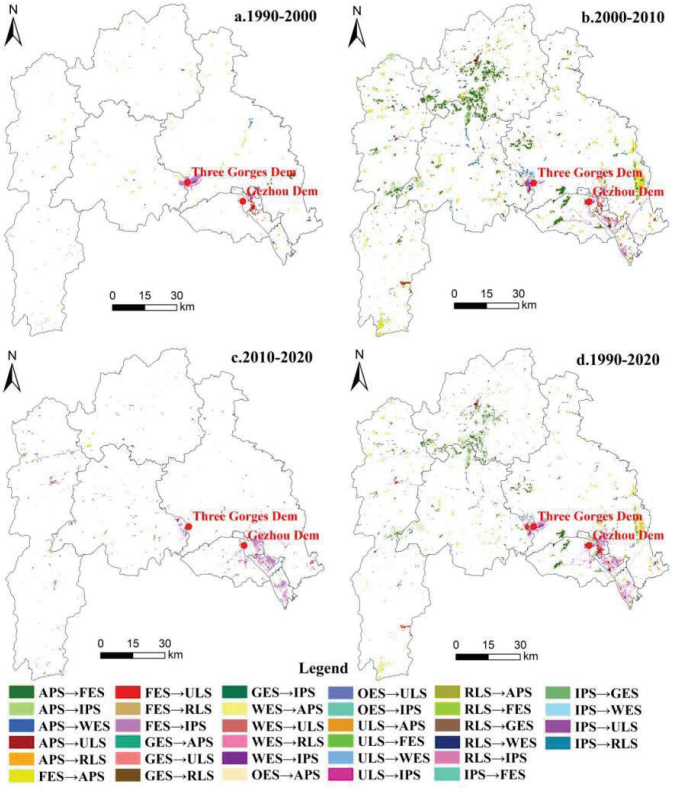

Figure 5. Spatial pattern evolution of PLES in the TGRA-HS between 1990 and 2020.

4.2. Characteristics of ESV Change

4.2.1. Quantity Characteristics of ESV Change from the perspective of PLES

According to Equations (3) and (4), the ESV of each spatial type in the TGRA-HS was calculated from 1990 to 2020 (Table 6). We could see that the total ESV of the PLES of the TGRA-HS in 1990, 2000, 2010, and 2020 was CNY 619.22 $\times$ 10^8, CNY 614.43 $\times$ 10^8, CNY 628.51 $\times$ 10^8, and CNY 621.39 $\times$ 10^8, respectively. The total ESV of the PLES showed a trend of floating change in the TGRA-HS, but remained relatively stable as a whole. Among them, the E-space contributed the most to the total ESV, with a proportion of more than 90% in different phases. The total ESV of E-space rose to a certain extent, increased by CNY 13.06 $\times$ 10^8. The total ESV of P-space and L-space decreased significantly from 1990 to 2020, with a value of CNY -9.73 $\times$ 10^8 and CNY -1.15 $\times$ 10^8, respectively. From the perspective of the corresponding secondary types, the total ESV of IPS and FES declined the most during the past 30 years, with a value of CNY 7.93 $\times$ 10^8 and CNY 7.56 $\times$ 10^8, respectively. The total ESV of APS, ULS, and RLS also declined significantly, and the total ESV of WES and GES increased by CNY 20.17 $\times$ 10^8 and CNY 0.45 $\times$ 10^8, respectively. At the same time, the GGP since 1998 has accelerated the improvement of ESV.

Table 6. Changes of ESV of PLES in the TGRA-HS between 1990 and 2020 calculated based on Equation (3) and (4) (unit: CNY 10^6).

Years/Period	P-space		L-space		E-space			
	APS	IPS	ULS	RLS	FES	GES	WES	OES
1990	1807.98	−29.96	−130.27	−11.71	54842.66	2852.42	2590.48	0.03
2000	1805.77	−232.62	−164.14	−12.54	54597.45	2852.05	2596.65	0.02
2010	1660.12	−384.79	−236.39	−14.91	54366.90	2902.79	4556.84	0.00
2020	1628.64	−823.90	−241.98	−15.41	54086.03	2897.82	4607.67	0.00
1990−2000	−2.21	−202.66	−33.87	−0.83	−245.21	−0.37	6.17	−0.01
2000−2010	−145.64	−152.17	−72.25	−2.37	−230.55	50.75	1960.20	−0.02
2010−2020	−31.49	−439.11	−5.59	−0.50	−280.87	−4.98	50.83	0.00
1990−2020	−179.34	−793.94	−111.71	−3.70	−756.62	45.40	2017.20	−0.03

4.2.2. Spatial Characteristics of ESV Change

According to the calculation results, the spatial characteristics of the ESV change in the TGRA-HS between 1990 and 2020 were obtained (Figure 6). The spatial pattern of the slight ESV area in the TGRA-HS was mainly distributed in the urban built-up area. It showed an obvious expansion trend with the development of urbanization and the construction of the TGP. The distribution pattern of the light and moderate ESV area was consistent with the spatial distribution of cultivated land, and most of them had been replaced by slight areas during the past 30 years. The spatial pattern of the severe ESV area was basically the same as the distribution of forestland. Additionally, the characteristics of spatial distribution tended to be fragmented from 1990 to 2020, which was related to the encroachment of forestland by construction land. The distribution pattern of extreme ESV area was consistent with the river. The population distribution in this region was relatively concentrated along the river banks with deep valleys and steep slopes, and the area of sloping farmland was large. People's daily life and agricultural production activities had destroyed the vegetation along the coast, causing serious water and soil loss.

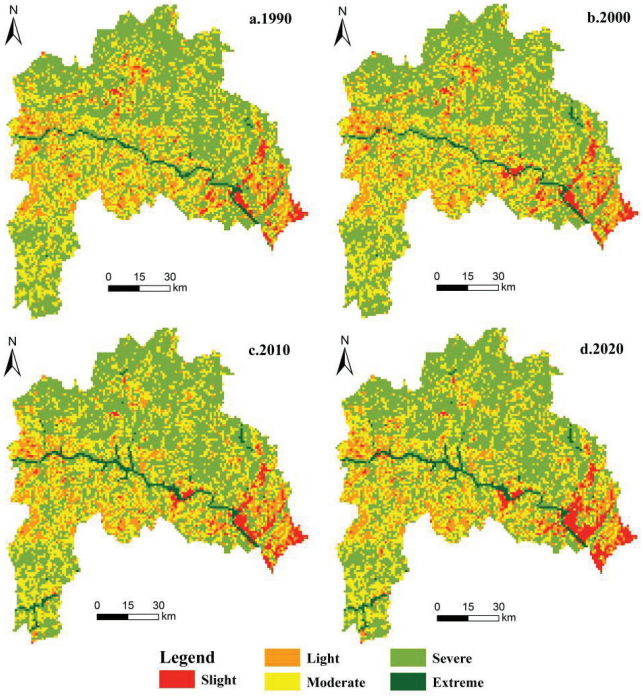

Figure 6. Spatial evolution of ESV in the TGRA-HS between 1990 and 2020.

4.3. The Effects of LUFT on Changes of ESV

According to Equation (5), the effects of LUFT on changes in ESV were calculated (Table 7). We could see that the transformation of PLES had brought about a decline in ESV in the TGRA-HS from 1990 to 2020. This mainly stemmed from the encroachment of P-space on E-space. The transition of E-space to P-space had the greatest impact on the reduction in ESV, and the proportion of contribution rates accounted for 82.76%. The transition of E-space to L-space was far less than that of P-space, and the proportion of the contribution rate was 12.68%. From the corresponding secondary type, the main reason for the decline in ESV in the TGRA-HS, stemmed from the encroachment of IPS and APS on FES, and the proportion of contribution rates in negative effects was 52.37% and 23.47%, respectively. Meanwhile, the transformation of PLES brought about an increase in ESV in the TGRA-HS from 1990 to 2020. This mainly stemmed from the encroachment of E-space on P-space. The transition of P-space to E-space had the greatest impact on the increase in ESV in the TGRA-HS, and the proportion of contribution rates accounted for 94.45%. From the corresponding secondary type, the main reason for the increase in ESV in the TGRA-HS stemmed from the increase in FES, WES, and GES, and the proportion of contribution rates in positive effects was 64.33%, 24.98%, and 5.14%, respectively.

Table 7. Main types and contribution rates of LUFT in the TGRA-HS between 1990 and 2020 calculated based on Equation (5).

Effect Type	Transition Type	Difference of ESV (CNY 10^6)	Contribution Rates (%)	Proportion of Contribution Rates (%)
Positive effects of ESV	APS → FES	747.41	0.358317	64.33
	APS → WES	290.21	0.139130	24.98
	APS → GES	59.70	0.028619	5.14
	ULS → WES	29.70	0.014240	2.56
	RLS → WES	14.25	0.006832	1.23
	ULS → FES	4.35	0.002085	0.37
	IPS → ULS	3.91	0.001875	0.34
	RLS → APS	3.78	0.001812	0.33
	RLS → FES	3.62	0.001738	0.31
	IPS → FES	3.03	0.001454	0.26
Negative effects of ESV	FES → IPS	−1016.67	−0.487402	52.37
	FES → APS	−455.63	−0.218434	23.47
	FES → ULS	−160.92	−0.077147	8.29
	WES → IPS	−69.08	−0.033119	3.56
	APS → ULS	−61.52	−0.029492	3.17
	WES → APS	−46.73	−0.022405	2.41
	WES → ULS	−40.87	−0.019594	2.11
	FES → RLS	−39.45	−0.018914	2.03
	RLS → IPS	−15.30	−0.007337	0.79
	GES → APS	−11.94	−0.005724	0.61
	APS → RLS	−10.64	−0.005100	0.55

In summary, the LUFT caused by human construction projects affects the spatiotemporal changes in the regional ESV, and the trends of the improvement and deterioration of ecosystem services can offset each other on the regional scale to keep the ESV relatively stable as a whole. However, the stability of the ESV does not mean that the eco-environment has not changed. The enhancement of LPS, IPS, and APS in the study area was the main reason for the decrease in ESV. Meanwhile, the improvement of ecosystem service functions was mainly achieved via the conservation of E-space and the GGP since 1998 in the TGRA. This shows that maintaining the stability of forestland, water land, and grass land ecosystems was crucial in improving the ESV in the TGRA. In addition, the transformation of L-space into E-space and P-space in the TGRA-HS also led to the improvement of ecosystem services. This is mainly due to the consolidation of rural settlements in recent years, but the proportion of contribution rates was relatively low.

5. Discussion

Existing research is more concerned with the calculation of ESV from the perspective of land use types, which may not reveal the mutual feedback relationship between anthropogenic interference and ecosystem services well. The PLES is a comprehensive method of dividing territorial space that can better reflect the comprehensive characteristics of ecosystem services with different land use types, and its layout and evolution have a profound impact on the regional ecosystem function. Taking the TGRA-HS as a study area, we explored the characteristics of LUFT, the spatiotemporal change of ESV, and the effects of LUFT on the change in ESV from the perspective of PLES by following the construction stage division of the TGP. This study revealed the mutual feedback relationship between human social systems and ecosystems well, making up for the shortcomings of the existing research.

5.1. Construction of the TGP and Stage Response

According to the stage deployment, the construction of the TGP can be divided into different stages, and there were obvious differences in the spatial pattern of PLES and its variation trend. The characteristic of LUFT was consistent with the period of project construction, national policies, and regional development plans in the TGRA-HS. Human activities, such as facility construction and resettlement, had a great impact on the structure and function of land use in the reservoir area. Before and after the construction of the TGP, the changes in the water level of the main stream of the Yangtze River were the most intuitive manifestation of the project's impact on the LUFT.

During the construction preparation and the start of the first phase of the project, the disturbance of the project was still small, and the LUFT was mainly driven by regional agricultural development planning and the early resettlement policy. In 1993, the resettlement of the TGRA began to be carried out on a large scale. The early resettlement strategy was local resettlement and local construction. To obtain food and income, the agricultural population reclaimed the sloping land spontaneously. In 2003, the TGP officially closed the sluice and stored water. The large-scale land use transition during this period was mainly driven by project water storage. The transformation of land use function mainly occurs in river valleys below 500 meters. The main reason for the increase in WES was that the reservoir area begun to store water after the Three Gorges Dam was built. In addition, driven by national policies such as the adjustment of resettlement policy and the pilot program of the "Two-oriented Society", FES and GES were restored and IPS and ULS were expanded. After 2010, the reservoir entered the stage of full operation, and the changes in land use patterns brought about by the construction of the project tended to be stable. Driven by national policies and regional development planning, the major functional areas divided the three western counties into key ecological function zones at the national level and restricted their development. The five eastern districts were key development zones at the provincial level with rapid urban development [60]. The development drew lessons from the past, and the economic development and ecological protection were more focused on diversity and coordination so as to achieve sustainable development. The project construction also brought about some policy responses to a certain extent. During the construction of the TGP, the country had successively implemented key ecological projects in the TGRA to mitigate the negative effects of the project. The territorial space ecological security system with forest vegetation dominated, and a combination of forest and grass was initially established to ensure the eco-environmental safety of the reservoir area and the safety of the reservoir operation. This also shows that maintaining the stability of forestland, water land, and grass land ecosystems was crucial to improving the ecosystem service function in the TGRA-HS.

5.2. Implications for Theory and Practice

This study put forward the LUFT from the perspective of PLES on the basis of the project construction stage division and the revised assessment methods of ESV. The quan-

titative assessment of ESV transforms ecological issues into indicators that are easily understood by the public, and which can help identify problems [61]. With the continuous deepening of ESV and function research, the quantitative assessment of ESV is becoming more and more mature [62,63]. In this study, we refer to the existing research of Xie et al. [64] to evaluate ESV in the TGRA-HS. It is generally assumed that the same type of land use has the same value of ecosystem services, but this ignores the potential impact of vegetation flourishing. However, the vegetation affects a variety of ecological processes, and ESV assessment that ignores vegetation growth will be very inaccurate. Therefore, this study relies on remote sensing images to determine the actual status of regional vegetation and uses the NDVI to revise the ESV realistically so as to obtain the accounting result of ESV with higher accuracy. At present, the revision methods of ESV are not unified, which deserves further discussion.

Meanwhile, this study provides a scientific reference to support and serve the layout optimization of the spatial development pattern and eco-environmental protection in the TGRA-HS. Additionally, it provides an important reference for understanding the effects of major conservancy projects on the ecosystem in reservoir areas, such as Bratsk Reservoir, Samara Reservoir, Smallwood Reservoir, Lake Guri, etc. The results are helpful in creating an incentive for people to understand ecosystem services and for policymakers to use, and they can effectively assist ecological restoration across the planning area [65]. Considering that project construction is an important but irreversible process affecting ESV in the reservoir area, policymakers should focus on the following recommendation during the construction process of large-scale conservancy projects. On the one hand, they should design reasonable targets for ecological protection and construction, design feasible plans and specific measures to promote the restoration of ecosystems and enhance the ecosystem service function so as to lay the ecological foundation for regional ecological security. On the other hand, they should strengthen the construction of projects related to ecological environmental construction and protection in the reservoir area, promote the smooth implementation of vegetation restoration and ecological corridor construction projects in the reservoir area, and improve the construction standards and ecological compensation.

5.3. Limitations and Future Works

Exploring the influencing mechanism of regional ecosystem services is helpful in guiding regional ecological construction. The research on the influencing factors of ESV can be roughly divided into two categories. One analyzes the spatiotemporal variation characteristics of ESV based on the transformation of land use patterns. The other is to select relevant factors, establish an index system, and use regression analysis or correlation analysis to discuss the main influencing factors of ESV. Additionally, the influencing factors can be divided into natural factors (including biological, climate, soil, and topography) and human factors (including land use transition and socio-economic development). In terms of human factors, changes in land use type, overall land use pattern and land development intensity will affect the level of ecosystem services [66]. Among them, the transition of land use function induced by anthropogenic interference (such as large-scale construction projects) is one of the most important influencing factors of ecosystem services, which will directly affect the change in ESV and the flow and interaction between ecosystem services. Due to the limitations of some basic data and research objects, this study mainly explored the effects of LUFT on changes in ESV during the construction of the TGP at the macro level. However, the driving mechanism of other potential factors on ESV evolution and the stability of the ecosystem have not been explored in depth, which is also an interesting direction for ecosystem service research. It is necessary to further study the driving mechanism of ESV evolution at each stage combined with the stages of economic and social development and to reveal the related issues of land use transition. In order to more accurately grasp the response of regional ecological environments to socio-economic development, the analysis of the driving mechanism needs to be further refined and quantified in the future.

6. Conclusions

(1) The transition of land use function from the perspective of PLES is the mapping of the evolution of the human–nature relationship in the spatial pattern, which reflects the evolution of the spatial pattern caused by human interference with the continuous development of society.

(2) From 1990 to 2020, the distribution pattern of PLES in the TGRA-HS was basically the same, and it was mainly dominated by FES; meanwhile, there were significant regional differences. The evolution of PLES showed the characteristics of a reduction in P-space and an expansion in L-space and E-space. The mutual transformation between P-space and E-space was the main form of PLES transformation in the TGRA-HS. The characteristics of structural transformation in different phases were obvious, which reflected the phases in the construction of the TGP and transformations brought about by socio-economic development.

(3) From 1990 to 2020, the total ESV showed a trend of floating change in the TGRA-HS but remained relatively stable as a whole. The E-space contributed the most to the total ESV, and increased by CNY 13.06×10^8. The IPS and FES declined the most during the past 30 years, with a decrease of CNY 7.93×10^8 and CNY 7.56×10^8, respectively. The LUFT caused by human project construction affects the spatiotemporal change of regional ESV. The spatial pattern of the slight ESV was mainly distributed in the urban built-up area, and it showed an obvious expansion trend with the development of urbanization and the construction of the TGP.

(4) The change in regional ESV induced by LUFT reveals the whole dynamic process of the positive and negative effects of human activities on ecosystem services, and the two effects offset each other to keep the ESV relatively stable as a whole. The main reason for the decline in the ESV stemmed from the encroachment of IPS and APS in FES, whose contribution rates were 52.37% and 23.47%, respectively. The TGRA should formulate differentiated spatial governance measures based on the in-depth implementation of the main functional zone strategy so as to promote the rational layout and integrated development of the PLES in the future.

Author Contributions: Conceptualization, F.P. and Q.W.; methodology, F.P., N.S. and Q.H.; investigation, all authors; resources, Q.W. and N.S.; writing—original draft preparation, F.P. and Q.W.; writing—review and editing, all authors. All authors have read and agreed to the published version of the manuscript.

Funding: This research was funded by the National Natural Science Foundation of China, grant number 42001229; the Research Project of Philosophy and Social Sciences in Colleges and Universities of Hubei Province, grant number 21Q093; Humanity and Social Science Key Program Foundation of Ministry of Education in China, grant number 18YJC790153; and the Science Research Foundation of Wuhan Institute of Technology, grant number K2021051.

Conflicts of Interest: The authors declare no conflict of interest.

References

1. Perring, M.; De Frenne, P.; Baeten, L.; Maes, S.; Depauw, L.; Blondeel, H.; Caron, M.; Verheyen, K. Global environmental change effects on ecosystems: The importance of land-use legacies. *Glob. Chang. Biol.* **2016**, *22*, 1361–1371. [CrossRef] [PubMed]
2. Güneralp, B.; Seto, K.; Ramachandran, M. Evidence of urban land teleconnections and impacts on hinterland. *Curr. Opin. Environ. Sustain.* **2013**, *5*, 445–451. [CrossRef]
3. Lynch, L.; Kangas, M.; Ballut, N.; Doucet, A.; Schoenecker, K.; Johnson, P.; Gharehaghaji, M.; Minor, E. Changes in land use and land cover along an urban-rural gradient influence floral resource availability. *Curr. Landsc. Ecol. Rep.* **2021**, *6*, 46–70. [CrossRef]
4. Liu, Y.; Huang, X.; Yang, H.; Zhong, T. Environmental effects of land-use/cover change caused by urbanization and policies in Southwest China Karst area: A case study of Guiyang. *Habitat Int.* **2014**, *44*, 339–348. [CrossRef]
5. Miller, J.R.; Grow, D.; Philyaw, L.S. Influence of historical land-use change on contemporary channel processes, form, and restoration. *Geosciences* **2021**, *11*, 423. [CrossRef]
6. Dewan, A.M.; Yamaguchi, Y. Land use and land cover change in Greater Dhaka, Bangladesh: Using remote sensing to promote sustainable urbanization. *Appl. Geogr.* **2009**, *29*, 390–401. [CrossRef]

7. Yang, Y.; Bao, W.; Li, Y.; Wang, Y.; Chen, Z. Land use transition and its eco-environmental effects in the Beijing–Tianjin–Hebei urban agglomeration: A production–living–ecological perspective. *Land* **2020**, *9*, 285. [CrossRef]
8. Allington, G.; Li, W.; Brown, D. Urbanization and environmental policy effects on the future availability of grazing re-sources on the Mongolian Plateau: Modeling socio-environmental system dynamics. *Environ. Sci. Policy* **2017**, *68*, 35–46. [CrossRef]
9. Powers, R.; Jetz, W. Global habitat loss and extinction risk of terrestrial vertebrates under future land-use-change scenarios. *Nat. Clim. Chang.* **2019**, *9*, 323–329. [CrossRef]
10. Das, S.; Angadi, D. Land use-land cover (LULC) transformation and its relation with land surface temperature changes: A case study of Barrackpore Subdivision, West Bengal, India. *Remote Sens. Appl.* **2020**, *19*, 100322. [CrossRef]
11. Groot, R. Function-analysis and valuation as a tool to assess land use conficts in planning for sustainable, multi-functional landscapes. *Landsc. Urban Plan.* **2006**, *75*, 175–186. [CrossRef]
12. Lambin, E.; Meyfroidt, P. Land use transitions: Socio-ecological feedback versus socio-economic change. *Land Use Policy* **2010**, *27*, 108–118. [CrossRef]
13. Asabere, S.; Acheampong, R.; Ashiagbor, G.; Beckers, S.; Keck, M.; Erasmi, S.; Schanze, J.; Sauer, D. Urbanization, land use transformation and spatio-environmental impacts: Analyses of trends and implications in major metropolitan regions of Ghana. *Land Use Policy* **2020**, *96*, 104707. [CrossRef]
14. Ge, D.; Long, H.; Zhang, Y.; Ma, L.; Li, T. Farmland transition and its influences on grain production in China. *Land Use Policy* **2018**, *70*, 94–105. [CrossRef]
15. Blüthgen, N.; Dormann, C.; Prati, D.; Klaus, V.; Kleinebecker, T.; Hölzel, N.; Alt, F.; Boch, S.; Gockel, S.; Hemp, A.; et al. A quantitative index of land-use intensity in grasslands: Integrating mowing, grazing and fertilization. *Basic Appl. Ecol.* **2012**, *13*, 207–220. [CrossRef]
16. Verburg, P.; Erb, K.; Mertz, O.; Espindola, G. Land system science: Between global challenges and local realities. *Curr. Opin. Environ. Sustain.* **2013**, *5*, 433–437. [CrossRef]
17. Laliberté, E.; Wells, J.A.; Declerck, F.; Metcalfe, D.J.; Catterall, C.P.; Queiroz, C.; Aubin, I.; Bonser, S.P.; Ding, Y.; Fraterrigo, J.M.; et al. Land use intensification reduces functional redundancy and response diversity in plant communities. *Ecol. Lett.* **2010**, *13*, 76–86. [CrossRef]
18. Basheer, M.; Boelens, L.; Bijl, R. Bus rapid transit system: A study of sustainable land-use transformation, urban density and economic impacts. *Sustainability* **2020**, *12*, 3376. [CrossRef]
19. Gogoi, P.; Vinoj, V.; Swain, D.; Roberts, G.; Dash, J.; Tripathy, S. Land use and land cover change effect on surface temperature over Eastern India. *Sci. Rep.* **2019**, *9*, 8859. [CrossRef]
20. Liu, Y.; Long, H.; Li, T.; Tu, S. Land use transitions and their effects on water environment in Huang-Huai-Hai Plain, China. *Land Use Policy* **2015**, *47*, 293–301. [CrossRef]
21. Nuissl, H.; Haase, D.; Lanzendorf, M.; Wittmer, H. Environmental impact assessment of urban land use transitions—A context-sensitive approach. *Land Use Policy* **2009**, *26*, 414–424. [CrossRef]
22. Estoque, R.; Murayama, Y. Landscape pattern and ecosystem service value changes: Implications for environmental sustainability planning for the rapidly urbanizing summer capital of the Philippines. *Landsc. Urban Plan.* **2013**, *116*, 60–72. [CrossRef]
23. Lambin, E.; Rounsevell, M.; Geist, H. Are agricultural land-use models able to predict changes in land-use intensity? *Agr. Ecosyst. Environ.* **2000**, *82*, 321–331. [CrossRef]
24. Chakraborty, D.; Reddy, M.; Tiwari, S.; Umapathy, G. Land Use Change Increases Wildlife Parasite Diversity in Anamalai Hills, Western Ghats, India. *Sci. Rep.* **2019**, *9*, 11975. [CrossRef]
25. López, S.; Wright, C.; Costanza, P. Environmental change in the equatorial Andes: Linking climate, land use and land cover transformations. *Remote Sens. Appl.* **2016**, *8*, 291–303. [CrossRef]
26. Duan, Y.; Xu, Y.; Huang, A.; Lu, L.; Ji, Z. Progress and prospects of "production-1iving-ecological" functions evaluation. *J. China Agric. Univ.* **2021**, *26*, 113–124.
27. Peng, J.; Lv, D.N.; Dong, J.Q.; Liu, Y.X.; Liu, Q.Y.; Li, B. Processes coupling and spatial integration: Characterizing ecological restoration of territorial space in view of landscape ecology. *J. Nat. Resour.* **2020**, *35*, 3–13.
28. Li, J.; Sun, W.; Li, M.; Meng, L. Coupling Coordination Degree of Production, Living and Ecological Spaces and Its Influencing Factors in the Yellow River Basin. *J. Clean. Prod.* **2021**, *298*, 126803. [CrossRef]
29. Costanza, R.; d'Arge, R.; de Groot, R.; Farber, S.; Grasso, M.; Hannon, B.; Limburg, K.; Naeem, S.; O'Neil, R.; Paruelo, J.; et al. The value of the world's ecosystem services and natural capital. *Nature* **1997**, *387*, 253–260. [CrossRef]
30. De Groot, R.; Wilson, M.; Boumans, R. A typology for the classification, description and valuation of ecosystem functions, goods and services. *Ecol. Econ.* **2002**, *41*, 393–408. [CrossRef]
31. Coatanza, R.; De Groot, R.; Sutton, P.; Van Der Ploeget, S.; Anderson, S.; Kubiszewski, I.; Farber, S.; Turner, R. Changes in the global value of ecosystem services. *Glob. Environ. Chang.* **2014**, *26*, 152–158. [CrossRef]
32. Liu, Y.; Long, H. Land use transitions and their dynamic mechanism: The case of the Huang-Huai-Hai Plain. *J. Geogr. Sci.* **2016**, *26*, 515–530. [CrossRef]
33. Nassl, M.; Löffler, J. Ecosystem services in coupled social–ecological systems: Closing the cycle of service provision and societal feedback. *Ambio* **2015**, *44*, 737–749. [CrossRef] [PubMed]
34. Ciftcioglu, G. Assessment of the relationship between ecosystem services and human wellbeing in the social-ecological landscapes of Lefke Region in North Cyprus. *Landsc. Ecol.* **2017**, *32*, 897–913. [CrossRef]

35. Toro, G.; Otero, M.; Clerici, N.; Szantoi, Z.; González-González, A.; Escobedo, F. Interacting municipal-level anthropogenic and ecological disturbances drive changes in Neotropical forest carbon storage. *Front. Environ. Sci.* **2022**, *10*, 937147. [CrossRef]
36. Lorenzen, M.; Orozco-Ramírez, Q.; Ramírez-Santiago, R.; Garza, G. Migration, socioeconomic transformation, and land-use change in Mexico's Mixteca Alta: Lessons for forest transition theory. *Land Use Policy* **2020**, *95*, 104580. [CrossRef]
37. Li, C.; Wu, J. Land use transformation and eco-environmental effects based on production-living-ecological spatial synergy: Evidence from Shaanxi Province, China. *Environ. Sci. Pollut. Res.* **2022**, *29*, 41492–41504. [CrossRef]
38. Long, H.; Liu, Y.; Hou, X.; Li, T.; Li, Y. Effects of land use transitions due to rapid urbanization on ecosystem services: Implications for urban planning in the new developing area of China. *Habitat Int.* **2014**, *44*, 536–544. [CrossRef]
39. Yin, D.; Li, X.; Li, G.; Zhang, J.; Yu, H. Spatio-temporal evolution of land use transition and its eco-environmental effects: A case study of the Yellow River Basin, China. *Land* **2020**, *9*, 514. [CrossRef]
40. Yu, S.; Deng, W.; Xu, Y.; Zhang, X.; Xiang, H. Evaluation of the production-living-ecology space function suitability of Pingshan County in the Taihang mountainous area, China. *J. Mt. Sci.* **2020**, *17*, 2562–2576. [CrossRef]
41. Qiu, L.; Pan, Y.; Zhu, J.; Amable, G.S.; Xu, B. Integrated analysis of urbanization-triggered land use change trajectory and implications for ecological land management: A case study in Fuyang, China. *Sci. Total Environ.* **2018**, *660*, 209–217. [CrossRef] [PubMed]
42. Gou, M.; Li, L.; Ouyang, S.; Wang, N.; La, L.; Liu, C.; Xiao, W. Identifying and analyzing ecosystem service bundles and their socioecological drivers in the Three Gorges Reservoir Area. *J. Clean. Prod.* **2021**, *307*, 127208. [CrossRef]
43. Li, S.; Liu, X.; Paudel, B.; Xu, F.; Deng, Q. Stable sediment retention and rapid economic growth occurred together from the end of the 1970s to 2015 in the Three Gorges Reservoir area. *Land Degrad. Dev.* **2021**, *32*, 3653–3665. [CrossRef]
44. Fu, B.; Wu, B.; Lü, Y.; Xu, Z. Three Gorges Project: Efforts and challenges for the environment. *Prog. Phys. Geog.* **2010**, *34*, 741–754. [CrossRef]
45. Amin, H.; Helmi, M. Impacts of land-use transformation on agriculture land in Afghanistan, Kabul city as case study. *Int. J. Environ. Sci. Sustain. Dev.* **2021**, *6*, 52. [CrossRef]
46. Bongaarts, J. Summary for policymakers of the global assessment report on biodiversity and ecosystem services of the Intergovernmental Science-Policy Platform on Biodiversity and Ecosystem Services. *Popul. Dev. Rev.* **2019**, *45*, 680–681. [CrossRef]
47. Chen, M.; Bai, Z.; Wang, Q.; Shi, Z. Habitat Quality Effect and Driving Mechanism of Land Use Transitions: A Case Study of Henan Water Source Area of the Middle Route of the South-to-North Water Transfer Project. *Land* **2021**, *10*, 796. [CrossRef]
48. Deng, Y.; Yang, R. Influence mechanism of production-living-ecological space changes in the urbanization process of Guangdong province, China. *Land* **2021**, *10*, 1357. [CrossRef]
49. Fu, X.; Wang, X.; Zhou, J.; Ma, J. Optimizing the Production-Living-Ecological Space for Reducing the Ecosystem Services Deficit. *Land* **2021**, *10*, 1001. [CrossRef]
50. Nelson, E.; Mendoza, G.; Regetz, J.; Polasky, S.; Tallis, H.; Cameron, D.R.; Chan, K.M.A.; Daily, G.C.; Goldstein, J.; Kareiva, P.M.; et al. Modeling multiple ecosystem services, biodiversity conservation, commodity production, and tradeoffs at landscape scales. *Front. Ecol. Environ.* **2009**, *7*, 4–11. [CrossRef]
51. Bennett, E.; Peterson, G.; Gordon, L. Understanding relationships among multiple ecosystem services. *Ecol. Lett.* **2009**, *12*, 1394–1404. [CrossRef] [PubMed]
52. Liu, J.; Liu, Y.; Li, Y. Classification evaluation and spatial-temporal analysis of "production-living-ecological" spaces in China. *Acta Geogr. Sin.* **2017**, *72*, 1290–1304. (In Chinese)
53. Meehan, T.; Gratton, C.; Diehl, E.; Hunt, N.; Mooney, D.; Ventura, S.; Barham, B.; Jackson, R. Ecosystem-service tradeoffs associated with switching from annual to perennial energy crops in riparian zones of the US Midwest. *PLoS ONE* **2013**, *8*, e80093. [CrossRef] [PubMed]
54. Chen, W.; Zhao, H.; Li, J.; Zhu, L.; Wang, Z.; Zeng, J. Land use transitions and the associated impacts on ecosystem services in the Middle Reaches of the Yangtze River Economic Belt in China based on the geo-informatic Tupu method. *Sci. Total Environ.* **2020**, *701*, 134690. [CrossRef]
55. Hu, M.; Li, Z.; Wang, Y.; Jiao, M.; Li, M.; Xia, B. Spatio-temporal changes in ecosystem service value in response to land-use/cover changes in the Pearl River Delta. *Resour. Conserv. Recycl.* **2019**, *149*, 106–114. [CrossRef]
56. Wang, W.; Guo, H.; Chuai, X.; Dai, C.; Lai, L.; Zhang, M. The impact of land use change on the temporospatial variations of ecosystems services value in China and an optimized land use solution. *Environ. Sci. Policy* **2014**, *44*, 62–72. [CrossRef]
57. Su, K.; Wei, D.; Lin, W. Evaluation of ecosystem services value and its implications for policy making in China: A case study of Fujian Province. *Ecol. Indic.* **2020**, *108*, 105752. [CrossRef]
58. Oliver, M.; Webster, R. A tutorial guide to geostatistics: Computing and modelling variograms and kriging. *Cetena* **2014**, *113*, 56–69. [CrossRef]
59. Hubei Provincial Statistics Bureau; National Bureau of Statistics Hubei Investigation Team. *Hubei Statistical Year Book*; China Statistics Press: Beijing, China, 2021.
60. Hubei Provincial People's Government. Hubei Province Main Functional Area Planning. 2012. Available online: https://www.hubei.gov.cn/zfwj/ezf/201303/t20130307_1711739.shtml (accessed on 17 January 2023).
61. Pan, F.; Song, M.; Wan, Q.; Yuan, L. A conservation planning framework for China's national key ecological function area based on ecological risk assessment. *Environ. Monit. Assess.* **2022**, *194*, 74. [CrossRef]

62. Mäler, K.; Aniyar, S.; Jansson, A. Accounting for the value of ecosystem assets and their services. *Implement. Environ. Acc.* **2013**, *28*, 187–205. [CrossRef]
63. Costanza, R.; De Groot, R.; Braat, L.; Kubiszewski, I.; Fioramonti, L.; Sutton, P.; Farber, S.; Grasso, M. Twenty years of ecosystem services: How far have we come and how far do we still need to go? *Ecosyst. Serv.* **2017**, *28*, 1–16. [CrossRef]
64. Xie, G.; Zhang, C.; Zhang, L.; Chen, W.; Li, S. Improvement of the evaluation method for ecosystem service value based on per unit area. *J. Nat. Resour.* **2015**, *30*, 1243–1254. (In Chinese)
65. De Groot, R.; Brander, L.; Ploeg, S.; Costanza, R.; Bernard, F.; Braat, L.; Christie, M.; Crossman, N.; Ghermandi, A.; Hein, L.; et al. Global estimates of the value of ecosystems and their services in monetary units. *Ecosyst. Serv.* **2012**, *1*, 50–61. [CrossRef]
66. Bryan, B.; Ye, Y.; Zhang, J.; Connor, J. Land-use change impacts on ecosystem services value: Incorporating the scarcity effects of supply and demand dynamics. *Ecosyst. Serv.* **2018**, *32*, 144–157. [CrossRef]

land

MDPI

Article

Response of Two Major Lakes in the Changtang National Nature Reserve, Tibetan Plateau to Climate and Anthropogenic Changes over the Past 50 Years

Zhilong Zhao [1,2], Zengzeng Hu [3,*], Jun Zhou [1], Ruliang Kan [1] and Wangjun Li [4]

[1] College of Economics and Management, China Three Gorges University, Yichang 443002, China
[2] Faculty of Geographical Science, Beijing Normal University, Beijing 100875, China
[3] Beijing Academy of Sciences and Technology, Beijing 100089, China
[4] School of Geography Science and Geomatics Engineering, Suzhou University of Science and Technology, Suzhou 215009, China
* Correspondence: huzengzeng@bjss.org.cn

Abstract: Areal changes in alpine lakes on the Tibetan Plateau (TP) are reliable indicators of climate change and anthropogenic disturbance. This study used long-term Landsat images and meteorological records to monitor the temporal evolution patterns of lakes within the Changtang National Nature Reserve between 1972 and 2021 and examine the climatic and anthropogenic impacts on lake area changes. The results revealed that the area of Lake LongmuCo and Lake Jiezechaqia significantly expanded by 12.81% and 12.88% from 1972 to 2021, respectively. After 1999, Lake LongmuCo and Lake Jiezechaqia entered into a period of rapid expansion. During 1972–2021, the annual mean temperature significantly increased at a rate of 0.05 °C/a, while the change in annual precipitation was not significant. The temperature change was a major contributor to the observed changes of Lake LongmuCo and Lake Jiezechaqia between 1972 and 2021, while human intervention also played a vital role during 2013–2021. The glaciers around these two lakes decreased by 21.81%, and the increase in water supply from warming-triggered glacier melting was a reason of expansion of Lake LongmuCo and Lake Jiezechaqia. The areas of the two artificial salt lakes affiliated with Lake LongmuCo and Lake Jiezechaqia were 0.24 km^2 and 2.67 km^2 in 2013 and rose to 0.51 km^2 and 9.80 km^2 in 2021, respectively. In particular, the continuous exploitations of salt lakes to extract lithium resources have retarded the rate of expansion of Lake LongmuCo and Lake Jiezechaqia. The dams constructed by industrial enterprises have blocked the expansion of Lake LongmuCo to the south. This paper sheds new light on the influences of recent human intervention and climatic variation on alpine lakes within the TP. Due to the importance of alpine lakes in the TP, we need more comprehensive and in-depth efforts to protect the lake ecosystems within the national nature reserves.

Keywords: lake area changes; climate change; anthropogenic activity; Tibetan Plateau; nature reserve; remote sensing monitoring

Citation: Zhao, Z.; Hu, Z.; Zhou, J.; Kan, R.; Li, W. Response of Two Major Lakes in the Changtang National Nature Reserve, Tibetan Plateau to Climate and Anthropogenic Changes over the Past 50 Years. *Land* **2023**, *12*, 267. https://doi.org/10.3390/land12020267

Academic Editor: Nir Krakauer

Received: 6 January 2023
Revised: 12 January 2023
Accepted: 15 January 2023
Published: 17 January 2023

1. Introduction

Lakes not only play important roles in the global hydrological system and biophysical environment [1–3] but also provide vital ecosystem services for the sustainable development of the global economy [3–6]. Lake area change is a reliable indicator of climate change and anthropogenic disturbance, especially lakes in arid and cold regions [7–9]. In recent decades, lakes worldwide have shown large and widespread variations in the context of accelerated climatic change and increasing anthropogenic impacts [9–13]. Major threats to lakes include the human use of land, such as farming, mining, spatial expansion of human settlements [4,14], and climatic variation, factors that influence the area, level, and volume of lakes, especially in different latitudes [4,7,14–20]. Protecting and restoring natural ecosystems, including lake ecosystems, is widely viewed as a win–win strategy for addressing

the challenges of human influence and climate change [4,12,21]. The establishment of protected areas is a major component of ecosystem conservation [22]. Globally, there were 261,200 Protected Areas in 2019 covering about 15% of the land area [23–25].

The Tibetan Plateau (TP) is considered the "Third pole" [26] and the "Asian water tower" [27]. There are currently ~1400 lakes on the TP, covering an area of approximately 5×10^4 km^2 [10,28]. Lake ecosystems in the TP have been severely altered by climatic warming and human activity [8,29]. Since the 1980s, a large number of nature reserves have been established to conserve natural ecosystems, including lake ecosystems, by restricting and prohibiting human activities [25,30]. In 2020, the Three-River-Source National Park, one of the first national parks in China, was established on the TP [25]. With the implementation of constructive projects to protect the ecological security of nature reserves on the TP, human activities showed positive impacts on the alpine ecosystems. However, there are still negative impacts of anthropogenic changes on ecosystems such as lake ecosystems [25]. Investigation of the lake spatio-temporal variability on the TP is essential for understanding the current state and future trajectory of lakes, evaluating water resources, and analyzing hydrologic processes in the context of climatic variation and anthropogenic intervention [8,28]. However, the paucity of historical lake area records and the physical difficulties of accessing results have severely limited our knowledge of the spatial patterns and processes of lakes in remote areas of the TP [8,9]. Fortunately, remote sensing (RS) has been widely used to examine lake dynamics and to incorporate more factors in analyses of climate change and human impact [25,31–34].

Numerous RS studies have reported that lake expansion since the late 1990s is one of the most outstanding environmental change events on the TP [10,34–36]. The lake expansion has been accelerated since the 2000s and has primarily occurred in areas of the Inner TP, such as the Changtang Plateau [34–37], while most of the lakes in the southern and eastern TP have experienced shrinkage over the last several decades [38–45]. Generally, climate factors were the major cause for the lake area changes on the TP, especially for lakes in the endorheic TP [40–45]. Moreover, climate change effects such as increased precipitation, rising temperature, glacial melting, and permafrost degradation have contributed to the lake changes in the TP in recent years [28,34–39]. However, research on the role of human activities in the lake changes is still lacking. In particular, researchers have generally focused on the influences of climate changes to lake changes in the Inner TP. Very limited studies have been conducted on the pivotal role of human intervention in the lake changes within the endorheic TP, such as the influences of the exploitation of salt lakes in the Changtang National Nature Reserve (CNNR) on lake changes.

Here, we selected two lakes (Lake LongmuCo and Lake Jiezechaqia) in the CNNR in the hinterland of the TP. These lakes are in one of the 25 National Key Ecological Function Areas in China and are also in one of the key implementation areas of the ecological conservation and restoration project in the TP ecological barrier area [46]. Furthermore, since Lake Jiezechaqia and Lake LongmuCo have the first and second lithium resource reserves in Tibet, respectively, two artificial salt lakes have been built around them by a state-owned enterprise. After the exploitation of salt lakes, these two lakes have become the only two lakes where lithium is being extracted at present in the CNNR, and the two largest lakes in Tibet for extracting lithium resources. Employing Landsat archive data and meteorological data, this study aimed to explore the patterns of area changes of lakes from 1972 to 2021 and to analyze the climatic and anthropogenic impacts on lake area changes. As a case study, this paper provides a better understanding of lake area change and its influencing factors within the TP.

2. Materials and Methods

2.1. Study Area

Lake LongmuCo (80°27.41′ E, 34°36.85′ N, 5005 m a.s.l.) and Lake Jiezechaqia (80°54.14′ E, 33°57.26′ N, 4527 m a.s.l.) are glacier-fed lakes [10]. They are located on the western edge of the CNNR [47,48] (Figure 1). Calculated from Landsat images, the

average areas of Lake LongmuCo and Lake Jiezechaqia were 106.80 km^2 and 114.98 km^2 in the period of 1972–2021, respectively. The nearest road to Lake LongmuCo is National Highway No. 219 (Figure 1).

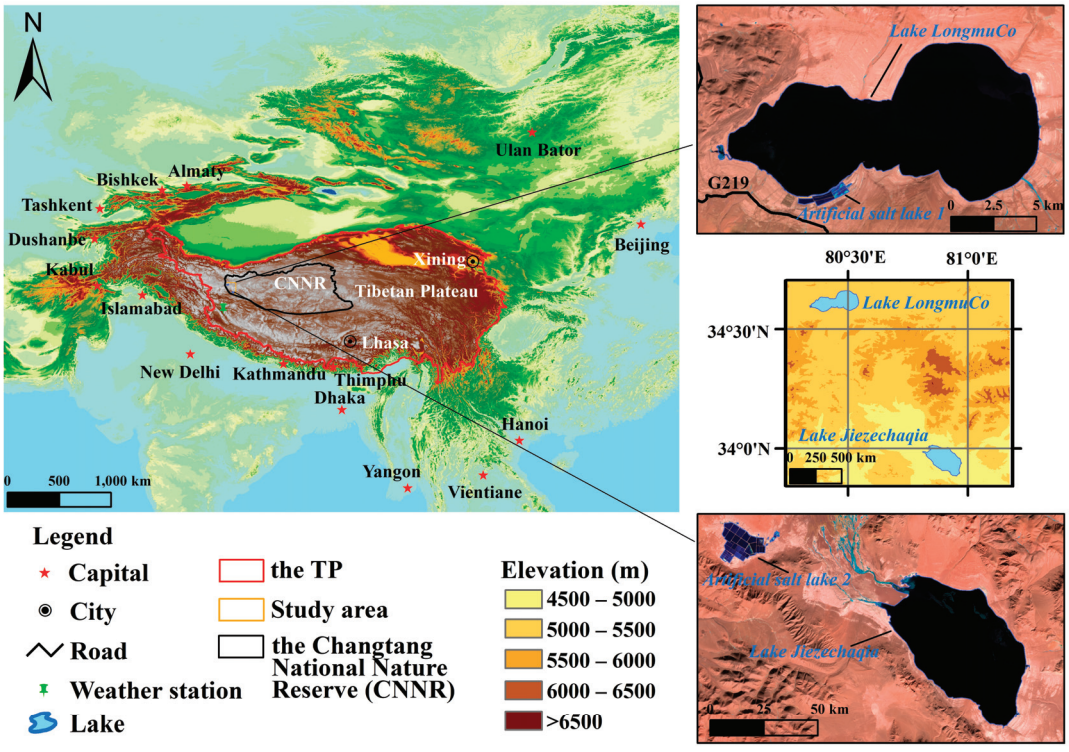

Figure 1. Locations of Lake LongmuCo and Lake Jiezechaqia and their surrounding topography.

CNNR, with a total area of 29.8 × 10^4 km^2, officially became a nature reserve in 1993 for protecting and restoring natural habitats, including grassland, desert steppe, wetland, and lake ecosystems. It will become a national park in the future. The climate type of the CNNR is a plateau continental climate. Annual mean temperature and annual precipitation around the areas of Lake LongmuCo and Lake Jiezechaqia are 1.06 °C and 72.88 mm, respectively [49].

2.2. Data and Processing

2.2.1. Remote Sensing (RS) Data

For lake area mapping, a total of 30 Landsat satellite images were used in this study (Table 1). These satellite data include one Landsat 1 MSS scene, ten Landsat 5 TM scenes, ten Landsat 7 ETM+ scenes, and nine Landsat 8 OLI scenes from 1972 to 2021, downloaded from the official website of the United States Geological Survey (http://glovis.usgs.gov, accessed on 1 August 2022). Among the 30 Landsat satellite image scenes, the maximum and minimum values of cloud cover were 25.80% and 0.72% (Table 1), respectively.

Since the change rate of lake extent on the TP was less than 2% from September to December, we chose RS data (Table 1) in this period each year for comparison of the interannual variability of lake area [9,50,51]. If there were several archived Landsat images available during the period from September to December each year, we selected the one with the lowest cloud cover for lake area mapping. However, the interpretation of lake extent was not performed if there were no high-quality archived images available.

Table 1. RS data used to derive the lake area.

Path	Row	Date	Name	Sensor Source	Resolution (m)	Cloud Cover (%)
156	36	19 December 1972	LM11560361972354AAA02	Landsat MSS	60	20.00
145	36	7 November 1987	LT51450361987311SGI00	Landsat TM	30	5.11
145	36	24 October 1988	LT51450361988298SGI00	Landsat TM	30	3.89
145	36	9 December 1993	LT51450361993343ISP00	Landsat TM	30	4.34
145	36	25 October 1994	LT51450361994298ISP00	Landsat TM	30	1.89
145	36	15 November 1996	LT51450361996320ISP00	Landsat TM	30	2.56
145	36	2 November 1997	LT51450361997306ISP00	Landsat TM	30	25.80
145	36	29 September 1999	LE71450361999272SGS01	Landsat ETM+	30	1.00
145	36	4 December 2000	LE71450362000339SGS00	Landsat ETM+	30	15.00
145	36	20 October 2001	LE71450362001293SGS00	Landsat ETM+	30	4.00
145	36	24 November 2002	LE71450362002328SGS05	Landsat ETM+	30	8.00
145	36	11 November 2003	LE71450362003315ASN01	Landsat ETM+	30	4.68
145	36	10 September 2004	LE71450362004254ASN01	Landsat ETM+	30	1.48
145	36	2 December 2005	LE71450362005336SGS00	Landsat ETM+	30	6.36
145	36	18 October 2006	LE71450362006291PFS00	Landsat ETM+	30	6.62
145	36	22 November 2007	LE71450362007326PFS00	Landsat ETM+	30	4.95
145	36	2 December 2008	LT51450362008337BJC00	Landsat TM	30	18.81
145	36	3 November 2009	LT51450362009307KHC00	Landsat TM	30	17.91
145	36	8 December 2010	LT51450362010342KHC00	Landsat TM	30	3.67
145	36	22 September 2011	LT51450362011265KHC00	Landsat TM	30	4.00
145	36	16 September 2012	LE71450362012260PFS00	Landsat ETM+	30	16.98
145	36	27 September 2013	LC81450362013270LGN01	Landsat OLI	30	1.53
145	36	17 November 2014	LC81450362014321LGN00	Landsat OLI	30	2.51
145	36	20 November 2015	LC81450362015324LGN00	Landsat OLI	30	1.80
145	36	8 December 2016	LC81450362016343LGN00	Landsat OLI	30	2.10
145	36	22 September 2017	LC81450362017265LGN00	Landsat OLI	30	2.43
145	36	25 September 2018	LC81450362018268LGN00	Landsat OLI	30	12.40
145	36	12 September 2019	LC81450362019255LGN02	Landsat OLI	30	1.19
145	36	30 September 2020	LC81450362020274LGN00	Landsat OLI	30	0.72
145	36	4 November 2021	LC81450362021308LGN00	Landsat OLI	30	9.65

2.2.2. Meteorological Data

In this study, the temperature and precipitation data were obtained from the China Meteorological Data Service Center (http://data.cma.cn, accessed on 5 August 2022). Among these data, we used the annual mean temperature and annual precipitation recorded at Shiquanhe Weather Station in the period of 1972–2021, the nearest meteorological station to Lake LongmuCo and Lake Jiezechaqia (Figure 1), to analyze the environmental impacts to lake changes.

2.2.3. Glacier Data

In this study, the glacier data were obtained from the first glacier inventory dataset of China (1987–2004) and the second glacier inventory dataset of China (2006–2011) [52]. Among these data, we analyzed the glacier area changes around the regions of Lake LongmuCo and Lake Jiezechaqia by comparison between the two glacier inventory datasets mentioned above.

2.2.4. Other Auxiliary Data

In this study, a 1:100,000 scale topographic map was used as the base image for geometric correction, and it was obtained from the Resource and Environment Science and Data Center (https://www.resdc.cn, accessed on 10 July 2022).

The digital elevation model (DEM) data with 30 m × 30 m spatial resolution were also obtained from the Resource and Environment Science and Data Center (https://www.resdc.cn, accessed on 2 August 2022), and the DEM data were used in drawing Figure 1.

The boundaries of the TP and the CNNR were obtained from Zhang et al. [53] and Zhang et al. [48], respectively, and these boundaries were also used in drawing Figure 1.

Lake volume change data were obtained from Zhang et al. [54] for analyzing volume changes of lakes within the study area. The lake area data were obtained from Zhang et al. [10] for data comparison.

2.2.5. Data Preparation

Using ENVI 5.3 software, the data preprocessing (Figure 2) of Landsat satellite images was divided into two steps: (1) geometric correction and (2) radiometric calibration and atmospheric correction. In Step (1), the value of root mean square error (RMSE) of each image was less than 0.5 pixels.

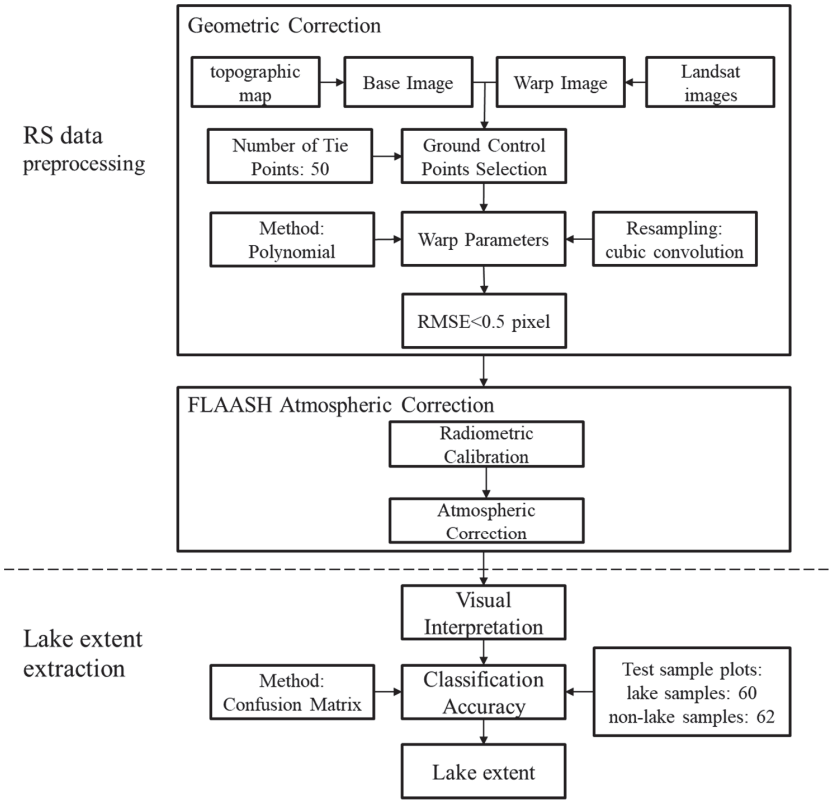

Figure 2. Workflow of lake area mapping.

After the steps mentioned above, 30 Landsat satellite images were used for the extraction of the extent of lakes. Then, we used the method of visual interpretation to delineate the selected lakes and non-lake land covers between 1972 and 2021 (Figure 2). Accuracy of lake extent was assessed by using the method of Confusion Matrix [55]. In this study, the overall accuracy of Lake LongmuCo and Lake Jiezechaqia extents in 2021 were 99.30% and 99.09%, k = 0.9826 and 0.9789; producer accuracies were 99.44% and 100.00%; and user accuracies were 98.01% and 97.21%, respectively.

2.2.6. Data Analysis

The equations used to calculate the changes in the lake area are as follows [56–58].

$$\alpha = \frac{S_{next} - S_{previous}}{S_{previous}} * 100\% \quad (1)$$

$$\beta = \frac{S_{next} - S_{previous}}{S_{previous}} * \frac{1}{T} * 100\% \quad (2)$$

In Equations (1) and (2), α (%) is the proportional change in the lake area and β (%) is the annual change rate. $S_{previous}$ (km^2) is the lake area in the previous period, S_{next} (km^2) is the lake area in the next time slot, and T (a) is the period in years. In this study, the above equations were used to explore the area changes of Lake LongmuCo, Lake Jiezechaqia, Artificial Salt Lake 1, and Artificial Salt Lake 2, respectively.

When analyzing the impacts of climate factors on lake area changes, a large number of studies used Pearson's correlation coefficient [31,58]. We also used this coefficient for analyzing environmental impacts on lake changes and for comparison between our results and other datasets.

The least squares method was often used in numerous studies to detect the overall trends and to divide a time series into different subperiods by providing several trend change points [59,60]. In this study, we used the operation code outlined by Tomé and Miranda [59] in the ENVI 5.3/IDL 8.5 software to explore the stage characteristics of lakes and climate factors.

3. Results

3.1. Pattern of Lake Changes

From 1972 to 2021, the average area of Lake LongmuCo was 106.80 km^2. The area of Lake LongmuCo was 100.60 km^2 in 1972 and rose to 113.48 km^2 in 2021 (Table S1), and it increased by 12.88 km^2 from 1972 to 2021. Over the same period, the proportional change in the area of Lake LongmuCo, α (%), was 12.81% (r = 0.929, p = 0.000 < 0.01) (Figure 3). This means that the annual rate of change in the lake area β (%), was 0.26%/a. Figure 3 shows that changes in Lake LongmuCo could be divided into two periods: (1) a slight expansion from 1972 to 1999; (2) a period of rapid expansion from 2000 to 2021. During 1972–1999, the area of Lake LongmuCo increased with a β (%) of 0.09%/a (r = 0.872, p = 0.005 < 0.01), while it increased with a β (%) of 0.43%/a (r = 0.998, p = 0.000 < 0.01) during 2000–2021.

During 1972–2021, the average area of Lake Jiezechaqia was 114.98 km^2. The area of Lake Jiezechaqia was 108.35 km^2 in 1972 and rose to an expanded 122.31 km^2 in 2021 (Table S1), and it increased by 13.96 km^2 from 1972 to 2021. Over the same period, α (%) of Lake Jiezechaqia was 12.88% (r = 0.924, p = 0.000 < 0.01) (Figure 3), and this means that β (%) was 0.26%/a. Figure 3 shows that changes in Lake Jiezechaqia also could be divided into two periods. During 1972–1999, a slight expansion occurred in Lake Jiezechaqia with a β (%) of 0.07%/a (r = 0.795, p = 0.058 < 0.1). During 2000–2021, a rapid expansion occurred in Lake Jiezechaqia with a β (%) of 0.47%/a (r = 0.992, p = 0.000 < 0.01), and the change rate of lake area in this period is similar to that of Lake LongmuCo, which is obviously higher than the change rate of 1972–1999.

3.2. Environmental Impacts on Lake Changes

From 1972 to 2021, a significant increase in annual mean temperature at a rate of 0.05 °C/a (r = 0.799, p = 0.000 < 0.01) demonstrated a progressively warmer climate throughout the basins of Lake LongmuCo and Lake Jiezechaqia and their surrounding areas (Figure 4). As shown in Figure 4, it can be seen that the annual precipitation of the study area fluctuated in the period of 1972–2021 (r = 0.031, p = 0.830 > 0.1). Over the past 50 years, the annual mean temperature and annual precipitation varied from −0.16 °C and 70.0 mm to 2.33 °C and 84.7 mm, respectively. During 1972–2021, the annual mean temperature reached a maximum in 2016 (3.65 °C), while the highest annual precipitation occurred in 2015 (138.2 mm). Furthermore, in the 1993–2021 period, the increased rate of annual mean temperature (0.06 °C/a, r = 0.598, p = 0.000 < 0.01) was twice as high as that (0.03 °C/a, r = 0.302, p = 0.092 < 0.1) in the period of 1972–1992.

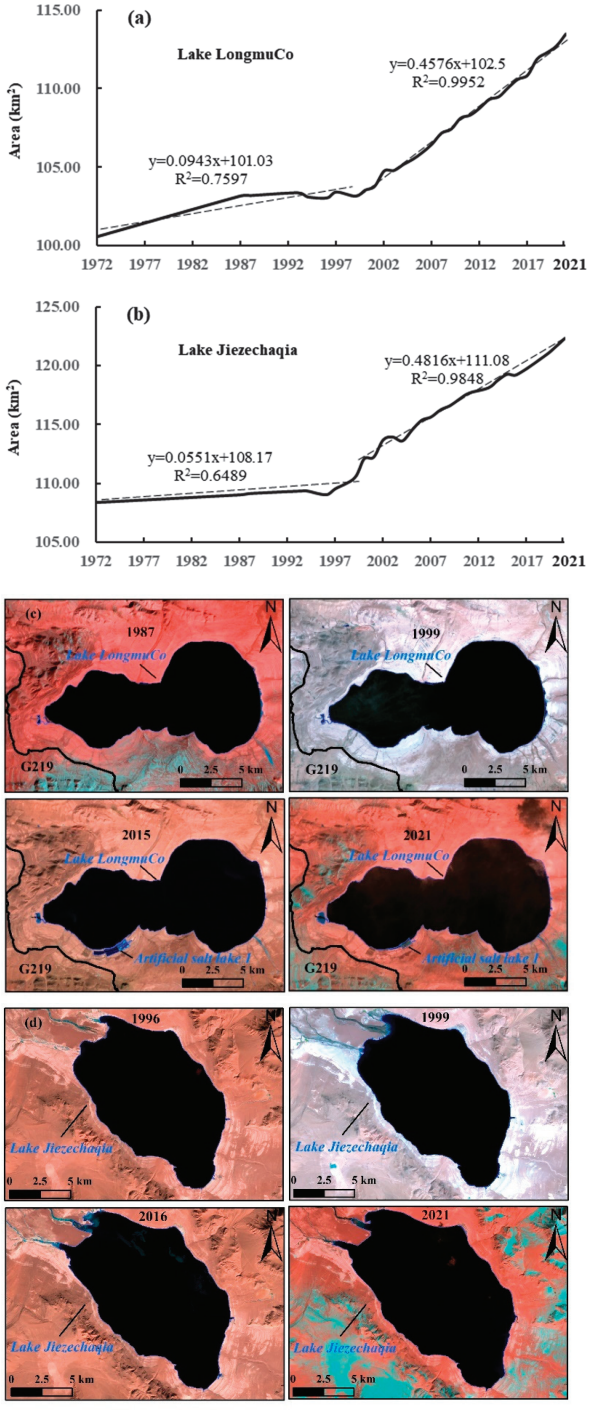

Figure 3. Area changes (**a**,**b**) and spatial distribution in different years (**c**,**d**) of Lake LongmuCo and Lake Jiezechaqia between 1972 and 2021.

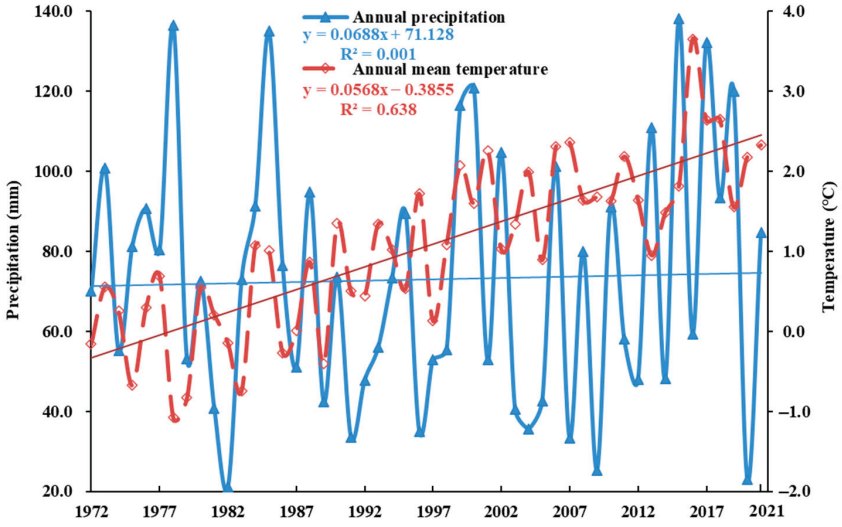

Figure 4. Changes in the annual mean temperature and annual precipitation around the study area during 1972–2021.

The results (Table 2) indicated positive correlations between temperature and areas of Lake LongmuCo and Lake Jiezechaqia, reaching the 99% confidence level. The good correlation implied that the annual mean temperature was likely a major contributor to the observed changes in the areas of Lake LongmuCo and Lake Jiezechaqia from 1972 to 2021. Table 2 also revealed that precipitation was not correlated with the areas of Lake LongmuCo and Lake Jiezechaqia. Furthermore, Lake LongmuCo and Lake Jiezechaqia are glacier-fed lakes [10,61] and the glaciers around these two lakes decreased by 21.81% in the first and second glacier inventories of China (Figure 5). The area of the largest glacier (Glacier Code: 5Z431I0075) around Lake LongmuCo and Lake Jiezechaqia decreased by 43.26%, while that of the smallest glacier (Glacier Code: 5Z431I0049) near these two lakes decreased by 95.53%. It seems that the increase in water supply from warming-triggered glacier melting was a reason for expansion of Lake LongmuCo and Lake Jiezechaqia [49].

Table 2. Pearson's correlation coefficients for lake area and climate factors.

Period	Lake	Annual Mean Temperature	Annual Precipitation
1972–2021	LongmuCo	0.588 **	0.180
1972–2021	Jiezechaqia	0.502 *	0.124

Notes: ** $p < 0.01$, * $p < 0.05$.

3.3. Human Impacts on Lake Changes

The TP reserves comprise 75% of China's lithium resources, primarily distributed in salt lake brine. In recent years, increasing numbers of salt lakes have been mined to obtain lithium resources, although these alpine lakes are very sensitive to human activities [9]. The extensive exploitation has resulted in severe changes in the lake area, lake function, and landscape of the TP [9,62]. The Lake LongmuCo and Lake Jiezechaqia reserves comprise 1.89 and 2.01 million tons of lithium resources, respectively [49]. After 2013, salts from the Lake LongmuCo and Lake Jiezechaqia began to be mined and industrialized (Figure 6).

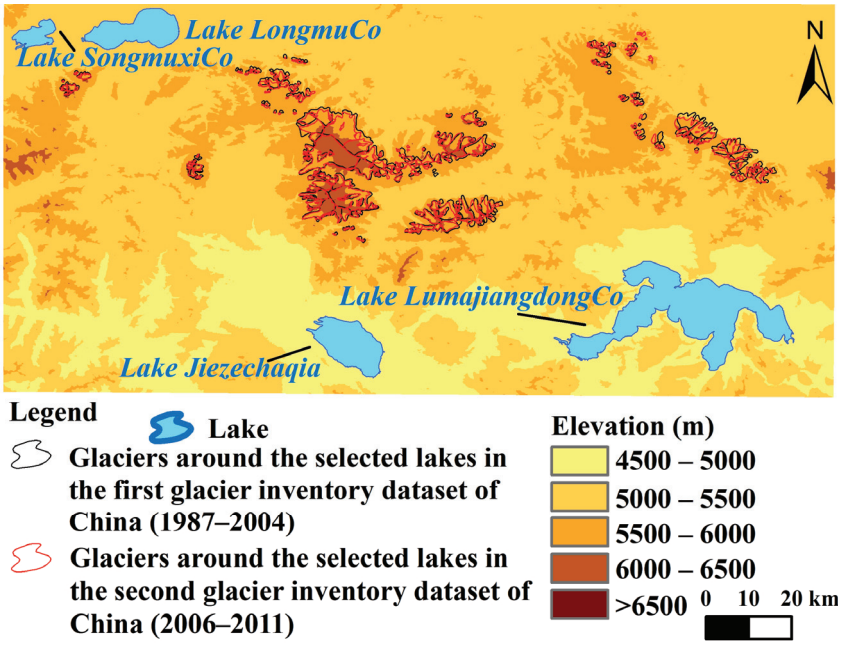

Figure 5. Area changes of glaciers around Lake LongmuCo and Lake Jiezechaqia.

More specifically, Figure 6 illustrated the changes in Lake LongmuCo and Lake Jiezechaqia exposed to the exploitation of lithium resources. Since 2013, one state-owned enterprise engaging in Lake LongmuCo exploitation has settled in and built dams to shift the water from Lake LongmuCo to an artificial salt lake (Figure 6). From 2013 to 2021, the average area of the Artificial Salt Lake 1 constructed by the state-owned enterprise was 0.88 km^2. The area of this artificial salt lake was 0.24 km^2 in 2013 and rose to 0.51 km^2 in 2021 (Table S1), and the maximum area of it occurred in 2015 (1.49 km^2). Figure 6 shows that the changes in the Artificial Salt Lake 1 can be divided into two periods: (1) a rapid expansion from 2013 to 2015; (2) a decrease from 2016 to 2021. During 2013–2015, the area of Artificial Salt Lake 1 increased, with a β (%) of 174.96%/a ($r = 0.928$, $p = 0.011 < 0.05$). During 2016–2021, the area of Artificial Salt Lake 1 decreased, with a β (%) of −9.36%/a ($r = -0.973$, $p = 0.003 < 0.01$).

In 2013, the enterprise that mined Lake LongmuCo also industrialized Lake Jiezechaqia and shifted water from Lake Jiezechaqia to Artificial Salt Lake 2 through a 20 km long pipeline. Different from the exploitation of Lake LongmuCo, Artificial Salt Lake 2 was not adjacent to Lake Jiezechaqia, and lay to the northwest of Lake Jiezechaqia. During 2013–2021, the average area of the Artificial Salt Lake 2 was 8.79 km^2 (Figure 6). The area of this artificial salt lake was 2.67 km^2 in 2013 and rose to 9.80 km^2 in 2021 (Table S1), and the maximum area of it occurred in 2017 (12.02 km^2). Figure 6 shows that changes in Artificial Salt Lake 2 also could be divided into two periods. During 2013–2017, a rapid expansion occurred in Artificial Salt Lake 2 with a β (%) of 70.04%/a ($r = 0.940$, $p = 0.017 < 0.05$). During 2018–2021, a slight decrease occurred in Artificial Salt Lake 2 with a β (%) of −3.69%/a ($r = -0.702$, $p = 0.149 > 0.1$).

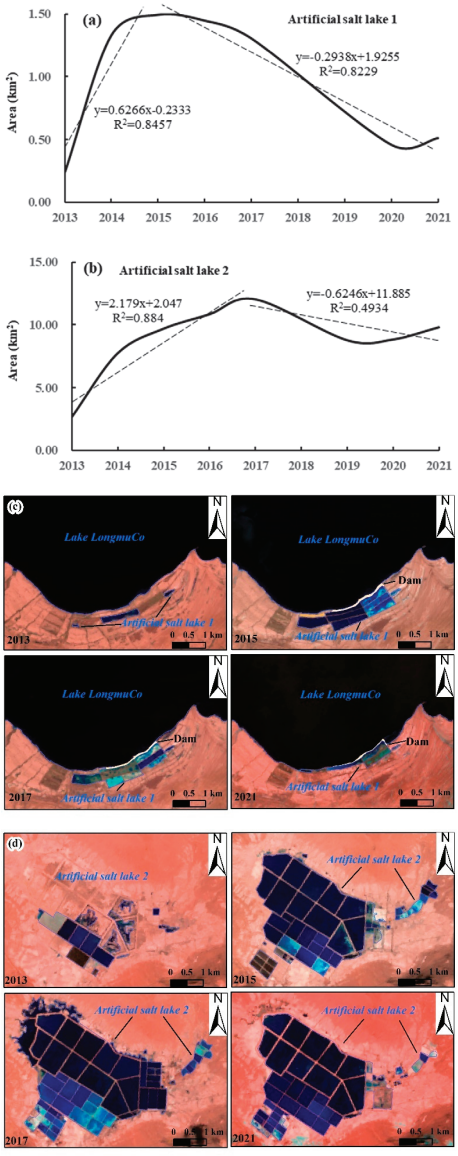

Figure 6. Area changes (**a**,**b**) and spatial distribution in different years (**c**,**d**) of the artificial salt lakes between 2013 and 2021.

Although the areas of the two artificial salt lakes have been shrinking in recent years, salt lake exploitations have spawned a host of complex environmental issues in the salt lake regions. Here, we selected two lakes (Lake SongmuxiCo and Lake LumajiangdongCo) in the CNNR to compare their area changes with that of Lake LongmuCo and Lake Jiezechaqia. These two lakes, like Lake LongmuCo and Lake Jiezechaqia, are also endorheic lakes and glacier-fed lakes [54]. The above four lakes could be observed on the same Landsat image. Among them, Lake SongmuxiCo is adjacent to Lake LongmuCo and Lake LumajiangdongCo is adjacent to Lake Jiezechaqia (Figure 5). Area changes of Lake SongmuxiCo and Lake LumajiangdongCo were mainly affected by climate change over the past several

decades [41–44,54], and according to Landsat image monitoring in this study, there was no exploitation of salt lakes in these two lakes in recent years. Figure 7 illustrated the area and water storage changes of Lake LongmuCo, Lake Jiezechaqia, Lake SongmuxiCo, and Lake LumajiangdongCo. From 1972 to 2021, the above four lakes all experienced lake expansion, Lake SongmuxiCo and Lake LumajiangdongCo expanded by more than 20%, while Lake LongmuCo and Lake Jiezechaqia only expanded by ~13% (Figure 7). After 2013, the β (%) of Lake LongmuCo and Lake Jiezechaqia was less than 0.5%/a, while the β (%) of Lake SongmuxiCo and Lake LumajiangdongCo was more than 1%/a (Figure 7). It seems that shifting the water from Lake LongmuCo and Lake Jiezechaqia to artificial salt lakes for extracting lithium has retarded the rate of expansion of these two lakes. During 2015–2019, when the salt lakes were developed, the change rates of water storage in Lake LongmuCo and Lake Jiezechaqia decreased by 7.68% and 40.05% compared with 2010–2015 (Figure 7). At the same time, the change rates of water storage in Lake SongmuxiCo and Lake LumajiangdongCo, which have no salt lake exploitations, increased by 48.44% and 6.95% compared with 2010–2015 (Figure 7). Then, in the period of 2017–2021, Lake LongmuCo inundated its south lakeshore outside the dams during its southward expansion (Figure 6). In other words, the dams that created Artificial Salt Lake 1 have blocked the expansion of Lake LongmuCo to the south (Figure 6). Next, the artificial salt lake exploitations have altered the landscape surface from grassland and saline alkali land to a water body [63]. Due to the vulnerability of the environment within Lake LongmuCo and Lake Jiezechaqia, as well as human intervention, the environmental processes of these lakes have been strongly influenced.

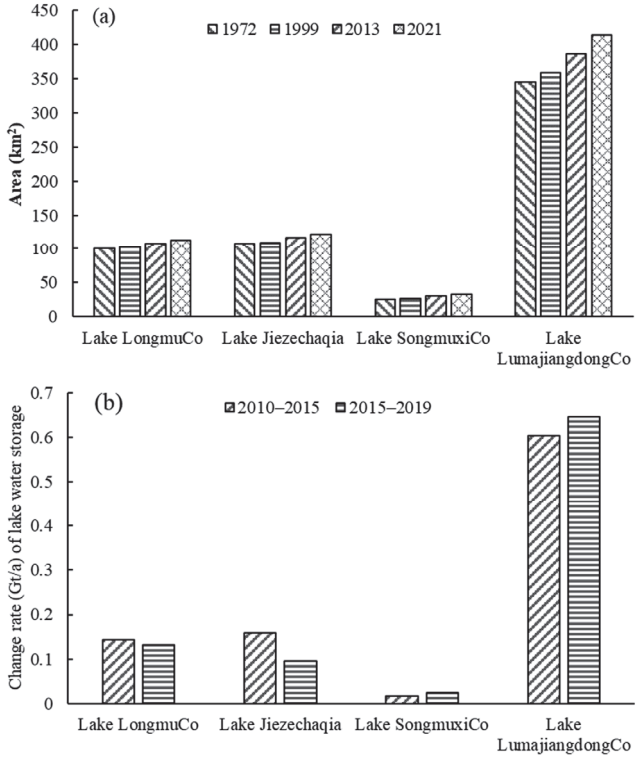

Figure 7. Comparison of area (**a**) and water storage (**b**) changes of Lake LongmuCo, Lake Jiezechaqia, Lake SongmuxiCo, and Lake LumajiangdongCo.

4. Discussion

Lakes are important indicators of the Earth's hydrological cycle [64]. A large number of studies have revealed that lake changes over the TP were characterized by strong spatio-temporal heterogeneity during the 1960s–2021 [10,35,65–69]. A long-term dataset for lakes on the TP was created by Zhang et al. [10] using Landsat imagery, and we compared our results with this dataset. Note that for the areas of Lake LongmuCo and Lake Jiezechaqia, the data obtained by Zhang et al. [10] and the data in this study were consistent (r = 0.996 and 0.999, $p = 0.000 < 0.01$). This means that the results of this study are credible. The area of Lake LongmuCo increased at a rate of 0.22%/a during 1970–2021 [10], and we found that the area of Lake LongmuCo increased at a rate of 0.26%/a during the same period. Our study confirmed the findings of Zhang et al. [10].

Over the past decades, lake expansion, especially in the Inner TP, has become one of the most prominent environmental change events on the TP [26,35]. Approximately three-quarters of the lakes on the TP showed noticeable expansion since the late 1990s and accelerated their expansion in the 2000s [38,68]. The year 2000 appeared to be a trend changing point for lake area changes on the TP [57]. We also found that Lake LongmuCo and Lake Jiezechaqia exhibited remarkable growth after 1999. Our study corroborated the findings of previous studies [35–38,66].

Over the TP, the annual mean temperature noticeably increased at a rate of 0.32 °C/decade since 1961 [67]. We found that the annual mean temperature significantly increased at a rate of 0.50 °C/decade since 1972 in the study area, and it was higher than that of the TP.

Numerous previous studies have shown that climate factors such as precipitation, warming-triggered glacial meltwater, air temperature, evapotranspiration, and warming-triggered permafrost melting were important contributors to lake changes over the TP in recent decades [10,24–26,34–39,63–66]. Moreover, the temperature was likely responsible for the observed lake changes on the Changtang Plateau [29,38,57,65]. We also found that Lake LongmuCo and Lake Jiezechaqia within the Changtang Plateau were sensitive to air temperature. Some researchers have noticed that there appears to be a positive spatial correlation between glacier melting and lake expansion [49,57,68,69]. We also found that Lake LongmuCo and Lake Jiezechaqia may receive an increased meltwater supply from glacier melting under the influence of warmer climates.

The natural ecosystems of the TP are very sensitive to human intervention [8,26,29,46,70], and the establishment of nature reserves has acted as an effective strategy for conserving ecosystems and restricting and prohibiting human activities [25–30]. The protected areas include various types of ecosystems, such as lakes, grasslands, and forests. Although the vast majority of lakes on the TP have been protected, there are still some lakes that have been developed by humans for economic profit [9,25]. A recent study indicated that the exploitation of salt lakes created a threat to the environment of the TP [9]. The dams constructed by industrial enterprises have altered water flow, affected the direction of lake changes, and disturbed local ecosystems [9,71]. In this study, we found that the artificial salt lake exploitations in the regions of Lake LongmuCo and Lake Jiezechaqia have retarded the rate of expansion of these two lakes during 2013–2021, and found that the dams of the artificial salt lake have blocked the expansion of Lake LongmuCo to the south.

5. Conclusions

This study used long-term Landsat imagery and meteorological records to monitor the temporal evolution patterns of two major lakes in the Changtang National Nature Reserve during 1972–2021 and examined climatic and anthropogenic impacts on lake area changes. Over nearly 50 years, the area of Lake LongmuCo and Lake Jiezechaqia significantly increased by 12.88 km^2 and 13.96 km^2, respectively. After 1999, Lake LongmuCo and Lake Jiezechaqia all entered into a period of rapid expansion. The annual mean temperature has been increasing since 1972 at a rate of 0.05 °C/a, while the change in annual precipitation was not significant. Furthermore, the annual mean temperature noticeably increased

at a rate of 0.06 °C/a during 1993–2021. Temperature was a major contributor to the observed lake changes over the basins of Lake LongmuCo and Lake Jiezechaqia between 1972 and 2021. And the glaciers around these two lakes decreased by 21.81%, the increase in water supply from warming-triggered glacier melting was a reason of expansion of Lake LongmuCo and Lake Jiezechaqia. With the mining exploitations of salt lakes since 2013, human activities directly contributed to the changes of Lake LongmuCo and Lake Jiezechaqia during 2013–2021. The areas of the two artificial salt lakes affiliated to Lake LongmuCo and Lake Jiezechaqia were 0.24 km^2 and 2.67 km^2 in 2013 and rose to 0.51 km^2 and 9.80 km^2 in 2021, respectively. Additionally, the maximum area of the two artificial salt lakes occurred in 2015 (1.49 km^2) and in 2017 (12.02 km^2), respectively. It seems that shifting the water from Lake LongmuCo and Lake Jiezechaqia to artificial salt lakes for extracting lithium has retarded the rate of expansion of these two lakes. The dams constructed by industrial enterprises have blocked the expansion of Lake LongmuCo to the south. These findings provide vital new light on the responses of lakes to climate change and anthropogenic activities. Now we need more comprehensive and in-depth efforts to protect lake ecosystems within the national nature reserves.

Supplementary Materials: The following supporting information can be downloaded at: https://www.mdpi.com/article/10.3390/land12020267/s1, Table S1: The measured lake areas in this study.

Author Contributions: Conceptualization, Z.Z. and Z.H.; methodology, Z.Z. and Z.H.; software, Z.Z. and J.Z.; validation, Z.H. and R.K.; formal analysis, Z.Z.; investigation, Z.Z. and Z.H.; resources, Z.Z.; data curation, Z.H.; writing—original draft preparation, Z.Z., Z.H., W.L. and J.Z.; writing—review and editing, Z.Z., Z.H., W.L. and R.K.; visualization, Z.Z. and Z.H.; supervision, Z.Z.; project administration, Z.Z.; funding acquisition, Z.Z. and Z.H. All authors have read and agreed to the published version of the manuscript.

Funding: This research was funded by the National Natural Science Foundation of China, grant number 42101293, and the Major Program of National Social Science Foundation of China, grant number 17ZDA158.

Data Availability Statement: The data presented in this study are available on request from the corresponding author.

Conflicts of Interest: The authors declare no conflict of interest.

References

1. Aysen, D.; Erhan, S.; Sehnaz, S. Evaluation of climate and human effects on the hydrology and water quality of Burdur Lake, Turkey. *J. Afr. Earth Sci.* **2019**, *158*, 103569.
2. Liu, W.; Ma, L.; Abuduwaili, J. Anthropogenic Influences on Environmental Changes of Lake Bosten, the Largest Inland Freshwater Lake in China. *Sustainability* **2020**, *12*, 711. [CrossRef]
3. Wang, J.D.; Sheng, Y.W.; Wada, Y. Little impact of the Three Gorges Dam on recent decadal lake decline across China's Yangtze Plain. *Water Resour. Res.* **2017**, *53*, 3854–3877. [CrossRef] [PubMed]
4. Wufu, A.; Wang, H.W.; Chen, Y.; Rusuli, Y.; Ma, L.G.; Yang, S.T.; Zhang, F.; Wang, D.; Li, Q.; Li, Y.B. Lake water volume fluctuations in response to climate change in Xinjiang, China from 2002 to 2018. *PeerJ* **2020**, *8*, e9683. [CrossRef]
5. Grant, L.; Vanderkelen, I.; Gudmundsson, L.; Tan, Z.L.; Perroud, M.; Stepanenko, M.V.; Debolskiy, V.A.; Droppers, B.; Janssen, B.G.A.; Woolway, I.R.; et al. Attribution of global lake systems change to anthropogenic forcing. *Nat. Geosci.* **2021**, *14*, 849–854. [CrossRef]
6. Yang, K.; Yu, Z.Y.; Luo, Y.; Zhou, X.L.; Shang, C.X. Spatial-Temporal Variation of Lake Surface Water Temperature and Its Driving Factors in Yunnan-Guizhou Plateau. *Water Resour. Res.* **2019**, *55*, 4688–4703. [CrossRef]
7. Liu, W.; Wu, J.L.; Zeng, H.A.; Ma, L. Geochemical evidence of human impacts on deep Lake Fuxian, southwest China. *Limnologica* **2014**, *45*, 1–6. [CrossRef]
8. Luo, S.X.; Song, C.Q.; Zhan, P.F.; Liu, K.; Chen, T.; Li, W.K.; Ke, L.H. Refined estimation of lake water level and storage changes on the Tibetan Plateau from ICESat/ICESat-2. *Catena* **2021**, *200*, 105177. [CrossRef]
9. Li, H.Y.; Mao, D.H.; Li, X.Y.; Wang, Z.M.; Wang, C.Z. Monitoring 40-Year Lake Area Changes of the Qaidam Basin, Tibetan Plateau, Using Landsat Time Series. *Remote Sens.* **2019**, *11*, 343. [CrossRef]
10. Zhang, G.Q.; Luo, W.; Chen, W.F.; Zheng, G.X. A robust but variable lake expansion on the Tibetan Plateau. *Sci. Bull.* **2019**, *64*, 1306–1309. [CrossRef]

11. Zhu, J.Y.; Song, C.Q.; Wang, J.D.; Ke, L.H. China's inland water dynamics: The significance of water body types. *Proc. Natl. Acad. Sci. USA* **2020**, *117*, 13876–13878. [CrossRef] [PubMed]
12. Cooley, S.W.; Ryan, J.C.; Smith, L.C. Human alteration of global surface water storage variability. *Nature* **2021**, *591*, 78–81. [CrossRef] [PubMed]
13. Mammides, C. A global assessment of the human pressure on the world's lakes. *Glob. Environ. Change* **2020**, *63*, 102084. [CrossRef]
14. Ebner, M.; Schirpke, U.; Tappeiner, U. How do anthropogenic pressures affect the provision of ecosystem services of small mountain lakes? *Anthropocene* **2022**, *38*, 100336. [CrossRef]
15. Zheng, W.X.; Zhang, E.L.; Wang, R.; Langdon, G.P. Human impacts alter driver–response relationships in lakes of Southwest China. *Limnol. Oceanogr.* **2022**, *67*, S390–S402. [CrossRef]
16. Zhang, Q.; Sannigrahi, S.; Bilintoh, M.T.; Zhang, R.; Xiong, B.; Tao, S.Q.; Bilsborrow, R.; Song, C.H. Understanding human-environment interrelationships under constrained land-use decisions with a spatially explicit agent-based model. *Anthropocene* **2022**, *38*, 100337. [CrossRef]
17. Wang, L.Z.; Wehrly, K.; Breck, E.J.; Kraft, S.L. Landscape based assessment of human disturbance for Michigan lakes. *Environ. Manag.* **2010**, *46*, 471–483. [CrossRef]
18. Musie, M.; Sen, S.; Chaubey, I. Hydrologic Responses to Climate Variability and Human Activities in Lake Ziway Basin, Ethiopia. *Water* **2020**, *12*, 164. [CrossRef]
19. Hong, C.P.; Burney, J.A.; Pongratz, J.; Nabel, J.E.M.S.; Mueller, N.D.; Jackson, R.B.; Davis, S.J. Global and regional drivers of land-use emissions in 1961–2017. *Nature* **2021**, *589*, 554–561. [CrossRef]
20. Winkler, K.; Fuchs, R.; Rounsevell, M.; Herold, M. Global land use changes are four times greater than previously estimated. *Nat. Commun.* **2021**, *12*, 2501. [CrossRef]
21. Girardin, C.A.J.; Jenkins, S.; Seddon, N.; Allen, M.; Lewis, S.L.; Wheeler, C.E.; Griscom, B.W.; Malhi, Y. Nature-based solutions can help cool the planet—If we act now. *Nature* **2021**, *593*, 191–194. [CrossRef] [PubMed]
22. Li, F.; Altermatt, F.; Yang, J.; An, S.; Li, A.; Zhang, X. Human activities' fingerprint on multitrophic biodiversity and ecosystem functions across a major river catchment in China. *Glob. Change Biol.* **2020**, *26*, 6867–6879. [CrossRef] [PubMed]
23. Huang, Z.H.; Peng, Y.J.; Wang, R.F.; Cui, G.F.; Zhang, B.; Lu, N.C. Exploring the Rapid Assessment Method for Nature Reserve Landscape Protection Effectiveness—A Case Study of Liancheng National Nature Reserve, Gansu, China. *Sustainability* **2021**, *13*, 3904. [CrossRef]
24. Shrestha, N.; Xu, X.T.; Meng, J.H.; Wang, Z.H. Vulnerabilities of protected lands in the face of climate and human footprint changes. *Nat. Commun.* **2021**, *12*, 1632. [CrossRef] [PubMed]
25. Li, S.C.; Su, S.; Liu, Y.X.; Zhou, X.W.; Luo, Q.X.; Paudel, B. Effectiveness of the Qilian Mountain Nature Reserve of China in Reducing Human Impacts. *Land* **2022**, *11*, 1071. [CrossRef]
26. Yao, T.D.; Thompson, L.G.; Mosbrugger, V.; Zhang, F.; Ma, Y.M.; Luo, T.X.; Xu, B.Q.; Yang, X.X.; Joswiak, D.R.; Wang, W.C.; et al. Third pole environment (TPE). *Environ. Dev.* **2012**, *3*, 52–64. [CrossRef]
27. Immerzeel, W.W.; van Beek, L.P.; Bierkens, M.F. Climate change will affect the Asian water towers. *Science* **2010**, *328*, 1382–1385. [CrossRef]
28. Zhang, G.Q.; Chen, W.F.; Xie, H.J. Tibetan Plateau's Lake level and volume changes from NASA's ICESat/ICESat-2 and Landsat Missions. *Geophys. Res. Lett.* **2019**, *46*, 13107–13118. [CrossRef]
29. Liang, J.; Lupien, L.R.; Xie, H.C.; Vachula, S.R.; Stevenson, A.M.; Han, B.P.; Liu, Q.Q.; He, Y.; Wang, M.D.; Liang, P.; et al. Lake ecosystem on the Qinghai–Tibetan Plateau severely altered by climatic warming and human activity. *Palaeogeogr. Palaeoclimatol. Palaeoecol.* **2021**, *576*, 110509. [CrossRef]
30. Li, S.; Zhang, H.; Zhou, X.; Yu, H.; Li, W. Enhancing protected areas for biodiversity and ecosystem services in the Qinghai–Tibet Plateau. *Ecosyst. Serv.* **2020**, *43*, 101090. [CrossRef]
31. Zhou, L.; Zhu, Y.N.; Du, M.Y.; Wang, S.Y.; He, C.C.; Luo, T.; Wu, J.J.; Zhang, J.; Yang, K. The Long-Time Variation of Lake in Typical Desert Area and Its Human and Climate Change Causes: A Case Study of the Hongjian Nur. *IEEE J. Sel. Top. Appl. Earth Obs. Remote Sens.* **2021**, *14*, 416–425. [CrossRef]
32. Felicia, C.; Omid, M.; Amir, A. Evidence of anthropogenic impacts on global drought frequency, duration, and intensity. *Nat. Commun.* **2021**, *12*, 2754.
33. Li, B.V.; Pimm, S.L. How China expanded its protected areas to conserve biodiversity. *Curr. Biol.* **2020**, *30*, R1334–R1340. [CrossRef]
34. Zhao, Z.L.; Zhang, Y.; Hu, Z.Z.; Nie, X.H. Contrasting Evolution Patterns of Endorheic and Exorheic Lakes on the Central Tibetan Plateau and Climate Cause Analysis during 1988–2017. *Water* **2021**, *13*, 1962. [CrossRef]
35. Yang, K.; Lu, H.; Yue, S.Y.; Zhang, G.Q.; Lei, Y.B.; La, Z.; Wang, W. Quantifying recent precipitation change and predicting lake expansion in the Inner Tibetan Plateau. *Clim. Change* **2018**, *147*, 149–163. [CrossRef]
36. Zhang, Z.; Chang, J.; Xu, C.Y.; Zhou, Y.; Wu, Y.; Chen, X.; Jiang, S.; Duan, Z. The response of lake area and vegetation cover variations to climate change over the Qinghai-Tibetan Plateau during the past 30 years. *Sci. Total Environ.* **2018**, *635*, 443–451. [CrossRef] [PubMed]
37. Song, C.Q.; Huang, B.; Ke, L.H.; Richards, K.S. Remote sensing of alpine lake water environment changes on the Tibetan Plateau and surroundings: A review. *ISPRS J. Photogramm. Remote Sens.* **2014**, *92*, 26–37. [CrossRef]

38. Dong, S.Y.; Peng, F.; You, Q.G.; Guo, J.; Xue, X. Lake dynamics and its relationship to climate change on the Tibetan Plateau over the last four decades. *Reg. Environ. Change* **2018**, *18*, 477–487. [CrossRef]
39. Woolway, R.I.; Kraemer, B.M.; Lenters, J.D.; Merchant, C.J.; O'Reilly, C.M.; Sharma, S. Global lake responses to climate change. *Nat. Rev. Earth Environ.* **2020**, *1*, 388–403. [CrossRef]
40. Zhang, G.Q.; Yao, T.D.; Chen, W.F.; Zheng, G.X.; Shum, C.K.; Yang, K.; Piao, S.L.; Sheng, Y.W.; Yi, S.; Li, J.L.; et al. Regional differences of lake evolution across China during 1960s–2015 and its natural and anthropogenic causes. *Remote Sens. Environ.* **2019**, *221*, 386–404. [CrossRef]
41. Zhang, G.Q.; Yao, T.D.; Xie, H.J.; Yang, K.; Zhu, L.P.; Shum, C.K.; Bolch, T.; Yi, S.; Allen, S.; Jiang, L.G.; et al. Response of Tibetan Plateau lakes to climate change: Trends, patterns, and mechanisms. *Earth-Sci. Rev.* **2020**, *208*, 103269. [CrossRef]
42. Lei, Y.B.; Yang, K.; Wang, B.; Sheng, Y.W.; Bird, B.W.; Zhang, G.Q.; Tian, L.D. Response of inland lake dynamics over the Tibetan Plateau to climate change. *Clim. Change* **2014**, *125*, 281–290. [CrossRef]
43. Wu, Y.H.; Zhu, L.P. The response of lake-glacier variations to climate change in Nam Co Catchment, central Tibetan Plateau, during 1970–2000. *J. Geogr. Sci.* **2008**, *18*, 177–189. [CrossRef]
44. Wang, X.; Siegert, F.; Zhou, A.G.; Franke, J. Glacier and glacial lake changes and their relationship in the context of climate change, Central Tibetan Plateau 1972–2010. *Glob. Planet. Change* **2013**, *111*, 246–257. [CrossRef]
45. Khadka, N.; Zhang, G.Q.; Thakuri, S. Glacial Lakes in the Nepal Himalaya: Inventory and Decadal Dynamics (1977–2017). *Remote Sens.* **2018**, *10*, 1913. [CrossRef]
46. Fu, B.J.; Ouyang, Z.Y.; Shi, P.; Fan, J.; Wang, X.D.; Zheng, H.; Zhao, W.W.; Wu, F. Current Condition and Protection Strategies of Qinghai-Tibet Plateau Ecological Security Barrier. *Bull. Chin. Acad. Sci.* **2021**, *36*, 1298–1306. (In Chinese with English Abstract)
47. Qiao, B.J.; Zhu, L.P. Differences and cause analysis of changes in lakes of different supply types in the north-western Tibetan Plateau. *Hydrol. Process.* **2017**, *31*, 2752–2763. [CrossRef]
48. Zhang, Y.L.; Wu, X.; Qi, W.; Li, S.C.; Bai, W.Q. Characteristics and protection effectiveness of nature reserves on the Tibetan Plateau, China. *Resour. Sci.* **2015**, *37*, 1455–1464. (In Chinese with English Abstract)
49. Li, Z.G.; Li, H.Z.; Wu, H.B.; Zhu, X.Y.; Li, X.X. Glaciers and lake changes (1991–2013) and their causes in the Jiezechaka Basin, northwest Tibetan Platea. *J. Arid Land Resour. Environ.* **2016**, *30*, 185–191. (In Chinese with English Abstract)
50. Li, J.L.; Sheng, Y.W.; Luo, J.C.; Shen, Z.F. Remotely sensed mapping of inland lake area changes in the Tibetan plateau. *J. Lake Sci.* **2011**, *23*, 311–320. (In Chinese with English Abstract)
51. Song, C.Q.; Sheng, Y.W. Contrasting evolution patterns between glacier-fed and non-glacier-fed lakes in the Tanggula Mountains and climate cause analysis. *Clim. Change* **2016**, *135*, 493–507. [CrossRef]
52. Guo, W.Q.; Liu, S.Y.; Xu, J.L.; Wu, L.Z.; Shangguan, D.H.; Yao, X.J.; Wei, J.F.; Bao, W.J.; Yu, P.C.; Liu, Q.; et al. The second Chinese glacier inventory: Data, methods and results. *J. Glaciol.* **2015**, *61*, 357–372. [CrossRef]
53. Zhang, Y.L.; Li, B.Y.; Zheng, D. Datasets of the Boundary and Area of the Tibetan Plateau. *Glob. Change Res. Data Publ. Repos.* **2014**, *69*, 164–168.
54. Zhang, G.Q.; Bolch, T.; Chen, W.F.; Crétaux, J.-F. Comprehensive estimation of lake volume changes on the Tibetan Plateau during 1976–2019 and basin-wide glacier contribution. *Sci. Total Environ.* **2021**, *772*, 145463. [CrossRef] [PubMed]
55. Xue, Z.S.; Lyu, X.G.; Chen, Z.K.; Zhang, Z.S.; Jiang, M.; Zhang, K.; Lyu, Y.L. Spatial and Temporal Changes of Wetlands on the Qinghai-Tibetan Plateau from the 1970s to 2010s. *Chin. Geogr. Sci.* **2018**, *28*, 935–945. [CrossRef]
56. Yang, C.Y.; Shen, W.S.; Wang, T. Spatial-temporal characteristics of cultivated land in Tibet in recent 30 years. *Trans. Chin. Soc. Agric. Eng.* **2015**, *31*, 264–271. (In Chinese with English Abstract)
57. Zhao, Z.L.; Liu, F.G.; Zhang, Y.L.; Liu, L.S.; Qi, W. The dynamic response of lakes in the Tuohepingco Basin of the Tibetan Plateau to climate change. *Environ. Earth Sci.* **2017**, *76*, 137. [CrossRef]
58. Nie, Y.; Zhang, Y.L.; Ding, M.J.; Liu, L.S.; Wang, Z.F. Lake change and its implication in the vicinity of Mt. Qomolangma (Everest), central high Himalayas, 1970–2009. *Environ. Earth Sci.* **2013**, *68*, 251–265. [CrossRef]
59. Tomé, A.R.; Miranda, P.M.A. Piecewise linear fitting and trend changing points of climate parameters. *Geophys. Res. Lett.* **2004**, *31*, 02207. [CrossRef]
60. Van, D.V.H.; Van, S.B.; De, T.R.; Hamdi, R.; Termonia, P. Modeling the scaling of short-duration precipitation extremes with temperature. *Earth Space Sci.* **2019**, *6*, 2031–2041.
61. Phan, V.; Lindenbergh, R.; Menenti, M. Geometric dependency of Tibetan lakes on glacial runoff. *Hydrol. Earth Syst. Sci.* **2013**, *17*, 4061–4077. [CrossRef]
62. Cai, Y.Q. Exploitation and Utilization of Salt Lake Mineral Resources in the Basin of Chaidamu. *CHN. Geol. Min. Econ.* **2003**, *2*, 11–13. (In Chinese with English Abstract)
63. Chen, Y.D.; Yang, Q.Y. Temporal and Spatial Characteristics and Driving Factors of Land Use/Cover Change in Tibet Autonomous Region. *J. Soil Water Conserv.* **2022**, *36*, 173–180. (In Chinese with English Abstract)
64. Mao, D.H.; Wang, Z.M.; Yang, H.; Li, H.Y.; Thompson, J.R.; Li, L.; Song, K.S.; Chen, B.; Gao, H.K.; Wu, J.G. Impacts of Climate Change on Tibetan Lakes: Patterns and Processes. *Remote Sens.* **2018**, *10*, 358. [CrossRef]
65. Qiao, B.J.; Zhu, L.P. Difference and cause analysis of water storage changes for glacier-fed and non-glacier-fed lakes on the Tibetan Plateau. *Sci. Total Environ.* **2019**, *693*, 133399. [CrossRef]

66. Lei, Y.B.; Yao, T.D.; Yang, K.; Bird, B.W.; Tian, L.D.; Zhang, X.W.; Wang, W.C.; Xiang, Y.; Dai, Y.F.; La, Z.; et al. An integrated investigation of lake storage and water level changes in the Paiku Co basin, central Himalayas. *J. Hydrol.* **2018**, *562*, 599–608. [CrossRef]
67. Song, Y.L.; Wang, C.Y.; Linderholm, H.W.; Tian, J.F.; Shi, Y.; Xu, J.X.; Liu, Y.J. Agricultural Adaptation to Global Warming in the Tibetan Plateau. *Int. J. Environ. Res. Public Health* **2019**, *16*, 3686. [CrossRef]
68. Li, L.; Li, J.; Yao, X.J.; Luo, J.; Huang, Y.S.; Feng, Y.Y. Changes of the three holy lakes in recent years and quantitative analysis of the influencing factors. *Quat. Int.* **2014**, *349*, 339–345. [CrossRef]
69. Yao, T.D.; Li, Z.G.; Yang, W.; Guo, X.J.; Zhu, L.P.; Kang, S.C.; Wu, Y.H.; Yu, W.S. Glacial distribution and mass balance in the Yarlung Zangbo River and its influence on lakes. *Chin. Sci. Bull.* **2010**, *55*, 2072–2078. [CrossRef]
70. Sun, H.Z.; Wang, J.Y.; Xiong, J.N.; Bian, J.H.; Jin, H.A.; Cheng, W.M.; Li, A.N. Vegetation change and its response to climate change in Yunnan Province, China. *Adv. Meteorol.* **2021**, *2021*, 8857589. [CrossRef]
71. Chen, K.; Bowler, J.M. Late Pleistocene evolution of salt lakes in the Qaidam Basin, Qinghai Province, China. *Palaeogeogr. Palaeoclimatol. Palaeoecol.* **1986**, *54*, 87–104.

land

MDPI

Article

Evaluation and Zoning of Cultivated Land Quality Based on a Space–Function–Environment

Fei Xu [1,*], Yaping Shao [1], Baogen Xu [1], Huan Li [2], Xuefeng Xie [3], Yan Xu [4] and Lijie Pu [5,6]

[1] Institute of Land and Urban-Rural Development, Zhejiang University of Finance & Economics, Hangzhou 310018, China
[2] Department of Land Resources Management, School of Public Administration, Zhejiang Gongshang University, Hangzhou 310018, China
[3] College of Geography and Environmental Sciences, Zhejiang Normal University, Jinhua 321004, China
[4] School of Geography Science and Geomatics Engineering, Suzhou University of Science and Technology, Suzhou 215009, China
[5] Key Laboratory of the Coastal Zone Exploitation and Protection, Ministry of Natural Resources, Nanjing 210023, China
[6] School of Geography and Ocean Science, Nanjing University, Nanjing 210023, China
* Correspondence: xufei16@zufe.edu.cn

Abstract: The multi-function characteristics of cultivated land have been widely recognized by researchers in China and globally, and it is important to provide a theoretical basis and practical reference for future research on the evaluation and zoning of cultivated land quality based on a space–function–environment perspective. Spearman rank correlation analysis and cluster analysis were used to categorize cultivated land by its quality. This study developed a theoretical evaluation framework of the space–function–environment quality for cultivated land and constructed a total of 23 indicators of cultivated land quality in three dimensions. The framework was applied to a case study that evaluated and zoned cultivated land quality based on a space–function–environment perspective. The results showed that the synergies and tradeoffs among spatial quality, functional quality and environmental quality, and the influences of the three on cultivated land quality are mutually restricted and act together. The cultivated land in Qujiang District can be divided into five types of areas according to the cold and hot spot analysis results of the secondary indexes of cultivated land spatial quality, functional quality and environmental quality. Based on these results, different protection schemes are proposed for different cultivated land qualities.

Keywords: land management; cultivated land resources; evaluation index; space–function–environment; cultivated land quality division

Citation: Xu, F.; Shao, Y.; Xu, B.; Li, H.; Xie, X.; Xu, Y.; Pu, L. Evaluation and Zoning of Cultivated Land Quality Based on a Space–Function–Environment. *Land* **2023**, *12*, 174. https://doi.org/10.3390/land12010174

Academic Editors: Shicheng Li, Chuanzhun Sun, Qi Zhang, Basanta Paudel and Lanhui Li

Received: 8 December 2022
Revised: 30 December 2022
Accepted: 31 December 2022
Published: 5 January 2023

1. Introduction

Cultivated land forms the material basis for the survival and development of human society. During the different periods of social development, there have been different concepts of the quality of cultivated land, from a single objective of crop production capacity and basic land capacity in the preliminary exploration stage to a comprehensive evaluation of productivity, suitability, carrying capacity, ecological security, environmental health and social development in more recent times (Table 1).

The United Nations Food and Agriculture Organization and the United Nations Environment Program put forward ten functions of land, which can be summarized into three categories, namely ecological function, production function and carrying function. Therefore, the land quality index system should include the ecological quality index system, the production quality index system and the bearing quality index system [1]. There is more discussion on land quality in the world. For example, the land quality index system jointly established by the Food and Agriculture Organization of the United Nations, the World

Bank, the United Nations Development Program and the United Nations Environment Program in 1995 considers land quality to be a range. It is the land condition related to agricultural production, forestry production, environmental protection, management and other land-use needs, and it is the ability to maintain the health of the ecosystem, animals and plants without soil degradation and other ecological environmental problems. Pieri et al. believed that land quality includes soil, climate and biological characteristics, as well as the land conditions and production capacity, together with the degree to which human needs are met [2]. Rossiter believed that land quality is a complex attribute of land and the ability of the land to meet the specific requirements of certain utilization types [3]. Costanza et al. published a paper on "The Value of World Ecosystem Services and Natural Capital", which provided a theoretical basis and basis for the measurement of the externality of cultivated land [4]. Bouma et al. defined land quality as the ratio of crop yield to potential yield under certain conditions [5]. At present, there are few studies on the protection of the trinity of cultivated land in China. Some scholars have sorted out the main practices of cultivated land protection in developed countries, including the corresponding system, cultivated land protection trend and management measures, and put forward corresponding suggestions for the protection of cultivated land in China [6,7]. Some elaborated the important influence, main content and the relationship among the three, and proposed multiple measures to build a new pattern of cultivated land protection [8–10]. From the perspective of system theory and public management, some scholars have conducted a preliminary study on the integrated supervision system of cultivated land quantity, quality and ecology [11–13]. In addition, many scholars discussed in their literature that the overall quality of cultivated land in China tends to decline from different angles [14–16].

Table 1. Conceptual understandings of cultivated land quality.

Development Period	Starting Point	Connotation of Cultivated Land Quality	Authors
1980s–1990s	Suitability and productivity	Only when land is used as one of the production modes of agriculture, forestry and animal husbandry can its production potential be brought into play, and the potential will not decline or be exhausted in the normal production process.	FAO [1] (1976)
		Land resource map is based on land potential and land quality evaluation.	Pieri C. et al. [2] (1995)
		The quality of cultivated land is a comprehensive attribute of cultivated land, which is mainly determined by the soil fertility of cultivated land and the location of cultivated land.	Rossiter D.G. et al. [3] (1996)
		The quality of cultivated land is the productivity level of cultivated land.	Costanza R. et al. [4] (1997)
		Cultivated land quality is a measure of soil, environment and field infrastructure.	Bouma et al. [5] (1998)
Early 21st Century	Ecological environment, carrying capacity and sustainability	The quality of cultivated land includes suitability, productive potential and actual productivity. Cultivated land quality is an indicator to measure the natural and environmental factors that affect cultivated land.	Yang H. et al. [6] (2000)
		The quality of cultivated land includes the quality of cultivated land background, health and economy. The quality of cultivated land includes ecology, production and bearing capacity. The quality of cultivated land includes the quality of cultivated land background, health and economy.	Lichtenberg E. et al. [7] (2008)
Near 21st Century	Comprehensive attribute	The quality of cultivated land is the overall function of nature, society, economy and technology. Cultivated land quality includes soil quality, spatial geography quality, management quality and economic quality.	Kong X.B. [8] (2014)
		The trinity quality view of quantity, quality and ecology of cultivated land includes three aspects: space quality, function quality and environmental quality.	Vasu D. et al. [9] (2018)

By distilling the definition of cultivated land quality from previous studies and understanding the need to protect all three facets of cultivated land quantity, quality and ecology, the evaluation of cultivated land quality can be seen to be best carried out from the

functional dimension. The multi-function characteristics of cultivated land—production, ecological, landscape and carrying function—have been widely recognized by researchers in China and globally. In recent years, experts and researchers have made progress in studies on cultivated land quality evaluation. The concepts and content of cultivated land quality are gradually expanding, and the evaluation purposes and methods have become more diversified. The content of cultivated land quality evaluation focuses on the evaluation of productivity, suitability, potential, environment and sustainable use. The evaluation indicators include site conditions, soil physical and chemical properties. The environment tends not to be comprehensively evaluated with regard to the quality of the cultivated land. Furthermore, less research on the value and application of the evaluation results of cultivated land quality has been carried out. The research on cultivated land protection tends to focus on protecting the overall quantity and improving the quality, whereas research on quality protection of local cultivated land through zoning needs to be further promoted.

On the basis of the existing research and from the perspective of the spatial layout, functional use and environmental protection of cultivated land, this study constructed a cultivated land quality evaluation index system based on the space–function–environment, which included three dimensions, eight levels and twenty-three indicator factors. The spatial, ecological and environmental indicators were added as important factors to expand the research scope of the cultivated land quality evaluation. The Qujiang District, Zhejiang Province, China, was used as an example to explore the application of the cultivated land quality evaluation. By analyzing the differences and aggregation characteristics of the quality of the indicators at all levels, a reasonable and effective zoning scheme for cultivated land quality was identified from the perspective of space, function and the environment. This study provides a theoretical basis and practical reference for research on cultivated land protection.

2. Materials and Methods

2.1. Study Area

The Qujiang District is located within the hilly basin area in the middle of Zhejiang Province, in eastern China (Figure 1). Each administrative village in the 2018 land-use status map of Qujiang District was used as a research unit, and the cultivated land was extracted as the minimum unit for the collection of basic data. The total area of the cultivated land accounted for 18.57% of the total land area of the region. There is multiple cropping with two crops a year, generally consisting of an early and late rice crop. Qujiang District was used as a pilot county for agricultural land grading and evaluation by the Ministry of Land and Resources. Therefore, it has complete agricultural land quality grading, a land quality geochemical survey, a land change survey and other data, which provide a good foundation for the development of the cultivated land space, function and environmental quality evaluation.

2.2. Data Sources

The main sources of the evaluation index data in this study were collected as follows: Basic data collection included the area of each plot, basic fertility, surface soil texture, soil organic matter content, soil pH, tillage layer thickness, irrigation assurance rate and altitude. We obtained the above data from the Bureau of Natural Resources and Planning, Bureau of Agriculture and Rural Affairs, Environmental Protection Agency and relevant websites. Data on the thickness of the effective soil layer, drainage conditions, soil heavy metals, white pollution, soil earthworms, fertilizer application amount of each administrative village, crop yield and planting conditions were obtained through field surveys and demographic data from the Statistical Yearbook. The shape, density, fragmentation, separation, atmospheric regulation, farmland attractiveness index, population carrying capacity and agricultural chemical fertilizer residue were calculated using relevant models [17–19]. According to the current situation of land use, cultivated land patches, remote sensing images and other

relevant data, the slope, field road accessibility and farming distance were obtained by combining remote sensing and GIS methods. Kriging interpolation was used to convert the collected survey point data into continuous areal attribute data in each evaluation unit [20].

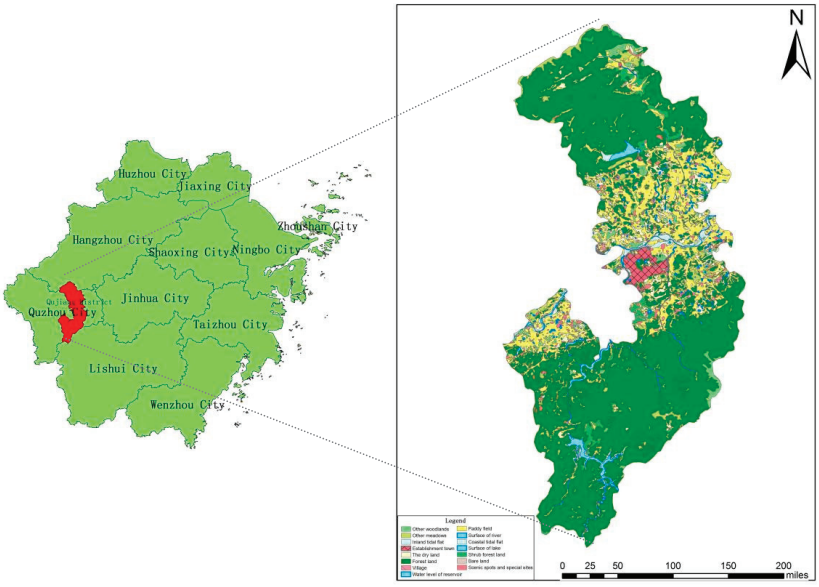

Figure 1. Administrative divisions of Qujiang District.

2.3. Research Method

2.3.1. Spearman Rank Correlation

This study selected eight indicators related to space quality, function quality and environmental quality; namely, scale, space characteristics, production function, ecological function, landscape function, carrying function, social environment and natural environment. In the analysis of these complex indicator relationships, if an increase in one indicator value was accompanied by a decrease in another indicator value, the two were considered to have a trade-off relationship. If the values of two indicators increased simultaneously with the interaction, they were regarded as having a collaborative relationship.

Spearman rank correlation is a common method used to analyze trade-offs and synergies. If the correlation coefficient is positive, it means that the relationship of indicators is synergistic; if the correlation coefficient is negative, the relationship of indicators are trade-offs. If the correlation is not significant, then the relationship of indicators is compatible [20,21]. The specific description of the correlation coefficient is:

Let n pairs of $\{(X_i,\ Y_i)\}$ data be represented.The pairs $\{(X_i)\}$ are rearranged in order to generate new data pairs $\{(X_i,\ Y_i)\}$, where $X_{(1)} < \cdots < X_{(n)}$ is the sequence opposite to X, but is the $Y_{(i)}$ concomitant of $X_{(i)}$. Suppose that when $X_{(j)}$ it is located at the kth position in the sequence, k is the rank of P_j. By analogy, the rank of Y_j is recorded as Q_j. The details are as follows:

$$r_s(X_i,\ Y_i) = 1 - \frac{6\sum_{i=1}^{n}(P_i - Q_i)^2}{n(n^2-1)} \tag{1}$$

In the formula, P_i Q_i indicates the ranking number of the ith attribute weight in the weight vector. If $r_s = 1$, it indicates that the rank between the attribute weight and the correlation coefficient is exactly the same, showing a positive correlation. If $r_s = -1$, the rank between them is completely opposite, showing a negative correlation. If $r_s = 0$, the

rank between them is completely independent. As the r_s value increases, the correlation between attribute weights and correlation coefficients improves.

2.3.2. Spatial Analysis Method

Through the correlation analysis of various indicators that affect the quality of cultivated land, we gained a preliminary understanding of the trade-offs and synergies among the indicators. On this basis, using Getis–Ord Gi* on the ArcGIS platform, this study analyzed the cold and hot spots of the cultivated land space–function–environment assessment index system and all of its secondary indicators, and identified the hot and cold spots for each indicator [22–25]. Hot spots refer to administrative villages with high cultivated land quality and good concentration in the study area, and vice versa. The specific calculation formula of Getis–Ord Gi* is as follows:

$$Gi^* = \frac{\sum_j^n W_{ij} X_j}{\sum_j^n X_j} \quad (2)$$

where Gi^* is the aggregation index of spatial unit i, W_{ij} is the spatial weight defined by distance, X_i, X_j is the attribute value of spatial units i and j, and n is the total number of spatial units.

$$Z(Gi^*) = \frac{Gi^* - E(Gi^*)}{\sqrt{Var(Gi^*)}} \quad (3)$$

where $Z(Gi^*)$ is the significance of the agglomeration index, $E(Gi^*)$ and $Var(Gi^*)$ are the mathematical expectation and variance of Gi^*, respectively. Where $Z(Gi^*) > 0$ indicates a positive spatial correlation and a tendency for spatial objects to cluster or agglomerate, the area showed as the hot spot district; where $Z(Gi^*) < 0$ indicates a negative spatial correlation and a tendency for objects to spatially disperse, the area showed as the cold spot district; $Z(Gi^*)$ is 0 indicates a situation where objects are randomly distributed. In this study, Finally, the ArcGIS overlay analysis tool was used to obtain the spatial distribution map of cold and hot spots in the comprehensive quality of cultivated land.

3. Results

3.1. Construction of Theoretical Framework for Cultivated Land Quality Evaluation

With the development and progress of society, the quality of cultivated land is no longer measured only from the traditional sense of high yield. The quality of cultivated land is related to the amount, shape and scale, as well as the spatial location, structure, relationship and other spatial elements of the cultivated land. However, the versatility of the cultivated land varies in different spaces. For example, in areas where the production function of the cultivated land is dominant, the production function and carrying function should be dominant to ensure food security, including quantity, quality, food safety supply and other aspects. In areas where the ecological and landscape qualities of the cultivated land are important, the ecological and landscape functions should be dominant, the ecological environmental protection and landscape aesthetics should be emphasized, and the traditional culture, modern culture and multi-cultural aspects should be combined for development. Therefore, priority should be given to the dominant function when evaluating the quality of cultivated land, and the function quality evaluation should combine functions using different weights. The cultivated land environment quality is an important standard to measure whether the cultivated land space quality and function quality meet the sustainable use of the cultivated land. Its indicators include the natural environment and the social environment. Physical, energy and other objective factors are generated by the natural environment, whereas the main factors of the social environment that affect the quality of the cultivated land include technology, capital investment and transportation.

The evaluation of cultivated land quality is thus a comprehensive process, which should establish a multi-level indicator system from multiple dimensions to judge the quality of the cultivated land, comprehensively and scientifically. The indicator system

constructed in this study was composed of spatial quality, functional quality and environmental quality. Differences were found in the evaluation directions of the three-dimensional indicator systems, evaluation means and calculated indicators. Therefore, the space quality, functional quality and environmental quality should not be confused when the indicators are established [22]. The evaluation dimensions of the cultivated land space, function and environmental quality are shown in Figure 2.

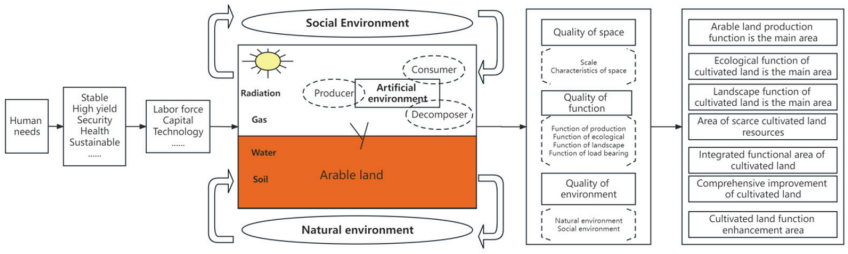

Figure 2. Structural diagram of cultivated land space–function–environmental quality evaluation system.

The evaluation system of the cultivated land space, function and environmental quality was multi-level. The space quality, function quality and environmental quality were all affected by external natural factors, such as light and temperature, weather, soil and biology. At the same time, the impact of human activities on the quality of the cultivated land could not be ignored. The various influencing factors were intertwined and complex. Therefore, when positioning the hierarchy, it should be subdivided based on dimensions. The subdivision rules should not only ensure the independence of each level but also realize the systematic nature of the whole hierarchy. On the basis of the three dimensions of space–function–environment, this study constructed a cultivated land quality evaluation system with eight levels: scale, spatial characteristics, production function, ecological function, landscape function, carrying function, social environment and natural environment.

3.2. Construction of Cultivated Land Space–Function–Environment Quality Evaluation Index System

The selection of the indicators is the key to an accurate evaluation of the quality of the cultivated land. Selection should meet the principles of combining science and feasibility, integrity and independence, comprehensiveness and pertinence, dynamics and stability to build a set of indicators that are interrelated and mutually restrictive and can comprehensively express the quality of cultivated land. At the government level, the Ministry of Agriculture has established a land productivity evaluation system, which uses 64 evaluation factors, including climate, soil, terrain, constraints and agricultural input. The Ministry of Land and Resources, by collecting relevant data from different counties and cities in various provinces, has divided the indicator areas, determined the farming system, the light temperature production potential index and yield ratio coefficient, and calculated the quality of the cultivated land in combination with the soil physical and chemical data, terrain and land use from field surveys. At the academic research level, researchers have built an indicator system for evaluating the quality of cultivated land from five levels of ecological and production functions: soil, climate, biodiversity, landscape and productivity [26]. Some researchers have established an evaluation system for cultivated land quality from the background, health and economy of the cultivated land. When evaluating the background quality of the cultivated land, they evaluated it from five levels: site conditions, soil physical and chemical properties, soil nutrient status, soil structure and management. When evaluating the health quality of the cultivated land, they selected two evaluation factors: soil environment and irrigation water quality pollution. When evaluating the economic quality of the cultivated land, they selected materials, labor and management along with five evaluation factors of input and policy effect [26,27]. Some researchers selected

climate, site conditions, soil physical and chemical properties, transportation, agricultural inputs, farming systems and policy measures to build a cultivated land quality evaluation system [28]. Some researchers selected 12 indicators, including weather, terrain and soil when building their land-use system health assessment framework [29]. There are other scholars who divided the farmland health evaluation index system into three aspects. The first was the quality of the farmland, which included 14 evaluation factors, such as physical properties, chemical properties and the farmland infrastructure conditions [30,31].

Using the three aspects that affect the quality of cultivated land, the present study conducted a comprehensive analysis from the perspective of combining human factors, resources and the environment. Space, function and the environment were selected to form a complete cultivated land quality evaluation index system. Combined with the data obtained from the study area and the analysis of the cultivated land space, function and environmental quality evaluation index system, the present study was able to determine a cultivated land quality evaluation index system in the Qujiang District (Table 2).

Table 2. Cultivated land space–function–environmental quality evaluation system.

Target Layer	Level 1 Indicators	Level 2 Indicators	Level 3 Indicators	Weight
Cultivated land quality	Space quality	Cultivated land scale	Area	0.0319
			Shape	0.0192
		Spatial characteristics of cultivated land	Density	0.0113
			Degree of fragmentation	0.0419
			Resolution	0.0179
	Functional quality	Production function	Basic fertility	0.0153
			Surface soil texture	0.0293
			Soil organic matter content	0.0676
			Soil pH	0.0641
			Thickness of tillage layer	0.0434
			Effective soil layer thickness	0.0149
			Irrigation assurance rate	0.0529
			Drainage conditions	0.0274
			Altitude	0.0161
			Slope	0.0375
		Ecological function	Atmospheric regulation	0.0830
		Landscape function	Farmland attractiveness index	0.0427
		Bearing function	Population carrying capacity	0.1537
		Social environment	Agricultural input	0.0494
			Field road accessibility	0.0345
	Environmental quality		Heavy metals in soil	0.0946
		Natural environment	White pollution	0.0336
			Soil earthworm	0.0178

3.3. Correlation Analysis and Zoning of Cultivated Land Space–Function–Environment Quality

The interaction of cultivated land space, function and environmental quality is influenced by natural factors, social factors and human factors. With the development and progress of society, a conflict between cultivated land protection and economic prosperity is growing. This conflict is not conducive to the protection and sustainable development of cultivated land and will eventually affect the sustainable development of human society, which requires a large area or high quality of cultivated land. The premise of cultivated land protection needs balance and coordination between cultivated land space, function and environment. Identifying the relationships among these three dimensions is important for implementing cultivated land protection, promoting regional coordination and achieving sustainable development.

Trade-offs and synergies often occur between small regions and large regions, short-term and long-term, and reversible and irreversible services. The current study mainly conducted trade-off and synergy analysis on the quality of the cultivated land in the study area. Therefore, from the perspective of space, combined with the imbalance of the

spatial distribution of cultivated land quality, diversity of functional types and human use selectivity, we used Spearman rank correlation and cold/hot spot analysis to analyze the spatial quality of the cultivated land. There was a trade-off between the functional quality and environmental quality and a synergistic relationship of mutual promotion or inhibition for the systematic analysis. Using the evaluation results of cultivated land space quality, functional quality and environmental quality, the current study identified the absolute value and positive and negative directions of the correlation coefficients and judged the relationship type and intensity characteristics among the cultivated land space quality, functional quality and environmental quality. At the same time, the spatial autocorrelation analysis was used to draw a spatial distribution map of the cultivated land quality evaluation results and to divide the cultivated land quality.

3.3.1. Space Quality Evaluation

In this study, the indicators used to measure the spatial quality of the cultivated land included the quality of the scale and the quality of the spatial characteristics, which were mainly determined using the five factors of area, shape, density, fragmentation and separation. The cultivated land with the highest score was the best, the cultivated land with the lowest score was the worst, and the cultivated land in the middle three grades was average. The high-quality area of the spatial characteristics was also located in the middle, and the scope of high-quality area was larger (Figure 3).

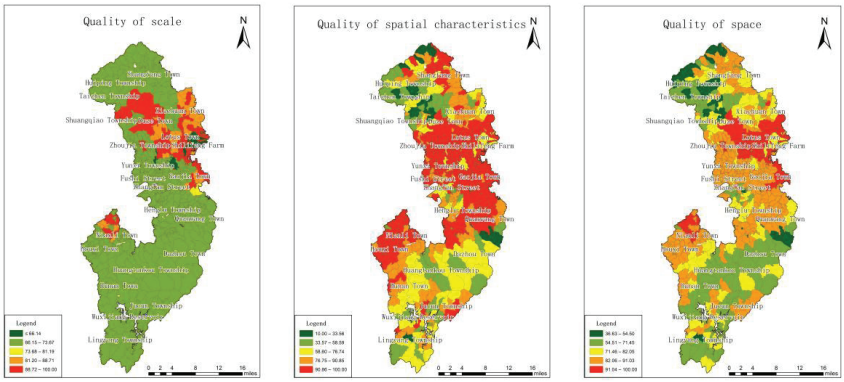

(a) Quality of scale

(b) Quality of spatial characteristics

(c) Quality of space

Figure 3. Scale, spatial characteristics and spatial quality evaluation of cultivated land.

The overall spatial quality of the cultivated land in Qujiang District was good. Most of the cultivated land was above the average level of the whole district. The cultivated land with high spatial quality was distributed in the central plain area, with good connectivity and regularity. However, the cultivated land in the southwest and northeast was located in mountainous areas, with undulating terrain and scattered distribution. Forming a good spatial association between the plots was difficult; thus, the spatial quality of the cultivated land was poor. The cultivated land with good space quality was conducive to the implementation of agricultural mechanization, especially large-scale agricultural mechanization. In contrast, the cultivated land with poor space quality was not conducive to agricultural mechanization, especially large-scale mechanized operations. Small agricultural mechanized operation could be considered for cultivated land with average space quality.

3.3.2. Function Quality Evaluation

In this study, the indicators for measuring cultivated land function quality included production function quality, ecological function quality, landscape function quality and

carrying function quality, which were mainly determined by 13 factors such as soil organic matter content, soil pH, atmospheric regulation and population carrying capacity. The score for the quality of the production function was divided into five grades by the natural breaks method, while the quality of ecological function, landscape function and carrying function was calculated by relevant models, and the quality was divided according to the rating standards. The high-quality area of cultivated land production function in Qujiang District was located in the middle, while the low-quality area was mainly located in Huiping Township and Taizhen Township. The high-quality areas of ecological function and landscape function were scattered over the central plain area, and the high-quality areas of carrying function were scattered over the whole area. The overall ecological function, landscape function and carrying function quality of Qujiang District were relatively low (Figure 4).

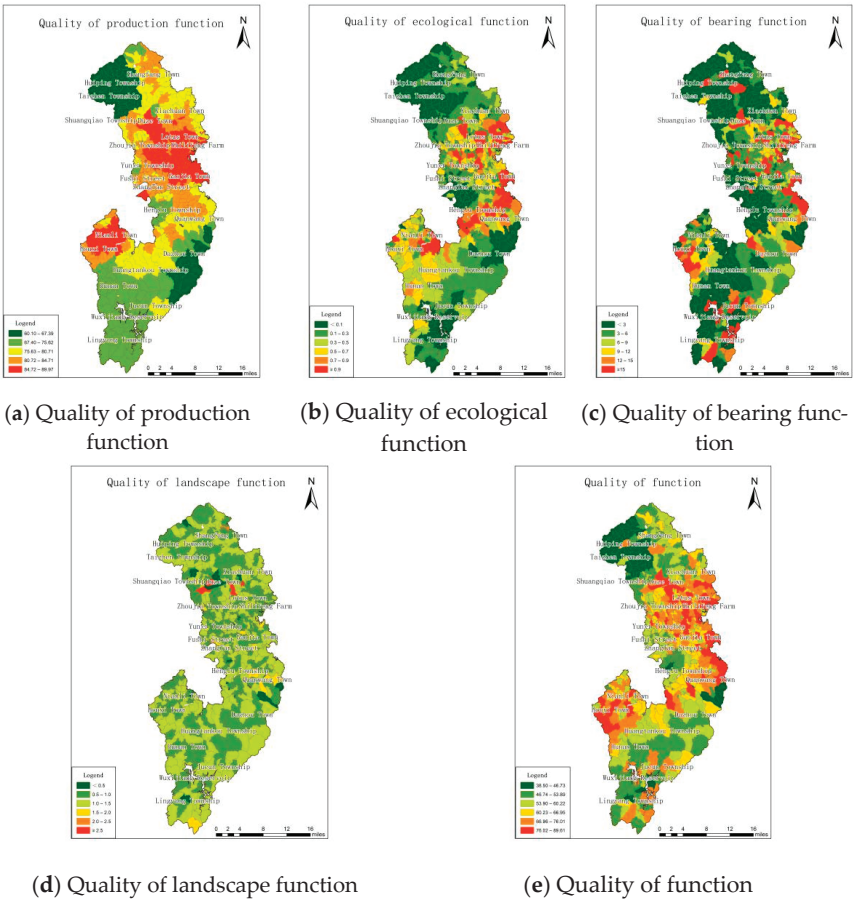

(**a**) Quality of production function

(**b**) Quality of ecological function

(**c**) Quality of bearing function

(**d**) Quality of landscape function

(**e**) Quality of function

Figure 4. Evaluation of cultivated land production function, ecological function, landscape function, carrying function and functional quality.

The overall cultivated land function quality in Qujiang District was average, and the score was mainly approximately 50 points. In addition, nearly 10% of the cultivated land was less than 50 points, which was mainly distributed in the southwest and north. Owing to the relatively biased terrain, fewer human activities and a high degree of non-agricultural cultivated land, the functional quality was poor. In the central region, close to the urban area, there was a large demand for agricultural products, and farmers tended to increase

investment and intensive farming; thus, the quality of the cultivated land function was good. The cultivated land with high functional quality is suitable for the development of food, cash crops, tourism and leisure agriculture. The relationship between food and cash crop production, agricultural production and leisure tourism should be properly handled to fully meet the basic needs of food and the increasing income for farmers. The limiting factors of cultivated land with poor functional quality should be addressed and its functional quality enhanced.

3.3.3. Environmental Quality Assessment

In this study, the indicators used to measure the environmental quality of the cultivated land included social and natural environmental quality, which were mainly determined by five factors: the residue of agricultural fertilizer, the accessibility of roads in the field, heavy metals in the soil, white pollution and earthworms in the soil. The scores for the quality of the social environment and the quality of the natural environment were divided into five grades using the natural breaks method. The high-quality area of cultivated land with regard to the social environment in Qujiang District was located in the south–central part, while the low-quality area was mainly located in the south. The overall quality of the natural environment in the Qujiang District was relatively high, although was relatively low in the central and northernmost areas (Figure 5).

Qujiang District had a good overall cultivated land environment quality. Most of the cultivated land environment quality was above the average level of the whole district. The area with the best environmental quality was located in the southwest. This was an eco-tourism area in Qujiang District, with convenient transportation, beautiful natural environment and less pollution. The central and northern regions were dominated by industrial development. Although the transportation was more convenient, the cultivated land environment quality was poor because of frequent human activities and more pollution sources. The cultivated land with high environmental quality should actively develop organic agricultural products and improve the production grade of agricultural products, as well as developing pollution-free agricultural products. The cultivated land with poor environmental quality should be strictly prohibited or restricted from producing agricultural products. At the same time, it is necessary to actively carry out farmland environmental restoration projects to improve the environmental quality of the cultivated land.

In general, the quality of the cultivated land in the central part of Qujiang District was the highest, followed by the southern part, while the northern part was relatively poor. The cultivated land with high comprehensive quality is the essence of cultivated land. It should not only be used efficiently but should also be strictly protected. It should be included in permanent basic farmland, whereby construction, occupation and destruction are strictly prohibited.

3.4. Analysis of Spatial Agglomeration Characteristics of Cultivated Land Quality Indicators

By analyzing the spatial distribution of cold and hot spots of the eight secondary indicators of cultivated land quality, this study found that the distribution of cold and hot spots in some different indicators were similar, such as scale, spatial characteristics and production function. The hot spots were mainly concentrated in the central plain area, while the cold spots were distributed in the northwest. One difference was that the production function in the south was a cold spot area, while the space characteristics in the south were insignificant. The cold and hot spots of the different indicators also varied greatly, such as the social environment and natural environment. For example, the cold spot area for the social environment was the hot spot area for the natural environment. The distribution of cold and hot spots of the landscape function in Qujiang District was not significant in most areas, and clustering was not statistically significant. Figure 6 shows the spatial distribution of the cold and hot spots that affected the quality of the cultivated land.

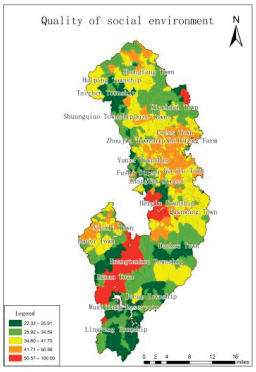

(**a**) Quality of social environment

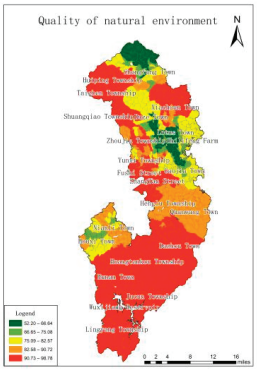

(**b**) Quality of natural environment

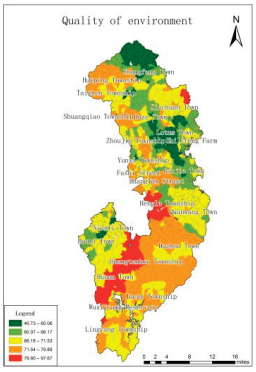

(**c**) Quality of environment

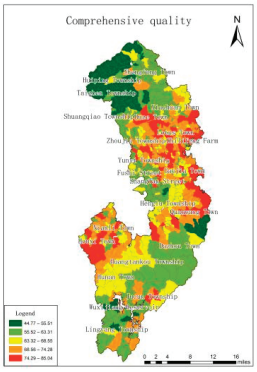

(**d**) Comprehensive quality

Figure 5. Social environment, natural environment and comprehensive quality evaluation results of cultivated land.

The distribution of the cold and hot spots of cultivated land space quality, functional quality and comprehensive quality was basically consistent. The center part was the hot spot area, the northwest was the cold spot area, while the hot spot area of environmental quality was located in the southwest, and the cold spot area was located in the center and northeast.

According to the analysis of cold and hot spots, the regions with hot spots in terms of scale, spatial characteristics, production function, carrying function and social environment were mainly in the central plain of Qujiang District, and these regions had large-scale production of cultivated land, priority protection of cultivated land and were the main food production areas. The hot spot area of ecological function was located in the south–central part of Qujiang District, which was suitable for the development of a cultivated land eco-tourism industry. The hot spots for the natural environment were located in the north and south of the area, and thus ecological environment protection should be carried out, such as returning farmland to forests. The cold spot area of each indicator shows the key areas for implementing the cultivated land protection system and is an important basis for quality zoning.

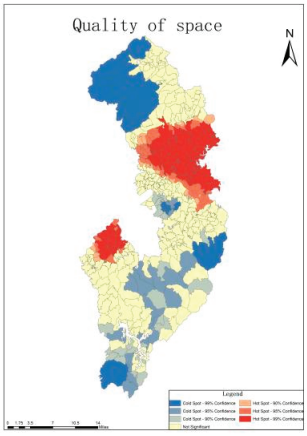

(**a**) Quality of space

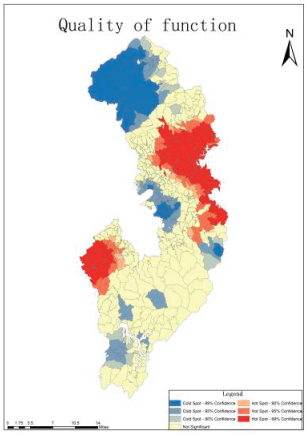

(**b**) Quality of function

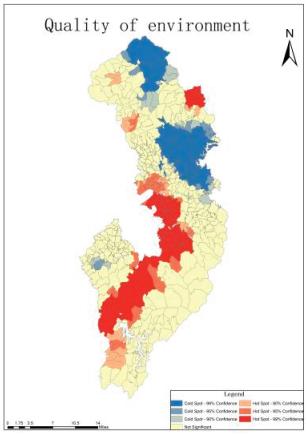

(**c**) Quality of environment

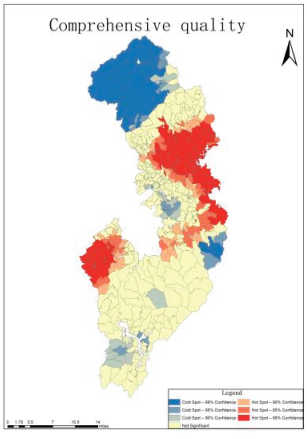

(**d**) Comprehensive quality

Figure 6. Spatial agglomeration and distribution of cold and hot spots in the spatial quality, functional quality and comprehensive quality of cultivated land in Qujiang District.

The cultivated land in Qujiang District was initially divided into seven types of areas (as shown in Figure 7): the main area of production function, the main area of ecological function, the main area of landscape function, the area of resource tension, the comprehensive functional area, the comprehensive rehabilitation area and the area of function improvement. The comprehensive quality score of cultivated land in each type of area is shown in Figure 8, and the quality results of each indicator in each type of area are shown in Figure 9. Using qualitative and quantitative analysis, the areas with a high degree of proximity were merged. The cultivated land in Qujiang District was then divided into five types of areas: the main area of production function, the main area of ecological and landscape function, the area of resource tension, the comprehensive functional area and the area of comprehensive improvement and function improvement.

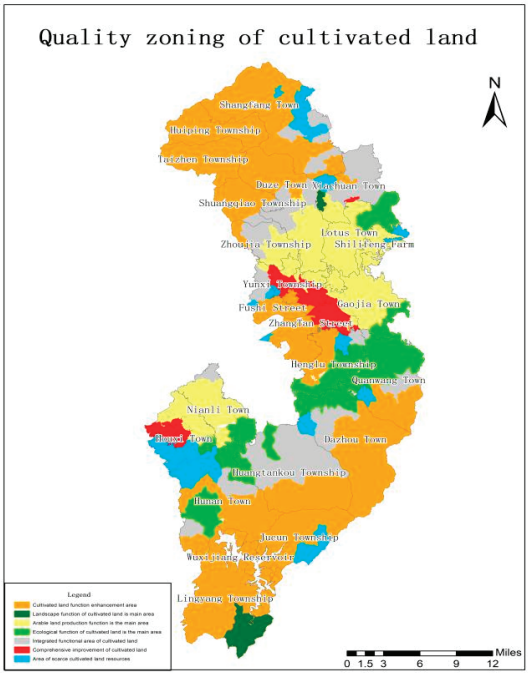

Figure 7. Quality zoning of cultivated land in Qujiang District.

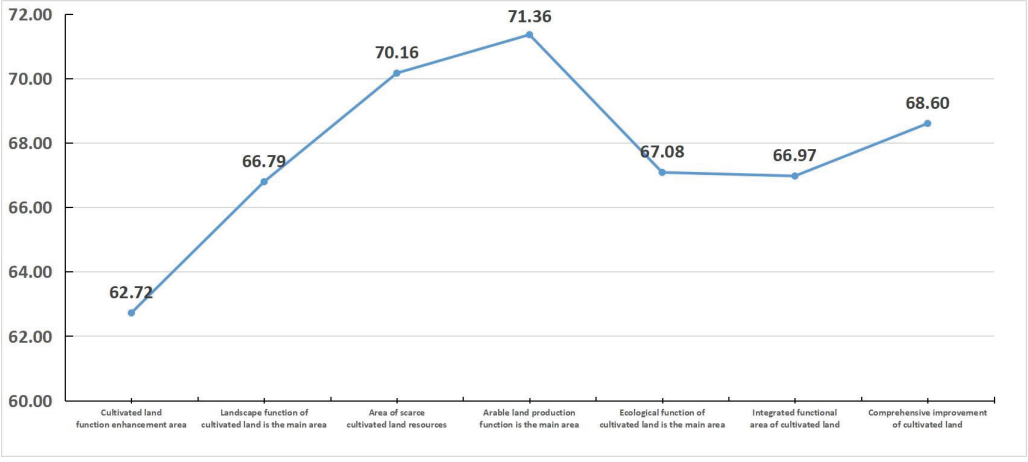

Figure 8. Comprehensive quality of cultivated land in various types of districts in Qujiang District.

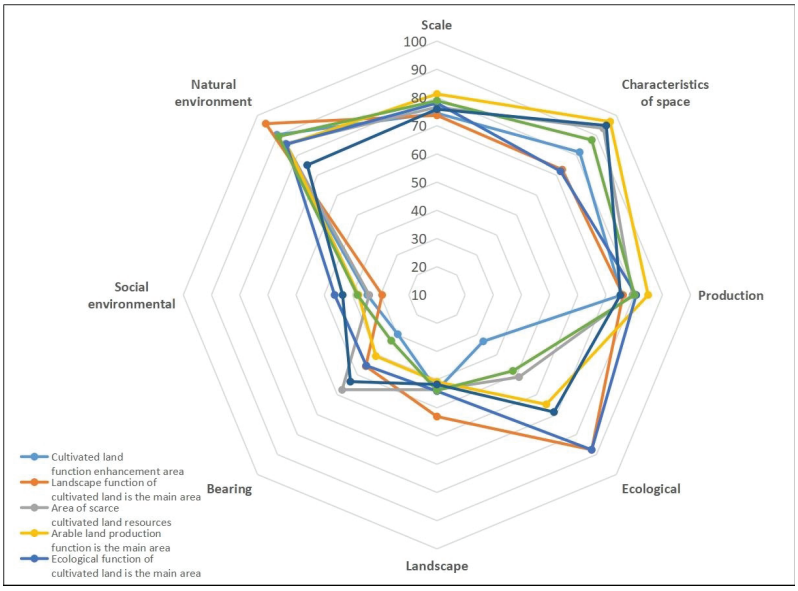

Figure 9. Quality map of various indicators of cultivated land in Qujiang District.

4. Discussion

The protection of cultivated land in the new era aims to focus more on the comprehensive protection of the trinity of the quantity, quality and ecology of cultivated land, strictly abide by the red line of cultivated land, ensure that the functional quality of cultivated land does not decline and maintain the balance between cultivated land and its surrounding environment. In the face of the huge economic benefits from farmland conversion, there is a gap between the implementation effect of cultivated land protection policies and the expected goals. There is an urgent need to improve the utilization mechanism of space, function and environment, and establish a system of cultivated land space, function and environmental protection. On the basis of the quality evaluation and zoning results of the space–function–environment of cultivated land, the following suggestions are put forward from this study.

4.1. Tradeoff and Cooperative Analysis of Cultivated Land Quality Index

Through calculation, the tradeoff and synergistic relationship among the indicators of cultivated land quality are shown below(Table 3).

Spearman rank correlation was applied to analyze the correlation properties of the indicators affecting cultivated land quality, and it was found that 15 of the 28 groups of relationships had significant positive correlation, 7 groups had insignificant correlation and 6 groups had significant negative correlation. Therefore, there were more synergistic relationships than tradeoff relationships. Specifically, in the spatial quality of cultivated land, there was a synergistic relationship between scale and spatial characteristics. In the quality of the cultivated land function, there was a synergistic relationship between production function, ecological function and bearing function, while the relationship between landscape function and production function was not significant. In the quality of the cultivated land environment, the social environment and the natural environment showed trade-offs.

Table 3. Spearman rank correlation statistical table of cultivated land quality indicators.

		Space Quality		Functional Quality				Environmental Quality	
		Cultivated Land Scale	**Spatial Characteristics of Cultivated Land**	**Production Function**	**Ecological Function**	**Landscape Function**	**Bearing Function**	**Social Environment**	**Natural Environment**
Space quality	Cultivated land scale	1	-	-	-	-	-	-	-
	Spatial characteristics of cultivated land	0.133 ** (0.002)	1	-	-	-	-	-	-
Functional quality	Production function	0.243 ** (0)	0.642 ** (0)	1	-	-	-	-	-
	Ecological function	0.091 (0.039)	0.578 ** (0)	0.413 ** (0)	1	-	-	-	-
	Landscape function	0.02 (0.646)	0.073 (0.095)	0.033 (0.452)	0.250 ** (0)	1	-	-	-
	Bearing function	0.148 ** (0.001)	0.335 ** (0)	0.250 ** (0)	0.454 ** (0)	0.198 ** (0)	1	-	-
Environmental quality	Social environment	0.122 ** (0.006)	0.401 ** (0)	0.451 ** (0)	−0.343 ** (0)	0.021 (0.635)	0.079 (0.073)	1	-
	Natural environment	**−0.387 ** (0)**	**−0.456 ** (0)**	**−0.530 ** (0)**	**0.316 ** (0)**	0.01 (0.815)	**−0.198 ** (0)**	**−0.416 ** (0)**	1

** The correlation is significant when the confidence (double measure) is 99%.

In addition, through comprehensive analysis, it was seen that spatial quality and functional quality had both synergistic and tradeoff relations. Scale had a synergistic relationship with production function and carrying function but had an insignificant relationship with ecological function and landscape function. The spatial characteristics showed a synergistic relationship with production function, ecological function and carrying function, but not a significant relationship with landscape function. There were both synergistic and tradeoff relations between spatial quality and environmental quality, both showing a synergistic relationship with social environment and a tradeoff relationship with natural environment. There was a synergistic relationship between functional quality and environmental quality as well as a tradeoff relationship between production function and social environment, and a tradeoff relationship between production function and natural environment. The ecological function and social environment showed a tradeoff relationship, and the natural environment showed a synergistic relationship. There was no significant relationship between landscape function and social environment and natural environment. The bearing function had an insignificant relationship with the social environment and a tradeoff relationship with the natural environment.

The scale and spatial characteristics were synergistic with production function, bearing function and social environment, indicating that the better the spatial quality of cultivated land, the greater the productive capacity of cultivated land, the more population that the cultivated land could satisfy, and the better the social environment could be formed. There was a synergistic relationship between the production function and the social environment, which indicated that the effect of human action on the production function of cultivated land was positive. The relationship between ecological function and natural environment was synergistic, which showed that they were complementary to each other.

Scale, spatial characteristics and natural environment in environmental quality were tradeoffs, indicating that the better the spatial quality was, the more easily the natural environment would be destroyed. Production function, carrying function and natural environment were trade-offs, indicating that the productive capacity and population carrying capacity of cultivated land in better natural environment were not large. However, ecological function and social environment were tradeoffs, which showed that human activities had a negative effect on ecological function.

4.2. Correlation Analysis

4.2.1. Correlation Analysis of Spatial Quality, Functional Quality and Environmental Quality of Cultivated Land

The correlation results of the indexes affecting the spatial quality, functional quality and environmental quality of the cultivated land revealed the following three points: First, the synergistic relationship between the scale and spatial characteristics representing the spatial quality of the cultivated land showed that the agglomeration effect formed by the scale and contiguity of the cultivated land had a positive effect on the quality of cultivated land. Secondly, according to the tradeoffs and synergies among the production function, ecological function, landscape function and carrying function, which represent the functional quality of cultivated land, it can be seen that there was a certain degree of positive influence among the functions of cultivated land, but the relationship between production function and landscape function was not significant. Thirdly, the tradeoff between the social environment and the natural environment, which represented the environmental quality of cultivated land, showed that the social environment and the natural environment became a set of conflicting indicators because the social development always occurred at the expense of the natural environment. It is incorrect to sum up the past experience of this development situation, and a sustainable development road must be found.

4.2.2. Correlation Analysis of Two Indexes Affecting Cultivated Land Quality

It can be seen from the correlation results of various indicators affecting cultivated land quality that there were synergistic and tradeoff relations among spatial quality, functional quality and environmental quality, indicating that the influences of the three on cultivated land quality were mutually restricted and act together. The quality of scale and spatial characteristics were synergistic with the production function, bearing function and social environment, indicating that the large-scale operation and management of cultivated land improved the production capacity of the cultivated land, and the positive impact on the social environment could not be ignored. The scale quality, spatial characteristic quality and the natural environment were all trade-offs, indicating that the land renovation project changed the original natural shape, thus destroying the natural environment. Production function and social environment were synergistic, which showed that production function and human activities were complementary. The production function, bearing function and natural environment were tradeoff relations, from the root showed that the formation of cultivated land was a kind of artificial transformation of nature behavior. The quality of cultivated land production function, bearing function and natural environment was a kind of relationship. Ecological function and natural environment were synergistic, which showed that they were complementary to each other. Ecological function and social environment were trade-offs, which showed that human activities had a negative effect on ecological function.

4.3. Cold and Hot Spot Analysis Results

The quality of cultivated land depends on the factors such as light temperature, water, soil and people, which differ greatly with the change of geographical environment. Therefore, it is necessary to analyze the indicators affecting cultivated land from the spatial distribution. It is of great significance to zoning cultivated land quality, giving full play to the agglomeration effect of cultivated land scale, formulating targeted protection measures and improving the efficiency of cultivated land use.

Based on the correlation analysis and cold and hot spot analysis, it could be seen that the hot spot areas, such as scale, spatial characteristics, production function, carrying function and social environment, were mainly in the central plain area of Qujiang District, which is the area of cultivated land large-scale production and cultivated land priority protection in the whole region, and was the main grain production area. The ecological function hotspot was located in the middle and south of Qujiang District, which was suitable for the development of cultivated land eco-tourism industry. The hot spots of

natural environment were located in the north and south of the district, which should be protected for ecological environment and suitable for returning farmland to forest. The cold point area of each index was the key area to implement the cultivated land protection system and the important basis for quality zoning.

4.4. Zoning Analysis of Cultivated Land Quality

According to the quality of cultivated land quality index, correlation and cold and hot spot analysis, the cultivated land quality of Qujiang District was divided into regions, which provided ideas for realizing differentiated protection and fine management and protection of cultivated land. According to the result of the quality division, the construction, utilization and protection of cultivated land were proposed from three aspects of economy, society and the environment.

In the social aspect, the cultivated land production function area, the cultivated land comprehensive improvement and function improvement area and the cultivated land resource shortage area should play their advantages in space, productivity and carrying capacity, ensure food security, develop modern agricultural industry and through strengthening agricultural infrastructure construction and cultivated land management level, establish centralized contiguously high standard farmland, maintain stable cultivated land area and improve the quality of cultivated land.

In terms of the economy, the cultivated land comprehensive functional area, which focuses on developing comprehensive agriculture and improving comprehensive agricultural production capacity, is a key area to develop into a modern agricultural demonstration area under the background of traditional agricultural transformation and upgrading.

In terms of the environment, the main area of cultivated land ecology and landscape function is the main area to maintain the balance of ecological environment, protect biodiversity protection and maintain the aesthetics of cultivated land landscape. At the same time, through the formation of characteristic agricultural industry, it drives the development of the agricultural economy and is an important area to help rural revitalization.

5. Conclusions

On the basis of the existing research results, this study combined the existing research on cultivated land quality and explored how to conduct comprehensive and systematic protection of cultivated land from the three aspects of space, function and environment. By clarifying the basic concepts, this study made a theoretical analysis of the relationship between the quantity, quality and ecology of cultivated land and the space, function and environment of cultivated land. The current study proposed a systematic theoretical framework for evaluating the space, function and environmental quality of cultivated land, constructed an indicator system and made an empirical application using the Qujiang District as the case area. The following conclusions are drawn.

The cultivated land quality evaluation results based on the space–function–environment have a supporting role in the development of modern agriculture. The cultivated land with good space quality is suitable for large-scale mechanized agricultural operation, the cultivated land with moderate space quality can be used for small-scale mechanized agricultural operation and the cultivated land with poor space quality is not suitable for mechanized operation. The cultivated land with high functional quality is suitable for the development of food, cash crops, tourism and other industries. The cultivated land with poor functional quality should identify its limiting factors and improve the functional quality of its cultivated land. The cultivated land with high environmental quality can produce high-grade organic agricultural products, as well as pollution-free agricultural products, while the cultivated land with poor environmental quality needs to strictly prohibit or restrict the production of edible agricultural products, and switch to industrial grain production or flower cultivation. The cultivated land with high comprehensive quality of space–function–environment should be classified as permanent basic farmland.

The trade-offs and synergies among the indicators of space–function–environment of the cultivated land are the basis for exploring zoning construction, utilization and protection measures based on cultivated land quality. The scale and spatial characteristics in spatial quality were synergistic with the production function, carrying function and social environment in the environmental quality, indicating that cultivated land with a better spatial quality also had a greater production capacity, which could support a greater population and form a better social environment. The relationship between the production function and social environment was also synergistic, which showed that the influence of human action on the production function of the cultivated land was positive. The ecological function and natural environment were synergistic, indicating that they also had a positive relationship. The scale, spatial characteristics and the natural environment in the environmental quality were trade-offs, indicating that if the spatial quality was better, the natural environment was more likely be damaged. The production function, carrying function and the natural environment were also trade-offs, which showed that few places had a high productive capacity and population carrying capacity of cultivated land and a good natural environment. The ecological function and social environment were trade-offs, which showed that human activities played a negative role in ecological function.

No significant relationship was found between landscape function and scale, spatial characteristics, production function, social environment, natural environment, ecological function and scale, carrying function and the social environment.

According to the cold and hot spot analysis of the secondary indicators of space quality, functional quality and environmental quality, cultivated land in the Qujiang District was divided into the main areas of cultivated land production function, ecological and landscape function, cultivated land resource tension, comprehensive improvement and function improvement of cultivated land and comprehensive functional areas of cultivated land. The main cultivated land production function area had the characteristics of large overall cultivated land area, relatively flat terrain, high plot connectivity and regularity, complete infrastructure and high comprehensive quality of the cultivated land. The main areas of cultivated land ecological and landscape functions were characterized by good ecological environment, beautiful landscape, scattered distribution of cultivated land and low farming efficiency. The cultivated land resource shortage area had the characteristics of a small, cultivated land area, dense population and cultivated land pollution. The comprehensive improvement and function improvement area of the cultivated land had the characteristics of inefficient use of the cultivated land, nonstandard layout and low comprehensive quality of the cultivated land.

Author Contributions: Conceptualization, F.X.; Methodology, X.X. and Y.X.; Writing—original draft, Y.S.; Supervision, B.X.; Project administration, H.L.; Funding acquisition, L.P. All authors have read and agreed to the published version of the manuscript.

Funding: This research was funded by the Natural Science Foundation of Zhejiang Province, China(LY21D010008,LQ21D010007), the National Natural Science Foundation of China (41701618, 42101068,41871083, 41230751), the Natural Science Foundation for Distinguished Young Scholars of Zhejiang Province, China (LR21G030001), the Natural Science Foundation of Guangdong Province, China (2020A1515010730), the Humanities and Social Science General Program sponsored by the Ministry of Education of China (22YJCZH208) and the Open Fund of Key Laboratory of Coastal Zone Exploitation and Protection, Ministry of Natural Resources (2019CZEPK09).

Data Availability Statement: The data presented in this study are available on request from the corresponding author.

Conflicts of Interest: The authors declare no conflict of interest.

References

1. FAO. *A Framework for Land Evaluation*; Soils Bulletin 32; Food and Agriculture Organization of the United Nations: Rome, Italy, 1976; p. 65.
2. Pieri, C.; Dumanski, J.; Hamblin, A.; Young, A. Land quality indicators. In *World Bank Discussion Papers*; World Bank: Washington, DC, USA, 1995; p. 315.
3. Rossiter, D.G. A theoretical framework for land evaluation. *Geoderma* **1996**, *72*, 165–190. [CrossRef]
4. Costanza, R.; d'Arge, R.; De Groot, R.; Farber, S.; Grasso, M.; Hannon, B.; Limburg, K.; Naeem, S.; O'neill, R.V.; Paruelo, J.; et al. The value of the world's ecosystem service and natural capital. *Nature* **1997**, *387*, 253–260. [CrossRef]
5. Bouma, J.; Droogers, P. A procedure to derive land quality indicators for sustainable agricultural production. *Geoderma* **1998**, *85*, 103–110. [CrossRef]
6. Yang, H.; Li, X. Cultivated land and food supply in China. *Land Use Policy* **2000**, *17*, 73–88. [CrossRef]
7. Lichtenberg, E.; Ding, C.R. Assessing farmland protection policy in China. *Land Use Policy* **2008**, *25*, 59–68. [CrossRef]
8. Kong, X.B. China must protect high-quality arable land. *Nature* **2014**, *506*, 7. [CrossRef]
9. Vasu, D.; Srivastava, R.; Patil, N.G. A comparative assessment of land suitability evaluation methods for agricultural land use planning at village level. *Land Use Policy* **2018**, *79*, 146–163. [CrossRef]
10. Ni, S.X.; Liu, Y.S. On the importance of cultivated land quality in the total cultivated land dynamic equilibrium. *Econ. Geogr.* **1998**, *18*, 83–85.
11. Matsom, P.A.; Parton, W.J.; Power, A.G.; Swift, M.J. Agricultural intensification and ecosystem properties. *Science* **1997**, *277*, 504–509. [CrossRef]
12. Hvistendahl, M. China's push to add by substracting fertilizer. *Science* **2010**, *327*, 801. [CrossRef]
13. Vitousek, P.M.; Naylor, R.; Crews, T.; David, M.B.; Drinkwater, L.E.; Holland, E.; Johnes, P.J.; Katzenberger, J.; Martinelli, L.A.; Matson, P.A.; et al. Nutrient imbalances in agricultural development. *Science* **2009**, *324*, 1519–1520. [CrossRef]
14. Guo, J.; Liu, X.; Zhang, Y.; Shen, J.; Han, W.; Zhang, W.; Christie, P.; Goulding, K.; Vitousek, P.; Zhang, F. Significant acidification in major Chinese croplands. *Science* **2010**, *327*, 1008–1010. [CrossRef]
15. Xu, Y.; Pu, L.J.; Zhang, R.; Zhu, M.; Zhang, M.; Bu, X.; Xie, X.; Wang, Y. Effects of agricultural reclamation on soil physicochemical properties in the mid-eastern coastal area of China. *Land* **2021**, *10*, 142. [CrossRef]
16. Xie, X.F.; Wu, T.; Zhu, M.; Jiang, J.J.; Xu, Y.; Wang, X.H.; Pu, L.J. Comparison of random forest and multiple linear regression models for estimation of soil extracellular enzyme activities in agricultural reclaimed coastal saline land. *Ecol. Indic.* **2021**, *120*, 106925. [CrossRef]
17. Uwizeyimana, H.; Wang, H.; Chen, W. Evaluation of combined noxious effects of siduron and cadmium on the earthworm Esisenafoetida. *Environ. Sci. Pollut. Res.* **2016**, *24*, 5349–5359. [CrossRef]
18. Zhao, F.J.; Ma, Y.; Zhu, Y.G.; Tang, Z.; McGrath, S.P. Soil contamination in China, current status and mitigation strategies. *Environ. Sci. Technol.* **2015**, *49*, 750. [CrossRef]
19. Wang, F.F.; Guan, Q.Y.; Tian, J.; Lin, J.K.; Yang, Y.Y.; Yang, L.Q.; Pan, N.H. Contamination characteristics, source apportionment, and health risk assessment of heavy metals in agricultural soil in the Hexi Corridor. *Catena* **2020**, *191*, 104573. [CrossRef]
20. Pearson, W.R.; Lipman, D.J. Improved tools for biological sequence comparison. *Proc. Natl. Acad. Sci. USA* **1988**, *85*, 16138–16143. [CrossRef]
21. Spearman, C. The proof and measurement of association between two things. *Am. J. Psychol.* **1904**, *15*, 72–101. [CrossRef]
22. Yang, Y.; Christakos, G.; Guo, M.W.; Xiao, L.; Huang, W. Space-time quantitative source apportionment of soil heavy metal concentration increments. *Environ. Pollut.* **2017**, *223*, 560–566. [CrossRef]
23. Guo, W.; Wu, T.; Jiang, G.; Pu, L.; Zhang, J.; Xu, F.; Yu, H.; Xie, X. Spatial distribution, environmental risk and safe utilization zoning of soil heavy metals in farmland, subtropical China. *Land* **2021**, *10*, 569. [CrossRef]
24. Rodríguez, J.P.; Beard, T.D., Jr.; Bennett, E.M.; Cumming, G.S.; Cork, S.J.; Agard, J.; Peterson, G.D. Trade-offs across space, time, and ecosystem services. *Ecol. Soc.* **2006**, *11*, 709–723. [CrossRef]
25. Getis, A.; Keith Ord, J. The Analysis of Spatial Association by Use of Distance Statistics. *Geogr. Anal.* **1992**, *24*, 189–206. [CrossRef]
26. Huan, L. *Introduction to the Research of Marginalization of Agricultural Land*, 1st ed.; China Social Sciences Press: Beijing, China, 2023; pp. 154–196.
27. Coyle, C.; Creamer, R.E.; Schulte, R.P.O.; O'Sullivan, L.; Jodan, P. A Functional Land Management conceptual framework under soil drainage and land use scenarios. *Environ. Sci. Policy* **2016**, *56*, 39–48. [CrossRef]
28. Akhtar, K.; Wang, W.Y.; Ren, G.X.; Khan, A.; Feng, Y.Z.; Yang, G.H.; Wang, H.Y. Integrated use of straw mulch with nitrogen fertilizer improves soil functionality and soybean production. *Environ. Int.* **2019**, *132*, 105092. [CrossRef]
29. Schellberg, J.; Hill, M.J.; Grehards, R.; Rothmund, M.; Braun, M. Precision agriculture on grassland: Applications, perspectives and constraints. *Eur. J. Agron.* **2008**, *29*, 59–71. [CrossRef]

30. Legaz, B.V.; De Souza, D.M.; Teixeira RF, M.; Antón, A.; Putman, B.; Sala, S. Soil quality, properties, and functions in life cycle assessment: An evaluation of models. *J. Clean. Prod.* **2017**, *140*, 502–515. [CrossRef]
31. Zhang, L.G.; Wang, Z.Q.; Chai, J.; Li, B.Q. Multifunction spatial differentiation and comprehensive zoningof cultivated land in Hubei Province. *Areal. Res. Dev.* **2019**, *38*, 125–130.

land

MDPI

Article

Priority to Self-Interest? Economic Development? Or Ecological Coordination? The Turnover of Local Officials and Environmental Governance in China

Yanjun Guo [1], Tuo Zhang [2,*] and Ruotong Li [1]

[1] China Academy of the Belt and Road Initiative, Beijing International Studies University, Beijing 100024, China
[2] Graduate School of Economics, Kyoto University, Kyoto 606-8501, Japan
* Correspondence: zhang.tuo.8p@kyoto-u.ac.jp

Abstract: Under the background of government-oriented environmental governance in China, the environmental effect of local official turnover has become an important issue. How to improve governmental governance is an important issue that profoundly affects local environmental governance. Based on a literature analysis, this paper establishes an environmental-effect identification equation to deeply analyze the environmental effect of local official turnover on private enterprises. Then, this paper empirically analyzes the effect of local personnel turnover on the environmental pollution control of private enterprises and the persistence of this effect. The results show that the turnover of local officials has a positive effect on the pollution control investment of private enterprises, but the effect is not persistent. The interest collusion between local officials and private enterprises tends to be one main reason to explain the environmental effect, and two different types of interest collusions are determined: priority to self-interest and economic development. The reasons why the positive effect cannot last for long may be attributed to a lack of systematic and effective institutions or temporary administrative measures. It is important to make local officials fully realize the "green wealth" value of the ecosystems, to change their economic priorities. Finally, this paper proposes countermeasures for local governments on personnel affairs to promote environmental governance.

Keywords: official turnover; environmental governance; collusion; environmental effect

Citation: Guo, Y.; Zhang, T.; Li, R. Priority to Self-Interest? Economic Development? Or Ecological Coordination? The Turnover of Local Officials and Environmental Governance in China. *Land* **2023**, *12*, 91. https://doi.org/10.3390/land12010091

Academic Editors: Chuanzhun Sun, Nir Krakauer, Shicheng Li, Qi Zhang, Basanta Paudel and Lanhui Li

Received: 4 October 2022
Revised: 23 December 2022
Accepted: 23 December 2022
Published: 27 December 2022

1. Introduction

The environmental issue is one of the most serious challenges that China has faced since the 1990s [1]. The current form of environmental governance in China is still government-oriented environmental governance. The central government's protection policies need to be implemented by local governments [2]. The responsibility of environmental governance is mainly assumed by local governments and their functional departments. Whether the local government can scientifically implement administrative law is directly related to the effectiveness of environmental governance. Environmental pollution is not only a problem of economic development but also refers to local government governance. The weakening of local government supervision is an important reason for the frequent occurrence of environmental problems. From early 2005 to 2007, the central government carried out four consecutive rounds of environmental law-enforcement inspections, which directly hit the increasingly prominent environmental pollution problems in China. In 2015, the trial Environmental Protection Inspection Program was promulgated. Environmental-protection inspection has become an important way to build an ecological civilization. Since 2015, the central government has successively launched two rounds of central government's supervision, and the "environmental storm" has once again had a wide impact on the whole society.

Environmental protection supervision from the central government brings huge pressure on local government through accountability interviews and official turnover, which

have a profound impact on the process of local environmental governance. Under such pressure, local officials pay more attention to environmental governance. The turnover of officials is one of the most noteworthy changes in local government governance, which not only affects regional economic growth [3–6], enterprise investment [7–10], utilization of foreign capital [11], enterprise R&D (Research and Development), and innovation [12] but also affects the governance of local environmental issues [13–16]. Local personnel turnover has become one of the most important factors affecting environmental governance. The research on the impact mechanism of local personnel turnover on environmental governance is gradually being deepened. However, at present, most of the research mainly uses personnel turnover to match the regional environmental data of cities or provinces for environmental effect analysis, though this matching analysis of personnel turnover and enterprise environmental data is still not perfect and needs to be further studied. There needs to be more study on the enterprise-level impacts and the length of time these impacts last.

This paper establishes an environmental-effect equation to empirically analyze the effect of official turnover on private enterprise pollution control. Based on theoretical analysis, this paper puts forward two hypotheses. Around these two hypotheses, this paper matches the personnel-turnover information of local officials with the data of heavily polluting enterprises and empirically verifies the validity of the two hypotheses through the environmental-effect equation. Then, this paper analyzes the empirical results of the environmental effects of official turnover on enterprises. Further, this paper discusses the impact mechanism of local personnel turnover on local environmental governance to explain how personnel turnover affects enterprise pollution control. At last, this paper provides a reference for environmental governance by optimizing the turnover and policy priority of local officials.

2. Theoretical Analysis and Hypotheses

The administrative intervention of local governments has been considered an important factor affecting the improvement of local environmental quality and the fulfillment of enterprises' environmental responsibilities [14,15]. It has been proven to some extent that the turnover of local officials can improve the local ecological environment. For example, the turnover of party secretaries (the top leader of a local government) can significantly reduce the number of local water-pollution incidents [15] and temporarily improve the air quality [16]. There are two main possible mechanisms for the local officials' turnover affecting the environmental pollution control. (1) The interest collusion mechanism, which contains two aspects, the direct breaking way and the indirect deterrent way. On the one hand, changing local officials breaks the interest collusion between polluting enterprises and the former leaders, thus, the supervision of polluting enterprises is strengthened, and the number of illegal pollution events is reduced [15]. On the other hand, while breaking some interest collusions between polluting enterprises and local officials, the turnover of officials also has a short-term "deterrent" that alerts other existing collusion interests to reduce their environmental illegal activities, to not be punished in this special time. Intercity turnover is more deterrent than same-city turnover [16]. (2) The economic tightening mechanism, which relates to the turnover of officials also having a temporary impact on local economic activities. It leads to a decline in the intensity of local economic activities [4,5], thereby indirectly reducing the pollution of the local environment. Environmental governance varies in different regions, but no matter which one of the two mechanisms works, the turnover of local officials has a certain positive effect on local environmental governance. Based on this, hypothesis 1 is proposed:

H1: *The turnover of officials may have a positive effect on the environmental governance of private enterprises*.

No matter whether from the perspective of collusion theory or from the perspective of the short-term impact of economic activities, the improving effect of local personnel turnover on private-enterprise pollution control appears to not be persistent. From the

perspective of collusion theory, if local officials collude with the private enterprises creating pollution, local officials act as an umbrella for the private enterprises that are creating pollution. When the officials who protect the private enterprise are replaced, some collusions between officials and the private enterprises creating pollution end, while other collusions are deterred. Thus, environmental governance is executed effectively, and the environmental conditions are improved. However, with the re-establishment of interest collusions, or the weakening of the deterrent effect, environmental-governance supervision is weakened, and the persistence of environmental improvement is not significant enough [16]. In another way, the turnover of officials may cause short-term economic fluctuations, and the investment in private business may drop, which accordingly reduce environmental pollution to a certain degree. After the short fluctuation, the local government runs smoothly, economic activities return to normal, and the investment intensity of the polluting private enterprises increases. Thus, environmental pollution is correspondingly deepened. Based on this, hypothesis 2 is proposed:

H2: *The effect of local official turnover on the environmental governance of private enterprises seems to not be persistent*.

3. Methodology and Data

3.1. Methodology

According to the existing literature [15–17], we take the local personnel turnover as a natural experiment to identify its impact on the pollution mitigation behaviors of heavily polluting firms. To be specific, the following linear model is used as our baseline model:

$$\begin{aligned} Mitigation_{ij} &= \beta_0 + \beta_1 Transfer_i + \Phi FirmAttr_{ij} + \Gamma OwnerAttr_{ij} \\ &\quad + \Lambda CityAttr_i + \varepsilon_{ij} \end{aligned} \tag{1}$$

The explained variable $Mitigation_{ij}$ is the investment of private enterprises for pollution control. "i" and "j" stand for different cities and different enterprises, respectively. $Transfer_i$ is the main explanatory variable; if the prefecture-level city where the enterprise is located has a turnover of the municipal party secretary in that year, there is $Transfer_i = 1$, otherwise, $Transfer_i = 0$. $FirmAttr_{ij}$ are control variables for firm characteristics, including firm size, profitability, firm age, etc. $OwnerAttr_{ij}$ are control variables for the characteristics of the firm owner, including the firm owner's age, gender, education level, etc. $CityAttr_{ij}$ are control variables for city-level characteristics, including the proportion of the secondary industry, economic development, fiscal deficit rate, etc. ε_{ij} is a random item. The main concern of this study is the coefficient β_1, which reflects the difference in the investment for pollution control by private enterprises in prefecture-level cities with official turnover or without official turnover.

In addition, when we use the equation mentioned above to test hypothesis 1, $Transfer_i$, as the main explanatory variable, stands for official turnover in the current year. When the equation above is used to test hypothesis 2, $Transfer_i$ stands for official turnover in the last year. We further use the regression equation above to figure out the differences in the effects brought about by different types of official turnover and to test the robustness of the model, referring to the inter-city turnover and the same-city turnover.

In addition to the normal linear model, we also use the Tobit regression [18] to avoid the problem of negative prediction. We build up the following Tobit model, where $Mitigation^*_{ij}$ is the latent dependent variable:

$$\begin{cases} Mitigation^*_{ij} = \beta_0 + \beta_1 Transfer_i + \Phi FirmAttr_{ij} + \Gamma OwnerAttr_{ij} + \Lambda CityAttr_{ij} + \varepsilon_{ij} \\ Mitigation_{ij} = max(0, Mitigation^*_{ij}) \end{cases} \tag{2}$$

We report the estimated results from both the OLS (Ordinary Least Squares) model and the Tobit model in Section 4.

3.2. Samples

The enterprise samples used in this study are the samples of China's private enterprise surveys in 2006, 2008, 2010, and 2012. China's private enterprise survey data adopt the method of cross-sectional stratified sampling survey and select 0.5% of the national private enterprise samples (with slight differences in different years) every two years for the survey. The samples are distributed in various industries and geographical areas. Therefore, this survey has been widely used in research on the operation of Chinese enterprises [19]. The data on the turnover of party secretaries in prefecture-level cities come from the database of Chinese political elites. The Chinese Political Elite Database includes the demographic information and political experience information of leaders of all prefecture-level cities and above in China since 1990 [20]. Other variables at the prefecture-city level are derived from the China Urban Statistical Yearbook.

In this paper, the samples are filtered according to the following three principles: (1) We exclude enterprises in the general service industry such as finance, accommodation, and catering as well as enterprises engaged in agriculture, forestry, animal husbandry, and fishery. We only retain three industries. One is the mining industry, another is the manufacturing industry, and the third one is the electricity, heat, gas, and water production and supply industry. (2) We also exclude the samples of municipalities directly under the central government and prefecture-level cities in Tibet, leaving only the samples of other prefecture-level cities. (3) We also remove the samples containing outliers through the program "winsorize" in Stata.

Considering the characteristics of the local government governance structure in China, previous studies on official turnover mostly used the turnover of local party committee secretaries to conduct simulation experiments [4,16]. Therefore, this study uses the turnover of municipal party committee secretaries as the research object. In this study, 40 party secretaries in these prefecture-level cities were transferred from the Chinese political elite database, accounting for 17% of total 230 surveyed cities (as shown in Appendix A, Table A1). Among these turnovers, 16 were transferred within the same city, accounting for 40%, and 24 were transferred from different places, accounting for 60%. The same-city transfers were usually the cases that the mayor was promoted to the secretary of the municipal party committee. There are many cases of transfers from other places, including from other prefecture-level cities in the same province and other provinces. Some of these are appointed by the provincial government or the central government.

3.3. Main Variables

In this paper, the measurement of corporate investment in pollution control is mainly based on the ratio of corporate investment in pollution control to operating income in the current year. It can remove the influence of inflation and control the fluctuation caused by the influence of scale. The descriptive statistics of the main variables used in this paper are shown in Table 1. (1) The proportion of investment in pollution control is the explained variable. The average value of the proportion of investment in pollution control to operating income is about 0.703, and the standard deviation is about 3.830, indicating that corporate investment in pollution control varies greatly in different cities or over time. (2) Official turnover is the main explanatory variable. Its value is 0 or 1. The average value is 0.213, referring to 1195 enterprise samples with turnover, about 21% of total 5600 enterprise samples (as shown in Appendix A, Table A1). (3) The others are control variables. The average profit rate of enterprises is about 8.148, and the standard deviation is about 15.505, indicating that the profit rate of heavily polluting enterprises seems very different. The average value of the proportion of sewage charges is 0.148, and the standard deviation is about 0.587, which shows that the heavily polluting enterprises have great differences in their expenditure on sewage charges.

Table 1. Descriptive statistics of variables.

Variables	Count	Mean	s. d.	Min	Max
Proportion of investment in pollution control (%)	5600	0.703	3.830	0.000	85.714
Official turnover (1 = have)	5600	0.213	0.410	0.000	1.000
Proportion of sewage charges (%)	5600	0.148	0.587	0.000	10.000
Average profit rate of enterprises (%)	5600	8.148	15.505	−100.000	100.000
Enterprise operating income (log)	5600	16.445	2.539	0.000	24.937
Enterprise age (year)	5600	8.031	4.930	0.000	27.000
Enterprise owner's age (year)	5600	46.062	8.433	15.000	90.000
Enterprise owner's college education (1 = yes)	5600	0.888	0.315	0.000	1.000
Enterprise owner's gender (1 = female)	5600	0.099	0.298	0.000	1.000
Proportion of secondary industry (%)	5600	50.825	9.155	15.700	85.920
GDP per capita (log)	5600	10.263	0.727	8.410	11.800
Fiscal deficit rate (%)	5600	0.994	1.166	−0.143	13.409

In this paper, the samples are divided into two groups with and without the turnover of the municipal party secretary, and the mean characteristics of the two groups are compared. Some descriptive statistics of the two groups are as follows: (1) The investment of the turnover group in pollution control is significantly higher than that of the non-turnover group. (2) There are a large number of truncated samples in both groups, and the median is 0. (3) Compared with the non-turnover group, the 75% quantile and 90% quantile of the turnover group were both higher than those of the non-turnover group.

4. Results and Discussion

4.1. Results

4.1.1. Empirical Results for Hypothesis 1

Based on regression Equations (1) and (2), different combinations of the control variables were controlled for empirical analysis, as shown in columns (1)–(4) in Table 2. Column (1) shows that the variables for firm characteristics, firm owner characteristics, and city characteristics were controlled. Column (2) shows that the variables for firm owner characteristics were controlled. Column (3) shows that the variables for firm characteristics were controlled. The effects of official turnover under different combinations of control variables were obtained (see Table 2). The results are as follows:

1. After controlling for the different explanatory variables listed in columns (1)–(4), official turnover still has a significant promoting effect on the investment of private enterprises in pollution control. As shown in Table 2, the turnover of the municipal party secretary increases the proportion of the investment in pollution control by 0.541. Moreover, the regression coefficients in columns (1)–(4) range from 0.541 to 0.583, which has a certain robustness.
2. The benchmark conclusion of this paper shows that the turnover of officials in prefecture-level cities may have a positive effect on the investment of local private enterprises in pollution control, which supports hypothesis 1. Investment in pollution control plays an important factor in environmental quality.

Table 2. The effect of municipal party secretary turnover on private enterprise pollution control investment: benchmark results.

	Proportion of Investment in Pollution Control (%)							
	(1)	(1)′	(2)	(2)′	(3)	(3)′	(4)	(4)′
	OLS	Tobit	OLS	Tobit	OLS	Tobit	OLS	Tobit
Official turnover in the current year (1 = have)	0.411 *** (0.142)	0.543 ** (0.222)	0.453 *** (0.150)	0.545 ** (0.237)	0.423 *** (0.148)	0.583 ** (0.232)	0.452 *** (0.150)	0.541 ** (0.238)
Environmental regulation								
Proportion of sewage charges (%)	1.783 *** (0.297)	2.479 *** (0.359)	1.494 *** (0.307)	2.499 *** (0.434)	1.791 *** (0.311)	2.491 *** (0.371)	1.497 *** (0.308)	2.513 *** (0.435)
Firm characteristics								
Average profit rate of enterprises (%)			0.016 ** (0.006)	0.034 *** (0.010)			0.015 ** (0.006)	0.033 *** (0.010)
Enterprise operating income (log)			0.050 ** (0.025)	0.613 *** (0.093)			0.050 * (0.025)	0.613 *** (0.095)
Enterprise age (year)			−0.028 *** (0.010)	−0.011 (0.018)			−0.024 ** (0.010)	−0.009 (0.018)
Firm owner characteristics								
Enterprise owner's age (year)					−0.012 ** (0.005)	0.007 (0.008)	−0.010 * (0.005)	−0.011 (0.010)
Enterprise owner's college education (1 = yes)					0.251 ** (0.119)	0.921 *** (0.260)	0.152 (0.125)	0.264 (0.265)
Enterprise owner's gender (1 = female)					−0.144 (0.186)	−0.795 ** (0.333)	−0.048 (0.204)	−0.441 (0.360)
City Characteristics								
Proportion of the secondary industry (%)			0.012 ** (0.006)	0.024 ** (0.012)	0.012 ** (0.006)	0.036 *** (0.011)	0.012 ** (0.006)	0.024 ** (0.012)
GDP per capita (log)			0.075 (0.092)	−0.075 (0.162)	0.098 (0.089)	0.166 (0.151)	0.079 (0.092)	−0.060 (0.163)
Fiscal deficit rate (%)			0.333 *** (0.089)	0.611 *** (0.133)	0.373 *** (0.091)	0.681 *** (0.135)	0.343 *** (0.091)	0.626 *** (0.136)
Samples	4758	4758	4073	4073	4407	4407	4043	4043
Log-likelihood	−11,959.6	−8059.3	−10,287.8	−6805.8	−11,131.3	−7454.0	−10,223.9	−6760.6
R-squared	0.112	0.027	0.099	0.040	0.128	0.033	0.099	0.040

Note: We report the marginal effect estimated by the Tobit model. The values in parentheses are heteroscedastic robust standard errors; *, **, and *** indicate significance at 10%, 5%, and 1% levels, respectively. The results by OLS are also reported in the table above.

4.1.2. Empirical Results for Hypothesis 2

To further explore the persistence of the effect of official turnover, according to the relevant research [16,17], the results of the previous year's turnover of municipal party secretaries were used as the main explanatory variable, and the rest of the settings are the same as those in Table 2. Based on regression Equations (1) and (2), different combinations of the control variables were controlled for empirical analysis (see Table 3). The results show that, in the second year after the turnover of the party secretary in prefecture-level cities, the effect of official turnover on the investment in pollution control by private enterprises seems to be not significant, as the value is only 0.096, which indicates that the official turnover may not have a persistent effect on the increase in the investment for pollution control. It appears that hypothesis 2 is supported.

Table 3. Persistence of the effects of official turnover.

	Proportion of Investment in Pollution Control (%)							
	(1)	(1)′	(2)	(2)′	(3)	(3)′	(4)	(4)′
	OLS	Tobit	OLS	Tobit	OLS	Tobit	OLS	Tobit
Official turnover in the former year (1 = have)	0.130 (0.109)	0.065 (0.168)	0.134 (0.124)	0.085 (0.185)	0.146 (0.119)	0.055 (0.175)	0.148 (0.128)	0.096 (0.189)
Environmental regulation								
Proportion of sewage charges (%)	1.622 *** (0.239)	2.199 *** (0.265)	1.262 *** (0.170)	2.145 *** (0.303)	1.643 *** (0.251)	2.220 *** (0.277)	1.263 *** (0.170)	2.151 *** (0.304)
Firm characteristics								
Average profit rate of enterprises (%)			0.002 (0.004)	0.010 (0.007)			0.002 (0.004)	0.009 (0.007)
Enterprise operating income (log)			0.047 * (0.025)	0.510 *** (0.107)			0.047 * (0.027)	0.510 *** (0.111)
Enterprise age (year)			−0.014 * (0.007)	0.001 (0.014)			−0.012 (0.008)	0.001 (0.015)
Firm owner characteristics								
Enterprise owner's age (year)					−0.004 (0.004)	0.016 ** (0.007)	−0.003 (0.005)	−0.001 (0.009)
Enterprise owner's college education (1 = yes)					0.306 *** (0.074)	0.833 *** (0.217)	0.208 *** (0.079)	0.256 (0.203)
Enterprise owner's gender (1 = female)					0.128 (0.214)	−0.315 (0.328)	0.217 (0.238)	−0.015 (0.368)
City Characteristics								
Proportion of the secondary industry (%)			0.009 (0.006)	0.015 (0.011)	0.008 (0.006)	0.021 ** (0.010)	0.009 (0.006)	0.015 (0.011)
GDP per capita (log)			−0.033 (0.106)	−0.172 (0.176)	0.029 (0.104)	0.086 (0.159)	−0.033 (0.105)	−0.164 (0.175)
Fiscal deficit rate (%)			0.192 ** (0.093)	0.374 *** (0.129)	0.223 ** (0.095)	0.430 *** (0.134)	0.194 ** (0.094)	0.375 *** (0.131)
Samples	3739	3739	3214	3214	3482	3482	3198	3198
Log-likelihood	−8644.8	−5966.4	−7410.0	−5017.9	−8064.6	−5521.1	−7377.0	−4993.5
R-squared	0.129	0.032	0.082	0.039	0.144	0.037	0.083	0.040

Note: We report the marginal effect estimated by the Tobit model. The values in parentheses are heteroscedastic robust standard errors; *, **, and *** indicate significance at 10%, 5%, and 1% levels, respectively. The results by OLS are also reported in this table above.

4.1.3. Further Robustness Test through Different Types of Official Turnover

Based on the regression Equations (1) and (2), we further figured out the differences between the effects brought about by the inter-city turnover and the same-city turnover and test the robustness of the model. It was a classification regression based on the two types, including transfer from different places and in the same city (see Table 4). In the samples of this study, about 40% of the replacement of party secretaries in prefecture-level cities belonged to the same-city transfer. Model stability was checked. The results show that the environmental effect brought by the official turnover transferred from different places is stronger than that of the same-city transfer. The transfer of municipal party secretaries from different places tends to significantly increase the investment of private enterprises in pollution control by 0.931, which is almost five times as high as the same-city transfer. Although same-city transfer also has a positive impact, its magnitude seems to be relatively small and insignificant.

Table 4. The differences in environmental effects between officials transferred from different places and transferred from the same city.

	Proportion of Investment in Pollution Control (%)							
	Inter-City Transfer				Same-City Transfer			
	(1)	(2)	(3)	(4)	(5)	(6)	(7)	(8)
	Tobit	Tobit	Tobit	Tobit	Tobit	Tobit	Tobit	Tobit
Official turnover in the current year (1 = have)	0.985 *** (0.379)	0.947 ** (0.388)	0.926 ** (0.379)	0.931 ** (0.389)	0.196 (0.218)	0.165 (0.241)	0.216 (0.220)	0.178 (0.242)
Environmental regulation								
Proportion of sewage charges (%)	2.495 *** (0.383)	2.536 *** (0.454)	2.520 *** (0.384)	2.551 *** (0.455)	2.181 *** (0.270)	2.117 *** (0.290)	2.194 *** (0.269)	2.122 *** (0.290)
Firm characteristics								
Average profit rate of enterprises (%)		0.032 *** (0.011)		0.031 *** (0.011)		0.014 ** (0.007)		0.013 ** (0.007)
Enterprise operating income (log)		0.635 *** (0.102)		0.636 *** (0.105)		0.503 *** (0.095)		0.503 *** (0.098)
Enterprise age (year)		−0.012 (0.019)		−0.011 (0.019)		0.002 (0.013)		0.003 (0.014)
Firm owner characteristics								
Enterprise owner's age (year)			0.008 (0.009)	−0.007 (0.011)			0.012 * (0.007)	−0.006 (0.008)
Enterprise owner's college education (1 = yes)			0.939 *** (0.245)	0.288 (0.241)			0.771 *** (0.233)	0.183 (0.237)
Enterprise owner's gender (1 = female)			−0.687 * (0.357)	−0.369 (0.387)			−0.482 (0.306)	−0.161 (0.343)
City Characteristics								
Proportion of the secondary industry (%)	0.031 ** (0.012)	0.023 * (0.013)	0.032 *** (0.012)	0.024 * (0.013)	0.026 *** (0.010)	0.017 * (0.010)	0.026 *** (0.010)	0.017 * (0.010)
GDP per capita (log)	0.201 (0.168)	−0.046 (0.182)	0.219 (0.170)	−0.025 (0.183)	0.115 (0.143)	−0.135 (0.157)	0.098 (0.144)	−0.130 (0.156)
Fiscal deficit rate (%)	0.685 *** (0.141)	0.606 *** (0.139)	0.699 *** (0.145)	0.620 *** (0.143)	0.450 *** (0.122)	0.407 *** (0.123)	0.447 *** (0.125)	0.413 *** (0.125)
Samples	3951	3624	3923	3605	4003	3663	3966	3636
Log-likelihood	−6689.4	−6046.6	−6638.3	−6014.5	−6389.6	−5775.1	−6331.0	−5739.0
R-squared	0.034	0.042	0.035	0.042	0.033	0.037	0.034	0.037

Note: We report the marginal effect estimated by the Tobit model. The values in parentheses are heteroscedastic robust standard errors; *, **, and *** indicate significance at 10%, 5%, and 1% levels, respectively. The results by OLS model are reported in Appendix A, Table A2.

4.2. Discussion

4.2.1. Deepening Analysis for the Formation of Interest Collusion between Local Officials and the Private Enterprises Creating Pollution

The big feature of the data in this paper is that they are just one kind of censored data, so there is a large number of zero points in the explained variable, and the data mostly do not obey the normal distribution, which may affect the robustness of the Tobit model [21,22]. Thus, we used Tobit and OLS models to convince each other and improve the robustness. The empirical results of the two models are relativey consistent. It can be believed that local officials play an important role in environmental governance. It appears that hypothesis 1 is supported by this research. The turnover of local officials may have a positive effect on environmental governance by enhancing the investment of private enterprises for pollution control. The interest collusion between local officials and private enterprises seems to be one of the most important reasons to explain the environmental effect brought about by the turnover of local officials. The existing collusion may hinder the government's enforcement of corporate investment in pollution control. However, more importantly, the key point is how these interest collusions form, which is especially urgent to be fully understood and necessary to be overcomed for improving environmental governance. As the policy maker, local officials' priority seems to be an internal deep motivation to choose whether to

collude or not with the private enterprises creating pollution. This could be interpreted in two ways, priority to self-interest or economic development, as shown below.

1. Priority to self-interest. When local officials give priority to self-interest and fetch illegal income from the private enterprises creating pollution, they would usually act as an umbrella for the private enterprises creating pollution. Lots of pollution activities may be ignored and, thus, escape from the relevant laws [23,24]. This kind of interest collusion may mainly come from local officials' pursuit of personal profit. Through all kinds of profit transmissions, interest collusion probably forms between local officials and the private enterprises creating pollution.
2. Priority to economic development. It is well-known that the "GDP only" preference is the long-standing policy orientation in China, which is the key performance measure for local officials. If local officials want to be promoted, they give priority to economic development, so environmental protection is usually neglected [25,26]. The private enterprises creating pollution sometimes play an important role in regional economic development, which reduces local officials' resolution to enhance environmental governance when they worry about the decline of local GDP growth. This kind of interest collusion may mainly be attributed to local officials' promotion, which makes local officials give priority to economic development, even though private enterprises create lots of pollution.

4.2.2. Key Points for Why the Positive Effect of Local Officials' Turnover on Environmental Governance Is Difficult to Keep

Hypothesis 2 is also supported by this research to some extent. It appears that the positive effect of local officials' turnover cannot last for long, which is not a good indication for us to improve environmental governance through local officials' turnover. It is totally necessary to figure out why the positive effect of local officials' turnover cannot last for long. It will help us to more efficiently take the way of local officials' turnover to improve environmental governance. The reasons why the positive effect of local officials' turnover cannot last for long may be summarized in two ways as below:

1. One reason may lie in the lack of systematic and effective institutions to prevent interest collusion. An interest collusion is usually difficult to be eliminated. It tends to be one complicated local relationship network when an interest collusion forms firmly. It appears more obvious that the deterrence of same-city transfer seems to be limited when we compare the differences in the environmental effects between inter-city transfer and same-city transfer [23,24]. Local promotion may just be the internal evolution of a local relationship network. Therefore, a set of systematic and effective institutions could help to thoroughly break through a local relationship network.
2. Another reason may be the temporary administrative measures taken for environmental supervision. Due to the "GDP only" preference, local officials usually take temporary administrative measures to reduce the aggravating pollution under the pressure of heavy environmental supervision from the central government. Local officials often take a one-size-fits-all approach to deal with this "environmental storm" supervision, which has a great effect on local economic development and social livelihood [27]. When one round of environmental supervision is finished, the measures of reducing pollution taken by local officials tend to be weakened. Long-term mechanisms may need to be strengthened [28]. The key point to coordinating economic development and environmental protection probably lies in making local officials realize that they can promote economic development through environmental protection.

4.2.3. One Possible Way to Coordinate Economic Development and Environmental Protection through Ecosystem "Green Wealth"

Further, more importantly, it is urgent to make officials fully aware of the multifunctionality of the ecosystems, which can provide multiple services at the same time [29–31]. Lucid waters and lush mountains are invaluable assets. For human beings, ecosystems not

only provide abundant material products and landscape tourism but also service functions such as climate regulation, water conservation, and pollution purification [32–35]. The value of an ecosystem's services is the "green wealth" of regional development, which is becoming an important part of regional economic development [36,37]. A sufficient scientific understanding of an ecosystem's functions and values seems to be an important basis for local officials to fundamentally change their development views. The "green wealth" of the ecosystem tends to be an important source of future regional development, which deserves all local officials' special attention. It is particularly noteworthy that the gradual formation of a national consensus on green development has made significant progress in ecological governance in China since the 18th National Congress of the Communist Party of China, with a rapid drop in pollution emissions [38].

5. Conclusions and Policy Implications

Under the current background of government-oriented environmental governance, it is of great importance to deeply study the effect of local personnel turnover on environmental governance and how to improve local government governance to effectively promote local environmental governance. Local governments mainly take charge of concrete environmental governance in China [39]. Focusing on the environmental effect of local personnel turnover, this paper matches the data of official turnover and private enterprises to analyze the environmental effect of official turnover on the enterprises. The conclusions are as follows:

1. Local officials' turnover may have a positive effect on the investment of private enterprises in pollution control. However, the effect of local officials' turnover on the investment in pollution control seems to not be persistent.
2. The interest collusion between local officials and private enterprises is one main reason to explain the environmental effect brought about by the turnover of local officials. The existing interest collusions may hinder the government's enforcement of corporate investment in pollution control. The formation of interest collusions probably lies in two different types: priority to self-interest and economic development given by local officials.
3. The reasons why the positive effect of local officials' turnover cannot last for long may refer to temporary administrative measures or a lack of systematic and effective institutions. The lack of systematic and effective institutions could not break through local relationship networks thoroughly. When environmental supervision is finished, the temporary measures for pollution control also tend to be weakened.
4. One possible way in the future to coordinate economic development and environmental protection is to fully realize the value of ecosystem "green wealth". The deep exploration of ecosystem "green wealth" may promote regional economic development.

The relevant conclusions of this paper have positive policy implications for how to improve local government governance to effectively promote local environmental governance as follows:

1. Personnel turnover may bring positive environmental effects to a certain extent. When interest collusion seriously hinders environmental governance, it is suggested to take the way of personnel turnover to overcome this issue. Meanwhile, it is also suggested to design a set of systematic and effective institutions and long-term measures to efficiently make full use of the personnel turnover policy. It is also suggested to take the way of inter-city transfer rather than same-city transfer to thoroughly break interest collusions.
2. It is necessary to consider the important role of local officials in environmental governance. The policy preferences of local officials usually have a great effect on environmental governance. Promoting local officials' priority from self-interest and GDP preference to the value of ecosystem services is an important way to promote environmental governance. Future work should test whether attitudes and understanding of "green wealth" in new officials affect the outcomes of environmental governance.

Author Contributions: Conceptualization, Y.G. and T.Z.; methodology, T.Z. and Y.G; software, T.Z.; validation, Y.G., T.Z. and R.L.; formal analysis, Y.G. and R.L.; investigation, T.Z. and Y.G.; resources, T.Z. and Y.G.; data curation, T.Z. and R.L.; writing—original draft preparation, Y.G. and R.L.; writing—review and editing, T.Z. and Y.G.; visualization, Y.G. and T.Z.; supervision, T.Z. and Y.G.; project administration, Y.G. and R.L.; funding acquisition, Y.G. and T.Z. All authors have read and agreed to the published version of the manuscript.

Funding: This research was supporteded by the Beijing International Studies University 2021 special scientific research project (Grant No. KYZX21A017), the National Social Science Foundation Major Project (Grant No. 22VMG012) and the National Natural Science Foundation of China (Grant No. 41931293).

Conflicts of Interest: The authors declare no conflict of interest.

Appendix A

Table A1. A summary of local official transfers during the research period.

Year	No. of Enterprise Surveyed	No. That Have Official Turnover	Share (%)	No. of Cities Surveyed	No. That Have Official Turnover	Share (%)
2006	1219	160	13%	88	16	18%
2008	1229	198	16%	80	13	16%
2010	1556	55	4%	42	3	7%
2012	1596	782	49%	20	8	40%
Total	5600	1195	21%	230	40	17%

Note: We would like to describe the detailed matching process, taking the sample in 2006 as an example. First, 1219 firms were surveyed by the Chinese Private Enterprise Survey (CPES) in that year. Second, we identified the location of these firms by their zip codes through the Baidu Open Map Service. We found that they were located in 88 Chinese cities. Third, we matched the 88 cities with the Chinese Political Elite Database (CPED). We found that 18% of the survey cities (16 cities) had transfers of local officials in the year 2006. Fourth, back to the CPES dataset, we found that 160 firms surveyed were located in cities with official transfers.

Table A2. The differences in environmental effects between officials transferred from different places and transferred from the same city through OLS.

	Proportion of Investment in Pollution Control (%)							
	Inter-City Transfer				Same-City Transfer			
	(1)	(2)	(3)	(4)	(5)	(6)	(7)	(8)
	OLS	OLS	OLS	OLS	OLS	OLS	OLS	OLS
Official turnover in the current year (1 = have)	0.791 *** (0.266)	0.776 *** (0.266)	0.763 *** (0.265)	0.761 *** (0.266)	0.092 (0.128)	0.147 (0.143)	0.091 (0.129)	0.159 (0.143)
Environmental regulation								
Proportion of sewage charges (%)	1.828 *** (0.321)	1.527 *** (0.320)	1.830 *** (0.322)	1.531 *** (0.321)	1.595 *** (0.244)	1.224 *** (0.168)	1.595 *** (0.244)	1.223 *** (0.169)
Firm characteristics								
Average profit rate of enterprises (%)		0.014 ** (0.007)		0.014 ** (0.007)		0.005 (0.004)		0.004 (0.004)
Enterprise operating income (log)		0.063** (0.026)		0.063** (0.027)		0.037 (0.025)		0.037 (0.026)
Enterprise age (year)		−0.029 *** (0.011)		−0.025 ** (0.011)		−0.014 * (0.007)		−0.012 (0.008)
Firm owner characteristics								
Enterprise owner's age (year)			−0.011 ** (0.005)	−0.009 (0.006)			−0.006 (0.004)	−0.005 (0.005)
Enterprise owner's college education (1 = yes)			0.300 *** (0.086)	0.199 ** (0.091)			0.210 * (0.112)	0.121 (0.118)
Enterprise owner's gender (1 = female)			−0.074 (0.203)	0.006 (0.221)			0.017 (0.192)	0.116 (0.215)

Table A2. *Cont.*

	Proportion of Investment in Pollution Control (%)							
	Inter-City Transfer				Same-City Transfer			
	(1)	(2)	(3)	(4)	(5)	(6)	(7)	(8)
	OLS	OLS	OLS	OLS	OLS	OLS	OLS	OLS
City Characteristics								
The proportion of the secondary industry (%)	0.009 (0.006)	0.012 * (0.006)	0.010 (0.006)	0.012 * (0.007)	0.010 * (0.005)	0.010 * (0.006)	0.010 * (0.005)	0.010 * (0.006)
GDP per capita (log)	0.141 (0.101)	0.112 (0.105)	0.157 (0.102)	0.119 (0.105)	0.034 (0.093)	−0.009 (0.094)	0.035 (0.093)	−0.009 (0.093)
Fiscal deficit rate (%)	0.377 *** (0.094)	0.339 *** (0.093)	0.394 *** (0.097)	0.349 *** (0.095)	0.225 *** (0.087)	0.208 ** (0.088)	0.231 *** (0.088)	0.213 ** (0.089)
Samples	3951	3624	3923	3605	4003	3663	3966	3636
Log-likelihood	−10,020.2	−9193.5	−9957.4	−9152.0	−9301.0	−8500.7	−9226.0	−8448.5
R-squared	0.139	0.107	0.141	0.108	0.125	0.074	0.127	0.074

Note: We report the marginal effect estimated by the OLS model. The values in parentheses are heteroscedastic robust standard errors; *, **, and *** indicate significance at 10%, 5%, and 1% levels, respectively.

References

1. Sun, D.Q.; Zhang, J.X.; Zhu, C.G.; Hu, Y.; Zhou, L. An assessment of China's ecological environment quality change and its spatial variation. *Acta Geogr. Sin.* **2012**, *12*, 1599–1610.
2. Long, S.; Hu, J. On environmental pollution from the perspective of government-enterprise collusion: A theoretical and empirical analysis. *J. Financ. Econ.* **2014**, *10*, 131–144.
3. Jones, B.; Olken, B. Do leaders matter? National leadership and growth since World War II. *Q. J. Econ.* **2005**, *3*, 835–864.
4. Wang, X.B.; Xu, X.X.; Li, X. Provincial governors' turnovers and economic growth: Evidence from China. *China Econ. Q.* **2009**, *4*, 1301–1328.
5. Cao, G.Y.; Zhou, L.A.; Weng, X. Effects of leadership turnovers on economic growth and the underlying mechanism—Evidence from prefectural-level jurisdiction. *China J. Econ.* **2019**, *4*, 102–126.
6. Ali, A.M. Political instability, policy uncertainty, and economic growth: An empirical investigation. *Atl. Econ. J.* **2001**, *29*, 87–106. [CrossRef]
7. Alesina, A.; Perotti, R. Income distribution, political instability, and investment. *Eur. Econ. Rev.* **1996**, *6*, 1203–1228. [CrossRef]
8. Julio, B.; Yook, Y. Political uncertainty and corporate investment cycles. *J. Financ.* **2012**, *1*, 45–83. [CrossRef]
9. Sun, J.X.; Zong, J.F. Does the governors' turnover affect the behavior and performance of corporations? *Ind. Econ. Res.* **2014**, *5*, 92–103.
10. Wang, P.; Li, C.Y. Turnover of government officials, entrepreneurs following and investment efficiency. *Soft Sci.* **2020**, *6*, 91–96.
11. Lei, G.Y.; Liu, M.; Wang, W.Z. The replacement of officials in power, uncertainty and utilizations of foreign capital. *Res. Econ. Manag.* **2017**, *3*, 24–35.
12. Li, H.J. Governor's turnover, bank credit and R&D investment. *Sci. Res. Manag.* **2018**, *11*, 158–165.
13. Hughes, S.B.; Anderson, A.; Golden, S. Corporate environmental disclosures: Are they useful in determining environmental performance? *J. Account. Public Policy* **2001**, *3*, 217–240. [CrossRef]
14. Zhang, G.F. Government intervention, environmental pollution and corporate environmental protection investment—Evidence from listed companies of heavy pollution industries. *Res. Econ. Manag.* **2013**, *9*, 38–44.
15. Liang, P.H.; Gao, N. Personnel turnover, legal environment and local environmental pollution. *Manag. World.* **2014**, *6*, 65–78.
16. Guo, F.; Shi, Q.L. Official turnover, collusion deterrent and temporary improvement of air quality. *Econ. Res. J.* **2017**, *7*, 155–168.
17. Liu, G.Q.; Yang, Z.Q.; Zhang, F.; Zhang, N. Environmental Tax Reform and Environmental Investment: A Quasi-Natural Experiment Based on China's Environmental Protection Tax Law. *Energy Econ.* **2022**, *109*, 106000. [CrossRef]
18. Amemiya, T. Tobit models: A Survey. *J. Econom.* **1984**, *24*, 3–61. [CrossRef]
19. Chen, G.; Lu, P.; Lin, Z.; Song, N. Introducing Chinese private enterprise survey: Points and prospects. *Nankai Bus. Rev. Int.* **2019**, *4*, 501–525. [CrossRef]
20. Jiang, J. Making bureaucracy work: Patronage networks, performance incentives, and economic development in China. *Am. J. Political Sci.* **2018**, *4*, 982–999. [CrossRef]
21. Arabmazar, A.; Schmidt, P. An investigation of the robustness of the Tobit estimator to non-normality. *Econometrica* **1982**, *50*, 1055–1063. [CrossRef]
22. Wilson, C.; Tisdell, C. OLS and Tobit estimates: When is substitution defensible operationally? In *Economic Theory, Applications and Issues, Working Paper No. 15*; The University of Queensland: Brisbane, Australia, 2002.
23. Nie, H.H.; Jiang, M.J. Coal mine accidents and collusion between local governments and firms: Evidence from provincial level panel data in China. *Econ. Res. J.* **2011**, *6*, 146–156.

24. Fan, Z.Y.; Tian, B.B. Collusion for evasion: Evidence from the rotation of NTBs' directors in China. *China Econ. Q.* **2016**, *4*, 1303–1328.
25. Zhou, L.A. Governing China's local officials: An analysis of promotion tournament model. *Econ. Res. J.* **2007**, *7*, 36–50.
26. Cai, F.; Du, Y.; Wang, M.Y. The political economy of emission in China: Will a low carbon growth be incentive compatible in next decade and beyond? *Econ. Res. J.* **2008**, *6*, 4–11+36.
27. Chen, S.Y.; Xie, Z. An inquiry into the win-win policy for economic development and environmental protection——Start with the Lin Yi Air Pollution Abatement Incident. *Chin. J. Environ. Manag.* **2015**, *4*, 14–20+33.
28. Zhang, T.; Xie, L. The protected polluters: Empirical evidence from the national environmental information disclosure program in China. *J. Clean. Prod.* **2020**, *258*, 120343. [CrossRef]
29. Hector, A.; Bagchi, R. Biodiversity and ecosystem multifunctionality. *Nature* **2007**, *448*, 188–190. [CrossRef]
30. Villéger, S.; Norman, W.H.; David, M. New multidimensional functional diversity indices for a multifaceted framework in functional ecology. *Ecology* **2008**, *8*, 2290–2301. [CrossRef]
31. Jing, X.; He, J.S. Relationship between biodiversity, ecosystem multifunctionality and multiserviceability: Literature overview and research advances. *Chin. J. Plant Ecol.* **2021**, *10*, 1094–1111. [CrossRef]
32. Ouyang, Z.Y.; Wang, R.S.; Zhao, J.Z. Evaluation of ecosystem service functions and their ecological economic value. *J. Appl. Ecol.* **1999**, *5*, 635–640.
33. Zhang, Z.Q.; Xu, Z.M.; Cheng, G.D. Evaluation of ecosystem services and natural capital value. *J. Ecol.* **2001**, *11*, 1918–1926.
34. He, H.; Chen, F.; Zhang, H.L. Research progress on ecosystem services. *J. China Agric. Univ.* **2009**, *6*, 41–45.
35. Xie, G.D.; Zhang, C.X.; Zhang, C.S.; Xiao, Y.; Lu, C.X. The value of ecosystem services in China. *Resour. Sci.* **2015**, *37*, 1740–1746.
36. Song, W.F.; Li, G.P.; Han, X.F. The Value of Ecosystem Services: Economic Theory Context and Modern Interpretation. *Sci. Technol. Manag. Res.* **2015**, *9*, 244–249.
37. Jiang, W.; Wu, T.; Fu, B.J. The value of ecosystem services in China: A systematic review for twenty years. *Ecosyst. Serv.* **2021**. [CrossRef]
38. Huan, Q.Z. Green transformation strategy requires clearer path selection. *People's Trib.* **2016**, *32*, 26–27.
39. Yang, J.; Xue, D.; Huang, G. The Changing Factors Affecting Local Environmental Governance in China: Evidence from a Study of Prefecture-Level Cities in Guangdong Province. *Int. J. Environ. Res. Public Health* **2020**, *17*, 3573. [CrossRef]

land

MDPI

Article

Identification of Land Use Conflicts in Shandong Province from an Ecological Security Perspective

Guanglong Dong [1], Zhonghao Liu [1], Yuanzhao Niu [2] and Wenya Jiang [3,*]

[1] School of Management Engineering, Shandong Jianzhu University, Jinan 250101, China
[2] Binhu New District Construction and Development Center in Xintai, Taian 271200, China
[3] Zhuhai Nature Resource and Planning Technology Center, Zhuhai 519000, China
* Correspondence: 2022025303@stu.sdjzu.edu.cn

Abstract: Accurate identification of land use conflicts is an important prerequisite for the rational allocation of land resources and optimizing the production–living–ecological space pattern. Previous studies used suitability assessment and landscape pattern indices to identify land use conflicts. However, research on land use conflict identification from the perspective of ecological security is insufficient and not conducive to regional ecological, environmental protection, and sustainable development. Based on ecological security, this study takes Shandong Province as an example and comprehensively evaluates the importance of ecosystem service function and environmental sensitivity. It identifies the ecological source, and extracts ecological corridors with a minimum cumulative resistance model from which ecological security patterns are constructed. It identifies land use conflicts through spatial overlay analysis of arable land and construction land. The results show that: (1) Shandong Province has formed an ecological security pattern of "two ecological barriers, two belts, and eight cores" with an area of 15,987 km^2. (2) The level of arable land–ecological space conflict is low, at 39.76%. The proportions of serious and moderate conflicts are 13.44% and 26.97%, respectively, distributed primarily on the Jiaodong Peninsula and the low hill areas of Ludong. (3) Construction land–ecological space conflict is reasonably stable and controllable, at 76.39%, occurring mainly around urban construction land, with serious and moderate conflict concentrated in the eastern coastal areas, mainly between rural settlements and ecologically safe space in the region. This study has important theoretical and practical reference values for identifying land use conflicts, protecting regional ecological security, and optimizing land use patterns.

Keywords: ecological security pattern; land use conflicts; ecosystem service function; ecological sensitivity; Shandong Province

Citation: Dong, G.; Liu, Z.; Niu, Y.; Jiang, W. Identification of Land Use Conflicts in Shandong Province from an Ecological Security Perspective. *Land* **2022**, *11*, 2196. https://doi.org/10.3390/land11122196

Academic Editor: Teodoro Semeraro

Received: 28 October 2022
Accepted: 1 December 2022
Published: 3 December 2022

1. Introduction

The concept of conflict, which first originated in sociology, refers to the psychological or behavioral contradictions that arise when two or more social units are incompatible or mutually exclusive in their goals [1]. With rapid urbanization and industrialization, increasing intensity of land development, and growing tension between people and land, scholars have introduced the concept of conflict into the field of land resources, resulting in the phrase "land use conflict" [2]. The concept of land use conflict can be traced back to 1970s. When the goals of different stakeholders in a specific land parcel were irreconcilable, land use conflict would occur. Land conflict can be understood as a dispute or abuse of land property rights [3]. Land use conflict refers to the contradictory state in the process of land resource utilization [1,4]. Li, Zhu [5] defined the conflict between agriculture and ecological functions as the space–time game generated in the process of agricultural activities and ecological protection. Based on stakeholder theory, Steinhäußer, Siebert [6] defined land use conflict as the inconsistency and disharmony between various stakeholders in the way and quantity of land use in the utilization of land resources, and the conflict between

various land use practices and the natural environment. Although there is no clear and unified concept of land use conflict, studies have generally accepted that land use conflict is caused by the multiplicity and finiteness of land resources and the diversity of demands [7]. Currently, land use conflicts have become a global issue [1,4,8–11]. Land use conflicts hinder the rational and sustainable use of land resources, exacerbate human–land conflicts, and are detrimental to sustainable development.

The study of land use conflicts is an important breakthrough in revealing the evolutionary mechanisms of complex human–land relations, and the accurate identification of land use conflicts is a core element of land use conflict research. As early as the 1970s, scholars carried out land use conflict identification employing interviews, field research, and participatory mapping [12–14]. In recent years, as land use conflicts have increased in intensity and scope and as technology has advanced, quantitative analysis methods are commonly used to identify land use conflicts [15–18]. Quantitative analysis can accurately identify the scale, intensity, spatial distribution, and change characteristics of land use conflicts, which can deepen our knowledge and understanding of land use conflicts and help us to take corresponding countermeasures to mediate land use conflicts. The two main categories include the landscape pattern method and the comprehensive evaluation method. Among them, the landscape pattern index method is based on land use data, and by analyzing the external pressure on the landscape, the degree of spatial exposure, and the spatial stability of the landscape, the rank and type of land use conflicts are judged comprehensively [19]. The integrated evaluation method focuses on the construction of an evaluation index system to comprehensively evaluate land use conflicts by considering the dimensions of land use suitability, propensity, competitiveness, and diversity of demand [20–23]. The above methods have achieved the quantitative identification of land use conflicts, promoted the development of land use conflict research, and provided inspiration for this study. However, the land use conflict identification described above belongs to the category of potential land use conflict identification, which reduces the significance of guidance for real land use. Land use conflicts are also closely related to socioeconomic development. Currently, China has proposed carbon neutrality and carbon peaking, and has an increased focus on the construction of ecological civilization, promoting the green development concept that green water and green mountains are precious, and that mountains, forests, fields, lakes, and grasses are a living community. Ecological security has received unprecedented attention, but research on the identification of land use conflicts from the perspective of ecological security is relatively lacking, making it difficult to effectively support the current allocation and use of land resources in China.

Shandong Province is a populous and economically powerful province in China. The rapid development of urbanization and industrialization has led to an increasingly prominent conflict between agricultural production, economic development, and ecological protection, a situation that serves as a microcosm of China. Taking Shandong Province as an example, this study attempts to construct an ecological security pattern based on the importance of ecosystem service function and ecological sensitivity and to quantitatively identify arable land–ecological space conflict and construction land–ecological space conflict from an ecological security perspective to provide a scientific reference for land use conflict mediation and optimization of the spatial pattern of the land in Shandong Province.

2. Study Area and Data Sources

2.1. Study Area

Shandong Province is geographically located at 34°22.9′ N–38°24.1′ N and 114°47.5′ E–122°42.3′ E (Figure 1), with a total land area of about 1.57×10^7 hm^2, accounting for about 1.63% of the total land area of China. Its topography is complex, with mountains in the center, hills in the east, and plains in the west and north. Shandong Province has a developed and rapidly developing economy, with a high level of industrialization and urbanization. With the growth of population and rapid urban expansion, the spatial pattern of land use has changed significantly. Shandong Province has more people, less

land, less water, and less forest, and the contradiction between land supply and demand is outstanding; the province is very short of forest and water resources, which are closely related to ecology, and the per capita wetland and forest possessions are among the 20th in China, the poor endowment of ecological resources coexists with the continuous increase in demand for land resources.

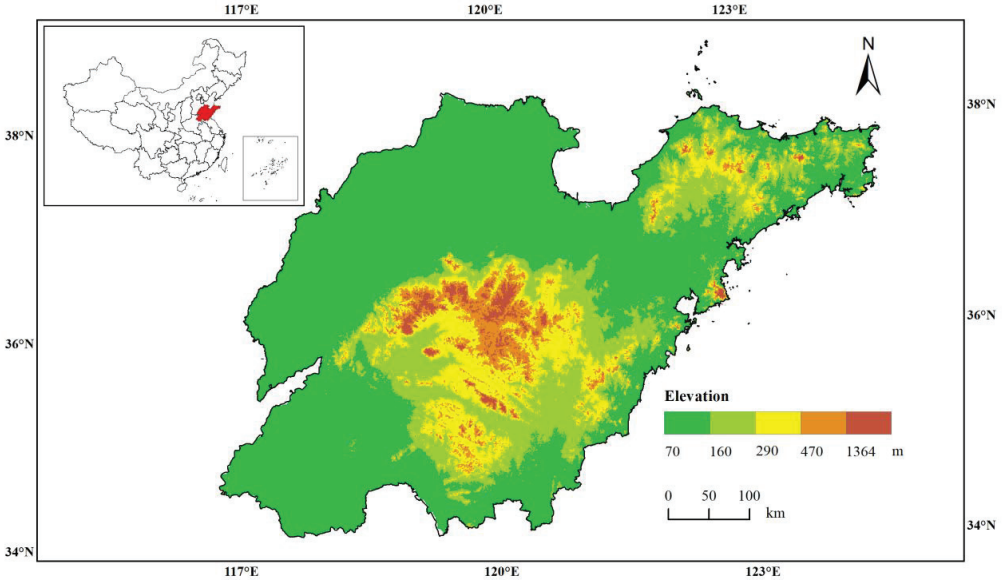

Figure 1. Location of study area.

2.2. Data Sources and Processing

The data used for the study mainly include DEM data from the ASTER GDEM data product of the geospatial data cloud platform (http://www.gscloud.cn/, accessed on 16 March 2022) with a spatial resolution of 30 m. The slope and relief amplitude were extracted through GIS spatial analysis tools; basic geographic data (rivers and waters, traffic roads) were obtained from the geospatial data cloud (https://www.gscloud.cn/, accessed on 16 March 2022); the locations of chemical plants and mines were obtained using the Google Maps coordinate selection system. The soil data were obtained from the Chinese soil dataset (V1.1) in the World Soil Database. Precipitation data were obtained from the National Meteorological Science Data Sharing Service Platform (http://data.cma.cn/index.html/, accessed on 18 March 2022) for 109 meteorological stations in and around the study area in 2020, and the precipitation in the study area was obtained by kriging interpolation. The annual scale mean values of net primary productivity of vegetation, land use data, and NDVI, all with a spatial resolution of 1 km, were obtained in 2020 from the Chinese Academy of Sciences Resource and Environment Science and Data Center (https://www.resdc.cn/, accessed on 18 March 2022).

3. Methodology

3.1. Evaluation of the Importance of Ecosystem Service Functions

Ecosystem service functions are the natural environmental conditions and functions that ecosystems and ecological processes create and maintain to ensure human survival. They include water conservation, soil and water conservation, wind and sand control, biodiversity, carbon fixation, and oxygen release. In line with relevant studies [24,25], combined with the guidelines for ecological protection red-line delineation and the background conditions of ecosystems and development needs in Shandong Province, this paper

comprehensively evaluates the importance of Shandong's ecosystem service functions in terms of water conservation, soil and water conservation, carbon fixation and oxygen release, and biodiversity conservation. The raster value corresponding to 30%, 50%, and 80% of the total value of ecosystem services is used as the cutoff point for the assessment of ecosystem service functions, which are classified into four levels: extremely important, highly important, moderately important, and generally important, and the measurement method of each ecosystem service function is shown in Table 1.

Table 1. Ecosystem service functions evaluation index system.

Ecosystem Service Functions	Calculation Formulas	Formula Parameters and Data-Related Notes
water conservation [24,25]	$WR = NPP_{mean} \times F_{sic} \times F_{pre} \times (1 - F_{slo})$	WR is the ecosystem water-support service capacity index, NPP_{mean} is the mean multiyear vegetation net primary productivity, F_{sic} is the soil infiltration factor, F_{pre} is a multiyear average precipitation factor, F_{slo} is the slope factor
soil and water conservation [26–28]	$S_{pro} = NPP_{mean} \times (1 - k) \times (1 - F_{slo})$	S_{pro} is the soil and water conservation service capability index, NPP_{mean} is the mean multiyear vegetation net primary productivity, F_{slo} is the slope factor,K is the soil erodibility factor
carbon fixation and oxygen release [29]	$Q_{tco_2} = \frac{M_{co_2}}{M_c} \times A \times C_c \times (AGB_{T2} - AGB_{T1})$	Q_{tco_2} is the amount of CO_2 fixed by the ecosystem, M_{co_2} is the coefficient of conversion of C to CO_2, A is the area of the ecosystem, C_c is the carbon conversion factor, AGB_{T2} for year $T2$ Biomass, AGB_{T1} for year $T1$ Biomass
biodiversity conservation [28,30]	$S_{bio} = NPP_{mean} \times F_{pre} \times F_{tem} \times (1 - F_{alt})$	S_{bio} indicates the capacity index for biodiversity conservation services; NPP_{mean}, F_{pre} parameters are calculated as given above, F_{tem} indicates temperature factor, F_{alt} indicates elevation factor

3.2. Evaluation of Ecological Sensitivity

Ecological sensitivity is the degree to which an ecosystem is sensitive to disturbance by natural and human activities in a region. It is used to reflect the ease with which ecological imbalances and ecological problems can occur when a regional ecosystem is disturbed [31]. There are high mountains in the middle of Shandong Province and low and gentle hills in the east. Therefore, there is a risk of soil erosion. The Yellow River Delta and other areas have a salinization problem. Therefore, the ecological sensitivity of Shandong Province was evaluated from two aspects: soil erosion and salinization. Referring to relevant studies [31–35], and in combination with the actual situation of the ecological environment and data availability in Shandong Province, seven evaluation indicators were selected to construct an ecological sensitivity evaluation index system (Table 2). On this basis, the geometric mean model was used to estimate the ecological sensitivity.

Table 2. Ecological sensitivity evaluation index system.

Ecological Sensitivities	Evaluation Indicators	Sensitivity Levels			
		Insensitive (1)	**Generally Sensitive (3)**	**Moderately Sensitive (5)**	**Highly Sensitive (7)**
Soil erosion [24,36,37]	rainfall erosivity ($J \cdot cm/m^2 \cdot h$)	<100	100–400	400–600	>600
	soil erodibility	gravel, sand, coarse sandy soil, fine sandy soil, clay	top sandy soil, loamy soil, loamy clay soil	sandy loam, chalky clay	sandy chalk, chalky soil
	relief amplitude(°)	0–50	50–300	300–500	>500
	vegetation coverage(%)	>60	40–60	20–40	<20
Salinization [38]	groundwater mineralization (g/L)	<5	5–18	18–25	>25
	depth of groundwater burial (m)	>5	3–5	1–3	<1
	soil textures	coarse sandy soil, fine sandy soil, clay	clay, loamy soils	loamy clay, chalky clay	sandy loam

3.3. Constructing Ecological Security Patterns

3.3.1. Identification of Ecological Sources

Ecological sources are areas of high habitat quality that contribute positively to the ecological environment and are the starting point for species maintenance and dispersal and the ecological protection floor [39]. In this paper, the importance of ecosystem service functions and ecological sensitivity layers are spatially overlaid using ArcGIS 10.5 software, and in line with Cannikin's law, extremely important ecosystem service functions and highly sensitive ecological areas are extracted as ecological source areas, while the Yellow River Delta National Nature Reserve and Nansi Lake Reserve are included in the ecological source areas. The source areas were also included in the Yellow River Delta National Nature Reserve and Nansi Lake Reserve.

3.3.2. Ecological Resistance Surface

The construction of the ecological resistance surface is the core of ecological corridor extraction, reflecting the spatial distribution of the intensity of resistance to ecological flows as they run between ecological functions [40]. The ecological processes of horizontal spatial movement of species and the flow and transfer of ecological functions are mainly influenced by the state of land cover and the degree of anthropogenic disturbance. Therefore, with reference to relevant studies [41–45], this paper selects eight evaluation indicators from two aspects of ecological attributes and ecological disturbances to construct an evaluation index system of ecological resistance (Table 3). According to the landscape resistance value of each resistance factor and the corresponding indicator weights, a weighted superposition is made in GIS software to obtain the spatial distribution of the ecological resistance surface.

Table 3. Resistance factors.

Type	Evaluation Factors (Weight)	Drag Coefficient			
		1	3	5	7
Ecological properties	Elevation (0.12)	<100 m	250–100 m	250–400 m	>400 m
	Slope (0.12)	<7°	7–15°	15–25°	>25°
	Land-cover types (0.2)	Wooded land, river water, lake water, scenic spots, and special sites	Garden, pond water, orchard, paddy field, other grassland, marshland, and dryland	Watered land, ditches, agricultural land for facilities, waterworks, fields, and canals	Railway land, road land, rural roads, established towns, villages, ports, and harbors
	Vegetation coverage (0.14)	>80%	60–80%	40–60%	<40%
Ecological disturbances	Distance from roads (0.1)	>800 m	400–800 m	200–400 m	<200 m
	Distance from railways (0.1)	>800 m	400–800 m	200–400 m	<200 m
	Distance from rural settlements (0.1)	>600 m	400–600 m	200–400 m	<200 m
	Distance from chemical plants, mines (0.12)	>800 m	400–800 m	200–400 m	<200 m

3.3.3. Ecological Corridors

A consensus has emerged in the field of ecological research regarding the achievement of ecological functions such as biodiversity conservation and pollution control through the construction of ecological corridors while meeting the growing human need for nature [46]. In this paper, the geometric center of an ecological source site is taken as the ecological source point, and the ecological resistance surface is used as the basis to simulate and calculate the minimum resistance that species need to overcome to move between source sites, thereby constructing an ecological corridor for biological flow, with the following calculation formula:

$$\mathrm{MCR} = f\min \sum_{j=n}^{i=m} \left(D_{ij} \times R_i\right) \tag{1}$$

In Equation (1), MCR is the minimum cumulative resistance value; D_{ij} is the spatial distance of a species from source j to landscape unit i; R_i is the coefficient of resistance of landscape unit i to the movement of a species; f denotes the positive correlation between the minimum cumulative resistance and the ecological process.

The interaction matrix between the ecological source patches was calculated through the gravity model (2) to quantitatively evaluate the interaction strength between the source patches so that the relative importance of potential corridors in the region could be judged more scientifically, and the potential corridors with highly important were considered optimal ecological corridors [47,48]. Simultaneously, to ensure connectivity between the source sites, the study area was combined with the actual situation to set up potential ecological corridors.

$$G_{ij} = \frac{N_i N_j}{D_{ij}^2} = \frac{\left[\frac{1}{P_i} \times ln(S_i)\right]\left[\frac{1}{P_i} \times ln(S_j)\right]}{\left(\frac{L_{ij}}{L_{max}}\right)^2} = \frac{L_{max}^2 ln(S_i S_j)}{L_{ij}^2 P_i P_j} \tag{2}$$

In Equation (2), G_{ij} is the interaction strength between patch i and patch j; N_i and N_j are the weighting coefficients of patch i and patch j, respectively; D_{ij} is the normalized resistance value of the potential corridor between patch i and patch j; P_i is the overall

resistance value of patch i; S_i is the area of patch i; L_{ij} is the cumulative resistance value of the potential corridor between patch i and patch j; and L_{max} is the maximum resistance value of all corridors in the study area.

3.3.4. Ecological Security Pattern

The ecological security pattern is derived from the coupling theory of spatial pattern and ecological process in landscape science, focusing on the potential landscape ecological pattern [49]. The ecological security pattern is a spatial configuration scheme to optimize the territorial spatial pattern of regional ecological space, which is of great significance for maintaining the integrity of the landscape pattern and regional ecological security [50], improving the quality and stability of the ecosystem, ensuring the sustainable supply of regional ecosystem services, and improving human well-being.

Therefore, based on the evaluation results of the importance of ecosystem service functions and ecological sensitivity, together with the extracted ecological sources and ecological corridors, this study comprehensively constructed an ecological security pattern including low, medium, high and extremely high levels of ecological security. Specifically, the 400 m buffer zone of the ecological sources and ecological corridors was taken as the low ecological safety level, while the high, medium, and low levels of the ecosystem service function importance and ecological sensitivity evaluation results and the 400–800 m buffer zone, 800–1200 m buffer zone, and 1200–1600 m buffer zone of the ecological corridors were taken as the medium, high, and extremely high ecological safety levels, respectively.

3.4. Land Use Conflicts Identification and Classifications

With the increase and diversification in land use demand, land resources are increasingly scarce, leading to a variety of land use conflicts. Among them, land use conflict mainly occurs between construction land and arable land, and ecological space and productive land (arable land and construction land). Combined with the current background of ecological civilization construction in China, land use conflict from the perspective of ecological security in this paper refers to the unreasonable occupation of ecological security space by human social and economic activities such as agricultural production and economic construction, which is mainly manifested as the mismatch and overlapping relationship among arable land, construction land, and ecological space [5,51]. The arable land–ecological space conflict is the occupation of ecological space by agricultural farming activities, expressed as the overlapping relationship between arable land and ecological space. The construction land–ecological space conflict is the occupation of ecological space by economic construction activities, expressed as the overlapping relationship between construction land and ecological space. The integrated land use conflict is the occupation of ecological space by agricultural farming, economic construction, and other human activities. The integrated land use conflict is the occupation of ecological space by economic activities such as farming and economic construction, manifested as the overlapping relationship among arable land, construction land, and ecological space, namely the superimposed result of the conflict between arable land and construction land, a comprehensive manifestation of the superimposed effect of land use conflict [52]. According to the overlapping relationship among arable land, construction land, and low, medium, high, and extremely high ecological safety levels, land use conflict is divided into four types: stable and controllable, mild conflict, moderate conflict, and serious conflict.

4. Results

4.1. Spatial Distribution Characteristics of Ecosystem Service Functions

The spatial differences in the importance of each individual ecosystem service function in the study area are evident(Figure 2). Among them, the extreme importance of carbon sequestration and oxygen release function is 13.02%, with a spatial distribution pattern of high in the east and low in the west, due to the abundant forest resources in the eastern region, while the northwestern region is a plain dominated by food production, and forest

resources are scarce. The proportion of areas with extremely important soil and water conservation functions is 10.46%, mainly in the eastern part of Shandong Province, which does not form a continuous distribution compared with the water conservation function, being mainly in the form of a point and block distribution. The importance of water conservation function is 9.72%, mainly in the southwest, northeastern Yanwei, and the central areas of Shandong Province, due to the high precipitation in the eastern coastal areas and the rich vegetation resources in the southwestern and central areas, which have strong water storage capacity. The extremely important areas of biodiversity account for 5.11% and are mainly distributed in the mountainous hills of south-central Shandong and the Yellow River Delta, mainly due to the good water and heat conditions, numerous mountains and high vegetation cover in these areas, while the low-value areas are distributed in urban built-up areas with high intensity of human activities.

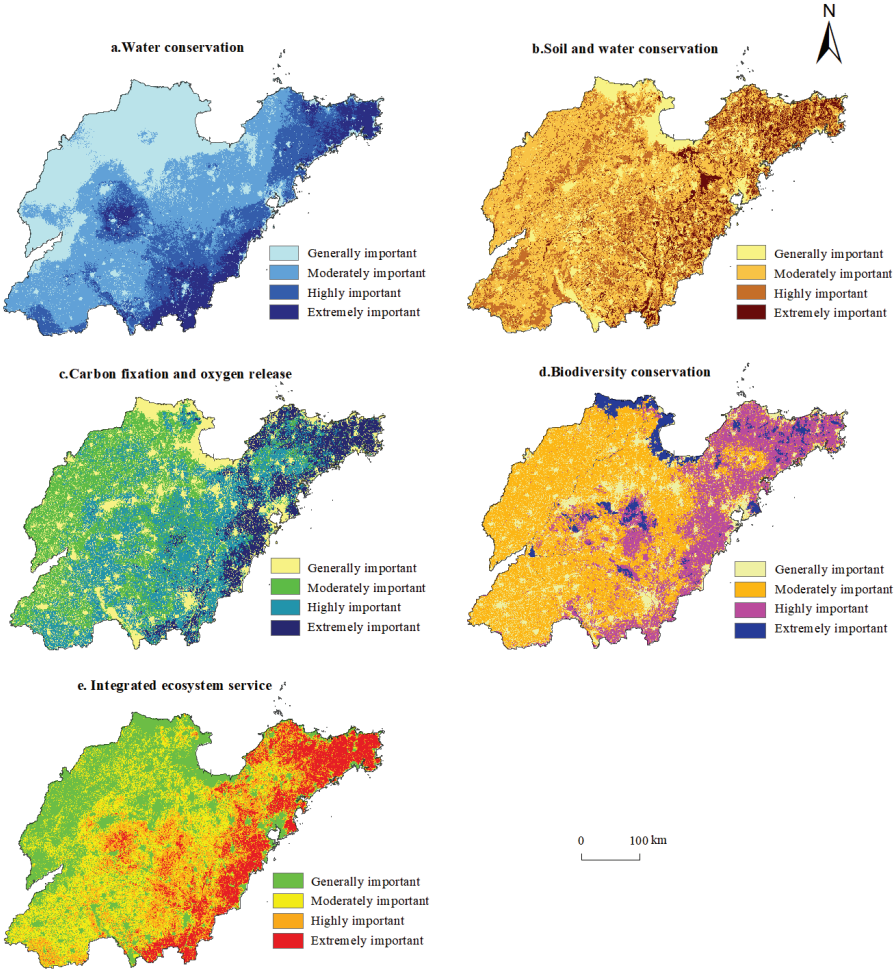

Figure 2. Spatial patterns of the importance of ecosystem service functions.

The importance of integrated ecosystem service functions in the study area shows a spatial distribution pattern of high in the east and low in the west. The area of extremely important ecosystem service function is 25,086 km^2, accounting for 16.17%, mainly in the

mountainous areas of central Shandong, the Jiaodong Peninsula, and the eastern coastal areas, which are rich in forest vegetation resources and have many rivers. The highly important area is 30,997 km^2, accounting for 19.98%, mainly located around the extremely important area. The areas of moderately important and general important account for 31.27% and 32.61% of the total area of the study area, respectively. The areas of moderately important and general important account for 31.27% and 32.61% of the total area of the study area, respectively, and are mainly located in the plains with fewer forest resources and in the built-up areas of cities and towns, which are more affected by human activities.

4.2. Spatial Distribution Characteristics of Ecological Sensitivities

As Figure 3 shows, the spatial distribution of ecological sensitivity in the study area varies widely. The highly and moderately sensitive area of soil erosion is 43,889 km^2, accounting for 28.29%, which indicates that the risk of soil erosion in the study area is higher. The area of highly sensitive areas is 11,775 km^2, accounting for 7.59%, and is mostly distributed in areas with high elevation slopes in the middle hills. The sensitivity to salinization is mainly dominated by nonsensitive areas, with an area of 146,187 km^2, accounting for 94.23%, of which the highly sensitive areas are mainly concentrated in the Yellow River Delta, which is affected by various hydrodynamic factors such as the Yellow River and the Bohai Sea, with shallow groundwater deposits, high mineralization, and high soil salinity.

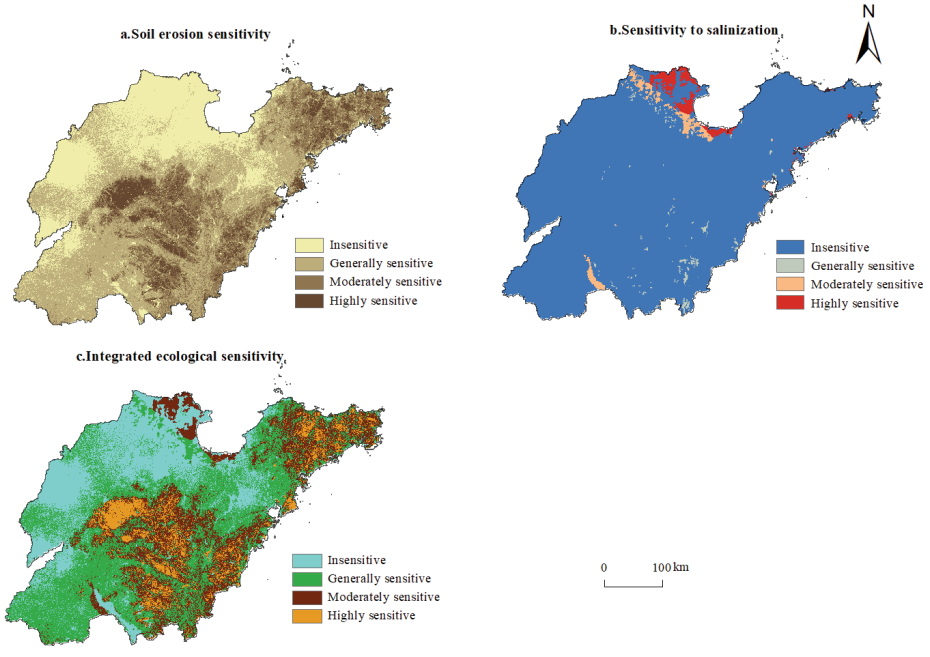

Figure 3. Spatial patterns of ecological sensitivity.

There is a significant difference in the proportion of each level of ecological sensitivity. The ecologically highly sensitive areas cover an area of 12,431 km^2, accounting for 8.01%, and are mostly located near mountains, hills, and rivers, with high vegetation cover in mountainous areas and sensitive and fragile ecology near water bodies, where human activities can easily cause damage to the ecological environment that is difficult to reverse. The ecologically sensitive and insensitive areas account for 41.37% and 27.90% of the total

area of the study area, respectively, and are mainly located in the western and northern parts of Shandong Plain and the built-up areas of cities and towns.

4.3. Ecological Sources and Corridors

According to Cannikin's law, after extracting the highly important ecosystem service functions and ecologically sensitive areas, and excluding the fragmented patches with an area of fewer than 5 km^2, we obtained eighteen ecological source areas, including the Yellow River Delta and the South Four Lakes Reserve (Figure 4a), with an area of 15,987 km^2, accounting for 10.26% of the total study area, mainly distributed in the mountainous hills of south-central Shandong, low mountainous hills in eastern Shandong, and the hills of the Jiaodong Peninsula.

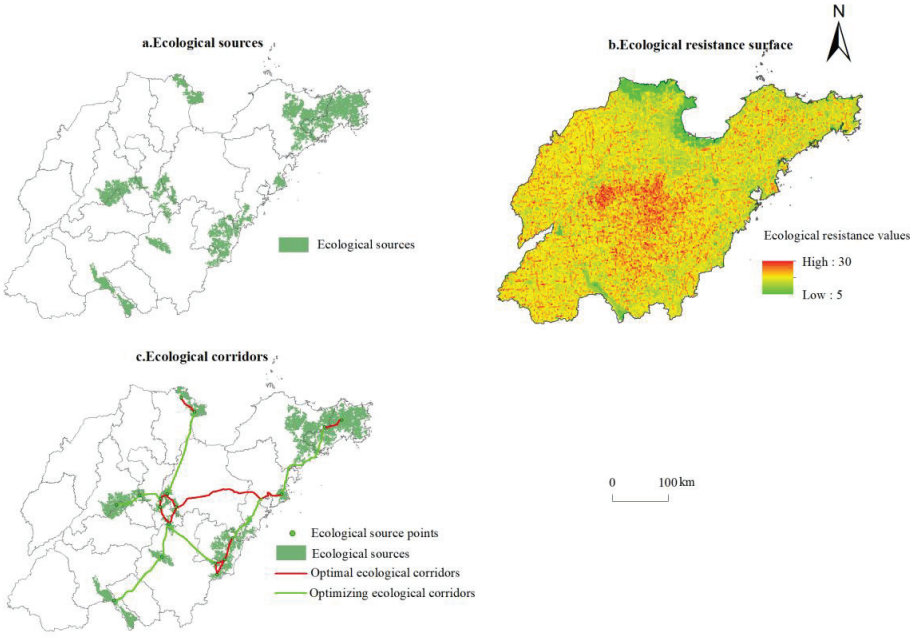

Figure 4. Ecological sources (**a**), ecological resistance surface (**b**), and ecological corridors (**c**).

Based on the landscape resistance values for each resistance factor and the corresponding index weights, the spatial distribution of ecological resistance was obtained by weighted superposition (Figure 4b). Additionally, 12 optimal ecological corridors, 587.43 km in length, were initially extracted by combining the ecological source areas with the minimum cumulative resistance model and the gravity model, mainly distributed in the mountainous hills of central Shandong and the Jiaodong Peninsula. The initial extracted optimal ecological corridors have problems such as disconnected landscape patches and intermittent ecological functions. Therefore, the disconnected ecological source points were further used as sources to find the subminimal resistance paths, and the strength of interaction and connectivity between ecological sources was comprehensively evaluated, resulting in seven optimizing ecological corridors of 681.78 km (Figure 4c).

4.4. Spatial Distribution Characteristics of Ecological Security Pattern

Figure 5 shows the ecological security pattern of the study area, with a low ecological safety-level spatial area of 22,107 km^2, accounting for 14.25% of the area, which mainly includes the ecological barriers of mountainous hills in south-central Shandong and low hills in eastern Shandong, covering the extremely important areas of water conservation,

biodiversity maintenance, soil and water conservation, carbon sequestration, and oxygen release ecological functions in Shandong Province, and highly sensitive areas of soil erosion and salinization, which maintain ecological safety. These areas have a good ecological environment and are rich in biodiversity. They are areas of high value for ecosystem service functions and ecological sensitivity. The spatial area of the medium ecological safety level is 41,251 km^2, accounting for 26.59%, which is widely distributed in the study area. These areas are ecologically fragile and serve as the conservation areas and protective barriers for ecological source lands and should be strengthened for ecological protection. The high ecological safety level covers 56,641 km^2, accounting for 36.51% of the total area. As a transitional zone between human activities and natural ecology, it should embody the integrated protection policy of "green water and green mountains are golden mountains," implement the concept of "green, open development," and promote the compatible and coordinated development of the three regional functions. The area of extremely high ecological safety level is 35,138 km^2, accounting for 22.65%, mainly in the construction land of the whole region and the plain areas of western and northern Shandong, where the ecological environment is poor due to the influence of human activities and background conditions. There is need to improve the level of intensive use, reduce the encroachment of ecological space, realize the combination of development, utilization, and protection, and build a green, ecological, and livable city.

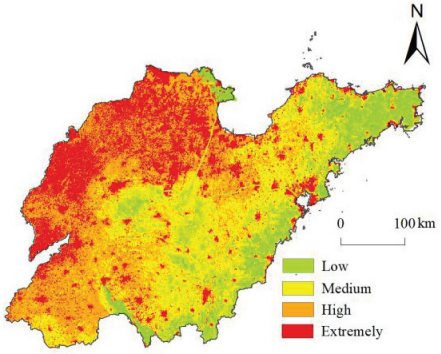

Figure 5. Ecological security pattern.

4.5. Spatial Distribution Characteristics of Land Use Conflict

4.5.1. Arable Land–Ecological Space Conflict

As Figure 6 shows, the distribution of Arable land–ecological space conflict in the study area is relatively concentrated and intense: first, because of the large area of arable land in Shandong Province, which accounts for 64.48%; second, because of the natural ecological environment in Shandong Province and the large area of ecological source land patches. Specifically, the areas of stable and controllable, mild, moderate, and serious conflicts are 20,327, 40,764, 27,649, and 13,775 km^2, respectively, among which, stable and controllable mild conflict is mainly distributed in the plain areas of western and northern Shandong. This is mainly because there is less ecological space, such as forest land, and land use in this region is mainly for farming and construction. Serious conflict and moderate conflict areas are mainly located in the Jiaodong Peninsula and the low hills of eastern Shandong, primarily because these areas are close to important water conservation functional areas, soil and water conservation functional areas, and biodiversity reserves, where the ecosystem service functions are high and ecological security is easily affected by human activities. Therefore, the conflict between arable land production and ecological protection is prominent.

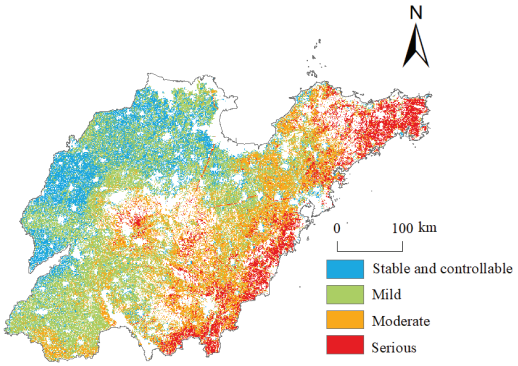

Figure 6. The conflict between arable land and ecological space.

4.5.2. Construction Land—Ecological Space Conflict

Construction land includes urban construction land, rural settlements, and other construction land. There is a clear spatial divergence in the intensity of land use conflict between the various types of construction land (Figure 7).

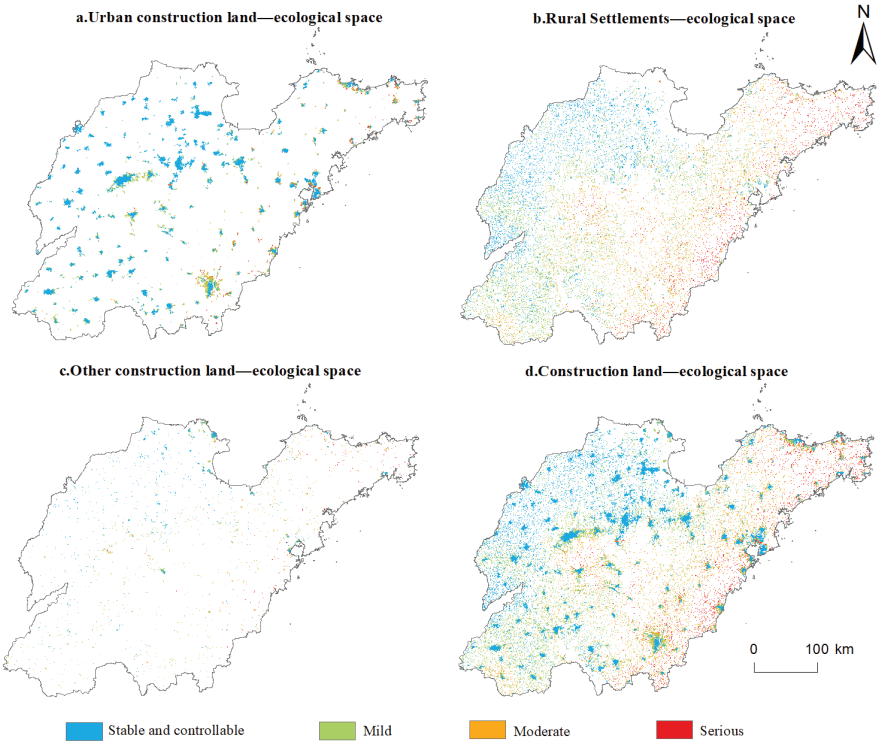

Figure 7. Construction land–ecological space conflict.

The intensity of urban construction land–ecological space conflict is mainly stable and controllable mild conflict, with an area constituting 89.13% of urban construction land, mainly distributed in urban built-up areas with a high level of ecological safety, where construction land is spatially adjacent to arable land. Therefore, the conflict between

construction land and ecological space is low. The area of serious and moderate conflict only accounts for 10.87% of urban construction land. This is mainly located in the suburban areas of the city. These areas are closer to forest land, waters, and other ecological space than the central urban areas, and human activities are likely to trigger ecological risks.

The areas of stable and controllable, mild, moderate, and serious conflicts among rural settlements–ecological space are 4235, 6172, 3372, and 1435 km^2, respectively. Of the total area, 31.60% is occupied by serious and moderate conflict, much higher than that of urban construction land use, mainly concentrated in the low hills of eastern Shandong and the hills of central Shandong. Compared with the spatial distribution pattern of large, concentrated, and contiguous land plots in cities and towns, the layout of rural settlements is scattered, especially in mountainous areas, where the scale is even smaller. Lack of planning and inadequate supervision result in phenomena such as "digging up hills to build houses," leading to intermittent damage to the ecological environment.

The areas of stable and controllable, mild, moderate, and serious conflicts in other lands for construction–ecological space conflict are 767, 842, 413, and 179 km^2, respectively, of which the proportion of serious and moderate conflict is much lower than that of urban construction land and rural settlements.

The areas of stable and controllable, mild, moderate, and serious conflicts in the construction land–ecological space conflict are 10,095, 8406, 4041, and 1676 km^2, respectively. Mild conflict and stable and controllable areas are mainly located in the Lucian Plain and the built-up areas of cities. The main reason is that these areas are relatively flat, densely populated, and less important in terms of ecosystem service functions, and are more suitable for urban construction. Serious and more-serious conflict areas are mainly located in Jinan, Linyi, and the coastal areas of the Jiaodong Peninsula, where urban development space is close to ecological space. For example, due to topography and other factors, the built-up area of Jinan is distributed in an east–west strip pattern, while its southern mountainous area is an important ecological barrier.

4.5.3. Integrated Land Use Conflict

As Figure 8 shows, the problems of arable land, construction land, and ecological space conflict are relatively serious in Shandong Province, with an overall spatial distribution pattern of high in the east and low in the west. Among them, the area of serious conflict zone is 15,342 km^2, accounting for 9.71%, mainly in Yantai, Weihai, Qingdao, Rizhao, and Linyi, in the low hills of eastern Shandong. These areas have a high level of urbanization, a developed economy, and a dense population. The arable land and construction land in these areas are close to forest land, water, and other ecological space, and land use conflicts are significant and concentrated. The comprehensive moderate land use conflict area is 31,608 km^2, accounting for 20.01%, mainly located in the mountainous hills of central Shandong and the western part of the low hills of eastern Shandong. The most serious areas of soil erosion are in Shandong Province, a highly ecologically sensitive area, leading to serious land use conflict. The area of land use conflict that is mild, stable, and controllable is 45,625 km^2, accounting for 50.30%, mainly distributed in the simple land use type and less economically developed western and northern plains of Shandong. The area of forest land in this region is 84 km^2, only 0.15% of the total area of the two regions, due to the lack of forest land resources, resulting in poor ecological background conditions in this region. Ecological functions are not pronounced, making land use conflict less obvious.

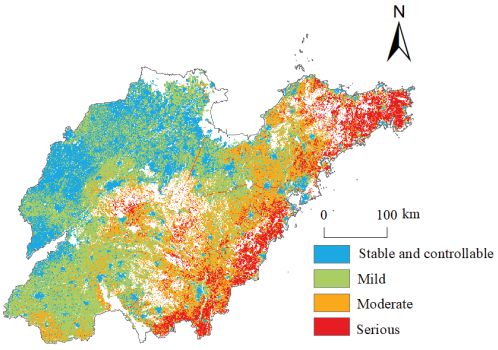

Figure 8. Integrated land use conflict in the study area.

5. Discussion

5.1. Arable Land–Ecological Space Conflict Management

The management of arable land–ecological space conflict is a matter of food security and ecological protection. At present, the world is in the midst of the greatest change in a century, with the Russia–Ukraine conflict and the global COVID-19 pandemic not only exacerbating regional tensions but also highlighting the importance of food security. China has also elevated the issue of food security to an unprecedented level, requiring strict protection of arable land with stringent measures and strict adherence to the red-line of 1.8 billion mu of arable land protection. However, ecological protection is an inevitable requirement for achieving sustainable development and has been incorporated into the significant strategy of the Five-in-One as an important part of the construction of ecological civilization. The western and northern plains of Shandong are important food production areas in Shandong Province and in China. The arable land–ecological space conflict is mainly stable and controllable with mild conflict, and the pressure of conflict management is low. However, it is noteworthy that Shandong Province is a region with serious water shortages. Therefore, in the process of arable land–ecological space conflict management, in addition to the principle of suitability, it is also necessary to consider water resource constraints, to reasonably determine the scale of arable land according to the water resource carrying capacity, and to guarantee ecological water. The Jiaodong Peninsula and the low hills in the eastern part of Shandong Province are the main areas of serious and moderate conflict between farmland and ecology. In this area, small, fragmented, noncontiguous, low-quality, and inconvenient farmland should be transferred out of the scope of basic farmland. High-quality, concentrated, and contiguous farmland should be added to the scope of permanent basic farmland. At the same time, the area, as the richest area in Shandong Province in terms of forest resources, includes the mountain area of Daze Mountain, Aishan Mountain, Asan Mountain, Kunbeishan Mountain, and Lushan Mountain, covering the Jiaonan Hills, the water-conserving area of the Jiaowei Plain, and the biodiversity-maintaining area of the Jiaodong Hills, along with various nature reserves and other areas in need of protection. Ecological protection of important areas, to strengthen the basic framework of multi–species, multi–functional, multi–benefit protective forests. The construction of ecological protection forest systems should be improved. Forest nurturing, replanting of sparse forest land, and transformation of inefficient forests should be carried out comprehensively. The structure of tree species should be improved; the quality of forests should be enhanced; the forest landscape should be upgraded; the capacity of forest carbon sinks should be improved; the ecological stability in the region should be reinforced.

5.2. Construction Land–Ecological Space Conflict Management

On the whole, the conflict between construction land and ecological space in Shandong Province is not serious, and the proportion of serious conflict is only 6.92%, mainly in the cities of Yantai, Weihai, Qingdao, Linyi, and Jinan, which are mostly close to the ecological protection red-line area of Shandong Province and are potential threats to the ecological environment. Yantai, Weihai, and Qingdao cities are located around the low hills of the eastern part of Shandong Province, and the area is large and the intensity of conflict between construction land and ecological space is high. The city of Linyi is characterized by "three major areas." Linyi City presents an ecological pattern of "three mountains and three lakes," strictly prohibiting the construction of disorderly encroachment on Mount Ni, Mount Meng, and Mount Yi, engaging in the environmental management in the watersheds of the Altar, Wen, and Yi rivers, implementing projects such as the protection of wetlands in the upper reaches, restoring polluted sites, improving the rural water environment, preventing and controlling urban water pollution, and monitoring and protecting coastal groundwater to improve the quality of the water. The quality of the environment has been improved. Jinan City has an ecological pattern of "multiple points in the north and south of the mountains," and as the capital city of Shandong Province, it is an important transportation hub and economic development center. The development and construction of urbanized areas should be transformed, the scale and structure of urban construction should be reasonably determined with an intensive and green orientation, and key industries should be guided to optimize their layout in areas with sufficient environmental capacity and good diffusion conditions. Key controls should be implemented in areas with dense populations, high intensity of resource development, and high intensity of pollutant emissions. Environmental governance and risk prevention and control need to be strengthened, and resilient, green, and low-carbon development should be promoted.

It should also be noted that, compared to urban construction land, rural settlements pose a greater threat to ecological space due to their wide area, scattered distribution, and direct proximity to ecological space. Therefore, attention should be given to the optimal reconfiguration of the three rural living spaces.

5.3. Limitations and Research Prospective

The construction of an ecological security pattern is the key to accurately identify land use conflicts. This paper uses a classical and highly recognized model to construct the ecological security pattern for Shandong Province [53]. Various methods such as circuit theory can be used to construct ecological security patterns [54,55]. However, this paper does not compare the differences among ecological security patterns constructed by different methods, which is worthy of further study.

In addition, this paper quantitatively identifies the scale, intensity, and spatial distribution of land use conflicts from the perspective of geography, and discusses some possible solutions. However, the connotation of land use conflict is rich, so future research can try to include land ownership and stakeholders in the research from more perspectives, such as political geography.

6. Conclusions

Ecological security is an important foundation for achieving green and sustainable development. Against the background of the current tensions and increasing conflict between people and land, the identification of land use conflict based on ecological security evaluation is a feasible path with important practical significance. The results indicate that in 2020, Shandong Province shows an obvious spatial mismatch between arable land, construction land, and ecological space. The areas of serious, moderate, mild conflict, and stable and controllable are 13,465, 27,113, 39,895, and 19,544 km^2, respectively, and the overall distribution is relatively concentrated, with serious and moderate conflict concentrated in the low hills of eastern Shandong, and mild conflict and stable and controllable

areas concentrated in the plains of western and northern Shandong. The areas of mild conflict and stability are concentrated in the eastern and northern plains of Shandong. The area of the construction land–ecological space serious conflict, moderate conflict, mild conflict, and stable and controllable areas are 1877, 4495, 9274, and 10,766 km^2, respectively, with an overall scattered distribution. Mild conflict and stable and controllable areas are widely distributed around the urban construction land. Serious and moderate conflict is concentrated in the eastern coastal areas. The land use types are mainly rural settlements. In general, the spatial distribution of land use conflict in Shandong Province shows obvious regional differences, with the coast being higher than the interior and the south higher than the north.

This paper evaluates the ecological security of Shandong Province based on the "serviceability importance" factor, which is not sufficiently comprehensive in the selection of ecosystem serviceability and ecological sensitivity factors. The identification of land use conflict between arable land and construction land is based on ecological security. However, only the conflict between arable land and construction land and ecological space is considered, not the conflict between the two, nor the conflict with other land use types. In future research, the evaluation system of ecological safety should be gradually improved, not only limited to the perspective of ecological priority, but also considering the identification of land use conflict from the perspective of sustainable development and carbon neutrality, and comprehensively considering the intensity of land use conflict among various categories.

Author Contributions: Conceptualization, G.D. and W.J.; methodology, Z.L., G.D., and Y.N.; formal analysis, G.D. and Z.L.; writing—original draft preparation, G.D. and Z.L.; writing—review and editing, G.D. and W.J.; funding acquisition, G.D. All authors have read and agreed to the published version of the manuscript.

Funding: This research was funded by the National Natural Science Foundation of China, grant number 41801173, Youth Innovation Science and Technology Support Plan of Colleges and Universities in Shandong Province, grant number 2021RW039, and Doctor Foundation of Shandong Jianzhu University, grant number XNBS 1803.

Data Availability Statement: The data presented in this study are available on request from the author.

Acknowledgments: Thanks to anonymous experts for their suggestions.

Conflicts of Interest: The authors declare no conflict of interest.

References

1. Zou, L.; Liu, Y.; Wang, J.; Yang, Y.; Wang, Y. Land use conflict identification and sustainable development scenario simulation on China's southeast coast. *J. Clean. Prod.* **2019**, *238*, 117899. [CrossRef]
2. Reuveny, R.; Maxwell, J.W.; Davis, J. On conflict over natural resources. *Ecol. Econ.* **2011**, *70*, 698–712. [CrossRef]
3. Hui, E.C.M.; Bao, H. The logic behind conflicts in land acquisitions in contemporary China: A framework based upon game theory. *Land Use Pol.* **2013**, *30*, 373–380. [CrossRef]
4. Campbell, D.J.; Gichohi, H.; Mwangi, A.; Chege, L. Land use conflict in Kajiado District, Kenya. *Land Use Pol.* **2000**, *17*, 337–348. [CrossRef]
5. Li, S.; Zhu, C.; Lin, Y.; Dong, B.; Chen, B.; Si, B.; Li, Y.; Deng, X.; Gan, M.; Zhang, J.; et al. Conflicts between agricultural and ecological functions and their driving mechanisms in agroforestry ecotone areas from the perspective of land use functions. *J. Clean. Prod.* **2021**, *317*, 128453. [CrossRef]
6. Steinhäußer, R.; Siebert, R.; Steinführer, A.; Hellmich, M. National and regional land-use conflicts in Germany from the perspective of stakeholders. *Land Use Pol.* **2015**, *49*, 183–194. [CrossRef]
7. Dong, G.; Ge, Y.; Jia, H.; Sun, C.; Pan, S. Land Use Multi-Suitability, Land Resource Scarcity and Diversity of Human Needs: A New Framework for Land Use Conflict Identification. *Land* **2021**, *10*, 1003. [CrossRef]
8. Zong, S.; Hu, Y.; Zhang, Y.; Wang, W. Identification of land use conflicts in China's coastal zones: From the perspective of ecological security. *Ocean Coast. Manag.* **2021**, *213*, 105841. [CrossRef]
9. Adam, Y.O.; Pretzsch, J.; Darr, D. Land use conflicts in central Sudan: Perception and local coping mechanisms. *Land Use Pol.* **2015**, *42*, 1–6. [CrossRef]
10. Andrew, J.S. Potential application of mediation to land use conflicts in small-scale mining. *J. Clean. Prod.* **2003**, *11*, 117–130. [CrossRef]

11. Milczarek-Andrzejewska, D.; Zawalińska, K.; Czarnecki, A. Land-use conflicts and the Common Agricultural Policy: Evidence from Poland. *Land Use Pol.* **2018**, *73*, 423–433. [CrossRef]
12. Henderson, S.R. Managing land-use conflict around urban centres: Australian poultry farmer attitudes towards relocation. *Appl. Geogr.* **2005**, *25*, 97–119. [CrossRef]
13. Orr, A.; Mwale, B. Adapting to Adjustment: Smallholder Livelihood Strategies in Southern Malawi. *World Dev.* **2001**, *29*, 1325–1343. [CrossRef]
14. Brown, G.; Raymond, C.M. Methods for identifying land use conflict potential using participatory mapping. *Landsc. Urban Plan.* **2014**, *122*, 196–208. [CrossRef]
15. Kim, I.; Arnhold, S. Mapping environmental land use conflict potentials and ecosystem services in agricultural watersheds. *Sci. Total Environ.* **2018**, *630*, 827–838. [CrossRef] [PubMed]
16. Cieślak, I. Identification of areas exposed to land use conflict with the use of multiple-criteria decision-making methods. *Land Use Pol.* **2019**, *89*, 104225. [CrossRef]
17. Karimi, A.; Brown, G. Assessing multiple approaches for modelling land-use conflict potential from participatory mapping data. *Land Use Pol.* **2017**, *67*, 253–267. [CrossRef]
18. Zhou, D.; Xu, J.; Lin, Z. Conflict or coordination? Assessing land use multi-functionalization using production-living-ecology analysis. *Sci. Total Environ.* **2017**, *577*, 136–147. [CrossRef]
19. Gao, Y.; Wang, J.; Zhang, M.; Li, S. Measurement and prediction of land use conflict in an opencast mining area. *Resour. Policy* **2021**, *71*, 101999. [CrossRef]
20. Iojă, C.I.; Niţă, M.R.; Vânău, G.O.; Onose, D.A.; Gavrilidis, A.A. Using multi-criteria analysis for the identification of spatial land-use conflicts in the Bucharest Metropolitan Area. *Ecol. Indic.* **2014**, *42*, 112–121. [CrossRef]
21. Jiang, S.; Meng, J.; Zhu, L. Spatial and temporal analyses of potential land use conflict under the constraints of water resources in the middle reaches of the Heihe River. *Land Use Pol.* **2020**, *97*, 104773. [CrossRef]
22. Jing, W.; Yu, K.; Wu, L.; Luo, P. Potential Land Use Conflict Identification Based on Improved Multi-Objective Suitability Evaluation. *Remote Sens.* **2021**, *13*, 2416. [CrossRef]
23. Lin, G.; Fu, J.; Jiang, D. Production–Living–Ecological Conflict Identification Using a Multiscale Integration Model Based on Spatial Suitability Analysis and Sustainable Development Evaluation: A Case Study of Ningbo, China. *Land* **2021**, *10*, 383. [CrossRef]
24. Wang, C.Y.; Delu, P. Zoning of Hangzhou Bay ecological red line using GIS-based multi-criteria decision analysis. *Ocean Coast. Manag.* **2017**, *139*, 42–50. [CrossRef]
25. Chen, Y.; Yue, W.; Zhang, L.J.A.E.S. Mapping of wetland reserve boundary in coastal zone utilizing spatial constraints assessment. *Acta Ecol. Sin.* **2018**, *38*, 900–908.
26. Gao, J.B.; Jiang, Y.; Wang, H.; Zuo, L.Y. Identification of Dominant Factors Affecting Soil Erosion and Water Yield within Ecological Red Line Areas. *Remote Sens.* **2020**, *12*, 399. [CrossRef]
27. Yang, Y.Q.; Ren, P.; Hong, B.T.J.R.; Basin, E.i.t.Y. The Study of Land Use Conflict Based on Ecological Security of the Chongqing Section of Three Gores Reservoir Area. **2019**, *28*, 322–332.
28. Li, Z.J.; Liu, Y.M.; Zeng, H. Application of the MaxEnt model in improving the accuracy of ecological red line identification: A case study of Zhanjiang, China. *Ecol. Indic.* **2022**, *137*, 108767. [CrossRef]
29. Yu, D.D.; Han, S.J. Ecosystem service status and changes of degraded natural reserves—A study from the Changbai Mountain Natural Reserve, China. *Ecosyst. Serv.* **2016**, *20*, 56–65. [CrossRef]
30. Sun, J.Q.; Huang, J.J.; Wang, Q.; Zhou, H. A method of delineating ecological red lines based on gray relational analysis and the minimum cumulative resistance model: A case study of Shawan District, China. *Environ. Res. Commun.* **2022**, *4*, 045009. [CrossRef]
31. Li, Y.; Shi, Y.; Qureshi, S.; Bruns, A.; Zhu, X.J.E.i. Applying the concept of spatial resilience to socio-ecological systems in the urban wetland interface. *Ecol. Indic.* **2014**, *42*, 135–146. [CrossRef]
32. Pan, F.; Tian, C.Y.; Shao, F.; Zhou, W.; Chen, F. Evaluation of ecological sensitivity in Karamay, Xinjiang, China. *J. Geogr. Sci.* **2012**, *22*, 329–345. [CrossRef]
33. Chi, Y.; Zhang, Z.W.; Gao, J.H.; Xie, Z.L.; Zhao, M.W.; Wang, E.K. Evaluating landscape ecological sensitivity of an estuarine island based on landscape pattern across temporal and spatial scales. *Ecol. Indic.* **2019**, *101*, 221–237. [CrossRef]
34. Jin, X.X.; Wei, L.Y.; Wang, Y.; Lu, Y.Q. Construction of ecological security pattern based on the importance of ecosystem service functions and ecological sensitivity assessment: A case study in Fengxian County of Jiangsu Province, China. *Environ. Dev. Sustain.* **2021**, *23*, 563–590. [CrossRef]
35. Cui, H.L.; Liu, M.; Chen, C. Ecological Restoration Strategies for the Topography of Loess Plateau Based on Adaptive Ecological Sensitivity Evaluation: A Case Study in Lanzhou, China. *Sustainability* **2022**, *14*, 17. [CrossRef]
36. Zhang, H.J.; Pang, Q.; Hua, Y.W.; Li, X.X.; Liu, K. Linking ecological red lines and public perceptions of ecosystem services to manage the ecological environment: A case study in the Fenghe River watershed of Xi'an. *Ecol. Indic.* **2020**, *113*, 106218. [CrossRef]
37. Luji, H.J.J.o.S.; Conservation, W. A Study on Rainfall in South China from the View of Soil Erosion. *J. Soil Water Conserv.* **1993**, *7*, 53–60. [CrossRef]

38. Wang, C.S.; Sun, G.Y.; Dang, L.J. Identifying Ecological Red Lines: A Case Study of the Coast in Liaoning Province. *Sustainability* **2015**, *7*, 9461–9477. [CrossRef]
39. Ding, M.M.; Liu, W.; Xiao, L.; Zhong, F.X.; Lu, N.; Zhang, J.; Zhang, Z.H.; Xu, X.L.; Wang, K.L. Construction and optimization strategy of ecological security pattern in a rapidly urbanizing region: A case study in central-south China. *Ecol. Indic.* **2022**, *136*, 13. [CrossRef]
40. Yang, Y.; Zhou, Y.R.; Feng, Z.; Wu, K.N. Making the Case for Parks: Construction of an Ecological Network of Urban Parks Based on Birds. *Land* **2022**, *11*, 1144. [CrossRef]
41. Dai, L.; Liu, Y.B.; Luo, X.Y. Integrating the MCR and DOI models to construct an ecological security network for the urban agglomeration around Poyang Lake, China. *Sci. Total Environ.* **2021**, *754*, 15. [CrossRef] [PubMed]
42. Li, F.; Ye, Y.P.; Song, B.W.; Wang, R.S. Evaluation of urban suitable ecological land based on the minimum cumulative resistance model: A case study from Changzhou, China. *Ecol. Model.* **2015**, *318*, 194–203. [CrossRef]
43. Hu, C.G.; Wang, Z.Y.; Wang, Y.; Sun, D.Q.; Zhang, J.X. Combining MSPA-MCR Model to Evaluate the Ecological Network in Wuhan, China. *Land* **2022**, *11*, 213. [CrossRef]
44. Yi, S.Q.; Zhou, Y.; Li, Q. A New Perspective for Urban Development Boundary Delineation Based on the MCR Model and CA-Markov Model. *Land* **2022**, *11*, 401. [CrossRef]
45. Xiao, S.C.; Wu, W.J.; Guo, J.; Ou, M.H.; Pueppke, S.G.; Ou, W.X.; Tao, Y. An evaluation framework for designing ecological security patterns and prioritizing ecological corridors: Application in Jiangsu Province, China. *Landsc. Ecol.* **2020**, *35*, 2517–2534. [CrossRef]
46. Popescu, O.C.; Tache, A.V.; Petrisor, A.I. Methodology for Identifying Ecological Corridors: A Spatial Planning Perspective. *Land* **2022**, *11*, 1013. [CrossRef]
47. Wanghe, K.Y.; Guo, X.L.; Wang, M.; Zhuang, H.F.; Ahmad, S.; Khan, T.U.; Xiao, Y.Q.; Luan, X.F.; Li, K. Gravity model toolbox: An automated and open-source ArcGIS tool to build and prioritize ecological corridors in urban landscapes. *Glob. Ecol. Conserv.* **2020**, *22*, 14. [CrossRef]
48. Wei, Q.Q.; Halike, A.; Yao, K.X.; Chen, L.M.; Balati, M. Construction and optimization of ecological security pattern in Ebinur Lake Basin based on MSPA-MCR models. *Ecol. Indic.* **2022**, *138*, 108857. [CrossRef]
49. Yu, K. Security patterns and surface model in landscape ecological planning. *Landsc. Urban Plan.* **1996**, *36*, 1–17. [CrossRef]
50. Peng, J.; Pan, Y.; Liu, Y.; Zhao, H.; Wang, Y. Linking ecological degradation risk to identify ecological security patterns in a rapidly urbanizing landscape. *Habitat Int.* **2018**, *71*, 110–124. [CrossRef]
51. Zhang, J.; Chen, Y.; Zhu, C.M.; Huang, B.B.; Gan, M.Y. Identification of Potential Land-Use Conflicts between Agricultural and Ecological Space in an Ecologically Fragile Area of Southeastern China. *Land* **2021**, *10*, 1011. [CrossRef]
52. Zou, L.L.; Liu, Y.S.; Wang, J.Y.; Yang, Y.Y. An analysis of land use conflict potentials based on ecological-production-living function in the southeast coastal area of China. *Ecol. Indic.* **2021**, *122*, 12. [CrossRef]
53. Chen, J.; Wang, S.; Zou, Y. Construction of an ecological security pattern based on ecosystem sensitivity and the importance of ecological services: A case study of the Guanzhong Plain urban agglomeration, China. *Ecol. Indic.* **2022**, *136*, 108688. [CrossRef]
54. Li, Y.; Liu, W.; Feng, Q.; Zhu, M.; Yang, L.; Zhang, J.; Yin, X. The role of land use change in affecting ecosystem services and the ecological security pattern of the Hexi Regions, Northwest China. *Sci. Total Environ.* **2023**, *855*, 158940. [CrossRef]
55. Li, Q.; Zhou, Y.; Yi, S. An integrated approach to constructing ecological security patterns and identifying ecological restoration and protection areas: A case study of Jingmen, China. *Ecol. Indic.* **2022**, *137*, 108723. [CrossRef]

land

MDPI

Article

Monitoring the Spatiotemporal Dynamics of Habitat Quality and Its Driving Factors Based on the Coupled NDVI-InVEST Model: A Case Study from the Tianshan Mountains in Xinjiang, China

Yayan Lu [1,2], Junhong Zhao [3], Jianwei Qi [1,2], Tianyu Rong [1,2], Zhi Wang [1,2,4], Zhaoping Yang [1,2] and Fang Han [1,2,*]

[1] State Key Laboratory of Desert and Oasis Ecology, Xinjiang Institute of Ecology and Geography, Chinese Academy of Sciences, Urumqi 830011, China
[2] University of Chinese Academy of Sciences, Beijing 100049, China
[3] Wenzhou Institute of Eco-environmental Sciences, Wenzhou 325088, China
[4] School of Management, Henan University of Science and Technology, Luoyang 471023, China
* Correspondence: hanfang@ms.xjb.ac.cn

Abstract: Globally, mountains have suffered enormous biodiversity loss and habitat degradation due to climate change and human activities. As an agent of biodiversity, evaluating habitat quality (HQ) change is an indispensable key step for regional ecological security and human well-being enhancement, especially for fragile mountain ecosystems in arid areas. In this study, we aimed to propose an integrated framework coupled with the Normalized Difference Vegetation Index (NDVI) and Integrated Valuation of Ecosystem Services and Tradeoffs (InVEST)-HQ module to improve the effectiveness and accuracy of HQ estimation. We highlighted the Tianshan Mountains in Xinjiang as an example to validate the model, as it is a typical representative of mountain ecosystems in the temperate arid zone. Specifically, we aimed to assess the spatiotemporal dynamics of HQ over the past two decades and investigate its influencing factors using a geographical detector model. The results show that, first, grassland and unused land were the main land-use types in the study area. The land-use transitions were mainly concentrated in grassland, woodland, water body, and unused land. Second, the total area of very important habitats and general habitats accounted for over 70% of the Tianshan Mountains. The average HQ decreased from 0.5044 to 0.4802 during 1995–2015. Third, the HQ exhibited significant spatial differentiation, and the Ili River Valley and Kaidu River Basin were the hot spots, while the south and east of the Tianshan Mountains were the cold spots. Habitat quality was strongly related to the terrain gradient, with an inverted "U" type. Protected areas of different categories played a vital role in biodiversity conservation. Finally, soil type, land-use change, precipitation, temperature, and grazing intensity were the dominant factors in response to HQ change for both the total Tianshan Mountains and sub-regions, followed by elevation, the relief degree of the land surface, gross domestic product, population density, and distance to tourism attractions. The interaction effects of the influencing factors were improved compared to the effects of the individual factors in each zone. Furthermore, these results provide decision-making criteria for formulating a scientific and systematic protection of ecology and restoration planning systems to enhance the capacity to address climate change.

Keywords: habitat quality; InVEST model; geographical detector model; Tianshan Mountains

Citation: Lu, Y.; Zhao, J.; Qi, J.; Rong, T.; Wang, Z.; Yang, Z.; Han, F. Monitoring the Spatiotemporal Dynamics of Habitat Quality and Its Driving Factors based on the Coupled NDVI-InVEST Model: A Case Study from the Tianshan Mountains in Xinjiang, China. *Land* **2022**, *11*, 1805. https://doi.org/10.3390/land11101805

Academic Editors: Shicheng Li, Chuanzhun Sun, Qi Zhang, Basanta Paudel and Lanhui Li

Received: 27 September 2022
Accepted: 14 October 2022
Published: 15 October 2022

1. Introduction

Biodiversity, which supports ecosystem processes, functions, and the continued delivery of ecosystem services, is fundamental to human health and well-being [1]. Although conservation efforts have been emphasized, habitat fragmentation, degeneration, and loss driven by human activities and climate change are still the greatest threats to global

biodiversity loss [2,3]. Habitat quality (HQ) is an effective decision-support tool for identifying conservation areas and evaluating their conservation status to provide welfare for people [4,5]. Therefore, there is an urgent need to monitor and assess the spatiotemporal dynamics of HQ and develop conservation management strategies that are significant for biodiversity conservation, ecosystem service function maintenance, ecological security pattern construction, and regional sustainable development.

Although mountains cover about 25% of the global area, mountains provide livelihoods for billions of people who live in or beyond mountain ranges [6,7]. Mountains are momentous pools of global biodiversity, are home to endemism and threatened species, and host about half of the global biodiversity hotspots [8]. Mountains supply multiple valuable ecosystem services as compared to those in other areas, such as water yield, climate regulation, carbon sequestration, soil retention, and natural habitats [1,7], which are the core elements of cultural diversity, human well-being, and sustainable development [6]. Mountain regions, particularly vulnerable ecosystems, are the first to be affected by global land-use change and climate change [9] and exhibit different degrees of decline in ecosystem services [10]. In arid and semi-arid regions, mountain ecosystems rich in vegetation are the focal points of biodiversity and ecological security [11]. The fragile and sensitive ecosystems in arid and semi-arid regions due to the extreme climate make it more difficult for ecological protection and restoration [12]. The Tianshan mountain range, known as the "Central Asian Water Tower", underpins a crucial biodiversity hotspot [13]. The visible climate warming has reached a level of 0.3 °C increase per decade in the Tianshan Mountains [14]. The changing climate has resulted in a series of serious ecological crises, including increased precipitation uncertainty, a retreat of approximately 97.52% of the glaciers [15], increased land-use conversion rates and intensities [16], and vegetation browning [17]. Meanwhile, the grazing pressures are amplified, leading to alterations in vegetation diversities, productivities, morphological structures, and distribution patterns [18]. To moderate the irreversible effects of climate change and anthropogenic disturbances, the Chinese government has released many ecological protection and restoration programs, such as the construction of the Three-North Shelterbelt, the Grain for Green Program, the Natural Forest Protection Project, and the Preventing and Controlling Sand Engineering. Nevertheless, knowledge gaps still exist in preventing habitat loss to improve the landscape health of the Tianshan mountain range. Thus, strengthening the research on mountain HQ in the context of global warming is of great significance for the ecological barrier construction of Central Asia and for the promotion of the sustainable development of the Silk Road Economic Belt.

Habitat quality is an important proxy for biodiversity and ecosystem services [19,20]. Traditional and typical regional biodiversity surveys have long been broadly used in HQ assessments [13]. Biodiversity surveys are time-consuming and costly, and the lack of long-term data makes it impossible to estimate temporal and spatial variations [21]. Thus, researchers have formulated synthetic index evaluation methods that provide flexibility to integrate field data [20]. Recently, it has become important to understand the distribution and degree of habitat threats [22,23]. The habitat quality module in the Integrated Valuation of Ecosystem Services and Tradeoffs (InVEST) is a powerful assessment tool that combines habitat suitability and intensity of threats [19]. It offers the opportunity for rapid and regular assessment of biodiversity status at different spatial scales from protected areas to the national scale [4,24], especially where there are poor species distribution data available [22,25]. However, habitat suitability and threat scores are deeply influenced by expert subjectivity and unilateralism [23]. To enhance the accuracy of the HQ assessment, species distribution models have been introduced into the InVEST-HQ model [25]. With the rapid development of remote sensing technology, moderate- to high-resolution data and monthly products support allow annual evaluations of species diversity and habitat conditions [26]. Given these, we proposed an integrated framework that combined the Normalized Difference Vegetation Index (NDVI) to modify the InVEST-HQ model, owing to the capacity of the NDVI for continuous monitoring of species richness [27].

In the present study, our primary objective was to construct an integrated and effective HQ evaluation system that coupled the NDVI and InVEST-HQ model to improve the accuracy of the evaluation results. We employed this model in the Tianshan Mountain Range, China, because it is crucial to maintain the ecological security in Western China. Habitat quality supervision and evaluation in arid and semi-arid mountain ecosystems are extremely important for biodiversity protection and regional sustainable development. The specific objectives of this research were to (1) evaluate the spatiotemporal dynamics of HQ in different periods; and (2) reveal the influencing factors using the geographical detector model at the grid scale.

2. Materials and Methods

2.1. Study Area

The Tianshan Mountains are the world's largest independent zonal mountain system, the largest mountain system in an arid region, and the farthest mountain system from the ocean [28]. It is one of the world's seven major mountain systems, connecting China, Kazakhstan, Kyrgyzstan, and Uzbekistan. The Tianshan Mountains in Xinjiang (TS) are located at 73°50′28″–95°33′56″ N and 39°24′40″–45°23′8″ E, with a total area of 23.53×10^4 km^2 (Figure 1). The elevation in TS ranges from 734 to 7380 m. The region includes not only high-altitude mountains but also some basins (e.g., Yurtus Basin) on the northern and southern slopes and valleys (e.g., Ili River Valley) in the western part of the TS [14]. The region has a typical continental climate, with an annual average temperature of 1.03 °C and annual average precipitation of 406.97 mm. The TS has all the typical mountain altitudinal natural zones in a temperate arid zone and is located in the mountains of Central Asia among the global biodiversity hotspots [29], the Global-200 ecoregions [30], and the priority areas for biodiversity conservation in the Tianshan Mountains–southwest Junggar Basin [31]. According to the "Guideline to Establish the Mechanism of Natural Protected Areas with National Parks as Backbone" released in 2019, there are 59 protected areas (PAs) in TS, including one World Natural Heritage site, nine nature reserves, and 49 nature parks, which account for 33.91 % of the protected areas in Xinjiang. The total area of PAs in the TS is 2307.46 km^2, accounting for 18.94 % of the study area. To quantitatively analyze the spatial variation, we divided the total Tianshan Mountains (TTS) into three sub-regions: the Middle Tianshan Mountains (MTS), the North Tianshan Mountains (NTS), and the East Tianshan Mountains (ETS).

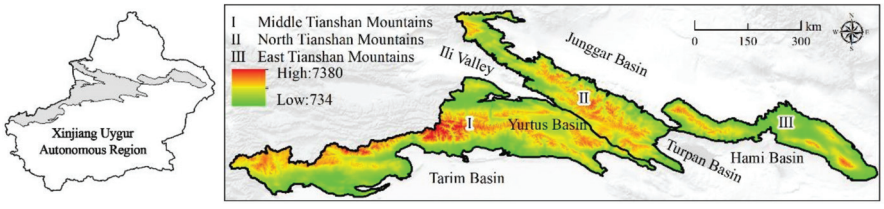

Figure 1. Location of study area (Map number: Xin S (2021) 023).

2.2. Data Sources

Land-use and monthly NDVI data from 1995, 2000, 2005, 2010, and 2015 were provided by the Resources and Environmental Sciences Data Center, Chinese Academy of Sciences (RESDC) (http://www.resdc.cn/, accessed on 25 January 2022). The land-use data had a spatial resolution of 30 m and an overall evaluation accuracy greater than 80% [16], which included 25 land-use categories, and we used ArcGIS10.5 to reclassify these categories into six primary types: cropland, woodland, grassland, water body, built-up land, and unused land. The monthly NDVI data with a resolution of 1 km were combined with the maximum value method to obtain the annual NDVI. The railway and highway data were obtained mainly from the National Catalogue Service for Geographic Information of China (https://www.webmap.cn/main.do?method=index, accessed on 21 April 2022)

and the National Earth System Science Data Center (http://www.geodata.cn/, accessed on 21 April 2022). The Digital Elevation Model (DEM) data were provided by the Geospatial Data Cloud (http://www.gscloud.cn/, accessed on 21 April 2022). The protected area boundaries, including the World Natural Heritage site, nature reserves, and nature parks, were acquired from the Forestry and Grassland Administration of the Xinjiang Uygur Autonomous Region.

2.3. Methods

2.3.1. Habitat Quality Evaluation

Land-use structure, intensity, and conversion cause global habitat fragmentation and loss [2,21]. Thus, the InVEST-HQ model, which combines information on land use and threats to biodiversity [19], has been widely used to evaluate the spatial distribution of habitat quality, habitat degradation, and habitat rarity. Vegetation coverage can influence the choice of habitat and the intensity of habitat use [22,32]. The NDVI was introduced to comprehensively evaluate HQ. Thus, the integrated HQ evaluation model was calculated as follows:

$$HQ_i = \text{Min}\left(NDVI_i \times Habitat_i \times 2, 1\right) \tag{1}$$

where HQ_i is the habitat quality of grid cell i; and $NDVI_i$ is the average annual $NDVI$ of grid cell i, ranging from 0 to 1. $Habitat_i$ is assessed by the InVEST habitat quality model as follows:

$$Habitat_{xj} = H_j \times \left[1 - \left(\frac{D_{xj}^z}{D_{xj}^z + k^z}\right)\right] \tag{2}$$

where H_j is the habitat suitability of land-use type j; z and k are scaling parameters; and D_{xj} is the total threat level in grid cell x with land-use type j.

$$D_{xj} = \sum_{r=1}^{R} \sum_{y=1}^{y_r} \left(\frac{\omega_r}{\sum_{r=1}^{n} \omega_r}\right) r_y i_{rxy} \beta_x S_{jr} \tag{3}$$

where r is threat source; R is the total number of threat sources; y indicates all grid cells on r's raster map; y_r is the set of grid cells on r's raster map; ω_r are threat weights; r_y is the value of threat factors in grid y; i_{rxy} is the impact of threat r that originates in grid cell y on habitat in grid cell x; and β_x is the accessibility of grid cell x. Besides, S_{jr} indicates the sensitivity of land use j to threat r where values closer to 1 indicate greater sensitivity.

Considering the importance of ecosystem protection and biodiversity maintenance of the study area, land-use accessibility is determined according to the different functional zones of the protected areas. Based on the control requirements of different functional zones in *Guiding Opinions on the Establishment of National Park-based Nature Reserve System* and previous research [33], the accessibility parameter β_x was assigned. The β_x value of the core control zones and general control zones is 0 and 0.5 in nature reserves, and it is 0.8 in general control zones of nature parks [33].

$$i_{rxy} = \begin{cases} 1 - \left(\frac{d_{xy}}{d_{r\ max}}\right) \ if\ linear \\ exp\left[-\left(\frac{2.99}{d_{r\ max}}\right) \times d_{xy}\right] \ if\ exponential \end{cases} \tag{4}$$

where d_{xy} is the linear distance between grid cells x and y and d_{rmax} is the maximum effective distance of the threat r's.

In order to ensure the conclusions conform to the reality of the study area, this research established an evaluation form containing the maximum influence distance and weight of the threat factors (Table 1), as well as the sensitivity of the different habitat types to different threat factors (Table 2), which are based on previous studies [34], the InVEST model user's guide [19], and experts' opinions.

Table 1. Maximum influence distance and weight of the threat factors in TS.

Threats	Maximum Influence Distance/km	Weight	Spatial Decay Type
Cropland	8	0.7	linear
Urban land	10	1	linear
Rural residential	6	0.6	linear
Other construction land	8	0.8	linear
Railway	4	0.5	linear
Highway	3	0.4	linear

Table 2. Sensitivity of different habitat types to different threat factors.

Land-Use Code	Habitat	Cropland	Urban Land	Rural Residential	Other Construction Land	Railway	Highway
10	0.3	0.0	0.6	0.4	0.3	0.5	0.4
21	1	0.8	0.9	0.8	0.8	0.8	0.7
22	0.9	0.6	0.7	0.6	0.5	0.6	0.5
23	0.8	0.7	0.8	0.7	0.6	0.8	0.7
24	0.7	0.7	0.8	0.7	0.6	0.7	0.6
31	0.9	0.5	0.6	0.5	0.4	0.5	0.6
32	0.8	0.6	0.7	0.6	0.4	0.5	0.6
33	0.7	0.7	0.8	0.7	0.6	0.5	0.6
41	1	0.1	0.7	0.6	0.5	0.5	0.4
42	1	0.1	0.7	0.6	0.5	0.5	0.4
43	1	0.1	0.7	0.6	0.5	0.5	0.4
44	1	0.1	0.1	0.2	0.1	0.5	0.4
45	0.8	0.7	0.8	0.6	0.5	0.5	0.4
51	0	0	0	0	0	0	0
52	0	0	0	0	0	0	0
53	0	0	0	0	0	0	0
61	0	0	0	0	0	0	0
62	0	0	0	0	0	0	0
63	0.1	0.1	0.1	0.1	0.1	0.2	0.2
64	0.8	0.1	0.5	0.6	0.4	0.5	0.7
65	0.1	0.1	0.1	0.1	0.1	0.2	0.2
66	0	0	0	0	0	0	0
67	0	0	0	0	0	0	0

Notes: 10 is cropland, 21 is forestland, 22 is shrub wood, 23 is sparse woods, 24 is other woodland, 31 is high coverage grassland, 32 is moderate coverage grassland, 33 is low coverage grassland, 41 is river and canal, 42 is lake, 43 is reservoir and pond, 44 is permanent glaciers, 45 is mudflats, 51 is urban land, 52 is rural settlements, 53 is other construction land, 61 is sand land, 62 is Gobi, 63 is saline-alkali lands, 64 is wetland, 65 is bare land, 66 is bare rock texture, and 67 is other unused land.

2.3.2. Terrain Factors

The changes in elevation and topography make a significant difference to the ecological environment of mountain areas [7]. The Terrain Niche Index (*TNI*) can comprehensively represent the elevation and slope characteristics of the study area [35], which was introduced to reveal the spatial distribution characteristics of HQ in different levels of terrain factors. It is calculated as follows:

$$TNI = lg\left[\left(E/\overline{E}+1\right) \times \left(S/\overline{S}+1\right)\right] \quad (5)$$

where *TNI* is the terrain niche index; E and S are the elevation and slope of each pixel; and $\overline{E}$ and $\overline{S}$ are the average elevation and slope of the study area. The greater the *TNI*, the higher the elevation and slope, and vice versa.

To eliminate the dimensional difference of HQ at a different *TNI*, the distribution index was used to explore the distribution characteristics of HQ. The *TNI* was divided into ten grades by natural breaks (jenks). It is calculated as follows:

$$P = (A_{ie}/A_i)/(A_e/A) \tag{6}$$

where P is the distribution index; A_{ie} is the areas of HQ in level i within *TNI* e; A_i is the total area of HQ in level I; A_e is the total area of *TNI* e; and A is the total study area. The greater the p value is, the more selective the terrain. The dominant terrain distribution at a certain level of HQ is where the p value is greater than 1, and vice versa.

2.3.3. Spatial Autocorrelation and Hot/Cold Spot Analysis

Spatial autocorrelation refers to the degree of relevance of an attribute of a geographic object in different spatial locations [22]. It contains global spatial autocorrelation and local spatial autocorrelation. The global Moran's I index was used to evaluate the global cluster characteristics of HQ. The value ranges from -1 to 1. The equation is as follows:

$$\text{Moran's } I = \frac{n\sum_{i=1}^{n}\sum_{j=1}^{n}(x_i-\overline{x})(x_j-\overline{x})}{\sum_{i=1}^{n}\sum_{j=1}^{n}w_{ij}\sum_{i=1}^{n}(x_i-\overline{x})^2} \tag{7}$$

where x_i and x_j are the habitat quality of grid cell i and j; $\overline{x}$ is the average habitat quality of study area; n is the total number of grid cells; and w_{ij} is the spatial weight matrix.

The hot spot analysis can be used to measure the spatial aggregation and differentiation characteristics of HQ, and whether and where high-value (hot spots) or low-value (cold spots) features cluster spatially. The Getis-Ord G_i^* index is calculated based on the ArcGIS platform. When the G_i^* value is significantly positive, the HQ show a high-value concentration, which is a hotspot area. While, when the G_i^* value is significantly negative, the HQ is a low-value aggregation, which is a cold spot area. The areas corresponding to the G_i^* values at the 99% or 95% significance levels are regarded as the hot spots (cold spots) or the sub-hot spots (sub-cold spots) [33]. The calculation formula is as follows:

$$G_i^* = \frac{\sum_{j=1}^{n}w_{ij}x_j - \overline{x}\sum_{j=1}^{n}w_{ij}}{S\sqrt{\frac{\left[n\sum_{j=1}^{n}w_{ij}^2-\left(\sum_{j=1}^{n}w_{ij}\right)^2\right]}{n-1}}} \tag{8}$$

where x_j is the HQ value of grid cell j; $\overline{x}$ is the average HQ value; w_{ij} is the spatial weight matrix between grid cell i and j; n is the total patch number; and S is the standard deviation of the HQ value.

2.3.4. Selection of Driving Factors

The spatiotemporal dynamics of HQ are widely influenced by natural and human factors. Soil plays a part in maintaining biodiversity, ecological conservation, and ecosystem services, as it provides habitat for the largest gene pool and diversity of species [36]. Land-use change, especially urban expansion, accelerates habitat degradation [22,23]. Moreover, the habitat types needed for species survival have been reduced and fragmented under the effects of climate change and land-use change [3,37]. Moreover, universally, overgrazing has caused grassland degradation and loss of biological diversity [18]. According to the natural conditions and development level of the study area, ten factors were selected based on previous studies (Table 3) [21,38,39]. The natural factors included soil type (SOL), annual mean precipitation (PRE), annual mean temperature (TEM), elevation (ELE), and relief degree of land surface (RDLS). The human factors included land-use type (LAND), gross domestic product (GDP), population density (PD), distance to tourism attractions (TOU), and grazing intensity (GI).

Table 3. Details of the driving factors.

Index	Code	Unit	Data Source and Calculation
Soil type	SOL	-	Data from RESDC
Annual mean precipitation	PRE	mm	Data from RESDC
Annual mean temperature	TEM	°C	Data from RESDC
Elevation	ELE	m	Data from the Geospatial Data Cloud (http://www.gscloud.cn, accessed on 21 April 2022)
Relief degree of land surface	RDLS	-	Extract from DEM
Land-use type	LAND	-	Data from RESDC
Gross domestic product	GPD	10^4CNY/km^2	Data from RESDC
Population density	PD	person/km^2	Data from RESDC
Distance to tourism attractions	TOU	m	The tourism attractions were obtained from the Department of Culture and Tourism of the Xinjiang Uygur Autonomous Region. It was calculated by ArcGIS "Euclidean distance" tool.
Grazing intensity	GI	heads/km^2	The livestock data was obtained from the XinJiang Statistical Yearbook. The grazing intensity was calculated based on literature (Li et al., 2014).

2.3.5. Geographical Detector Model

The geographical detector model [40] has been widely used to detect spatially stratified heterogeneity and its driving factors in the fields of ecology and ecosystem services [39]. The model includes factor detection, interaction detection, risk detection, and ecological detection. Factor detection was applied to reveal the relative importance of driving factors on the HQ, and interaction detection was used to explore the interaction effects between the two factors (Table 4). The model is easily accessible on the website (http://www.geodetector.cn/, accessed on 21 April 2022). To maximize the utilization of useful spatial information and enhance the effectiveness of factor detection, it is of great importance to discretize continuous spatial data using the most appropriate discretization method. The optimal parameter-based geographical detector model (OPGD) provides an optimal solution for spatial data discretization, finding the number of spatial strata, and the spatial scale parameter [41]. It can further extract geographical characteristics and information over professional experience, as it supplies the best parameter combination when the geographical detector model is applied. The "GD" package in R 4.1.0 was used for the computation of the OPGD model (https://cran.r-project.org/web/packages/GD/, accessed on 21 April 2022). These factors were classified by the OPGD model in R 4.1.0, except soil type and land-use type.

Table 4. Types of interaction between driving factors (Xs).

Description	Interaction
$q(X1 \cap X2) < \text{Min}(q(X1), q(X2))$	Weaken, nonlinear
$\text{Min}(q(X1), q(X2)) < q(X1 \cap X2) < \text{Max}(q(X1), q(X2))$	Weaken, univariate, nonlinear
$q(X1 \cap X2) > \text{Max}(q(X1), q(X2))$	Enhance, linear, bivariate
$q(X1 \cap X2) = q(X1) + q(X2)$	Independent
$q(X1 \cap X2) > q(X1) + q(X2)$	Enhance, nonlinear

3. Results

3.1. Validation of Habitat Quality

It is necessary to test the effectiveness of the modified HQ model for assessing biodiversity. The species richness was used to characterize biodiversity, which was obtained from the literature [13,42]. The fitting results (Figure 2) showed that this model showed a highly significant Pearson's r (0.69, $p < 0.01$) and regression slope values (14.558, $p < 0.01$), with an $R^2 = 0.48$, indicating that there was a good linear relationship between the two. Thus, this model can be applied to the field of biodiversity estimation.

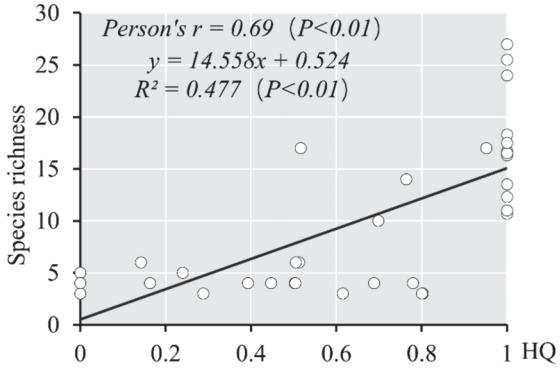

Figure 2. The validation of habitat quality based on species richness.

3.2. Land-Use Change from 1995–2015

Grassland was the dominant land-use type of the TS, and its total area accounted for almost 60%, followed by unused land (Figure 3). The land-use structure underwent a rapid change during the study period. The areas of cropland, grassland, built-up land, and unused land showed a tendency to increase to varying degrees. The area of grassland and unused land increased the most, reaching 10,345.98 km^2 (7.45%) and 3382.57 km^2 (5.38%), respectively, and the area of construction land increased the fastest (285.91%). The area of woodland and water body decreased by 3919.17 km^2 (30%) and 11,091.12 km^2 (65.54%), respectively. Overall, the area of artificial landscape (e.g., cropland and built-up land) increased by 1283.62 km^2 (37.55%), while the areas of natural landscape (e.g., woodland, grassland, water body, and unused land) decreased by 1281.74 km^2 (0.55%).

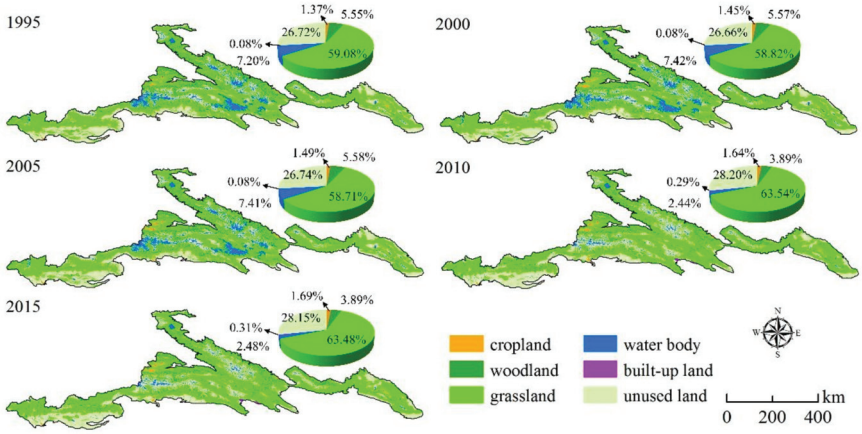

Figure 3. The land-use change from 1995 to 2015.

As shown in Figure 4, land-use transitions can be divided into two stages—smooth change (1995–2005) and fast change (2005–2015). From 1995 to 2005, the grassland was mostly transformed into other land-use types, which mainly contained unused land (1085.59 km^2), cropland (760.72 km^2), and woodland (758.29 km^2). The area of unused land transferred out up to 1452.12 km^2. From 2005 to 2015, a large amount of unused land was converted to grassland, with an area of 18,563.39 km^2. The area of grassland and water body decreased rapidly by 19,711.91 km^2 and 13,521.97 km^2, respectively. Water bodies were mainly converted into unused land and grassland, while grassland was mainly transformed into unused land and woodland. Overall, under the background of global

climate change, ecological land, such as woodlands, grasslands, and water bodies, became more vulnerable. This result is consistent with Wei's research [16].

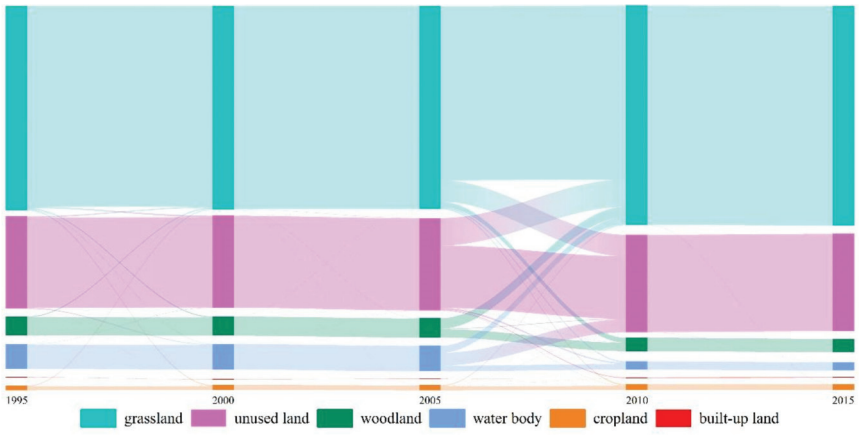

Figure 4. Land-use transitions from 1995 to 2015.

3.3. Spatiotemporal Change in Habitat Quality

The HQ was divided into four different levels using the equal interval method in ArcGIS 10.5 (Table 5): L1—very important habitat (0.75–1.0); L2—important habitat (0.5–0.75); L3—moderately important habitat (0.25–0.5); and L4—general habitat (0–0.25).

Table 5. The area of different habitat quality levels.

Classification	Level	Value	Area (%)				
			1995	2000	2005	2010	2015
Very important habitat	L1	0.75~1.0	37.08	37.76	36.15	37.05	35.23
Important habitat	L2	0.5~0.75	10.65	9.60	11.78	10.87	10.69
Moderately important habitat	L3	0.25~0.5	16.86	15.76	16.47	15.29	14.98
General habitat	L4	0.0~0.25	35.41	36.88	35.61	36.78	39.10

The spatial distribution pattern of HQ in the TS was relatively stable from 1995 to 2015 (Figure 5), with few large areas with significant changes; but, there was still small-scale fluctuation. The NTS had a higher HQ (0.68), followed by the MTS (0.44) and the ETS (0.40). The very important habitat was mainly distributed in the Ili River Valley and the southern edge of the Junggar Basin. These regions were the main distribution areas of forests and grasslands in the TS. The average altitude was above 2700 m and was less disturbed by human activities, which is consistent with previous research [24,43]. The general habitat was mainly distributed in the transitional belt between the southern slope of the middle Tianshan Mountains and the Tarim Basin, which is close to the Taklimakan Desert. There were Gobi desert and bare rock areas with sparse vegetation.

From 1995 to 2015 (Table 5), the average values of the HQ in the TS were 0.5044, 0.5032, 0.5011, 0.4983, and 0.4802, which were at the middle level, with a slight decrease. The HQ of the TS was mainly dominated by very important habitats and general habitats, followed by moderately important habitats and important habitats. In the last 20 years, the areas of L1 and L3 decreased by 1.85 % and 1.88 %, respectively, while the area of L4 increased by 3.69 %, which was mainly due to the substantial glacier shrinkage in the TS caused by rapid warming [15]. The area of L2 was relatively stable.

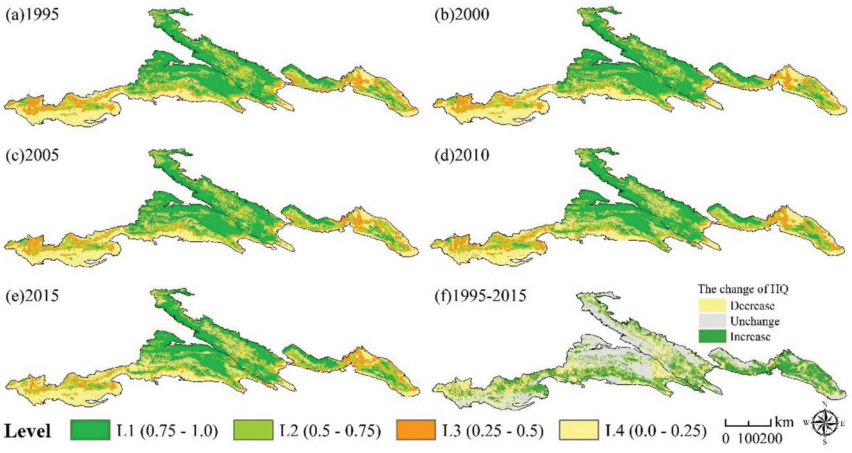

Figure 5. The change in habitat quality from 1995 to 2015. Notes: (**a**)~(**e**) are the spatial distribution of different habitat quality levels in 1995, 2000, 2005, 2010, and 2015, respectively; (**f**) is the change of habitat quality from 1995 to 2015.

Altogether, the area with improved HQ reached 30.35% of the study area, mainly in the east. Meanwhile, almost 30.15% of the region faced HQ degradation to different degrees, which was more evident in the western region. The fluctuating change in HQ threatens the biodiversity and ecological security of the Tianshan Mountains.

3.4. The Spatial Heterogeneity of the Habitat Quality

A total of 61,315 grids of 2 × 2 km^2 were generated with the "fish net" tool in ArcGIS10.5. From 1995 to 2015, the Global Moran's I ($p < 0.01$) values were 0.9024, 0.9034, 0.8989, 0.9028, and 0.9003, respectively, indicating that there was a significant spatial agglomeration of HQ in the TS, but the spatial agglomeration tended to weaken, with a slight decrease in Global Moran's I.

The Getis-Ord G_i^* was used to identify the spatial heterogeneity in HQ in the TS. There were three non-uniform units (Figure 6): hot spots, cold spots, and random areas. The hot spot areas were mainly distributed in the Ili River Valley and Kaidu River Basin, while the cold spot areas were mainly distributed in the south and east of the Tianshan Mountains. The proportion of hot spot areas in 1995–2015 were 29.62%, 29.75%, 28.79%, 29.6%, and 29.02%, respectively, showing a downward trend. Meanwhile, the proportions of the cold spot areas were 28.40%, 28.90%, 28.17%, 28.63%, and 28.91%, respectively, showing an increasing trend. The proportions of random areas were 41.98%, 41.35%, 43.04%, 41.73%, and 42.07%, respectively. The hot spot areas of PAs in the TS were 17,856 km^2, accounting for 25.51% of the total hot spot areas, suggesting that PAs play an important role in maintaining regional biodiversity [24].

3.5. Habitat Quality in Relation to Different PAs

Considering that the boundaries of the World Natural Heritage site were almost the same as those of the nature reserves or nature parks, the HQ of the World Natural Heritage site was not compared, to avoid repeated calculations. Overall, the HQ was strongly affected by the protection level (Figure 7a). Specifically, the nature parks (0.78) had the highest HQ, followed by nature reserves (0.68), the priority areas for biodiversity conservation in the Tianshan Mountains–southwest Junggar Basin (0.65), total Tianshan Mountains (0.50), and unprotected areas (0.47). The average HQ of the PAs was higher than 0.6, whereas that of the unprotected areas was lower than 0.5. Clearly, the establishment of PAs was distinguished in safeguarding important habitats. From 2005 to 2015, the HQ values of the different PA categories fluctuated slightly and were entirely stable. The HQ

of the nature parks increased slightly, whereas that of the other PAs showed a downward trend. Among them, the HQ of the nature reserves decreased the most due to the shrinkage of substantial glaciers, up to 0.18, and it was lower than that of the priority areas for biodiversity conservation in the Tianshan Mountains–southwest Junggar Basin.

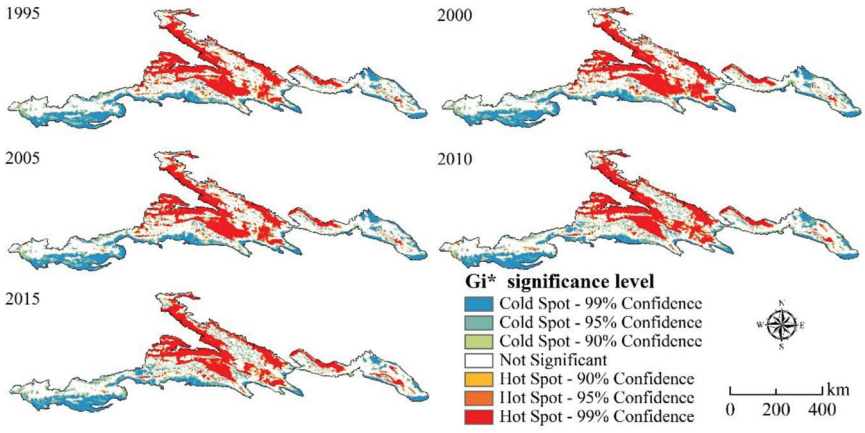

Figure 6. Getis-Ord G_i^* scores of habitat quality.

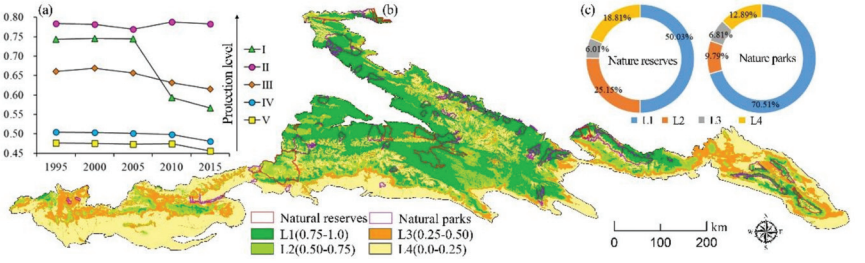

Figure 7. The change in habitat quality of the different PA categories (**a**), the average habitat quality from 1995 to 2015 (**b**), and the proportion of each different habitat quality level of the nature reserves and nature parks (**c**). Notes: I is nature reserve, II is nature park, III is the priority areas for biodiversity conservation in the Tianshan Mountains–southwest Junggar Basin, IV is total Tianshan Mountains, and V is unprotected areas.

In terms of the spatial pattern and habitat level (Figure 7b,c), most of the nature reserves and nature parks were distributed in the region of very important habitats and important habitats, both of which covered more than 75% of the area. Nature reserves were mainly distributed in the region of very important habitats, followed by important habitats. Nature parks had an overwhelming superiority of very important habitats, indicating that nature reserves and nature parks play a vital role in supporting ecological security. Nevertheless, conservation effectiveness and design need to be extended beyond the existing PA network to protect an adequate representation of species and habitats [44]. Moreover, we should not only get information on how much area needs protection, but, more importantly, also where to protect biodiversity and habitats.

3.6. Habitat Quality Variation in Terrain Gradient

From 1995 to 2015, the HQ at different terrain niches presented three characteristics. First, the HQ showed an inverted "U" type (Figure 8). It increased at TNI 1–5 and decreased at TNI 6–10. The important habitats were mainly distributed at TNI 3–8, which were the main distribution areas of ecological land, such as grassland, forest, and water bodies.

Therefore, people should give importance to the monitoring of HQ in these terrain gradient areas. The structure and composition of land use were relatively stable. Second, the HQ impairment and constancy areas increased with the terrain niche index, while the gain areas changed slightly. Third, the distribution index of L1 was greater than 1 at TNI 3–7, which showed a dominant distribution, but habitat quality L4 showed the opposite trend. The distribution index of L2 appeared to be dominant when the TNI was greater than 5. In general, landscape heterogeneity increased at moderate to high terrain levels compared to the low terrain levels in arid mountain ecosystems, indicating that they can support more species, habitat richness, and habitat diversity.

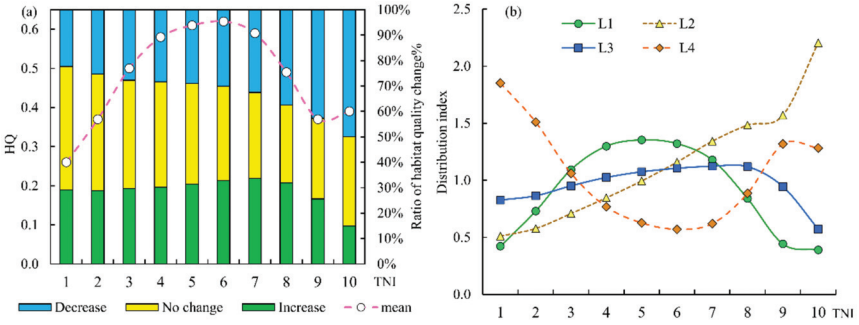

Figure 8. The habitat quality change from 1995 to 2015 (**a**), and the distribution index of habitat quality level at different terrain niches (**b**).

3.7. Driving Factors of Habitat Quality

3.7.1. Comparison of Driving Factors in the Different Sub-Regions

The geographical detector model was utilized to analyze the driving factors ($q < 0.01$) of HQ in the TS (Figure 9). For the TTS, the driving factors from highest to lowest were SOL, LAND, PRE, TEM, GI, ELE, GDP, RDLS, PD, and TOU. In general, the effect of natural factors on HQ was significantly higher than that of socioeconomic factors. The effects of LAND (−14.93%), PRE (−22.17 %), GDP (−26.36 %), PD (−40.12 %), TOU (−14.76 %), and GI (−31.12 %) all showed a downward trend, while the effects of TEM (11.55 %) and ELE (56.06 %) showed an upward trend, and the effects of SOIL (2.80 %) and RDLS (1.97 %) were relatively stable.

For the ETS, the value of SOL was up to 0.6, and other factors were in the range of 0.2–0.5, besides TOU. The effects of LAND (−10.97 %), PRE (−35.73 %), GDP (−25.66 %), PD (−23.79 %), TOU (−43.93 %), and GI (−27.24 %) all showed a downward trend, while the effects of TEM (11.91 %), ELE (45.48 %), and RDLS (11.91 %) showed an upward trend, and the effect of SOL (3.54 %) showed slight fluctuations.

For the NTS, the first two driving factors were LAND and SOL, and TEM, PRE, ELE, GDP, GI, PD, TOU, and RDLS followed. The effects of LAND (−10.47 %), PRE (−69.01 %), RDLS (−17.32 %), PD (−14.73 %), TOU (−21.19 %), and GI (−35.22 %) all showed a downward trend, and the effects of SOL (12.83 %), TEM (69.01 %), ELE (43.30 %), and GDP (9.16 %) showed an upward trend.

For the MTS, the SOL, LAND, PRE, GI, and TEM were the main influencing factors, followed by ELE, GDP, PD, RDLS, and TOU. The effects of LAND (−18.70 %) and PD (−61.14 %) showed a downward trend, and the effects of TEM (7.60 %), ELE (43.84 %), RDLS (13.87 %), TOU (18.74 %), and GI (11.33 %) showed an upward trend. The effects of SOL (3.94 %), PRE (4.64 %), and GDP (0.95 %) remained almost unchanged.

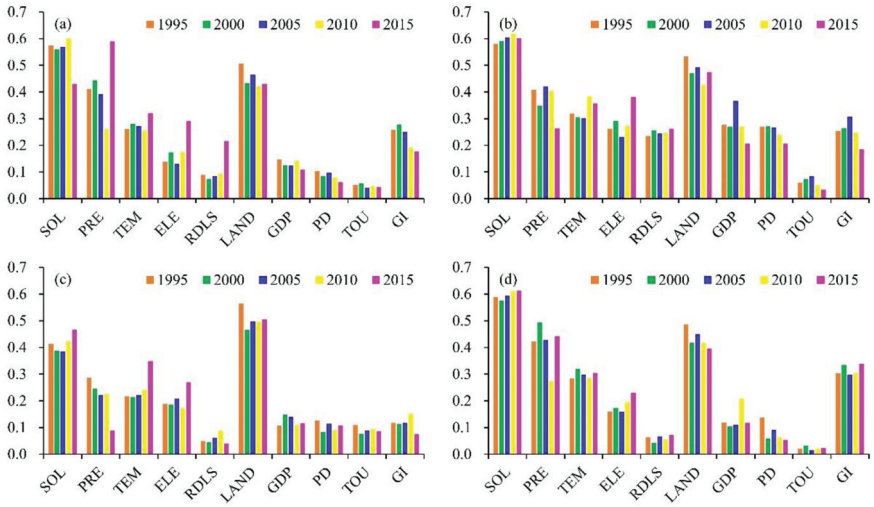

Figure 9. The PD value of each factor from 1995 to 2015: (**a**) the total Tianshan Mountains area, (**b**) the east Tianshan Mountains, (**c**) the north Tianshan Mountains, and (**d**) the middle Tianshan Mountains.

Our study revealed that both natural factors and anthropogenic activities have varying degrees of effects on HQ, but the influence of natural factors is significantly stronger than human activities. Soil properties, such as soil nutrient status, soil acidification state, and soil moisture, are significant preconditions for vegetation growth. The soil types on the north and south slopes of Tianshan show obvious differences, with the north slope being rich in organic matter and favorable for plant growth, while the south slope is mostly desert and meadow soils, which are not favorable for vegetation growth. Climate factors play a more important role in vegetation sensitivity and resilience in arid and semi-arid regions, and climate variability challenges the stability of vegetation. Abundant precipitation in the Ili Valley and high-altitude mountain areas promotes greening of vegetation, while strong evaporation in the southern Tian Shan, especially in the Taklamakan Desert, inhibits plant growth. Land-use change affects biodiversity by increasing the probability of habitat conversion and fragmentation and lowers the viability of species. Population and economic activities were mainly distributed in piedmont oasis areas because of the high elevation of the TS, and overall, the population density and economic activity intensity were at very low levels. Although the tourist numbers and tourism economy in Xinjiang grew rapidly, the level and scale of tourism development is relatively low compared to those of eastern and central China [45]. Meanwhile, the government planned to cultivate the Tianshan Mountains into a nature-based ecotourism corridor [46]. Grazing is the main use of pastures in the Tian Shan region. Grazing, especially heavy grazing, changes the habitat size and connectivity, threatening the survival of species.

3.7.2. Spatial Interactions between Driving Factors

It is widely accepted that HQ is comprehensively affected by multiple factors; thus, the interaction detector was taken into consideration. The results suggested that the interaction effects on the spatial distribution pattern of HQ were higher than those of single factors for both the total Tianshan Mountains and sub-regions, which showed a double-factor and nonlinear enhancement (Table 6). Overall, the interaction between soil type and land use had the strongest explanatory power because they were the main driving factors. Subsequently, some indistinctive influence factors, such as GDP, PD, and ELE, showed a strong explanatory power in the dynamic interaction processes, demonstrating that HQ was very sensitive to minor changes when the ecosystems were subjected to external disturbances.

Table 6. The dominant interactions between two driving factors in different zones.

Year	Zone	Main Interaction Detector
1995	TTS	SOL∩LAND, GI∩LAND, GI∩SOL
	ETS	SOL∩LAND, GDP∩SOL, PRE∩LAND
	NTS	SOL∩LAND, PRE∩LAND, GI∩LAND
	MTS	SOL∩LAND, GI∩SOL, ELE∩SOL
2000	TTS	SOL∩LAND, PRE∩LAND, GI∩SOL
	ETS	SOL∩LAND, GDP∩SOL, PD∩SOL
	NTS	SOL∩LAND, PRE∩LAND, GI∩LAND
	MTS	GI∩SOL, SOL∩LAND, ELE∩PRE
2005	TTS	SOL∩LAND, GI∩SOL, GDP∩SOL
	ETS	GDP∩SOL, SOL∩LAND, PD∩SOL
	NTS	SOL∩LAND, ELE∩LAND, GI∩LAND
	MTS	SOL∩LAND, GI∩SOL, ELE∩SOL
2010	TTS	SOL∩LAND, ELE∩SOL, GDP∩SOL
	ETS	SOL∩LAND, GDP∩SOL, PD∩SOL
	NTS	SOL∩LAND, PRE∩LAND, GI∩LAND
	MTS	ELE∩SOL, GI∩SOL, GDP∩SOL
2015	TTS	SOL∩LAND, ELE∩SOL, GDP∩SOL
	ETS	SOL∩LAND, ELE∩SOL, PD∩SOL
	NTS	SOL∩LAND, ELE∩LAND, TEM∩LAND
	MTS	ELE∩SOL, GI∩SOL, ELE∩PRE

4. Discussion

4.1. Climate Change and Anthropogenic Activity Implications

Based on the results, the core driving factors were soil, climate change, land-use change, and grazing. These basic properties (e.g., particle size distribution, clay content, organic matter, and mineral content) in soil support the terrestrial ecosystem and have a great and persistent influence on HQ [47]. Moreover, the impacts of climate change and land-cover change on soil function cannot be ignored [48]. Global biodiversity is affected by climate change and land-use change [3], causing geographic range shifts, expansions and contractions, and decreasing species habitat availability [2,49]. The land-use structure changes, shift in spatial distribution, and increase in intensity of the changes lead to the landscape being dispersed and fragmented, affecting the natural state and integrity of the ecosystem [16]. The interaction effects between climate change and land-use change increased the risk of habitat loss and fragmentation. Thus, appropriate land-use exploitation seems to be a long-term measure to mitigate the impacts of climate change on biodiversity [37]. The leading use of grasslands is in the form of grazing to maintain millions of livelihoods. However, increasing heavy grazing pressure alters plant community composition, diversity, and productivity [18]. Overgrazing is globally regarded as a booster of land degradation and surface erosion [50], which appears to be devastating for biodiversity protection, ecosystem multifunctionality maintenance, and ecosystem services supply, given that rehabilitation is difficult and takes a long time [48]. Hence, grazing pressure management strategies should be strengthened to achieve the goal of grassland ecological restoration.

4.2. The Gap between Conservation Expectations and Reality

A network of PAs is the cornerstone of global biodiversity and plays a key role in preserving rare and endangered species and ecosystems [9]. Consistent with a previous study [24], our results revealed that PAs provide very important habitat protection. There still exist some gaps, as shown in the following: first, the increased fluctuation in habitat quality in the PAs brings challenges to a stable range of species; and second, there is a large spatial mismatch between the distribution of important habitats and PAs.

Poor management is a significant challenge for the PAs in China [51]. As protected species in PAs have specific and strict demands for habitat types and quality, they have

limited adaptive capacity to climate change [52]. To enhance the conservation effectiveness of PAs, we suggest the design of a framework for the quantification of the efficiency as the basic requirement and normalization measure [9]. However, it is even more important to strengthen the prediction of climate change impacts on habitats and formulate corresponding strategies to enhance the ability of PAs to adapt to climate change [53].

It has been reported that climate change will expose 84% of mountain species to extinction. Thus, increasing representation in high-elevation reserves is of great value to achieve biodiversity targets after 2020 [49]. It is an urgent and important task to integrate important habitats into the ecological conservation redlines and in the restricted zones in the national ecological function zoning. Forest and grass departments should investigate and identify important habitats and ecosystems and establish an optimized adjustment plan for PAs to repair the ecological gaps in the PA network [51]. Furthermore, integrating protected areas to establish national parks can balance the conflict between ecological conservation and regional development.

4.3. Limitations and Future Work

This study integrated the NDVI and InVEST-HQ module to assess the temporal and spatial variation in HQ over the past 20 years in the Tianshan Mountain ranges. The findings of this study provide further information to expand HQ research on mountain biodiversity and ecosystem services. Despite the merits of our framework, this research still had some limitations that should be addressed in the future. First, owing to the difficulty in obtaining historical threat data, some had to be replaced by adjacent years. In addition, some important threat factors, such as pasture distribution and mining sites, were not calculated in the InVEST-HQ model. Second, with the popular application of remote sensing technology, it could provide a large-scale analysis, long time series, and multiple types of observation data for biodiversity research. The potential and effectiveness of other ecological remote sensing parameters for HQ monitoring and assessment were not compared with NDVI, such as the Enhanced Vegetation Index, Leaf Area Index. Third, future climate change and land-use change scenario simulations and predictions would have been of great value [23,34]. Thus, in the future, it is necessary to make a prediction of HQ to support policy recommendations and guidance for land-use spatial optimization and regional development.

5. Conclusions

Understanding the temporal and spatial variation in HQ and its associated driving factors is the basis for biodiversity conservation and ecosystem management in the context of climate change. This study coupled the NDVI and InVEST-HQ module with higher effectiveness to investigate the HQ change over space and time in the Tianshan Mountains in Xinjiang from 1995 to 2015. The following were found: (1) Natural habitats, such as grassland, was the main body of the research area, and changed the fastest both spatially and quantitatively from 1995 to 2015, as compared to the other habitats. (2) The spatial patterns of the habitats were stable, with the largest areas comprising very important habitats and general habitats, although a slight tendency toward habitat degradation and loss should be highly emphasized. The NTS had a better HQ score than that of the MTS and ETS. (3) The spatial heterogeneity of HQ in the Tianshan Mountains was evident, with the hot spot areas clustered in the Ili River Valley and Kaidu River Basin, and the cold spot areas distributed in the south and east of the Tianshan Mountains. The HQ behaved as an inverted "U" type in the different terrain gradients. Protected areas, such as nature reserves, natural parks, and priority areas for biodiversity conservation, were important for biodiversity protection in the Tianshan ranges, with a HQ score of over 0.5. (4) Natural factors (e.g., soil and climate change) were determined to be the mainstays of HQ, and human factors (e.g., land use and grazing) accelerated the fluctuation in habitat change. Their interaction effects increased conspicuously compared to the those of the single factors. In conclusion, HQ varies due to an elaborate mechanism. Thus, understanding the

mechanisms behind the effects of climate change and human activities on mountain HQ will contribute to dynamic governance. These results provide a scientific basis for land-use planning that is adapted to climate change, for the optimal adjustment of PAs, which play a critical role in maintaining mountainous biodiversity and ecosystems.

Author Contributions: Conceptualization, Y.L. and F.H.; methodology, Y.L. and J.Z.; software, J.Z. and Z.W.; validation, Y.L. and Z.Y.; formal analysis, Y.L. and T.R.; investigation, Y.L.; data curation, J.Q.; writing—original draft preparation, Y.L.; writing—review and editing, F.H. and T.R.; visualization, Z.W. and J.Q.; supervision, Z.Y.; project administration, Z.Y.; funding acquisition, F.H. All authors have read and agreed to the published version of the manuscript.

Funding: This research was funded by the Second Tibetan Plateau Scientific Expedition and Research Program (STEP), Grant No. 2019QZKK0401 and the National Natural Science Foundation of China (No. 41971192).

Institutional Review Board Statement: Not applicable.

Informed Consent Statement: Not applicable.

Data Availability Statement: Not applicable.

Conflicts of Interest: The authors declare no conflict of interest.

References

1. Duraiappah, A.K.; Naeem, S.; Agardy, T.; Ash, N.J.; Cooper, H.D.; Díaz, S.; Faith, D.P.; Mace, G.; McNeely, J.A.; Mooney, H.A.; et al. *Ecosystems and Human Well-Being: Biodiversity Synthesis*; World Resources Institute: Washington, DC, USA, 2005; p. 86.
2. Powers, R.P.; Jetz, W. Global habitat loss and extinction risk of terrestrial vertebrates under future land-use-change scenarios. *Nat. Clim. Chang.* **2019**, *9*, 323–329. [CrossRef]
3. Heikkinen, R.K.; Kartano, L.; Leikola, N.; Aalto, J.; Aapala, K.; Kuusela, S.; Virkkala, R. High-latitude EU Habitats Directive species at risk due to climate change and land use. *Glob. Ecol. Conserv.* **2021**, *28*, e01664. [CrossRef]
4. Moreira, M.; Fonseca, C.; Vergílio, M.; Calado, H.; Gil, A. Spatial assessment of habitat conservation status in a Macaronesian island based on the InVEST model: A case study of Pico Island (Azores, Portugal). *Land Use Policy* **2018**, *78*, 637–649. [CrossRef]
5. Maes, J.; Paracchini, M.L.; Zulian, G.; Dunbar, M.B.; Alkemade, R. Synergies and trade-offs between ecosystem service supply, biodiversity, and habitat conservation status in Europe. *Biol. Conserv.* **2012**, *155*, 1–12. [CrossRef]
6. Payne, D.; Spehn, E.M.; Snethlage, M.; Fischer, M. Opportunities for research on mountain biodiversity under global change. *Curr. Opin. Environ. Sustain.* **2017**, *29*, 40–47. [CrossRef]
7. Yu, Y.; Li, J.; Zhou, Z.; Ma, X.; Zhang, X. Response of multiple mountain ecosystem services on environmental gradients: How to respond, and where should be priority conservation? *J. Clean. Prod.* **2021**, *278*, 123264. [CrossRef]
8. Kohler, T.; Maselli, D. (Eds.) *Mountains and Climate Change. From Understanding to Action*, 3rd ed.; Geographica Bernensia: Bern, Switzerland, 2012.
9. Vincent, C.; Fernandes, R.F.; Cardoso, A.R.; Broennimann, O.; Di Cola, V.; D'Amen, M.; Ursenbacher, S.; Schmidt, B.R.; Pradervand, J.-N.; Pellissier, L.; et al. Climate and land-use changes reshuffle politically-weighted priority areas of mountain biodiversity. *Glob. Ecol. Conserv.* **2019**, *17*, e00589. [CrossRef]
10. Grêt-Regamey, A.; Weibel, B. Global assessment of mountain ecosystem services using earth observation data. *Ecosyst. Serv.* **2020**, *46*, 101213. [CrossRef]
11. Bernardino, P.N.; De Keersmaecker, W.; Fensholt, R.; Verbesselt, J.; Somers, B.; Horion, S.; Silva, T. Global-scale characterization of turning points in arid and semi-arid ecosystem functioning. *Glob. Ecol. Biogeogr.* **2020**, *29*, 1230–1245. [CrossRef]
12. McNeely, J.A. Biodiversity in arid regions: Values and perceptions. *J. Arid. Environ.* **2003**, *54*, 61–70. [CrossRef]
13. Zhang, H.X.; Zhang, M.L. Spatial Patterns of Species Diversity and Phylogenetic Structure of Plant Communities in the Tianshan Mountains, Arid Central Asia. *Front. Plant Sci.* **2017**, *8*, 2134. [CrossRef] [PubMed]
14. Fan, M.; Xu, J.; Chen, Y.; Li, W. Reconstructing high-resolution temperature for the past 40 years in the Tianshan Mountains, China based on the Earth system data products. *Atmos. Res.* **2021**, *253*, 105493. [CrossRef]
15. Chen, Y.; Li, W.; Deng, H.; Fang, G.; Li, Z. Changes in Central Asia's Water Tower: Past, Present and Future. *Sci. Rep.* **2016**, *6*, 35458. [CrossRef]
16. Wei, H.; Xiong, L.; Tang, G.; Strobl, J.; Xue, K. Spatial–temporal variation of land use and land cover change in the glacial affected area of the Tianshan Mountains. *Catena* **2021**, *202*, 105256. [CrossRef]
17. Li, Y.; Chen, Y.; Sun, F.; Li, Z. Recent vegetation browning and its drivers on Tianshan Mountain, Central Asia. *Ecol. Indic.* **2021**, *129*, 107912. [CrossRef]
18. Zhao, W.Y.; Li, J.L.; Qi, J.G. Changes in vegetation diversity and structure in response to heavy grazing pressure in the northern Tianshan Mountains, China. *J. Arid. Environ.* **2007**, *68*, 465–479. [CrossRef]

19. Sharp, R.; Tallis, H.T.; Ricketts, T.; Guerry, A.D.; Wood, S.A.; Chaplin-Kramer, R.; Nelson, E.; Ennaanay, D.; Wolny, S.; Olwero, N.; et al. *InVEST+ VERSION+ User's Guide*; The Natural Capital Project; Stanford University: Stanford, CA, USA; University of Minnesota: Minneapolis, MN, USA; The Nature Conservancy, and World Wildlife Fund: Arlington, VT, USA, 2015.
20. Riedler, B.; Lang, S. A spatially explicit patch model of habitat quality, integrating spatio-structural indicators. *Ecol. Indic.* **2018**, *94*, 128–141. [CrossRef]
21. Sun, X.; Jiang, Z.; Liu, F.; Zhang, D. Monitoring spatio-temporal dynamics of habitat quality in Nansihu Lake basin, eastern China, from 1980 to 2015. *Ecol. Indic.* **2019**, *102*, 716–723. [CrossRef]
22. Zhu, C.; Zhang, X.; Zhou, M.; He, S.; Gan, M.; Yang, L.; Wang, K. Impacts of urbanization and landscape pattern on habitat quality using OLS and GWR models in Hangzhou, China. *Ecol. Indic.* **2020**, *117*, 106654. [CrossRef]
23. He, J.; Huang, J.; Li, C. The evaluation for the impact of land use change on habitat quality: A joint contribution of cellular automata scenario simulation and habitat quality assessment model. *Ecol. Model.* **2017**, *366*, 58–67. [CrossRef]
24. Sallustio, L.; De Toni, A.; Strollo, A.; Di Febbraro, M.; Gissi, E.; Casella, L.; Geneletti, D.; Munafò, M.; Vizzarri, M.; Marchetti, M. Assessing habitat quality in relation to the spatial distribution of protected areas in Italy. *J. Environ. Manag.* **2017**, *201*, 129–137. [CrossRef] [PubMed]
25. Di Febbraro, M.; Sallustio, L.; Vizzarri, M.; De Rosa, D.; De Lisio, L.; Loy, A.; Eichelberger, B.A.; Marchetti, M. Expert-based and correlative models to map habitat quality: Which gives better support to conservation planning? *Glob. Ecol. Conserv.* **2018**, *16*, e00513. [CrossRef]
26. Nagendra, H.; Lucas, R.; Honrado, J.P.; Jongman, R.H.G.; Tarantino, C.; Adamo, M.; Mairota, P. Remote sensing for conservation monitoring: Assessing protected areas, habitat extent, habitat condition, species diversity, and threats. *Ecol. Indic.* **2013**, *33*, 45–59. [CrossRef]
27. Pettorelli, N.; Ryan, S.; Mueller, T.; Bunnefeld, N.; Jedrzejewska, B.; Lima, M.; Kausrud, K. The Normalized Difference Vegetation Index (NDVI): Unforeseen successes in animal ecology. *Clim. Res.* **2011**, *46*, 15–27. [CrossRef]
28. Aizen, V.; Aizen, E.; Melack, J.; Dozier, J. Climatic and Hydrologic Changes in the Tien Shan, Central Asia. *J. Clim.* **1997**, *10*, 1393–1404. [CrossRef]
29. Mittermeier, R.A.; Turner, W.R.; Larsen, F.W.; Brooks, T.M.; Gascon, C. Global Biodiversity Conservation: The Critical Role of Hotspots. In *Biodiversity Hotspots*; Springer: Berlin/Heidelberg, Germany, 2011; pp. 3–22. [CrossRef]
30. Olson, D.M.; Dinerstein, E. The Global 200: Priority ecoregions for global conservation. *Ann. Mo. Bot. Gard.* **2002**, *89*, 199–224. [CrossRef]
31. Ministry of Ecology and Environment of People's Republic of China. *China National Biodiversity Conservation Strategy and Action Plan (2011–2030)*; China Environmental Science Press: Beijing, China, 2010.
32. Shui, Y.; Lu, H.; Wang, H.; Yan, Y.; Wu, G. Assessment of habitat quality on the basis of land cover and NDVI changes in Lhasa River Basin (in Chinese). *Acta Ecol. Sin.* **2018**, *38*, 8949–8954. [CrossRef]
33. Zhao, X.; Wang, J.; Su, J.; Sun, W.; Jin, W. Assessment of habitat quality and degradation degree based on InVEST model and Moran index in Gansu Province, China. *Trans. Chin. Soc. Agric. Eng.* **2020**, *36*, 301–308. (In Chinese) [CrossRef]
34. Liu, F.T.; Xu, E.Q. Comparison of spatial-temporal evolution of habitat quality between Xinjiang Corps and Non-corps Region based on land use. *Chin. J. Appl. Ecol.* **2020**, *31*, 2341–2351. (In Chinese) [CrossRef]
35. Xue, L.; Zhu, B.; Wu, Y.; Wei, G.; Liao, S.; Yang, C.; Wang, J.; Zhang, H.; Ren, L.; Han, Q. Dynamic projection of ecological risk in the Manas River basin based on terrain gradients. *Sci. Total Environ.* **2019**, *653*, 283–293. [CrossRef]
36. McBratney, A.; Field, D.J.; Koch, A. The dimensions of soil security. *Geoderma* **2014**, *213*, 203–213. [CrossRef]
37. Hülber, K.; Kuttner, M.; Moser, D.; Rabitsch, W.; Schindler, S.; Wessely, J.; Gattringer, A.; Essl, F.; Dullinger, S. Habitat availability disproportionally amplifies climate change risks for lowland compared to alpine species. *Glob. Ecol. Conserv.* **2020**, *23*, e01113. [CrossRef]
38. Liu, C.; Wang, C.; Liu, L. Spatio-temporal variation on habitat quality and its mechanism within the transitional area of the Three Natural Zones: A case study in Yuzhong county. *Geogr. Res.* **2018**, *37*, 419–432. (In Chinese) [CrossRef]
39. Fang, L.; Wang, L.; Chen, W.; Sun, J.; Cao, Q.; Wang, S.; Wang, L. Identifying the impacts of natural and human factors on ecosystem service in the Yangtze and Yellow River Basins. *J. Clean. Prod.* **2021**, *314*, 127995. [CrossRef]
40. Wang, J.-F.; Zhang, T.-L.; Fu, B.-J. A measure of spatial stratified heterogeneity. *Ecol. Indic.* **2016**, *67*, 250–256. [CrossRef]
41. Song, Y.; Wang, J.; Ge, Y.; Xu, C. An optimal parameters-based geographical detector model enhances geographic characteristics of explanatory variables for spatial heterogeneity analysis: Cases with different types of spatial data. *GISci. Remote Sens.* **2020**, *57*, 593–610. [CrossRef]
42. Zhang, H.; Qian, Y.; Wu, Z.; Wang, Z. Vegetation-environment relationships between northern slope of Karlik Mountain and Naomaohu Basin, East Tianshan Mountains. *Chin. Geogr. Sci.* **2012**, *22*, 288–301. [CrossRef]
43. Yang, Y. Evolution of habitat quality and association with land-use changes in mountainous areas: A case study of the Taihang Mountains in Hebei Province, China. *Ecol. Indic.* **2021**, *129*, 107967. [CrossRef]
44. De Alban, J.D.T.; Leong, B.P.I.; Venegas-Li, R.; Connette, G.M.; Jamaludin, J.; Latt, K.T.; Oswald, P.; Reeder, C.; Webb, E.L. Conservation beyond the existing protected area network is required to improve species and habitat representation in a global biodiversity hotspot. *Biol. Conserv.* **2021**, *257*, 109105. [CrossRef]
45. Wang, T.; Wu, P.; Ge, Q.; Ning, Z. Ticket prices and revenue levels of tourist attractions in China: Spatial differentiation between prefectural units. *Tour. Manag.* **2021**, *83*, 104214. [CrossRef]

46. Xinjiang Uygur Autonomous Region Development and Reform Commission; Xinjiang Uygur Autonomous Region Tourism Development Commission. *Xinjiang Uygur Autonomous Region Thirteenth Five-Year Plan for Tourism Development*; Xinjiang Uygur Autonomous Region Development and Reform Commission; Xinjiang Uygur Autonomous Region Tourism Development Commission: Urumqi, China, 2017.
47. Jost, E.; Schonhart, M.; Skalsky, R.; Balkovic, J.; Schmid, E.; Mitter, H. Dynamic soil functions assessment employing land use and climate scenarios at regional scale. *J. Environ. Manag.* **2021**, *287*, 112318. [CrossRef] [PubMed]
48. Albaladejo, J.; Díaz-Pereira, E.; de Vente, J. Eco-Holistic Soil Conservation to support Land Degradation Neutrality and the Sustainable Development Goals. *Catena* **2021**, *196*, 104823. [CrossRef]
49. Manes, S.; Costello, M.J.; Beckett, H.; Debnath, A.; Devenish-Nelson, E.; Grey, K.-A.; Jenkins, R.; Khan, T.M.; Kiessling, W.; Krause, C.; et al. Endemism increases species' climate change risk in areas of global biodiversity importance. *Biol. Conserv.* **2021**, *257*, 109070. [CrossRef]
50. Donovan, M.; Monaghan, R. Impacts of grazing on ground cover, soil physical properties and soil loss via surface erosion: A novel geospatial modelling approach. *J. Environ. Manag.* **2021**, *287*, 112206. [CrossRef]
51. Zhang, L.; Luo, Z.; Mallon, D.; Li, C.; Jiang, Z. Biodiversity conservation status in China's growing protected areas. *Biol. Conserv.* **2017**, *210*, 89–100. [CrossRef]
52. Li, X.; Clinton, N.; Si, Y.; Liao, J.; Liang, L.; Gong, P. Projected impacts of climate change on protected birds and nature reserves in China. *Sci. Bull.* **2015**, *60*, 1644–1653. [CrossRef]
53. Tanner-McAllister, S.L.; Rhodes, J.; Hockings, M. Managing for climate change on protected areas: An adaptive management decision making framework. *J. Environ. Manag.* **2017**, *204*, 510–518. [CrossRef]

land

MDPI

Article

The Evolution and Determinants of Ecosystem Services in Guizhou—A Typical Karst Mountainous Area in Southwest China

Lu Jiao [1], Rui Yang [2,*], Yinling Zhang [3], Jian Yin [4] and Jiayu Huang [1]

[1] College of Big Data Application and Economics, Guizhou University of Finance and Economics, Guiyang 550025, China; jiaolu@mail.gufe.edu.cn (L.J.); huangjiayu@mail.gufe.edu.cn (J.H.)
[2] College of Public Management, Guizhou University of Finance and Economics, Guiyang 550025, China
[3] School of Tourism and Culture Industry, Chengdu University, Chengdu 610106, China; zhangyinling@cdu.edu.cn
[4] West China Modernization Research Center, Guizhou University of Finance and Economics, Guiyang 550025, China; jiany@mail.gufe.edu.cn
* Correspondence: yangrui@mail.gufe.edu.cn

Abstract: Due to rapid urbanization and economic development, the natural environment and ecological processes have been significantly affected by human activities. Especially in ecologically fragile karst areas, the ecosystems are more sensitive to external disturbances and have a hard time recovering, thus studies on the ecosystem services in these areas are significant. In view of this, we took Guizhou (a typical karst province) as the research area, evaluated the ecosystem service value (ESV) according to reclassified land uses and revised equivalent factors, and investigated the determinants of ecosystem services based on geographic detection. It was found that the total ESV showed a prominent increase trend, increasing from 152.55 billion CNY in 2000 to 285.50 billion CNY in 2020. The rise of grain prices due to growing social demands was the main factor in driving the increase of ESV. Spatially, the ESVs of central and western Guizhou were lower with cold spots appearing around human gathering areas, while that of southern and southeastern Guizhou were higher with hot spots that formed in continually distributed woodland. Moreover, the ESV per unit area and its change rate in karst regions were always lower than that in non-karst areas. Precipitation and temperature were the dominant nature factors while cultivation and population density were the main anthropogenic effects driving the evolution of ecosystem services. Therefore, positive human activities as well as rational and efficient land-use should be guided to promote the coordinated and high-quality development of ecology and the economy.

Keywords: karst region; land-use change; ecosystem service value; spatial autocorrelation; geographical detector

Citation: Jiao, L.; Yang, R.; Zhang, Y.; Yin, J.; Huang, J. The Evolution and Determinants of Ecosystem Services in Guizhou—A Typical Karst Mountainous Area in Southwest China. *Land* **2022**, *11*, 1164. https://doi.org/10.3390/land11081164

Academic Editors: Shicheng Li, Chuanzhun Sun, Qi Zhang, Basanta Paudel and Lanhui Li

Received: 25 June 2022
Accepted: 24 July 2022
Published: 27 July 2022

1. Introduction

Ecosystem services refer to the direct and indirect natural environmental conditions and effects provided by ecosystem and ecological processes to maintain human existence [1–3], including provisioning, regulating, and supporting, as well as cultural services [4]. However, with the intensification of human activities, ecosystem services have been increasingly affected by land-use change, economic development, population growth, urbanization, and industrialization [5]. Research shows that over the past 50 years, about 60% of global ecosystem degradations are caused by population growth and urbanization [6,7]. Although governments from countries have adopted a series of environmental protection policies to restore ecosystem functions [8–10], and some achievements have been made, the ecological and environmental problems cannot be ignored. The ecosystem service value (ESV) is the monetized embodiment of the service provided by natural ecosystems

and is considered as a favorable indicator to evaluate regional sustainable development. In the face of severe resource constraints and global warming, converting ecological resources and advantages into ecological assets and economic advantages is particularly important. It means that the accurate accounting of ESV has new practical significance.

Land is an indispensable carrier for supporting urban economic, social, and cultural activities. Land use and cover change (LUCC) could be the most direct manifestation of human impact on the environment. Especially since rapid industrialization and urbanization, land use patterns and intensity have dramatically varied. The structure and function of ecosystems, as well as the ecological processes, have been changed by LUCC [11], and consequently, led to changes in the ESV. Polasky et al. [12] pointed out that the increase in cultivated land is the main reason for the decline of ESV in partial areas of the United States. Gashaw et al. [13] found that land use is closely related to the value of individual ecosystem services; for instance, the conversion of forest to arable land leads to a decrease in gas and climate regulation but an increase in food production and biodiversity conservation. Urbanization also has a great impact on ecosystem services [14,15] and could be reflected in land-use change, e.g., the occupation of ecological land such as high-quality cultivated land by urban construction affects the function of food supply [16,17]. Similarly, the degradation and reduction of wetlands caused by urban expansion has led to a significant decrease in biodiversity [18]. Therefore, as a bridge connecting natural ecosystems and human socioeconomic systems, LUCC and its impacts on both sides have been widely considered in ecosystem services studies [19].

There are two main types of methods for ESV valuation based on land-use change [20]. One is the functional value evaluation method, which uses the per unit price of ecological products to calculate the value of each ecosystem function by adopting economic valuation techniques such as shadow projects, market pricing, carbon taxes, etc. [21]. Due to the specific considerations of the different ecological processes, products, and parameters, this method could be more accurate, but is complex and more suitable for small-scale studies [22,23]. The other is the equivalent factor method, which uses the economic value of the cropland products per unit area as one equivalent value, thereby defining the value coefficients of different lands and multiplying that with each land area to obtain the ESV [24]. Given the lesser data requirement and statistical convenience, this method is mainly used in large-scale assessments [25]. With the development of remote sensing technology, satellite images and aerial photographs are widely applied to ESV research [26,27], thus the spatial and temporal distribution pattern of ESV and the relevant influencing factors have been given more attention [28]. Research shows that [29–31], under different climate conditions, vegetation coverage, and urbanization levels, ESVs present obvious spatial heterogeneity, which in China is gradually increasing from the northwest to the southeast and is extremely high in the southwest and northeast [29]. Besides, Li et al. [32] investigated the spatiotemporal changes of ESVs in China and identified the cold–hot spot areas. It was found that high-value hot spots were mainly distributed in the west, while low-value cold spots were situated around the coastal areas, indicating that urbanization plays an important role in the distribution of ESV.

The scope and object of ESV studies have also gradually expanded, covering small administrative divisions [33,34] to national [35] and even global views [24]; or focusing on natural geomorphic units, such as watersheds [23], plains [36], and oases [37]; as well as ecosystem scales, including forests [38], wetlands [39], and farmland [40]. In addition, more and more attention has been paid to specific areas—for instance, karst regions. Hu et al. [41] evaluated the ESVs of karst regions in China during 1992–2015 and found obvious spatial variations, which increased in the northwest and northern southwest but decreased in the northeast and eastern southwest. Chen et al. [42] focused on karst regions in southwest China, estimated the ESVs based on land-use data from 1980 to 2018, and found that ESVs increased at early stages and decreased thereafter. In terms of spatial distribution, ESVs in the west were higher, while that in the other regions presented high–low alternating characteristics from west to east, showing significant spatial autocorrelations during the

study period. There are also studies of provinces and cities in karst regions, such as Guizhou [43], Guangxi [44] and Chengdu [45]; however, it is not sufficient and deep enough, and is especially lacking in mechanism research through the comprehensive consideration of nature conditions and human factors driving the evolution of ecosystem services. Due to the special hydrologic and geological conditions in karst areas, it is easy to form a complex landform and fragile ecological environment, which could further restrict human activities and jointly determine the distribution of vegetation and land use. This significantly varies in non-karst areas and was less focused on in previous studies. Furthermore, the karst in China is mainly distributed in the southwestern economically-backward areas, where the demands of economic development and ecological protection are both urgent. Balancing the relationship between ecology and economy is very important. Therefore, this study aims to investigate land-use change and its corresponding ESV evolution in karst areas, and to explore the key natural factors and anthropogenic effects. The results could provide scientific data support and decision-making references for the optimization of land use, the improvement of ecosystem stability, and, finally, the coordinated development of ecology and economy.

2. Materials and Methods

2.1. Study Area

Guizhou province is located in southwest China, with a latitude and longitude of 24°37′–29°13′ N, 103°36′–109°35′ E (Figure 1), and the total area is approximately 176,093 km^2. It is a mountainous area with high-altitude, low-latitude, and typical karst landforms. The geomorphologic types are dominated by plateau mountains, hills, and basins, with highly undulating terrain, which makes the surface cut in varying degrees. The karst here is widely developed and carbonate outcrops almost 2/3 of the total area (Figure 1b), thus it is an ecologically-fragile area and the vegetation structure has poor stability [46]. The total average elevation is about 1100 m, presenting a general pattern that is higher in the west, lower in the east, and tilts from the middle to the north, east, and south. The topography can be roughly divided into three steps with each average elevation being 1500 m, 800–1500 m, and 800 m, respectively. As in the middle and low-latitude transition zone of the eastern Yunnan–Guizhou Plateau, the climate here is relatively complex. It is influenced by atmospheric circulation and topography, and is divided into a south subtropical climate, a middle subtropical climate, a north subtropical climate, and a warm temperate climate. Most of the study area is located in the middle subtropical and northern subtropical climatic regions, with an annual average temperature of 15 °C, an annual sunshine duration of 1100–1400 h, and an annual average rainfall of 1100–1300 mm. Meanwhile, based on the upper reaches of the Pearl River and the Yangtze River in China, the water resources in Guizhou are relatively rich. However, the engineering water shortage is prominent due to weak water storage capacity from the geological particularity of karst [47].

Guizhou includes one provincial capital city (Guiyang) and eight prefecture cities, with a total permanent population of 37.56 million in 2000 and 38.58 million in 2020. The most populous cities are Bijie (17.89% of the total), Zunyi (17.13%), and Guiyang (15.53%), among which Guiyang has the largest population density. The economics of Guizhou has always been relatively backwards and is lower than the average level of China. Due to the implementation of the "Western Development" strategy in 2000, the socioeconomic development of Guizhou has been significantly improved, which result in the urbanization rate increasing from 23.87% in 2000 to 53.15% in 2020 and the gross domestic product (GDP) increasing from 102.99 billion CNY (2759 CNY per capita) to 1782.66 billion CNY (46,267 CNY per capita), resulting in Guizhou jumping to the forefront of China in terms of its economic growth rate for several years. However, the rapid development of socioeconomic activities also intensified land use and cover changes, thereby increasing the risk of ecosystem functions being damaged and weakened.

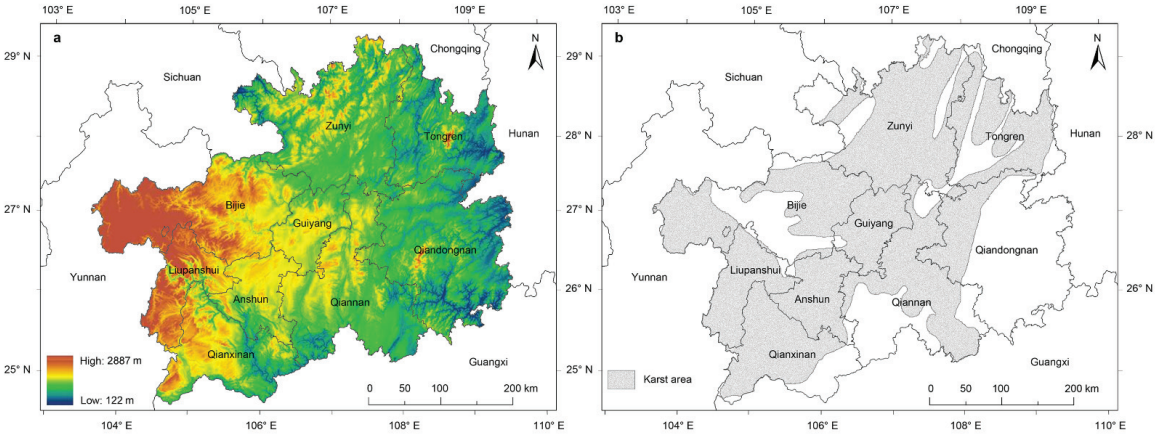

Figure 1. Location and districts of Guizhou province with topographic condition (**a**) and karst distribution (**b**).

In sum, Guizhou is characterized by both ecological vulnerability and a backwards economy, challenging it with the dual tasks of ecological protection and economic development. Therefore, we took Guizhou as the study area, evaluated the ESV according to reclassified land uses and revised equivalent factors, and investigated the determinants of the ecosystem services based on geographic detection. The results could provide an important reference and inspiration for the coordinated and sustainable development of ecology and the economy in similar areas.

2.2. Data Sources and Pre-Processing

In this study, land-use data with a resolution of 1 × 1 km for five periods of 2000, 2005, 2010, 2015, and 2020 were obtained from the Resource and Environment Science and Data Center (RESDC, http://www.resdc.cn, (accessed on 27 July 2021)). According to pre-processing, each land area was extracted and the land, of which was proportional to less than 2%, was merged into the corresponding primary land category to facilitate the statistical analysis; thus, the land-use data were reclassified into nine types, including paddy field, dry land, forest land, shrubbery, sparse wood, grassland, water area, building land, and barren land. Meanwhile, based on previous studies and by combining the regional characteristics of Guizhou with the available data, we preset nine main indicators, including precipitation, temperature, normalized difference vegetation index (NDVI), elevation, slope, lithology, cultivation, population density (PopDensity), and per capita GDP (PerGDP), to comprehensively study the effects of natural factors and human activity on the spatial differentiation of ESV. Among them, elevation and slope were extracted through the DEM data with a resolution of 30 × 30 m, which were obtained from the Geospatial Data Cloud (http://www.gscloud.cn, (accessed on 27 July 2021)). Cultivation was represented by the proportion of farmland per unit area. The rest of the information for the precipitation, temperature, NDVI, lithology, PopDensity, and PerGDP spatialized data, and the administrative boundary vector data, were collected from RESDC. The data above were mainly pre-processed in the ArcGIS 10.7 platform. A fishnet with a grid resolution of 3 × 3 km was created to cut each attribute layer in the study area, and a total of 20,095 grid cells were obtained. The attribute values of every grid corresponding to all layers were measured and extracted to facilitate a subsequent spatial analysis.

In addition, the other relevant socioeconomic development statistics were collected from the Guizhou Provincial Statistical Yearbook, China Agricultural Statistical Yearbook, and China Agricultural Price Survey Yearbook. In order to eliminate the influence of

inflation factors on the results, all economic data were revised using the purchasing power index to be comparable to the price in 2000.

2.3. Methods

The framework and procedure adopted in this study are presented in Figure 2. The first step was model selection and data processing. The equivalent factor method was selected based on the available data in Guizhou to assess the ESV, and the equivalent coefficients were revised according to the regional productive and economic factors to get more accurate evaluation results. Thereafter, the land uses were extracted and reclassified based on remote sensing images to suit the selected method, and to highlight the changes in major land uses in Guizhou and their impact on the ESV. The second step was to calculate the ESV, investigate the temporal changes of the ESV, and adopt a sensitivity analysis to verify the applicability of the revised equivalent coefficients. The third step was to match the ESV to the space based on the land-use data and ESV calculation results, reveal its distribution characteristics, and explore the ESV spatial clustering through the spatial autocorrelation analysis. The fourth step was based on the analysis results of the ESV and the selected influencing factors to identify the importance of different natural conditions and human effects. From these steps, the evolution and determinants of ecosystem services in Guizhou could be obtained. The main methods of each step are detailed as below.

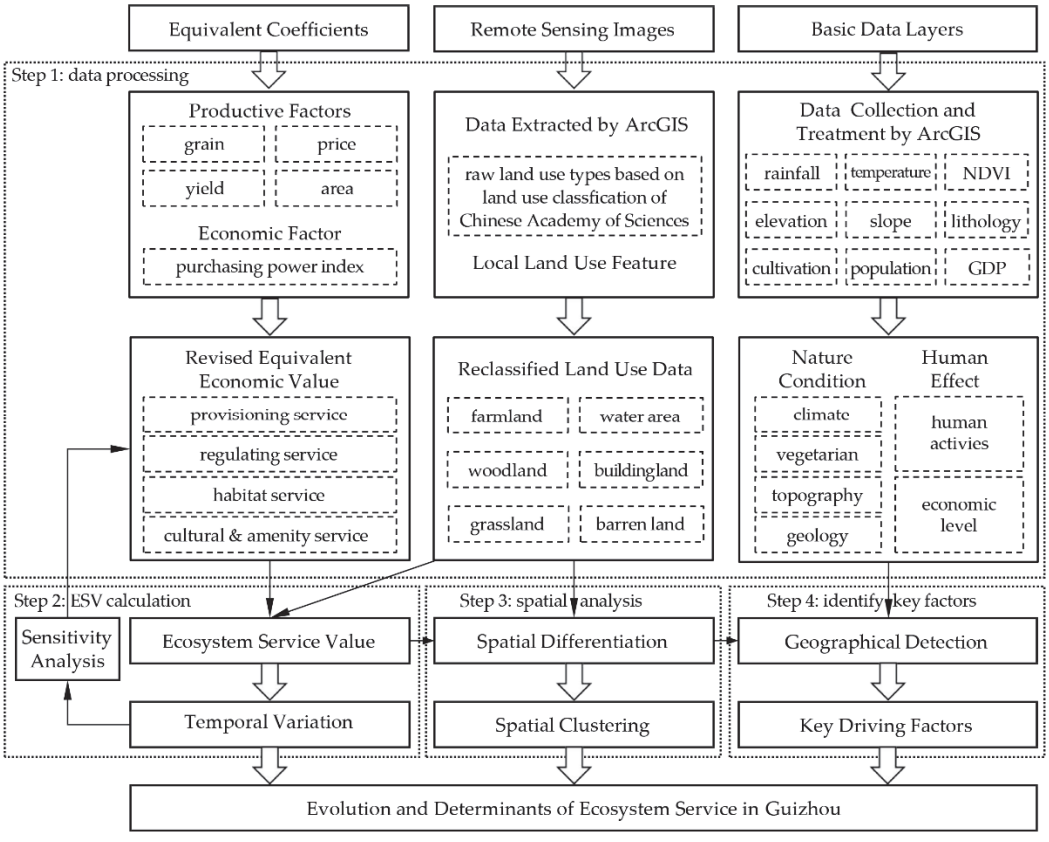

Figure 2. Framework and procedure adopted in this study.

2.3.1. Assessment of Ecosystem Service Value

The equivalent factor method originated from Costanza et al.'s [1] evaluation of the global ESV in 1997, which was adapted for research in China. Xie et al. [20] modified the equivalent value coefficients based on the questionnaire survey results of 200 ecologists, and obtained the ecological service value per unit area of terrestrial ecosystems in China, which include forestland, grassland, cropland, wetland, waterbodies, and bare land. Since this method requires few data and adopts relatively uniform standard parameters, the calculation is easy to operate and the results are intuitive and comparable. It is more conducive to analyze the impact of the macro-scale land-use change on ESV evolution. Therefore, the ESV was assessed using the equivalent factor method in this study. Based on the previous studies and combined with the land-use features in Guizhou, nine ecosystems were identified based on land reclassification, merging the land with area that was proportional to less than 2% into a corresponding primary category. Since the ecosystem service of building land is weak, the relevant ESV was considered as 0. The equivalent coefficients of ESV for the rest of the ecosystem and each ecosystem service was decided upon according to previous studies [41,48] and presented in Table 1.

Table 1. The equivalent coefficients of the ecosystem service value for different land uses.

Ecosystem Service		Farmland		Woodland			Grassland	Water Area	Barren Land
Primary Type	Secondary Type	Paddy Field	Dry Land	Forest Land	Shrubbery	Sparse Wood			
Provisioning service	Food	1.36	0.85	0.29	0.19	0.38	0.22	0.80	0.01
	Materials	0.09	0.40	0.66	0.43	0.56	0.33	0.23	0.03
	Water	−2.63	0.02	0.34	0.22	0.31	0.18	8.29	0.02
Regulating service	Air quality regulation	1.11	0.67	2.17	1.41	1.97	1.14	0.77	0.11
	Climate regulation	0.57	0.36	6.50	4.23	5.21	3.02	2.29	0.10
	Waste treatment	0.17	0.10	1.93	1.28	1.72	1.00	5.55	0.31
	Regulation of water flows	2.72	0.27	4.74	3.35	3.82	2.21	102.24	0.21
	Erosion prevention	0.01	1.03	2.65	1.72	2.40	1.39	0.93	0.13
	Maintenance of soil fertility	0.19	0.12	0.20	0.13	0.18	0.11	0.07	0.01
Habitat Service		0.21	0.13	2.41	1.57	2.18	1.27	2.55	0.12
Cultural and amenity service		0.09	0.06	1.06	0.69	0.96	0.56	1.89	0.05
Total		3.89	4.01	22.95	15.22	19.69	11.43	125.61	1.10

Specifically, one equivalent coefficient of ESV is defined as 1/7 of the economic value of farmland's grain per unit area yield, i.e., the monetary embodiment of the equivalent ecological services. According to previous studies [20,41,48], it is generally average data that originates from the national scale over a certain time. For different regions and periods, the variations in productive and economic factors, such as grain types, sown area, yield and prices, etc., could lead to significant differences in the ESV. In order to improve the accuracy of ESV evaluation, scholars modified the equivalent value of ecosystem services in a variety of ways, e.g., comparing grain yield, net profit, normalized difference vegetation index, net primary productivity, precipitation, soil conservation, willingness to pay [49], and so on, making adjustments with global, national, and regional average levels—and in correspondence with expert experience. Therefore, considering the differences in grain products and yields as well as the changes in demand and grain price over time in Guizhou, the equivalent economic value of ecosystem services, i.e., the economic value for one ESV equivalent coefficient, was confirmed through the following formula and presented in Table 2:

$$E_a = P_a \frac{1}{7} \sum_t \frac{m_t p_t q_t}{M} \quad (1)$$

where E_a denotes the economic value of ecosystem services corresponding to one equivalent coefficient in year a (CNY/ha); t is the type of grain in the research area (mainly rice, corn, and wheat in Guizhou); m_t, p_t, and q_t represent the sown area (ha), average price (CNY/t), and per unit area yield (t/ha) of each type of grain, respectively; M is the total sown area of

grain (ha); and P_a is the purchasing power index in year a based on 2000, which was used to revise the current price to a comparable price.

Table 2. The equivalent economic value of ecosystem services revised by the purchasing power index.

Item	2000	2005	2010	2015	2020
Economic value of one equivalent coefficient at current price (CNY/ha)	651.32	1002.48	1282.88	1613.49	1864.55
Purchasing Power Index *	1.00	0.94	0.81	0.71	0.63
Economic value of one equivalent coefficient of comparable price (CNY/ha)	651.32	937.54	1038.31	1137.98	1178.38

* Purchasing Power Index = Reciprocal of the Consumer Price Index (CPI), based on 2000.

Combining Tables 1 and 2, the value coefficient per unit area for each service of different ecosystems in different years as well as the corresponding ESV could be calculated according to the following formulas:

$$ESV_{ij} = VC_{ij}A_i = e_{ij}E_aA_i \quad (2)$$

$$ESV = \sum_i \sum_j ESV_{ij} \quad (3)$$

where ESV denotes the ecosystem service value (CNY); i and j refer to the type of ecosystems and ecosystem services, respectively; VC_{ij} is the value coefficient per unit area for service j in ecosystem i (CNY/ha); A_i is the area of ecosystem i (ha); e_{ij} is the equivalent coefficient of ESV shown in Table 1; and E_a is the economic value for one ESV equivalent coefficient shown in Table 2 (CNY/ha).

2.3.2. Sensitivity Analysis

It is indispensable to conduct a sensitivity analysis to verify the elasticity between the equivalent value coefficient (VC) of different ecosystems and the total ESV, where the VC was adjusted by increasing or reducing by 50%, respectively, to ascertain the corresponding change in total ESV [50]. The calculation formula is:

$$CS = \left| \frac{(ESV' - ESV)/ESV}{(VC_i' - VC_i)/VC_i} \right| \quad (4)$$

where CS is the sensitivity coefficient; VC and VC' represent the initial and adjusted value coefficient, respectively; ESV and ESV′ denote the total ecosystem service value before and after the adjustment; and i is the type of ecosystems. If $CS < 1$, indicating ESV is inelastic for VC, the research results are credible.

2.3.3. Spatial Autocorrelation Analysis

A spatial autocorrelation analysis is generally used to explore the spatial distribution characteristics and heterogeneity of the ESV, including global and local autocorrelations [51]. Specifically, the global autocorrelation is mainly used to measure the spatial correlation and similarity of the attribute values of adjacent grids over an entire region, while the local autocorrelation is used to reflect the local spatial association and identify the hot spots and cold spots [52]. In this study, the Global Moran's I and Univariate local Moran's I were applied to characterize the spatial aggregation or discrete distribution of ESV in Guizhou using GeoDa software. Permutation tests (9999) were used for the statistical significance assessment [53]. The calculation is as follows:

$$I = \frac{\sum_{i=1}^{n} \sum_{j=1}^{n} \omega_{ij}(x_i - \overline{x})(x_j - \overline{x})}{S^2\left(\sum_i \sum_j \omega_{ij}\right)} \quad (5)$$

$$I_i = \frac{(x_i - \overline{x}) \sum_{j=1}^{n} \omega_{ij}(x_i - \overline{x})}{S^2} \quad (6)$$

$$S^2 = \frac{1}{n} \sum_{i=1}^{n} (x_i - \overline{x})^2 \quad (7)$$

where I and I_i denote the Global Moran's I and univariate local Moran's I; n is the number of grid cells; x_i and x_j represent the measured values of grid i and j; $\overline{x}$ is the average value of the grids; ω_{ij} is the standardized spatial weight matrix between grid i and j; and S^2 is the variance. The global Moran's I ranges from -1 to 1. If I is positive, the ESVs tend to cluster together spatially (high values cluster together or low values cluster near to each other), while if I is negative, high values will repel other high values and tend to be near low values; the spatial autocorrelation is more significant when the I absolute value is larger. If I is near zero, the ESV is randomly distributed with no correlation in space.

2.3.4. Geographic Detection

Geographic detection can be used to detect the stratified heterogeneity of the subject being studied or reveal the possible causality between two variables by analyzing the coupling of their spatial distributions [54]. A Geodetector model [55] was applied to explore the correlations between ESV (Y) and the potential driving factors (Xs, nine selected indicators as mentioned above) in this study. Fishnet cutting and stratified sampling were conducted by ArcGIS to extract the corresponding grid values of the ESV and that of the various driving factors. A statistical analysis was then performed through the Geodetector model to identify dominant factors and their interactions with the ESV. Specifically, the factor detector was used to measure the contribution of factors to ESV spatial distribution, while the interaction detector was applied to assess whether the interaction of pairwise factors would weaken or enhance the explanatory power for the ESV spatial distribution. The factor detector model can be expressed as follow:

$$q = 1 - \frac{1}{N\sigma^2} \sum_{h=1}^{L} N_h \sigma_h^2 \quad (8)$$

where q is the explanatory power of factor X on ESV spatial distribution; h is the partition of factor X; L is the number of partitions; N and σ^2 represent the number of samples and the discrete variance in the entire region; and N_h and ${\sigma_h}^2$ are the number of samples and the discrete variance in h layer, respectively. The value range of q is [0,1]. If the stratification is generated by factor X, the larger the q is, the stronger the impact of this factor on the ESV spatial distribution. When q is 0, it means there is no spatial relationship between X and Y.

3. Results

3.1. Land-Use Changes in Guizhou Province from 2000 to 2020

For more specific studies, land-use data in Guizhou were extracted and reclassified into nine types, including paddy field, dry land, forest land, shrubbery, sparse wood, grassland, water area, building land, and barren land. Moreover, considering that carbonate rocks are widely distributed in Guizhou and form the typical karst geological and geomorphic features, which may have a significantly different impact on vegetation distribution and land use compared with non-karst regions, we further divided the study area into karst and non-karst regions (Figure 1b) for comparative analysis. The area and proportion of different land uses as well as land-use changes from 2000 to 2020 are presented in Table 3 and Figure 3. The dominant land uses in Guizhou were woodland, farmland, and grassland, among which woodland (including forest, shrubbery, and sparse wood) was the most widely distributed. Due to the positive ecological policies, woodland always represented more than 1/2 of the total area, followed by farmland (including paddy field and dry land) with a proportion of over 1/4. The water area and building land were very small, while barren land was the smallest—with the proportion only being about 0.02%.

Table 3. The area (km^2) of each land use and its proportion (%) in different regions in Guizhou province.

Year	Region	Farmland		Woodland			Grassland	Water Area	Building Land	Barren Land
		Paddy Field	Dry Land	Forest Land	Shrubbery	Sparse Wood				
2000	Karst	9619 [a] (8.30) [P]	24,923 (21.50)	12,519 (10.80)	29,779 (25.69)	16,629 (14.35)	21,670 (18.70)	287 (0.25)	470 (0.41)	14 (0.01)
	Non-karst	5141 (8.54)	9714 (16.14)	11,246 (18.69)	13,466 (22.38)	9994 (16.61)	10,375 (17.24)	125 (0.21)	92 (0.15)	30 (0.05)
	All region	14,760 (8.38)	34,637 (19.67)	23,765 (13.50)	43,245 (24.56)	26,623 (15.12)	32,045 (18.20)	412 (0.23)	562 (0.32)	44 (0.02)
2005	Karst	9521 (8.21)	25,000 (21.57)	12,620 (10.89)	29,847 (25.75)	17,155 (14.80)	20,973 (18.09)	294 (0.25)	487 (0.42)	13 (0.01)
	Non-karst	5085 (8.45)	9820 (16.32)	11,234 (18.67)	13,560 (22.53)	10,286 (17.09)	9958 (16.55)	124 (0.21)	92 (0.15)	24 (0.04)
	All region	14,606 (8.29)	34,820 (19.77)	23,854 (13.55)	43,407 (24.65)	27,441 (15.58)	30,931 (17.57)	418 (0.24)	579 (0.33)	37 (0.02)
2010	Karst	9482 (8.18)	24,926 (21.50)	12,648 (10.91)	29,784 (25.70)	17,186 (14.83)	21,002 (18.12)	324 (0.28)	545 (0.47)	13 (0.01)
	Non-karst	5082 (8.44)	9785 (16.26)	11,282 (18.75)	13,643 (22.67)	10,290 (17.10)	9819 (16.32)	161 (0.27)	97 (0.16)	24 (0.04)
	All region	14,564 (8.27)	34,711 (19.71)	23,930 (13.59)	43,427 (24.66)	27,476 (15.60)	30,821 (17.50)	485 (0.28)	642 (0.36)	37 (0.02)
2015	Karst	9245 (7.98)	24,725 (21.33)	12,614 (10.88)	29,690 (25.61)	17,126 (14.78)	20,865 (18.00)	342 (0.30)	1291 (1.11)	12 (0.01)
	Non-karst	5016 (8.33)	9720 (16.15)	11,273 (18.73)	13,604 (22.60)	10,272 (17.07)	9780 (16.25)	177 (0.29)	316 (0.53)	25 (0.04)
	All region	14,261 (8.10)	34,445 (19.56)	23,887 (13.56)	43,294 (24.59)	27,398 (15.56)	30,645 (17.40)	519 (0.29)	1607 (0.91)	37 (0.02)
2020	Karst	8294 (7.16)	25,303 (21.83)	14,558 (12.56)	29,940 (25.83)	13,489 (11.64)	21,650 (18.68)	743 (0.64)	1925 (1.66)	8 (0.01)
	Non-karst	4877 (8.10)	9810 (16.30)	12,125 (20.15)	13,408 (22.28)	9507 (15.80)	9534 (15.84)	446 (0.74)	453 (0.75)	23 (0.04)
	All region	13,171 (7.48)	35,113 (19.94)	26,683 (15.15)	43,348 (24.62)	22,996 (13.06)	31,184 (17.71)	1189 (0.68)	2378 (1.35)	31 (0.02)

[a] Area of each land use (km^2). [P] Area proportion of each land use (%).

In terms of temporal change, the area of woodland, farmland, grassland, and barren land declined overall during the research period, decreasing by 2.24%, 0.65%, 2.69%, and 29.55%, respectively. Among them, farmland roughly declined period by period, with a maximum decreasing rate of 1.15% from 2010 to 2015. Woodland increased in the early stages and reached a maximum area proportion of 53.85% in 2010; after that, it gradually reduced to a minimum area proportion of 52.83% in 2020, which was opposite to grassland. The total decreasing rate of barren land was the highest, but the change amount was less than 10 km^2 due to the smallest total area. Contrarily, water area and building land increased significantly, in which, building land presented the highest total change rate—over 300%—increasing from 562 km^2 in 2000 to 2378 km^2 in 2020, and growing the fastest from 2010 to 2015 with a rate of 150.31%. Water area exhibited a similar variation trend with building land and had a maximum increasing rate of 129.09% during the last stage. The continuous implementation of the Grain to Green Project in Guizhou is the main reason for the decrease in farmland and the increase in woodland during the early stages, while the rapid urbanization development in the last decade is the key factor that caused the rapid increase in building land. Moreover, the increase in water area is mainly caused by the water storage in reservoirs in the Central Guizhou Water Conservancy Project.

Given the unique karst mountain landform in Guizhou, the land surface is cut to varying degrees and fluctuates greatly, thus forming an obviously fragmented distribution of land use. According to Figure 3, woodland was mainly distributed in the north, east, and south of Guizhou, including some contiguously-distributed forest in the natural reserves, such as the Subtropical Evergreen Broad-leaved Forest National Nature Reserve in the north, Anlong Xianheping National Forest Park in the southwest, and Fanjing Mountain National Nature Reserve in the east. Grassland was more spread out in the western region with higher altitudes, and this type was mostly alpine meadows. Farmland was scattered in gentle slopes and low-lying areas and was closely related to the population distribution. Bijie and Zunyi had the largest population as well as the top three land areas among the nine cities in Guizhou and thus accounted for nearly 40% of the total farmland. Water

area was concentrated in the rivers, lakes, and reservoirs of the Wujiang River system and Hongshuihe River system, while building land was intensively distributed in each central city area, especially within the Central Guizhou Cities Group.

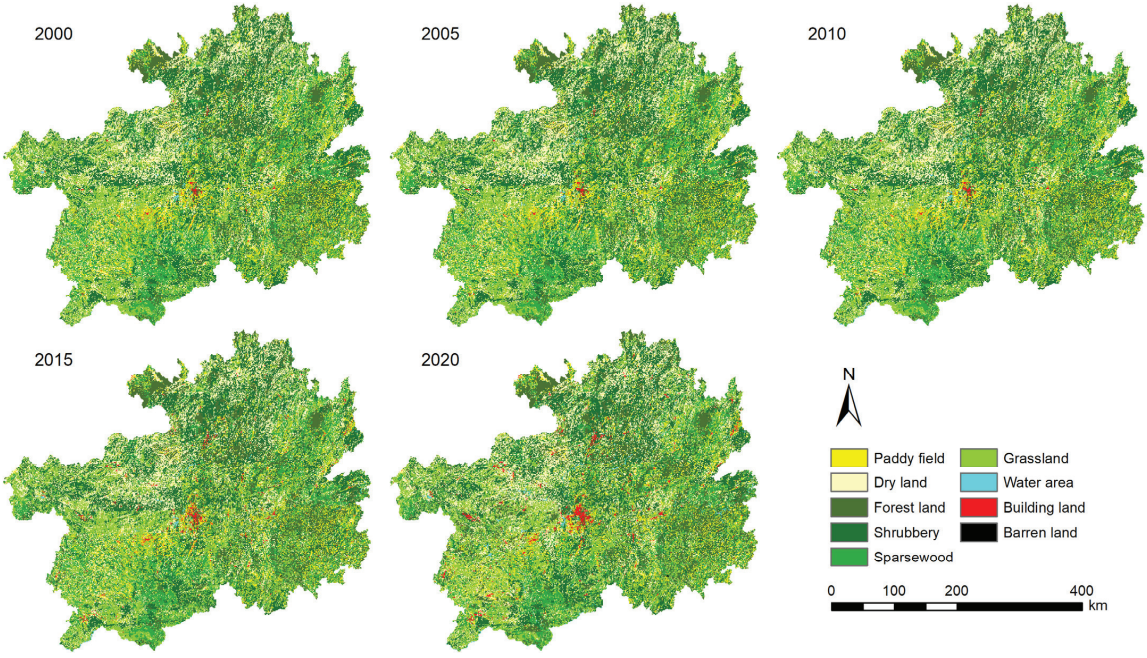

Figure 3. The land-use changes in Guizhou province from 2000 to 2020.

Moreover, it is interesting that the land-use distribution had large differences between karst and non-karst regions. For instance, the proportion of paddy fields in farmland was lower in karst regions than in non-karst areas, while that of dry land was reversed. This is because carbonate rock is resistant to physical weathering but easily dissolved and lost through chemical erosion, thereby causing the slowness of the soil-forming process and thus the shallow and discontinuous soil. In general, paddy fields require thicker and relatively concentrated soil relative to dry land, thus representing the distribution features as above. Similarly, in karst regions the proportion of grassland was higher but that of woodland was lower compared to non-karst areas. Meanwhile, the proportion of shrubbery in woodland was significantly higher in karst regions than in non-karst areas. In addition to soil differences, these land-use distribution characteristics are also related to the extensively developed fissures and pipes in karst regions, where rainfall tends to move underground with less surface water storage and weak soil-water holding capacity, which is more suitable for the development of low-water-demand grassland and shrubbery.

3.2. Temporal Variations of Ecosystem Service Value in Guizhou Province from 2000 to 2020

3.2.1. Variations of Ecosystem Service Value in Different Ecosystems

During the research period, the total ESV in Guizhou showed a significant increase from 152.55 billion CNY in 2000 to 285.50 billion CNY in 2020 (Table 4), with an overall growth rate of 87.15%. Among that, the ESV grew the fastest from 2000 to 2005 at an increment of 67.86 billion CNY and a growth rate of 44.48% which was more than half of the overall increase. Thereafter, the ESV growth gradually slowed down and reached a minimum growth rate of 11.42% from 2015 to 2020. Since the economic value of farmland's grain per unit area yield determines the equivalent economic value of ecosystem services,

the rise in grain unit price (comparable price) could be the key factor for the continuous increase of ESV.

Table 4. The ecosystem service value (billion CNY) of each land use and its proportion (%) in Guizhou province.

Land Use Type	2000		2005		2010		2015		2020	
	ESV	%	ESV	%	ESV	%	ESV	%	ESV	%
Paddy field	3.74	2.45	5.33	2.42	5.88	2.40	6.31	2.35	6.04	2.11
Dry land	9.05	5.93	13.09	5.94	14.45	5.90	15.72	5.86	16.59	5.81
Forest land	35.52	23.29	51.33	23.29	57.02	23.27	62.39	23.27	72.16	25.28
Shrubbery	42.87	28.10	61.94	28.10	68.63	28.00	74.99	27.97	77.74	27.23
Sparse wood	34.14	22.38	50.66	22.98	56.17	22.92	61.39	22.90	53.36	18.69
Grassland	23.86	15.64	33.15	15.04	36.58	14.93	39.86	14.87	42.00	14.71
Water area	3.37	2.21	4.92	2.23	6.33	2.58	7.42	2.77	17.60	6.16
Barren land	0.00	0.00	0.00	0.00	0.00	0.00	0.01	0.00	0.00	0.00
Total	152.55	100.00	220.41	100.00	245.07	100.00	268.08	100.00	285.50	100.00

Structurally, significant differences in the ESVs among different land uses appeared. As mentioned above, the dominant types of land use in Guizhou were woodland, farmland, and grassland, with their ESV accounting for 93.83–97.79% of the total ESV, and thus playing a decisive role in ecosystem services. In particular, woodland made the greatest contribution, providing 71.20–74.37% of the total ESV (Table 4), while its area only accounted for 52.83–53.85% of the total area (Table 3). Due to the increase in the equivalent economic value of ecosystem services, the ESV of each land use always maintained a rising trend during the study period, except for paddy fields and sparse woods during 2015–2020. However, the detailed contribution of each land use to the total ESV varied differently over time. The area of farmland and grassland gradually decreased, causing its ESV proportion in the total ESV to continuously decrease from 8.38% and 15.64% in 2000 to 7.92% and 14.71% in 2020, respectively. The area of woodland increased during the early stages, leading its ESV proportion in the total ESV to increase from 73.77% in 2000 to 74.37% in 2005, and then gradually decrease to 71.2% in 2020, which was accompanied by the decrease of its area. The above reduced ESV was mainly replaced by the ESV provided from water areas. Though its area was small, water area provided the highest growth rate of ESV, with its proportion climbing from 2.21% up to 6.16% in the total ESV, which was close to the ESV provided by farmland and even exceeded the ESV from paddy fields or dry land, indicating that water area plays more and more of an important role in ecosystem services.

3.2.2. Sensitivity Analysis of the Variations of Ecosystem Service Value

The ranking of the ESV sensitivity index for each land use is woodland, grassland, farmland, water area, and barren land (Table 5). In the subclass of land use, the highest ESV sensitivity index appears in shrubbery as 0.2810, meaning that the shrubbery in woodland is more sensitive to changes in the ESV equivalent coefficient than other land uses. This is because of the large area of shrubbery in the study area as well as its higher ESV coefficient. Overall, all the ESV sensitivity coefficients are much less than 1.00, indicating that changes in the ESV equivalent coefficients have less impact on the total ESV. Therefore, the ESV equivalent coefficients in this study are basically reliable and applicable, thus the results are credible.

Table 5. The sensitivity index resulting from adjustment of equivalent coefficient.

Ecosystem	Sensitivity Index				
	2000	**2005**	**2010**	**2015**	**2020**
Paddy field	0.0245	0.0242	0.0240	0.0235	0.0211
Dry land	0.0593	0.0594	0.0590	0.0586	0.0581
Forest land	0.2329	0.2329	0.2327	0.2327	0.2528
Shrubbery	0.2810	0.2810	0.2800	0.2797	0.2723
Sparse wood	0.2238	0.2298	0.2292	0.2290	0.1869
Grassland	0.1564	0.1504	0.1493	0.1487	0.1471
Water area	0.0221	0.0223	0.0258	0.0277	0.0616
Barren land	0.0000	0.0000	0.0000	0.0000	0.0000

3.2.3. Changes in the Value of Individual Ecosystem Services

From 2000 to 2020, the value of each ecosystem service always presented an upward trend, however, the changes in their proportions in the total ESV showed great differences (Table 6). In terms of the primary type, regulating services were dominant and continuously increased, reaching the highest value of 226.79 billion CNY and the largest proportion of 79.44% in the total ESV in 2020. The value of cultural and amenity services were the lowest, with its maximum proportion being only about 4.39% in the total ESV. The change in provisioning services was consistent with regulating services, where the value and proportion increased simultaneously. However, in habitat services as well as cultural and amenity services, the values gradually increased but their proportions showed an opposite change, reducing by 0.34% and 0.13% in the total ESV during the study period.

Table 6. The value of individual ecosystem services (billion CNY) and its proportion (%) in Guizhou province.

Ecosystem Service	2000		2005		2010		2015		2020	
	ESV	**%**	**ESV**	**%**	**ESV**	**%**	**ESV**	**%**	**ESV**	**%**
Providing Food	5.35	3.51	7.71	3.50	8.53	3.48	9.26	3.46	9.46	3.31
Providing Materials	4.89	3.20	7.06	3.20	7.82	3.19	8.54	3.18	8.83	3.09
Providing Water	−0.20	−0.13	−0.24	−0.11	−0.19	−0.08	−0.10	−0.04	0.86	0.30
Air quality regulation	15.73	10.31	22.70	10.30	25.15	10.26	27.44	10.23	28.16	9.86
Climate regulation	38.73	25.39	55.96	25.39	62.03	25.31	67.76	25.28	69.96	24.50
Waste treatment	12.20	8.00	17.63	8.00	19.57	7.99	21.40	7.98	22.40	7.85
Regulation of water flows	33.98	22.27	49.08	22.27	55.09	22.48	60.52	22.58	70.15	24.57
Erosion prevention	18.37	12.04	26.55	12.04	29.41	12.00	32.12	11.98	33.14	11.61
Maintenance of soil fertility	1.67	1.10	2.41	1.09	2.67	1.09	2.91	1.09	2.99	1.05
Habitat Services	15.15	9.93	21.88	9.93	24.27	9.90	26.51	9.89	27.39	9.59
Cultural and amenity services	6.69	4.39	9.67	4.39	10.72	4.38	11.72	4.37	12.17	4.26

For the secondary type of ecosystem service, the ranking of value is as follows: Climate regulation services > Regulation services of water flow > Erosion prevention services > Air quality regulation services > Habitat services > Waste treatment services > Cultural and amenity services > Providing food services > Providing materials services > Maintenance services of soil fertility > Providing water services. Except for the regulation services of water flow exceeding climate regulation services in 2020, the order of individual ecosystem services during the whole period was exactly the same, indicating that the ecosystem structure and function were relatively stable. Climate regulation services had the highest value and were the most dominant ecosystem service, accounting for 47.66% of the total ESV. The lowest value was found in providing water services, which were even negative from 2000 to 2015, manifesting as the utilization and consumption of water resources. The value of providing water services did not turn positive until the substantial increase of water area in 2020, but still only provided 0.30% of the total ESV. Moreover, the value

proportions of regulation services of water flow and providing water services gradually increased, which mainly came from the contribution of the increased water area. Inversely, the value proportions of the remaining ecosystem services all decreased from 2000 to 2020, in which the value proportion of the climate regulation services decreased the most, while that of maintenance services of soil fertility decreased the least.

3.3. Spatial Characteristics of Ecosystem Service Values in Guizhou Province from 2000 to 2020

3.3.1. Spatial Distribution and Variations of Ecosystem Service Values

Based on the data and methods above, the ESVs of Guizhou from 2000 to 2020 were further assigned into grids with values of lowest, low, medium, high, and highest to express the spatial distribution characteristics (Figure 4).

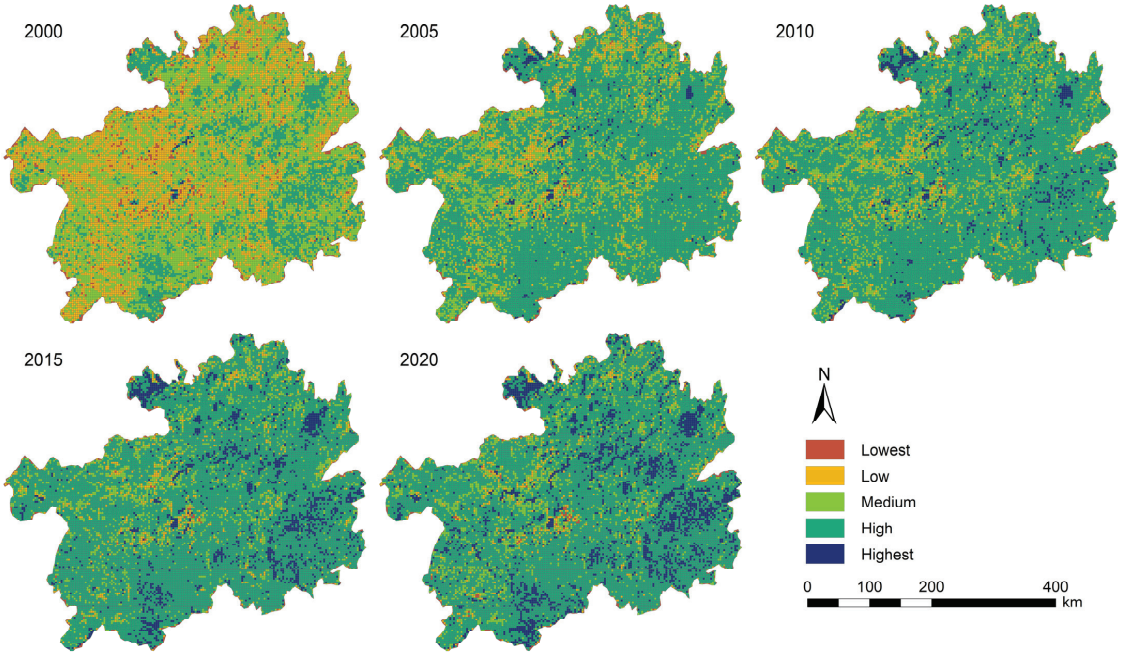

Figure 4. The spatiotemporal differentiation of ecosystem service values in Guizhou province from 2000 to 2020.

The ESVs in Guizhou were generally higher in the east and lower in the west. In 2000, it was dominated by medium and low values, accounting for 45.67% and 30.64% of the total area, respectively, among which low values were mainly distributed in western Guizhou. High values were scattered like plaques in the east and southeast, as well as having a small distribution in the northern and southern edges, which accounted for about 17.79% of the total area. The lowest and highest values were few, while the former was distributed as points near the downtown area and the latter was concentrated in the water area in the central Guizhou reservoirs and the Wujiang River basin. In 2005 and 2010, the medium and low value areas were significantly concentrated in the west; instead, high value areas expanded rapidly on the original basis, and were concentrated and continuously distributed in eastern, southeastern, and southern Guizhou with absolute dominance—and gradually spread to the central and western regions. In 2015 and 2020, the medium and low values were further reduced to 12.09–12.10% and 3.59–4.45% of the total area, and the high values covered 67.33–71.17% of the total area, while the original high value areas in 2000 were gradually transformed into the highest value areas, which accounted for 13.64%

of the total area in 2020. The lowest value areas showed little changes during the early stages but increased slightly in 2020 and concentrated near the urban agglomeration of central Guizhou due to urban development and building land expansion. Overall, the spatial differentiation of ESV above is greatly correlated with the topography that is higher in the west and lower in the east, as well as being correlated with the distribution of land use in Guizhou. The temporal evolution of this spatial differentiation is largely affected by the increased equivalent economic value of ecosystem services.

Furthermore, by comparing karst regions with non-karst areas, we found some special and interesting results (Table 7). In karst regions, the total amount of ESV was higher because of its larger area. However, the average ESV per unit area in karst regions was always lower than in non-karst areas. Similarly, the annual change rate of the ESV was lower in karst areas but higher in non-karst areas, meaning there was a slower growth of the ESV in karst areas. This indicates that geological bases, such as lithology, may have specific effects on the spatial differences and the evolution of ESVs.

Table 7. The ecosystem service values (billion CNY) and its annual change rate (%) of different regions in Guizhou province.

Region	ESV					Annual Change Rate				
	2000	2005	2010	2015	2020	2000–2005	2005–2010	2010–2015	2015–2020	2000–2020
Karst (total)	96.99	140.22	155.70	170.15	180.28	8.92%	2.21%	1.86%	1.19%	4.29%
Karst (CNY/ha) *	8367.40	12,097.49	13,433.09	14,679.14	15,553.61	-	-	-	-	-
Non-karst (total)	55.56	80.19	89.36	97.93	105.21	8.86%	2.29%	1.92%	1.49%	4.47%
Non-karst (CNY/ha) *	9232.49	13,324.27	14,848.69	16,272.06	17,482.15	-	-	-	-	-

* Average ecosystem service value per unit area in karst and non-karst regions.

3.3.2. Spatial Autocorrelation Analysis of Ecosystem Service Value

According to Geoda software, a global autocorrelation analysis was performed to further explore the spatial distribution and agglomeration of ESVs in the study area. As shown in Figure 5, Moran's *I* during the study period was always greater than 0, indicating a positive spatial autocorrelation and agglomeration in ESVs, with high values being adjacent to each other and low values concentrated together. Meanwhile, Moran's *I* gradually decreased from 2000 to 2020, meaning that the spatial differences of the ESVs were enhanced and the spatial heterogeneity became larger, especially at the end of the study period, the value points are more scattered, corresponding to the lowest Moran's *I* on the scatter plot. Moreover, the value points are mainly distributed in the first and third quadrants, and are more concentrated in the third quadrant, indicating smaller differences between the grids in low value areas. Some of the value points extend along the trend line to the first quadrant, especially in 2020, meaning that the value of some grids increased and were obviously higher than other adjacent grids; this is just matching the rapid evolution of the highest value areas in 2020, as mentioned above.

As can be seen from the cluster map (Figure 6), the difference in the ESV spatial agglomeration in Guizhou was not significant from 2000 to 2015, indicating that the ecosystem structure was relatively stable. ESV hot spots (high–high value areas) were mainly distributed in the east and southeast, and gradually extend along the northwest and southwest directions, showing similarity with the ">" type distribution characteristics. Woodland in these areas was widely distributed, with good ecological integrity and strong ecological service function, which is extremely important for maintaining and improving the regional ecological environment. ESV cold spots (low–low value areas) were mainly distributed in central and northern Guizhou. The land uses in these areas were mainly farmland, accompanied by a large amount of building land with a large population density and strong human disturbance. In addition to protecting basic farmland and ensuring ecological land, the rational development and utilization of urban building land should not be neglected. In 2020, the ESV spatial agglomeration evolved some differences, roughly showing a small contraction of the distribution range of hot spots and cold spots. However, the cold spots in central Guizhou appeared local expansion and connection, which were mainly caused

by the rapid agglomeration and development of the cities in central Guizhou, and thus the expanded building land. In future developments, special attention should be paid to the conservation and restoration of ecosystem services in these regions.

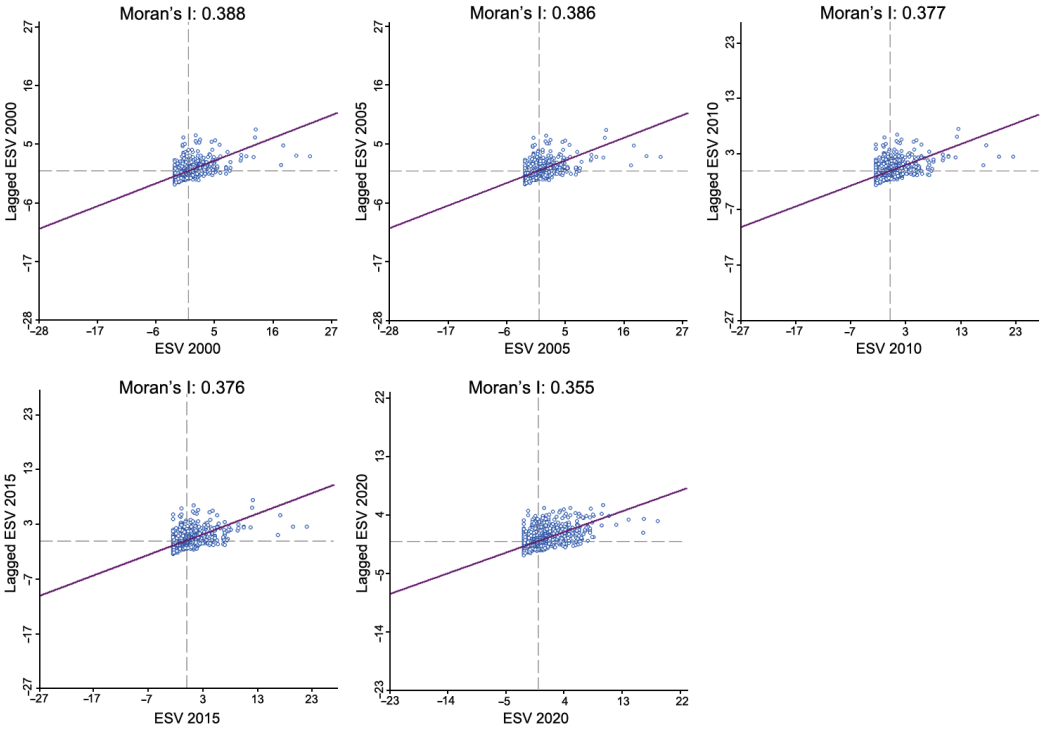

Figure 5. The changes in Global Moran's *I* of ecosystem service values in Guizhou province from 2000 to 2020.

3.3.3. Geographical Detection of Spatial Differentiation in Ecosystem Service Values

From the results above, it can be found that ESVs in Guizhou showed obvious spatial differentiation, which is mostly formed under the combination of natural factors such as climate, vegetation, topography, and geology, as well as human activities. On the basis of this, nine potential driving factors were selected for "Factor detection" and "Interaction detection" according to the Geodetector model to further clarify the contribution of these factors to the ecosystem service spatial heterogeneity. The factor detection results (Table 8) show that each factor has a significant correlation with the spatial distribution of the ESVs, but the respective contribution varies greatly. The multi-year average q value is overall ordered as Precipitation > Temperature > Cultivation > Elevation > PopDensity > NDVI > Slope > Lithology > PerGDP. Among them, Precipitation has the strongest interpretation of the ESV spatial distribution, with each q value exceeding 0.7, followed by Temperature, in which the minimum q value also reaches above 0.6, indicating that climate plays a crucial role in the ESV spatial distribution. In addition, the factors with q values that reach above 0.5 include Elevation, Cultivation, and PopDensity, implying that topography is also a key control factor; furthermore, the influence of human tillage and population density, which reflect the intensity of human activity, cannot be ignored.

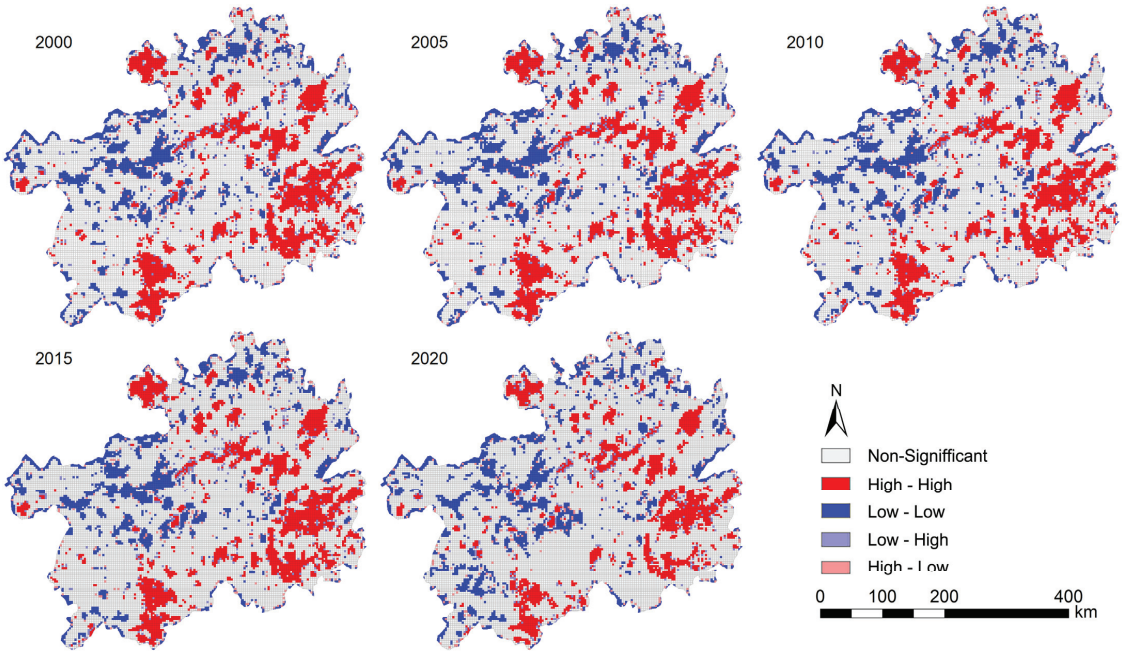

Figure 6. The local indicators of spatial association cluster maps of ecosystem service values in Guizhou province from 2000 to 2020.

Table 8. The *q* statistic and *p* value of nine factors according to geographical detection.

Factor	2000		2005		2010		2015		2020	
	q Statistic	*p* Value	*q* Statistic	*p* Value	*q* Statistic	*p* Value	*q* Statistic	*p* Value	*q* Statistic	*p* Value
Precipitation	0.7820	0.0000	0.7786	0.0000	0.7757	0.0000	0.7687	0.0000	0.7068	0.0000
Temperature	0.6892	0.0000	0.6894	0.0000	0.6831	0.0000	0.6742	0.0000	0.6153	0.0000
NDVI	0.2232	0.0000	0.2426	0.0000	0.2794	0.0000	0.2675	0.0000	0.2472	0.0000
Elevation	0.6363	0.0000	0.6356	0.0000	0.6299	0.0000	0.6243	0.0000	0.5838	0.0000
Slope	0.1617	0.0000	0.1619	0.0000	0.1605	0.0000	0.1584	0.0000	0.1439	0.0000
Lithology	0.1370	0.0000	0.1368	0.0000	0.1355	0.0000	0.1340	0.0000	0.1244	0.0000
Cultivation	0.6552	0.0000	0.6493	0.0000	0.6428	0.0000	0.6346	0.0000	0.5812	0.0000
PopDensity	0.6477	0.0000	0.5032	0.0000	0.6331	0.0000	0.6163	0.0000	0.3611	0.0000
PerGDP	0.1228	0.0000	0.1246	0.0000	0.1293	0.0000	0.0332	0.0000	0.1285	0.0000

Interaction detection is used to investigate whether the combination of any two factors enhance or weaken the strength of the separate interpretation of the ESV spatial distribution. It is shown that each interaction *q* value is greater than that of a single factor, which further indicates that the spatial distribution of ESVs in Guizhou is the result of the combination of multiple factors. Given the complexity of the data group, we only list the strongest interaction factors in each period (Table 9). The interaction between Precipitation and Lithology, Precipitation and NDVI, and Precipitation and Temperature showed the strongest interpretation of the ESV spatial distribution, with interaction *q* values all above 0.72, indicating the basic role of natural factors on ESV spatial patterns. The interaction of Precipitation ∩ Lithology is the most prominent, with the highest interaction *q* value of 0.7950, implying that the difference in lithology would have a great impact on the spatial pattern of ESV under the same precipitation conditions.

Table 9. The dominant interaction factors driving the spatial differentiation in ecosystem service values.

Year	Interaction Factors	Interaction q	Interaction Result
2000	Precipitation ∩ Lithology	0.7950	Enhance, bi-
2005	Precipitation ∩ NDVI	0.7937	Enhance, bi-
2010	Precipitation ∩ Lithology	0.7889	Enhance, bi-
2015	Precipitation ∩ Lithology	0.7820	Enhance, bi-
2020	Precipitation ∩ Temperature	0.7202	Enhance, bi-

4. Discussion

4.1. Mechanism of the Temporal Variation of Ecosystem Service Value

4.1.1. Social Demand

In the assessment of ESV, while the equivalent coefficient is determined, the change of ESV per unit area under the same land use depends on the equivalent economic value of ecosystem services, i.e., determined by the economic value of grain yield per unit area of farmland [29]. In many studies [33,36,42], to focus more on the effect of land-use change on the ESV, the multi-annual average grain price is usually used in the ESV calculation to deduct the impact of price changes on ESV. According to the results of such studies, the ESV variations are generally small, unless there is a large change in land use. Actually, ESV is also the value expression of ecosystem services, which means that the temporal changes and regional differences in grain prices may often bring about huge differences in the ESV [56–58]; this cannot be ignored, especially in the ESV evaluation over long timescales. In this study, ESV continuously increased mainly due to the rise of grain unit prices (comparable price). Supposing there is no conversion among different land uses, the increase of ESV caused by the increase of comparable grain unit prices from 2000 to 2020 could be 123.49 billion CNY, about 92.86% of the existing total increment. After deducting the impact of the purchasing power index on prices, this change is largely the value expression of social demand. That is to say, with the development of society and the economy, the disposable personal income and living standards are gradually improved, so thus the quantity and quality of consumer demand enhanced [59]. For ecosystem services, people also potentially have a higher willingness and ability to pay, thus representing a higher ESV.

4.1.2. Land-Use Change

There are significant differences in the ecosystem services under various land uses, corresponding to different ESV equivalent coefficients [20], e.g., the equivalent coefficients of forest land and dry land have a 5-fold gap, while that of water area is even 31-times higher than dry land in this study. In addition, building land is mostly considered a none ecosystem service, thus the ESV is zero [60–62]. It follows that, once land use changes, so will ecosystem services and their corresponding value. The staged growth of ESV, where it was faster earlier but slower later in Guizhou, is determined by both the rise of grain prices and the change of land use together. From 2000 to 2010, the continuous afforestation and the Grain to Green Project in Guizhou caused an increase of woodland and thus promoted the growth of total ESV due to the higher ESV equivalent coefficient, which corresponded to a faster growth rate. Obviously, the increase of woodland has a positive effect on ESV. A similar change is particularly significant according to the study of Han et al. [52], in which the land use transfer is dominated by vegetation restoration and has significantly promoted the growth of ESV by nearly 20%. However, during 2010–2020, the development of Guizhou was accelerated and the urbanization rate climbed up rapidly. A large area of land was occupied by the exploitation of building land, offsetting some of the ESV increment caused by rising grain prices, and thus showing a slower growth rate. While in those studies that did not consider the price factors, the transfer of other land to building land usually leads to a direct decline in ESV [34], or maintains a relatively stable ESV

through the compensation of ecological land during urban construction [63]. In this study, if the impact of price changes is excluded, the total ESV will increase by 5.25 billion CNY, which is about 3.95% of the current increment. It shows that, despite the recent acceleration of urban construction, the evolution of land use in Guizhou during the research period has an overall positive role on ecosystem services. However, special attention should also be paid to the rational exploitation and efficient utilization of building land to ensure the coordinated and sustainable development of the economy and ecology.

4.2. Driving Factors for the Spatial Differentiation in Ecosystem Service Values

4.2.1. Climate and Vegetation

Climate and vegetation significantly influence ecosystem diversity. Precipitation and temperature are the most intuitive and prominent features of climate, in which the differences in precipitation and temperature among regions constitute an important basis for the spatial differentiation of vegetation and ecosystems. Moreover, as the producer of ecosystems, vegetation determines the complexity of ecosystem structure to a large extent. In general, areas with abundant water and heat conditions are more suitable for developing forest vegetation and forming more complex ecosystems. With the decrease of water and heat, the natural vegetation gradually evolves to grassland and even desert, the ecosystem structure tends to be simple [64], thus the ecosystem services are weakened and the corresponding value is reduced. The precipitation and temperature in Guizhou vary greatly in different regions and are characterized by the monsoon climate. The water and heat are abundant in the east with an average annual rainfall and temperature of 900–1300 mm and 16–18 °C; while that of the western area are lower, about 800–1100 mm and 10–14 °C, respectively. Therefore, the ESV is higher in the east and lower in the west, and the high-value areas are mainly concentrated in the lush forest in eastern and southeastern Guizhou, forming ESV hot spots. This is also well confirmed by the highest *q*-values of precipitation and temperature according to the geographical detection in this study. The ESV spatial differentiation driven by climate is particularly evident in large-scale studies. According to Xie et al. [29], the ESV in China exhibits a distribution rule corresponding to the zonal vegetation and climate, which gradually decreases from southeastern forest areas with abundant rainfall to northwestern arid vegetation areas and desert, and the difference is significant. Similar to this study, the spatial differentiation of ESV on a meso-scale [36] and small-scale [65] also reflects the effects of topography and regional microclimate, but this spatial difference is much smaller than that of large-scale studies.

4.2.2. Topography and Geology

Topographical and geological conditions have multiple effects on ecosystems. Complex topography is an important factor in causing regional climate differences. The study of Wu et al. [66] on the Qinghai–Tibet Plateau shows that the ESV decreased with an increase in the elevation gradient, and the ESV decreased first and then increased based on the gradient of the slope and terrain niche index, which indicates that the ESV has a significant correlation with the topography. Generally, in the troposphere, air temperature will gradually decrease with the rise of altitude, while the precipitation will increase slightly within a certain elevation range but decrease rapidly thereafter. This is also an important reason for the low average annual temperature and rainfall in the high-altitude area of western Guizhou, which corresponds to the preponderant distribution of alpine meadows and thus the lower ESV. The western mountain land extends along the Miaoling mountains to central Guizhou and slopes to the north, east, and south, leading to gradually increases in water and heat as well as the development of forests—so the ESV is generally higher. On the other hand, the slope and lithology also affect the formation and development of soil as well as the redistribution of surface water and groundwater. Through a study of ESV in northern Guangxi, Zhang et al. [65] found that geology is fundamentally important for ecosystem services and the special geological conditions of karst have different effects on ESV compared to non-karst areas. In karst areas, carbonate rocks are easily dissolved by

chemical weathering and transfer with water flow because of its rapid reaction kinetics, leaving less soil parent material, and the soil formation process is slow [67]. Meanwhile, soil particles are also prone to be eroded by water flow on steep mountains, resulting in more debris from primary minerals but less secondary clay minerals in slope soil and the corresponding weak soil water-holding capacity [68]. In addition, widely developed karst fissures will further promote the transfer of surface water underground [69]. However, in the intermountain depression, part of the flushed soil particles accumulate to form a relatively thick soil layer. All the above-mentioned reasons significantly affect the regional distribution of vegetation, thereby explaining the lower ESV per unit area in karst areas than non-karst areas, and the lower ESV on high-slope areas than low-lying areas. To sum up, due to the specific geological and hydrological conditions [70], karst regions are usually characterized by a lack of surface runoff [71], thin soil layer [72], serious soil erosion [73], and weak fertility [74], resulting in low environmental carrying capacity and weak anti-interference ability, as well as poor ecosystem stability [74], with slow vegetation recovery and development, thus showing lower ESV growth than that in non-karst areas.

4.2.3. Human Activities

In addition to the above natural conditions, human activities are also a key factor for local spatial differences in ESV. Guo et al. [75] found that ESV is affected by a combination of the natural environment and human activity, where population is the most important influencing factor of ESV, and the influence of human activities on ESV may be further strengthened through rapid economic development. In our research, the Geodetector results also indicate that there is a high spatial correlation between agricultural activity and population density with ESV. In high altitude mountains and nature reserves, e.g., Fanjing Mountain National Nature Reserve, it is less populated with no cultivation and few disturbances to the ecosystem, natural vegetation such as alpine grassland and native forests are widespread, and the ESV is relatively high. In the foothills with low altitudes and slow slopes, as well as relatively flat areas, which are suitable for farming, the population is concentrated and the vegetation is dominated by farmland as well as sparse wood, shrubbery, and grassland, which are converted from farmland according to the Grain to Green Project, showing relatively low ESV. Especially in Bijie City, which is located in the west of Guizhou and has the largest population as well as the third largest area in the province—most of which are high altitude mountains—the population and farmland are mainly concentrated in the low terrain districts and counties, thus low value areas of ESV are continuously distributed, thereby forming cold spots. In addition, in the central city area of each administrative region, there is a dense population and intense urban construction, and the land use is dominated by building land—except for a small amount of park and greenbelt—thereby presenting the lowest ESV. This is also the main reason for the continuous distribution of ESV cold spots in the Central Guizhou Cities Group. It can be seen that in areas with complex terrain, human activity not only affects ecosystem services but are also restricted by natural conditions. Especially under rapid development, special attention should be paid to avoid irrational development and disorderly human disturbances, which could lead to ecological and environmental destruction and degradation of similar karst mountain areas like Guizhou, and even induce natural and socioeconomic problems such as disaster and poverty [76].

5. Conclusions

During the study period, ESV in Guizhou shows a continuous upward trend, and the increase was faster during the early stages but slowed down during the later stages. Rising social demand reflected by grain prices is the leading factor for ESV increase, contributing to about 92.86% of increment. During the first decade, the continuous implementation of the Grain to Green Project significantly promoted the growth of woodland, which even reached 53.85% of total area, and thus accelerated the rise of ESV. Rapid social and economic development during the latter decade increased the demand for building land, causing over

a three-fold rise relative to that in 2000, offsetting some of the growth in ESV. Influenced by natural conditions and human activities, ESV spatial differentiation is significant, with a higher ESV in northern, eastern, and southern regions, and lower ESV in the west. The highest value areas are concentrated in eastern and southeastern Guizhou, which have abundant water and heat conditions and less human activity, thereby forming ESV hot spots. The lowest value areas are continuously distributed in the western mountains with poor water and heat conditions and densely-populated areas in central and western Guizhou, forming cold spots.

Consequently, the spatial and temporal change of ESV is a combination of the results of natural conditions, such as climate, topography, and geology, as well as human activities, such as agricultural activities and urban construction. Natural conditions constitute the basis of ecosystems and ensure the service ceiling they can provide, which is difficult to intervene in. Human activities affect the stability of ecosystem services and determine its lower limit. Positive ecological policies can improve the stability of ecosystem services, and unreasonable development, especially in ecologically sensitive and fragile karst areas, will significantly weaken ecosystem services, which are difficult to recovery. Considering the limitation of land resources and the inevitability of social development, we should persevere in the coordinated development of ecology, society, and the economy: consolidating the achievements of afforestation and protecting ecological land to ensure ecological security, strictly sticking to the farmland red line to ensure food security, and scientifically planning of building land to improve comprehensive land-use efficiency, thereby to achieve high-quality economic development.

This study comprehensively considers the limiting effects of natural conditions and the effects of human activity. Moreover, social demands obviously influenced the value embodiment of ecosystem services and was also taken into account. This could provide methodological references for similar research. In this study, we only investigated the temporal changes of social demands and the relevant impact on ESV; however, the spatial differences of social demands also have significant implications for ecological compensation and economic coordination between regions, which we will take into account in further research.

Author Contributions: Conceptualization and methodology, R.Y. and L.J.; software, L.J., Y.Z. and J.Y.; validation, R.Y.; formal analysis, L.J.; investigation and resources, L.J. and J.H.; data curation, R.Y.; writing—original draft preparation, L.J.; writing—review and editing, R.Y. All authors have read and agreed to the published version of the manuscript.

Funding: This research was supported by National Natural Science Foundation of China (41807366); Guizhou Provincial Science and Technology Projects (Qiankehe Basic [2019] 1048, Qiankehe Platform Talent [2018] 5774-026); Guizhou Provincial Philosophy and Social Science Planning Project (18GZQN03).

Institutional Review Board Statement: Not applicable.

Informed Consent Statement: Not applicable.

Data Availability Statement: Data supporting reported results are available from the corresponding author on request.

Acknowledgments: The authors are very grateful to the editors and anonymous reviewers for their constructive comments on improving this paper.

Conflicts of Interest: The authors declare no conflict of interest.

References

1. Costanza, R.; d'Arge, R.; de Groot, R.; Farber, S.; Grasso, M.; Hannon, B.; Limburg, K.; Naeem, S.; O'Neill, R.V.; Paruelo, J.; et al. The value of the world's ecosystem services and natural capital. *Nature* **1997**, *387*, 253–260. [CrossRef]
2. Nelson, E.; Mendoza, G.; Regetz, J.; Polasky, S.; Tallis, H.; Cameron, D.R.; Chan, K.M.A.; Daily, G.C.; Goldstein, J.; Kareiva, P.M.; et al. Modeling Multiple Ecosystem Services, Biodiversity Conservation, Commodity Production, and Tradeoffs at Landscape Scales. *Front. Ecol. Environ.* **2009**, *7*, 4–11. [CrossRef]
3. Englund, O.; Berndes, G.; Cederberg, C. How to Analyse Ecosystem Services in Landscapes-A Systematic Review. *Ecol. Indic.* **2017**, *73*, 492–504. [CrossRef]
4. Millennium Ecosystem Assessment. How have ecosystem services and their uses changed? In *Ecosystems and Human Well-Being: Synthesis*; Island Press: Washington, DC, USA, 2005; pp. 39–48.
5. Wang, X.; Yan, F.Q.; Zeng, Y.W.; Chen, M.; Su, F.Z.; Cui, Y.K. Changes in Ecosystems and Ecosystem Services in the Guangdong-Hong Kong-Macao Greater Bay Area since the Reform and Opening Up in China. *Remote Sens.* **2021**, *13*, 1611. [CrossRef]
6. Harris, J.M. Global environmental challenges of the twenty-first century: Resources, consumption, and sustainable solutions. *Ecol. Econ.* **2004**, *50*, 315–316. [CrossRef]
7. Wu, J.; Jin, X.; Feng, Z.; Chen, T.; Wang, C.; Feng, D.; Lv, J. Relationship of Ecosystem Services in the Beijing-Tianjin-Hebei Region Based on the Production Possibility Frontier. *Land* **2021**, *10*, 881. [CrossRef]
8. Deng, L.; Shangguan, Z.P.; Li, R. Effects of the Grain-for-Green program on soil erosion in China. *Int. J. Sediment Res.* **2012**, *27*, 120–127. [CrossRef]
9. Bai, Y.; Jiang, B.; Wang, M.; Li, H.; Alatalo, J.M.; Huang, S.F. New ecological redline policy (ERP) to secure ecosystem services in China. *Land Use Policy* **2016**, *55*, 348–351. [CrossRef]
10. Yan, D.; Zhong, C.J. Characteristic of rocky desertification and comprehensive improving model in karst peak-cluster depression in Guohua, Guangxi, China. *Procedia Environ. Sci.* **2011**, *10*, 2449–2452.
11. Zhao, L.; Liu, J.P.; Tian, X.Z. The temporal and spatial variation of the value of ecosystem services of the Naoli River Basin ecosystem during the last 60 years. *Acta Ecol. Sin.* **2013**, *33*, 3169–3176. [CrossRef]
12. Polasky, S.; Nelson, E.; Pennington, D.; Kris, A. The Impact of Land-Use Change on Ecosystem Services, Biodiversity and Returns to Landowners: A Case Study in the State of Minnesota. *Environ. Resour. Econ.* **2011**, *48*, 219–242. [CrossRef]
13. Gashaw, T.; Tulu, T.; Argaw, M.; Abeyou, W.; Tolessa, T.; Kindu, M. Estimating the impacts of land use/land cover changes on Ecosystem Service Values: The case of the Andassa watershed in the Upper Blue Nile basin of Ethiopia. *Ecosyst. Serv.* **2018**, *31*, 219–228. [CrossRef]
14. Luo, S.F.; Yan, W.D. Evolution and driving force analysis of ecosystem service values in Guangxi Beibu Gulf coastal areas, China. *Acta. Ecol. Sin.* **2018**, *38*, 3248–3259.
15. Li, L.; Wu, D.F.; Wang, F.; Liu, Y.Y.; Liu, Y.H.; Qian, L.X. Prediction and tradeoff analysis of ecosystem service value in the rapidly urbanizing Foshan City of China: A case study. *Acta. Ecol. Sin.* **2020**, *40*, 9023–9036.
16. Jiang, L.; Deng, X.; Seto, K.C. The impact of urban expansion on agricultural land use intensity in China. *Land Use Policy* **2013**, *35*, 33–39. [CrossRef]
17. Huang, Z.H.; Du, X.J.; Castillo, C.S.Z. How does urbanization affect farmland protection? Evidence from China. *Resour. Conserv. Recycl.* **2019**, *145*, 139–147. [CrossRef]
18. Yan, F.; Zhang, S. Ecosystem service decline in response to wetland loss in the Sanjiang Plain, Northeast China. *Ecol. Eng.* **2019**, *130*, 117–121. [CrossRef]
19. Zhao, M.; Cheng, W.M.; Huang, K.; Wang, N.; Liu, Q.Y. Research on land cover change in Beijing–Tianjin–Hebei region during the last 10 years based on different geomorphic units. *J. Nat. Resour.* **2016**, *31*, 252–264.
20. Xie, G.D.; Zeng, L.; Lu, C.X.; Xiao, Y.; Chen, C. Expert Knowledge based Valuation Method of Ecosystem Services in China. *J. Nat. Resour.* **2008**, *23*, 911–919.
21. Lin, W.P.; Xu, D.; Guo, P.P.; Wang, D.; Li, L.B.; Gao, J. Exploring variations of ecosystem service value in Hangzhou Bay Wetland, Eastern China. *Ecosyst. Serv.* **2019**, *37*, 100944. [CrossRef]
22. Remme, R.P.; Edens, B.; Schroter, M.; Hein, L. Monetary accounting of ecosystem services: A test case for Limburg province, the Netherlands. *Ecol. Econ.* **2015**, *112*, 116–128. [CrossRef]
23. Wu, C.; Ma, G.; Yang, W.; Zhou, Y.; Peng, F.; Wang, J.; Yu, F. Assessment of Ecosystem Service Value and Its Differences in the Yellow River Basin and Yangtze River Basin. *Sustainability* **2021**, *13*, 3822. [CrossRef]
24. Costanza, R.; de Groot, R.; Sutton, P.; van der Ploeg, S.; Anderson, S.J.; Kubiszewski, I.; Farber, S.; Turner, R.K. Changes in the global value of ecosystem services. *Glob. Environ. Chang* **2014**, *26*, 152–158. [CrossRef]
25. Richardson, L.; Loomis, J.; Kroeger, T.; Casey, F. The role of benefit transfer in ecosystem service valuation. *Ecol. Econ.* **2015**, *115*, 51–58. [CrossRef]
26. Cabello, J.; Fernandez, N.; Alcaraz-Segura, D.; Oyonarte, C.; Pineiro, G.; Altesor, A.; Delibes, M.; Paruelo, M.G. The ecosystem functioning dimension in conservation: Insights from remote sensing. *Biodivers. Conserv.* **2012**, *21*, 3287–3305. [CrossRef]
27. Lang, Y.Q.; Song, W. Quantifying and mapping the responses of selected ecosystem services to projected land use changes. *Ecol. Indic.* **2019**, *102*, 186–198. [CrossRef]
28. Chen, W.; Zeng, J.; Zhong, M.; Pan, S. Coupling Analysis of Ecosystem Services Value and Economic Development in the Yangtze River Economic Belt: A Case Study in Hunan Province, China. *Remote Sens.* **2021**, *13*, 1552. [CrossRef]

29. Xie, G.D.; Zhang, C.X.; Xiao, Y.; Lu, C.X. The value of ecosystem services in China. *Resour. Sci.* **2015**, *37*, 1740–1746.
30. Liu, W.; Zhan, J.Y.; Zhao, F.; Yan, H.M.; Zhang, F.; Wei, X.Q. Impacts of urbanization-induced land-use changes on ecosystem services: A case study of the Pearl River Delta Metropolitan Region, China. *Ecol. Indic.* **2019**, *98*, 228–238. [CrossRef]
31. Chen, F.Y.; Li, L.; Niu, J.Q.; Lin, A.W.; Chen, S.Y.; Hao, L. Evaluating ecosystem services supply and demand dynamics and ecological zoning management in Wuhan, China. *Int. J. Environ. Res. Public Health* **2019**, *16*, 2332. [CrossRef]
32. Li, G.D.; Fang, C.L.; Wang, S.J. Exploring spatiotemporal changes in ecosystem service values and hotspots in China. *Sci. Total Environ.* **2016**, *545–546*, 609–620. [CrossRef]
33. Ye, Y.; Zhang, J.; Wang, T.; Bai, H.; Wang, X.; Zhao, W. Changes in Land-Use and Ecosystem Service Value in Guangdong Province, Southern China, from 1990 to 2018. *Land* **2021**, *10*, 426. [CrossRef]
34. Rahman, M.M.; Szabó, G. Impact of Land Use and Land Cover Changes on Urban Ecosystem Service Value in Dhaka, Bangladesh. *Land* **2021**, *10*, 793. [CrossRef]
35. Guan, Q.C.; Hao, J.M.; Shi, X.J.; Gao, Y.; Wang, H.L.; Li, M. Study on the change of ecological land and ecosystem service value in China. *J. Nat. Resour.* **2018**, *33*, 195–207.
36. Zhou, Y.; Zhang, X.; Yu, H.; Liu, Q.; Xu, L. Land Use-Driven Changes in Ecosystem Service Values and Simulation of Future Scenarios: A Case Study of the Qinghai-Tibet Plateau. *Sustainability* **2021**, *13*, 4079. [CrossRef]
37. Tan, Z.; Guan, Q.Y.; Lin, J.K.; Yang, L.Q.; Lou, H.P.; Ma, Y.R.; Tian, J.; Wang, Q.Z.; Wang, N. The response and simulation of ecosystem services value to land use/land cover in an oasis, Northwest China. *Ecol. Indic.* **2020**, *118*, 106711. [CrossRef]
38. Taye, F.A.; Folkersen, M.V.; Fleming, C.M.; Buckwell, A.; Mackey, B.; Diwakar, K.C.; Le, D.; Le, D.; Hasan, S.; Ange, C.S. The economic values of global forest ecosystem services: A meta-analysis. *Ecol. Econ.* **2021**, *189*, 107145. [CrossRef]
39. Ma, X.F.; Zhu, J.T.; Zhang, H.B.; Yan, W.; Zhao, C.Y. Trade-offs and synergies in ecosystem service values of inland lake wetlands in Central Asia under land use/cover change: A case study on Ebinur Lake, China. *Glob. Ecol. Conserv.* **2020**, *24*, e01253. [CrossRef]
40. Russo, D.; Bosso, L.; Ancillotto, L. Novel perspectives on bat insectivory highlight the value of this ecosystem service in farmland: Research frontiers and management implications. *Agric. Ecosyst. Environ.* **2018**, *266*, 31–38. [CrossRef]
41. Hu, Z.Y.; Wang, S.J.; Bai, X.Y.; Luo, G.J.; Li, Q.; Wu, L.H.; Yang, Y.J.; Tian, S.Q.; Li, C.J.; Deng, Y.H. Changes in ecosystem service values in karst areas of China. *Agr. Ecosyst. Environ.* **2020**, *301*, 107026. [CrossRef]
42. Chen, W.; Zhang, X.P.; Huang, Y.S. Spatial and temporal changes in ecosystem service values in karst areas in southwestern China based on land use changes. *Environ. Sci. Pollut. R.* **2021**, *28*, 45724–45738. [CrossRef] [PubMed]
43. Zhang, T.F.; Wang, L.C.; Su, W.C.; Liang, Y.H.; Shao, J.X.; Zeng, C.F. Analysis of ecological service value in vulnerable karst area of southwestern Guizhou. *Adv. Mater. Res.* **2012**, *1477*, 2241–2244. [CrossRef]
44. Zhang, M.Y.; Wang, K.L.; Liu, H.Y.; Chen, H.S.; Zhang, C.H.; Yue, Y.M. Responses of ecosystem service values to landscape pattern change in typical Karst area of northwest Guangxi, China. *Chin. J. Appl. Ecol.* **2010**, *21*, 1174–1179.
45. Dai, X.; Johnson, B.A.; Luo, P.L.; Yang, K.; Yao, Y.Z. Estimation of urban ecosystem services value: A case study of Chengdu, southwestern China. *Remote Sens.* **2021**, *13*, 207. [CrossRef]
46. Zhang, Y.H.; Xu, X.L.; Li, Z.W.; Liu, M.X.; Xu, C.H.; Zhang, R.F.; Luo, W. Effects of vegetation restoration on soil quality in degraded karst landscapes of southwest China. *Sci. Total Environ.* **2019**, *650*, 2657–2665. [CrossRef]
47. Peng, T.; Wang, S.J. Effects of land use, land cover and rainfall regimes on the surface runoff and soil loss on karst slopes in southwest China. *Catena* **2012**, *90*, 53–62. [CrossRef]
48. Xie, G.D.; Zhang, C.X.; Zhen, L.; Zhang, L.M. Dynamic changes in the value of China's ecosystem services. *Ecosyst. Serv.* **2017**, *26*, 146–154. [CrossRef]
49. Wang, Y.; Shataer, R.; Xia, T.T.; Chang, X.; Zhen, H.; Li, Z. Evaluation on the Change Characteristics of Ecosystem Service Function in the Northern Xinjiang Based on Land Use Change. *Sustainability* **2021**, *13*, 9679. [CrossRef]
50. Hu, H.; Liu, W.; Cao, M. Impact of Land Use and Land Cover Changes on Ecosystem Services in Menglun, Xishuangbanna, Southwest China. *Environ. Monit. Assess.* **2007**, *146*, 147–156. [CrossRef]
51. Hu, X.; Wu, C.; Hong, W.; Qiu, R.; Qi, X. Impact of land-use change on ecosystem service values and their effects under different intervention scenarios in Fuzhou City, China. *Geosci. J.* **2013**, *17*, 497–504. [CrossRef]
52. Han, X.J.; Yu, J.L.; Shi, L.N.; Zhao, X.C.; Wang, J.J. Spatiotemporal evolution of ecosystem service values in an area dominated by vegetation restoration: Quantification and mechanisms. *Ecol. Indic.* **2021**, *131*, 108191. [CrossRef]
53. Anselin, L. Local indicators of spatial associationa-LISA. *Geogr. Anal.* **1995**, *27*, 93–115. [CrossRef]
54. Wang, J.F.; Zhang, T.L.; Fu, B.J. A measure of spatial stratified heterogeneity. *Ecol. Indic.* **2016**, *67*, 250–256. [CrossRef]
55. Wang, R.S.; Pan, H.Y.; Liu, Y.H.; Tang, Y.P.; Zhang, Z.F.; Ma, H.J. Evolution and driving force of ecosystem service value based on dynamic equivalent in Leshan City. *Acta. Ecol. Sin.* **2022**, *42*, 76–90.
56. Hu, M.M.; Li, Z.T.; Wang, Y.F.; Jiao, M.Y.; Li, M.; Xia, B.C. Spatio-temporal changes in ecosystem service value in response to land-use/ cover changes in the Pearl River Delta. *Resour. Conserv. Recy.* **2019**, *149*, 106–114. [CrossRef]
57. Jiang, W.; Wu, T.; Fu, B.J. The value of ecosystem services in China: A systematic review for twenty years. *Ecosyst. Serv.* **2021**, *52*, 101365. [CrossRef]
58. Liu, H.; Wu, J.; Liao, M. Ecosystem service trade-offs upstream and downstream of a dam: A case study of the Danjiangkou dam, China. *Arab. J. Geosic.* **2019**, *12*, 17. [CrossRef]
59. Yu, L.; Lyu, Y.; Chen, C.; Choguill, C.L. Environmental deterioration in rapid urbanisation: Evidence from assessment of ecosystem service value in Wujiang, Suzhou. *Environ. Dev. Sustain.* **2021**, *23*, 331–349. [CrossRef]

60. Qiu, H.H.; Hu, B.Q.; Zhang, Z. Impacts of land use change on ecosystem service value based on SDGs report–Taking Guangxi as an example. *Ecol. Indic.* **2021**, *133*, 108366. [CrossRef]
61. Hu, Z.N.; Yang, X.; Yang, J.J.; Yuan, J.; Zhang, Z.Y. Linking landscape pattern, ecosystem service value, and human well-being in Xishuangbanna, southwest China: Insights from a coupling coordination model. *Golb. Ecol. Conserv.* **2021**, *27*, e01583. [CrossRef]
62. Liu, B.; Pan, L.B.; Qi, Y.; Guan, X.; Li, J.S. Land Use and Land Cover Change in the Yellow River Basin from 1980 to 2015 and Its Impact on the Ecosystem Services. *Land* **2021**, *10*, 1080. [CrossRef]
63. Zhao, D.Y.; Xiao, M.Z.; Huang, C.B.; Liang, Y.; Yang, Z.T. Land Use Scenario Simulation and Ecosystem Service Management for Different Regional Development Models of the Beibu Gulf Area, China. *Remote Sens.* **2021**, *13*, 3161. [CrossRef]
64. Wen, L.; Song, T.Q.; Du, H.; Wang, K.L.; Peng, W.X.; Zeng, F.P.; Zeng, Z.X.; He, T.G. The succession characteristics and its driving mechanism of plant community in karst region, Southwest China. *Acta. Ecol. Sin.* **2015**, *35*, 5822–5833.
65. Zhang, M.Y.; Wang, K.L.; Liu, H.Y.; Zhang, C.H.; Yue, Y.M.; Qi, X.K. Effect of ecological engineering projects on ecosystem services in a karst region: A case study of northwest Guangxi, China. *J. Clean Prod.* **2018**, *183*, 831–842. [CrossRef]
66. Wu, J.H.; Wang, G.Z.; Chen, W.X.; Pan, S.P.; Zeng, J. Terrain gradient variations in the ecosystem services value of the Qinghai-Tibet Plateau, China. *Glob. Ecol. Conserv.* **2022**, *34*, e02008. [CrossRef]
67. Liu, W.J.; Liu, C.Q.; Zhao, Z.Q.; Li, L.B.; Tu, C.L.; Liu, T.Z. The weathering and soil formation process in karstic area, southwest China: A study on Strontium isotope geochemistry of yellow and limestone soil profiles. *J. Earth Environ.* **2011**, *2*, 331–336.
68. Yuan, D.X. Aspects on the new round land and resources survey in karst rock desertification areas of South China. *Garsologica Sin.* **2000**, *19*, 103–108.
69. Zhang, W.; Chen, H.S.; Wang, K.L.; Zhang, J.G. Spatial variability of surface soil water in typical depressions between hills in karst region in dry season. *Acta. Pedol. Sin.* **2006**, *43*, 554–562.
70. Jiang, Z.C.; Lian, Y.Q.; Qin, X.Q. Rocky desertification in Southwest China: Impacts, causes, and restoration. *Earth Sci. Rev.* **2014**, *132*, 1–12. [CrossRef]
71. Wu, L.H.; Wang, S.J.; Bai, X.Y.; Tian, Y.C.; Zeng, C.; Luo, G.J.; He, S.Y. Quantitative assessment of the impacts of climate change and human activities on runoff changes in a typical Karst watershed, SW China. *Sci. Total Environ.* **2017**, *601–602*, 1449–1465. [CrossRef]
72. Ouyang, Z.W.; Song, T.Q.; Peng, W.X.; Du, H.; Zeng, F.P. Spatial heterogeneity of soil main mineral composition in manmade forest in karst peak-cluster depression region. *J. Hunan Agric. Univ.* **2011**, *37*, 325–328. [CrossRef]
73. Zeng, C.; Wang, S.; Bai, X.; Li, Y.; Tian, Y.; Li, Y.; Wu, L.; Luo, G. Soil erosion evolution and spatial correlation analysis in a typical karst geomorphology, using RUSLE with GIS. *Solid Earth* **2017**, *8*, 721–736. [CrossRef]
74. Xiong, K.N.; Chi, Y.K. The problems of South China Karst ecosystem in southern China and the countermeasures. *Ecol. Econ.* **2015**, *31*, 23–30.
75. Guo, C.; Gao, J.; Zhou, B.; Yang, J. Factors of the Ecosystem Service Value in Water Conservation Areas Considering the Natural Environment and Human Activities: A Case Study of Funiu Mountain, China. *Int. J. Environ. Res. Public Health* **2021**, *18*, 11074. [CrossRef] [PubMed]
76. Wang, R.; Cai, Y.L. Management modes of degraded ecosystem in southwest Karst area of China. *Chin. J. Appl. Ecol.* **2010**, *21*, 1070–1080.

land

MDPI

Article

Effects of Land-Use Change on the Pollination Services for Litchi and Longan Orchards: A Case Study of Huizhou, China

Qinhua Ke [1], Shuang Chen [1], Dandan Zhao [1], Minting Li [1] and Chuanzhun Sun [1,2,*]

[1] School of Public Management, South China Agricultural University, Guangzhou 510642, China; tsinhua0517@163.com (Q.K.); chenshuang20220701@163.com (S.C.); zhaodandan0903@163.com (D.Z.); hn_lmting@163.com (M.L.)
[2] Key Laboratory of Natural Resources Monitoring in Tropical and Subtropical Area of South China, Ministry of Natural Resources, Guangzhou 510815, China
* Correspondence: suncz@scau.edu.cn

Abstract: Land-use change has a significant impact on the structure and function of ecosystems and is an important reason for the imbalance between the supply and demand of ecosystem services. Pollination services are indispensable functions of ecosystems. In recent years, land-use change has caused a decline in the abundance of pollinators, thereby affecting the supply of pollination services, which has been a major concern for governments and scholars. Currently, there is an insufficient exploration of the impact mechanism of land-use change on pollination services. The application of a pollination service evaluation model based on land-use data uses a large amount of empirical data, which greatly affects the accuracy of regional evaluation results. This study uses Huizhou as a representative example. Remote sensing images from 2015 and 2019 were used to interpret the land-use data of the region, and the spatiotemporal changes in the land use were then analyzed. Due to their high pollination dependence, litchi and longan were selected as the research objects. Basic data such as the main pollinator species of litchi and longan and floral plant species were obtained through field sampling surveys. The InVEST model was used to evaluate the abundance of pollinators in litchi and longan orchards, and the abundance of pollinators was used to represent the value of pollination services in litchi and longan orchards. Then, the Hotspot analysis method was used to analyze the change in the spatial pattern of the pollinator abundance in litchi and longan orchards. The main influencing factors of pollination service in litchi and longan orchards were analyzed by a Geographical detector. Finally, we have explored the impact mechanism of land-use change on pollination services. The following are the results of this research. The pollinator abundance in the orchards of litchi and longan and their buffer zones in Huizhou decreased by 6.64% and 13.94% from 2015 to 2019, respectively. The wild bee abundance in forest land and rainfed cropland decreased by varying degrees. The spatial aggregation characteristics of pollinator abundance in litchi and longan orchards demonstrated an increase in cold spots, whereas the hot spots decreased and were more dispersed. In the study area, the area change and land-use change of natural or semi-natural habitats, such as forest land, rainfed cropland, and grassland, affected the pollination services for litchi and longan orchards. Within the types of changing land-use, the change of forest land has the greatest impact on litchi and longan pollination services. The impact degrees of Forest land area, rainfed cropland area, area under litchi and longan orchards, and forest landscape fragmentation on the pollination services for litchi and longan orchards were 0.20, 0.16, 0.21, and 0.26, respectively.

Keywords: land-use change; pollination service; InVEST model; litchi and longan

Citation: Ke, Q.; Chen, S.; Zhao, D.; Li, M.; Sun, C. Effects of Land-Use Change on the Pollination Services for Litchi and Longan Orchards: A Case Study of Huizhou, China. *Land* **2022**, *11*, 1073. https://doi.org/10.3390/land11071073

Academic Editor: Marta Debolini

Received: 29 May 2022
Accepted: 6 July 2022
Published: 14 July 2022

1. Introduction

Ecosystem services are the benefits obtained by human beings from ecosystems, and they form the basis of human survival. They are also closely related to human well-being [1–3]. The results of the Millennium Ecosystem Assessment [4] showed that the

Earth's natural ecosystems provide services worth approximately 15 trillion pounds per year to humans. Pollination is a basic ecosystem service that plays an important role in crop yields and food security [5]. Globally, 85% of flowering plants require animal pollination [6]. Pollinator-dependent crop production in global agriculture has increased by 300% in the last 50 years, making human survival more reliant on the food supply brought about by pollination [7].

In recent years, an increasing number of international organizations and scholars have begun to study the impact of land use and its changes on pollination services. Globally, numerous cases have demonstrated that land-use change, intensive agricultural management, pesticide use, environmental pollution, invasive alien species, pathogens, and climate change have the most negative impacts on pollinators [8]. In response to the decline in the number of pollinators and the loss of pollination services, the Intergovernmental Science-Policy Platform on Biodiversity and Ecosystem Services (IPBES), a follow-up to the Millennium Ecosystem Assessment (MEA) and a policy driven by the United Nations Environment Programme (UNEP), have taken up 'pollinator, pollination, and food production assessment' as a top priority for rapid assessments in the program of work from 2014–2018, with 'multiple threats, drivers, and mitigation measures such as land-use change' as the main component in 2013.

Studies have found that the habitat loss and fragmentation caused by land-use change are the most important factors driving the decline of pollinators [9–11]. In terms of the impact of land-use change on pollination services, some scholars have emphasized habitat factors and studied pollination services from the perspective of habitat isolation [12] and habitat fragmentation [13]. For example, Ricketts et al. conducted a meta-analysis of 23 studies on 17 crops across five continents [12]. The results showed that habitat isolation had a significantly negative impact on the abundance of wild bees. Tscharntke et al. found that habitat allocation in broken landscapes only affected populations in simple landscapes, but not those in complex landscapes [13]. Other scholars have studied the impacts of landscape heterogeneity, habitat type, habitat loss, and different degrees of disturbance on pollinators in forest land, and have proposed countermeasures such as improving the diversity of the habitat types of pollinators, adopting low-intensity habitat management methods, and planning the landscape heterogeneity of different geomorphologic types [14–17].

Using the concept model of land-use and pollination service evaluation proposed by Kremen et al. [18], the pollination module of the Integrated Valuation of Ecosystem Services and Trade-offs (InVEST) model has been widely used. The research focus has shifted from land-use change and the spatialization of pollination services to a quantitative relationship between land-use change and pollination services [11,19–21]. Based on the land-use map, this module derives an index of the abundance of wild bees in the region by using the nesting preference of wild bees for different land-use types, the availability of floral resources for different land-use types, and the foraging distances of wild bees. The index of the abundance of wild bees was used to represent the value of pollination services in litchi and longan orchards.

Currently, there are some shortcomings with respect to the impact of land-use changes on pollination services. For example, when relevant data, such as the pollinator species and floral plant species, are applied to different regions using large amounts of empirical data, the accuracy of calculating the pollinator abundance index is reduced, which will cause the evaluation results of land-use change on pollination service to be inconsistent with reality. Additionally, research on the influence mechanism of land-use change on pollination services is currently insufficient. Based on land-use and related biophysical data, this study used the InVEST model to evaluate the regional pollination services quantitatively and spatially. Furthermore, this study explored the influence mechanism of land use and its change on the pollination services for longan and litchi. Through remote sensing interpretation and field investigation, further basic data, such as litchi and longan orchard patches, the pollinator species of litchi and longan, and the number of pollinators

and flowering plants with different land-use types, were obtained to improve the accuracy of the evaluation of the pollination services.

2. Materials and Methods

2.1. Study Area

Huizhou is located between 22°24′–23°57′ N and 113°51′–115°28′ E and belongs to the subtropical monsoon humid climate zone in South China (Figure 1). The annual average temperature is 22 °C, the annual average precipitation is 1770 mm, and the frost-free period lasts up to 350 days. Forest land accounts for 63.67% of the area of Huizhou, with a forest coverage rate of 90.4%, and is mainly distributed in the eastern and northwestern regions. Irrigated cropland and rainfed cropland are more contiguous, accounting for 16.01% and 7.29% of the area, respectively. Construction land accounted for 7.5% and is primarily distributed in the southwest and central areas. Various land types in the region are conducive to the development of agriculture and forestry. Litchi and longan are highly dependent on pollination. In this study, the relevant biophysical parameters of pollination service evaluations of longan and litchi orchards in the villages, such as the species and number of pollinators for litchi and longan as well as the species of flowering plants and their vegetation coverage, were obtained from a field sampling survey of four typical villages. The villages are located in the town of Jimei, Boluo County. The land-use types and planting structure of the villages are consistent with the overall scenario of Huizhou.

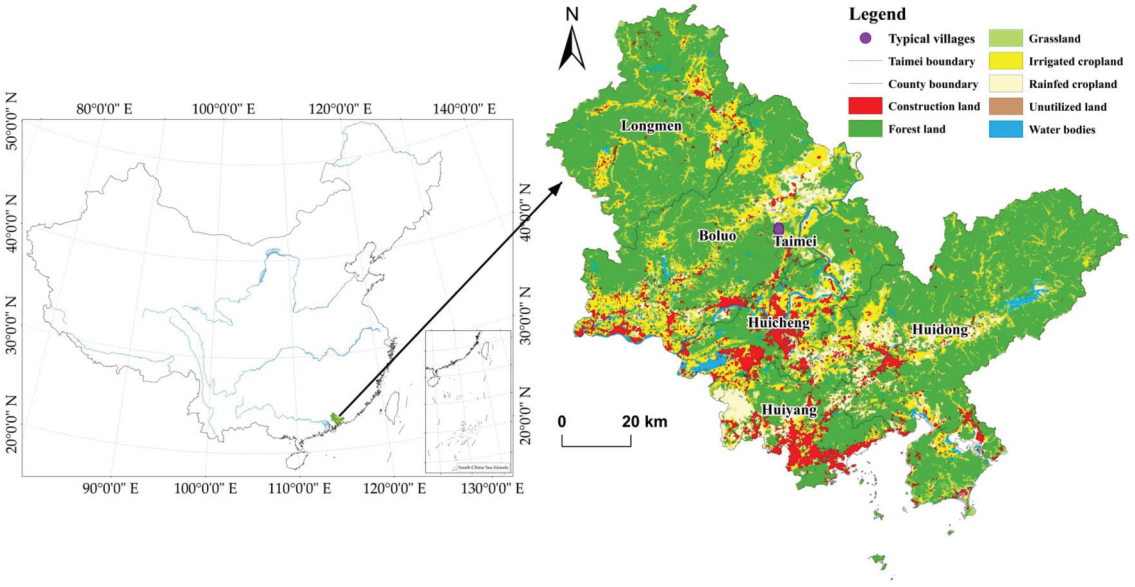

Figure 1. Location of the study area.

2.2. Data Sources

2.2.1. Remote Sensing Interpretation of Longan and Litchi Orchards

According to the data released by Huizhou Natural Resources Department, litchi and longan orchards accounted for 22.54% of all orchards in Huizhou in 2019. The dependence of litchi and longan on insect pollination was 0.97 and 0.81, respectively [22]. Therefore, the pollination services of insects have an important impact on the yield of litchi and longan. We could more effectively study the impact of land-use change on pollination services in litchi and longan orchards in across a large-scale area. Referring to Wang et al. [23], this study used Sentinel-2A optical images to identify the samples of litchi and longan orchards (Table S1) in Huizhou. Sentinel-1A radar images were used to calculate the

backscattering and coherence coefficient of the land class to improve its classification accuracy. Images were obtained from the Copernicus Open Access Hub (previously known as Sentinel Scientific Data Hub) (https://scihub.copernicus.eu/, accessed from May to December 2015 and from March to December 2019). The preprocessed images were first fused, and the classification and information extraction of litchi and longan orchards in Huizhou was realized using the support vector machine (SVM) classification according to the number of samples and their attribute characteristics (Figure 2). The overall accuracy of the classification in 2015 and 2019 was 92.61% and 93%, respectively, and the Kappa coefficients were 0.88 and 0.89, respectively. The classification accuracies for the litchi and longan orchards were 79.79% and 83.72%, respectively, and the classification accuracy for other land types was more than 70%.

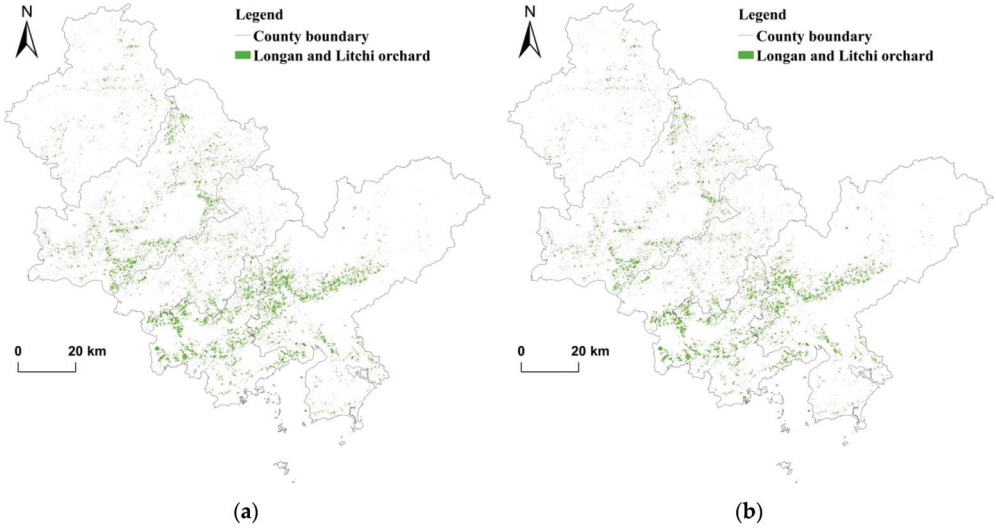

Figure 2. Spatial distribution of longan and litchi orchards in the study region in 2015–2019. (**a**) 2015; (**b**) 2019.

2.2.2. Biophysical Data for the Evaluation of Pollination Services

The population data of pollinators for litchi and longan were obtained by field surveys using the sweeping net method [24,25]. The biophysical parameters of wild bees, such as the body length of wild bees, the activity of wild bees in different seasons, and the preference of wild bees for nesting in different land-use types, come from the literature, books [26,27], and the China Bee Database, Institute of Zoology, Chinese Academy of Sciences (http://www.zoology.csdb.cn/dba/cnbee, accessed on 29 May 2022).

The nesting suitability of the land-use types was expressed by the diversity of pollinators within the land-use types. The diversity data of pollinators in the land-use types were obtained using the trap method through field sampling surveys [28]. The data on species and vegetation coverage of floral plants were obtained using the two-point sampling method and five-point sampling method [29]. Data on the ability of the plants to provide nectar and pollen were obtained from relevant books [30].

2.2.3. Land-Use Data

The data for remote sensing interpretation of the land use were obtained from the Resource and Environment Science and Data Center, Chinese Academy of Sciences (http://www.resdc.cn/, accessed in 2015 and 2020), with an accuracy of 30 × 30 m. In this study, five first-class classifications were reserved for forest land, grassland, water bodies,

construction land, and unutilized land, and two second-class classifications for irrigated cropland and rainfed cropland.

2.3. Methods

2.3.1. InVEST-Pollination Module

The Pollination module of the InVEST model first simulates the nesting suitability and availability of floral resources of land-use types in the landscape by using the nesting preference of wild bees, the abundance of flowering plants, and the biophysical parameters of wild bees such as in different land uses. The biophysical parameters are the activity of wild bees in different seasons, their foraging distance, and the relative abundance of wild bees. The module then estimates the abundance index of wild bees. The abundance index is between 0 and 1, and a higher value, which means closer to 1, indicated higher wild bee abundance. The abundance index of wild bees is used to represent the value of pollination services, to quantitatively evaluate the regional pollination service [31]. The abundance index of wild bees is expressed by the following equation [32]:

$$P_{x\beta} = N_j \frac{\sum_{m=1}^{M} F_{jm} e^{\frac{-D_{mx}}{\alpha_\beta}}}{\sum_{m=1}^{M} e^{\frac{-D_{mx}}{\alpha_\beta}}} \quad (1)$$

In this equation, $P_{x\beta}$ is the abundance index of wild bees; N_j is the nesting suitability of land-use type j, and F_j is the availability of floral resources of land-use type j; D_{mx} is the Euclidean distance between the grid unit m and x; and α_β is the expected foraging distance of wild bee β.

In this study, the main pollinators of litchi and longan referred to the results of field sampling surveys, as shown in Table S2 in the Supplementary Materials, including 16 pollinators. The Pollination module sets wild bees as important pollinators, without considering cultivated bees. Therefore, this paper only studies the pollination services of litchi and longan of six main wild bees.

Foraging distance, the seasonal activity of the six main wild bees, and the proportion of wild bees are shown in Table S5 in the Supplementary Materials. The foraging distance of the pollinators was calculated according to Gathmann [33]. The seasonal activity index of wild bees was found to be between 0 and 1, and a higher value indicated stronger activity. The proportion of wild bees was obtained from field sampling surveys.

Table S6 in the Supplementary Materials shows the nesting suitability and availability of floral resources of land-use types. The nesting suitability index ranged from 0 to 1, and the larger the value, the more suitable it was for wild bee nesting. The availability index of floral resources ranges from 0 to 1, and the greater the value, the more floral resources.

2.3.2. Hotspot Analyses

Hotspot analyses are widely applied in ecological analyses, and they were used to identify the locations of statistically significant hotspots and cold spots. Hotspots and cold spots are statistically significant spatial clusters of high values and low values, respectively [34]. The G_i^* index is the coefficient for Hotspot analyses. It is based on partial spatial autocorrelation using a distance weighted matrix, which can detect aggregates of high-value areas and low-value areas [20]. The G_i^* can be standardized to $Z(G_i^*)$. The G_i^* and $Z(G_i^*)$ index are expressed by the following equation [35]:

$$G_i^* = \frac{\sum_j^n w_{ij} x_j}{\sum_j^n x_j} \quad (2)$$

$$Z(G_i^*) = \frac{G_i^* - E(G_i^*)}{\sqrt{VAR(G_i^*)}} \quad (3)$$

In these two equations, n is the total amount of the spatial unit, x_j is the attribute value of the spatial unit in a partial spatial area, w_{ij} is the distance weight between units i and j, $E(G_i^*)$ is the mathematical expectation of G_i^*, and $VAR(G_i^*)$ is the variance of G_i^* [20].

In addition, <−1.65 or >+1.65, <−1.96 or >+1.96, and <−2.58 or >+2.58 are critical $Z(G_i^*)$-scores for 90, 95, and 99% confidence levels, respectively.

2.3.3. Geographical Detector (Geodetector)

Geodetector (http://www.geodetector.org/, accessed in 2015) was created by Wang et al. [36] and used in this study to detect the main influencing factors of the pollination services for litchi and longan orchards and to reveal the underlying driving mechanism. The Geodetector uses q-statistics to measure the impact degree of independent variable X (influencing factors) on dependent variable Y (pollination service). Q-statistic was calculated as follows [37]:

$$q = 1 - \frac{\sum_{h=1}^{L} N_h \sigma_h^2}{N\sigma^2} \quad (4)$$

where $h = 1, 2, \ldots, L$ is a given class (stratum) of an independent variable; L is the number of classes; N_h and N are the numbers of samples in class h and entire study area, respectively; and σ_h^2 and σ^2 are the variance of dependent variable in class h and the entire study area, respectively. Ranging from 0 to 1, the higher the q value is, the stronger the influence of this factor on the dependent variable. Otherwise, the influence is weaker [38]. By estimating the value of q-statistic corresponding to the interaction of two independent variables, Geodetector can also quantify the degree of the interactive impact of each pair of conditioning factors on the dependent variable [39]. As is shown in Table 1, based on the comparison of this value with the individually estimated values, the type of interaction can be then determined.

Table 1. Types of interaction between independent variables.

Description	Interaction Type
$q(X1 \cap X2) < \text{Min}[q(X1), q(X2)]$	Nonlinear-weaken
$\text{Min}[q(X1), q(X2)] < q(X1 \cap X2) < \text{Max}[q(X1), q(X2)]$	Univariate-weaken
$q(X1 \cap X2) > \text{Max}[q(X1), q(X2)]$	Bivariate-enhanced
$q(X1 \cap X2) = q(X1) + q(X2)$	Independent
$q(X1 \cap X2) > q(X1) + q(X2)$	Nonlinear-enhanced

3. Results

3.1. Land Use and Its Change in Huizhou

3.1.1. Characteristics of Land-Use Changes

During 2015–2019, the area of the land-use types suitable for nesting by pollinators and that of the land-use types with floral resources demonstrated a downward trend. Specifically, the irrigated cropland area decreased by 22.11 km^2, and the forest land and rainfed cropland decreased by 16.9 km^2 and 15.42 km^2, respectively (Table 2, Figure 3). Forest land was still dominant in Huizhou, whereas the construction land area exceeded that of rainfed cropland, increasing by 65.48 km^2 (8.39%). The increased area of construction land is primarily attributed to the transfer of forest land, irrigated cropland, and rained cropland (the transferred areas are 25.20 km^2, 24.35 km^2, and 18.40 km^2, respectively), which are concentrated in the central and southwestern regions of the study area. The area of the constructed land converted to forest land was 8.85 km^2, which was distributed in the central region. Due to the implementation of ecological restoration in large quarries, the forest land resources have increased to some extent.

3.1.2. Longan and Litchi Orchards and Their Characteristics

Longan and litchi orchards in Huizhou are mainly distributed in the low-altitude areas. Along with the rural residential areas and farming areas, they have a zonal distri-

bution, which is widely dispersed and fragmented (Figure 4). The orchards are densely distributed in the central, western, and southwestern regions, and are rarely distributed in the northern Luofu and Nankun Mountains, the central Xiangtou Mountain, and the eastern Lianhua Mountain.

Table 2. Land-use Areas and their Proportions in Huizhou, 2015–2019.

Land-Use Types	2015		2019		2015–2019
	Area (km^2)	Proportion (%)	Area (km^2)	Proportion (%)	Changing Range (km^2)
Irrigated cropland	1827.77	16.21	1805.66	16.01	−22.11
Rainfed cropland	837.41	7.43	821.99	7.29	−15.42
Forest land	7197.46	63.82	7180.56	63.67	−16.90
Grassland	265.45	2.35	263.74	2.34	−1.71
Water bodies	367.07	3.25	357.72	3.17	−9.35
Construction land	780.73	6.92	846.21	7.50	65.48
Unutilized land	1.51	0.01	1.52	0.01	0.01

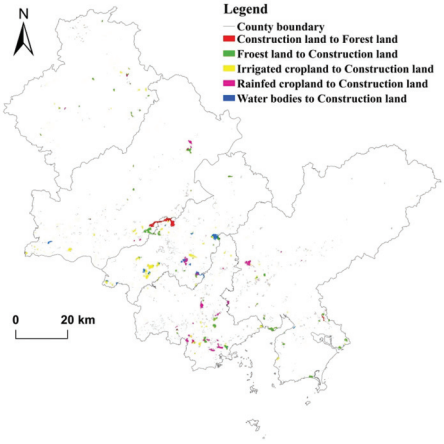

Figure 3. Spatiotemporal distribution of the main land-use conversions in the study region from 2015 to 2019.

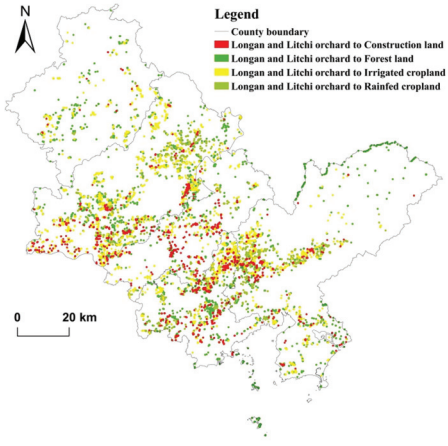

Figure 4. Spatiotemporal distribution of the main conversions of the longan and litchi orchards in the study region from 2015 to 2019.

In terms of quantity, during 2015–2019, the area of the orchards decreased by 31.72 km^2, which is a reduction of 12.22%. In terms of spatial distribution, the decreasing areas of the orchards were concentrated in the central, western, and southwestern regions. The overlap ratio of the reduction in the area of the orchards and that of rural expansion reached 33.86%, which was primarily distributed in the western and urban regions of the study area, and adjacent to the economically developed areas. The overlap area between the area of reduction of the orchards and the planting area of cultivated land was as high as 15.06 km^2, and the scale ratio was as high as 47.48%. This is primarily distributed in the agricultural counties of the study area.

3.2. Characteristics of the Spatiotemporal Change of Wild Bee Abundance of Litchi and Longan in Huizhou

3.2.1. Characteristics of Quantitative Change of the Wild Bee Abundance of Litchi and Longan

Since the foraging distance of wild bees is 1000 m, the research scope was set to litchi and longan orchards and their outward extension area (buffer zone). Then, the abundance of wild bees in litchi and longan orchards and their buffer zone was counted. As is shown in Table 3, the results demonstrated that the total wild bee abundance in the buffer zone decreased by 13.94% between 2015 and 2019, whereas the abundance decreased by 6.64% in the litchi and longan orchards. The wild bee abundance in forest land or rainfed cropland in the buffer zone and the entire region decreased by varying degrees. However, the rate of change of wild bee abundance in forest land in the buffer zone was greater than that in the whole region, and that in rainfed croplands in the whole region was greater than that in the buffer zone.

Table 3. Abundance of wild bee in litchi and longan orchards and their buffer zones in Huizhou, 2015–2019.

	2015	2019	Rate of Change
Total in the buffer zone	116,830.28	100,530.53	−13.94%
Total in litchi and longan orchards	442.33	412.93	−6.64%
Average in rainfed cropland of the buffer zone	0.0063	0.0057	−9.52%
Standard deviation in rainfed cropland of the buffer zone	0.0026	0.0024	−0.08%
Average in rainfed cropland of the whole region	0.0059	0.0053	−10.17%
Standard deviation in rainfed cropland of the whole region	0.0028	0.0026	−0.07%
Average in the forest land of the buffer zone	0.0214	0.0196	−8.41%
Standard deviation in the forest land of the buffer zone	0.0038	0.0036	−0.05%
Average in the forest land of the whole region	0.0218	0.0202	−7.34%
Standard deviation in the forest land of the whole region	0.0039	0.0037	−0.05%

Unit: pixel 900 $m^{2.}$

3.2.2. Changes in the Spatial Pattern of Wild Bee Abundance for Litchi and Longan Orchards in Huizhou

As is shown in Figure 5, the hotspots of wild bee abundance decreased significantly from 2015 to 2019, whereas the cold spots increased slightly. From the perspective of spatial distribution, the hotspots are closely related to the distribution of litchi and longan orchards. These orchards were mostly located at the foot of the mountain and adjacent to the forest land, which provided suitable nesting sites. The cold spot areas were mainly distributed in farming and built-up areas. The hotspots of wild bee abundance become dispersed in the midwestern and southwestern regions. In the central region, some cold spots were converted to hot spots.

3.2.3. Influencing Factors Analysis of Pollination Service for Litchi and Longan Orchards

The results of the Geodetector analyses are shown in Table 4. The forest land area, rainfed cropland area, litchi and longan orchards area, and forest landscape fragmentation were the dominant influencing factors of the pollination services for litchi and longan

orchards, whose impact degrees on the pollination services were 0.20, 0.16, 0.21, and 0.26, respectively. Other Influencing factors did not have a significant effect on the pollination services. Forest land area and litchi and longan orchards area jointly affected the pollination services for litchi and longan orchards, and the degree of the interactive impact of these two factors on the pollination services was 0.50, which was the maximum interactive impact degree.

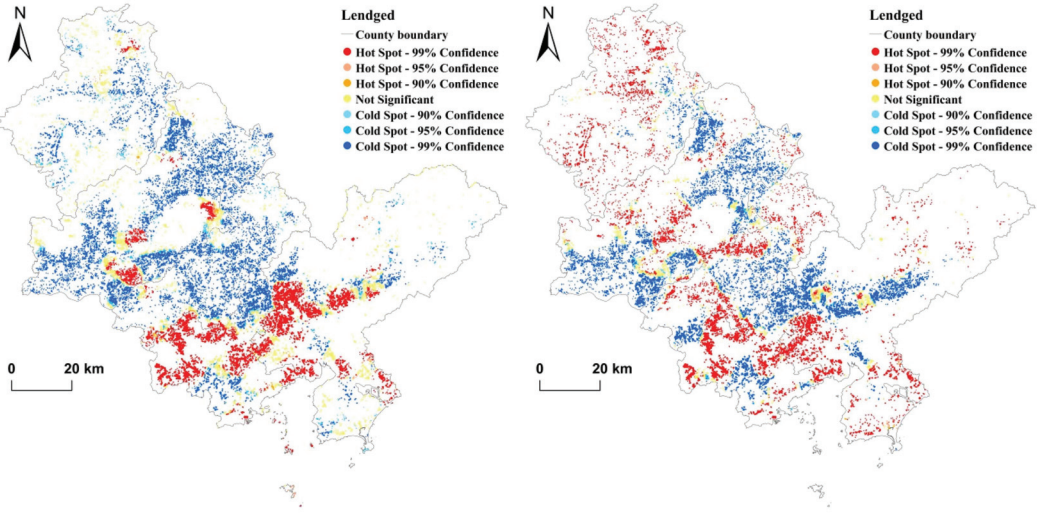

Figure 5. Spatial distribution of hotspots of the wild bees of longan and litchi in the study region in 2015–2019. (**a**) 2015; (**b**) 2019.

Table 4. Interaction between influencing factors on the pollination services for litchi and longan.

Influencing Factors	Forest Land Area	Grassland Area	Rainfed Cropland Area	Litchi and Longan Orchards Area	Forest Fragmentation Degree	Grass Fragmentation Degree	Rainfed Cropland Fragmentation Degree
Forest land area	0.20						
Grassland area	0.34 *	0.02					
Rainfed cropland area	0.39 *	0.19	0.16				
Litchi and longan orchards area	0.50 *	0.25 *	0.27	0.21			
Forest fragmentation degree	0.36	0.32 *	0.37	0.44	0.26		
Grass fragmentation degree	0.29 *	0.05	0.19	0.23	0.30	0.03	
Rainfed cropland fragmentation degree	0.30	0.12	0.22	0.26	0.32	0.14	0.10

* indicates that the interaction between the factors is a nonlinear enhancement type, while the others are a double-factor enhancement type.

3.3. Effects of Land-Use Change on the Pollination Services for Litchi and Longan Orchards

As shown in Table 5, the abundance index of wild bees in forest land decreased by 2.03 as the forest land area decreased by 16.90 km^2. As shown in Table 6, the conversion of forest land to irrigated cropland per 1 km^2 reduced the abundance index of wild bees by 1.55. The reasons for the decrease in wild bee abundance in the orchards may be summarized as follows. First, the large-scale decrease in the litchi and longan orchards led to a reduction in the nectar-pollen resources in the region. Second, a large amount of construction land occupied suitable nesting sites for wild bees and floral resources. The superposition of the two reasons resulted in a decrease in the wild bee abundance of litchi and longan in forestland. Moreover, the litchi and longan orchards are primarily distributed along the foot of the mountain, and the decrease in their area has a greater impact on the wild

bee abundance in the adjacent forest land. Therefore, the rate of change in the wild bee abundance of litchi and longan in the buffer zone was greater than that in the whole region (Table 3).

Table 5. Land-use types and wild bee abundance index for litchi and longan in the buffer zone of Huizhou, 2015–2019.

Land-Use Types	Area Change 2015–2019 (km^2)	Wild Bee Abundance Index (sum) in Land-Use Types		
		2015	2019	Abundance Index Change of Wild Bee
Irrigated cropland	−22.11	0.00	0.00	0.00
Rainfed cropland	−15.42	7.04	6.32	−0.72
Forest land	−16.90	23.82	21.78	−2.03
Grassland	−1.71	10.63	9.60	−1.03
Water bodies	−9.35	0.00	0.00	0.00
Construction land	65.48	0.00	0.00	0.00
Unutilized land	0.01	0.00	0.00	0.00
Litchi and longan orchards	31.72	1.70	1.84	0.14

Table 6. Correlation between land-use conversion and the change in wild bee abundance index for litchi and longan in the buffer zone from 2015 to 2019.

Types of Land-Use Conversion	Area Change (km^2)	Abundance Index Change of Wild Bee	Abundance Index Change of Wild Bee per Unit Area
Construction land to Rainfed cropland	14.68	11.93	0.81
Forest land to Construction land	20.95	−18.40	−0.88
Rainfed cropland to Construction land	16.94	−5.56	−0.33
Forest land to Irrigated cropland	3.19	−4.95	−1.55
Irrigated cropland to Forest land	3.08	2.92	0.95
Irrigated cropland to Construction land	19.29	−0.12	−0.01
Water bodies to Construction land	7.59	−0.08	−0.01

From the perspective of spatial distribution (Figure 5), the hotspots are closely related to the distribution of litchi and longan orchards. These orchards were mostly located at the foot of the mountain and adjacent to the forest land, which provided suitable nesting sites. The abundance of wild bees was extremely high considering the large number of nectar-pollen resources in the orchards. The cold spot areas were mainly distributed in farming and built-up areas. Here, the wild bee abundance of the litchi and longan orchards was low due to the flat terrain, the cross-distribution of cultivated and construction lands, and the penetration of water areas. The hotspots of wild bee abundance become dispersed in the midwestern and southwestern regions. These two regions were the main areas with a reduction in the litchi and longan orchards, and the main areas where forestland and rainfed cropland were converted to construction land. The primary reasons for this may be a reduction in the nectar-pollen plant resources and habitat fragmentation. In the central region, some cold spots were converted to hot spots because of the ecological restoration carried out in this region. Construction land was converted to forest land, resulting in an increased habitat for wild bees, thereby increasing the abundance of the wild bees of the litchi and longan orchards.

A summary of this section is as follows: The areas where the pollination services decreased and increased significantly were mainly concentrated in the central, southwestern, and southeastern parts of the study area. The reason for the decrease was that forest land and rainfed cropland were converted to construction land, and the reason for the increase was that construction land was converted to forestland and rainfed cropland. Among the forest land, grassland, and rainfed cropland, the wild bee abundance for litchi and longan orchards decreased in forest land and was the highest for every unit reduction.

3.4. Influence Mechanism of Land-Use Change on the Pollination Services for Litchi and Longan Orchards

The Pollination module of the InVEST model estimates the abundance index of wild bees by using the nesting preference of wild bees, the abundance of flowering plants in different land uses, and the foraging distances of wild bees. The abundance index of wild bees was used to represent the value of pollination services for litchi and longan orchards. Therefore, the change in land-use types will directly affect the results of the abundance index of wild bees. In the study area, the land-use types with a high nesting suitability and availability of floral resources are converted to the land-use types with low nesting suitability and availability of floral resources, such as forest land converted to construction land, which will reduce the nesting suitability and availability of floral resources. The results will reduce the abundance of wild bees. In the study area, the area change and land-use change of natural or semi-natural habitats, such as forest land, rainfed cropland, and grassland, affected the pollination services for litchi and longan orchards. The reduction of forest land area and the conversion of forest land to construction land have the greatest impact on the pollination service of litchi and longan orchards (Tables 5 and 6). In the study area, the impact degrees of forest land area and forest landscape fragmentation on the pollination services of litchi and longan orchards were 0.20 and 0.26, respectively (Figure 6). The degree of the interactive impact of forest land area and litchi and longan orchards area on the pollination services was 0.50 and that of forest fragmentation degree and litchi and longan orchards area on the pollination services was 0.44. It is again confirmed that in the change of land-use types, the change of forest land had the greatest impact on the pollination service of litchi and longan orchards in the study area.

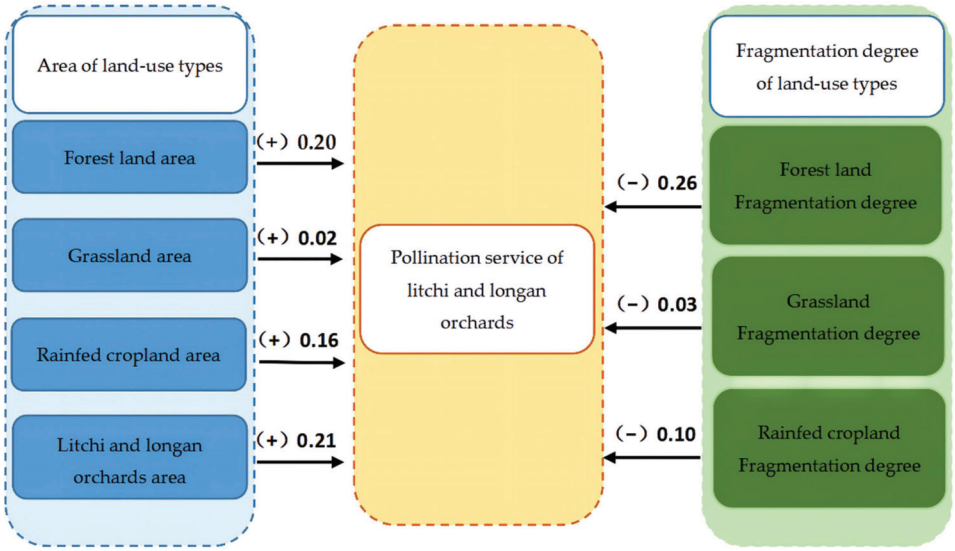

Figure 6. Influence mechanism of land use and its change on the pollination services for litchi and longan orchards. (Note: the influencing factors of the two types shown in the figure are the area of land use type and the landscape fragmentation of land use type. Numbers indicate their respective impact degrees on the pollination services of litchi and longan orchards, ranging from 0 to 1. (+) indicates positive impact, and (−) indicates negative impact).

4. Discussion

4.1. Comparison of the Results with Other Studies

Our research shows that the change of forest land has the greatest impact on the pollination service of litchi and longan orchards in the study area. However, Groff et al.

suggested that the proportion of deciduous/mixed forest was positively correlated with bee abundance, while the proportion of coniferous forest was negatively correlated with bee abundance [40]. This paper did not consider that the effects of different types of forest land on pollination services in litchi and longan orchards might be different. In future studies, the assessment results of pollinator abundance can be more comprehensive by refining the land classification.

This paper shows that area change and land-use change of natural or semi-natural habitats affect the pollination services for litchi and longan orchards in the study area, which is consistent with the research results of many scholars [18,21,41,42]. However, our research does not consider the climatic factors. According to the research results of Polce et al. [43], the climate is one of the most important factors affecting the distribution of the pollinators. Therefore, the determination of a method for incorporating climate factors into the assessment system based on the InVEST model is an important research direction. Another analysis result of this paper is that landscape fragmentation has a great impact on the pollination services in the study area, which is consistent with the research results of Garibaldi et al. [44] and Tscharntke et al. [13]. However, Kennedy et al. found that the effects of landscape configuration on bee abundance were weak [42]. The difference between the results of this study and that of Kennedy et al. may be related to the scale of the study area.

4.2. Methods Application and Improvement

In this study, further basic data for the pollination service evaluation were obtained through remote sensing interpretation and field investigation, and the accuracy of the pollination service evaluation was improved. This study used the InVEST model to evaluate the regional pollination services quantitatively and spatially. Furthermore, the influence of land use and its change on the pollination services for litchi and longan was discussed using the Geodetector. However, a limitation of this study is that although some important parameters (such as the population data of pollinators in litchi and longan orchards) were derived from the survey, several parameters (such as the foraging distance of the pollinators) were derived from empirical values, which require further validation. Groff et al. evaluated the InVEST Crop Pollination model performance with parameters informed by four approaches and found that uninformed optimization improved model performance by 29% compared to an expert opinion-informed model, while a sensitivity-analysis informed optimization improved model performance by 54% [40]. In future studies, we can learn from their proposed methods to obtain these parameters and improve the credibility of pollination service assessment results. Polce et al. integrated a species distribution model (SDM) with a pollination service model (PSM) to derive the availability of pollinators for crop pollination and combined the Lonsdorf model [32] to derive the pollination services [43]. One of the innovations in their approach was the application of pollinator records data rather than expert knowledge to predict the pollinator occurrence [43], which can improve the accuracy of pollination service evaluations. In this study, further basic data—such as the pollinator species of litchi and longan, and the number of pollinators and flowering plants with different land-use types—for the pollination service evaluation were obtained through the field sampling survey, and the accuracy of the pollination service evaluation was improved. When there is a lack of pollinator records, the field sampling survey method used in this paper is of reference value for other studies. Another innovation in their methods is their inclusion of the managed pollinator supply. In contrast, our study only considers the pollination services of wild bees for litchi and longan orchards and not those of domesticated bees, which will inevitably affect the authenticity of the pollination service assessment results. The impact of managed honeybees on pollination services in litchi and longan orchards should be considered in future research. Local farm management and landscape structure are two drivers which influence wild bee abundance [18]. This paper does not include agricultural management in the assessment of the pollination services for

litchi and longan orchards. In the future, we must consider the influence of field type and field diversity [42] on pollination services in litchi and longan orchards.

The InVEST-pollination module represents pollination services based on the abundance of pollinators and has not yet been able to evaluate the quantity of the supply capacity of pollination services. Future research may further realize the conversion from assessments of pollinator abundance to assessments of the quantity of pollination services. At the same time, due to the lack of influencing factors outside the study area on pollination services, pollination services around the region may be underestimated. Future research may address this issue by expanding the study area outward (buffer zone) and incorporating it into the assessment.

5. Conclusions

(1) The area of land use types suitable for nesting by pollinators and the area of land-use types with nectar-pollen plant resources demonstrated a downward trend from 2015 to 2019. Forest land and rainfed cropland were reduced by 16.9 km^2 and 15.42 km^2, respectively, primarily due to the conversion of these lands to construction land. The reduced area was concentrated in the central and southwest regions. Owing to ecological restorations, 8.848 km^2 of construction land was converted to forest land. The area of litchi and longan orchards decreased by 31.72 km^2, which is a reduction of 12.22%. The reduction areas were primarily concentrated in the central, western, and southwestern regions.

(2) The pollinator abundance in the litchi and longan orchards and their buffer zones decreased by 6.64% and 13.94%, respectively, between 2015 and 2019. The pollinator abundance in forest land and rainfed cropland decreased to varying degrees. The cold spots increased in space, whereas the hot spots decreased in size and became more dispersed. The decrease in the pollinator abundance was mainly concentrated in the midwestern and southwestern regions. The main reasons for this may be the decrease in the area of litchi and longan orchards, forest lands, and rainfed croplands, as well as landscape fragmentation.

(3) Forest land area, rainfed cropland area, litchi and longan orchards area, and forest landscape fragmentation were the dominant Influencing factors of the pollination services for litchi and longan orchards, whose impact degrees on the pollination services were 0.20, 0.16, 0.21, and 0.26, respectively. Forest land area and litchi and longan orchards area will jointly affect the pollination services for litchi and longan orchards, and the degree of the interactive impact of these two factors on the pollination services is 0.50, which is the maximum interactive impact degree. In the study area, the area change and land-use change of natural or semi-natural habitats, such as forest land, rainfed cropland, and grassland, affected the pollination services for litchi and longan orchards. The reduction of forest land area and the conversion of forest land to construction land have the greatest impact on the pollination services of litchi and longan orchards.

Supplementary Materials: The following supporting information can be downloaded at: https://www.mdpi.com/article/10.3390/land11071073/s1, Table S1: Samples of litchi and longan orchards; Table S2: Main pollinators species of litchi and longan; Table S3: The ability of plants to provide pollen and nectar and Vegetation survey results in flowering period of litchi and longan; Table S4: Richness of pollinators in land-use types; Table S5: Biophysical parameters and relative abundance of wild bees in Huizhou, 2015–2019; Table S6: Nested suitability and availability of nectar-pollen plant resources of the land-use types in Huizhou, 2015–2019.

Author Contributions: All authors listed have made a substantial, direct, and intellectual contribution to the work and approved it for publication. All authors have read and agreed to the published version of the manuscript.

Funding: This research was funded by National Social Sciences Foundation of China, grant number 20CGL063.

Data Availability Statement: The data presented in this study are available on request from the authors.

Acknowledgments: Thanks to anonymous experts for their suggestions.

Conflicts of Interest: The authors declare no conflict of interest.

References

1. Costanza, R.; d'Arge, R.; de Groot, R.; Farber, S.; Grasso, M.; Hannon, B.; Limburg, K.; Naeem, S.; O'Neill, R.V.; Paruelo, J.; et al. The value of the world's ecosystem services and natural capital. *Ecol. Econ.* **1998**, *25*, 3–15. [CrossRef]
2. Daily, G.C. Nature's Services: Societal Dependence on Natural Ecosystems (1997). In *The Future of Nature: Documents of Global Change*, 1st ed.; Robin, L., Sörlin, S., Warde, P., Eds.; Yale University Press: New Haven, CT, USA, 2003; pp. 454–464.
3. Assessment, M.E. *Ecosystems and Human Well-Being: Wetlands and Water*, 1st ed.; World Resources Institute: Washington, DC, USA, 2005; 80p.
4. Assessment, M.E. *Ecosystems and Human Well-Being: A Framework for Assessment*, 1st ed.; Island Press: Washington, DC, USA, 2003; 245p.
5. Otieno, M.; Steffan-Dewenter, I.; Potts, S.G.; Kinuthia, W.; Garratt, M. Enhancing legume crop pollination and natural pest regulation for improved food security in changing African landscapes. *Glob. Food Secur.* **2020**, *26*, 100394. [CrossRef]
6. Ollerton, J.; Winfree, R.; Tarrant, S. How many flowering plants are pollinated by animals? *Oikos* **2011**, *120*, 321–326. [CrossRef]
7. Tian, Y.; Lan, C.; Xu, J.; Li, X.; Li, J. Assessment of pollination and China's implementation strategies within the IPBES framework. *Biodivers. Sci.* **2016**, *24*, 1084. [CrossRef]
8. Potts, S.G.; Biesmeijer, J.C.; Kremen, C.; Neumann, P.; Schweiger, O.; Kunin, W.E. Global pollinator declines: Trends, impacts and drivers. *Trends Ecol. Evol.* **2010**, *25*, 345–353. [CrossRef] [PubMed]
9. Betts, M.G.; Hadley, A.S.; Kormann, U. *The Landscape Ecology of Pollination*; Springer: New York, NY, USA, 2019; Volume 34, pp. 961–966.
10. Dalsgaard, B. Land-use and climate impacts on plant–pollinator interactions and pollination services. *Diversity* **2020**, *12*, 168. [CrossRef]
11. Rahimi, E.; Barghjelveh, S.; Dong, P. Using the Lonsdorf model for estimating habitat loss and fragmentation effects on pollination service. *Ecol. Process.* **2021**, *10*, 22. [CrossRef]
12. Ricketts, T.H.; Regetz, J.; Steffan-Dewenter, I.; Cunningham, S.A.; Kremen, C.; Bogdanski, A.; Gemmill-Herren, B.; Greenleaf, S.S.; Klein, A.M.; Mayfield, M.M. Landscape effects on crop pollination services: Are there general patterns? *Ecol. Lett.* **2008**, *11*, 499–515. [CrossRef]
13. Tscharntke, T.; Klein, A.M.; Kruess, A.; Steffan-Dewenter, I.; Thies, C. Landscape perspectives on agricultural intensification and biodiversity–ecosystem service management. *Ecol. Lett.* **2005**, *8*, 857–874. [CrossRef]
14. Lázaro, A.; Fuster, F.; Alomar, D.; Totland, Ø. Disentangling direct and indirect effects of habitat fragmentation on wild plants' pollinator visits and seed production. *Ecol. Appl.* **2020**, *30*, e02099. [CrossRef]
15. Olynyk, M.; Westwood, A.R.; Koper, N. Effects of natural habitat loss and edge effects on wild bees and pollination services in remnant prairies. *Environ. Entomol.* **2021**, *50*, 732–743. [CrossRef] [PubMed]
16. Wu, P.; Song, X.; Xia, B.; Xu, H.; Liu, Y. Temporal-spatial dynamics of wild bee diversity in agricultural landscapes in Changping District, Beijing. *Chin. J. Eco-Agric.* **2018**, *26*, 357–366.
17. Wang, M.; Lu, X.; Cui, Y.; Wang, M.; Ding, S. Effects of woodland types with different levels of human disturbance on pollinators: A case study in Gongyi, Henan, China. *Acta Ecol. Sin.* **2018**, *38*, 464–474.
18. Kremen, C.; Williams, N.M.; Aizen, M.A.; Gemmill-Herren, B.; LeBuhn, G.; Minckley, R.; Packer, L.; Potts, S.G.; Roulston, T.a.; Steffan-Dewenter, I. Pollination and other ecosystem services produced by mobile organisms: A conceptual framework for the effects of land-use change. *Ecol. Lett.* **2007**, *10*, 299–314. [CrossRef]
19. Zhang, R.; Wang, D.; Zhou, M.; Cai, Y. Pollination service analysis of Chongming wild bee based on InVEST model. *J. Anhui Agric. Univ.* **2018**, *45*, 37–44.
20. Sun, C.; Zhen, L.; Wang, C.; Hu, J.; Du, B. Biodiversity simulation of Poyang Lake wetlands by InVEST model under different scenarios. *Resour. Environ. Yangtze Basin* **2015**, *24*, 1119–1125.
21. Zulian, G.; Maes, J.; Paracchini, M.L. Linking land cover data and crop yields for mapping and assessment of pollination services in Europe. *Land* **2013**, *2*, 472–492. [CrossRef]
22. Liu, P.; Wu, J.; Li, H.; Lin, S. Evaluation of economic value of agricultural bee pollination in China. *Sci. Agric. Sin.* **2011**, *24*, 5117–5123.
23. Wang, C.; Li, B.; Zhu, R.; Chang, S. Study on tree species identification by combining Sentinel-1 and JL101A images. *For. Eng.* **2020**, *36*, 40–48.
24. Fang, W.; Zen, J.; Jiang, B. Compare the Pollination effects of Litchi chinensis and Dimocarpus longan by Apis mellifera Hgustica and A. cerana cerana. *Apic. China* **2011**, *62*, 51–53.
25. Zhong, Y.; Zhao, D.; Gao, J.; Wang, Y.; Liu, J. Study of Pollinating Insect of Dimocarpus longana. *Apic. China* **2014**, *65*, 61–63.
26. Zhang, W.; Li, Y. *Insect Ecology in China*, 2nd ed.; Chongqing University Press: Chongqing, China, 2019; 692p.
27. Michener, C.D. *The Bees of the World*, 2nd ed.; JHU Press: Baltimore, MD, USA, 2007; 953p.

28. Vrdoljak, S.M.; Samways, M.J. Optimising coloured pan traps to survey flower visiting insects. *J. Insect Conserv.* **2012**, *16*, 345–354. [CrossRef]
29. Fang, J.; Wang, X.; Shen, Z.; Tang, Z.; He, J.; Yu, D.; Jiang, Y.; Wang, Z.; Zheng, C.; Zhu, J.; et al. The main contents, methods and technical specifications of plant community investigation. *J. Biodivers.* **2009**, *6*, 533–548.
30. Ke, X. *Botany of Nectar Plants*, 1st ed.; China Agricultural Press: Beijing, China, 1995; 226p.
31. InVEST. Natural Capital Project. Available online: https://naturalcapitalproject.stanford.edu/software/invest (accessed on 17 June 2022).
32. Lonsdorf, E.; Kremen, C.; Ricketts, T.; Winfree, R.; Williams, N.; Greenleaf, S. Modelling pollination services across agricultural landscapes. *Ann. Bot.* **2009**, *103*, 1589–1600. [CrossRef]
33. Gathmann, A.; Tscharntke, T. Foraging ranges of solitary bees. *J. Anim. Ecol.* **2002**, *71*, 757–764. [CrossRef]
34. Li, G.; Fang, C.; Wang, S. Exploring spatiotemporal changes in ecosystem-service values and hotspots in China. *Sci. Total Environ.* **2016**, *545–546*, 609–620. [CrossRef]
35. Getis, A.; Ord, K. The Analysis of Spatial Association by Use of Distance Statistics. *Geogr. Anal.* **1992**, *24*, 189–206. [CrossRef]
36. Wang, J.; Zhang, T.; Fu, B. A measure of spatial stratified heterogeneity. *Ecol. Indic.* **2016**, *67*, 250–256. [CrossRef]
37. Wang, J.; Xu, C. Geodetector: Principle and prospective. *Acta Geogr. Sin.* **2017**, *72*, 116–134.
38. Zhang, X.; Liao, L.; Xu, Z.; Zhang, J.; Chi, M.; Lan, S.; Gan, Q. Interactive Effects on Habitat Quality Using InVEST and GeoDetector Models in Wenzhou, China. *Land* **2022**, *11*, 630. [CrossRef]
39. Polykretis, C.a.C.; Grillakis, M.G.a.C.; Argyriou, A.V.a.C.; Papadopoulos, N.G.a.C.; Alexakis, D.D.a.C. Integrating multivariate (Geodetector) and bivariate (iv) statistics for hybrid landslide susceptibility modeling: A case of the vicinity of pinios artificial lake, ilia, greece. *Land* **2021**, *10*, 973. [CrossRef]
40. Groff, S.C.; Loftin, C.S.; Drummond, F.; Bushmann, S.; McGill, B. Parameterization of the InVEST Crop Pollination Model to spatially predict abundance of wild blueberry (Vaccinium angustifolium Aiton) native bee pollinators in Maine, USA. *Environ. Model. Softw.* **2016**, *79*, 1–9. [CrossRef]
41. Steffan-Dewenter, I.; Munzenberg, U.; Burger, C.T.; Tscharntke, T. Scale-dependent effects of landscape context on three pollinator guilds. *Ecology* **2002**, *83*, 1421–1432. [CrossRef]
42. Kennedy, C.M.; Lonsdorf, E.; Neel, M.C.; Williams, N.M.; Ricketts, T.H.; Winfree, R.; Bommarco, R.; Brittain, C.; Burley, A.L.; Cariveau, D.; et al. A global quantitative synthesis of local and landscape effects on wild bee pollinators in agroecosystems. *Ecol. Lett.* **2013**, *16*, 584–599. [CrossRef] [PubMed]
43. Polce, C.; Termansen, M.; Aguirre-Gutiérrez, J.; Boatman, N.D.; Budge, G.E.; Crowe, A.; Garratt, M.P.; Pietravalle, S.; Potts, S.G.; Ramirez, J.; et al. Species Distribution Models for Crop Pollination: A Modelling Framework Applied to Great Britain. *PLoS ONE* **2013**, *8*, e76308. [CrossRef]
44. Garibaldi, L.A.; Steffan-Dewenter, I.; Kremen, C.; Morales, J.M.; Bommarco, R.; Cunningham, S.A.; Carvalheiro, L.s.G.; Chacoff, N.P.; Dudenhoffer, J.H.; Greenleaf, S.S.; et al. Stability of pollination services decreases with isolation from natural areas despite honey bee visits. *Ecol. Lett.* **2011**, *14*, 1062–1072. [CrossRef]

land

MDPI

Article

Degradation or Restoration? The Temporal-Spatial Evolution of Ecosystem Services and Its Determinants in the Yellow River Basin, China

Bowen Zhang [1,2], Ying Wang [1,2,*], Jiangfeng Li [1] and Liang Zheng [3]

[1] School of Public Administration, China University of Geosciences, Wuhan 430074, China; bw.zhang@cug.edu.cn (B.Z.); jfli@cug.edu.cn (J.L.)
[2] The Key Laboratory of the Ministry of Natural Resources for Legal Research, Wuhan 430074, China
[3] Changjiang Institute of Survey, Planning, Design and Research, Wuhan 430024, China; zl@cug.edu.cn
* Correspondence: yingwang0610@cug.edu.cn

Abstract: Ecosystem services (ESs) are irreplaceable natural resources, and their value is closely related to global change and to human well-being. Research on ecosystem services value (ESV) and its influencing factors can help rationalize ecological regulatory policies, and is especially relevant in such an ecologically significant region as the Yellow River Basin (YRB). In this study, the ecological contribution model was used to measure the contribution of intrinsic land use change to ESV, the bivariate spatial autocorrelation model was applied to investigate the relationship between land use degree and ESV, and the geographical detector model (GDM) and geographically weighted regression (GWR) were applied to reveal the impact of natural and socio-economic factors on ESV. Results showed that: (1) The total ESV increased slightly, but there were notable changes in spatial patterns of ESV in the YRB. (2) Land use changes can directly lead to ESV restoration or degradation, among which, conversion from grassland to forest land and conversion from unused land to grassland are vital for ESV restoration in the YRB, while degradation of grassland is the key factor for ESV deterioration. (3) According to GDM, NDVI is the most influential factor affecting ESV spatial heterogeneity, and the combined effect of multiple factors can exacerbate ESV spatial heterogeneity. (4) GWR reveals that NDVI is always positively correlated with ESV, GDP is mainly positively correlated with ESV, and population density is mainly negatively correlated with ESV, while positive and negative correlation areas for other factors are roughly equal. The findings can provide theoretical support and scientific guidance for ecological regulation in the YRB.

Keywords: ecosystem services value (ESV); natural and socio-economic factors; ecological contribution model; geographical detector model (GDM); geographically weighted regression (GWR); Yellow River Basin (YRB)

Citation: Zhang, B.; Wang, Y.; Li, J.; Zheng, L. Degradation or Restoration? The Temporal-Spatial Evolution of Ecosystem Services and Its Determinants in the Yellow River Basin, China. *Land* **2022**, *11*, 863. https://doi.org/10.3390/land11060863

Academic Editors: Shicheng Li, Chuanzhun Sun, Qi Zhang, Basanta Paudel and Lanhui Li

Received: 11 May 2022
Accepted: 5 June 2022
Published: 7 June 2022

1. Introduction

Ecosystem services (ESs) refer to all benefits obtained by humans from the natural environment [1]. The ecosystem services value (ESV) is a measure of ESs and is an important indicator of ecological health, which includes transfer of ESs into practical applications [2]. To ensure territorial ecological security, adapt to global climate change, and achieve high-quality development, it is essential to monitor and maintain ESV [3]. However, with socio-economic development and population growth, high-intensity human activities have had a huge impact on ecosystems [4], resulting in a slew of global ecosystem deterioration issues such as climate change [5], ozone layer destruction [6], biodiversity loss [7], water pollution [8] and land desertification [9]. With the increasing prominence of environmental issues, there exists an urgent need to investigate the spatiotemporal evolution of regional ESV and its influencing factors, in order to achieve a balance between ecosystems and socio-economic sustainable development.

Many studies have shown that ESV is vulnerable to multiple impacts from natural changes and human activities, with land use and cover change (LUCC) being the most important influencing factor on terrestrial ESV [10–12]. Changes in land use type cause changes in basic ecological elements, hence influencing ESV directly, although the underlying relationships are complex [13]. Statistical analysis, correlation analysis, regression analysis, redundancy analysis, principal component analysis, and other methods have been employed to explore the relationship between LUCC and ESV [14–17]. Wang et al. [18], for example, used a geographically weighted regression (GWR) model to investigate the effect of LUCC on ESV, finding that forest land and grassland had the greatest effect on ESV. Using bivariate spatial autocorrelation, Lei et al. [19] explored the link between land use degree and ESV and discovered a negative correlation. However, most studies have explored only the effect of area of different land use types on ESV, or the effect of land use degree on overall ESV. Using an ecological contribution model of land use change, we attempted to reveal the potential impact on ESV changes of transformation processes of land use type. In addition, we employed a bivariate spatial autocorrelation model to investigate the relationship between degree of land use and the value of each ES, in order to uncover a more nuanced relationship between them.

Furthermore, a number of natural and socio-economic factors have a substantial impact on overall ESV through exerting varied effects on the inherent aspects of ESs [20,21]. For example, Zhang et al. [22] found that an increase in average precipitation leads to an increase in lake and wetland area, which in turn leads to an improvement in regional ESV. Dai et al. [23] showed that when population density exceeds a threshold, there is a risk of ecological undersupply, which has a negative impact on ESV. When studying the effects of natural and socio-economic factors on ESV, it is necessary to consider a wide range of factors and their interactions. The geographical detector model (GDM) is a new statistical method for revealing the impact of multiple influencing factors and their linkages on a geographical phenomenon [24]. It has two major advantages. First, it can identify relationships between a complex set of factors and a wide range of geographical phenomena, without any assumptions or restrictions regarding independent and dependent variables, allowing it to be used without removing multi-collinear factors [24–26]. Second, it can quantitatively extract the implicit interrelationships between pairs of factors and obtain useful findings [27]. The GDM is now widely utilized in a variety of disciplines, and an increasing number of researchers have employed it to investigate the factors that influence ESV [28,29]. In this study, the GDM's Factor Detector and Interaction Detector tools were used to reveal the relative roles of the multiple natural and socio-economic factors, as well as their interactions. However, the GDM can only quantify the effect magnitude of various factors, and the directions of influence could not be determined [30]. To investigate the direction and spatial variation of each factor's effect on ESV, we further adopted the GWR, which can capture the correlation between spatial objects themselves, as well as reflect the spatial heterogeneity and direction of influence at different geographical locations through the regression coefficient [31].

The Yellow River Basin (YRB) is a key ecological barrier and economic belt in China, and plays a critical role in China's socio-economic development and ecological security [32]. In recent years, the Chinese government has placed high priority on ecological conservation and the green development of the YRB, implementing initiatives such as the Three-North Shelterbelt Project, the "Grain-for-Green" and Natural Forest Protection programs, which have begun to bear fruit [33–35]. However, some areas of ecological degradation still exist in the YRB, where the ESs have been severely damaged. For example, the Shaanxi-Gansu-Ningxia region, in the upper and middle of the YRB, suffers from severe soil erosion and a fragile ecological environment [36]. Severe silt deposition frequently generates river overhangs in the lower YRB, flooding is frequent, and ESs are grave danger [37]. To optimize the YRB's ecological structure and promote high-quality development, it is critical to identify the vulnerable ESV areas in the YRB and reveal their influencing factors. Specifically, the objectives of our study are: (1) to map the spatial distribution of ESV and

identify vulnerable areas of ESV in the YRB; (2) to quantify the impact of LUCC on ESV and reveal the extent of that impact; (3) to investigate the impact of natural and socio-economic factors on ESV, and reveal the interactions of multiple factors; and (4) to propose relevant recommendations based on the findings.

2. Materials and Methods

2.1. Overview of the Study Area

The Yellow River is the second longest river in China, with a total length of 5464 km. It is a major biodiversity gathering region as well as an ecological security barrier within China. This study defines the provinces through which the Yellow River flows, viewing the YRB in a broad sense, based on the Yellow River and physical geographic watersheds, with the provincial administrative regions considered as the units. Since most of Sichuan Province belongs to the Yangtze River Basin, the other eight provinces where the Yellow River flows were used as research areas in this study (Figure 1). The terrain in the YRB is complex. With an average altitude of around 4000 m, the western region is made up of a succession of mountains with permanent snow and glacier landforms. The central region has a loess landform with loose soil and considerable soil erosion, with an average altitude of 1000 m to 2000 m. The Yellow River's alluvial plain makes up the majority of the eastern area. The overall ecological quality in the YRB is poor due to substantial land degradation including soil erosion and desertification. It is critical to evaluate the YRB's ecological condition, identify its ecological weak spots, to provide scientific guidance for ecological protection and spatial management, and build its ecological barrier status.

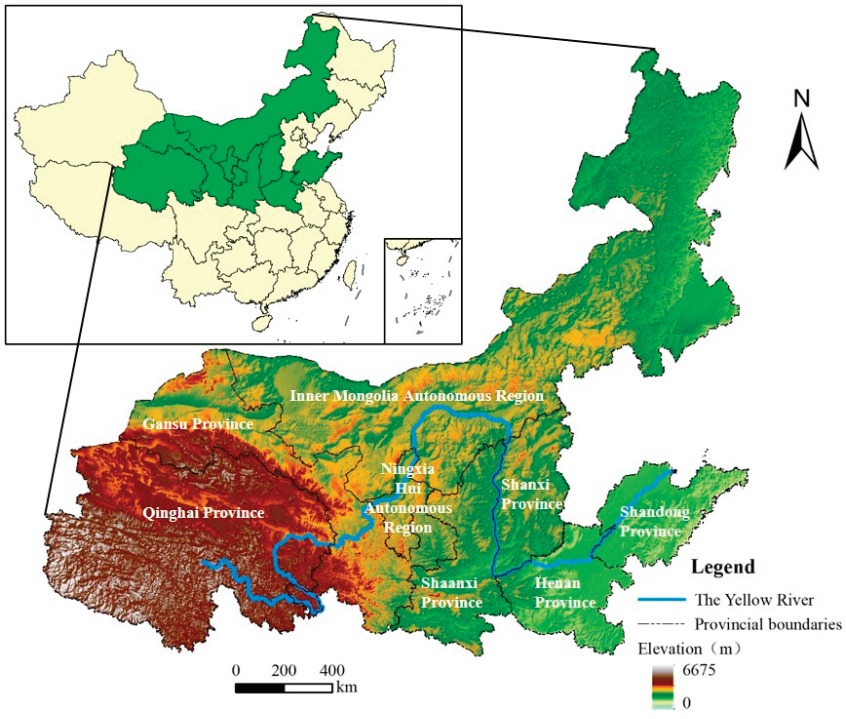

Figure 1. The location of the YRB.

2.2. Data Sources

This study used basic geographical data, such as LUCC, administrative boundaries, grain yield per unit area and grain price, and data on natural and socio-economic factors of ESV change (Table 1). The LUCC data of 1990, 2000, 2010 and 2018, with a spatial

resolution of 30 m × 30 m, were obtained from the Resources and Environmental Sciences and Data Center, Chinese Academy of Sciences (https://www.resdc.cn/ (accessed on 20 November 2021)). The original LUCC data contains 29 land use types, which we reclassified into 6 categories (i.e., cropland, forest land, grassland, water bodies, and unused land). The administrative boundary data of each administrative unit was taken from the 1:400,000 database of the National Geomatics Center of China (http://www.ngcc.cn/ngcc/ (accessed on 22 November 2021)). Using sown area and grain yield, grain yield per unit area was estimated, with data coming from the statistical yearbook of each region. The grain price data came from the China Agricultural Product Price Survey Yearbook.

Table 1. List of basic data information.

Type	Name	Source	Year	Precision
Statistics	Grain sown area Grain yield Grain price	Statistical Yearbook	2018	Provincial
Vectors	Administrative boundary River map Road map City location	The 1:400,000 database of the National Geomatics Center of China (http://www.ngcc.cn/ngcc/ (accessed on 22 November 2021))	2017	-
Rasters	LUCC	The Resources and Environmental Sciences and Data Center, Chinese Academy of Sciences (https://www.resdc.cn/ (accessed on 20 November 2021))	1990, 2000, 2010, 2018	30 m
	DEM		-	250 m
	Precipitation		2015	1 km
	NDVI		2018	
	Population density		2015	
	GDP			

The natural factors included elevation, slope, aspect, soil types, soil erosion, precipitation, temperature, vegetation types, and NDVI. Socio-economic factors included population density, GDP, road maps, river maps, railway maps, county location, city location, and provincial capital location. The DEM was processed in ArcGIS 10.7 to produce the elevation, slope, and aspect maps. The Euclidean Distance Tool of ArcGIS 10.7 was used to create the distance maps. Data for other influencing factors were obtained from the Resources and Environmental Sciences and Data Center, Chinese Academy of Sciences. Finally, using the ArcGIS 10.7 software, all the data were converted to raster data with a resolution of 1000 m × 1000 m, and the influencing factors data were discretized to type data sets according to Jenks (Figure 2). In addition, the mapping and tabulation were processed at the prefecture-level city scale.

2.3. Methods

2.3.1. LUCC Evolution Analysis Model

(1) Land use transfer matrix

The transfer matrix of land use can depict the changes in various land use types through time and the amount of change from one land use type to another [38]. It is based on a grid-by-grid description of the change from the initial state to the final state, reflecting the transformation of land use from moment T to moment T + 1, which can reveal the spatial and temporal evolution of land use patterns. The transfer matrix is described as follows:

$$S_{ij} = \begin{bmatrix} s_{11} & s_{12} & \cdots & s_{1n} \\ s_{21} & s_{22} & \cdots & s_{2n} \\ \cdots & \cdots & \cdots & \cdots \\ s_{n1} & s_{n2} & \cdots & s_{nn} \end{bmatrix} \quad (1)$$

where S_{ij} represents the area of LUCC change from type i to type j, and s_{nn} denotes the LUCC type before and after transfer.

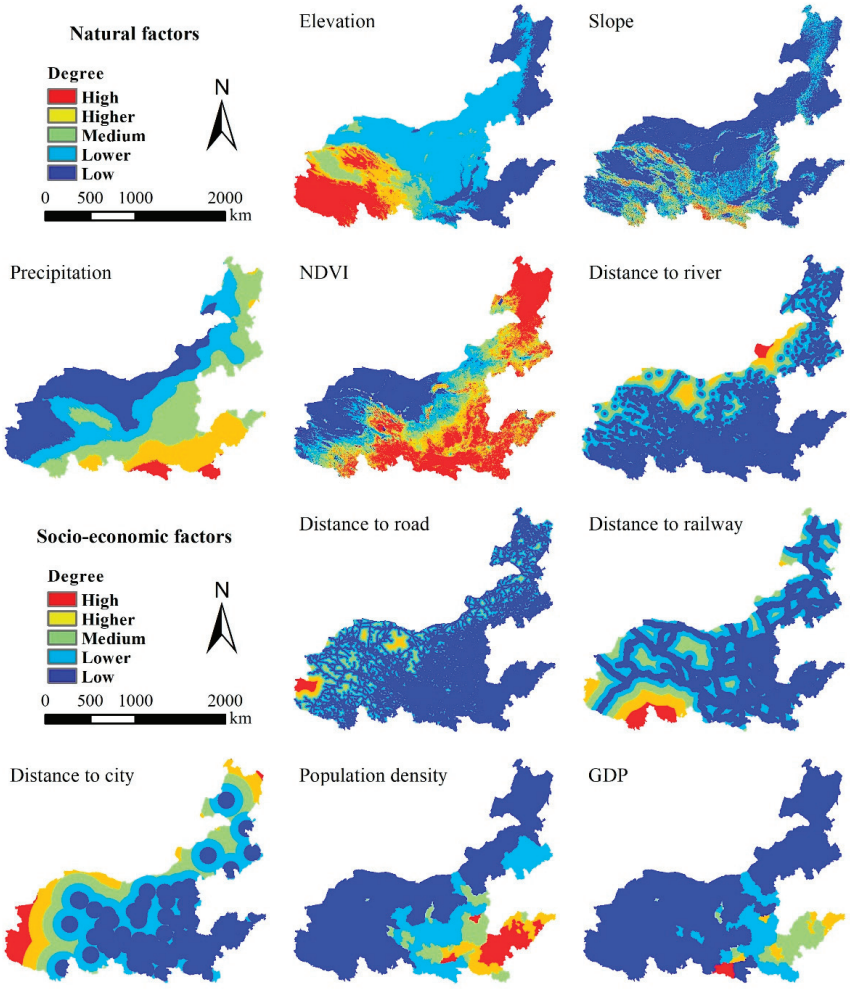

Figure 2. Influencing factors of ESV change.

(2) Calculation of land use degree

The comprehensive index of land use degree is a metric for assessing the extent to which land is used by humans. Different land use types were assigned to distinct values to represent the level of human utilization [39]. Specifically, built-up land was graded 4, cropland graded 3, forest land, grassland and water bodies were graded 2, and unused land was graded 1. The formula is as follows:

$$L = \sum_{i=1}^{n} A_i C_i \quad (2)$$

where L is the comprehensive index of land use degree; A_i is the grade of different land use type, and C_i is the proportion of land use type i to the total area.

2.3.2. ESV Evaluation Model

To evaluate ESV, this study adopted the value coefficient method modified by Xie et al. [40]. Specifically, the economic value of food supply provided by cropland was defined as the standard value, and the ESV of all other land use types was converted into equivalent values corresponding to the standard value. The economic value of food supply equals to 1/7 of the estimated value of grain yield in the YRB, which can be estimated based on the grain yield per unit area of the YRB and the average grain price in 2018, which is 2.08×10^5 CNY·km^{-2}·a^{-1} (1 USD = 6.70 CNY). The value of each type of ESs provided by different land use types is shown in Table 2. The ESV and its changes in the YRB can be estimated with the following formulas:

$$ESV = \sum_{i=1}^{n}(LUC_i \times VC_i) \quad (3)$$

$$AESV = \frac{\sum_{i=1}^{n}(LUC_i \times VC_i)}{\sum_{i=1}^{n} LUC_i} \quad (4)$$

$$C = \frac{ESV_{t2} - ESV_{t1}}{ESV_{t1}} \times 100\% \quad (5)$$

where ESV is ecosystem services value (CNY), $AESV$ is the average ESV (CNY·km^{-2}), VC_i is the ESV coefficient from land use type i, and LUC_i is the area of land use type i, C is the rate of change of ESV, ESV_{t1} and ESV_{t2} represent ESV at t_1 and t_2, respectively (CNY).

Table 2. ESV coefficient of different land use type in the YRB (CNY·km^{-2}·a^{-1}).

Ecosystem Services		Cropland	Forest Land	Grassland	Water Bodies	Unused Land
Supply services	Food supply	2083.02	687.40	895.70	926.94	41.66
	Raw material	812.38	6207.40	749.89	614.49	83.32
Regulation services	Gas regulation	1499.77	8998.65	3124.53	3041.21	124.98
	Climate regulation	2020.53	8477.90	3249.51	16,257.98	270.79
	Hydrological regulation	1603.92	8519.55	3166.19	33,547.05	145.81
	Waste disposal	2895.40	3582.80	2749.59	30,464.18	541.59
Support services	Soil conservation	3062.04	8373.74	4665.97	2499.62	354.11
	Biodiversity maintenance	2124.68	9394.42	3895.25	7415.55	833.21
Cultural services	Aesthetic landscape	354.11	4332.68	1812.23	9508.99	499.93
Total		16,455.86	58,574.54	24,308.85	104,276.02	2895.40

2.3.3. ESV Changes in Response to LUCC

(1) Ecological contribution model of land use change

To calculate how land use change contributes to ESV change, we used the ecological contribution model of land use change. This method can clearly show the direction and extent of the contribution of different land use changes to ESV change, and facilitate the identification of the main types of land use change that affect ESV [41]. Its formula is as follows:

$$EL_{i-j} = \frac{(VC_j - VC_i) \times LUC_{i-j}}{\sum_{i=1}^{n}\sum_{j=1}^{n}\left[(VC_j - VC_i) \times LUC_{i-j}\right]} \quad (6)$$

where EL_{i-j} is the contribution of land use change to ESV change, VC_i and VC_j is the coefficient from ESs type i and type j, LUC_{i-j} is the total area converted from land use type i to type j.

(2) Bivariate spatial autocorrelation model

LUCC can cause ESV variation. The local bivariate spatial autocorrelation proposed by Anselin [42] was used to investigate the spatial correlation between land use degree and ESV. Its formula is as follows:

$$I_{kl}^{i} = z_k^i \sum_j w_{ij} z_l^j \tag{7}$$

where w_{ij} is the spatial weight matrix, X_k^i represents the value of attribute i of unit k, X_l^j represents the value of attribute l to unit j, $\overline{X_k}$ and $\overline{X_l}$ are the average values of attributes k and l, respectively, σ_k and σ_l are the variances of attributes k and l, respectively.

2.3.4. Geographical Detector Model (GDM)

In this study, the average ESV was taken as the dependent variable, 17 natural and socio-economic factors were taken as independent variables, and the GDM was used to investigate the individual impacts of each factor and their interactions, as well as the degree of impact on spatial heterogeneity of the average ESV in the YRB.

The GDM is composed of Factor Detector, Interaction Detector, Risk Detector and Ecological Detector, which can be used to detect spatial heterogeneity and its influencing factors [24]. In this study, the Factor Detector and Interaction Detector tools were used to explore the impact of natural and socio-economic factors on ESV.

(1) Factor Detector

The Factor Detector uses the relationship between the within-strata variance and the variance of the entire region to measure the explanatory degrees of independent to dependent variables. The formula is as follows:

$$q = 1 - \frac{1}{N\sigma^2} \sum_{h=1}^{L} N_h \sigma_h^2 \tag{8}$$

where q measures the influence degree of each influencing factor on the dependent variable ESV, and its value is within [0, 1]. The larger the q value, the stronger the influence of the factor on ESV. $h = 1, 2, \ldots, L$ represents the strata of influencing factors. N_h and N are the number of samples in strata h and the entire region, respectively. σ_h^2 and σ^2 are the variance of influencing factors in strata h and the entire region, respectively.

(2) Interaction Detector

The Interaction Detector is used to quantify the interaction between different factors, i.e., wheter two factors have stronger or weaker effects on ESV when combined than when considered separately. The interaction effects of influencing factors were judged by the relationship between $q(x_i \cap x_j)$, $q(x_i)$, and $q(x_j)$ based on the following formulas:

If $\min(q(x_i), q(x_j)) < q(x_i \cap x_j) < \max(q(x_i), q(x_j))$, it represents single-factor nonlinear weakening.
If $q(x_i \cap x_j) > \max(q(x_i), q(x_j))$, it represents two-factor enhancement.
If $q(x_i \cap x_j) > q(x_i) + q(x_j)$, it represents nonlinear enhancement.
If $q(x_i \cap x_j) = q(x_i) + q(x_j)$, it represents mutual independence.

2.3.5. Geographically Weighted Regression (GWR)

By establishing the local regression equation in each grid, GWR can be used to study the correlation between multiple variables with spatial distribution characteristics to a dependent variable. In this study, GWR described the correlation between ESV and natural socio-economic factors, and reflected the spatial heterogeneity and direction of influence through the regression coefficient within each grid [31]. Its formula is as follows:

$$y_i = \beta_o(u_i, v_i) + \sum_{k=1}^{p} \beta_k(u_i, v_i) x_{ik} + \xi_i \tag{9}$$

where: y_i is the ESV in grid i, (u_i, v_i) is the space coordinates of grid i, β_o and β_k is the o and k regression coefficient in the grid, x_{ik} is the kth independent variable for the ith site, ξ_i is the residual value in the grid i.

In this study, ten factors that passed the test for multi-collinearity were screened as independent variables and regressed with average ESV as the dependent variable by the GWR model. The results show an adjusted R^2 value of 0.82, which indicates that the GWR model fits well for exploration of the ESV and its influencing factors, and the results can be used to explain the spatial heterogeneity of the influencing factors of ESV.

3. Results

3.1. Characteristics of LUCC Evolution in the YRB

3.1.1. Land Use Dynamics from 1990 to 2018 in the YRB

The land use transfer matrix (Figure 3) shows that the dominant land use types in the YRB are grassland, cropland, and unused land, with these three types accounting for over 80% of the total area during 1990–2018. The percentage of water bodies in the study area is roughly 2%, with a modest increase every year. Built-up land has increased substantially, nearly doubling from 1990 to 2018. Cropland area expanded greatly between 1990 and 2000, then declined, maintaining a marginal overall increase. Overall, the total amount of forest land has fluctuated and increased. Between 1990 and 2010, the amount of grassland declined significantly, especially between 2000 and 2010, when it decreased by 44,325 km^2. However, since 2010, the downward trend has reversed and its area has gradually increased.

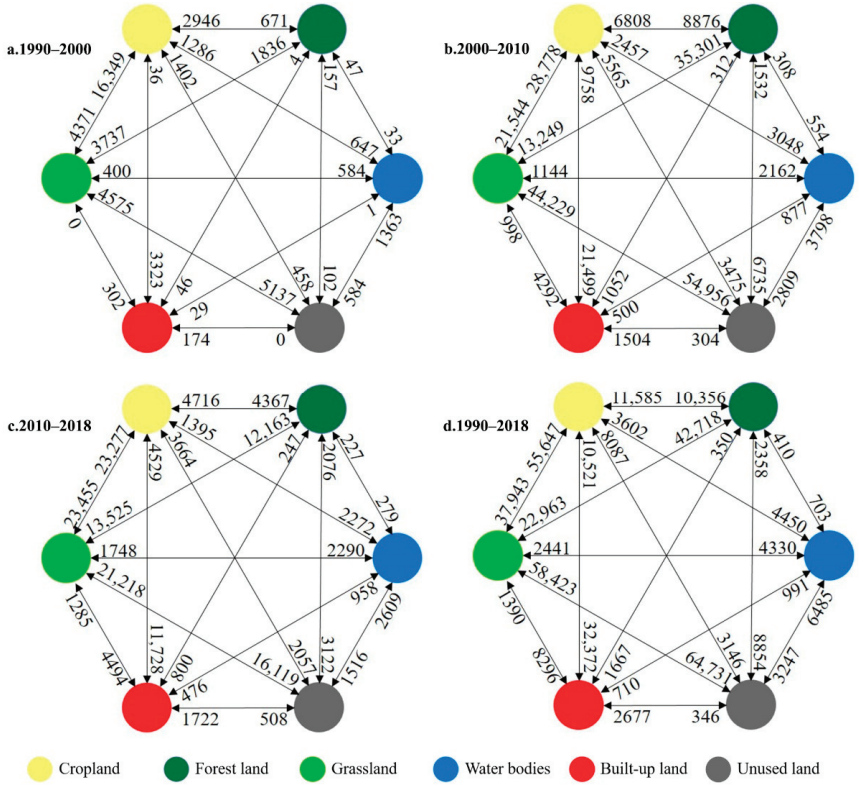

Figure 3. Land use transfer matrix in the YRB during 1990–2018 (km^2).

3.1.2. Land Use Degree in the YRB

The land use degree of the YRB increased gradually over time, rising from 1.9650 to 1.9861. Meanwhile, more than 90% of the cities studied exhibited a growing trend in land use during the study period. After more than 20 years of development, only cities in the Inner Mongolia

Autonomous Region and along the boundary between eastern Gansu Province and central Shaanxi Province have seen a decline in land use. During 1990–2018, the Alxa League had the lowest degree of land use, at around 1.1275. The cities with the highest degree of land use changed over time, with Zhoukou City (3.1615), Shangqiu City (3.1697), Liaocheng City (3.2066), and again Liaocheng City (3.2105) being the highest in 1990, 2000, 2010, and 2018, respectively. These three cities are located in Henan or Shandong Provinces, near coastal areas with developed agriculture or industry.

3.2. Temporal and Spatial Variations of ESV in the YRB

As shown in Figure 4, the lower ESV area in the YRB is concentrated in the northwest, and the high value area is concentrated in the northeast. According to the calculation results, the average ESV was 227.29 $\times$ 10^4, 226.35 $\times$ 10^4, 227.22 $\times$ 10^4, and 227.43 $\times$ 10^4 CNY·km^{-2} in 1990, 2000, 2010, and 2018, respectively. The regulation services had the highest value, accounting for more than 50% of the total ESV, and that with cultural services it followed a changing pattern of falling and growth over the study period. Eventually, their values change from 356.81 $\times$ 10^{10} CNY and 49.03 $\times$ 10^{10} CNY to 359.01 $\times$ 10^{10} CNY and 49.16 $\times$ 10^{10} CNY, respectively. Support services, on the other hand, steadily declined from 211.68 $\times$ 10^{10} CNY to 209.77 $\times$ 10^{10} CNY. In addition, supply services fluctuated, but their overall value remained consistent at roughly 62.51 $\times$ 10^{10} CNY.

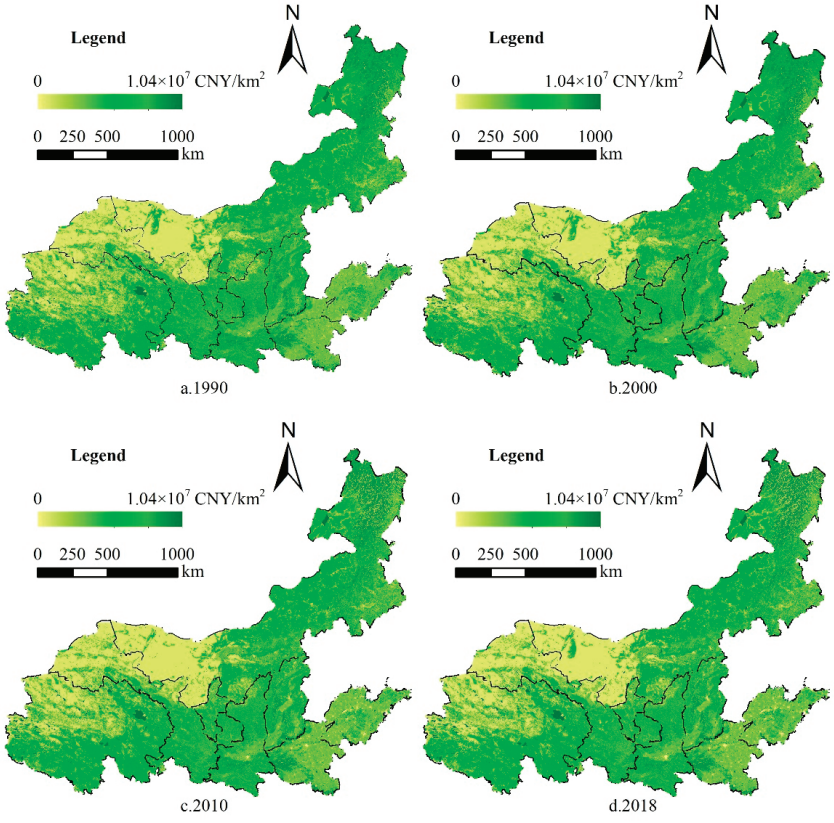

Figure 4. Spatial distribution of ESV per unit area in the YRB during 1990–2018.

The ESV remained stable in most areas of the YRB during the study period, with only a small number of areas improving or deteriorating (Figure 5). Specifically, the overall changes from 1990 to 2000 were minor, dominated by ESV deterioration, and were sporadic

across the region. From 2000 to 2010, nearly 10% of the regions changed in ESV, accounting for more than 70% of the regional changes during the whole study period. The Central Inner Mongolia Autonomous Region, and Shanxi and Henan Provinces were characterized by deterioration, while Qinghai and Shaanxi Provinces were characterized by improvement. The northeastern Inner Mongolia Autonomous Region showed mixed changes. From 2010 to 2018, ESV remained stable, with changes concentrated in south Gansu Province. In general, the ESV of YRB fluctuated during the study period, with an overall increase of 0.06%.

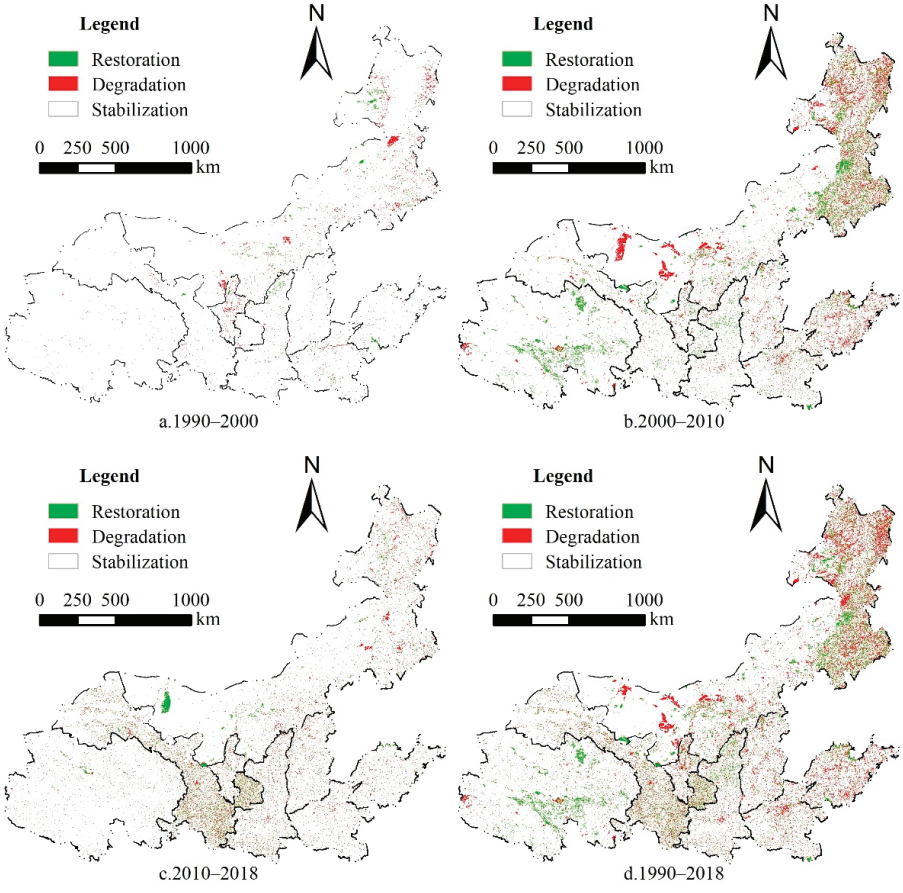

Figure 5. ESV changes in different study periods.

3.3. Impact of LUCC on ESV

3.3.1. Ecological Contribution Rate of LUCC on ESV

ESV in the YRB was 680.03 × 10^{10} CNY, 677.22 × 10^{10} CNY, 678.91 × 10^{10} CNY, and 680.45 × 10^{10} CNY, respectively (Table 3). Grassland and forest land each contributed more than 40% and 30% of ESV, respectively. The contribution of forest land increased, while that of grassland decreased over time. The contribution of cropland remained consistent at around 13%, while the contribution of unused land was the lowest.

Different land use activities lead to different changes in ESV. Conversion from land use types with high value coefficients to those with low value coefficients will deteriorate ESV, while the opposite will improve ESV. According to the calculation results of Formula (6), a total of 30 pairs of land use type changes resulted in ESV variation (Table 4), of which half improved ESV and the other half deteriorated ESV.

Table 3. ESV coefficient of different land use type in the YRB (CNY·km^{-2}·a^{-1}).

Type	1990		2000		2010		2018	
	ESV	Proportion	ESV	Proportion	ESV	Proportion	ESV	Proportion
	10^8 CNY	%	10^8 CNY	%	10^8 CNY	%	10^8 CNY	%
Cropland	8846.56	13.01	9053.06	13.37	8969.53	13.19	8865.89	13.03
Forest land	21,233.50	31.22	20,990.48	31.00	22,040.78	32.42	21,843.85	32.10
Grassland	29,731.38	43.72	29,460.94	43.50	28,383.45	41.75	28,453.66	41.82
Water bodies	6006.40	8.83	6035.81	8.91	6371.68	9.37	6689.31	9.83
Unused land	2185.46	3.21	2181.44	3.22	2215.17	3.26	2192.11	3.22
Total	68,003.31	100.00	67,721.73	100.00	67,980.62	100.00	68,044.81	100.00

Table 4. Contribution rate of land use change to ESV in the YRB during 1990–2018.

Land Use Change	1990–2000			2000–2010			2010–2018			1990–2018		
	Variation	Improvement	Deterioration	Variation	Improvement	Deterioration	Variation	Improvement	Deterioration	Variation	Improvement	Deterioration
	10^8 CNY	%	%	10^8 CNY	%	%	10^8 CNY	%	%	10^8 CNY	%	%
1→2	28.26	5.71		373.85	9.33		183.93	8.05		436.18	8.01	
1→3	34.33	6.93		169.18	4.22		184.19	8.06		297.97	5.47	
1→4	56.82	11.47		267.68	6.68		199.53	8.73		390.80	7.17	
1→5	−54.68		7.04	−353.78		9.44	−192.99		8.69	−532.71		9.85
1→6	−6.21		0.80	−47.12		1.26	−27.89		1.26	−42.66		0.79
2→1	−124.08		15.97	−286.74		7.65	−198.63		8.94	−487.94		9.02
2→3	−128.05		16.48	−453.99		12.11	−463.44		20.86	−786.84		14.55
2→4	1.51	0.30		25.32	0.63		12.75	0.56		32.13	0.59	
2→5	−2.69		0.35	−61.62		1.64	−46.86		2.11	−97.64		1.81
2→6	−5.68		0.73	−375.00		10.01	−173.83		7.82	−492.98		9.12
3→1	−128.39		16.52	−225.99		6.03	−182.79		8.23	−437.00		8.08
3→2	62.91	12.70		1209.61	30.19		416.77	18.23		1463.76	26.87	
3→4	46.70	9.43		172.89	4.31		183.12	8.01		346.26	6.36	
3→5	−7.34		0.94	−104.33		2.78	−109.24		4.92	−201.67		3.73
3→6	−110.00		14.16	−1176.80		31.40	−345.16		15.54	−1386.11		25.64
4→1	−112.94		14.54	−215.77		5.76	−122.51		5.51	−316.33		5.85
4→2	−2.15		0.28	−14.08		0.38	−10.37		0.47	−18.74		0.35
4→3	−31.99		4.12	−91.48		2.44	−139.78		6.29	−195.20		3.61
4→5	−3.02		0.39	−52.14		1.39	−49.64		2.23	−74.04		1.37
4→6	−59.21		7.62	−284.78		7.60	−153.69		6.92	−329.18		6.09
5→1	0.59	0.12		160.58	4.01		74.53	3.26		173.13	3.18	
5→2	0.23	0.05		18.28	0.46		14.47	0.63		20.50	0.38	
5→3	0.00	0.00		24.26	0.61		31.24	1.37		33.79	0.62	
5→4	0.10	0.02		91.45	2.28		99.90	4.37		103.34	1.90	
5→6	0.00	0.00		0.88	0.02		1.47	0.06		1.00	0.02	
6→1	19.01	3.84		75.46	1.88		49.69	2.17		109.66	2.01	
6→2	8.74	1.76		85.30	2.13		115.59	5.06		131.29	2.41	
6→3	97.97	19.78		947.10	23.64		454.35	19.88		1251.04	22.96	
6→4	138.18	27.90		385.04	9.61		264.50	11.57		657.45	12.07	
6→5	−0.50		0.06	−4.35		0.12	−4.99		0.22	−7.75		0.14

Note: 1–6 represent cropland, forest land, grassland, water bodies, built-up land and unused land, respectively. 1→2 represents land use type change from cropland to forest land, and other conversion types follow the same pattern.

The value coefficients of land use types determine the direction of ecological contribution of land use change, while the conversion area dominates the magnitude of contribution. Conversion from grassland to forest land and conversion from unused land to grassland during 1990–2018 were the key causes of ecosystem improvement, with their contribution rate more than 20%. Unused land converted into water bodies was a primary factor in ESV improvement, with a contribution rate of more than 10%. The conversion from cropland to forest land, grassland, and water bodies, as well as conversion from grassland to water bodies were minor factors for ESV improvement, with a contribution of more than 5%. Other land use change types contributed no more than 5% to ESV improvement and had only a negligible effect.

Conversion from grassland to unused land was the key cause of ESV deterioration, contributing more than 25%. Another primary factor for ESV degradation was the conversion of forest land to grassland, with a contribution rate of more than 10%. Furthermore, the occupation of cropland by expansion of built-up land, the conversion of forest land to grassland and unused land, the conversion of grassland to cropland, and the conversion of water bodies to cropland and unused land had less impact on ESV deterioration, with a contribution of more than 5%. Other land use change types contributed no more than 5% to the ESV deterioration.

3.3.2. Bivariate Spatial Autocorrelation between Land Use Degree and ESV

Using the GeoDa spatial analysis tool, a Queen spatial connectivity matrix was generated to calculate the global spatial autocorrelation index for land use degree and the value of each ESs in different years. As shown in Table 5, Moran's I for all ESs and land use degree was negative, except for supply services, indicating that there was a significant positive spatial correlation between supply services and degree of land use. This is because supply services are composed of food production and raw material, both of which are linked to the extent of cropland reclamation and built-up land expansion. As a result, increasing degree of land use results in improved supply services. Furthermore, there is a significant negative spatial correlation between land use degree and support services and cultural services, which are intimately linked to the natural ecosystem and its aesthetic landscape. There is no doubt that human efforts to strengthen land use have a negative influence on the natural environment, so the increase in degree of land use leads to a decrease in support and cultural services. The relationship between land use degree and regulation services was negative but not significant.

Table 5. Bivariate spatial autocorrelation between land use degree and ESV.

Index		Comprehensive Index of Land Use Degree		
		Moran's I	**Z**	***p*-Value**
1990	Supply services	0.4360	7.8729	0.0010
	Regulation services	−0.0045	−0.1379	0.4640
	Support services	−0.1067	−2.0931	0.0200
	Cultural services	−0.3836	−6.8991	0.0010
2000	Supply services	0.4299	7.7624	0.0010
	Regulation services	−0.0121	−0.2860	0.3870
	Support services	−0.1106	−2.1650	0.0150
	Cultural services	−0.3825	−6.8704	0.0010
2010	Supply services	0.3603	6.5781	0.0010
	Regulation services	−0.046	−0.9580	0.1790
	Support services	−0.1821	−3.5213	0.0010
	Cultural services	−0.4051	−7.2955	0.0010
2018	Supply services	0.3333	6.1278	0.0010
	Regulation services	−0.0545	−1.1116	0.1440
	Support services	−0.2004	−3.8674	0.0010
	Cultural services	−0.4081	−7.3436	0.0010

3.4. Impact of Natural and Socio-Economic Factors on ESV

3.4.1. Relative Effects and Interactions of Influencing Factors

Factor Detector results (Table 6) show that both natural and socio-economic factors affected the spatial heterogeneity of average ESV in the YRB, and the impact size of different factors changed slightly each year. NDVI had the greatest impact on the spatial heterogeneity of average ESV, with q values of higher than 0.55 for each year. Meanwhile, the q values of precipitation and population density were above 0.20, which were the primarily reasons for spatial heterogeneity of average ESV. In contrast, the q values of slope, distance to road, distance to railway and distance to city were less than 0.10, and had smaller effects on the spatial heterogeneity of average ESV.

As revealed by the Interaction Detector (Table 7), the interaction effects between all pairs of factors selected were greater than those of each factor separately. As a result, the spatial heterogeneity of the average ESV in the YRB was caused by the mutual influence of multiple factors, and their interactions exacerbated the spatial heterogeneity. Specifically,

the interaction between NDVI and other factors had the strongest impact on average ESV. The q values of NDVI ∩ population density were the highest (q = 0.6605), and thus had the strongest impact on the spatial heterogeneity of ESV. Following that were NDVI ∩ GDP (q = 0.6564) and NDVI ∩ elevation (q = 0.6302). There were 14 interaction combinations with q values greater than 0.5, five were natural factor combinations, nine were natural and socio-economic factor combinations, with no combinations between socio-economic factors.

Table 6. The results of Factor Detector for the spatial heterogeneity of average ESV in the YRB during 1990–2018.

Factors	1990		2000		2010		2018	
	q	*p*-Value	*q*	*p*-Value	*q*	*p*-Value	*q*	*p*-Value
Elevation	0.1140	0.0000	0.1105	0.0000	0.0998	0.0000	0.0961	0.0000
Slope	0.0717	0.0000	0.0717	0.0000	0.0825	0.0000	0.0829	0.0000
Precipitation	0.3861	0.0000	0.3873	0.0000	0.4066	0.0000	0.4031	0.0000
NDVI	0.5511	0.0000	0.5522	0.0000	0.5590	0.0000	0.5562	0.0000
Population density	0.2785	0.0000	0.2810	0.0000	0.2630	0.0000	0.2591	0.0000
GDP	0.1496	0.0000	0.1520	0.0000	0.1494	0.0000	0.1459	0.0000
Distance to road	0.0900	0.0000	0.0912	0.0000	0.0936	0.0000	0.0927	0.0000
Distance to river	0.1470	0.0000	0.1471	0.0000	0.1663	0.0000	0.1637	0.0000
Distance to railway	0.0183	0.0000	0.0188	0.0000	0.0231	0.0000	0.0228	0.0000
Distance to city	0.0448	0.0000	0.0454	0.0000	0.0472	0.0000	0.0475	0.0000

Table 7. The results of Interaction Detector for the spatial heterogeneity of average ESV in the YRB.

$X_i \cap X_j$	$q(X_i)$	$q(X_j)$	$q(X_i \cap X_j)$	Interaction Types
$X_1 \cap X_3$	0.0961	0.4033	0.5650	Nonlinear enhancement
$X_1 \cap X_4$	0.0961	0.5560	0.6302	Two-factor enhancement
$X_1 \cap X_5$	0.0961	0.2592	0.6024	Nonlinear enhancement
$X_1 \cap X_6$	0.0961	0.1459	0.5750	Nonlinear enhancement
$X_2 \cap X_4$	0.0829	0.5560	0.5829	Two-factor enhancement
$X_3 \cap X_4$	0.4033	0.5560	0.5952	Two-factor enhancement
$X_3 \cap X_5$	0.4033	0.2592	0.5251	Two-factor enhancement
$X_3 \cap X_6$	0.4033	0.1459	0.5017	Two-factor enhancement
$X_4 \cap X_5$	0.5560	0.2592	0.6605	Two-factor enhancement
$X_4 \cap X_6$	0.5560	0.1459	0.6564	Two-factor enhancement
$X_4 \cap X_7$	0.5560	0.0929	0.5758	Two-factor enhancement
$X_4 \cap X_8$	0.5560	0.1638	0.5810	Two-factor enhancement
$X_4 \cap X_9$	0.5560	0.0228	0.5852	Nonlinear enhancement
$X_4 \cap X_{10}$	0.5560	0.0475	0.6174	Nonlinear enhancement

Note: X_1—elevation, X_2—slope, X_3—precipitation, X_4—NDVI, X_5—population density, X_6—GDP, X_7—distance to road, X_8—distance to river, X_9—distance to railway, and X_{10}—distance to city.

3.4.2. Spatial Distribution of the Effects of Influencing Factors

Figure 6 depicts the spatial variation of the regression coefficients of each influence factor based on GWR results. The regression coefficients of NDVI are all greater than zero, meaning that NDVI is always positively correlated with ESV. Regression coefficients of GDP are generally greater than zero, indicating that the influence of GDP on ESV is mainly positive. In contrast, the regression coefficients of population density are generally less than zero, indicating that the influence of population density on ESV is mainly negative. In addition, other factors showed approximately equal areas of positive and negative correlation with ESV. Among them, the effects of elevation, precipitation, distance to road and distance to city on ESV were mainly positive in the west and negative in the east. The effects of slope and distance to railway on ESV showed mainly negative correlations in the west and positive correlations in the east, while the distance to river showed positive correlation in the center and negative correlations in the east and west.

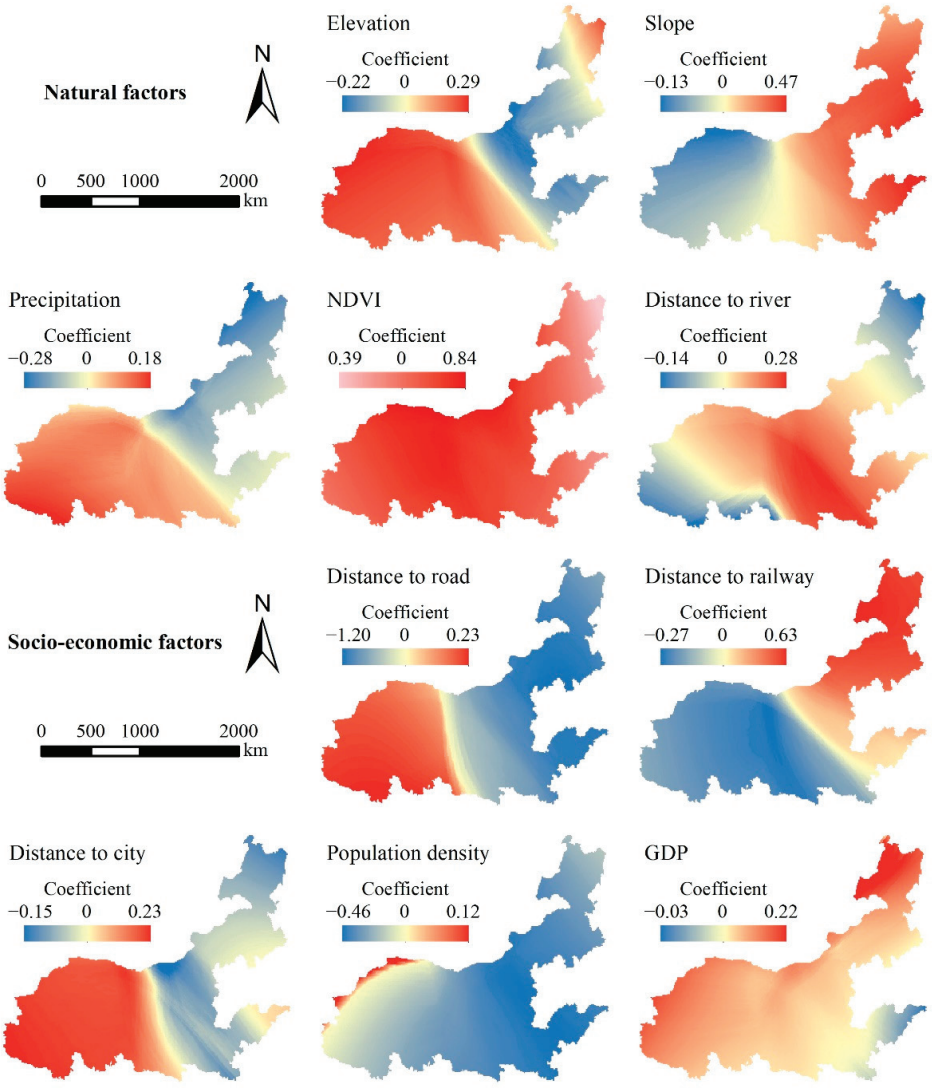

Figure 6. Spatial distribution of regression coefficients of influencing factors.

4. Discussion

4.1. Temporal-Spatial Evolution of ESV and Its Determinants

The findings of this study show that the northeastern part of the YRB with high vegetation cover had the highest average ESV, while the northwest part with scarce water resources and three large deserts had the lowest average ESV, which is consistent with the research of Cui et al. [43] and Zhang et al. [44]. Meanwhile, most scholars believe that the conservation of ecological lands such as forest land, grassland and water bodies is particularly important for the stability of ESV [34,35].

In terms of time, the ESV in the YRB clearly deteriorated from 1990 to 2000, owing to people's lack of awareness of the importance of their ecological environment and the failure to take effective ecological protection measures, resulting in the disorderly expansion of built-up land and the continuous degradation of forest land and grassland [45]. Since 2000, China has gradually strengthened ecological management, particularly through a

series of afforestation and soil conservation projects, which have improved the ecological environment of the YRB [46]. These ecological protection projects have shown preliminary results, indicating the state's important role in ecological regulation [47–49].

Overall, the total ESV of the YRB has remained stable, but the results show significant spatial heterogeneity, with some parts improving and others deteriorating. It was the balance of improvement and deterioration across the region that kept the ESV of the YRB relatively stable [50]. Regions with improved ESV were scattered across the YRB, all of them in areas showing an expansion of built-up land, and where at least one type of ecological land use had also increased. This suggests that the expansion of built-up land has been widespread, and that focusing on the cultivation of ecological land to allow orderly expansion of construction land can help to achieve the goal of ESV improvement [51,52]. Socio-economic development is based on the consumption of various resources, and land exploitation is inevitable. Our results show that any change in land use type resulted in a moderate or substantial change in ESV, exerting a direct impact on ESV. Specifically, the conversion of grassland to forest land was the major reason for ESV improvement in YRB, accounting for more than 25% of the total increase (Table 4), due to the much higher ESV per unit area of forest land than grassland (Table 2), and the large conversion areas (Figure 3). This was made possible by the implementation of projects such as the Three-North Shelterbelt Project, the "Grain-for-Green" and Natural Forest Protection programs, which resulted in a net increase in the area of forest land [53]. In particular, the Three-North Shelterbelt Project has been promoting large-scale afforestation since its implementation and has contributed greatly to ESV growth [54]. Meanwhile, the areas with deteriorating ESV were mainly concentrated in the eastern part of the YRB, and these areas showed a decline in forest land and grassland, and a significant increase in built-up land. Grassland degradation was the major factor in the deterioration of ESV in the YRB, accounting for more than 25% of the reduction (Table 4). Because of the fragile ecological environment of the YRB, with the frequent natural disasters such as floods and mudslides, grassland, a relatively ecologically fragile area, is vulnerable to destruction [33]. Additionally, human activities such as irrational use of water resources, overgrazing and overexploitation have exacerbated the degradation of grassland [55]. Therefore, in future construction, it is necessary to continue to supervise the implementation of these ecological projects, to strengthen the protection and construction of ecological land, and to formulate protection policies tailored to ecological degradation areas in order to ensure steady ecological improvement.

Research on ESV has become a hot topic in the process of building an ecological civilization. Most recent studies have found that changes in ESV are the result of a combination of natural and socio-economic factors [10,56]. Different factors can have varying impacts on ESV, and the combination of multiple factors can produce more complex effects [20]. From the perspective of sustainable development, positive impacts should be promoted and negative impacts should be suppressed [57]. Therefore, identifying the ways in which different factors contribute to ESV is essential for precise policy-making and the formulation of reasonable ecological regulatory measures. In this study, we used GDM and GWR models to explore in depth the impacts on ESV of multiple natural socioeconomic factors.

The results revealed that NDVI was the relative strongest influencing factor for spatial heterogeneity of ESV, which is consistent with the findings of Sun et al. [36]. Meanwhile, NDVI is the only factor that positively affected ESV in all regions. Because NDVI is an indicator of vegetation growth status [58], and abundant vegetation growth and cover are beneficial to ESV [59], therefore, NDVI had a relatively strong effect on ESV with a positive correlation across the whole area. Due to the different geographic conditions, there was spatial variability in the effects on ESV of all other factors. Overall, compared with socio-economic factors, natural factors dominated the influence on ESV. This is in line with the findings of Han et al., who suggested that various types of natural factors influence the structure, distribution, growth, and succession of biomes on a large scale, thus influencing ESV at a macroscopic level [49]. Nevertheless, the impact of socio-economic factors on ESV cannot be ignored, especially population density, which is the most influential of the

socio-economic factors. Population growth will lead to an increased demand for built-up land, food, and other necessities. In such a case, it will lead to LUCC and eventually influence ESV [51]. Therefore, in the practice of enhancing ESV, human interference should be minimized and the regulation of natural elements prioritized [60].

Furthermore, the results of the Interaction Detector revealed that the interaction effect of any two factors was greater than each factor alone, and the interaction type was dominated by two-factor enhancement, indicating that spatial heterogeneity of ESV in the YRB was the result of the combined effect of multiple factors. This is consistent with previous studies, which showed that combining various variables increased their influence on ESV [11,61,62]. It was noted that 9 of the 14 pairs of interaction combinations with q values over 0.5 are interactions of nature and socio-economics, which means that in terms of interaction, the joint effect of nature and socio-economic factors has a stronger influence on ESV. Therefore, in ecological regulation, attention should be paid to the harmonious coexistence of man and nature, and to the combined effect of different regulation methods in order to maximize overall benefits and thus increase the efficiency of ecological improvement initiatives.

4.2. Policy Implication

Based on an in-depth analysis of the temporal-spatial evolution of ESV and its influencing factors, this study proposes three practical policy recommendations for the YRB. First, our study indicated that both in ecological improvement or deterioration areas, built-up land generally showed a trend for expansion, while the maintenance of ecological land such as forest land and water bodies can keep ESV stable. Therefore, an ecological monitoring mechanism can be established in the YRB to dynamically monitor various types of ecological land. The first priority is to monitor its area and limit the conversion of ecological land to other land uses. Ecological quality monitoring should also be enhanced for areas with ecological significance, and timely regulation should be carried out when their quality declines.

Second, the positive effect of the state as the main body to regulate ecology has already been shown, and the implementation of ecological conservation or restoration programs, such as the Three-North Shelterbelt Project, the "Grain-for-Green" Program and the Natural Forest Protection Program should be strengthened. Aside from policies applied to the entire region, specific programs should be designed and implemented in ecologically fragile areas based on their type of ecological vulnerability. For example, in water-scarce areas, a system of compensated use of water resources that matches socio-economic development should be implemented to conserve and control water in a comprehensive manner. In areas with severe land degradation, the local government should identify the type of land degradation, and implement unified planning and treatment in a piecemeal manner according to the classification results. In addition, areas prone to natural disasters should be designated as disaster management zones, requiring strict environmental control to prevent human activities from aggravating disasters.

Third, since natural ecosystems have the ability to self-heal, an ecological assessment mechanism can be established in the YRB, and different measures can be taken based on the assessment results to maintain or improve the ecological environment for different ecological zones. For example, in ecologically sound areas, ESV can be stabilized by limiting human activities, especially those that are polluting and destructive. In contrast, human interventions such as afforestation and engineering restoration are needed to rehabilitate the ecological environment in areas that have lost the ability to restore themselves.

4.3. Limitation

The YRB is an important ecological region within China. We investigated the temporal and spatial heterogeneity of its ESV, identified the ecologically fragile areas of the basin, evaluated the influencing factors, and proposed policy recommendations for improving the ecosystems of the YRB. Our findings may provide a basis for decision-making for ecological governance and regulation in the YRB.

However, there were some limitations to our study. First, we only classified the land use data into six primary categories without further subdividing it, which would tend to make the results biased. In the future, a more detailed classification of land use types should be performed to calculate ESV more accurately, such as dividing cropland into paddy fields, dryland, and irrigated land, and dividing forest land into tree forest, bamboo forest, shrub land, etc. Second, due to the limitation of data acquisition, the influencing factors used may not have been comprehensive enough, and policy or institutional factors were not taken into account. More data should be collected in the future to allow a more thorough investigation of the factors influencing ESV.

5. Conclusions

In this study, we investigated the temporal–spatial evolution of ESV and its determinants in the YRB, based on the ecological contribution, bivariate spatial autocorrelation, and geographical detector models. We found that the ESV of the YRB fluctuated during the study period, with an overall increase of 0.06%. Land use change exhibited a direct and dominant effect on ESV, with conversion of grassland to forest land and conversion of unused land to grassland being the dominant factors in ESV improvement, and conversion of grassland to unused land being the main cause of ESV deterioration. In addition, natural and socio-economic factors had a subtle influence on ecological elements, which gradually affected ESV. Furthermore, the differences in geographical location made the effect of natural socio-economic factors on ESV spatially heterogeneous. These results revealed that the adjustment of land use types in ecological management practices is a dominant factor in maintaining and improving ESV. At the same time, when formulating optimal land management policies, practical and efficient policies should be developed according to local conditions, to promote ESV improvement.

Author Contributions: Conceptualization, B.Z. and L.Z.; methodology, B.Z.; software, B.Z.; validation, B.Z., Y.W. and J.L.; formal analysis, B.Z.; investigation, B.Z. and L.Z.; resources, B.Z.; data curation, B.Z. and L.Z.; writing—original draft preparation, B.Z.; writing—review and editing, Y.W. and J.L.; visualization, B.Z.; supervision, J.L.; project administration, Y.W.; funding acquisition, J.L. All authors have read and agreed to the published version of the manuscript.

Funding: This research was funded by National Natural Science Foundation of China (Grant No. 41901213) and the Natural Science Foundation of Hubei Province (Grant No. 2020CFB856).

Data Availability Statement: The LUCC data were obtained from the Resources and Environmental Sciences and Data Center, Chinese Academy of Sciences (https://www.resdc.cn/ (accessed on 20 November 2021)). The administrative boundary data were obtained from the 1:400,000 database of the National Geomatics Center of China (http://www.ngcc.cn/ngcc/ (accessed on 22 November 2021)). The grain yield per unit area and grain price data were obtained Statistical Yearbooks of each province. Data for other influencing factors were obtained from the Resources and Environmental Sciences and Data Center, Chinese Academy of Sciences (https://www.resdc.cn/ (accessed on 20 November 2021)).

Acknowledgments: The authors are grateful to the editor and the learned reviewers for their valuable comments and suggestions.

Conflicts of Interest: The authors declare no conflict of interest.

References

1. Costanza, R.; d'Arge, R.; de Groot, R.; Farber, S.; Grasso, M.; Hannon, B.; Limburg, K.; Naeem, S.; O'Neill, R.V.; Paruelo, J.; et al. The value of the world's ecosystem services and natural capital. *Nature* **1997**, *387*, 253–260. [CrossRef]
2. Li, W.; Wang, L.; Yang, X.; Liang, T.; Zhang, Q.; Liao, X.; White, J.R.; Rinklebe, J. Interactive influences of meteorological and socioeconomic factors on ecosystem service values in a river basin with different geomorphic features. *Sci. Total Environ.* **2022**, *829*, 154595. [CrossRef] [PubMed]
3. Shang, Y.; Wang, D.; Liu, S.; Li, H. Spatial-Temporal Variation and Mechanisms Causing Spatial Differentiation of Ecosystem Services in Ecologically Fragile Regions Based on Value Evaluation: A Case Study of Western Jilin, China. *Land* **2022**, *11*, 629. [CrossRef]

4. Vitousek, P.M.; Mooney, H.A.; Lubchenco, J.; Melillo, J.M. Human domination of earth's ecosystems. *Science* **1997**, *277*, 494–499. [CrossRef]
5. Kintisch, E.; Kerr, R.A. Global warming, hotter than ever. *Science* **2007**, *318*, 1846–1847. [CrossRef]
6. Prather, M.; Midgley, P.; Rowland, F.; Stolarski, R. The ozone layer: The road not taken. *Nature* **1996**, *381*, 551–554. [CrossRef]
7. Butchart, S.H.M.; Walpole, M.; Collen, B.; Van Strien, A.; Scharlemann, J.P.W.; Almond, R.E.A.; Baillie, J.E.M.; Bomhard, B.; Brown, C.; Bruno, J.; et al. Global Biodiversity: Indicators of Recent Declines. *Science* **2010**, *328*, 1164–1168. [CrossRef] [PubMed]
8. Gao, W.; Du, Z.P.; Yan, C.A.; Chen, Y. Evaluating net ecosystem services value of a polluted lake: A case study of Lake Dianchi. *Acta Ecol. Sin.* **2019**, *39*, 1748–1757. [CrossRef]
9. Huang, J.P.; Zhang, G.L.; Zhang, Y.T.; Guan, X.D.; Wei, Y.; Guo, R.X. Global desertification vulnerability to climate change and human activities. *Land Degrad. Dev.* **2020**, *31*, 1380–1391. [CrossRef]
10. Li, Y.; Feng, Y.; Peng, F.; Chen, S.D. Pattern evolvement of ecological land in Tianjin based on geodetector. *Econ. Geogr.* **2017**, *37*, 180–189. [CrossRef]
11. Fang, L.L.; Wang, L.C.; Chen, W.X.; Jia, S.; Cao, Q.; Wang, S.Q.; Wang, L.Z. Identifying the impacts of natural and human factors on ecosystem service in the Yangtze and Yellow River Basins. *J. Clean. Prod.* **2021**, *314*, 127995. [CrossRef]
12. Zhang, X.L.; Jin, X.B.; Liang, X.Y.; Ren, J.; Han, B.; Liu, J.P.; Fan, Y.T.; Zhou, Y.K. Implications of land sparing and sharing for maintaining regional ecosystem services: An empirical study from a suitable area for agricultural production in China. *Sci. Total Environ.* **2022**, *820*, 153330. [CrossRef]
13. Akhtar, M.; Zhao, Y.; Gao, G.; Gulzar, Q.; Hussain, A.; Samie, A. Assessment of ecosystem services value in response to prevailing and future land use/cover changes in Lahore, Pakistan. *Reg. Sustain.* **2020**, *1*, 37–47. [CrossRef]
14. He, Y.Y.; Kuang, Y.Q.; Zhao, Y.L.; Ruan, Z. Spatial correlation between ecosystem services and human disturbances: A case study of the Guangdong–Hong Kong–Macao Greater Bay Area, China. *Remote Sens.* **2021**, *13*, 1174. [CrossRef]
15. Salata, S.; Grillenzoni, C. A spatial evaluation of multifunctional ecosystem service networks using principal component analysis: A case of study in Turin, Italy. *Ecol. Indic.* **2021**, *127*, 107758. [CrossRef]
16. Yang, Y.J.; Zhang, H.; Zhao, X.Q.; Chen, Z.Z.; Wang, A.G.; Zhao, E.L.; Cao, H. Effects of urbanization on ecosystem services in the Shandong Peninsula urban agglomeration in China: The case of Weifang City. *Urban Sci.* **2021**, *5*, 54. [CrossRef]
17. Yu, H.S.; Yang, J.; Sun, D.Q.; Li, T.; Liu, Y.J. Spatial responses of ecosystem service value during the development of urban agglomerations. *Land* **2022**, *11*, 165. [CrossRef]
18. Wang, Y.H.; Dai, E.F.; Yin, L.; Ma, L. Land use/land cover change and the effects on ecosystem services in the Hengduan Mountain region, China. *Ecosyst. Serv.* **2018**, *34*, 55–67. [CrossRef]
19. Lei, J.R.; Chen, Z.Z.; Wu, T.T.; Li, Y.L.; Yang, Q.; Chen, X.H. Spatial autocorrelation pattern analysis of land use and the value of ecosystem services in northeast Hainan island. *Acta Ecol. Sin.* **2019**, *39*, 2366–2377. [CrossRef]
20. Liu, Z.T.; Wu, R.; Chen, Y.X.; Fang, C.L.; Wang, S.J. Factors of ecosystem service values in a fast-developing region in China: Insights from the joint impacts of human activities and natural conditions. *J. Clean. Prod.* **2021**, *297*, 126588. [CrossRef]
21. Chen, M.; Lu, Y.; Ling, L.; Wan, Y.; Luo, Z.; Huang, H.; Chen, M.; Lu, Y.; Ling, L.; Wan, Y.; et al. Drivers of changes in ecosystem service values in Ganjiang upstream watershed. *Land Use Policy* **2015**, *47*, 247–252. [CrossRef]
22. Zhang, F.; Yushanjiang, A.; Jing, Y.Q. Assessing and predicting changes of the ecosystem service values based on land use/cover change in Ebinur Lake Wetland National Nature Reserve, Xinjiang, China. *Sci. Total Environ.* **2019**, *656*, 1133–1144. [CrossRef] [PubMed]
23. Dai, X.; Wang, L.C.; Huang, C.B.; Fang, L.L.; Wang, S.Q.; Wang, L.Z. Spatio-temporal variations of ecosystem services in the urban agglomerations in the middle reaches of the Yangtze River, China. *Ecol. Indic.* **2020**, *115*, 106394. [CrossRef]
24. Wang, J.F.; Xu, C.D. Geodetector: Principle and prospective. *Acta Geogr. Sinca* **2017**, *72*, 116–134. [CrossRef]
25. Liu, X.Q.; Wang, H.; Wang, X.P.; Bai, M.; He, D.H. Driving factors and their interactions of carabid beetle distribution based on the geographical detector method. *Ecol. Indic.* **2021**, *133*, 108393. [CrossRef]
26. Wang, X.M.; Meng, Q.Y.; Zhang, L.L.; Hu, D. Evaluation of urban green space in terms of thermal environmental benefits using geographical detector analysis. *Int. J. Appl. Earth Obs. Geoinf.* **2021**, *105*, 102610. [CrossRef]
27. Ju, H.R.; Zhang, Z.X.; Zuo, L.J.; Wang, J.F.; Zhang, S.R.; Wang, X.; Zhao, X.L. Driving forces and their interactions of built-up land expansion based on the geographical detector—A case study of Beijing, China. *Int. J. Geogr. Inf. Sci.* **2016**, *30*, 2188–2207. [CrossRef]
28. Liao, J.J.; Yu, C.Y.; Feng, Z.; Zhao, H.F.; Wu, K.N.; Ma, X.Y. Spatial differentiation characteristics and driving factors of agricultural eco-efficiency in Chinese provinces from the perspective of ecosystem services. *J. Clean. Prod.* **2020**, *288*, 125466. [CrossRef]
29. He, J.H.; Pan, Z.Z.; Liu, D.F.; Guo, X.N. Exploring the regional differences of ecosystem health and its driving factors in China. *Sci. Total Environ.* **2019**, *673*, 553–564. [CrossRef]
30. Zhan, D.; Kwan, M.-P.; Zhang, W.; Yu, X.; Meng, B.; Liu, Q. The driving factors of air quality index in China. *J. Clean. Prod.* **2018**, *197*, 1342–1351. [CrossRef]
31. Liu, Y.; Liu, S.; Sun, Y.; Sun, J.; Wang, F.; Li, M. Effect of grazing exclusion on ecosystem services dynamics, trade-offs and synergies in Northern Tibet. *Ecol. Eng.* **2022**, *179*, 106638. [CrossRef]
32. Lu, D.D.; Sun, D.Q. Development and management tasks of the Yellow River Basin: A preliminary understanding and suggestion. *Acta Geogr. Sinca* **2019**, *74*, 2431–2436. [CrossRef]

33. Zhang, X.; Liu, K.; Wang, S.; Wu, T.; Li, X.; Wang, J.; Wang, D.; Zhu, H.; Tan, C.; Ji, Y. Spatiotemporal evolution of ecological vulnerability in the Yellow River Basin under ecological restoration initiatives. *Ecol. Indic.* **2022**, *135*, 108586. [CrossRef]
34. Jia, G.Y.; Hu, W.M.; Zhang, B.; Li, G.; Shen, S.Y.; Gao, Z.H.; Li, Y. Assessing impacts of the Ecological Retreat project on water conservation in the Yellow River Basin. *Sci. Total Environ.* **2022**, *828*, 154483. [CrossRef]
35. Yin, D.Y.; Li, X.S.; Li, G.E.; Zhang, J.; Yu, H.C. Spatio-temporal evolution of land use transition and its eco-environmental effects: A case study of the Yellow River Basin, China. *Land* **2020**, *9*, 514. [CrossRef]
36. Sun, M.H.; Niu, W.H.; Zhang, B.B.; Geng, Q.L.; Yu, Q. Spatial-temporal evolution and responses of ecosystem service value under land use change in the Yellow River Basin: A case study of Shaanxi-Gansu-Ningxia region, Northwest China. *Chin. J. Appl. Ecol.* **2021**, *32*, 3913–3922. [CrossRef]
37. Zhang, J.L.; Shang, Y.Z.; Liu, J.X.; Fu, J.; Cui, M. Improved ecological development model for lower Yellow River floodplain, China. *Water Sci. Eng.* **2020**, *13*, 275–285. [CrossRef]
38. Zhu, H.Y.; Li, X.B. Discussion on the index method of regional land use change. *Acta Geogr. Sinca* **2003**, *58*, 643–650. [CrossRef]
39. Zhuang, D.F.; Liu, J.Y. Study on the model of regional differentiation of land use degree in China. *J. Nat. Resour.* **1997**, *12*, 105–111. [CrossRef]
40. Xie, G.D.; Zhen, L.; Lu, C.X.; Xiao, Y.; Chen, C. Expert knowledge based valuation method of ecosystem services in China. *J. Nat. Resour.* **2008**, *23*, 911–919. [CrossRef]
41. Liang, Y.; Zhang, Z.X.; Zhao, X.L.; Liu, B.; Wang, X.; Wen, Q.K.; Zuo, L.J.; Liu, F.; Xu, J.Y.; Hu, S.G. Have changes to unused land in China improved or exacerbated its environmental quality in the past three decades? *Sustainability* **2016**, *8*, 184. [CrossRef]
42. Anselin, L.; Syabri, I.; Smirnov, O. Visualizing multivariate spatial correlation with dynamically linked windows. In Proceedings of the CSISS Workshop on New Tools for Spatial Data Analysis, Santa Barbara, CA, USA, 10–11 May 2002.
43. Cui, F.Q.; Tang, H.Q.; Zhang, Q.; Wang, B.J.; Dai, L.W. Integrating ecosystem services supply and demand into optimized management at different scales: A case study in Hulunbuir, China. *Ecosyst. Serv.* **2019**, *39*, 100984. [CrossRef]
44. Zhang, X.Y.; Xu, D.Y.; Wang, Z.Y.; Zhang, Y. Balance of water supply and consumption during ecological restoration in arid regions of Inner Mongolia, China. *J. Arid. Environ.* **2021**, *186*, 104406. [CrossRef]
45. Cui, J.; Zhu, M.S.; Liang, Y.; Qin, G.J.; Li, J.; Liu, Y.H. Land use/land cover change and their driving factors in the Yellow River Basin of Shandong Province based on google earth Engine from 2000 to 2020. *ISPRS Int. J. Geo-Inf.* **2022**, *11*, 163. [CrossRef]
46. Ji, Q.; Liang, W.; Fu, B.; Zhang, W.; Yan, J.; Lü, Y.; Yue, C.; Jin, Z.; Lan, Z.; Li, S.; et al. Mapping land use/cover dynamics of the Yellow River Basin from 1986 to 2018 supported by google earth engine. *Remote Sens.* **2021**, *13*, 1299. [CrossRef]
47. Xu, C.; Jiang, Y.N.; Su, Z.H.; Liu, Y.J.; Lyu, J.Y. Assessing the impacts of Grain-for-Green Programme on ecosystem services in Jinghe River basin, China. *Ecol. Indic.* **2022**, *137*, 108757. [CrossRef]
48. Yang, Q.Y.; Gao, D.; Song, D.Y.; Li, Y. Environmental regulation, pollution reduction and green innovation: The case of the Chinese Water Ecological Civilization City Pilot policy. *Econ. Syst.* **2021**, *45*, 100911. [CrossRef]
49. Han, X.J.; Yu, J.L.; Shi, L.N.; Zhao, X.C.; Wang, J.J. Spatiotemporal evolution of ecosystem service values in an area dominated by vegetation restoration: Quantification and mechanisms. *Ecol. Indic.* **2021**, *131*, 108191. [CrossRef]
50. Zhai, T.L.; Zhang, D.; Zhao, C.C. How to optimize ecological compensation to alleviate environmental injustice in different cities in the Yellow River Basin? A case of integrating ecosystem service supply, demand and flow. *Sustain. Cities Soc.* **2021**, *75*, 103341. [CrossRef]
51. Pan, N.H.; Guan, Q.Y.; Wang, Q.Z.; Sun, Y.F.; Li, H.C.; Ma, Y.R. Spatial differentiation and driving mechanisms in ecosystem service value of Arid Region: A case study in the middle and lower reaches of Shule River Basin, NW China. *J. Clean. Prod.* **2021**, *319*, 128718. [CrossRef]
52. Abera, W.; Tamene, L.; Kassawmar, T.; Mulatu, K.; Kassa, H.; Quintero, M. Impacts of land use and land cover dynamics on ecosystem services in the Yayo coffee forest biosphere reserve, southwestern Ethiopia. *Ecosyst. Serv.* **2021**, *50*, 101338. [CrossRef]
53. Wang, L.-J.; Ma, S.; Zhao, Y.-G.; Zhang, J.-C. Ecological restoration projects did not increase the value of all ecosystem services in Northeast China. *For. Ecol. Manag.* **2021**, *495*, 119340. [CrossRef]
54. Chu, X.; Zhan, J.; Li, Z.; Zhang, F.; Qi, W. Assessment on forest carbon sequestration in the Three-North Shelterbelt Program region, China. *J. Clean. Prod.* **2019**, *215*, 382–389. [CrossRef]
55. Liu, B.; Pan, L.; Qi, Y.; Guan, X.; Li, J. Land Use and Land Cover Change in the Yellow River Basin from 1980 to 2015 and Its Impact on the Ecosystem Services. *Land* **2021**, *10*, 1080. [CrossRef]
56. Ma, X.F.; Zhu, J.T.; Zhang, H.B.; Yan, W.; Zhao, C.Y. Trade-offs and synergies in ecosystem service values of inland lake wetlands in Central Asia under land use/cover change: A case study on Ebinur Lake, China. *Glob. Ecol. Conserv.* **2020**, *24*, e01253. [CrossRef]
57. Qi, Y.; Lian, X.H.; Wang, H.W.; Zhang, J.L.; Yang, R. Dynamic mechanism between human activities and ecosystem services: A case study of Qinghai lake watershed, China. *Ecol. Indic.* **2020**, *117*, 106528. [CrossRef]
58. Wang, X.Z.; Wu, J.Z.; Liu, Y.L.; Hai, X.Y.; Shanguan, Z.P.; Deng, L. Driving factors of ecosystem services and their spatiotemporal change assessment based on land use types in the Loess Plateau. *J. Environ. Manag.* **2022**, *311*, 114835. [CrossRef] [PubMed]
59. Liu, W.; Zhan, J.Y.; Zhao, F.; Wang, C.; Zhang, F.; Teng, Y.M.; Chu, X.; Kumi, M.A. Spatio-temporal variations of ecosystem services and their drivers in the Pearl River Delta, China. *J. Clean. Prod.* **2022**, *337*, 130466. [CrossRef]
60. Huang, M.Y.; Yue, W.Z.; Fang, B.; Feng, S.R. Scale response characteristics and geographic exploration mechanism of spatial differentiation of ecosystem service values in Dabie Mountain area, central China from 1970 to 2015. *Acta Geogr. Sinca* **2019**, *74*, 1904–1920. [CrossRef]

61. Gao, J.B.; Jiang, Y.; Anker, Y. Contribution analysis on spatial tradeoff/synergy of Karst soil conservation and water retention for various geomorphological types: Geographical detector application. *Ecol. Indic.* **2021**, *125*, 107470. [CrossRef]
62. Sannigrahi, S.; Zhang, Q.; Pilla, F.; Joshi, P.K.; Basu, B.; Keesstra, S.; Roy, P.S.; Wang, Y.; Sutton, P.C.; Chakraborti, S.; et al. Responses of ecosystem services to natural and anthropogenic forcings: A spatial regression based assessment in the world's largest mangrove ecosystem. *Sci. Total Environ.* **2020**, *715*, 137004. [CrossRef] [PubMed]

land

MDPI

Article

Quantifying and Analyzing the Responses of Habitat Quality to Land Use Change in Guangdong Province, China over the Past 40 Years

Hanwen Zhang [1] and Yanqing Lang [2,3,*]

[1] College of Landscape and Art, Jiangxi Agricultural University, Nanchang 330045, China; zhanghanwen0717@163.com
[2] Key Laboratory for Urban Habitat Environmental Science and Technology, School of Environment and Energy, Peking University Shenzhen Graduate School, Shenzhen 518055, China
[3] Shenzhen New Land Tool Planning & Architectural Design Co., Ltd., Shenzhen 518172, China
* Correspondence: langyq@pku.edu.cn

Abstract: Guangdong Province is an important ecological barrier and the primary pillar of economic development in China. Driven by high-speed urbanization and industrialization, unreasonable land use change in Guangdong Province has exacerbated habitat degradation and loss, seriously affecting habitat quality. Thus, taking Guangdong Province as the study area, this paper quantifies the response of habitat quality on land use change using the Integrated Valuation of Ecosystem Services and Tradeoffs (InVEST) model and constructs a contribution index (CI). The following conclusions can be drawn from the results: (1) The habitat quality exhibits a spatial distribution pattern of low quality in plain areas and high quality in hilly and mountainous areas. (2) The annual average habitat quality gradually decreases from 1980 to 2020, with a total decrease of 0.0351 and a reduction rate of 4.83%; (3) The impact of land use change on habitat quality is mainly negative, and the habitat quality mainly decreases by the conversion of forest land to orchards, paddy field to urban land, and forest land to dry land, with CI values of −24.09, −11.67, and −8.04, respectively. Preventing the destruction of natural forests, increasing the diversity of plantation orchards, and rationalizing and mitigating the growth rate of construction land are key to maintaining and improving the habitat quality.

Keywords: land use change; habitat quality; habitat degradation; Guangdong Province

Citation: Zhang, H.; Lang, Y. Quantifying and Analyzing the Responses of Habitat Quality to Land Use Change in Guangdong Province, China over the Past 40 Years. *Land* **2022**, *11*, 817. https://doi.org/10.3390/land11060817

Academic Editors: Shicheng Li, Chuanzhun Sun, Qi Zhang, Basanta Paudel and Lanhui Li

Received: 18 April 2022
Accepted: 28 May 2022
Published: 31 May 2022

1. Introduction

Habitat denotes the natural environment that provides living space for human beings and other species [1]. It is the guarantee and basic environment for biological survival and reproduction and is the premise of all ecosystem functions and services [2,3]. Habitat quality denotes the ability of a habitat to provide suitable and sustainable living conditions for biological individuals or populations [4]. It reflects the regional biodiversity and ecological service levels. Moreover, it is also an important representation of regional ecological security and ecological health [5,6]. Habitat quality depends on natural and geographical conditions as well as human activities. On the one hand, the natural and geographical conditions determine the basis of habitats, such as the type of habitat, biodiversity, the quality of the biological living environment, and the ability to provide the biological survival and development requirements [7,8]. On the other hand, human activities change the structure, nature, and ecological processes of a habitat [9]. Land is a carrier of human activities that can directly record the patterns of land use change driven by the social economy. On the premise that geographical conditions are not easy to change in the short term, land use change alters the pattern and function of the regional habitat and affects the material circulation and energy flow within the habitat, ultimately causing change to habitat quality [10–14]. When land use type and structure changes are accelerated, habitat

fragmentation, degradation, and even loss can occur, leading to the continuous decline of habitat quality [15–18].

As an important ecological barrier and the primary pillar of economic development in China, the northern Nanling Mountains and the southern coastal zone in Guangdong province occupies an important position in China's national ecological security strategic pattern of "two screens and three belts" [19,20]. Moreover, Guangdong affords the highest economic development and urbanization levels in China [21]. Recently, the contradiction between economic development and ecological protection in Guangdong has become increasingly prominent [22]. On the one hand, although Guangdong Province has the highest level of economy and urbanization in China, the economic development of the province is extremely uneven [23]. In 2020, the gross domestic product (GDP) of the Pearl River Delta (PRD) region in Guangdong Province accounted for 85.17% of the total GDP of Guangdong Province and gathered 62.15% of the province's resident population, and these two figures are on a gradual increase [24,25]. Driven by urbanization, industrialization, and population agglomeration, construction land, industrial and mining land, and infrastructure land are increasing, which not only destroys the integrity of land but also sequesters other land use types [26–29], further intensifies the degradation and even habitat loss, which seriously affects the habitat quality and hinders sustainable economic development and ecological civilization construction [30]. On the other hand, the ecological environment in Guangdong is relatively fragile due to its special geographical location. The hilly and mountainous areas in northern Guangdong Province are prone to soil water erosion under typhoons and rainstorms, and the simple forest structure in Guangdong Province leads to ecological vulnerability [31]. Since 2000, a series of measures have been taken in Guangdong Province to address the problem of soil erosion. Among them, the planting of economic forests and soil conservation forests can effectively combat soil erosion [32], but the impact of such measures on habitat quality is unknown. Therefore, the response mechanisms of habitat quality under continuous land use change in Guangdong Province urgently need to be clarified. Quantitative research on the response of habitat quality to land use and exploration of the relationship between land use change and habitat quality in Guangdong Province are helpful for figuring out the response mechanism of habitat quality to land use change and can provide theoretical support and scientific reference for the rational land-development and utilization as well as of habitat quality improvement, which is of great significance to Maintaining the national ecological security pattern barrier system and ensuring the coordinated and sustainable development of the ecological socioeconomic system [12,33,34]. Currently, most quantitative studies focus on the PRD and the Guangdong-Hong Kong-Macao Greater Bay Area [18,35], and less attention is paid to the entire Guangdong.

Currently, the quantitative research on the response of global habitat quality to land use change is mainly performed on the macro and micro levels.

At the micro-level, studies have revealed the responses of habitat quality to land use change with measured data, such as species quantity, soil properties, and species types. For example, through field investigation, Verheyen et al. [36] and Newbold et al. [16] determined that land use change will affect the division and distribution of herb and wood plant species. The measured data can accurately characterize the impact of land use change on habitat quality. However, the acquisition of measured data is difficult and spatially discontinuous, which is unsuitable for macro-scale promotion.

At the macro level, quantitative research is mainly divided into three aspects. The first is correlation analysis, which mainly analyzes the relation between land use change (e.g., landscape index, land use change degree, pattern change index) and habitat quality change (HQC) [37–40]. Studies showed that urban land expansion, agricultural land expansion, and landscape fragmentation are significantly related to habitat quality reduction in Southwest Ethiopia and the Baotou–Ordos–Yulin urban agglomeration in China [41,42]. The second is evaluating the HQC caused by the land use changes. One way of determining this is by assigning values to different land types to represent their habitat quality and then directly

comparing the differences before and after land use conversion [43,44]; Another way is to evaluate the habitat quality in two or more years using an evaluation model and then analyzing the change of habitat quality in the area with land use change [45,46]. Finally, a prospective study can be performed to determine the future habitat quality. Evaluation of the future habitat quality under different land use scenarios can help optimize the land use scheme and provide the most appropriate land use scenarios for different goal orientations [47–49]. Notably, among the latter two categories of research, the Integrated Valuation of Ecosystem Services and Tradeoffs (InVEST) model is most commonly used due to its convenience, pertinence, and applicability [11,38,50]. It can replace the exhaustive methods and quickly test the habitat quality and quantity. The running data in the model is mainly the land use data, which can better characterize the relation between land use and habitat quality. The accuracy and effectiveness of this model have been widely recognized, and it is deemed suitable for the study of the impact of land use change on habitat quality [51–53].

Therefore, taking Guangdong Province as the study area, we conducted a quantitative analysis of the response of habitat quality to land use change over a long time-span. First, the habitat quality from 1980 to 2020 was determined using the InVEST model. Then, the influence degree index (IDI) and contribution index (CI) were established to quantitatively analyze the response of the habitat quality to land use change. The study aims to: (1) analyze the temporal and spatial evolution characteristics of land use change in Guangdong Province over the last 40 years; (2) determine the temporal and spatial variation characteristics of habitat quality in the study area; and (3) quantitatively analyze the response of habitat quality to land use change and reveal the patterns of land change causing HQC.

2. Materials and Methods

2.1. Study Area

Guangdong Province is located in the southernmost part of the Chinese mainland (Figure 1), between 20°13′ N–25°31′ N and 109°45′ E–117°20′ E. It is adjacent to Fujian in the east, Jiangxi, Hunan in the north, Guangxi in the west, Hong Kong and Macao in the south, and faces Hainan across the sea to the southwest [54]. The total land area of the Guangdong Province is 179,800 km^2. The terrain is high in the north and low in the south. The landform types are complex and diverse. Moreover, hills and mountains are common in the north, while plains and platforms are common in the south. The climate conditions are complex, belonging to the middle subtropical monsoon climate zone, the south subtropical monsoon climate zone, and the tropical monsoon climate zone, with long summers and warm winters, abundant rainfall, large stream flows, and a long flood season. The surface water resources are abundant, but the temporal and spatial distribution is uneven [55]. Meteorological disasters such as rainstorms and floods, tropical cyclones, strong convective weather, lightning strikes, and high temperatures, regularly occur. These disasters have long periods, high frequencies, and can cause heavy damage. From north to south, the soil type transitions from red to lateritic red soil to brick red soil. From north to south, the vegetation is subtropical evergreen broad-leaved forest, subtropical seasonal rain forest, and tropical seasonal rain forest from north to south.

Guangdong comprises 21 prefecture-level cities and is divided into four sub-regions, including nine cities in PRD, including Guangzhou, Foshan, Zhaoqing, Shenzhen, Dongguan, Huizhou, Zhuhai, Zhongshan, and Jiangmen, three cities in western Guangdong (WG), including Zhanjiang, Maoming, and Yangjiang, four cities in eastern Guangdong (EG), including Shantou, Jieyang, Chaozhou and Shanwei, and five cities in northern Guangdong (NG), including Shaoguan, Qingyuan, Yunfu, Meizhou, and Heyuan. In 2020, the urbanization rate of Guangdong reached 74.15%, exhibiting the highest urbanization rate except for Beijing, Tianjin, and Hebei [25]. Among the sub-regions, the population of PRD is the largest, reaching 77.95 million, and the populations of EG, WG, and NG are 16.39, 15.76, and 15.92 million, respectively. The urbanization rate of Shenzhen, Foshan, Dong-

guan, Zhuhai, Zhongshan, and Guangzhou exceeds 85%. Notably, the urbanization rate of Shenzhen has reached 99.54%, thereby representing the city with the highest urbanization rate in China [24]. In 2020, the GDP of the Guangdong Province was 11,076.094 billion yuan, ranking first in China. Specifically, the GDPs of Shenzhen, Guangzhou, and Foshan were more than 100 billion Yuan, respectively, and that of other cities ranged from 10 to 100 billion Yuan [24].

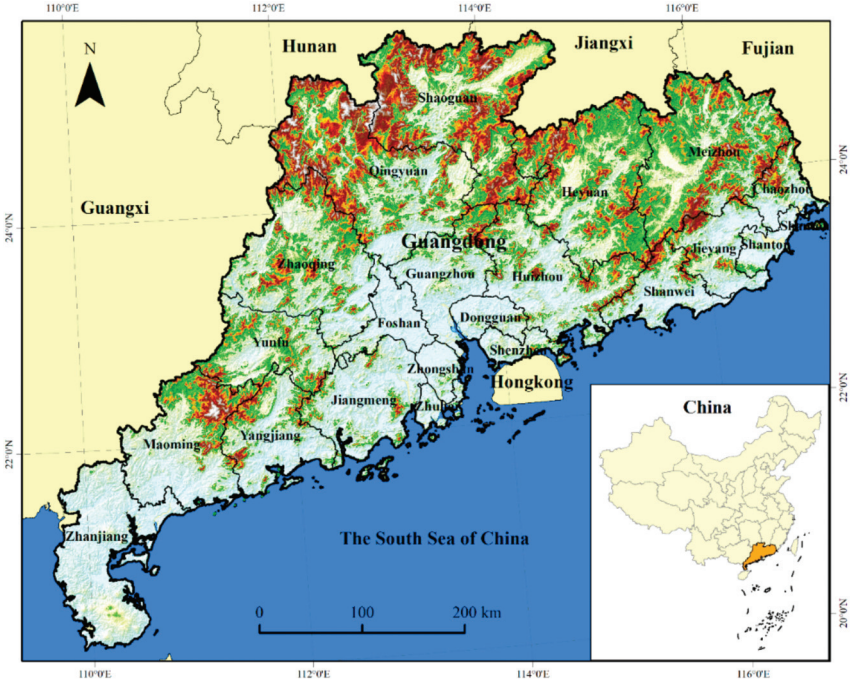

Figure 1. Geographical location of Guangdong province, China.

2.2. Data Sources

The used the following data sources were employed:

(1) Land use data. The land use data were obtained from the Resource and Environmental Science and Data Center, Chinese Academy of Science (http://www.resdc.cn/, accessed on 1 February 2022), with a time resolution of 10 years and a 1000-m spatial resolution, including five years of data in 1980, 1990, 2000, 2010, and 2020. The dataset is based on Landsat TM/ETM+ remote sensing image data, compliments of Liu's and other Chinese land use remote sensing cartographic classification systems, and was generated by the human-computer interactive interpretation of land use change remote sensing information [56,57]. Each phase of data was subject to a unified quality inspection. Ten percent of the counties were randomly selected nationwide, and the data classification results were verified through field investigation. The classification and total accuracies were evaluated using a confusion matrix. The land use types were divided into six first-class types and 25 second-class types. Among them, the comprehensive evaluation accuracy of the first-class types of land use was more than 93%, and the comprehensive classification accuracy of the second-class types was more than 91% [57,58]. According to the data requirements herein, the land use types were reclassified into ten categories: paddy field, dry land, forest land, orchard, grassland, water and wetland, urban land, rural settlement, other construction land, and idle land.

2.3. Study Design

Herein, we analyzed the land use change and its effects on habitat quality from 1980 to 2020 in Guangdong Provence, China. First, we analyzed the long-time spatiotemporal dynamic changes of land use using the atlas analysis method. Then, we assessed the habitat quality in the corresponding year of land use using the Habitat Quality module (HQM) in the InVEST model and clarified the habitat change and its degradation using the hotspots analysis method (Getis-Ord G*index). Finally, we established IDI to represent the impact of annual land use change per unit area on HQC and CI to denote the total contribution of each land use type change on the HQC. Figure 2 shows the study design.

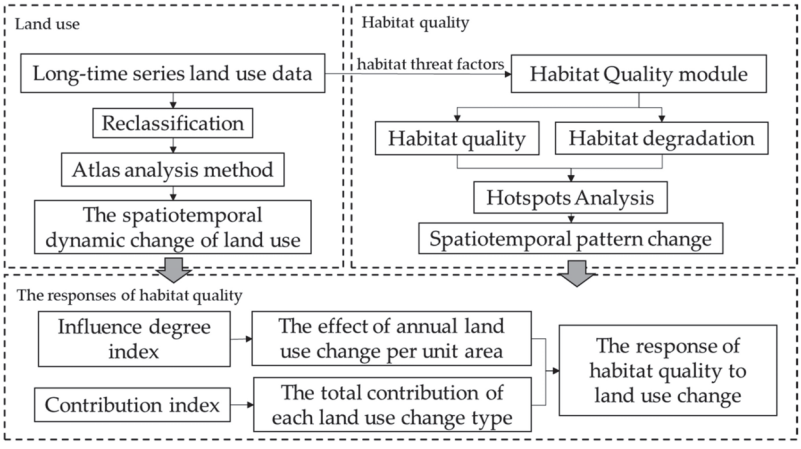

Figure 2. Illustration of the research design.

2.4. Methods

2.4.1. Atlas Analysis Method

The land use data used herein are raster data. Each land use type has a corresponding unique code (paddy field, dry land, forest land, orchard, grassland, water and wetland, urban land, rural settlement, other construction land, and idle land are sequentially numbered from 1 to 10). Thus, an atlas analysis method was used to calculate the land use change; the specific formula is as follows:

$$M = 100A + B \tag{1}$$

where A is the land use type code before converting, and B is the land use type code after converting. M is the code of the land use change type. $A = B$ denotes that the land use type does not change; $A \neq B$ denotes that land use type has changed.

The area of land use change is calculated in the formulas as follows:

$$A_i = C_i \times 10^6 \tag{2}$$

where A_i is the area of land use change type i, with unit m^2, and C_i is the total count of land use change type i, i.e., the raster count of M corresponding to the land use change type i.

2.4.2. Habitat Quality Assessment Model

The HQM in the InVEST model is selected to evaluate habitat quality. The module suggests that the habitat quality depends on a habitat's proximity to human land uses and the intensity of these land uses. Habitat quality degrades with increasing intensity of nearby land use. Thus, the more frequent the human activity, the higher the intensity of land use and the worse the habitat quality [59,60]. This module, which produces a habitat quality

map by combining the information of land use data and habitat threat factors, allows the rapid assessment of the status of and change in a proxy for more detailed measures of the biodiversity status.

The assessment principle of the HQM is as follows: First, habitat degradation is calculated depending on the sensitivity of different land types to threat factors and the intensity of external threats. The specific calculation formula is as follows:

$$D_{xj} = \sum_{r=1}^{r} \sum_{y=1}^{y} \left(\frac{\omega_r}{\sum_{r=1}^{r} \omega_r} \right) r_y i_{rxy} \beta_x S_{jr} \tag{3}$$

$$i_{rxy} = 1 - \left(\frac{d_{xy}}{d_{r\max}} \right) \text{ if linear, or } i_{rxy} = \exp\left[-\left(\frac{2.99}{d_{r\max}} \right) d_{xy} \right] \text{ if exponential} \tag{4}$$

where D_{xj} is the habitat degradation of the land use type j in a grid cell x ranging from 0 to 1. The larger the D_{xj} value, the higher the habitat degradation degree. ω_r represents the weight of each threat factor (ranging from 0 to 1); r_y denotes the effect of threat r that originates in grid cell y, essentially representing the intensity of threat factors. Additionally, i_{rxy} represents the distance between the habitat and the threat source and the impact of the threat across the space; β_x is the factor that may mitigate the impact of threats on the habitat through various protection policies; S_{jr} indicates the sensitivity of the land type j to the threat factor r, where values closer to 1 indicate greater sensitivity; r is the habitat threat factor; y indicates all grid cells on the raster map of r; d_{xy} is the distance between grid cell x and y; $d_{r\max}$ is the influence range of the threat factors.

Then, the habitat quality based on the above-calculated habitat degradation and the suitability of different habitat types to the threat factors can be calculated as follows:

$$Q_{xj} = H_j \left[1 - \left(\frac{D_{xj}^2}{D_{xj}^2 + k^2} \right) \right] \tag{5}$$

where Q_{xj} is the habitat quality of the grid x in the land use type j, which ranges between 0 and 1, the higher the value, the higher the habitat quality; H_j denotes the habitat suitability of the grid x in the land use type j, whose range is [0, 1] and k is the half-saturation constant.

According to the principle of the HQM: paddy fields, dry land, orchard, urban land, rural settlement, other construction land, and idle land are considered threat factors. The data involved in the model mainly include the maximum threat distance, weight and decay of threat factors, habitat suitability, and the sensitivity of different habitat types to threat factors. The above parameter data mainly refer to the model reference values in the InVEST User's Guide and the research results of relevant scholars in similar areas [35,46,53,61,62] (Tables 1 and 2).

Table 1. Threat factor property sheet.

Threat Factor	Maximum Threat Distance (km)	Weight	Decay
Paddy field	4	0.7	linear
Dry land	3	0.6	linear
Orchard	3	0.5	linear
Urban land	10	0.3	exponential
Rural settlements	5	0.2	exponential
Other construction land	4	0.6	exponential
Idle land	6	0.5	linear

Note: Maximum threat distance is the maximum distance over which each threat affects habitat quality (measured in km). The impact of each degradation source will decline to zero at this maximum distance. Weight is the impact of each threat on habitat quality, relative to other threats; Decay is the type of spatial decay for the threat and can be either "linear" or "exponential" [60].

Table 2. Habitat score of each land use type.

Habitat Type	Habitat	PF	DL	ORC	UL	RS	OCL	IL
PF	0.4	0	1	0.3	0.8	0.7	0.8	0.4
DL	0.2	1	0	0.2	0.8	0.6	0.9	0.5
FL	1	0.6	0.7	0.5	0.3	0.4	0.5	0.2
ORC	0.5	0.3	0.5	0	0.5	0.6	0.7	0.3
GL	1	0.6	0.7	0.5	0.6	0.5	0.4	0.6
W&W	1	0.7	0.5	0.3	0.5	0.4	0.4	0.3
UL	0	0.05	0.1	0.1	0	0	0.1	0.1
RS	0	0.7	0.7	0.5	0	0	0.9	0.1
OCL	0.3	0.2	0.2	0.3	0.4	0.5	0	0
IL	0.6	0.5	0.55	0.6	0.3	0.35	0.6	0

Note: PF is paddy field; DL is dry land; FL is forest land; ORC is orchard; GL is grassland; W&W is water and wetland; UL is urban land; RS is rural settlement; OCL is other construction land; and IL is idle land; Habitat refers to habitat suitability, and each land use type is assigned a relative habitat suitability score from 0 to 1.

2.4.3. Hotspots Analysis

The hotspots analysis method was used to illustrate the spatial clustering distribution characteristics of the HQC. The Getis–Ord G* index was employed to identify statistically significant spatial clusters of high values (hotspots) and low values (cold spots) of HQC:

$$G_i^* = \frac{\sum_{j=1}^{n} w_{ij}x_j - \overline{x}\sum_{j=1}^{n} w_{ij}}{S\sqrt{\frac{\left[n\sum_{j=1}^{n} w_{ij}^2 - \left(\sum_{j=1}^{n} w_{ij}\right)\right]^2}{n-1}}} \quad (6)$$

where G_i* is the G* value of pixel i in the HQC raster data, and x_j is the HQC value. Additionally, w_{ij} is the spatial weight matrix of pixel i and pixel j defined by the distance rules. If i and j are adjacent, their spatial weight is 1; otherwise is 0. x denotes the average HQC value; S is the standard deviation of the HQC value, and n is the total count of the pixel. The G* values are calculated using the ArcGIS 10.5 platform. When the G* value was significantly positive, the HQC exhibited a high-value concentration, indicating a hotspot area. In contrast, when the G* value was significantly negative, the HQC exhibited a low-value aggregation, denoting a cold spot area. The significance level was used to identify the hotspots and cold spots, and the areas corresponding to the G* value greater than or equal to 90% of the significance level were regarded as the hotspots and the cold spots.

2.4.4. Assessment of the Contribution of Land Use Change to Habitat Quality

We tailored the CI proposed by Zhang et al. [46] and Wu et al. [63]: First, IDI was established to represent the HQC caused by the annual land use change per unit. To more accurately evaluate the impact of land use change on habitat quality, we divided 1980–2020 into four periods: 1980–1990, 1990–2000, 2000–2010, and 2010–2020. The HQC caused by the unit land use change in the study area from 1980 to 2020 is obtained by calculating the mean IDI of these four periods. The calculation formula is as follows:

$$IDI_i = \frac{1}{4}\sum_{j=1}^{4}\frac{1}{10}\left(\Delta Q_{ij}/SA_{ij}\right) \quad (7)$$

where IDI_i denotes the HQC caused by the annual land use change type i per unit area, ΔQ_{ij} is the total HQC caused by land use change type i in period j, and SA_{ij} is the total area of land use change type i in period j. When $IDI_i > 0$, the land use change type i positively impacts the HQC and improves habitat quality. The higher its value, the greater is its positive impact and the more the improvement on the habitat quality. When $IDI_i < 0$, the land use change type i negatively impacts the habitat quality and reduces the habitat quality. The greater its absolute value, the greater its negative impact, and the more habitat quality is reduced. When $IDI_i = 0$, the land use change type i has no impact on the habitat quality.

Then, using IDIs, we calculated the CI of each land use change type to determine the contribution of different land use change types to HQC. The specific calculation formula is as follows:

$$CI_i = IDI_i \times PA_i * 40 \quad (8)$$

where CI_i is the contribution of the land use change type i on the habitat quality from 1980 to 2020, and PA_i is the percentage of land use change type i in the total area of the land use change from 1980 to 2020. When $CI_i > 0$, the land use change type i positively impacts the habitat quality, plays a positive role on HQC, and improves the habitat quality of the region. The larger its value, the more the habitat quality is improved. When $CI_i < 0$, the land use change type i negatively impacts the habitat quality; the greater its absolute value is, the more the habitat quality is reduced. When $CI_i = 0$, the contribution of the land use change type i to HQC is 0.

3. Results

3.1. Land Use Change in Guangdong

Between 1980 and 2020, the main land use types were cultivated land (dry land and paddy field) and woodland (forest land and orchard) (Figure 3). Specifically, the woodland area and cultivated land annually accounted for more than 55% and 22%, respectively. Spatially, woodland was mainly distributed in the hills and mountains in WG, EG, and NG, while cultivated land was concentrated in the plain areas along PRD and was scattered in other sub-regions.

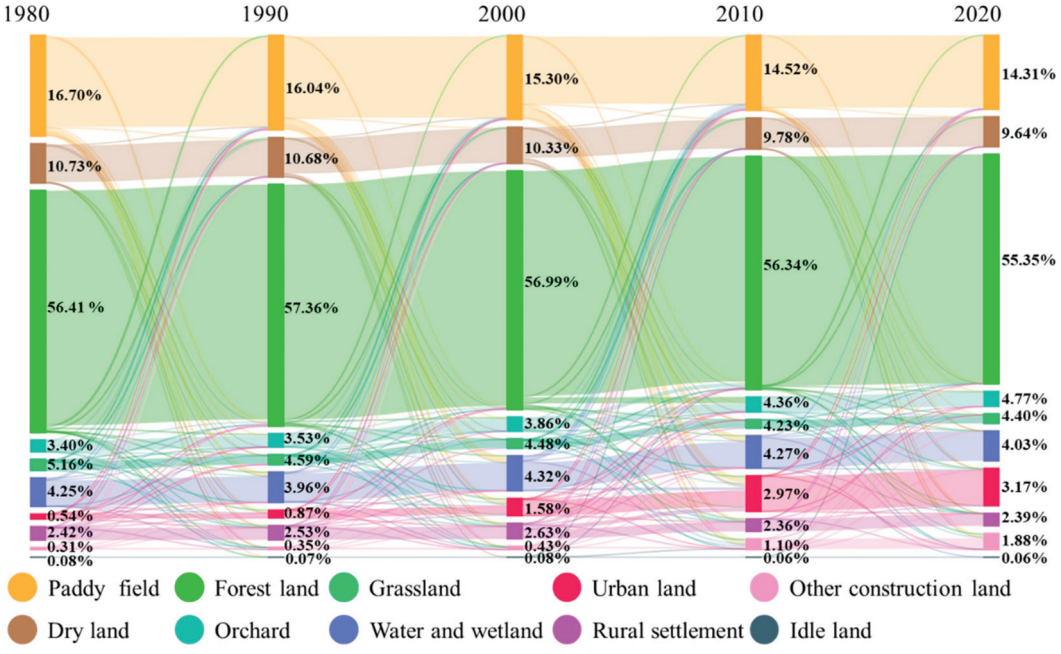

Figure 3. Dynamic change of land use in Guangdong from 1980 to 2020. (Note: The percentage in the figure indicates area proportion of each land use type).

Over the past 40 years, the area of each land use type has greatly varied with time (Figure 3). Orchards, urban land, and other construction land showed a continuous growth trend, with the area increasing by 2423, 4652, and 2779 km^2, respectively, achieving corresponding growth rates of 40.36%, 491.24%, and 506.19%, Urban land exhibited the largest area increment. The areas of the remaining land use types decreased to varying degrees. The largest reduction observed was in paddy fields, with a decrease of 4211 km^2 (14.27%);

followed by dry land, forest land, and grassland, with decreases of 1932 km^2 (10.19%), 1884 km^2 (1.89%), and 1358 km^2 (14.88%), respectively. The water and wetland, rural settlement, and idle land areas exhibited relatively small decreases of 391 km^2 (5.20%), 53 km^2 (1.24%), and 25 km^2 (18.52%), respectively. Furthermore, the change of most land use types after 2000 (later stage) was greater than that before 2000 (early stage), and the land use change was more active in the later stage.

From 1980 to 2020, the spatiotemporal conversion of the land use in the study area exhibited the following characteristics (Figures 3 and 4):

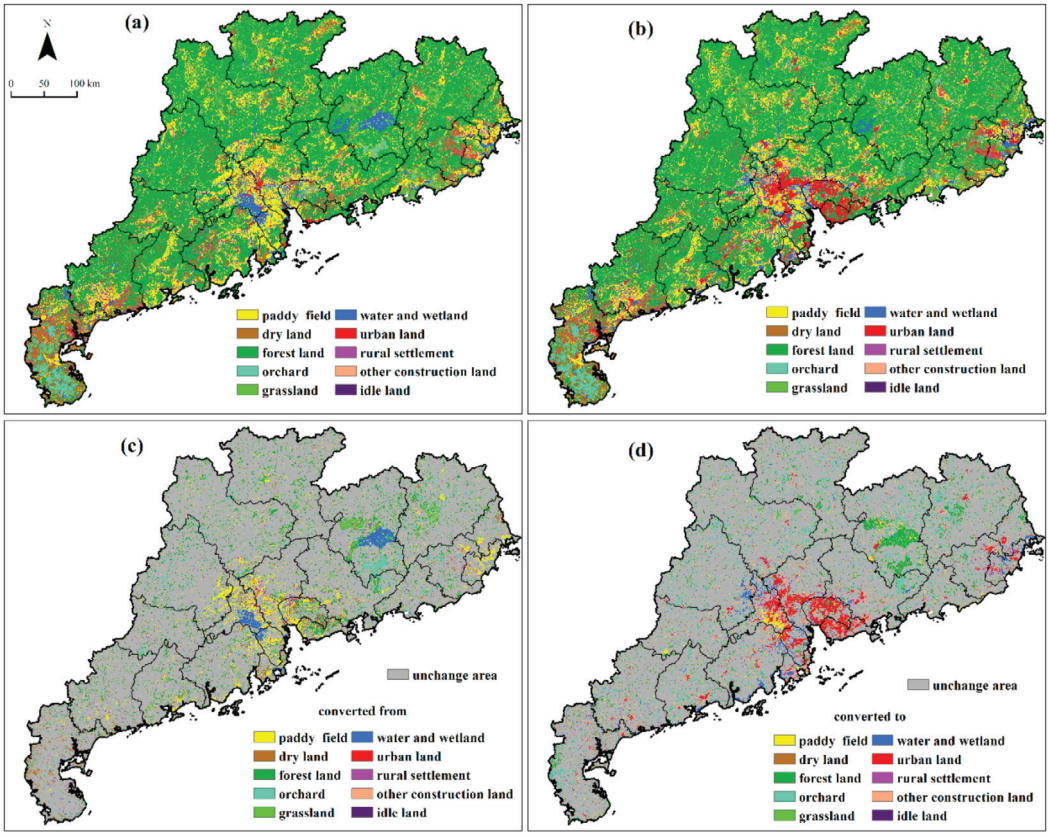

Figure 4. Land use spatial distribution in 1980 (**a**) and 2020 (**b**) and land use converted in (**c**) and out (**d**) from 1980 to 2020.

(1) Large-scale construction land in the PRD continued to expand. This expansion was mainly reflected in the conversion of a large area of paddy fields, dry land, and forest land into urban land and other construction land. Specifically, 2075 and 964 km^2 of paddy fields were converted to urban land and other construction land, respectively, of which 1340 km^2 was mainly distributed and concentrated in the plain area of PRD. Additionally, 863 km^2 and 472 km^2 of dry land have been converted to urban land and other construction land, respectively; the former was concentrated in the PRD (670 km^2), while the latter was scattered throughout the whole region. Furthermore, 556 km^2 and 873 km^2 of forest lands were converted to urban land and other construction land, respectively, which was mainly distributed in the plain area of PRD (501 km^2 and 2446 km^2). Moreover, the rural settlement area exhibited a net decrease, mainly due to the imbalance between the 1121 km^2 of land converted into rural settlements and the 1174 km^2 that was converted out, among which

487 km^2 was converted to urban land, which was mainly distributed in the plain area of PRD.

(2) Large-scale changes in woodland occurred in NG. These changes are mainly manifested in the mutual conversion of forest land and orchard in hills and mountainous areas where 3511 km^2 of forest land was converted into orchards, of which 2054 km^2 is distributed in NG. In contrast, 1429 km^2 of orchard land was converted to forest land, of which 895 km^2 is distributed in NG. Additionally, large areas of conversion into and out of forest land and other land occurred. For example, 1040 km^2 of paddy field and 901 km^2 of dry land were converted into forest land; the former is mainly distributed in NG (589 km^2), while the latter was mainly distributed in WG; 980 km^2 of water and wetland area was converted into forest land, among which, 861 km^2 is distributed in NG. In addition, 964, 899, and 771 km^2 of forest lands were converted to paddy fields, grassland, and dry land, respectively, which is mainly distributed in NG (563, 527, and 264 km^2).

(3) The mutual conversion of paddy fields to and from water and wetland occurred along rivers and coastal areas. Among them, 1409 km^2 of paddy field was converted to water and wetland, including 1007 km^2 distributed in the PRD, which is along the banks of the Xijiang River, Dongjiang River, and Beijiang River, and the coastal areas of Jiangmen and Zhuhai. Additionally, 210 and 102 km^2 are distributed in the coastal areas of EG and WG. Moreover, 594 km^2 of water and wetland was converted to paddy fields, of which 470 km^2 is distributed along the Xijiang River and Beijiang River.

3.2. Habitat Quality and Degradation

3.2.1. Variation in Habitat Quality

From 1980 to 2020, the annual average habitat quality of Guangdong was above 0.6 (Figure 4). Spatially, the habitat quality was between 0 and 1. The distribution pattern exhibited a low habitat quality in plain areas and high habitat quality in the hilly and mountainous areas. Higher habitat quality was observed in the Pearl River Estuary and inland areas. Habitat quality was divided into five levels according to its value: level-1 (0–0.2), level-2 (0.2–0.4), level-3 (0.4–0.6), level-4 (0.6–0.8) and level-5 (0.8–1). The habitat quality of the study area is mainly level-5 (the area for each year accounts for more than 55%), level-1 (the area for each year accounts for more than 14%), and level-2 (the area for each year accounts for more than 15%).

The habitat quality of the four sub-regions in the study area (Figure 5) shows that the annual average habitat quality in NG is the highest, above 0.7 in each year, and the habitat quality in WG is the lowest, below 0.6 in each year. Additionally, the annual average habitat quality in EG and PRD ranges between 0.6 and 0.7 in each year. Spatially, the habitat quality of the four regions is mostly exhibits three levels: level-1, level-2, and level-5 (Figure 6). Over the past 40 years, the habitat quality in the Guangdong Province has gradually decreased with time. The annual average habitat quality decreased by 0.0351, which is equivalent to a reduction rate of 4.83%. The habitat quality of all sub-regions decreased to varying degrees. Among them, the annual average habitat quality decreased the most in PRD, which was –0.0549 (7.88%), and decreased by 0.0287 (3.46%), 0.0276 (4.34%), and 0.0205 (3.57%) in NG, EG, and WG, respectively.

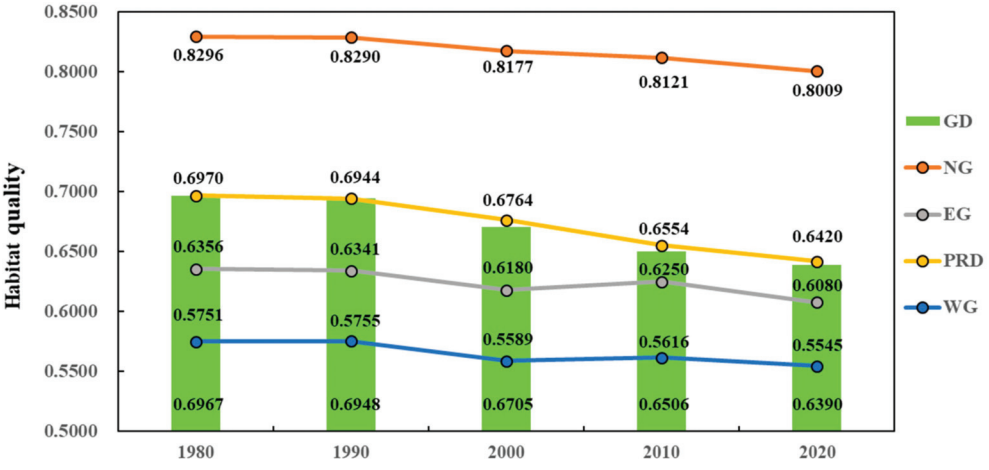

Figure 5. Annual average habitat quality of Guangdong and its sub-regions from 1980 to 2020. (Note: GD refers to Guangdong; NG refers to northern Guangdong; EG refers to eastern Guangdong; PRD refers to Pearl River Delta; WG refers to western Guangdong (WG)).

Spatially (Figure 7), from 1980 to 2020, the habitat quality of 80.33% of the regions in the Guangdong Province decreased to varying degrees, with a reduction amount between 0 and 1, of which 70.99% of the regions decreased between 0 and 0.1, 4.53% of the regions decreased between 0.1 and 0.2, and 1.85%, 2.24% and 1.03% of the regions decreased between 0.4 and 0.5, 0.5 and 0.6, and 0.6 and 0.7, respectively. High of reduction values were mainly distributed in southern Guangzhou, the eastern Foshan, Dongguan, and Shenzhen with a flat terrain around the plain area of PRD, as well as Heyuan and Meizhou in NG. High reduction values were also sporadically distributed in other areas, while low reduction values were distributed throughout the entire region. The habitat quality in 16.39% of the regions increased to varying degrees, with the increment ranging from 0 to 1, of which 12.33% of the regions increased between 0 and 0.1, 1.07% of the regions increment between 0.4 and 0.5. The area for the other increments was small. High and low values of the incremental increases are sporadically distributed in the whole region. Finally, the habitat quality in 3.28% of the regions did not change, mainly in the areas with unchanged land use.

3.2.2. Habitat Degradation

The annual average habitat degradation in the Guangdong Province was more than 0.02 (Figure 8). Specifically, the habitat degradation in WG was the highest, with a value of more than 0.025 per year, while that in NG was the lowest, with a value of less than 0.02 per year. The habitat degradation in PRD was generally between 0.02–0.025. Spatially, the habitat degradation is between 0 and 1. High-value areas were mainly distributed in the low altitude and flat terrain in the PRD, WG, and EG. In contrast, low-value areas were mainly distributed in areas with relatively high altitudes and large slopes (Figure 9).

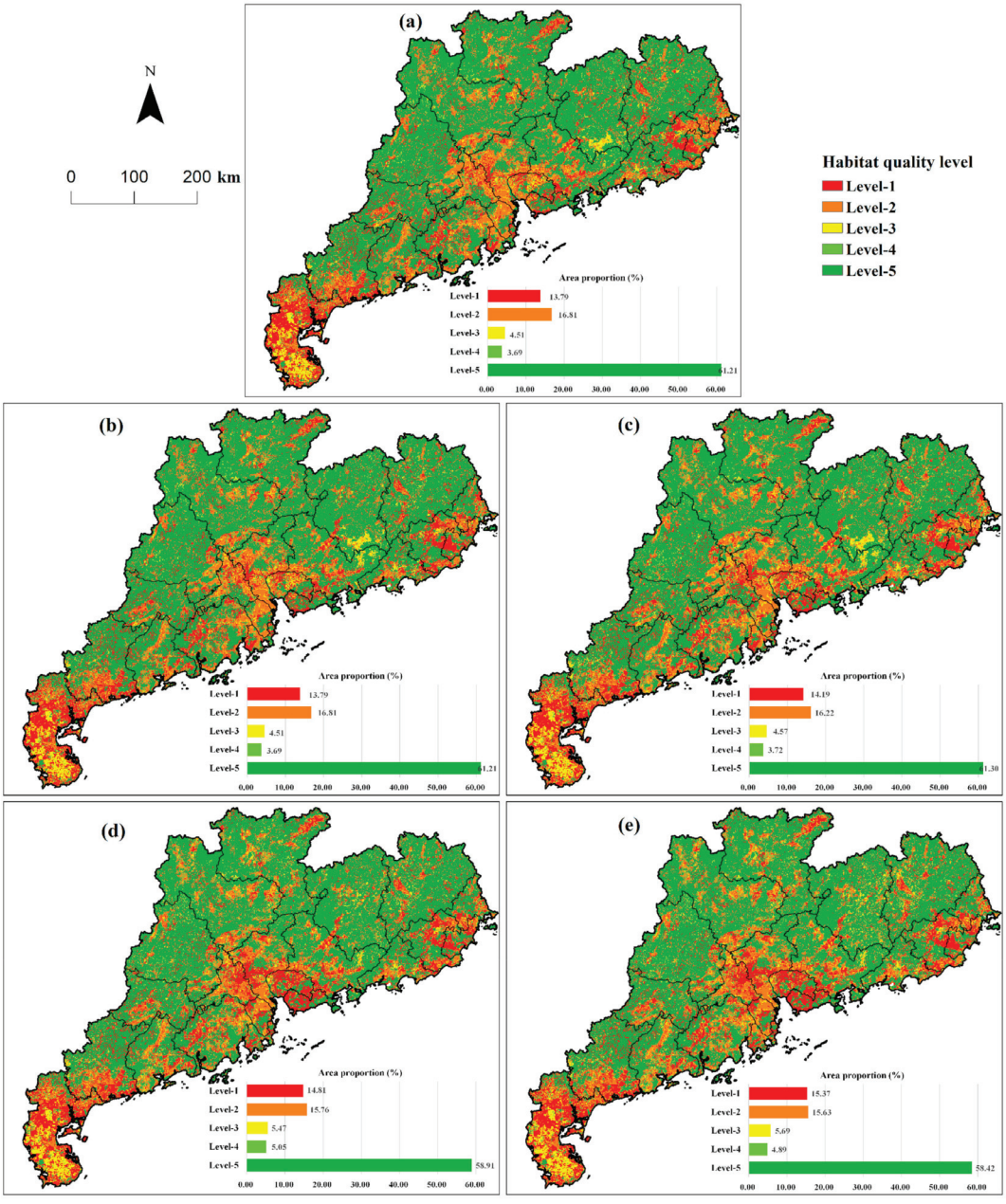

Figure 6. Spatial distribution of habitat quality levels in Guangdong: 1980 (**a**); 1990 (**b**); 2000 (**c**); 2010 (**d**); 2020 (**e**).

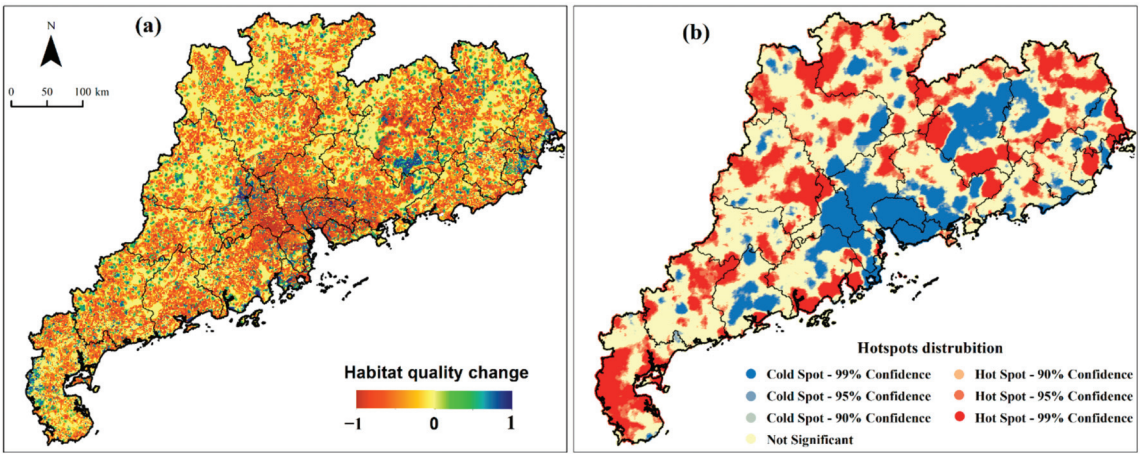

Figure 7. The habitat quality change (**a**) and its hotspots distribution (**b**) from 1980 to 2020. (Note: 99% Confidence refers to at the 99% significant level; 95% Confidence refers to at the 95% significant level; 90% Confidence refers to at the 90% significant level).

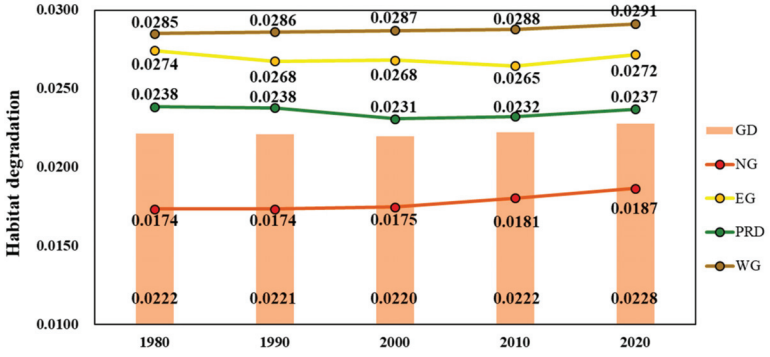

Figure 8. Annual average habitat degradation of Guangdong and its sub-regions from 1980 to 2020. (Note: GD refers to Guangdong; NG refers to northern Guangdong; EG refers to eastern Guangdong; PRD refers to Pearl River Delta; WG refers to western Guangdong).

From 1980 to 2020, the annual average habitat degradation of the Guangdong Province first decreased and then increased (Figure 8). The overall change exhibited a "concave" curve. The curve rebounded after reaching the lowest value in 2000. The habitat degradation decreased in the early stage and continued to increase in the later stage. The annual average habitat degradation increased by 0.0006 (2.79%). The habitat degradation of EG and the PRD decreased by 0.0003 (0.94%) and 0.0001 (0.57%), respectively, while that of NG and WG increased by 0.0013 (7.58%) and 0.0006 (2.19%), respectively.

Spatially, from 1980 to 2020, habitat degradation in 33.75% of the regions decreased (Figure 9f). The reduced high-value areas were mainly distributed in PRD, and the low-value areas were scattered throughout the entire region; the habitat degradation in 66.21% of the regions exhibited an increasing trend. The high-value areas are mainly distributed along the periphery of the plain area of PRD, and Heyuan and Meizhou in NG, and were scattered in other areas. Low-value areas were scattered throughout the entire region. Furthermore, habitat degradation remained unchanged in 0.04% of the regions.

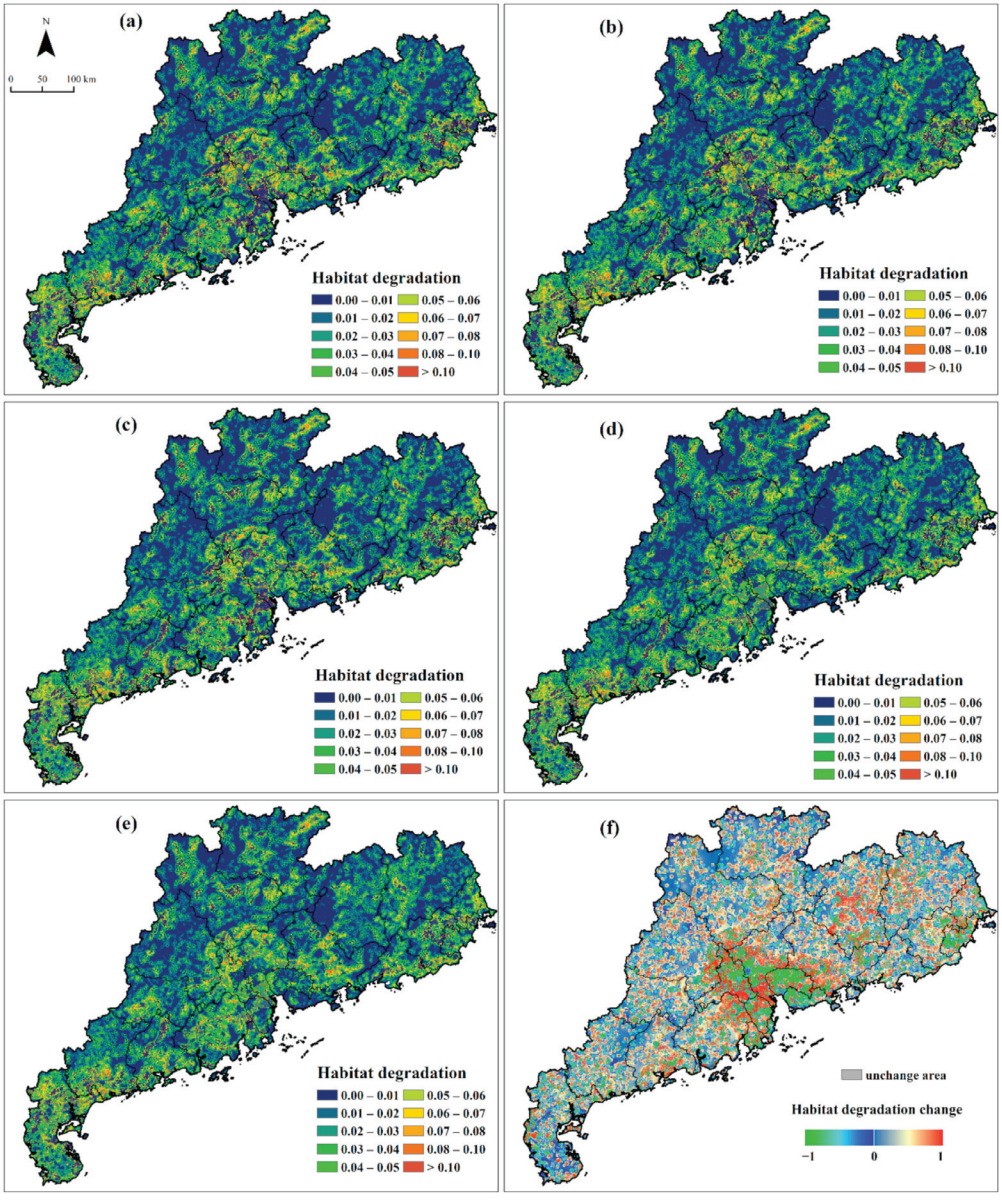

Figure 9. Spatial distribution of habitat degradation in 1980 (**a**), 1990 (**b**), 2000 (**c**), 2010 (**d**), 2020 (**e**) and habitat degradation change from 1980 to 2020 (**f**).

3.3. The Impact of Land Use Change on Habitat Quality

3.3.1. IDIs of Different Land Use Change Types

The depiction of the average habitat quality of different land use types in the selected year (Figure 10), shows that the annual average habitat qualities of forest land, grassland, water and wetland were larger, all above 0.8; while those of paddy field, orchard, idle land, and other construction land is between 0.2 and 0.6, and those of dry land, urban land, and rural settlement were the smallest, all below 0.2. From 1980 to 2020, the annual average habitat quality for each land use type has decreased to varying degrees. The largest

reduction was observed for water and wetland, with a decrease of 0.0519 and a decrease rate of 5.99%, followed by forest land, grassland, and idle land, with decreases of 0.0186 (1.94%), 0.0296 (3.20%) and 0.0186 (3.39%), respectively. The HQC for other land use types was relatively small, no more than 0.01.

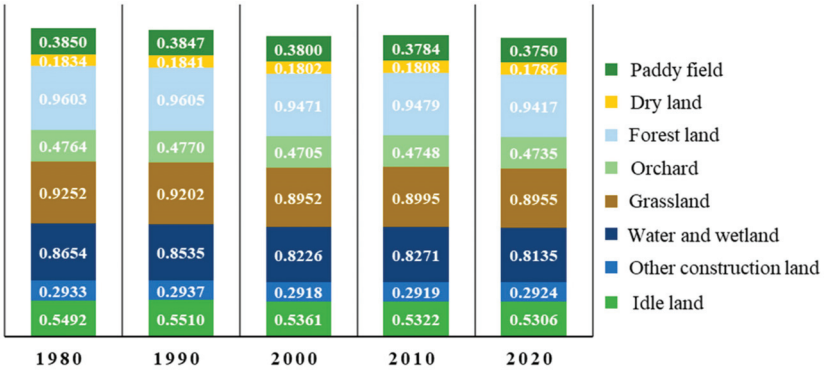

Figure 10. Annual average habitat quality of different land use types from 1980 to 2020. (Note: the annual average habitat quality of urban land and rural settlement is 0).

Land use change has both positive and negative impacts on habitat quality. Table 3 shows that the conversion of forest land, grassland, and water and wetland to dry land, urban land, rural settlement, and other construction land negatively impact habitat quality. The conversion of forest land to urban land afforded the most negative impact, with an IDI value of −0.0903, followed by the conversion of grassland to urban land, with an IDI value of −0.0858. The IDIs of other types were also below −0.05. Furthermore, the conversion of forest land to dry land and idle land to rural settlement negatively affected the habitat quality, with IDIs of less than −0.05.

Table 3. The IDIs of different land use change types.

		After Convert									
		PF	**DL**	**FL**	**ORC**	**GL**	**W&W**	**UL**	**RS**	**OCL**	**IL**
Before convert	PF	-	−0.0158	0.0504	0.0101	0.0441	0.0396	−0.0378	−0.0380	−0.0091	0.0122
	DL	0.0137	-	0.0670	0.0263	0.0621	0.0665	−0.0172	−0.0175	0.0120	0.0358
	FL	−0.0523	−0.0701	-	−0.0461	−0.0007	0.0000	−0.0903	−0.0811	−0.0590	−0.0300
	ORC	−0.0126	−0.0251	0.0448	-	0.0413	0.0369	−0.0462	−0.0468	−0.0174	-
	GL	−0.0466	−0.0657	−0.0005	−0.0406	-	−0.0011	−0.0858	−0.0808	−0.0542	−0.0355
	W&W	−0.0436	−0.0638	−0.0020	−0.0318	−0.0012	-	−0.0870	−0.0833	−0.0555	−0.0392
	UL	0.0375	0.0167	0.0924	0.0449	0.0949	0.0917	-	0.0000	0.0294	-
	RS	0.0379	0.0178	0.0866	0.0452	0.0793	0.0770	0.0000	-	0.0290	0.0582
	OCL	0.0093	−0.0111	0.0577	0.0181	0.0506	0.0556	−0.0294	−0.0292	-	-
	IL	−0.0128	−0.0343	0.0252	−0.0063	0.0386	0.0386	-	−0.0570	−0.0228	-

Note: PF is paddy field; DL is dry land; FL is forest land; ORC is orchard; GL is grassland; W&W is water and wetland; UL is urban land; RS is rural settlement; OCL is other construction land; and IL is idle land.

The conversions of dry land, urban land, rural settlement, and other construction land to forest land, grassland, and water and wetland positively impacted the habitat quality, with IDIs all above 0.05. The conversion of urban land to forest land, grassland, water and wetland afforded the greatest positive impact, with IDIs values of above 0.09. Additionally, the conversions of paddy fields to forest land, and rural settlement to idle land have great positive impacts on habitat quality, with IDIs of above 0.05. The absolute value of IDI for other land use change types was below 0.05, which exerts a relatively small positive or negative impact on the habitat quality.

3.3.2. CIs of Different Land Use Change Types

From the perspective of CIs (Table 4), the contribution of land use change to habitat quality is mainly negative. The total CI is −100.24, where −56.20 is attributed to the conversion of forest land to other land use types, and −32.49 is caused by the conversion of the other land use types (except for forest land) to construction land. Specifically, the CI of the conversion of forest land to orchards is the most negative, with a CI value of −24.09, accounting for 24.03% of the total negative CI, followed by the conversion of paddy fields to urban land, and forest land to dry land, with CI values (percentage of total negative CI) of −11.67 (11.64%) and −8.04 (8.02%), respectively. Additionally, the negative contributions associated with the conversion of forest land to paddy fields, forest land to dry land, and water and wetland to urban land are large, and their respective CIs are less than −1.

Table 4. The CIs of land use change to habitat quality from 1980 to 2020.

		2020									
		PF	**DL**	**FL**	**ORC**	**GL**	**W&W**	**UA**	**RS**	**OCL**	**IL**
1980	PF	-	−0.54	7.79	0.32	0.88	8.31	−11.67	−3.52	−1.31	0.00
	DL	0.46	-	8.98	1.44	0.83	2.42	−2.21	−0.68	0.84	0.01
	FL	−7.50	−8.04	-	−24.09	−0.09	0.00	−7.47	−1.33	−7.66	−0.03
	ORC	−0.26	−0.26	9.53	-	0.32	0.36	−1.50	−0.22	−0.34	-
	GL	−1.64	−1.43	−0.11	−1.76	-	−0.01	−1.26	−0.29	−1.50	−0.01
	W&W	−3.85	−0.73	−0.29	−0.66	−0.01	-	−4.45	−0.72	−2.33	−0.03
	UA	0.05	0.02	0.29	0.03	0.00	0.20	-	0.00	0.09	-
	RS	1.59	0.45	1.13	0.13	0.26	0.48	0.00	-	0.27	0.02
	OCL	0.03	−0.03	0.16	0.02	0.02	0.40	−0.39	−0.06	-	-
	IL	0.00	−0.01	0.02	−0.01	0.05	0.02	-	0.00	−0.05	-

Note: PF is paddy field; DL is dry land; FL is forest land; ORC is orchard; GL is grassland; W&W is water and wetland; UL is urban land; RS is rural settlement; OCL is other construction land; and IL is idle land.

The positive contribution of land use change to the habitat quality constitutes less than half of the negative contribution, which is 48.24. Of this, 27.91 stems from the conversion of other land types to forest land. The CI of converting orchard to forest land is the largest, with a value of 9.53, followed by the conversions from paddy field to forest land, dry land to forest land, and paddy field to water and wetland, with CIs of 7.79, 8.98, and 8.31, respectively, The CI values of other land use change types do not exceed 1.

The CIs in each sub-region of the study area significantly differ. Table 5 shows that positive contribution mainly occurs in NG and PRD. The contribution in these two sub-regions accounts for more than 70% of the total positive contribution, while the positive contribution in EG and WG is relatively small. Moreover, the CI value associated with the conversion from orchard to forest land is the largest in NG, the conversion from paddy field to water and wetland is the largest in EG and PRD, and that from dry land to forest land is the largest in WG.

The negative contribution mainly occurs in NG and PRD, accounting for 32.6% and 49.15% of the total negative contribution, respectively. The negative contribution is relatively small in EG and WG. The land use change types causing habitat quality reduction in each sub-region are different. For example, the habitat quality reduction in NG is mainly caused by the conversion of forest land to other land use types (with CI value of −24.27), among which the CI value of forest land to orchard is −14.03. The degradation of the habitat quality in EG is mainly caused by the conversion of paddy fields to construction land, and the conversion of forest land into other land use types. The CI values of the conversion of paddy fields to urban land and forest land to orchards are the smallest, which are −1.30 and −1.25, respectively. The habitat quality reduction in PRD is mainly due to the conversion of other land use types to construction land, among which the CI value of paddy field to urban land is the smallest. The habitat quality reduction in WG mainly

occurs due to the conversion of forest land into other land use types, among which the CI value of forest land to dry land is the smallest.

Table 5. The CIs in four sub-regions of Guangdong from 1980 to 2020.

Sub-Region	Positive Contribution			Negative Contribution		
	Total CI	Main Converted Types and Their CIs		Total CI	Main Converted Types and Their CIs	
NG	4.2326	PF ct FL	4.38	−8.1772	FL ct PF	−4.38
		PF ct W&W	0.53		FL ct DL	−2.75
		DL ct FL	2.55		FL ct ORC	−14.03
		ORC ct FL	5.97		FL ct OCL	−2.54
EG	1.1185	PF ct FL	0.40	−1.8485	PF ct UL	−1.30
		PF ct W&W	1.24		PF ct RS	−0.59
		DL ct FL	1.07		FL ct DL	−0.94
		ORC ct FL	0.58		FL ct ORC	−1.25
PRD	4.2622	PF ct FL	1.99	−12.3288	PF ct UL	−9.02
		PF ct W&W	5.94		FL ct ORC	−6.23
		DL ct FL	1.92		FL ct UL	−6.73
		ORC ct FL	2.29		W&W ct UL	−4.22
WG	2.4460	PF ct FL	1.03	−2.7286	FL ct PF	−1.02
		DL ct FL	3.44		FL ct DL	−2.50
		DL ct ORC	1.06		FL ct ORC	−2.58
		DL ct W&W	0.80		FLct OCL	−0.76

Note: GD refers to Guangdong; NG refers to northern Guangdong; EG refers to eastern Guangdong; PRD refers to Pearl River Delta; WG refers to western Guangdong. PF is paddy field; DL is dry land; FL is forest land; ORC is orchard; W&W is water and wetland; UL is urban land; RS is rural settlement; and OCL is other construction land. "ct" refers to "convert to", therefore, "PF ct FL" means "paddy field convert to forest land".

4. Discussion

4.1. The Verification of Habitat Quality

The habitat quality value assessed herein is considered a continuous variable in HQM. It is a dimensionless comprehensive indicator with a range of 0–1. The assessment values of the habitat quality are not field observations, and the accuracy of the assessment results cannot be verified by direct comparison with the actual observation values. Moreover, field observations are used in the evaluation index systems to assess the habitat quality, and systems that are too subjective will afford large differences in results and are therefore less suitable for validating of the habitat quality assessed by HQM. Therefore, we cross-validated our assessment results by comparing with the HQM-assessed results of other scholars in the whole and part of the study area (Table 6).

The comparison results show that differences are present in the respective habitat quality assessment values in the same areas, but the overall differences are not significant, none of them exceeded ± 0.1 compared with our study results. Additionally, the trends of change over time are consistent. Therefore, it is reasonable to assume that the HQM is applicable to the habitat quality assessment in the study area and that our assessment results can effectively describe the status and changes in habitat quality in the study area.

The differences in the habitat quality assessment results mainly stem from the selection of threat factors and the parameters settings. The threat factors selection and the parameter settings, most of them refer to the InVEST User's Guide and other scholars, and the parameters and threat factors for the same study area exhibit little difference.

Table 6. The assessment results of habitat quality within Guangdong Province of other scholars.

Region	Threat Factors	Results	Comparison
Guangdong–Hong Kong–Macao Greater Bay Area (GBA)	Bare land, Built-up areas, Cropland, Railway, Trunk road, Primary road, Secondary road, Industry activity, Residential [35].	• The annual average habitat quality was 0.61, 0.60, 0.59, 0.60 and 0.60 in 1995, 2000, 2005, 2010 and 2015, respectively; • The high habitat quality was mainly distributed in the outer ring of the GBA, and low habitat quality were concentrated in the central areas of the GBA.	• Their results in the GBA lower 0.04–0.07 than ours in PRD; • The spatiotemporal change trends were consistent.
	Cultivate land, Construction land, and Idle land [64].	• The annual average habitat quality of the GBA in 1980, 1995, 2005 and 2015 was 0.79, 0.78, 0.76 and 0.74, respectively; • Low-values in the central and south-central parts and high-values in the surrounding margins	• Their result higher 0.05–0.1 than our results; • The spatiotemporal change trends were consistent.
	Paddy field, Upland field, Urban land, Rural settlement, Construction land, Sand, Bare ground [65].	• The annual average habitat quality in 2005, 2010, 2015 and 2018 was 0.613, 0.604, 0.600 and 0.595, respectively; • The habitat quality of the GBA shows a circular distribution of low in the central part and high in the surrounding area.	• Their result higher 0.04–0.1 than our results; • The spatiotemporal change trends were consistent.
Pearl River Delta (PRD)	Construction land, Idle land [66].	• The annual average habitat quality was 0.6 in 2020; • Habitat quality was relatively high in the west and northeast of PRD, while low in the central.	• Similar to our results in the PRD; • Share the same distribution characteristics
	Cropland, City/town, Rural settlements, Other construction land, Unused land, Land reclamation [63].	• From 1990–2018, the annual average habitat quality dropped from 0.7181 to 0.6672; • High-values distributed in the surrounding area, while low-values distributed in the central area.	• Close to our results; • The spatiotemporal change trends were consistent.

Table 6. *Cont.*

Region	Threat Factors	Results	Comparison
Guangdong Province	Cultivate land, Construction land, and Idle land [67].	• The area proportion of low-level (0–0.33) increased from 3.5–6.7% from 1980–2010, that of high-level (0.34–0.66) increased from 69.4–69.3%, moderate-level (0.66–1) decreased from 27.1 to 21.2%. • Low-value areas were clustered and distributed mainly in the plain areas of the PRD, with higher habitat quality in western, northern, and eastern Guangdong.	• Their results were higher than our results. Our results showed that the area proportions of three level were 15.14, 20.67 and 64.18% in 1980, respectively, from 1980–2010, the area proportion of low-level area increased to 17.58%, while that of high-level and moderate-level decreased to 20.04 and 62.38%, respectively; • Share a same change trend that the habitat quality gradually decreases with time.

4.2. Degradation of the Habitat Quality and the Policy Implications

Regarding the impact of land use change on habitat quality, land use change can either improve or reduce habitat quality. In most cases, the positive impact of mutual conversion between two land use types is less than the negative impact (Table 3), demonstrating that restoring the habitat quality to its original state is difficult. Land use types with high habitat quality (e.g., forest; grassland; and water and wetland) are mostly unspoiled natural ecosystems, which are complete and stable, and they have a certain ability to restore and maintain stability and are vulnerable to the negative impact of the land use change. In contrast, land use types with low habitat quality (e.g., orchard; cultivated land; and settlements) are mostly semi-natural and artificial ecosystems, which are greatly affected by human activities. The conversion from a high-quality to low-quality land use type is very destructive, and it directly changes the type, nature, and layout of ecosystems; a natural ecosystem gradually becomes a semi-natural and an artificial ecosystem. Even if water and soil conservation projects can promote the restoration of the ecosystem, man-made selective planting causes the simple structure of the forest land and grassland to directly affect the biodiversity, further demonstrating that the habitat quality cannot be restored to its original state.

The regional HQC is related to not only IDIs but also the area of land use change type. The three main land use change types that cause the decline of habitat quality are forest land to orchards, paddy fields to urban land, and forest land to dry land. Among them, the conversion of forest land to dry land affords the largest IDI and affords relatively large conversion areas. Therefore, this land use change type significantly negatively impacts the HQC. Notably, the IDIs of the conversion of forest land to orchard and paddy field to urban land are relatively small, but due to the large conversion area, the CIs of these two land use change types are very large. Therefore, two approaches are introduced to better restore the ecosystem and improve the habitat quality. First, for land use types with high habitat quality, the conversion to the known land use types with low habitat quality should be slowed. For different land use types, measures to improve habitat quality should be targeted. For example, for economic forests and water conservation forests, not only their water and soil conservation and economic benefits but also the diversity of species should be considered. Second, the habitat quality of land use types with low habitat quality is easy to improve. Measures such as employing reasonable farming methods of cultivated land and increasing the internal green areas within an urban land will improve the habitat quality.

4.3. The Merits and Limitations of This Study

This study quantitatively evaluates the response of habitat quality to land use change in Guangdong Province over the past 40 years. Moreover, it analyzes the main land use change types causing HQC and briefly analyzes the relation between land use and habitat quality. The study results can serve as a reference for land use planning, ecosystem restoration, and biodiversity protection in the Guangdong Province. The limitations of this study are as follows. First, the regional scale research can only explain the relationship between land use change and habitat quality change in the province. Although the research results provide reference value, more specific response measures need to be carefully studied from a finer scale. Second, the InVEST model itself has limitations. The model evaluation only considers the direct relationship between natural factors and habitat quality, while human factors, a known important factor affecting the regional habitat quality, do not directly participate in the evaluation of the habitat quality.

5. Conclusions

Using the land use data from 1980 to 2020 and the InVEST model, we analyzed the temporal and spatial evolution characteristics of land use in the Guangdong Province, evaluated the regional habitat quality, and revealed its temporal and spatial change characteristics. We established CI to reveal the response of habitat quality to land use change. The results from 1980 to 2020 reveal the following. (1) The land use change in Guangdong Province exhibited obvious temporal and spatial evolution characteristics, including large-scale expansion of the construction land in plain areas, large-scale conversion into and out of forest land in hilly and mountainous areas, and the mutual conversion of paddy field and water and wetland in coastal and river areas; (2) The habitat quality of the Guangdong Province presented a spatial distribution pattern of low quality in plain areas and high quality in hilly and mountainous areas. The habitat quality gradually decreased with time, and the decrease was larger in the later stage compared to the early stage, which decreased by 0.0351, with a reduction rate of 4.83%; (3) The negative contribution of land use change to HQC is about twice the positive contribution. The decline of the habitat quality in Guangdong Province is mainly due to the conversion of forest land to orchards, paddy fields to urban land and forest land to dry land, with CIs of −24.09, −11.67, and −8.04, respectively. Analyzing the CIs and the relationship between land use and habitat quality, this study presented targeted habitat quality restoration measures, providing a scientific reference for land use management and habitat protection in the study area.

Author Contributions: Conceptualization, H.Z. and Y.L.; methodology, H.Z. and Y.L.; software, H.Z.; validation, H.Z.; formal analysis, H.Z.; resources, Y.L.; data curation, Y.L.; writing—original draft preparation, Y.L.; writing—review and editing, Y.L.; supervision, Y.L.; project administration, Y.L.; funding acquisition, Y.L. All authors have read and agreed to the published version of the manuscript.

Funding: This research was funded by the National Natural Science Foundation of China (42071204) and the Guangdong Basic and Applied Basic Research Foundation (2019A1515011661).

Institutional Review Board Statement: Not applicable.

Informed Consent Statement: Not applicable.

Data Availability Statement: The data used to support the findings of this study are available from the corresponding author upon request.

Conflicts of Interest: The authors declare no conflict of interest.

References

1. Krausman, P.R. Some basic principles of habitat use. *Ida. For. Wildl. Range Exp. Stn. Bull.* **1999**, *70*, 85–90.
2. Kija, H.K.; Ogutu, J.O.; Mangewa, L.J.; Bukombe, J.; Verones, F.; Graae, B.J.; Kideghesho, J.R.; Said, M.Y.; Nzunda, E.F. Spatio-Temporal Changes in Wildlife Habitat Quality in the Greater Serengeti Ecosystem. *Sustainability* **2020**, *12*, 2440. [CrossRef]
3. Zhang, H.; Zhang, C.; Hu, T.; Zhang, M.; Ren, X.; Hou, L. Exploration of roadway factors and habitat quality using InVEST. *Transp. Res. Part D Transp. Environ.* **2020**, *87*, 102551. [CrossRef]

4. Kunwar, R.M.; Evans, A.; Mainali, J.; Ansari, A.S.; Rimal, B.; Bussmann, R.W. Change in forest and vegetation cover influencing distribution and uses of plants in the Kailash Sacred Landscape, Nepal. *Environ. Dev. Sustain.* **2020**, *22*, 1397–1412. [CrossRef]
5. Ahmadi Mirghaed, F.; Souri, B. Relationships between habitat quality and ecological properties across Ziarat Basin in northern Iran. *Environ. Dev. Sustain.* **2021**, *23*, 16192–16207. [CrossRef]
6. Bai, L.; Xiu, C.; Feng, X.; Liu, D. Influence of urbanization on regional habitat quality: A case study of Changchun City. *Habitat Int.* **2019**, *93*, 102042. [CrossRef]
7. Lee, D.-J.; Jeon, S.W. Estimating Changes in Habitat Quality through Land-Use Predictions: Case Study of Roe Deer (Capreolus pygargus tianschanicus) in Jeju Island. *Sustainability* **2020**, *12*, 10123. [CrossRef]
8. Rybicki, J.; Hanski, I. Speciesarea relationships and extinctions caused by habitat loss and fragmentation. *Ecol. Lett.* **2013**, *16*, 27–38. [CrossRef]
9. Song, C.; Lee, W.-K.; Lim, C.-H.; Jeon, S.W.; Kim, J. Habitat Quality Valuation Using InVEST Model in Jeju Island. *J. Korea Soc. Environ. Restor. Technol.* **2015**, *18*, 1–11. [CrossRef]
10. Janus, J.; Bozek, P. Land abandonment in Poland after the collapse of socialism: Over a quarter of a century of increasing tree cover on agricultural land. *Ecol. Eng.* **2019**, *138*, 106–117. [CrossRef]
11. Sharma, R.; Nehren, U.; Rahman, S.; Meyer, M.; Rimal, B.; Aria Seta, G.; Baral, H. Modeling Land Use and Land Cover Changes and Their Effects on Biodiversity in Central Kalimantan, Indonesia. *Land* **2018**, *7*, 57. [CrossRef]
12. Gao, Y.; Ma, L.; Liu, J.; Zhuang, Z.; Huang, Q.; Li, M. Constructing Ecological Networks Based on Habitat Quality Assessment: A Case Study of Changzhou, China. *Sci. Rep.* **2017**, *7*, 46073. [CrossRef] [PubMed]
13. Guo, Z.W.; Zhang, L.; Li, Y.M. Increased Dependence of Humans on Ecosystem Services and Biodiversity. *PLoS ONE* **2010**, *5*, e13113. [CrossRef] [PubMed]
14. Liu, Y.; Huang, X.J.; Yang, H.; Zhong, T.Y. Environmental effects of land-use/cover change caused by urbanization and policies in Southwest China Karst area A case study of Guiyang. *Habitat Int.* **2014**, *44*, 339–348. [CrossRef]
15. Ding, Q.; Chen, Y.; Bu, L.; Ye, Y. Multi-Scenario Analysis of Habitat Quality in the Yellow River Delta by Coupling FLUS with InVEST Model. *Int. J. Environ. Res. Public Health* **2021**, *18*, 2389. [CrossRef]
16. Newbold, T.; Hudson, L.N.; Hill, S.L.L.; Contu, S.; Lysenko, I.; Senior, R.A.; Boerger, L.; Bennett, D.J.; Choimes, A.; Collen, B.; et al. Global effects of land use on local terrestrial biodiversity. *Nature* **2015**, *520*, 45–50. [CrossRef]
17. Ramaswami, A. Unpacking the Urban Infrastructure Nexus with Environment, Health, Livability, Well-Being, and Equity Comment. *One Earth* **2020**, *2*, 120–124. [CrossRef]
18. Wang, H.; Tang, L.; Qiu, Q.; Chen, H. Assessing the Impacts of Urban Expansion on Habitat Quality by Combining the Concepts of Land Use, Landscape, and Habitat in Two Urban Agglomerations in China. *Sustainability* **2020**, *12*, 4346. [CrossRef]
19. Du, Y.; Qin, W.; Sun, J.; Wang, X.; Gu, H. Spatial Pattern and Influencing Factors of Regional Ecological Civilisation Construction in China. *Chin. Geogr. Sci.* **2020**, *30*, 776–790. [CrossRef]
20. Gai, M.; Wang, X.; Qi, C. Spatiotemporal Evolution and Influencing Factors of Ecological Civilization Construction in China. *Complexity* **2020**, *2020*, 8829144. [CrossRef]
21. Ye, Y.; Li, S.; Zhang, H.; Su, Y.; Wu, Q.; Wang, C. Spatial-Temporal Dynamics of the Economic Efficiency of Construction Land in the Pearl River Delta Megalopolis from 1998 to 2012. *Sustainability* **2017**, *10*, 63. [CrossRef]
22. Ye, Y.; Zhang, J.; Wang, T.; Bai, H.; Wang, X.; Zhao, W. Changes in Land-Use and Ecosystem Service Value in Guangdong Province, Southern China, from 1990 to 2018. *Land* **2021**, *10*, 426. [CrossRef]
23. Li, C.; Kuang, Y.; Huang, N.; Zhang, C. The long-term relationship between population growth and vegetation cover: An empirical analysis based on the panel data of 21 cities in Guangdong Province, China. *Int. J. Environ. Res. Public Health* **2013**, *10*, 660–677. [CrossRef] [PubMed]
24. National Bureau of Statistics of China. *China Statistical Yearbook*; China Statistics Press: Beijing, China, 2021.
25. Statistics Bureau of Guangdong Province. *Guangdong Statistical Yearbook*; China Statistics Press: Beijing, China, 2021.
26. Xu, F.; Wang, Z.; Chi, G.; Zhang, Z. The impacts of population and agglomeration development on land use intensity: New evidence behind urbanization in China. *Land Use Policy* **2020**, *95*, 104639. [CrossRef]
27. Liu, J.; Ning, J.; Kuang, W.; Xu, X.; Zhang, S.; Yan, C.; Li, R.; Wu, S.; Hu, Y.; Du, G.; et al. Spatio-temporal patterns and characteristics of land-use change in China during 2010–2015. *Acta Geogr. Sin.* **2018**, *28*, 16.
28. Seto, K.C.; Fragkias, M.; Guneralp, B.; Reilly, M.K. A Meta-Analysis of Global Urban Land Expansion. *PLoS ONE* **2011**, *6*, e23777. [CrossRef] [PubMed]
29. Song, M.; Wu, Y.; Chen, L. Does the land titling program promote rural housing land transfer in China? Evidence from household surveys in Hubei Province. *Land Use Policy* **2020**, *97*, 104701. [CrossRef]
30. Lai, Y.; Huang, G.; Chen, S.; Lin, S.; Lin, W.; Lyu, J. Land Use Dynamics and Optimization from 2000 to 2020 in East Guangdong Province, China. *Sustainability* **2021**, *13*, 3473. [CrossRef]
31. Ren, H.; Chen, H.; Li, L.; Li, P.; Hou, C.; Wan, H.; Zhang, Q.; Zhang, P. Spatial and temporal patterns of carbon storage from 1992 to 2002 in forest ecosystems in Guangdong, Southern China. *Plant Soil* **2013**, *363*, 123–138. [CrossRef]
32. Department of Water Resources of Guangdong Province. *Bulletin of Soil and Water Conservation of Guangdong Province*; Department of Water Resources of Guangdong Province: Guangzhou, China, 2020.
33. Fan, X.; Gu, X.; Yu, H.; Long, A.; Tiando, D.S.; Ou, S.; Li, J.; Rong, Y.; Tang, G.; Zheng, Y.; et al. The Spatial and Temporal Evolution and Drivers of Habitat Quality in the Hung River Valley. *Land* **2021**, *10*, 1369. [CrossRef]

34. Huang, J.; Tang, Z.; Liu, D.; He, J. Ecological response to urban development in a changing socio-economic and climate context: Policy implications for balancing regional development and habitat conservation. *Land Use Policy* **2020**, *97*, 104772. [CrossRef]
35. Wu, L.; Sun, C.; Fan, F. Estimating the Characteristic Spatiotemporal Variation in Habitat Quality Using the InVEST Model—A Case Study from Guangdong–Hong Kong–Macao Greater Bay Area. *Remote Sens.* **2021**, *13*, 1008. [CrossRef]
36. Verheyen, H.K. Legacies of the past in the present-day forest biodiversity: A review of past land-use effects on forest plant species composition and diversity. *Ecol. Res.* **2007**, *22*, 361–371.
37. Han, Y.; Kang, W.; Thorne, J.; Song, Y. Modeling the effects of landscape patterns of current forests on the habitat quality of historical remnants in a highly urbanized area. *Urban For. Urban Green.* **2019**, *41*, 354–363. [CrossRef]
38. Mengist, W.; Soromessa, T.; Feyisa, G.L. Landscape change effects on habitat quality in a forest biosphere reserve: Implications for the conservation of native habitats. *J. Clean. Prod.* **2021**, *329*, 129778. [CrossRef]
39. Sieber, A.; Uvarov, N.V.; Baskin, L.M.; Radeloff, V.C.; Bateman, B.L.; Pankov, A.B.; Kuemmerle, T. Post-Soviet land-use change effects on large mammals' habitat in European Russia. *Biol. Conserv.* **2015**, *191*, 567–576. [CrossRef]
40. Yang, J.; Li, S.; Lu, H. Quantitative Influence of Land-Use Changes and Urban Expansion Intensity on Landscape Pattern in Qingdao, China: Implications for Urban Sustainability. *Sustainability* **2019**, *11*, 6174. [CrossRef]
41. Berta Aneseyee, A.; Noszczyk, T.; Soromessa, T.; Elias, E. The InVEST Habitat Quality Model Associated with Land Use/Cover Changes: A Qualitative Case Study of the Winike Watershed in the Omo-Gibe Basin, Southwest Ethiopia. *Remote Sens.* **2020**, *12*, 1103. [CrossRef]
42. Song, S.; Liu, Z.; He, C.; Lu, W. Evaluating the effects of urban expansion on natural habitat quality by coupling localized shared socioeconomic pathways and the land use scenario dynamics-urban model. *Ecol. Indic.* **2020**, *112*, 106071. [CrossRef]
43. Nie, C.; Yang, J.; Huang, C. Assessing the Habitat Quality of Aquatic Environments in Urban Beijing. *Procedia Environ. Sci.* **2016**, *36*, 162–168. [CrossRef]
44. Santelmann, M.; Freemark, K.; Sifneos, J.; White, D. Assessing effects of alternative agricultural practices on wildlife habitat in Iowa, USA. *Agric. Ecosyst. Environ.* **2006**, *113*, 243–253. [CrossRef]
45. Sallustio, L.; De Toni, A.; Strollo, A.; Di Febbraro, M.; Gissi, E.; Casella, L.; Geneletti, D.; Munafo, M.; Vizzarri, M.; Marchetti, M. Assessing habitat quality in relation to the spatial distribution of protected areas in Italy. *J. Environ. Manag.* **2017**, *201*, 129–137. [CrossRef] [PubMed]
46. Zhang, X.; Song, W.; Lang, Y.; Feng, X.; Yuan, Q.; Wang, J. Land use changes in the coastal zone of China's Hebei Province and the corresponding impacts on habitat quality. *Land Use Policy* **2020**, *99*, 104957. [CrossRef]
47. He, J.; Huang, J.; Li, C. The evaluation for the impact of land use change on habitat quality: A joint contribution of cellular automata scenario simulation and habitat quality assessment model. *Ecol. Model.* **2017**, *366*, 58–67. [CrossRef]
48. Li, F.; Wang, L.; Chen, Z.; Clarke, K.C.; Li, M.; Jiang, P. Extending the SLEUTH model to integrate habitat quality into urban growth simulation. *J. Environ. Manag.* **2018**, *217*, 486–498. [CrossRef] [PubMed]
49. Tang, F.; Fu, M.; Wang, L.; Zhang, P. Land-use change in Changli County, China: Predicting its spatio-temporal evolution in habitat quality. *Ecol. Indic.* **2020**, *117*, 106719. [CrossRef]
50. Moreira, M.; Fonseca, C.; Vergílio, M.; Calado, H.; Gil, A. Spatial assessment of habitat conservation status in a Macaronesian island based on the InVEST model: A case study of Pico Island (Azores, Portugal). *Land Use Policy* **2018**, *78*, 637–649. [CrossRef]
51. De Simone, S.; Sigura, M.; Boscutti, F. Patterns of biodiversity and habitat sensitivity in agricultural landscapes. *J. Environ. Plan. Manag.* **2017**, *60*, 1173–1192. [CrossRef]
52. Li, M.; Zhou, Y.; Xiao, P.; Tian, Y.; Huang, H.; Xiao, L. Evolution of Habitat Quality and Its Topographic Gradient Effect in Northwest Hubei Province from 2000 to 2020 Based on the InVEST Model. *Land* **2021**, *10*, 857. [CrossRef]
53. Polasky, S.; Nelson, E.; Pennington, D.; Johnson, K.A. The Impact of Land-Use Change on Ecosystem Services, Biodiversity and Returns to Landowners: A Case Study in the State of Minnesota. *Environ. Resour. Econ.* **2011**, *48*, 219–242. [CrossRef]
54. Shobairi, S.O.R.; Li, M. Dynamic Modelling of VFC from 2000 to 2010 Using NDVI and DMSP/OLS Time Series: A Study in Guangdong Province, China. *J. Geogr. Inf. Syst.* **2016**, *08*, 205–223. [CrossRef]
55. Zheng, J.Y.; Yin, Y.H.; Li, B.Y. A new scheme for climate regionalization in China. *Acta Geogr. Sin.* **2010**, *65*, 3–12.
56. Kuang, W.; Liu, J.; Dong, J.; Chi, W.; Zhang, C. The rapid and massive urban and industrial land expansions in China between 1990 and 2010: A CLUD-based analysis of their trajectories, patterns, and drivers. *Landsc. Urban Plan.* **2016**, *145*, 21–33. [CrossRef]
57. Liu, J.; Liu, M.; Deng, X.; Zhuang, D.; Zhang, Z.; Luo, D. The land use and land cover change database and its relative studies in China. *J. Geogr. Sci.* **2002**, *12*, 275–282.
58. Jia, N.; Liu, J.; Kuang, W.; Xu, X.; Jing, N. Spatiotemporal patterns and characteristics of land-use change in China during 2010–2015. *J. Geogr. Sci.* **2018**, *28*, 547–562.
59. Tallis, H. *Natural Capital: Theory and Practice of Mapping Ecosystem Services*; Oxford University Press: Oxford, UK, 2011.
60. Sharp, R.; Chaplin-Kramer, R.; Wood, S.; Guerry, A.; Douglass, J. *InVEST User's Guide*; Stanford University: Stanford, CA, USA; University of Minnesota: Minneapolis, MN, USA; The Nature Conservancy: Arlington, VA, USA; World Wildlife Fund: Minneapolis, MN, USA, 2018.
61. Zhang, H.B.; Wu, F.E.; Zhang, Y.N.; Han, S.; Liu, Y.Q. Spatial and temporal changes of habitat quality in Jiangsu Yancheng wetland national nature reserve—Rare birds of China. *Appl. Ecol. Environ. Res.* **2019**, *17*, 4807–4821. [CrossRef]
62. Zhang, L.; Hu, N. Spatial Variation and Terrain Gradient Effect of Ecosystem Services in Heihe River Basin over the Past 20 Years. *Sustainability* **2021**, *13*, 11271. [CrossRef]

63. Wu, J.; Li, X.; Luo, Y.; Zhang, D. Spatiotemporal Effects of Urban Sprawl on Habitat Quality in the Pearl River Delta from 1990 to 2018. *Sci. Rep.* **2021**, *11*, 13981. [CrossRef]
64. Liu, H.; Lin, M.; Zhou, R.; Zhong, L. Spatial and temporal evolution of habitat quality in Guangdong-Hong Kong-Macao Greater Bay Area based on InVEST model. *Ecol. Sci.* **2021**, *40*, 82–91. (In Chinese)
65. Jiang, W.; Wu, J. Spatio-temporal evolution of habitat quality in Guangdong-Hong Kong-Macao Greater Bay Area based on regional GDP and population spatial distribution. *Acta Ecol. Sin.* **2021**, *41*, 1747–1757.
66. Chen, C.; Zhang, Q.; Yang, X.; Li, R.; Xin, C. Habitat Quality Assessment of Waterfowl Ecological Corridors in the Pearl River Delta Based on InVEST Model. *For. Environ. Sci.* **2021**, *37*, 25–30. (In Chinese)
67. Lu, Y.; Li, T.; Gong, J. Attribution of habitat quality in different geomorphological types in Guangdong Province. *Ecol. Sci.* **2022**, *41*, 24–32. (In Chinese)

land

MDPI

Article

Variations and Mutual Relations of Vegetation–Soil–Microbes of Alpine Meadow in the Qinghai-Tibet Plateau under Degradation and Cultivation

Yueju Zhang [1], Mingjun Ding [1,2], Hua Zhang [1,2,*], Nengyu Wang [1], Fan Xiao [1], Ziping Yu [1], Peng Huang [1] and Fu Zou [1]

[1] Key Laboratory of Poyang Lake Wetland and Watershed Research, Ministry of Education, School of Geography and Environment, Jiangxi Normal University, Nanchang 330022, China; 2020zyj@jxnu.edu.cn (Y.Z.); dingmj@jxnu.edu.cn (M.D.); 202040100085@jxnu.edu.cn (N.W.); xiaofan2019@jxnu.edu.cn (F.X.); 202040100086@jxnu.edu.cn (Z.Y.); huangpeng2021@jxnu.edu.cn (P.H.); zoufu@jxnu.edu.cn (F.Z.)

[2] Jiangxi Provincial Key Laboratory of Poyang Lake Comprehensive Management and Resource Development, Jiangxi Normal University, Nanchang 330022, China

* Correspondence: zhangh2013@jxnu.edu.cn

Abstract: Artificial cultivation had been applied to recover the meadow suffering from serious degradation in the Qinghai–Tibet Plateau. Studies focusing only on the changes in vegetation, soil and microbes along the meadow degradation were insufficient, and artificial cultivation as an important part of succession was always neglected. Here, the variables of vegetation, soil, and soil bacteria are surveyed in four types of alpine meadow in the protected lands of the Qinghai–Tibet Plateau: intact alpine meadow (IAM), moderate degradation alpine meadow (MDAM), extreme degradation alpine meadow (black soil beach (BSB)), and artificial alpine grassland (AAG). The results indicated that degradation and cultivation significantly changed the characteristics of the vegetation community, physicochemical features of the soil, and soil bacterial community diversity. Soil bacteria took a considerably longer time to adapt to degradation and cultivation than vegetation and soil. Compared to IAM and BSB, ADAM and AAG had more specific bacteria identified by ANOVA and LEfSe analysis, implying an unstable state. Combined with vegetation and soil variables, it was speculated that the unstable AAG was not significantly improved from the degraded meadow, and also lagged significantly compared to IAM. Correlation analysis revealed that aboveground biomass, species richness, vegetation coverage, SOC, C/N, BD, WC, and pH were significantly associated with bacterial diversity under community level. Aboveground biomass was an effective indicator for soil bacterial gene copies. Redundancy analysis demonstrated that the soil bacterial community is mainly regulated by the vegetation coverage, Gleason index, Simpson index, TN, TP, and pH under phylum and genus level. Partial mantel test analysis indicated that the physicochemical features of the soil were the most important factor correlating with the soil bacterial community along the degradation and cultivation, compared to other environmental factors.

Keywords: alpine meadow; the Qinghai–Tibet Plateau; vegetation community characteristics; soil physicochemical features; soil bacterial community; degradation; cultivation

Citation: Zhang, Y.; Ding, M.; Zhang, H.; Wang, N.; Xiao, F.; Yu, Z.; Huang, P.; Zou, F. Variations and Mutual Relations of Vegetation–Soil–Microbes of Alpine Meadow in the Qinghai-Tibet Plateau under Degradation and Cultivation. *Land* **2022**, *11*, 396. https://doi.org/10.3390/land11030396

Academic Editors: Shicheng Li, Chuanzhun Sun, Qi Zhang, Basanta Paudel and Lanhui Li

Received: 11 February 2022
Accepted: 5 March 2022
Published: 8 March 2022

1. Introduction

As the zonal vegetation types, alpine meadows and steppe cover more than 70% of the total area of the Qinghai–Tibet Plateau (QTP) [1]. They not only support livelihoods for the local people, but also provide a significant mass of ecosystem services, such as carbon storage, erosion control, and climate regulation from local to regional scales [2]. Sustained by global climate change and intense human activity, alpine meadows and steppe have been subjected to severe soil degradation [1,3]. The alpine meadows accounting for 38%

of the grassland area and covering more than 700,000 km^2 in the QTP provide greater biodiversity, productivity and are more sensitive to the soil degradation [4,5]. Therefore, the degradation of the alpine meadow can cause a greater loss of biomass and productivity, which will produce a profound effect on local livestock and the regional climate. It is worth noting that more than 30% of alpine meadows have experienced degradation or severe degradation in recent decades, which has been attracting a lot of interest [6].

The changes in vegetation community characteristics directly mirror the degradation of the alpine meadow. Species composition changes, a decline in diversity, and biomass decrease always accompany soil degradation [4,7]. Reduced vegetation coverage resulted in increasing availability of light [8], which decreases soil moisture and causes a ripple effect, such as increases in soil pH and bulk density [9,10], organic carbon and total nitrogen loss [1,11]. Soil microorganisms facilitate the release of nutrients, decomposition of organic matter, and participation in the cycle of carbon and nitrogen [12]. Their short life cycle produces extraordinary sensitivity to the microenvironment, which results in their terrific response to environmental stress and ecological change, especially in the alpine meadow [9,13]. Previous studies have proven that microbial community composition changes accompany soil degradation or degraded patch formation [13,14].

The changes in vegetation community characteristics, soil properties and multifunctionality with the degradation of the alpine meadow have been fully explored in recent decades [5,7,15–20], while variations in soil microorganisms under soil degradation gained preliminary recognition [21]. The extremely degraded alpine meadows, known as "black beach" are always transformed into artificial grassland to improve grass productivity and relieve the grazing pressure on the natural meadow [22,23]. However, as a significant improvement for alpine meadow degradation artificial cultivation was always neglected in previous studies [6,9]. This is not conducive to fully and accurately understanding the changing rules of soil factors in the degradation and cultivation of alpine meadow. Additionally, literature has emerged that offers contradictory findings about similar studies; for example, Luo et al. [24] believed that meadow degradation had no effect on the alpha diversity of soil bacteria, whereas Li et al. [13] found that there was significant change in the alpha diversity during meadow degradation; it was suggested that both vegetation and soil environmental factors affected the composition of the soil microbial community during alpine meadow degradation [9], while vegetation factors were proven to have no effect on the soil bacterial community in alpine meadow [13]. Furthermore, the relationships between soil microbes and factors under different taxonomic levels were always neglected in previous studies. Therefore, more research needs to be executed to thoroughly clarify the change and coupling of environmental factors relating to alpine meadow degradation and artificial cultivation.

This study aimed to determine the changes and paired relations of vegetation–soil–microbes during the degradation and artificial cultivation of alpine meadow. Specifically, we: (1) ascertained the variations in vegetation community characteristics and soil features relating to alpine meadow degradation and artificial cultivation; (2) explored the changes in composition, predicted function, and diversity of soil bacteria; (3) evaluated the paired relations of vegetation–soil–microbes and compared the importance of different environmental factors to regulate the bacterial community under different taxonomic levels. This study provides an important opportunity to advance the understanding of vegetation–soil–microbes relationships in the alpine meadow during degradation and cultivation, and offers some insights for the restoration and management of degraded alpine meadow on the QTP.

2. Materials and Methods

2.1. Sampling Area

The sampling sites were scattered in Dalag County (98°15′29″~100°32′41″ E to 32°36′42″~34°15′20″ N, 4200 m ASL), and situated on the southern part of the source area of the Yellow River and the hinterland of the Qinghai–Tibet Plateau, China (Figure 1).

The area is characteristic of the alpine sub-humid plateau climate, with an annual mean precipitation and temperature of 540.6 mm and −1.3 °C, respectively. Dalag County is one of the typical alpine meadow regions on the Qinghai–Tibet Plateau and is one of the seriously degraded meadow areas on the Yellow River source [25]. Typical vegetation types, including intact alpine meadow (IAM), moderately degraded meadow (MDAM), extremely degraded meadow (black soil beach (BSB)), and artificial alpine grassland (AAG), were adopted. According to the field conditions and previous study [1], the intact alpine meadow (IAM) featured >90% vegetation coverage, averages 5 cm tall, and >80% edible forage coverage; characteristics of approved MADM included 50–70% vegetation coverage and 20–50% edible forage coverage; the vegetation and edible forage coverage of the BSB were below 50% and 5%, respectively. Selected AAG was mainly covered by *Elymus nutans*, and distributed flat land (Table S1).

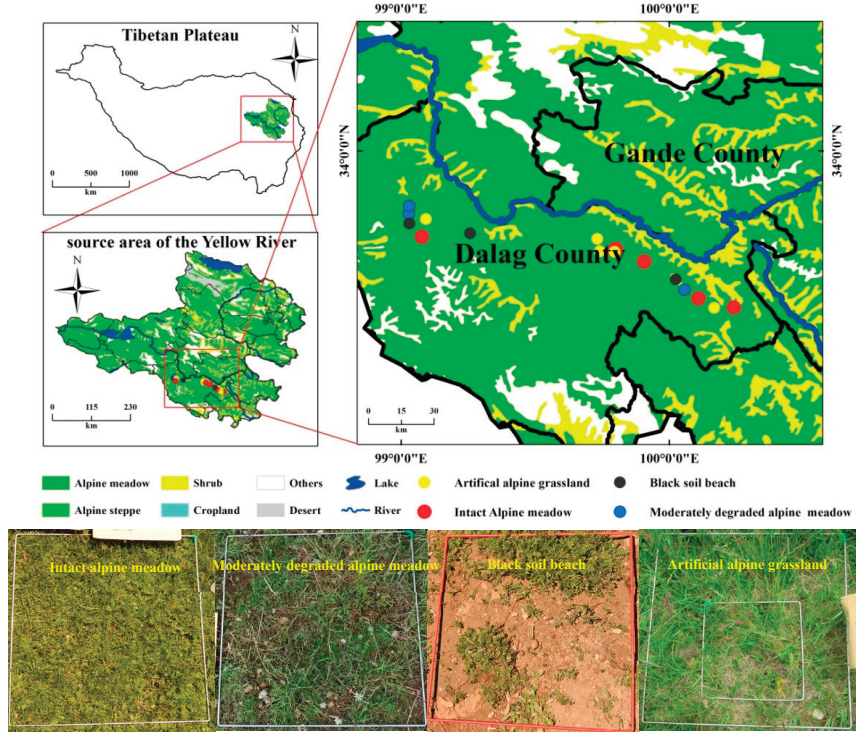

Figure 1. Study sites in the three-river source area of the Qinghai–Tibet Plateau. The border of the Qinghai–Tibet plateau quoted from Zhang et al. [26]; the border of the Three-River-Source National Park quoted from Wei (2018) [27].

2.2. Vegetation Investigation and Soil Sampling

In August 2019, 6–11 typical plots (50 × 100 m) were applied to each style with different degradation and cultivation levels, and three random quadrats (50 × 50 cm) (replicates) about 20 m apart were arranged within each plot. Information including the slope and altitude in each plot was also recorded. In addition, the vegetation coverage, species name, coverage, richness, and height in each quadrat were investigated. Aboveground biomass was also collected and weighted after drying at 65 °C for 24 h. Furthermore, the Shannon–Wiener index, Simpson index, Gleason index, and Pielou index were calculated in terms of the established protocol [28]. After the vegetation investigation, two steel cutting rings (5 cm diameter, 100 cm^3 volume) were employed to determine the soil bulk density and moisture in each quadrat (0–10 cm). One homogenized soil sample from each quadrat

was collected by soil anger with 3.5 cm diameter (0–10 cm). The homogenized samples were sieved (<2 mm) to remove stones, roots and other materials. The sieved sample was divided into two parts; one part was air-dried for physicochemical analysis, and the other part was stored at −20 °C. Three soil samples from three quadrats in the same plot were homogenized to one sample for DNA extraction.

2.3. Soil Physicochemical Analyses

The collected soil was air-dried and texture analyses (>63 mm (sand), 4–63 mm (silt), <4 mm (clay)) were performed using a Mastersizer 2000 laser diffractometer that was capable of analyzing particles with sizes between 0.02 and 2000 mm [29]; soil pH and electrical conductivity (EC) were measured with a pH and conductivity meter in a soil-to-water ratio of 1:2.5; soil organic carbon (SOC; g kg^{-1}) was determined using the dichromate oxidation method [30]; total nitrogen (TN, g kg^{-1}) was measured by the Kjeldahl method [31]; soil total phosphorus (TP) and potassium were determined colorimetrically after wet digestion with H_2SO_4 and $HClO_4$ [6]; soil total potassium (TK) was determined by the flame emission method with a flame photometer [9].

2.4. Soil DNA Extraction and Sequencing

Total genomic DNA in the soil was extracted with the E.Z.N.A.® soil DNA Kit (Omega Bio-tek, Norcross, GA, USA) following the manufacturer's instructions. The metagenomic DNA was utilized as a template for quantitative PCR using the Applied Biosystems 7500 sequence detection equipment, in which SYBR green is used to identify the amplicons quantitatively. To check DNA extract 1% agarose gel was used. The universal primers 338F (5′-ACTCCTACGGGAGGCAGCAG-3′) and 806R (5′-GGACTACHVGGGTWTCTAAT-3′) were adopted to amplify the hypervariable region V3-V4 of the bacterial 16S rRNA gene [32]. The PCR amplification was executed as follows: denaturizing for 3 min at 95 °C, followed by 27 cycles of denaturing at 95 °C for 30 s, annealing 30 s at 55 °C, extension 45 s at 72 °C, single extension for 10 min at 72 °C, and ending at 4 °C. After triplicate PCR reactions, the product was extracted from 2% agarose gel, and purified with the AxyPrep DNA Gel Extraction Kit (Axygen Biosciences, Union City, CA, USA). Purified amplicons were pooled in equimolar and paired-end sequenced (2 × 300 bp) on an Illumina MiSeq platform (Illumina, San Diego, CA, USA), and sequenced following the standard protocols by Majorbio Bio-Pharm Technology Co., Ltd. (Shanghai, China). The raw reads were deposited into the NMDC Sequence Read Archive (SRA) database (Accession Number: NMDC10017903).

2.5. MiSeq Processing and Bioinformatics Analysis

The original DNA fragments were demultiplexed, quality-filtered by Trimmomatic and FLASH-merged as follows: reads less than 50 bp and containing ambiguous characters were eliminated; reads that could not be assembled were also discarded. Operational taxonomic units (OTUs) with ≥97% similarity were clustered using UPARSE version 7.1 software [33]. Each OTUs was examined by RDP Classifier according to the SSU-rRNA SILVA database with a confidence threshold of 0.7 [9]. The samples were normalized by standardizing with the least data. The QIIME program was used to calculate microbial community diversity indices. Ultimately, a total of 1,530,555 high-quality, chimera-free 16S gene sequences ranged from 41,054 to 61,867 per sample were obtained.

2.6. Statistical Analysis

The descriptive statistics were compiled to form a multi-element database using PASW (IBM Inc., Armonk, NY, USA). A one-way analysis of variation (ANOVA) with Duncan's method was used to compare the data concerning the vegetation and soil bacterial community characteristics and soil physicochemical features among different degradations and under cultivation. Analyses of paired relationships among vegetation community characteristics, soil bacterial community characteristics, and soil physicochemical features were performed using Pearson correlations, which were visualized by Originpro 21 (Origin-

Lab Corporation, Northampton, MA, USA). A Soil Texture Triangle coordinate plot was also performed in Originpro 21. The ANOVA with the least significant difference (LSD) multiple comparisons post-hoc test was applied to characterize the differences in the relative abundance of the same bacteria among different degradations and cultivation. Bacterial data were analyzed by the principal coordinate analysis (PCoA) with Bray–Curtis dissimilarity. Specific species among different groups were identified by using a linear discriminant analysis effect size (LEfSe) method [9]. The effects of vegetation community characteristics and soil physicochemical features on the soil bacterial composition based on different ecological scales were tested by redundancy analysis (RDA) and the Monte Carlo Permutation test, and executed in the vegan package of R [33]. Independent variables with VIF < 10 were analyzed by RDA [11]. Furthermore, the correlations between soil bacterial community Unweighted or Weighted uniFrac distance matrices and the environmental variables distance matrices were measured by using a partial Mantel test in R (vegan package). The bacterial community functions were analyzed and predicted using FAPROTAX (http://www.zoology.ubc.ca/louca/FAPROTAX (accessed on 5 November 2021).

3. Results

3.1. Variations in Vegetation and Soil Variables under Degradation and Cultivation

With the degree of meadow degradation increasing, the frequency and importance value of *Cyperaceae* and *Gramineae* are decreasing, *Asteraceae* and other toxic and noxious species are gradually occupying a principal position, and Gramineae plants such as *Elymus nutans Griseb*, *Poa pratensis* L., and *Puccinellia tenuiflora (Griseb.) Scribn. et Merr*. are the preferred species for artificial cultivation (Table S1). Specially, the vegetation characteristics varied among different levels of degradation and cultivation (Table 1). The coverages are significantly decreased from IAM to BSB, and the AAG coverage is equivalent to the MDAM coverage. The Gleason index is gradually and significantly decreasing in the order of IAM (2.01), MDAM (1.76), BSB (1.21), and AAG (0.89). In terms of Shannon–Wiener index, there is no significant difference between IAM (1.90) and BSB (1.83), and it is significantly higher in MDAM (2.10) and lower in AAG (1.56), while the opposite result is found for the Simpson index. The Pielou indexes do not significantly differ among MDAM (0.80), BSB (0.83), and AAG (0.83). The above-ground biomass of IAM is 253.02 g m^{-2}, which is 3.80, 5.34, 2.87 times higher than that of MDAM (66.51 g m^{-2}), BSB (47.38 g m^{-2}), and AAG (88.10 g m^{-2}).

As for soil physiochemical features, what stands out in the table is the difference between IAM and other types of meadow. The pH in IAM is significantly lower than other types of meadow, while EC, BD, WC, TOC, TN, TP are significantly higher. As two stages of degradation, the levels of all soil physicochemical features in MDAM and BSB do not show significant differences. Closer inspection of the Table 1 shows that some soil physicochemical features, such as EC, WC and TP in AAG, present certain advantages over the degraded meadows (MDAM and BSB). In addition, although the content of TOC in AAG does not show significant differences from the degraded meadows, its mean value (4.09 g kg^{-1}) is slightly higher. It is noteworthy that the content of TP (821.63 mg kg^{-1}) is comparable to the content of IAM (811.58 mg kg^{-1}), and significantly higher than that of MDAM (643.40 mg kg^{-1}) and BSB (697.55 mg kg^{-1}). The content of TK maintains homogeneity among different degradations and cultivation. The results, as shown in Figure S1, indicate that the soil particle size distributions of IAM and AAG are more concentrated than those of MDAM and BSB, being imprisoned in the frames of sandy loam, loam, and silty loam as classified by the international soil classification system.

Table 1. Calculated statistics for vegetation–soil–bacteria variables of the alpine meadow under degradation and cultivation (means ± the standard deviation).

	Variables	IAM	MDAM	BSB	AAG
Vegetation	Coverage (%)	96.42 ± 2.34 a	44.21 ± 15.22 b	31.67 ± 12.13 c	55.56 ± 10.97 b
	Gleason index	2.01 ± 0.31 a	1.76 ± 0.30 b	1.21 ± 0.29 c	0.89 ± 0.27 d
	Shannon–Wiener index	1.90 ± 0.20 a	2.10 ± 0.17 b	1.83 ± 0.18 a	1.56 ± 0.16 c
	Simpson index	0.16 ± 0.04 a	0.11 ± 0.02 b	0.17 ± 0.05 a	0.26 ± 0.05 c
	Pielou index	0.74 ± 0.05 a	0.80 ± 0.03 b	0.83 ± 0.09 b	0.83 ± 0.08 b
	Aboveground biomass (g m^{-2})	253.02 ± 53.80 a	66.51 ± 78.43 b	47.38 ± 30.93 c	88.10 ± 23.39 b
Soil	pH	5.65 ± 0.27 a	6.81 ± 0.58 b	6.67 ± 0.68 b	6.58 ± 0.66 b
	EC (μS cm^{-1})	192.87 ± 112.48 a	100.03 ± 72.68 c	136.11 ± 55.72 bc	144.53 ± 79.13 abc
	BD (g cm^{-3})	0.68 ± 0.20 a	1.20 ± 0.14 b	1.08 ± 0.16 b	1.13 ± 0.19 b
	WC	0.86 ± 0.26 a	0.26 ± 0.09 c	0.37 ± 0.10 bc	0.43 ± 0.15 b
	TOC (g kg^{-1})	9.12 ± 3.04 a	3.17 ± 0.70 b	3.74 ± 1.19 b	4.09 ± 1.04 b
	TN (%)	0.74 ± 0.25 a	0.30 ± 0.06 b	0.40 ± 0.22 b	0.40 ± 0.07 b
	TP (mg kg^{-1})	811.58 ± 147.31 a	643.40 ± 143.75 b	697.55 ± 130.62 b	821.63 ± 226.64 a
	TK (%)	1.95 ± 0.22 a	2.24 ± 0.34 a	2.13 ± 0.34 a	2.08 ± 0.31 a
Soil bacteria	Sobs ($\times 10^{-3}$)	2.70 ± 0.20 a	2.77 ± 0.11 ab	3.07 ± 0.12 c	3.04 ± 0.21 bc
	Shannon	6.28 ± 0.22 a	6.50 ± 0.05 ab	6.62 ± 0.06 b	6.67 ± 1.15 b
	Simpson ($\times 10^{-3}$)	7.65 ± 6.09 a	3.87 ± 0.22 a	3.93 ± 0.35 a	3.49 ± 1.02 a
	Ace ($\times 10^{3}$)	3.74 ± 0.30 a	3.87 ± 0.15 ab	4.24 ± 0.15 b	4.06 ± 0.26 ab
	Chao ($\times 10^{3}$)	3.73 ± 0.29 a	3.87 ± 0.12 a	4.25 ± 0.11 b	4.04 ± 0.24 ab
	Coverage (%)	97.40 ± 0.23 a	97.32 ± 0.11 ab	97.04 ± 0.09 b	97.27 ± 0.21 ab
	Shannon even	0.79 ± 0.02 a	0.82 ± 0.00 b	0.82 ± 0.00 b	0.83 ± 0.01 b
	Simpson even	0.06 ± 0.02 a	0.09 ± 0.01 ab	0.08 ± 0.01 ab	0.10 ± 0.03 b
	Quantity ($\times 10^{9}$ copies g^{-1})	27.30 ± 8.02 a	17.58 ± 1.03 b	23.01 ± 10.17 b	4.32 ± 0.97 c

IAM, intact alpine meadow; MDAM, moderately degraded alpine meadow; BSB, black soil beach; AAG, artificial grassland; EC, electrical conductivity; BD, bulk density; WC, water content; TOC, total organic carbon; TN, total nitrogen; TP, total phosphorus; TK, total potassium. Different lowercase letters in the same row indicate significant differences ($p < 0.05$).

3.2. Changes in Soil Bacterial Diversity, Composition, Structure, and Predicted Functions

In general, the response of soil bacterial alpha diversity indexes to degradation and cultivation lags behind soil and vegetation variables. Most indexes, except for Simpson's diversity index in IAM, are significantly lower than those of other types of alpine meadow. Similarly to the soil physicochemical features, most of the indexes, except for the Sobs and Chao richness index between MDAM and BSB, do not show significant differences. Sobs and Chao richness in MDAM is comparable to that in IAM, but significantly lower than that in BSB. There is a remarkable result that the alpha diversity indexes in AAG have no significant difference from the degraded meadows (MDAM and BSB). The gene copy number in IAM (2.73×10^{10} copies g^{-1}) is observed to be significantly higher than other types of alpine meadow, and the gene copy number in AAG is the lowest (4.32×10^{10} copies g^{-1}). The result, as presented in Figure 2, demonstrate that the four types of alpine meadow significantly differed from each other based on PCoA with the Bray–Curtis distance (ANOSIM: R = 0.670, $p = 0.001$; Adonis: $R^2 = 0.550$, $p = 0.001$). It can also be seen that the bacterial communities in MDAM and BSB have greater similarity, separately from AAG and IAM.

The bacterial composition and their significant differences at the phylum and genus level (relative abundance > 0.01%) are visually presented in Figure 3. At the phylum level, Proteobacteria is the most abundant in all samples, and the average abundance is not significantly different among different degradations and cultivation, but its average abundance in MDAM (21.38%) is significantly lower than that in IAM (29.10%), BSB (26.93%), and AAG (34.93%). The other phyla with relative abundance >0.01% follow the order: Actinobacteria (10.30–30.47%), Acidobacteria (18.10–24.99%), Chloroflexi (7.72–12.59%), Gemmatimonates (2.44–6.31%), Bacteroidetes (1.80–4.79%), Firmicutes (0.70–6.18%), Rolubacteria (1.40–3.11%), Verrucomicrobia (1.13–2.14%), Nitrosporea (0.76–1.47%), and Patescibacteria (0.27–1.47%). The abundance of some phyla such as Actinobacteria, Chloroflexi, Gem-

matimonates, Bacteroidetes among different groups present significant differences, and higher abundances are identified in AAG and MDAM (Figure 3c). At the genus level, representatives of 44 common genera (56.89–64.71%) are ranked based on the average abundance >0.01. The most interesting aspect is that most genera among the four groups exhibit significant variability in their abundance (Figure 3b). In addition, genera abundance in IAM and MDAM present more significant differences, whereas genera abundance in BSB and MDAM demonstrate less significant variations (Figure 3d).

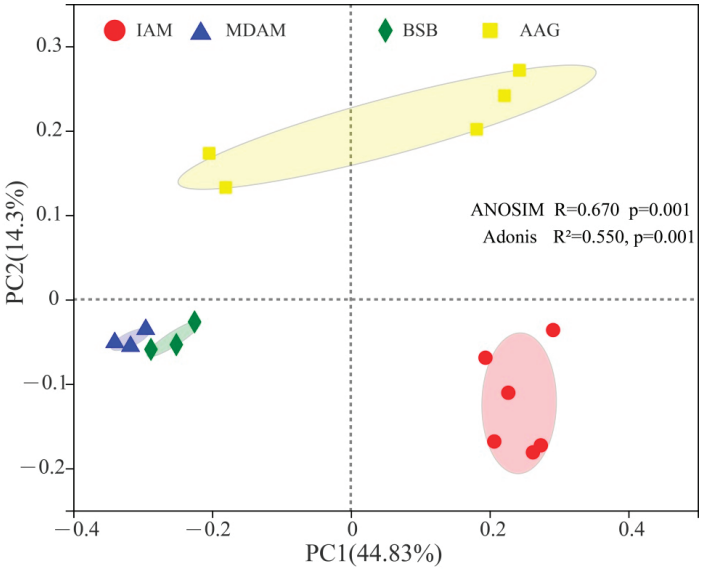

Figure 2. Principal coordinates analysis (PCoA) of bacterial communities in the alpine meadows with different groups based on the Bray–Curtis distances. IAM, intact alpine meadow; MDAM, moderately degraded alpine meadow; BSB, black soil beach; AAG, artificial grassland.

In terms of bacterial structure, IAM has more unique bacteria, followed by AAG, BSB, and MDAM from OTU level to phylum level (Table 2). Moreover, IAM and AAG have more common bacteria, accounting for 59.95%, 26.89%, 19.59%, 14.57%, 12.57%, 7.32, and 3.33% of the total common bacteria, respectively, from OTU level to phylum level. The abundance of common bacteria in different groups is also different. The linear discriminant analysis effect size (LEfSe) is applied to further identify the characterization of the different abundances and their associated categories among different groups (Figure 4). Forty-five bacteria are identified with LDA (linear discriminant analysis) scores over 4.0, exhibiting significant differences among different groups. Most specialized bacteria are significantly numerous in MDAM (15 bacteria) and AAG (17 bacteria), while the minority are numerous in IAM (7 bacteria) and BSB (6 bacteria). More specifically, Gemmatimonadetes (phylum, class, order, family), norank_f_Gemmatimonadaceae (genus), Bacteroidetes (phylum, class), Solibacterales (order), Solibacterales_Subgroup_3 (family), Subgroup_7 (order), and norank_o_Subgroup_7 (family, genus) are numerous in AAG; Gaiellales (order), norank_o_Gaiellales (family, genus), norank_c_Actinobacteria (family, order, genus), Chloroflexi (phylum, class), KD4-96 (class), norank_c_KD4-96 (order, family, genus) are abundant in BSB; Bacilli (class), Bacillales (order), Bacillaceae (family), Bacillus (genus) have the maximum abundance in IAM; Actinobacteria (phylum, class) concentrate in BSB.

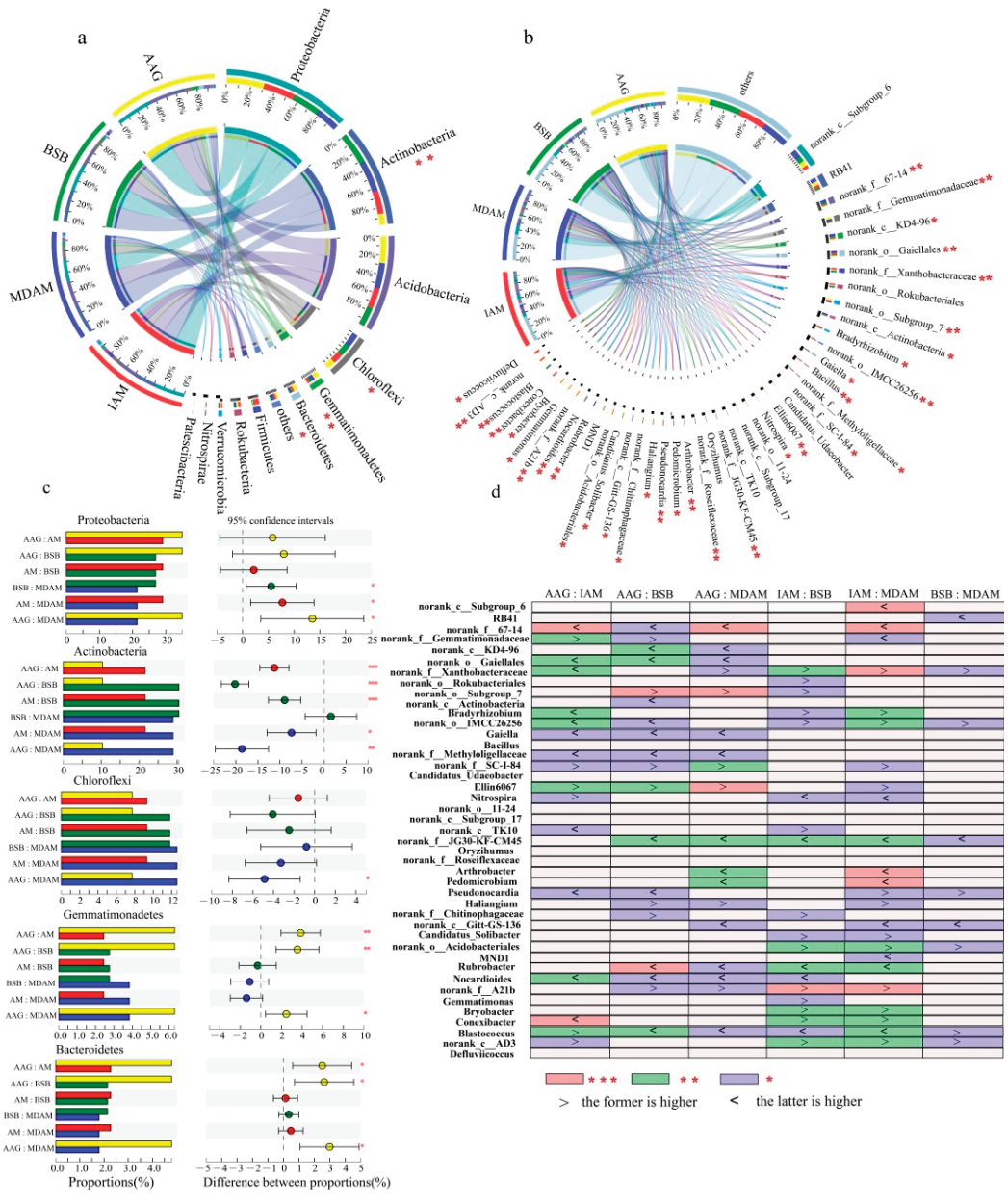

Figure 3. The relative abundance of the dominant bacterial (**a**,**b**) at the phyla and genus level and their composition variations (**c**,**d**) in alpine meadows with different groups. Phyla or genera with a relative abundance of less than 0.01 in all samples were classified as others. *** <0.001; ** <0.01; * <0.05. IAM, intact alpine meadow; MDAM, oderately degraded alpine meadow; BSB, black soil beach; AAG, artificial grassland.

Table 2. Distribution of total bacteria, unique, and common in different groups.

Levels	IAM	MDAM	BSB	AAG	Common	AAG&IAM
Phylum	35 (2)	32 (0)	34 (0)	37 (1)	30	1
Class	98 (3)	88 (1)	94 (1)	104 (2)	82	6
Order	251 (16)	214 (2)	232 (4)	268 (11)	191	24
Family	429 (34)	347 (4)	379 (4)	439 (19)	302	44
Genus	748 (60)	589 (12)	654 (13)	773 (37)	485	95
Species	1643 (138)	1271 (26)	1408 (45)	1713 (89)	978	263
OTU	5477 (997)	4092 (254)	4567 (283)	6072 (636)	2070	1241

The number in brackets indicates the unique bacteria in different groups; IAM, intact alpine meadow; MDAM, moderately degraded alpine meadow; BSB, black soil beach; AAG, artificial grassland.

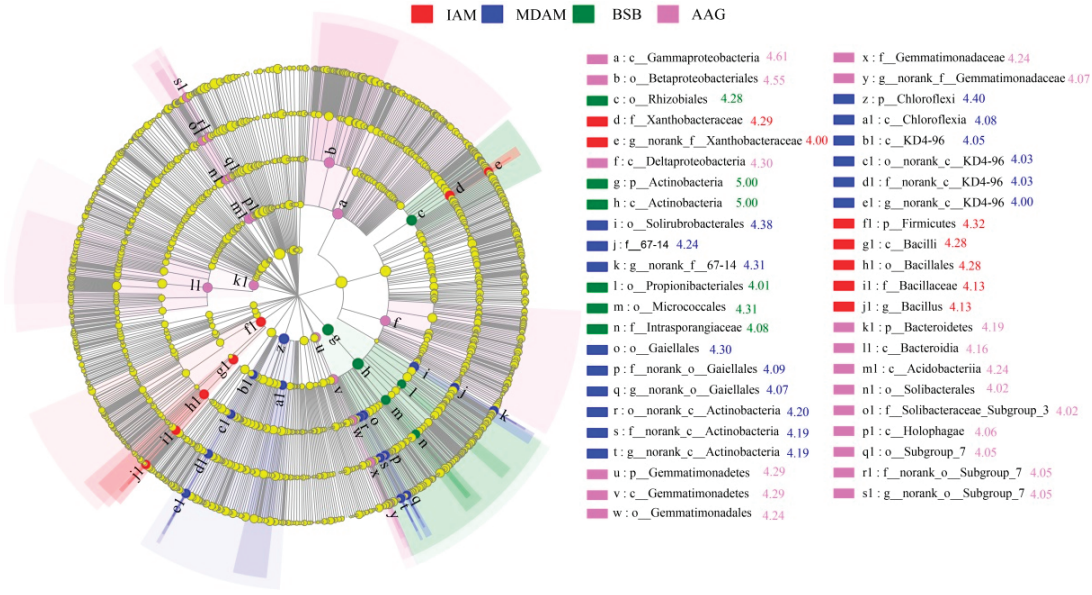

Figure 4. Linear discriminant analysis effect size (LEfSe) analysis of microbial abundance in different types of alpine meadow, identified with a threshold value of 4.0. The LDA scores are listed after the legend. IAM, intact alpine meadow; MDAM, moderately degraded alpine meadow; BSB, black soil beach; AAG, artificial grassland.

The function proportions of the bacteria in soils among different groups are predicated based on the Functional Annotation of Prokaryotic Taxa (FAPROTAX 1.2.4) database. The functions related to the carbon and nitrogen cycle, human pathogens, and plant pathogens are main interests in this study. The proportions of all selected functions except 'plant_pathogen', 'human_pathogens', 'nitrate_denitrification' are significantly different among different groups (Figure 5). With the degradation of the alpine meadow, chemoheterotrophy and aerobic chemoheterotrophy show a significant upward trend, and nitrate reduction shows a trend of first increasing then decreasing. AAG shows more remarkable advantages in nitrification and aerobic ammonia oxidation, and IAM exhibits great strength in nitrogen fixation. AAG is roughly comparable to IAM in aerobic ammonia oxidation, phototrophy, photoautotrophy, nitrate respiration, and methanotrophy, but has significant advantages over degraded meadows.

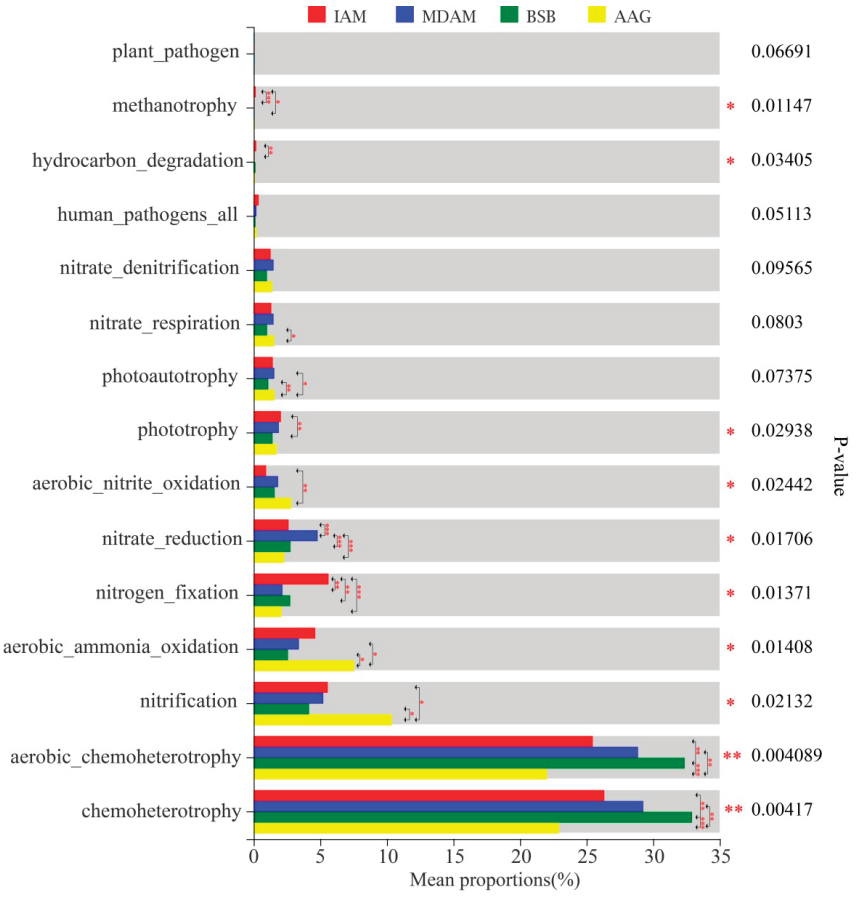

Figure 5. Comparison of the predicted microbial functions among different types of alpine meadows based on the FAPROTAX database (*** $p < 0.001$; ** $p < 0.01$; * $p < 0.05$); IAM, intact alpine meadow; MDAM, moderately degraded alpine meadow; BSB, black soil beach; AAG, artificial grassland.

3.3. Relationships between Microbial Community and Environmental Variables under Different Taxonomic Level

The inter- and intra-relationships among vegetation–soil–bacteria variables are shown in Figure 6. It is apparent that intra-group correlations are stronger than inter-group correlations. The inter-relationships should be more concerned. The vegetation diversity indexes do not show significant correlation with the corresponding microbial alpha diversity indexes, except richness indexes. A significant negative correlation was found between species richness, the Gleason index for vegetation community, and the Sobs and Chao richness index for microbial communities. In addition, there is a significant correlation between vegetation above-ground biomass, and most microbial alpha diversity indexes, indicating that it is an important impact factor at the microbial community scale. Closer inspection of the figure shows that gene copy number has a significant positive correlation with vegetation above-ground biomass. Further analysis reveals that soil pH, WC, and C/N are important factors significantly correlating with microbial alpha diversity indexes. Meanwhile, the Shannon and Simpson diversity index and the Shannon evenness index are the most sensitive factors significantly correlating with the soil physicochemical features. Gene copy number has a significant positive correlation with TN, TOC and WC, and a negative correlation with soil BD and pH. Vegetation coverage and above-ground biomass

are closely related to the majority of soil physicochemical features. Together, these results provide important insights that soil pH, WC, TN, TOC, C/N, BD, vegetation coverage, and above-ground biomass are the important factors closely associated with microbial diversity and biomass at the community level.

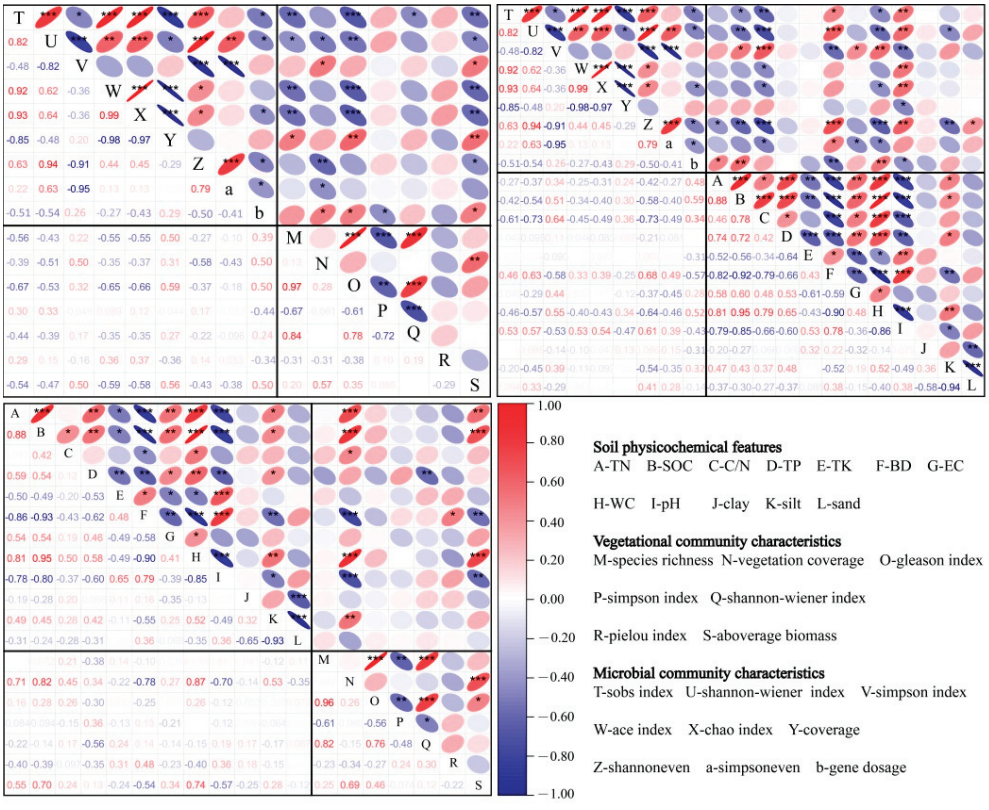

Figure 6. Correlation analysis among soil physicochemical features, vegetation community characteristics, and microbial community characteristics of the alpine meadow. *** $p < 0.001$; ** $p < 0.01$; * $p < 0.05$. IAM, intact alpine meadow; MDAM, moderately degraded alpine meadow; BSB, black soil beach; AAG, artificial grassland; EC, electrical conductivity; BD, bulk density; WC, water content; TOC, total organic carbon; TN, total nitrogen; TP, total phosphorus; TK, total potassium.

The effects of the environmental variables on the microbial community are explained by a redundancy analysis (RDA) based on the phylum and genus level (Figure 7). At the phylum level, two coordinate axes explain 47.12% and 18.70% of the variation, respectively. Gleason and Simpson index of the vegetation community and TP are the key factors affecting the composition of bacterial communities significantly. At the genus level, two coordinate axes only represent 27.94% and 16.67% of the variation. Coverage and the Simpson index of the vegetation community and TN, TP, and pH in soils were significantly associated with bacterial communities. Furthermore, the partial Mental test was applied to explore the relationships between environmental matrixes and bacterial communities at the phylum and genus level (Table 3). Soil physicochemical features are significantly associated with bacterial community composition across all samples. In contrast, bacterial community distance is not significantly correlated with vegetation community characteristics, topographic factors, and the combination of vegetation community characteristics and topographic factors when soil physicochemical features are used as a control based on

Weighted UniFrac distance. Therefore, minor differences in bacterial community compositions are generally observed among pairs of samples with the close soil environment. It is also apparent that vegetation community characteristics have closer relationships with bacterial communities than the topographic factors (Table 3). Closer inspection of the table shows that the correlations between soil physicochemical features, vegetation community characteristics and bacterial community are more pronounced at the genus level than that at the phylum level, but the opposite result is detected from the correlation between the topographic factors and bacterial community.

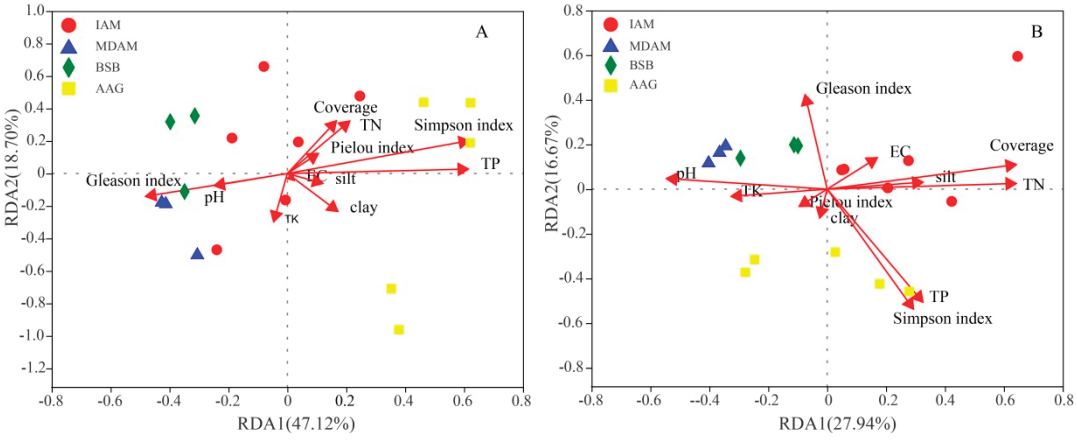

Figure 7. Redundancy analysis (RDA) of soil microbial communities and environmental factors based on phyla level (**A**) and genus level (**B**) in alpine meadow. The red arrows represent the direction and significance of environmental factors with microbial community structures. IAM, intact alpine meadow; MDAM, moderately degraded alpine meadow; BSB, black soil beach; AAG, artificial grassland; EC, electrical conductivity; TN, total nitrogen; TP, total phosphorus; TK, total potassium.

Table 3. The results of correlation between soil bacterial community UniFrac distance and environmental variables using partial Mantel test analysis under phyla level and genus level.

		Control Factor	Weighted UniFrac Distance		Unweighted UniFrac Distance	
			r	*p*-Value	r	*p*-Value
phyla	S	V + T	0.4515	0.004	0.2910	0.011
	V	S + T	0.1339	0.144	0.2246	0.033
	T	S + V	−0.0852	0.785	0.2543	0.008
	V + T	S	−0.0335	0.592	0.3211	0.005
	S + T	V	0.3103	0.011	0.3504	0.004
	S + V	T	0.4664	0.001	0.3420	0.002
Genus	S	V + T	0.5464	0.001	0.4636	0.001
	V	S + T	0.2189	0.068	0.3664	0.003
	T	S + V	−0.0567	0.654	−0.0186	0.531
	V + T	S	0.0403	0.334	0.2064	0.027
	S + T	V	0.4011	0.002	0.3781	0.003
	S + V	T	0.5826	0.001	0.5356	0.001

S, soil physicochemical features; V, vegetation community characteristics; T, topographic factors. *p*-values are based on 9999 permutations.

4. Discussion

4.1. Degradation and Cultivation Significantly Changes the Biotic and Abiotic Components

Changes in the dominant species and vegetation coverage were the preferred evidence for identifying vegetation degradation [1]. With the meadow degradation, the sedge was

gradually replaced by miscellaneous and toxic grasses (Table S1) [4]. It was found that the coverage, species richness, and aboveground biomass significantly decreased with meadow degradation [34], which was verified in our study (Table 1). However, the Shannon–Wiener index and Simpson index had the highest and lowest levels in MDAM. This result might be explained by the fact that the importance value of each vegetation species was equivalent and there was no absolute competitive ability of any vegetation species in the community. It had been suggested that the moderate degradation stage was a transitional point for meadow degradation, with this transition mainly mirrored in the soil physiochemical features (Table 1) [35,36]. The level of all investigated physiochemical features dramatically changed before the MDAM stage and remained stable after the MDAM, except TK (Table 1). This result might be explained by the fact that the increased sand content and decreased clay content in the soil reduced its moisture retention capacity and denitrification with the onset of degradation, resulting in leaching losses of soil nutrition (Table 1) [21,37]. Artificial cultivation was used as an available restoration strategy for improving plant and soil resilience in degraded meadow and alleviating the conflict of grass storage on the Qinghai–Tibet Plateau [38]. Xing et al. [39] showed that artificial cultivation significantly improved the vegetation and soil environment compared to BSB. In this study, the improvement was insignificant and mainly occurred in the soil environment. Gao et al. [40] believed that highly degraded grassland could be restored by revegetated grassland through 16–18 years' recovery. Moreover, the improvements were inconsistent between soil physicochemical features, vegetation community characteristics, and soil quality lagged behind the vegetation quality under restoration (Tables 2 and 3) [40].

Soil bacteria are important in the natural cycle of organic matter, soil formation, and soil fertility [41]. The composition and structure of soil bacteria will ultimately affect these functions [42]. In this study, similar dominant bacteria were also found as in the previous studies, regardless of relative abundance discrepancies [9,13]. The relative abundance of dominate soil bacteria including Proteobacteria, Actinobacteria, Chloroflexi, Gemmatimonadetes, and Bacteroidetes significantly varied suffered from degradation and cultivation. Proteobacteria, widely recognized as copiotrophic bacteria, had the lowest abundance in MDAM possibly due to the low-fertility and alkaline soil in a cold environment (Figure 3c; Table 1) [14,43]. The relative abundance of Actinobacteria, which prefer to survive and reproduce in a neutral or alkaline environment, decreased with degradation and cultivation (Figure 3) [6,9,36]. The significant change in Chloroflexi mainly occurred between MDAM and AAG (Figure 3c). The reason for this was not clear, but it might have something to do with oxidation of inorganic carbon and degradation of macromolecules such as cellulose [44]. The variation of Gemmatimonadetes was consistent with Bacteroidetes and mainly concentrated in AAG (Figures 3 and 4). Deuruyn et al. [45] believed that Gemmatimonadetes preferred environments with low soil moisture, while Bacteroidetes preferred anaerobic environments with high moisture [46]. Therefore, we deduced that these two bacteria concentrated in AAG were possibly related to the specific nitrogen utilization in artificial grassland independent of soil moisture [47,48]. Other dominant bacteria such as Acidobacteria, Firmicutes, Rokubacteria, Verrucomicrobia, Nitrospire, and Patescibacteria, possibly characteristic of wider ecological amplitude and higher interference resistance, were stable in the process of succession [6,11]. At the genus level, the relative abundance of most of soil bacteria differed throughout the four alpine grasslands, indicating a filtering effect of the environmental conditions (Figure 3b) [41]. This also suggested that bacteria at the genus level were more sensitive to the environmental conditions compared to those at the phylum level. MDAM and AAG had more significantly differentiated species, possibly due to the unstable environment in these stages (Figures 3b and 4). Previous studies paid more attention to the differentiated species of shared bacteria among different environments [9,13,41]. The unique bacteria were also identified among different succession stages in our study. Although AAG had more differentiated species, it also had more unique bacteria regardless of different taxonomic units (Table 2). Epsilonbacteraeota was identified as a unique phylum in the AAG, which was

characteristic of autotrophic, motile, thermophilic and possibly absorbed nitrogen from ammonium taken up from the environment or created from ambient nitrate and nitrite by utilizing a range of function redox modules [49]. In addition, AAG and IAM covered more common bacteria regardless of taxonomic units, indicating a possibly improving microbial environment in the AAG (Table 2). Microbial functional genes are more sensitive to environmental disturbance [50,51]. Consistent with the previous studies, Chemoheterotrophy, aerobic chemoheterotrophy, and nitrification were the dominant functional bacteria groups under degradation and cultivation (Figure 5) [9,13]. With the degradation, the proportions of chemoheterotrophy, aerobic chemoherotrophy, and methanotrophy increased and carbon was reduced (Figure 6; Table 1). However, the drastic increase occurred between the IAM and MDAM stages and moderately increased subsequently, consistent with the variations in most of soil physicochemical features [13]. It was also found that IAM had the highest nitrogen fixation capacity (Figure 5). These findings suggested the superiority of IAM in carbon and nitrogen fixation [3,23,52]. The abundance of nitrification, aerobic ammonia oxidation, and aerobic nitrite oxidation increased at AAG, which facilitated the formation and accumulation of nitrogen assimilated by crops [52]. An implication of this was the possibility that artificial cultivation improved the geochemical cycling of nitrogen. Degradation had potential effects on bacteria involved in nitrate reduction and MDAM was an inflection point for this function (Figure 5). The high abundance of nitrogen reduction functional bacteria suggested soil nitrogen emissions [53]. Therefore, MDAM was possibly the key stage for nitrogen loss under meadow degradation and required more attention. Therefore, the restoration of degraded meadows should be arranged before the MDAM stage.

4.2. The Relationships among the Biotic and Abiotic Factors under Different Taxonomic Level

The correlation analysis suggested interactions among soil physicochemical features, vegetation community characteristics, and bacterial diversities at the community level (Figure 6). TN, SOC, BD, and WC interacted with the vegetation coverage and aboveground biomass. Degradation of vegetation coverage increased the loss of TN and SOC stocks [23]. Grazing or rodent activity reduced aboveground biomass and impeded root system growth, resulting in a reduction in SOM inputs [54]. BD was a necessary indicator for predicting TN and SOC, and was affected by vegetation coverage and above-ground biomass [23]. Degradation directly resulted in the synergistic variation of vegetation coverage and WC [55]. The above indicators, pH, and the Gleason index were also found to interact with soil bacterial diversities and biomass (Figure 6). Previous studies had verified that SOC, WC, BD, and pH had a high explanatory power for soil bacterial communities [33,41]. Above-ground biomass, species richness, and coverage of vegetation community also significantly affected the soil bacterial community [5,56]. Gene copy numbers, widely used to represent absolute microbial abundance, decreased accompanied by meadow degradation [57,58]. Interestingly, there was a positive correlation between the gene copy numbers of soil bacterial communities and vegetation above-ground biomass ($p < 0.05$). Correlation was also significantly positive between vegetation coverage, the Gleason index, TN, TOC, WC, and negative with the Simpson index, pH, and BD.

Correlations between environmental factors and soil bacterial compositions were changed at the phylum and genus level (Figure 7). This finding was also reported by Zhou et al. [6]. It was found that only the Gleason index, Simpson index, and TP were significantly related to the soil bacterial structure at the phylum level, while vegetation coverage, Simpson index, TN, TP, and pH were closely associated with the soil bacterial structure at the genus level ($p < 0.05$). Other environmental factors, such as SOC, BD, and WC, were not key environmental factors for the soil bacterial structure [2]. In accordance with the present results, previous studies have demonstrated that TP was the key factor of microbial growth [59,60]. Another implication from our result was that the distribution of plant species in different communities resulted in different soil bacterial compositions. More pronounced environmental factors were detected at the genus level, possibly due to greater variability of soil bacterial species among different habitats (Figure 5). These

driving factors identified in this study were not exactly consistent with other studies. This discrepancy might be due to the different study sites, sampling times, and study areas with complex interactions of environmental factors [6,9]. The composition of the soil microbial community was affected by vegetation, soil, and topographic characteristics [6,61]. Furthermore, the effect of soil physicochemical features on the soil microbial community was always considered to outweigh the effect of vegetation community characteristics [5,9]. In this study, topographic factors were also considered due to sampling sites with varied topographic factors. Soil physicochemical features had closer relations than vegetation community characteristics on soil bacterial communities, regardless of the phylum or genus level, which also broadly supported the work of other studies in this area [9,21]. Although vegetation destruction was the initial symptom of meadow degradation, soil nutrients varied more than other environmental variables and became the crucial driver of soil microbial community composition change [9,13]. Zhang et al. [62] also concluded that there was a lag effect of vegetation characteristics on soil bacterial communities. Moreover, topographic factors had the least relation with soil bacterial communities in comparison to soil and vegetation characteristics. The relationship between topographic factors and the soil bacterial community was equivalent to an indirect interaction. Topography modified soil bacterial communities predominantly through its effect on the soil's physicochemical features [63].

5. Conclusions

Meadow degradation and artificial cultivation greatly changed the vegetation, soil, and microbe variables. Synchrony existed between the deterioration of soil vegetation before the MDAM stage. Improved soil quality lagged behind the vegetation quality after cultivation. Soil bacteria response to degradation and cultivation lagged behind soil and vegetation variables. The soil bacterial community structures were altered dramatically with the levels of degradation and cultivation. The dominant bacteria among different degradation and cultivation levels were similar with significantly differentiated relative abundance. A one-way analysis of variation (ANOVA) and linear discriminate analysis (LDA) effect size (LEfSe) analysis indicated that MDAM and AAG were the transitional and unstable stages for meadow reverse succession, and had more specific bacteria. One of the more significant findings to emerge from this study was that AAG also had prominent unique bacteria and more bacteria in common with IAM. FAPROTAX prediction analysis suggested that bacterial function in MDAM had potential effects on nitrate reduction, while bacteria function in AAG facilitated the formation of nitrate easily assimilated by plants. The unstable AAG was not significantly improving from degraded meadow, and also lagged a large gap to IAM. The relationships among the biotic and abiotic factors under different taxonomic levels varied. Above-ground biomass, species richness, vegetation coverage, SOC, C/N, BD, WC, and pH were significantly correlated with soil bacterial diversities. Above-ground biomass was an effective indicator for predicting soil bacterial biomass. The soil bacterial compositions were mostly connected to the TP and Simpson index when both phylum and genus levels were considered. Moreover, soil factors had closer relations with soil bacterial communities than vegetation and topographical factors regardless of phylum or genus levels.

Supplementary Materials: The following supporting information can be downloaded at: https://www.mdpi.com/article/10.3390/land11030396/s1; Figure S1: Soil texture triangle coordinates of different types of alpine meadow, based on the international soil classification system; Table S1: Basic information of the alpine meadow under degradation and cultivation.

Author Contributions: Conceptualization, H.Z. and M.D.; methodology, Y.Z.; software, Y.Z.; validation, H.Z. and M.D.; formal analysis, Y.Z.; investigation, H.Z., Y.Z., Z.Y., F.X., P.H. and F.Z.; resources, H.Z. and M.D.; data curation, H.Z.; writing—original draft preparation, Y.Z.; writing—review and editing, H.Z.; visualization, Y.Z., N.W. and F.X.; supervision, H.Z.; project administration, M.D. All authors have read and agreed to the published version of the manuscript.

Funding: This research was funded by the Second Tibetan Plateau Scientific Expedition and Research, grant number 2019QZKK0603 and National Natural Science Foundation of China, grant number 42061018.

Institutional Review Board Statement: Not applicable.

Informed Consent Statement: Not applicable.

Data Availability Statement: Data are contained within the article.

Conflicts of Interest: The authors declare no conflict of interest.

References

1. You, Q.; Xue, X.; Peng, F.; Xu, M.; Duan, H.; Dong, S. Comparison of ecosystem characteristics between degraded and intact alpine meadow in the Qinghai-Tibetan Plateau, China. *Ecol. Eng.* **2014**, *71*, 133–143. [CrossRef]
2. Xu, Y.; Dong, S.; Gao, X.; Yang, M.; Li, S.; Shen, H.; Xiao, J.; Han, Y.; Zhang, J.; Li, Y.; et al. Aboveground community composition and soil moisture play determining roles in restoring ecosystem multifunctionality of alpine steppe on Qinghai-Tibetan Plateau. *Agric. Ecosyst. Environ.* **2020**, *305*, 107163. [CrossRef]
3. Wang, X.T.; Zang, C.; Liao, L.R.; Wang, J.; Yu, L.H.; Zhang, X.Z. Effects of Degradation of Alpine Meadow on Soil Microbial Genes in Nitrogen Transformation in Qinghai-Tibet Plateau. *B. Soil Water Conserv.* **2020**, *40*, 8–13. (In Chinese with English Abstract)
4. Hao, A.H.; Xue, X.; Peng, F.; You, Q.G.; Liao, J.; Duan, H.C.; Huang, C.H.; Dong, S.Y. Different vegetation and soil degradation characteristics of a typical grassland in the Qinghai-Tibetan Plateau. *Acta Ecol. Sin.* **2020**, *40*, 964–975. (In Chinese with English Abstract)
5. Wang, J.; Wang, X.; Liu, G.; Wang, G.; Zhang, C. Grazing-to-fencing conversion affects soil microbial composition, functional profiles by altering plant functional groups in a Tibetan alpine meadow. *Appl. Soil Ecol.* **2021**, *166*, 104008. [CrossRef]
6. Zhou, H.; Zhang, D.; Jiang, Z.; Sun, P.; Xiao, H.; Yuxin, W.; Chen, J. Changes in the soil microbial communities of alpine steppe at Qinghai-Tibetan Plateau under different degradation levels. *Sci. Total Environ.* **2018**, *651*, 2281–2291. [CrossRef]
7. Wu, G.-L.; Ren, G.-H.; Dong, Q.-M.; Shi, J.-J.; Wang, Y.-L. Above- and Belowground Response along Degradation Gradient in an Alpine Grassland of the Qinghai-Tibetan Plateau. *CLEAN–Soil Air Water* **2013**, *42*, 319–323. [CrossRef]
8. Zhang, L.; Unteregelsbacher, S.; Hafner, S.; Xu, X.; Schleuss, P.-M.; Miehe, G.; Kuzyakov, Y. Fate of Organic and Inorganic Nitrogen in Crusted and Non-Crusted Kobresia Grasslands. *Land Degrad. Dev.* **2016**, *28*, 166–174. [CrossRef]
9. Li, H.; Qiu, Y.; Yao, T.; Han, D.; Gao, Y.; Zhang, J.; Ma, Y.; Zhang, H.; Yang, X. Nutrients available in the soil regulate the changes of soil microbial community alongside degradation of alpine meadows in the northeast of the Qinghai-Tibet Plateau. *Sci. Total Environ.* **2021**, *792*, 148363. [CrossRef]
10. Dai, L.; Yuan, Y.; Guo, X.; Du, Y.; Ke, X.; Zhang, F.; Li, Y.; Li, Q.; Lin, L.; Zhou, H.; et al. Soil water retention in alpine meadows under different degradation stages on the northeastern Qinghai-Tibet Plateau. *J. Hydrol.* **2020**, *590*, 125397. [CrossRef]
11. Gao, X.; Dong, S.; Xu, Y.; Li, Y.; Li, S.; Wu, S.; Shen, H.; Liu, S.; Fry, E.L. Revegetation significantly increased the bacterial-fungal interactions in different successional stages of alpine grasslands on the Qinghai-Tibetan Plateau. *CATENA* **2021**, *205*, 105385. [CrossRef]
12. Dai, Y.T.; Yan, Z.J.; Xie, J.H.; Wu, H.X.; Xu, L.B.; Hou, X.Y.; Gao, L.; Cui, Y.W. Soil bacteria diversity in rhizosphere under two types of vegetation restoration based on high throughput sequencing. *Acta Pedol. Sin.* **2017**, *54*, 735–748.
13. Li, S.X.; Wang, Y.L.; Wang, Y.Q.; Yin, Y.L. Response of soil bacterial community characteristics on alpine meadow degradation. *Biodiv. Sci.* **2021**, *29*, 53–64.
14. Che, R.; Wang, Y.; Li, K.; Xu, Z.; Hu, J.; Wang, F.; Rui, Y.; Li, L.; Pang, Z.; Cui, X. Degraded patch formation significantly changed microbial community composition in alpine meadow soils. *Soil Tillage Res.* **2019**, *195*, 104426. [CrossRef]
15. Zhou, H.K.; Zhao, X.Q.; Zhou, L.; Liu, W.; Li, Y.N.; Tang, Y.H. Characteristics of vegetation degradation and soil degradation in alpine meadow on Tibetan Plateau. *Acta Pratacul. Sin.* **2005**, *3*, 31–40. (In Chinese with English Abstract)
16. Du, Y.; Cao, G.; Wang, Q.; Wang, C. Effects of grazing on surface characteristics and soil physical properties in alpine meadow. *Mt. Res.* **2007**, *3*, 338–343. (In Chinese with English Abstract)
17. Li, Y.K.; Han, F.; Ran, F.; Bao, S.K.; Zhou, H.K. Effects of alpine meadow degradation on soil nutrients and soil enzyme activities in the Three-river Source region. Chinese. *J. Grassl.* **2008**, *4*, 51–58. (In Chinese with English Abstract)
18. Zhou, H.K.; Zhao, X.Q.; Wen, J.; Chen, Z.; Yao, B.Q.; Yang, Y.W.; Xu, W.X.; Duan, J.C. Characteristics of vegetation degradation and soil degradation on alpine steppe in the source region of Yellow River. *Acta Pratacul. Sin.* **2012**, *21*, 1–11. (In Chinese with English Abstract)
19. Xue, X.; You, Q.; Peng, F.; Dong, S.; Duan, H. Experimental Warming Aggravates Degradation-Induced Topsoil Drought in Alpine Meadows of the Qinghai-Tibetan Plateau. *Land Degrad. Dev.* **2017**, *28*, 2343–2353. [CrossRef]
20. Pan, T.; Hou, S.; Liu, Y.J.; Tan, Q.H.; Liu, Y.H.; Gao, X.F. Influence of degradation on soil water availability in an alpine swamp meadow on the eastern edge of the Tibetan Plateau. *Sci. Total Environ.* **2020**, *722*, 137677. [CrossRef]
21. Li, Y.; Wang, S.; Jiang, L.; Zhang, L.; Cui, S.; Meng, F.; Wang, Q.; Li, X.; Zhou, Y. Changes of soil microbial community under different degraded gradients of alpine meadow. *Agric. Ecosyst. Environ.* **2016**, *222*, 213–222. [CrossRef]

22. Shang, Z.H.; Dong, Q.M.; Shi, J.J.; Zhou, H.K.; Dong, S.K.; Shao, X.Q.; Li, S.X.; Wang, Y.L.; Ma, Y.S.; Ding, L.M.; et al. Research progress in recent ten years of ecological restoration for "black soil land" degraded grassland on Tibetan Plateau—Concurrently discuss of ecological restoration in Sanjiangyuan Region. *Acta Agrestia Sin.* **2018**, *1*, 1–21. (In Chinese with English Abstract)
23. Liu, X.; Wang, Z.; Zheng, K.; Han, C.; Li, L.; Sheng, H.; Ma, Z. Changes in soil carbon and nitrogen stocks following degradation of alpine grasslands on the Qinghai-Tibetan Plateau: A meta-analysis. *Land Degrad. Dev.* **2020**, *32*, 1262–1273. [CrossRef]
24. Luo, Z.; Liu, J.; Jia, T.; Chai, B.; Wu, T. Soil Bacterial Community Response and Nitrogen Cycling Variations Associated with Subalpine Meadow Degradation on the Loess Plateau, China. *Appl. Environ. Microbiol.* **2020**, *86*, e00180-20. [CrossRef] [PubMed]
25. Du, C.J.; Zhang, Y.L.; Liu, L.S.; Wang, Z.F.; Zhang, J.; Zhou, Q. Herdsmen' s adaptation to alpine grassland degradation: A case study of Dalag County, China. *Resour. Sci.* **2009**, *31*, 973–979. (In Chinese with English Abstract)
26. Wei, Y. Establishing Developing and Applying of the Space-Air-Field Integrated Eco-Monitoring and Data Infrastructure of the Three-River-Source National Park. In *The Boundaries of the Source Regions in Sanjiangyuan Region*; National Tibetan Plateau Data Center: Beijing, China, 2018; CSTR: 18406.11. Geogra.tpdc.270009. [CrossRef]
27. Zhang, Y.L.; Li, B.Y.; Liu, L.S.; Zheng, D. Redetermine the region and boundaries of Tibetan Plateau. *Geogra. Res.* **2021**, *40*, 1543–1553.
28. Li, J.; Wang, H.; Hu, J.; Zhai, B.J.; Ren, X.N.; Wang, C.L. Plant species diversity and its relationship with environmental factors in Ningwu Laoshifu Sea wetland. *Chin. J. Ecol.* **2021**, *40*, 950–958. (In Chinese with English Abstract)
29. Zhang, H.; Jiang, Y.; Ding, M.; Xie, Z. Level, source identification, and risk analysis of heavy metal in surface sediments from river-lake ecosystems in the Poyang Lake, China. *Environ. Sci. Pollut. Res.* **2017**, *24*, 21902–21916. [CrossRef]
30. Nelson, D.W.; Sommers, L.E. Total carbon, organic carbon, and organic matter. In *Methods of Soil Analysis*; Page, A.L., Miller, R.H., Keeney, D.R., Eds.; American Society of Agronomy: Madison, WI, USA, 1982; pp. 539–579.
31. Bao, S. *Agricultural Chemical Analysis of Soil*; China Agriculture Press: Beijing, China, 2000; pp. 14–16, 70–89.
32. Zhang, N.N.; Zhong, B.; Zhao, C.Z.; Wang, E.T.; Wang, Y.J.; Chen, D.M.; Shi, F.S. Change of soil physicochemical properties, bacterial community and aggregation during desertification of grasslands in the Tibetan Plateau. *Eur. J. Soil Sci.* **2020**, *72*, 274–288. [CrossRef]
33. Edgar, R.C. UPARSE: Highly accurate OTU sequences from microbial amplicon reads. *Nat. Methods* **2013**, *10*, 996–998. [CrossRef]
34. Liu, X.N.; Sun, J.L.; Zhang, D.G.; Pu, X.P.; Xu, G.P. A study on the community structure and plant diversity of alpine meadow under different degrees of degradation in Eastern Qilian Mountains. *Acta Pratacul. Sin.* **2008**, *17*, 1–11. (In Chinese with English Abstract)
35. Yang, Y.W.; Li, X.L.; Zhou, X.H.; Qin, Y.J.; Shi, Y.Y.; Li, C.Y.; Zhou, H.K. Study on the relationship between plant community degradation and soil environmental characteristics in alpine meadow. *Acta Agrestia Sin.* **2016**, *4*, 1211–1217. (In Chinese with English Abstract)
36. Li, C.Y.; Lai, C.M.; Peng, F.; Xue, X.; You, Q.; Zhang, W.; Liu, F. Productivity and community structure of alpine meadow at different degraded levels in the Northern Luhe Watershed of the Tibetan Plateau. *Pratacul. Sci.* **2019**, *36*, 1044–1052. (In Chinese with English Abstract)
37. Li, Y.J.; Liu, J.; Xu, C.L.; Cao, W.X. Effects of different degradation degrees on soil inorganic nitrogen and urease activity in alpine meadow. *Acta Pratacul. Sin.* **2018**, *27*, 45–53. (In Chinese with English Abstract)
38. Wei, X.; Li, Y.; Wu, P.F. Effects of artificial grasslands with different forage species on soil nematode communities on the Qinghai-Tibetan Plateau. *Acta Ecol. Sin.* **2022**, *42*, 1–17. (In Chinese with English Abstract)
39. Xing, Y.F.; Wang, X.L.; Liu, Y.Q.; Hua, R.; Wang, C.; Wu, J.L.; Shi, J.J. Characteristics of plant community and soil organic carbon and nitrogen in artificial grassland with different planting years. *Acta Agrestia Sin.* **2020**, *28*, 521–528. (In Chinese with English Abstract)
40. Gao, X.; Dong, S.; Xu, Y.; Wu, S.; Wu, X.; Zhang, X.; Zhi, Y.; Li, S.; Liu, S.; Li, Y.; et al. Resilience of revegetated grassland for restoring severely degraded alpine meadows is driven by plant and soil quality along recovery time: A case study from the Three-river Headwater Area of Qinghai-Tibetan Plateau. *Agric. Ecosyst. Environ.* **2019**, *279*, 169–177. [CrossRef]
41. Jiang, H.; Chen, Y.; Hu, Y.; Wang, Z.; Lu, X. Soil Bacterial Communities and Diversity in Alpine Grasslands on the Tibetan Plateau Based on 16S rRNA Gene Sequencing. *Front. Ecol. Evol.* **2021**, *9*, 630722. [CrossRef]
42. Bier, R.L.; Bernhardt, E.S.; Boot, C.M.; Graham, E.; Hall, E.K.; Lennon, J.T.; Nemergut, D.R.; Osborne, B.B.; González, C.R.; Schimel, J.P.; et al. Linking microbial community structure and microbial processes: An empirical and conceptual overview. *FEMS Microbiol. Ecol.* **2015**, *91*, fiv113. [CrossRef]
43. Thomson, B.C.; Ostle, N.; McNamara, N.; Bailey, M.J.; Whiteley, A.; Griffiths, R.I.; Ostle, N. Vegetation Affects the Relative Abundances of Dominant Soil Bacterial Taxa and Soil Respiration Rates in an Upland Grassland Soil. *Microb. Ecol.* **2009**, *59*, 335–343. [CrossRef]
44. Xian, W.D.; Zhang, X.T.; Li, W.J. Research status and prospect on bacterial phylum Chloroflexi. *Acta Microbiol. Sin.* **2020**, *60*, 1801–1820. (In Chinese with English Abstract)
45. DeBruyn, J.M.; Nixon, L.T.; Fawaz, M.N.; Johnson, A.M.; Radosevich, M. Global Biogeography and Quantitative Seasonal Dynamics of Gemmatimonadetes in Soil. *Appl. Environ. Microbiol.* **2011**, *77*, 6295–6300. [CrossRef] [PubMed]
46. Lu, M. Effects of Napahai Wetland Degradation on Soil Microbial Community Structure and Diversity. Ph.D. Thesis, Beijing Forestry University, Beijing, China, 2018.

47. Guo, Y.; Gong, H.; Guo, X. Rhizosphere bacterial community of Typha angustifolia L. and water quality in a river wetland supplied with reclaimed water. *Appl. Microbiol. Biotechnol.* **2014**, *99*, 2883–2893. [CrossRef] [PubMed]
48. Sun, H.F.; Li, X.L.; Jin, L.Q.; Li, C.Y.; Zhang, J. Change over time in soil microbial diversity of artificial grassland in the Yellow River source zone. *Acta Pratacul. Sin.* **2021**, *30*, 46–58. (In Chinese with English Abstract)
49. Waite, D.W.; Vanwonterghem, I.; Rinke, C.; Parks, D.H.; Zhang, Y.; Takai, K.; Sievert, S.M.; Simon, J.; Campbell, B.J.; Hanson, T.E.; et al. Comparative Genomic Analysis of the Class Epsilonproteobacteria and Proposed Reclassification to Epsilonbacteraeota (phyl. nov.). *Front. Microbiol.* **2017**, *8*, 682. [CrossRef]
50. Ma, X.; Zhang, Q.; Zheng, M.; Gao, Y.; Yuan, T.; Hale, L.; Van Nostrand, J.D.; Zhou, J.; Wan, S.; Yang, Y. Microbial functional traits are sensitive indicators of mild disturbance by lamb grazing. *ISME J.* **2019**, *13*, 1370–1373. [CrossRef]
51. Wu, M.-H.; Chen, S.-Y.; Chen, J.-W.; Xue, K.; Chen, S.-L.; Wang, X.-M.; Chen, T.; Kang, S.-C.; Rui, J.-P.; Thies, J.E.; et al. Reduced microbial stability in the active layer is associated with carbon loss under alpine permafrost degradation. *Proc. Natl. Acad. Sci. USA* **2021**, *118*, e2025321118. [CrossRef]
52. Yang, Y.D.; Zhang, M.C. Hu teria and Archaea in a North China agricultural soil. *Acta Ecol. Sin.* **2017**, *37*, 3636–3646. (In Chinese with English Abstract)
53. Yin, S.; Chen, D.; Chen, L.; Edis, R. Dissimilatory nitrate reduction to ammonium and responsible microorganisms in two Chinese and Australian paddy soils. *Soil Biol. Biochem.* **2002**, *34*, 1131–1137. [CrossRef]
54. Pang, X.P.; Guo, Z.G. Effects of plateau pika disturbance levels on the plant diversity and biomass of an alpine meadow. *Grassl. Sci.* **2018**, *64*, 159–166. (In Chinese with English Abstract) [CrossRef]
55. Wang, J.; Liu, G.; Zhang, C.; Wang, G. Effect of long-term destocking on soil fungal functional groups and interactions with plants. *Plant Soil* **2020**, *448*, 495–508. [CrossRef]
56. Chen, Y.-L.; Ding, J.-Z.; Peng, Y.-F.; Li, F.; Yang, G.-B.; Liu, L.; Qin, S.-Q.; Fang, K.; Yang, Y.-H. Patterns and drivers of soil microbial communities in Tibetan alpine and global terrestrial ecosystems. *J. Biogeogr.* **2016**, *43*, 2027–2039. [CrossRef]
57. Hu, A.; Nie, Y.; Yu, G.; Han, C.; He, J.; He, N.; Liu, S.; Deng, J.; Shen, W.; Zhang, G. Diurnal Temperature Variation and Plants Drive Latitudinal Patterns in Seasonal Dynamics of Soil Microbial Community. *Front. Microbiol.* **2019**, *10*, 674. [CrossRef] [PubMed]
58. Du, Y.; Ke, X.; Dai, L.; Cao, G.; Zhou, H.; Guo, X. Moderate grazing increased alpine meadow soils bacterial abundance and diversity index on the Tibetan Plateau. *Ecol. Evol.* **2020**, *10*, 8681–8687. [CrossRef]
59. Liu, L.; Gundersen, P.; Zhang, T.; Mo, J. Effects of phosphorus addition on soil microbial biomass and community composition in three forest types in tropical China. *Soil Biol. Biochem.* **2012**, *44*, 31–38. [CrossRef]
60. Quast, C.; Pruesse, E.; Yilmaz, P.; Gerken, J.; Schweer, T.; Yarza, P.; Peplies, J.; Glöckner, F.O. The SILVA ribosomal RNA gene database project: Improved data processing and web-based tools. *Nucleic Acids Res.* **2013**, *41*, 590–596. [CrossRef]
61. Ma, J.P.; Pang, D.B.; Chen, L.; Wan, H.Y.; Chen, G.L.; Li, X.B. Characteristics of soil microbial community structure under different altitude vegetation in Helan Mountain. *Acta Ecol. Sin.* **2022**, *2*, 1–10. (In Chinese with English Abstract)
62. Zhang, C.; Liu, G.; Song, Z.; Wang, J.; Guo, L. Interactions of soil bacteria and fungi with plants during long-term grazing exclusion in semiarid grasslands. *Soil Biol. Biochem.* **2018**, *124*, 47–58. [CrossRef]
63. Yuan, X.C.; Liu, H.Y.; Zeng, Q.X.; Chen, W.W.; Chen, J.M.; Xu, J.H.; Chen, Y.M.; Lin, K.M. Soil organic nitrogen depolymerase activity and its influencing factors of Pinus huangshanensis under different elevations in Wuyi Mountain. *Acta Ecol. Sin.* **2022**, *4*, 1–11. (In Chinese with English Abstract)

MDPI
St. Alban-Anlage 66
4052 Basel
Switzerland
www.mdpi.com

Land Editorial Office
E-mail: land@mdpi.com
www.mdpi.com/journal/land

Academic Open
Access Publishing

mdpi.com

ISBN 978-3-7258-0558-7